AD_____

Award Number: DAMD17-99-1-9402

TITLE: Training Program in the Molecular Basis of Breast Cancer Research

PRINCIPAL INVESTIGATOR: Wen-Hwa Lee, Ph.D.

CONTRACTING ORGANIZATION: The University of Texas Health Science Center at San Antonio
San Antonio, Texas 78284-7828

REPORT DATE: August 2001

TYPE OF REPORT: Annual Summary

PREPARED FOR: U.S. Army Medical Research and Materiel Command
Fort Detrick, Maryland 21702-5012

REPORT DOCUMENTATION PAGE

Form Approved
OMB No. 074-0188

1. AGENCY USE ONLY (Leave blank)	2. REPORT DATE	3. REPORT TYPE AND DATES COVERED
	August 2001	Annual Summary (1 Aug 00 - 31 Jul 01)

4. TITLE AND SUBTITLE
Training Program in the Molecular Basis of Breast Cancer Research

5. FUNDING NUMBERS
DAMD17-99-1-9402

6. AUTHOR(S)
Wen-Hwa Lee, Ph.D.

7. PERFORMING ORGANIZATION NAME(S) AND ADDRESS(ES)
The University of Texas Health Science Center at San Antonio
San Antonio, Texas 78284-7828

E-Mail: **grants@uthscsa.edu**

8. PERFORMING ORGANIZATION REPORT NUMBER

9. SPONSORING / MONITORING AGENCY NAME(S) AND ADDRESS(ES)
U.S. Army Medical Research and Materiel Command
Fort Detrick, Maryland 21702-5012

10. SPONSORING / MONITORING AGENCY REPORT NUMBER

11. SUPPLEMENTARY NOTES
Report contains color

12a. DISTRIBUTION / AVAILABILITY STATEMENT
Approved for Public Release; Distribution Unlimited

12b. DISTRIBUTION CODE

13. ABSTRACT *(Maximum 200 Words)*

The objective of the program is to train highly qualified doctoral students in the genetic, cellular, and molecular basis of Breast Cancer. The training program, conducted within the Molecular Medicine Ph.D. Program, was administered by a select group of faculty whose research projects were intimately involved in breast cancer. An additional goal of the program was to promote synergistic interactions between the various laboratories engaged in breast cancer research. Breast cancer meetings, Molecular Medicine Distinguished Seminar Series were integral parts of the training program for students supported by the Breast Cancer Training Program. The major strengths of the program were the high quality of the Program faculty, and the interactive nature of the Breast Cancer research community in San Antonio. The program faculty, organized into three subprograms, encompassed scientists and physicians studying different aspects of breast cancer and cancer therapy, as well as fundamental mechanisms of DNA repair, cell growth and cell differentiation. Key research accomplishments during the 1999-00 reporting period were: **1)** publication of 30 peer-reviewed articles by students in the program; **2)** two DOD BCRP pre-doctoral grants awarded to students in the program; **3)** the addition of five new highly qualified faculty; and **4)** four faculty awarded DOD BCRP Idea grants; **5)** five Ph.D. students supported by the program graduated.

14. SUBJECT TERMS	15. NUMBER OF PAGES
breast cancer, research training, cancer therapy, DNA repair and tumor suppressor genes, cell growth regulation and cell differentiation	250
	16. PRICE CODE

17. SECURITY CLASSIFICATION OF REPORT	18. SECURITY CLASSIFICATION OF THIS PAGE	19. SECURITY CLASSIFICATION OF ABSTRACT	20. LIMITATION OF ABSTRACT
Unclassified	Unclassified	Unclassified	Unlimited

Table of Contents

INTRODUCTION

Brief Description of the Training Program and Its Objectives

The goal of the program is to establish at the University of Texas Health Science Center in San Antonio an in-depth training program in the Molecular Genetics of Breast Cancer. The most important goal of the program is to train highly qualified Ph.D. students in the genetic, cellular, and molecular basis of Breast Cancer. Toward these ends, the program has been extremely successful. Based on the publication record of our trainees, our expectation for significant discoveries is being realized. During the reporting period, students supported by the training program achieved a total of 19 publications relevant to breast cancer.

The training program was conducted within the Molecular Medicine Ph.D. Program by a select group of faculty whose research projects are relevant to breast cancer. An additional goal of the program was to promote synergistic interactions between the various laboratories engaged in breast cancer research. An important meeting was the Annual Breast Cancer Symposium held in San Antonio. All students supported by the program were required to attend. Finally, an outstanding Molecular Medicine Seminar Series sponsored by the Department of Molecular Medicine was also a requirement for all trainees. The following seminars in this series were pertinent to breast cancer:

- Fall Semester: 2000

Richard Behringer	"Genetic Regulation of Mammalian Sexual Development"
Leonard P. Freedman	"Mechanisms of Transcriptional Activation by Nuclear Hormone Receptors"
Gregg L. Semenza	"Hypoxia-Inducible Factor 1 and the Pathophysiology of Ischemic and Neoplastic Disease"
Marian B. Carlson	"Snf1/AMPK Kinases, Glucose Signaling, and RNA Pol II Holoenzymes"
Jeremy W. Thorner	"A Novel Checkpoint Pathway that Couples Cell Cycle Progression to Assembly of the Cytokinesis Apparatus"
Virginia A. Zakian	"A Tale of Two Helicases: Effects on Telomeres and Ribosomal DNA"
Gordon L. Hager	"The Dynamic Interaction of Nuclear Receptors with Chromatin: Studies with Living Cells and Reconstituted Templates"
Jerry L. Workman	"Multiprotein Complexes that Regulate Transcription by Modifying Chromatin"
Michael O. Hengartner	"Roads to Ruin: Regulation of Apoptosis in C. *Elegans*"
Michael Simons	"Down Cronus" Gullet: Is Selective Digestion Possible: Selective Regulation of Proteasome Function"
Michael M. Cox	"RecA Protein and the Repair of Stalled Replication Forks"
Joachim Herz	"Signaling by ApoE Receptors in the Brain"

- Spring Semester: 2001

Jeffrey C. Hansen	"Core Histone Acetylation: Tails First"
Lawrence A. Donehower	"Does p53 Regulate Organismal Aging"
Terry L. Orr-Weaver	"Developmental Regulation of DNA Replication"
Arnold J. Berk	"Lessons in Transcription Control From Adenovirus"

Hannah Klein	"DNA Damage Checkpoints and Recombination Mutants"
Martha S. Cyert	"Calcium and Calcineurin Dependent Signal Transduction Pathways in Yeast"
Sankar Mitra	"Interaction Among Base Excision Repair Proteins in Repair of Oxidative DNA Damage"
Xiao-Fan Wang	"TGF-β Signaling Mechanisms"
Chiaho Shih	"Human Hepatitis B Virus Variants"
Joyce L. Hamlin	"Mechanisms of Gross Genetic Instability in Cancer"
Lester Lau	"Angiogenesis and Signaling Through Integrin Receptors"
Mina Bissell	"The Structural Basis of Tissue Specificity: The Role of Extracellular Matrix in Normal and Malignant Breast"
Jerard Hurwitz	"*In Vitro* Studies on Eukaryotic Replecation"
Ramiro Ramirez-Solis	"Functional Genomics in the Mouse"
Jeffrey L. Brodsky	"Molecular Chaperones and Protein Quality Control"
Jay H. Chung	"DNA Damage-Induced Activation of Cds1 (Chk2) Kinase: Implications for Cancer"

Breast Cancer Research Programs and Faculty.

One of the major strengths of the program is the high quality of the Program faculty, and the interactive nature of the Breast Cancer research community in San Antonio, which encompass scientists and physicians studying different aspects of breast cancer and cancer therapy, as well as fundamental mechanisms of to maintain genomic stability, cell growth, differentiation and molecular genetics. These faculty groupings are listed below; detailed descriptions of individual research programs were included in the original application.

Breast Cancer Research Training Faculty

W.-H. Lee, Ph.D. (Director)
C. Kent Osborne, M.D. (Co-Director)
Powell H. Brown, M.D., Ph.D.
Peter O'Connell, Ph.D.
Gary M. Clark, Ph.D.
Suzanne Fuqua, Ph.D.
Alan Tomkinson, Ph.D.
E. Lee, Ph.D.
W.-H. Lee, Ph.D.
Z. Dave Sharp, Ph.D.
Patrick Sung, Ph.D.
Greg R. Mundy
Bettie Sue Masters, Ph.D.
Bandana Chatterjee, Ph.D.
Arun K. Roy, Ph.D.
Judy M. Teale, Ph.D.
Peter M. Ravdin, M.D. Ph.D.
Phang-Lang Chen, Ph.D
Renee Yew, Ph.D.
Tom Boyer, Ph.D.
Maria Gazynska, Ph.D.
Paul Hasty, DVM
Jan Vijg, Ph.D.

**Tadayoshi Bessho, Ph.D., Assistant Professor, Department of Molecular Medicine
**Sung Eun Lee, Ph.D., Assistant Professor, Department of Molecular Medicine

** New faculty additions

Relationship between the Breast Cancer Training Program and the Molecular Medicine Graduate Ph.D. Program

The Breast Cancer Training Program was implemented within the context of the Molecular Medicine Graduate Ph.D. Program. The Molecular Medicine Ph.D. Program is an interdisciplinary Ph.D. training program in the Graduate School of Biomedical Sciences at the UTHSCSA. For the academic year 2000-01, there were a total of 50 students enrolled in the Molecular Medicine Program -- 46 Ph.D. and 4 M.S.

The Breast Cancer Training program takes advantage of the internationally recognized breast cancer research programs existing in the institution for many years, and offers a unique opportunity for students interested in starting careers in breast cancer research. The participating scientists in this breast cancer program represent diverse departments including the Divisions of Medical Oncology, Endocrinology in the Department of Medicine, and the Departments of Cellular and Structural Biology, and Biochemistry. In addition, the University of Texas Institute of Biotechnology and the San Antonio Cancer Institute (SACI), an NIH-designated Cancer Center, represent outstanding resources for training opportunities in clinical and basic science research. The national and international reputation of the participating faculty serve to attract a large number of excellent applicants to the breast cancer research track in the Molecular Medicine program.

The rationale for administering the breast cancer training program in the Molecular Medicine Ph.D. program was based on several important criteria: (1) The Molecular Medicine curriculum is specifically designed to provide basic science training while integrating fundamental principles of molecular biology with modern medicine. A Molecular Medicine Core course provides students with the mechanisms underlying human disease and provides intensive review of specific diseases (including breast cancer) that may serve as models for how human diseases can be studied at the molecular genetic level. (2) The Molecular Medicine program requires the participation of both clinical and basic scientists in the training process. The inclusion of MDs on all student advisory committees insures that every graduate of the program has a clear perspective on the clinical relevance of the basic research in their program that, in most instances, will serve as a guide for the project. (3) The Molecular Medicine program is an interdepartmental, interdisciplinary program that offers flexibility to students in terms of research laboratories, advisors and committee members. This arrangement offers a real potential for synergism in breast cancer research not possible in traditional department-bound programs. In summary, the Ph.D. program in Molecular Medicine offers a near perfect environment for Ph.D. training in breast cancer and has attracted many well-qualified applicants.

Research Support for Program Faculty

An essential component of maintaining a successful and aggressive training program in Breast Cancer Research is the continued research funding of the individual Program Faculty laboratories. The faculty have been extremely successful in obtaining research funding, including over $16 million in total direct costs for the 2000-2001 reporting period.

Key Research Accomplishments:

Research grants awarded to members of the faculty by the Defense Department's Breast Cancer Research Program (BCRP).

Tom Boyer, Ph.D., Career Development Award

Project Title: Regulation of BRCA1 function by DNA damage-induced site-specific phosphorylation.
Project Period 06/01/02 - 05/31/06
Project Total: $176,516 Total for entire project

Considerable evidence implicates DNA-damage-induced site-specific phosporylation of BRCA1 as a critical regulator of its caretaker properties. We hypothesize that DNA damage-induced site-specific phosphorylation of BRCA1 regulates its transcription and/or DNA double-strand break repair activities.

Renee Yew, Ph.D., Career Development Award

Project Title: The role of BRCA1-dependent ubiquitination in Breast Cancer
Project Period: 06/01/02 - 05/31/06
Project Total: $181,960

Mutational inactivation of the BRCA1 gene accounts for a large percentage of hereditary breast cancer. Although the BRCA1 gene product has been implicated to function in a number of different cellular processes including DNA repair and transcription, it is still unclear how BRCA1 biochemically mediates its cellular function as a tumor suppressor protein. It has been suggested that the BRCA1 gene product functions as an ubiquitin protein ligase or E3 enzyme in a manner similar to a growing number of proteins that comprise a family of ring finger proteins. If this putative E3 activity of BRCA1 can be shown to be a physiological function of full length BRCA1 in the cell, this could greatly aid in determining the molecular mechanisms by which BRCA1 mediates its cellular function.

Paul Hasty, DVM, Idea Award

Project Title: Development of anti-cancer therapeutics that disrupt the RAD51-BRCA2 complex.
Project Period: 01/01/02 - 12/31/04
Project Total: $433,500

RAD51 is important for repairing double-strand breaks in DNA by recombination; interestingly, this function is likely to be essential since mammalian cells deleted for RAD51 exhibit chromosomal instability, are unable to sustain proliferation and senesce or die. Our specific aims are: characterize antp-26mer for biological activity on tissue culture cells, perform a deletion and substitution analysis on the antp-26mer, and test peptides for potential as anti-cancer therapeutics in mice.

- *Predoctoral Breast Cancer Research Awards to Supported Trainees*

Predoctoral training grants awarded to current trainees by the Defense Department's Breast Cancer Research Program (BCRP):

Stefan Sigurdsson *training in Dr. Patrick Sung's laboratory.*

Project Title: Functions of Human Rad51 and Other Recombination Factors In DNA Double-Strand Break Repair.
Project Period: 03/01/01 – 02/28/04
Total Award: $61,110

Homologous recombination and recombinational repair of DNA double-strand breaks are mediated by proteins of the *RAD52* epistasis group. Rad51 is a key factor in these processes and the protein can assemble on ssDNA substrates to form a nucleoprotein filament. With the help from other factors, the Rad51-ssDNA nucleoprotein filament searches for a DNA homlog and catalyzes formation of a heteroduplex DNA joint with the homolog. The biochemical reaction that forms heteroduplex DNA joints is called "homologous DNA pairing and strand exchange." A number of Rad51-like proteins are known in human cells, but their function in recombination and DNA repair is currently unknown. I have shown that two of these Rad51-like proteins, Rad51B and Rad51C, are associated in a stable heterodimer. I will further define the homologous DNA pairing and strand exchange activity of human Rad51. In addition, a variety of experiments will be conducted to test the hypothesis that the Rad51B-Rad51C complex promotes the assembly of the Rad51-ssDNA nucleoprotein filament and enhances the efficiency of Rad51-mediated homologous DNA pairing and strand exchange. The information garnered from this study should contribute significantly to our understanding of how DNA double-strand breaks are repaired in human cells.

Stephen Van Komen, *training in Dr. Patrick Sung's laboratory.*

Project Title: Functional Interactions of Human Rad54 with the Rad51 Recombinase
Project Period: 03/01/01 – 02/28/03
Total Award: $60,345

Homologous recombination is essential for the accurate repair of DNA double-strand breaks. Products of the BRCA1 and BRCA2 breast and ovarian susceptibility genes have recently been shown to associate with key members of the recombinational machinery including the Rad51 recombinase. Rad51 is homologous to the bacterial homologous DNA pairing and strand exchange enzyme, RecA. Unlike RecA, yeast Rad51 has little ability to promote pairing between homologous linear ssDNA and covalently closed duplex to form an important recombination intermediate known as a D-loop. Importantly, yeast Rad54, another recombination factor, promotes robust D-loop formation by Rad51. Recently, I have shown that yeast Rad54 uses the free energy from ATP hydrolysis to remodel DNA structure in a fashion that generates both positively and negatively supercoiled domains in the DNA template, and that DNA supercoiling by Rad54 is important for the D-loop reaction. Given the conservation between yeast and human recombination factors, I hypothesize that human Rad54 supercoils DNA and promotes D-loop formation with human Rad51 in a similar manner. Using highly purified human Rad51 and Rad54 proteins, I will study the functional interactions between these two factors in D-loop formation and in supercoiling DNA. The results from these studies will be important for understanding the human recombinational machinery and may provide a system for dissecting the role of BRCA1, BRCA2, and other tumor suppressors in recombination and DNA double-strand break repair.

Sean Post, *training in Dr. E. Lee's laboratory.*

Project Title: Phosphorylation of hRad17 by ATR is required for cell cycle checkpoint activation
Project Period: 01/01/02 - 12/31/04
Total Award: $61,342

The goal of this study is to determine the relationship between ATR, hRad17, Chk2, and BRCA1 and demonstrate how these potential protein networks regulate checkpoint activation. Based on the reuqirement of SpRad3 and SpRad17 for checkpoint activation through SpCds1 in fission yeast and the ability of Chk2 to phosphorylate BRCA2 Ser988 in humans, it is my hypothesis that ATR mediated phosphorylation of hRad17 is required to activate cell cycle checkpoints, through Chk2 and BRCA1.

Karen Block, *training in Dr. Renee Yew's laboratory.*

Project Title: The role of Ubiquitin-Mediated Proteolysis of cyclin D in Breast Cancer
Project Period: 01/01/02-12/31/04
Project Total: $65,636

Recent studies have indicated that cyclin D protein levels are modulated post-transcriptionally by the ubiquitin-mediated protein degradation pathway. The specific E2 and E3 enzymes postulated to target cyclin D for ubiquitination are the ubiquitin conjugating enzyme, CDC34, and the ubiquitin protein ligase called SCF (Skp1, cullin, F-box, ring protiein). We will define and characterize how the regulation of CDC34-SCF activity modulates cyclin D proteolysis during the normal cell cycle and in breast cancer cells.

Graduates During the Reporting Period (A description of their research and future plans is below)

David Levin, Ph.D.

Linda deGraffenried, Ph.D.

Qing Zhong, Ph.D.

Shang Li, Ph.D.

Suh-Chin(Jackie) Lin, Ph.D.

Lei Zheng, Ph.D.

Reportable Outcomes

Supported Trainees, Research Description and Publications

The following outstanding group of trainees was supported on the Breast Cancer Training Program during the final reporting period.

Reporting Period 8/1/00 – 7/31/01

***Sean Post – 4th year
Teresa Motycka – 4th year
Deanna Jansen – 3rd year
Shang Li – 5th year
Qing Zhong – 5th year
Horng-Ru Lin – 3rd year
Song Zhao – 5th year

Lei Zheng – 5th year
Guikai Wu – 3rd year
***Stefan Sigurdsson – 4th year

*** Mr. Sigurdsson was supported for only a part of the reporting period since he as was placed on his DOD BRCP predoctoral fellowship (see below). Mr. Post recently was award a DOD BRCP predoctoral fellowship, and will be replaced on the training grant by an qualified trainee. In addition, Mr. Van Komen, a previous trainee, is also supported by his DOD BRCP predoctoral fellowship (see below). In addition to Mr. Post, Ms. Karen Block was also awarded a fellowship (see below for a full description).

The accomplishments of these students and their mentors are outstanding examples of how small investments in student training can be amplified in programs grounded in excellence.

The 2000-2001 academic year marks the eighth full year of operation for the Molecular Medicine Ph.D. Program, and is the sixth one for the Training Program in the Molecular Basis of Breast Cancer Research. The availability of highly qualified applicants to the Molecular Medicine Program was excellent. Overall, 77 applications were received for admission to the Fall 2000 entering class. Fourteen new students began classes in August of 2000. The total number of students at the start of the Fall semester 2000 in the Molecular Medicine Ph.D. Program at all levels was 50, which includes 18 women, and 1 minority.

Project Summaries and Publications of Ph.D. Trainees

- ***David Levin*** ***Mentor -- Dr. Alan Tomkinson***

DNA joining events are required to maintain the integrity of the genome. Three human genes encoding DNA ligases have been identified. David is identifying the cellular functions involving the product of the LIG1 gene. Previous studies have implicated DNA ligase I in DNA replication and some pathways of DNA repair. During DNA replication, DNA ligase I presumably functions to join Okazaki fragments. However, under physiological salt conditions, DNA ligase I does not interact with DNA. It is Mr. Levin's working hypothesis that DNA ligase I involvement in different DNA metabolic pathways is mediated by specific protein-protein interactions which serve to recruit DNA ligase I to the DNA substrate. To detect proteins that bind to DNA ligase I, David has fractionated a HeLa nuclear extract by DNA ligase I affinity chromatography. PCNA was specifically retained by the DNA ligase I matrix. To confirm that DNA ligase I and PCNA interact directly, Mr. Levin found that in vitro translated and purified recombinant PCNA bind to the DNA ligase I matrix. In similar experiments, he has shown that DNA ligase I interacts with a GST (glutathione S transferase)-PCNA fusion protein but not with GST. Using in vitro translated deleted versions of DNA ligase I, Mr. Levin determined that the amino terminal 120 residues of this polypeptide are required for the interaction with PCNA. During DNA replication PCNA acts as a homotrimer that encircles DNA and tethers the DNA polymerase to its template. He showed that DNA ligase I forms a stable complex with PCNA that is topologically linked to a DNA duplex. Thus, it appears that PCNA can also tether DNA ligase I to its DNA substrate. A manuscript describing these studies has been published in the Proc. Natl. Acad. Sci. U.S.A.

In addition to interacting with PCNA, the amino terminal domain of DNA ligase I also mediates the localization of this enzyme to replication foci. To determine whether these are separable functions David fine mapped the region that interacts with PCNA and, in collaboration with Dr.

Montecucco's group, the region required for recruitment to replication foci. Since the same 19 amino acids are necessary and sufficient for both functions and the same changes in amino acid sequence inactivate both functions, we conclude that DNA ligase I is recruited to replication foci by its interaction with PCNA. A manuscript describing these studies has been published in the EMBO Journal.

In recent studies, Mr. Levin has a constructed a mutant version of DNA ligase I that does not interact with PCNA. Importantly the amino acid substitutions do not affect the catalytic activity of DNA ligase I. By transfecting cDNAs encoding the mutant and wild type DNA ligase I into a DNA ligase I-mutant cell line, he has demonstrated the biological significance of the DNA ligase I/PCNA interaction in DNA replication and long patch base excision repair.

This project is relevant to breast cancer since problems with DNA replication and repair undoubtedly underlie the genomic instability associated with tumor formation.

Publications:

Levin, D. S., McKenna, A. E., Motycka, T. A., Matsumoto, Y. & Tomkinson, A. E. (2000) Interaction between PCNA and DNA ligase I is critical for joining of Okazaki fragments and long-patch base-excision repair. *Curr Biol* **10,** 919-22.

Tomkinson, A. E., Chen, L., Dong, Z., Leppard, J. B., **Levin, D. S.**, Mackey, Z. B. & Motycka, T. A. (2001) Completion of base excision repair by mammalian DNA ligases. Interaction between PCNA and DNA ligase I is critical for joining of Okazaki fragments and long-patch base-excision repair. *Prog Nucleic Acid Res Mol Biol* **68,** 151-64.

Dr. Levin earned his Ph.D. in Molecular Medicine in the summer of 2000, and finishing additional work in a post-doctoral position in Tomkinson's laboratory. He is currently looking at other post-doctoral positions upon completion of his current work.

- ***John Leppard*** ***Mentor -- Alan Tomkinson***

Three genes, *LIG1*, *LIG3* and *LIG4*, encoding DNA ligases have been identified in the mammalian genome. Unlike the *LIG1* and *LIG4* genes, there are no homologues of the *LIG3* gene in lower eukaryotes such as yeast. Biochemical and genetic studies suggest that DNA ligase III participates in base excision repair and the repair of DNA single-strand break. A feature of DNA ligase III that distinguishes it from other eukaryotic DNA ligases is a zinc finger. In published studies we have shown that this zinc finger binds preferentially to nicks in duplex DNA and allows DNA ligase III to efficiently ligate nicks at physiological salt concentrations. These studies will be extended by determining how the zinc finger of DNA ligase III binds to DNA single-strand breaks but does not hinder access of the catalytic domain of DNA ligase III to ligatable nicks. Furthermore, we will reconstitute the base excision and single-strand break repair pathways mediated by DNA ligase III and elucidate the functional consequences of interactions between DNA ligase III and other DNA repair proteins such as Xrcc1, DNA polymerase beta and poly (ADP-ribose) polymerase that participate in these repair pathways.

Mr. Leppard's research is relevant to breast cancer since genomic instability is likely to be involved at several stages during the progression to malignant breast cancer. Methods to intervene and stabilize the genome could prevent progression and spread of the disease. In addition, information about DNA repair processes in normal and cancer cells may lead to the

development of treatment regimes that more effectively kill cancer cells and minimize damage to normal tissues and cells.

Publications:

Tomkinson, A. E., Chen, L., Dong, Z., **Leppard, J. B.**, Levin, D. S., Mackey, Z. B. & Motycka, T. A. (2001) Completion of base excision repair by mammalian DNA ligases. *Prog Nucleic Acid Res Mol Biol* **68,** 151-64.

- ***Teresa Motycka*** ***Mentor -- Alan Tomkinson***

The repair of DNA double strand breaks (DSBs) is critical for maintaining genomic stability. These cytotoxic lesions can be repaired by two different processes, one of which occurs by end-to end joining whereas the other process involves a homologous duplex. Genetic studies in Saccharomyces cerevisiae have identified a group of genes known as the *RAD52* epistasis group that are involved in the repair of DSBs by homologous recombination. The identification of mammalian homologs of these genes indicates that this type of repair is conserved among eukaryotes. The severe phenotype of yeast *rad52* strains suggests that the *RAD52* gene product plays key role in recombinational repair of DSBs. To understand how human Rad52 protein functions, we have fractionated a HeLa cell nuclear extract by hRad52-affinity chromatography and identified proteins that were specifically retained by the resin. A protein implicated in Rad52-dependent recombination pathway by yeast genetic studies was identified by immunoblotting. Two other proteins were identified by amino acid sequencing. One of these proteins is conserved in yeast but encoded by an ORF of unknown function. Inactivation of the gene encoding that protein results in hypersensitivity to DNA damaging agents suggesting that we have identified a novel DNA repair gene.

An understanding of the mechanisms of DSB in mammalian cells is relevant to breast cancer because the accumulating evidence linking the products of the breast cancer susceptibility genes, *BRCA1* and *BRCA2*, with DSB repair.

Publications:

Levin DS, McKenna AE, **Motycka TA**, Matsumoto Y, Tomkinson AE. Interaction between PCNA and DNA ligase I is critical for joining of Okazaki fragments and long-patch base-excision repair. Curr Biol. (2000) 10(15):919-22.

Tomkinson, A.E., Chen, L., Dong, Z., Leppard, J.B., Levin, D.S., Mackey, Z.B., **Motycka, T.A.** Completion of Base Excision Repair by Mammalian DNA Ligases. Progress in Nucleic Acid Research and Molecular Biology (2001) 68: 151-164.

- ***Linda DeGraffenried*** ***Mentor -- Dr. Suzanne Fuqua***

Ms. deGraffenried's current project is to determine the cis-acting sequences responsible for the regulation of the human estrogen receptor gene. Deletion and site-directed mutagenesis of the ER promoter combined with transient transfection assays have revealed elements located proximal as well as distal to the primary transcriptional start site to be responsible. Mobility gel shift analysis suggests that a number of factors in whole cell extracts from ER-positive MCF-7 cells bind to the ER promoter between nucleotides -245 and -192, as indicated by the formation of four specific protein/DNA complexes. This region of the promoter contains a GC box

between -223 bp and -211 bp as well as a non-consensus binding site for Sp1 between -203 bp and -192 bp. Antibodies to the transcription factors Sp1 and Sp3 supershift two of the specific complexes. Co-transfection of expression plasmids for Sp1 and Sp3 with an ER promoter-driven luciferase reporter plasmid into Sp1-void *Drosophila* SL2 cells induces a one-hundred- and a thirty-fold activation of the ER promoter, respectively. Transient transfection assays using linker-scanner mutants of the ER promoter spanning -245 bp to -182 bp also suggest an important role for elements flanking the Sp binding sites in the regulation of ER gene transcription. A detailed elucidation of these elements as well as the DNA-binding proteins that mediate transcriptional response will be characterized.

This project is directly relevant to breast cancer. Elucidating the basis for regulation of ER expression is an important issue in breast cancer research.

Dr. deGraffenried earned her Ph.D. in Molecular Medicine in 2000, and is has a recently been appointed as a research instructor in the Department of Medicine at the UTHSCSA. She is currently working on signal transduction in the insulin response pathway specifically that involving PI3 kinase and PDK pathways in breast cancer cells.

- ***Jill Gilroy*** ***Mentor – Dr. Hanna Abboud***

Signal transduction pathways are a vital part of development, proliferation, and tumorigenesis. In my work, I am interested in the involvement of growth factors, primarily Platelet Derived Growth Factor (PDGF) and its receptor (PDGFR), in signaling pathways. PDGFRs are tyrosine kinase receptors and upon stimulation dimerize and autophosphorylate, which in turn induces many downstream signaling molecules including, Mitogen Activated Protien Kinase (MAPK), and Phosphatidylinositol 3-kinase (PI3K). One of my goals was to determine the role of PI3K and MAPK in mediating biological processes such as cell migration and proliferation by PDGFR activation. Activation of PI3K was assayed using thin layer chromtography of anti-phosphotyrosine immunoprecipitates. MAPK activation was measured by immune complex assay of MAPK immunoprecipitates and SDS-PAGE using anti-phospho-MAPK antibodies. Functional assays, chemotaxis and ^{3}H-thymidine assays, were also preformed to test for cell migration and proliferation respectively. Inhibitors of MAPK and PI3K were also used in these studies to further show the involvement of these pathways in the aforementioned biological processes.

This project is relevant to breast cancer since signal transduction pathways are a vital part of tumorigenesis.

Ghosh Choudhury G, **Ricono JM** Increased effect of interferon gamma on PDGF-induced c-fos gene transcription in glomerular mesangial cells: differential effect of the transcriptional coactivator CBP on STAT1alpha activation. *Biochem Biophys Res Commun* 2000 273:1069-77

Gooch, J. L., Tang, Y., **Ricono, J. M.** & Abboud, H. E. (2001) Insulin-like Growth Factor-I Induces Renal Cell Hypertrophy via a Calcineurin-dependent Mechanism. *J Biol Chem* **276,** 42492-500.

Ricono, J. M., Arar, M., Ghosh Choudhury, G. & Abboud, H. E. (2001) Effect of Platelet-Derived Growth Factor (PDGF) Isoforms in Rat Metanephric Mesenchymal Cells. *Am J Physiol Renal Physiol* **8,** 8.

Also, please note that Ms. JM Gilroy is publishing under her married name (JM Ricono)

- ***Suh-Chin(Jackie) Lin*** ***Mentor -- Dr. Eva Lee***

The tumor suppressor gene, p53, is frequently mutated in human tumors, including breast carcinoma. P53 null mice develop multiple spontaneous tumors, predominantly lymphoma and sarcoma, within the first 6 months of age. To establish a mouse model of p53-mediated mammary tumor development, Ms. Lin initiated a bigenetic approach employing the cre-loxp system. Through gene targeting in embryonic stem (ES) cells, mice carrying floxed p53 genes in which exons 5 and 6 are flanked by the loxp sequence were generated. A second mouse line carrying a cre transgene under the control of mouse mammary tumor virus LTR (MMTV-cre) has also been generated. Floxed p53 mice were mated with MMTV-cre transgenic mice to produce mice with p53 inactivation in mammary tissue. Indeed, we observed p53 excision in the tissues of double transgenic mice. In addition, adenoviral vectors carrying cre recombinase are being used to inactivate p53. These approaches should provide a mouse mammary tumor model for studies of mammary tumor progression resulting from p53 mutation and for testing therapeutic interventions of mammary tumorigenesis. The resulting mice have demonstrated interesting patterns of tumor development including those of the mammary gland. These animals will be valuable models for testing new approaches to breast cancer treatment and understanding its etiology.

Upon DNA damage, p53 protein becomes phosphorylated and stabilized, leading to subsequent activation of cell cycle checkpoints. It has been shown that ATM is required for IR induced phosphorylation on Ser15 residue of p53. Based on the involvement of p53 in mammary tumorigenesis and on the higher risk of ATM carriers for breast cancer, we have carried out studies to address the cancer susceptibility of ATM heterozygous and ATM null mammary epithelial cells by transplanting mammary gland to wild-type sibling mice. Initial studies have indicated differential checkpoint and apoptotic responses in cells harboring ATM mutation. These studies will establish whether ATM plays important roles in mammary tumorigenesis.

Both of these projects are highly relevant to breast cancer, especially the Ms. Lin's animal models which hold promise in terms of new therapies for breast cancer and its metastases.

Lin, S. C., Skapek, S. X., Papermaster, D. S., Hankin, M. & Lee, E. Y. (2001) The proliferative and apoptotic activities of E2F1 in the mouse retina. *Oncogene* **20,** 7073-84.

Zhao, S., Weng, Y. C., Yuan, S. S., Lin, Y. T., Hsu, H. C., **Lin, S. C.**, Gerbino, E., Song, M. H., Zdzienicka, M. Z., Gatti, R. A., Shay, J. W., Ziv, Y., Shiloh, Y. & Lee, E. Y. (2000) Functional link between ataxia-telangiectasia and Nijmegen breakage syndrome gene products. *Nature* **405,** 473-7.

Ms. Lin successfully defended her dissertation on December 18, 2000, and continues as a post-doctoral fellow in Dr. Lee's laboratory extending her work on the development of important animal models for human cancer.

- ***Sean Post*** ***Mentor -- Dr. Eva Lee***

Recent studies indicate that breast cancer susceptibility genes,BRCA1 and BRCA2, are involved in DNA repair. Cells harboring mutations in either gene are hypersensitive to ionizing radiation (IR). Extensive genetic evidence in yeast indicates that DNA double-stranded breaks are processed by Rad50/Mre11 nuclease complex. It has also been shown that in response to IR, Rad50 assembles into nuclear foci. In mammalian cells, such IR-induced Rad50 foci are not

observed in cells established from Nijmegen breakage syndrome (NBS). We and others have shown that the protein product of gene mutated in NBS, Nibrin, forms a stable complex with Rad50/Mre11 and the complex possesses nuclear activity. The E. Lee laboratory demonstrated that IR-induced Rad50 redistribution requires ATM kinase activity. Rad50 is phosphorylated upon IR. Their preliminary studies indicate that such IR-induced Rad50 foci formation and phosphorylation are defective in A-T cells. In addition, IR-induced Rad50 foci formation is aberrant in some sporadiac cancers that express normal ATM, Rad50, Mre11, nibrin, BRCA1 and BRCA2 suggesting involvement of additional protein in this DNA damage response.

Mr. Post is a fourth year graduate student who is characterizing IR-induced Rad50 phosphorylation. How phosphorylation affects Rad50 function will be studied. In addition, cross-linking experiments will be carried out to investigate whether there is defective Rad50 protein complex formation in breast cancer cells. These studies will provide insights into the role of ATM kinase cascade in the assembly of double-stranded breakage repair protein. Furthermore, characterization of components in the repair protein complex may lead to the identification of additional players involved in breast carcinoma.

These projects are highly relevant to breast cancer since genomic instability is a hallmark of cancer and is thought to be a major contributor to the tumorigenic process. Mr. Post's research will contribute toward a greater understanding of the mechanisms responsible for maintaining genomic integrity that is undoubtedly involved in breast cancer development and progression.

Post, S., Weng, Y. C., Cimprich, K., Chen, L. B., Xu, Y. & Lee, E. Y. (2001) Phosphorylation of serines 635 and 645 of human Rad17 is cell cycle regulated and is required for G(1)/S checkpoint activation in response to DNA damage *Proc Natl Acad Sci U S A* **98,** 13102-7.

- ***Song Zhao*** ***Mentor – Dr. Eva Lee***

Mr. Zhao is working on the functional interactions between ATM and DNA repair proteins with a focus on NBS1. Ataxia-telangiectasia (A-T) and Nijmegen breakage syndrome (NBS) are recessive genetic disorders with susceptibility to cancer and similar cellular phenotypes. The protein product of the gene responsible for A-T, designated ATM, is a member of a family of kinases characterized by a carboxy-terminal phosphatidylinositol 3-kinase-like domain. The NBS1 protein is specifically mutated in patients with Nijmegen breakage syndrome and forms a complex with the DNA repair proteins Rad50 and Mrel1. Mr. Song has shown that phosphorylation of NBS1, induced by ionizing radiation, requires catalytically active ATM. Complexes containing ATM and NBS1 exist in vivo in both untreated cells and cells treated with ionizing radiation. He, along with others in the lab, have identified two residues of NBS1, Ser 278 and Ser 343 that are phosphorylated in vitro by ATM and whose modification in vivo is essential for the cellular response to DNA damage. This response includes S-phase checkpoint activation, formation of the NBS1/Mrel1/Rad50 nuclear foci and rescue of hypersensitivity to ionizing radiation. Together, these results demonstrate a biochemical link between cell-cycle checkpoints activated by DNA damage and DNA repair in two genetic diseases with overlapping phenotypes

Publications:

Song Zhao, Weng YC, Yuan SS, Lin YT, Hsu HC, Lin SC, Gerbino E, Song MH, Zdzienicka MZ, Gatti RA, Shay JW, Ziv Y, Shiloh Y, Lee EY. Functional link between ataxia-telangiectasia and Nijmegen breakage syndrome gene products. (2000) *Nature* 405:473-7

- ***Shang Li*** ***Mentor -- Dr. Wen-Hwa Lee***

Mutations of the *BRCA1* gene predispose women to the development of breast cancer. The *BRCA1* gene product [BRCA1] is a nuclear phosphoprotein whose cellular function is poorly understood. The C-terminal region of the BRCA1 protein contains an activation domain and two repeats termed BRCT (for BRCA1 C-terminal). In his recent work, Mr. Li identified a BRCT-interacting protein previously identified as CtIP, a protein that interacts with the C-terminal-binding protein (CtBP) of E1A. Together, CtIP and CtBP are postulated to form a transcription corepressor complex. The ability of BRCA1 to transactivate the p21 promoter can be inactivated by mutation of the C-terminal conserved BRCT domains. To explore the mechanisms of this BRCA1 function, the BRCT domains were used as bait in a yeast two-hybrid screen. A known protein, CtIP, a co-repressor with CtBP, was found. CtIP interacts specifically with the BRCT domains of BRCA1, both *in vitro* and *in vivo*, and tumor-derived mutations abolished these interactions. The association of BRCA1 with CtIP was also abrogated in cells treated with DNA-damaging agents including UV, γ-irradiation and adriamycin, a response correlated with BRCA1 phosphorylation. The transactivation of the p21 promoter by BRCA1 was diminished by expression of exogenous CtIP and CtBP. These results suggest that the binding of the BRCT domains of BRCA1 to CtIP/CtBP is critical in mediating transcriptional regulation of p21 in response to DNA damage.

This project is directly relevant to breast cancer since it involves the study of a protein whose function appears to central to the mobilizing the response of cells to DNA damage. Perturbations in the systems that maintain genomic integrity underlie initiation and progression of most cancers, including those of the breast.

During the summer of 2000, Dr. Li accepted a post-doctoral position in Dr. Elizabeth Blackburn's laboratory at Department of Biochemistry and Biophysics, University of California, San Francisco.

Publications:

Zheng, L., **Li, S.**, Boyer, T. G., and Lee, W. H., Lessons learned from BRCA1 and BRCA2, *Oncogene, 19*, 6159 (2000).

Zheng, L., Pan, H., **Li, S.**, Flesken-Nikitin, A., Chen, P. L., Boyer, T. G., and Lee, W. H., Sequence-specific transcriptional corepressor function for BRCA1 through a novel zinc finger protein, ZBRK1, *Mol Cell, 6*, 757 (2000).

Li, S., Ting, N. S., Zheng, L., Chen, P. L., Ziv, Y., Shiloh, Y., Lee, E. Y., and Lee, W. H., Functional link of BRCA1 and ataxia telangiectasia gene product in DNA damage response, *Nature, 406*, 210 (2000).

Dr. Li defended his dissertation in Fall of 2000. He has taken a post doctoral position in the laboratory of Dr. Elizabeth Blackburn in the department of biochemistry and biophysics at the UCSF. He is working on a novel cancer therapy involving a mutated telomere RNA template.

- ***Qing Zhong*** ***Mentor -- Dr. Wen-Hwa Lee***

One of Mr. Zhong's project in Dr. Lee's laboratory is a study of the tumor suppressor protein, TSG101. *tsg101* was identified as a tumor susceptibility gene by homozygous function inactivation of allelic loci in mouse 3T3 fibroblasts. To confirm its relevance to breast cancer that was originally reported, antibodies specific for the putative gene product were prepared and used to identify cellular 46 kDa TSG101 protein. A full size 46 kDa TSG101 protein was

detected in a panel of 10 breast cancer cell lines and 2 normal breast epithelial cell lines with the same antibodies. A full-length *TSG101* mRNA was also detected using rtPCR. These results indicate that homozygous intragenic deletion of *TSG101* is rare in breast cancer cells. In more recent work, Mr. Zhong demonstrated that TSG101 is a cytoplasmic protein that translocates to the nucleus during S phase of the cell cycle. Interestingly, TSG101 is distributed mainly around the chromosomes during M phase. Microinjection of antibodies selective for TSG101 during G1 or S results in cell cycle arrest and overexpression leads to cell death. These data indicate that neoplastic transformation due to lack of TSG101 could be due to a bypass of cell cycle checkpoints.

Another more recent interest of Mr. Zhong is the role of the breast tumor suppressor BRCA1 in cancer formation. *BRCA1*, encodes a tumor suppressor that is mutated in familial breast and ovarian cancers. Mr. Zhong's work showed that BRCA1 interacts *in vitro* and *in vivo* with human Rad50, which forms a complex with hMre11 and p95/nibrin. BRCA1 was detected in discrete foci in the nucleus that colocalize with hRad50 after irradiation. Formation of irradiation-induced foci positive for BRCA1, hRad50, hMre11 or p95 were dramatically reduced in HCC1937 breast cancer cells carrying a homozygous mutation in *BRCA1*, but was restored by transfection of wild-type *BRCA1*. Ectopic expression of wild-type, but not mutated *BRCA1* in these cells rendered them less sensitive to the DNA damage agent, methyl methanesulfonate. These data suggest that BRCA1 is important for the cellular responses to DNA damage that are mediated by the hRad50-hMre11-p95 complex.

Mr. Zhong's work on BRCA1 is highly relevant for breast cancer research. By understanding the interaction and functional role of BRCA1 in the DNA repair process could lead to a greater understanding of its role in tumorigenesis and to new forms of cancer therapy aimed at interactions with the repair proteins.

Publications:

Dr. Zhong successfully defended his dissertation in November, 2000. He is currently completing additional work toward publications related to his doctoral research as a postdoctoral fellow in Dr. Wen-Hwa Lee's laboratory.

- ***Lei Zheng*** ***Mentor -- Dr.Wen-Hwa Lee***

Lei accomplished a significant amount of work during this training period. His main goal was to elucidate the molecular basis of genomic instability that occurs in most of human cancers including breast cancer. He started working on a novel mitotic phase specific protein, Hec1, by demonstrating that Hec1 interacts with retinoblastoma protein for maintaining the genomic stability that was published in Mol. Cell. Biol. (1999). He then developed a method to examine the level of chromosome instability by using retrovirus carrying both positive and negative selectable marker that integrated randomly into individual chromosomes, and the frequency of loss of this selectable chromosomal marker (LOM) was measured. The results showed that normal mouse embryonic stem cells had a very low frequency of LOM, which was less than 10-8/cell/generation. In Rb-/- mouse ES cells, the frequency was increased to approximately 10-5/cell/generation, while in Rb+/- ES cells, the frequency was approximately 10-7/cell/generation. LOM was mainly mediated through chromosomal mechanisms and not due to point mutations. These results therefore revealed that Rb, with a haploinsufficiency, plays a critical role in the maintenance of chromosome stability. The mystery of why Rb heterozygous carriers have early onset tumor formation with high penetrance can be, at least, partially explained by this novel activity. This work was recently submitted for publication in Cancer Research.

Publications:

Zheng L,, Andrea Flesken-Nikitin, Phang-Lang Chen and Wen-Hwa Lee. Deficiency of Retinoblastoma gene in mouse embryonic stem cells leads to genetic instability. Cancer Research , (2002).

Zheng L, Chen Y, Riley DJ, Chen P-L, and Lee W-H: Retinoblastoma protein enhances the fidelity of chromosome segregation mediated by a novel coiled-coil protein, hsHec1p. Mol. Cell. Biol., 20: 3529-3537 (2000).

Li S, Ting N S.Y., **Zheng L**, Chen P-L, Ziv Y, Shiloh Y, Lee E Y-H, and Lee W-H: Functional link of BRCA1 and ataxia-telangiectasia gene product in DNA damage response. Nature, 406: 210-215, (2000).

Zheng L, Pan H, Li S, Flesken-Nikitin A, Chen P-L, Boyer T, and Lee W-H: A novel zinc-finger protein, ZBRK1, represses transcription of the GADD45 gene mediated by BRCA1. Molecular Cell, 6: 757-768 (2000).

Zheng L, Li S, Boyer TG, and Lee W-H: Lessons Learned From BRCA1and BRCA2. Oncogene, 19: 6159 - 6175 (2000).

Dr. Zheng successfully defended his Ph.D. dissertation in Novermber, 2000. Lei is currently working on a project involving regulators of gene transcription in Dr. Robert Roeder's at the I Laboratory of Biochemistry and Molecular Biology, The Rockefeller University, New York. Since he discovered that BRCA1 represses expression of many specific genes regulated by ZBRK1 repressor (Mol. Cell, 2000), he wants to extend this line of understanding by further training in transcriptional regulation using biochemical approaches.

- ***Horng-Ru Lin***

BRCA1 or BRCA2 germline mutations predispose women to early onset, familial breast cancer. Current studies on BRCA1 and BRCA2 suggest their roles in the maintenance of genome integrity. However, in contrast to the clear studies of BRCA1, there has been very little characterization of the BRCA2 protein and evidence that speaks to a dynamic function of BRCA2 in this regard. That is, the intrinsic biological nature of the BRCA2 protein remains enigmatic. Therefore, this project is to try to reveal the physiological function of the BRCA2 protein by characterizing its posttranslational processing, such as phosphorylation.

The novelty of the work lies in the following. First, it demonstrates BRCA2 is a phosphoprotein in vivo. Second, BRCA2 is hyperphosphorylated specifically in mitosis. Third, dephosphorylation of BRCA2 corresponds to the timing of cells' exit from mitosis. These findings imply that BRCA2 may play an important role in mitosis. To further characterize the phosphorylated amino acids of bRCA2 will provide fresh insights into functional study of BRCA2.

- ***Stephen Van Komen*** ***Mentor – Dr. Patrick Sung***

In yeast homologous recombination, Rad54, a member of Swi2/Snf2 family of proteins, functionally cooperates with the Rad51 recombinase in making D-loop, the first DNA joint formed between recombining chromosomes. Our biochemical studies have indicated that yeast Rad54 modulates DNA topology at the expense of ATP hydrolysis, producing extensive

unconstrained supercoils in DNA. This supercoiling ability is likely to be indispensable for D-loop formation. Given the high degree of structural and functional conservation among yeast and human recombination factors, we hypothesize that human Rad51 and Rad54 also function together to make D-loop. This hypothesis is being tested with human Rad51 and Rad54 proteins purified from insect cells infected with recombinant baculoviruses. In addition, whether human Rad54 has ATP hydrolysis-driven DNA supercoiling ability is also being examined. Our work is directly relevant to breast cancer, since recent studies have implicated the breast tumor suppressor BRCA2 in modulating the activities of the recombination machinery via Rad51.

Mr. Van Komen's research is directly relevant to breast cancer since double strand breaks in DNA and their repair is an issue pertinent to breast cancer. Since the tumor suppressor, BRCA2, interacts with Rad51, it is critically important to understand the biochemistry of this important enzyme in DNA repair.

Van Komen, S., Petukhova, G., Sigurdsson, S., Stratton, S., and Sung, P., Superhelicity-driven homologous DNA pairing by yeast recombination factors Rad51 and Rad54, *Mol Cell, 6*, 563 (2000).

Sung, P., Trujillo, K. M., and **Van Komen, S.**, Recombination factors of Saccharomyces cerevisiae, *Mutat Res, 451*, 257 (2000).

- **Deanna Jansen**

Ms. Jansen's husband was transferred to a new military base and, for family reasons, she decided to withdraw from the program. At some point, she plans to complete her Ph.D. training.

- **Stefan Sigurdsson** **Mentor – Dr. Patrick Sung**

The RAD51 encoded product exhibits structural and functional similarities to the Escherichia coli recombination protein RecA. RecA promotes the pairing and strand exchange between homologous DNA molecules to form heteroduplex DNA. We have shown that hRad51 also makes DNA joints avidly and promotes highly efficient DNA strand exchange. Two Rad51-like proteins, Rad51B and Rad51C, are found associated in a heterodimeric complex. We have co-expressed the Rad51B and Rad51C proteins in insect cells and purified the Rad51B-Rad51C complex to near homogeneity. Biochemical experiments have revealed that Rad51B-Rad51C binds DNA and enhances the recombinase activity of the Rad51 protein. This recombination mediator function of Rad51B-Rad51C is likely indispensable for efficient recombination in vivo. Recently, hRad51 was shown to interact with the breast tumor suppressor BRCA2. The biochemical studies in our laboratory should be useful for understanding the molecular basis of breast tumor suppression by the recombination machinery.

Publications:

Stefan Sigurdsson, Stephen Van Komen, Wendy Bussen, David Schild, Joanna S. Albala, and Patrick Sung. (2001) Mediator function of the human Rad51B-Rad51C complex in Rad51/RPA-catalyzed DNA strand exchange. Genes & Development, in the press.

Van Komen S, Petukhova G, **Sigurdsson S**, Stratton S, Sung P. Superhelicity-driven homologous DNA pairing by yeast recombination factors Rad51 and Rad54. (2000) *Mol Cell* 6:563-72

Stefan Sigurdsson, Trujillo K, Song B, Stratton S, Sung P. Basis for avid homologous DNA strand exchange by human Rad51 and RPA (2000) J. Biol. Chem. 276: 8798-806

Guikai Wu **Mentor – Dr. Phang-Lang Chen**

Nijmegan breakage syndrome (NBS), a chromosomal instability disorder, is characterized in part by cellular hypersensitivity to ionizing radiation. The NBS1 gene product, p95 (NBS1 or nibrin) forms a complex with Rad50 and Mre11. Cells deficient in the formation of this complex are defective in DNA double-strand break repair, cell cycle checkpoint control, and telomere length maintenance. How the NBS1 complex is involved in telomere length maintenance remains unclear. In published studies the Chen laboratory showed that NBS1 and Mre11 co-localize with TRF1 in PML nuclear bodies in telomerase-negative immortalized cells during G2 phase of the cell cycle. Significantly, the NBS1/TRF1 foci undergo active BrdU incorporation during late S/G2 transition, suggesting a novel role for NBS1 in telomere lengthening in telomerase-negative immortalized cell lines. These results suggest that NBS1 may be invovled in alternative lengthening of telomeres in telomerase-hegative immortalized cells. Given that multiple key players in homolgous recombination area localized to PML bodies in telomerase-hegative immortalized cells, it is reasonable to speculate that active DNA synthesis in these nuclear domains in late S/G2 may reflect a telomere maintenance process potentially involving a homologous recombination. Mr. Wu will investigate the mechanistic details of how these factors work in concert. An understanding of the mechanisms of telomere length maintenance is relevant to breast cancer.

Publications:

Wu G, Lee W-H, and Chen P-L. NBS1 and TRF1 Colocalize at Promyelocytic Leukemia Bodies during Late S/G2 Phases in Immortalized Telomerase-negative Cells. (2000) J Biol Chem 275:39, 30618-30622

Changes to the Program Faculty:

Removals: None

Additions: The following investigators have been added to the faculty. All have expertise and funded research programs relevant to breast cancer as indicated by their descriptions below and appended NIH Biosketches.

Tadayoshi Bessho, Ph.D., Assistant Professor, Department of Molecular Medicine.

The interstrand crosslink DNA damage is believed to be the cytotoxic lesions produced by various chemotherapeutic agents, such as *cis*-diamminedichloroplatinum (II) (cisplatin) and melphalan. In fact, the enhanced removal of crosslink DNA is one of the major contributing factors in acquired drug resistance to cisplatin and melphalan. Clearly, an understanding of the molecular mechanism for removal of crosslink DNA damage in humans will be necessary for devising an effective regimen to overcome acquired drug resistance and for the development of better anticancer drugs. Currently, little is known about how the interstrand crosslink DNA damage is removed in mammalian cells. Extensive genetic studies show that Chinese hamster ovary cell lines defective in ERCC1 and ERCC4 (XPF) are extremely sensitive to bifunctional DNA crosslinking agents. These data indicate that the XPF/ERCC1 complex is needed for crosslink repair. The genetic data have also implicated that the involvement of the XRCC2 and XRCC3 protein in crosslink repair. XRCC2 and XRCC3 are needed for homologous

recombination and the repair of double strand breaks by homologous recombination. To decipher the mechanism of crosslink repair in mammalian cells, we have recently developed a cell free crosslink repair system that is specifically dependent on XPF, ERCC1, and XRCC3. The roles of XPF/ERCC1 complex, XRCC2 and XRCC3 in the removal of the interstrand crosslink DNA damage will be defined. The proposed studies should shed some light on the understanding of the molecular mechanism of crosslink repair in mammalian cells, and they will also provide basis for the eventual reconstitution of the crosslink repair reaction with purified factors.

Trainees in Dr. Bessho's laboratory will have the opportunity to use multiple approaches to study the mechanisms involved in the above areas of DNA repair. Since many of the agents under study are used in cancer therapy, an understanding of how cancer cells, including those of the breast, evade these therapies is an important work that trainees can pursue.

Sang Eun Lee, Ph.D., Assistant Professor, Department of Molecular Medicine.

Ionizing radiation and radio-mimetic chemicals induce a variety of DNA lesions, the most lethal of which is the DNA double-strand break (DSB). A single misrepaired or unrepaired DSB can cause a variety of catastrophic consequences including gene inactivation, translocations, loss of large portions of the genome and oncogenic transformation as well as cell death. All organisms have thus evolved an intricate network of systems for repairing chromosome breaks. The importance of these processes is underscored by the fact that several human diseases, which are characterized by immune dysfunctions and strong cancer predisposition, are caused by mutations in DSB repair genes. The focus of this research is to identify and characterize the genetic components of a novel DSB repair process, which is independent on the Rad52 and Ku proteins and apparently modulated by mismatch repair (MMR) factors. To gain further insight into this newly discovered DSB repair pathway, we propose a molecular genetic approach to identify and characterize the additional components of this pathway in *Saccharomyces cerevisiae*. Since the genetic components and the basic mechanism of DSB repair processes are remarkably conserved from yeast to humans, these studies should set the stage for dissecting the equivalent pathway in humans.

Trainees in Dr. S. Lee's laboratory will have the opportunity to use the most up-to-date genetic approaches to identify important players in the above DNA repair pathways. Elucidating these novel players and potential mechanisms of action will allow trainees to make major contributions in breast cancer research.

Changes in the Program Courses: None during the last funding period.

SUMMARY: The Breast Cancer Training Program made excellent progress toward attracting and retaining excellently qualified students in breast cancer research. The students received a high level of training in the modern research methods and theory. A total of 19 publications on breast cancer was achieved by students supported by the program. Two more of our students obtained predoctoral training awards from the Defense Department's Breast Cancer Research Program, raising the total to four. There were new faculty additions that will greatly expanded the training opportunities in Breast Cancer Research in the areas of DNA repair and breast cancer metastasis. Combined with the basic instruction they receive in the Molecular Medicine Ph.D. Program, students will graduate as highly skilled researchers who will be competitive for post doctoral positions in the premiere breast cancer laboratories in the world.

Appendix: NIH Biosketches and Reprints of Trainee Publications.

BIOGRAPHICAL SKETCH

Provide the following information for the key personnel in the order listed for Form Page 2.
Photocopy this page or follow this format for each person.

NAME	POSITION TITLE
E. Paul Hasty, D.V.M.	Associate Professor

EDUCATION/TRAINING *(Begin with baccalaureate or other initial professional education, such as nursing, and include postdoctoral training.)*

INSTITUTION AND LOCATION	DEGREE *(if applicable)*	YEAR(s)	FIELD OF STUDY
Texas A&M University, College Station, TX	B.S.	1985	Veterinary Medicine
Texas A&M University, College Station, TX	D.V.M.	1987	Veterinary Medicine
Baylor College of Medicine, Houston, Tx	Postdoc	1992	Molecular Medicine

RESEARCH AND PROFESSIONAL EXPERIENCE: Concluding with present position, list, in chronological order, previous employment, experience, and honors. Include present membership on any Federal Government public advisory committee. List, in chronological order, the titles, all authors, and complete references to all publications during the past three years and to representative earlier publications pertinent to this application. If the list of publications in the last three years exceeds two pages, select the most pertinent publications. **DO NOT EXCEED TWO PAGES.**

Professional Positions:

1987 – 1992 Postdoctoral Fellow, Institute for Molecular Genetics, Baylor College of Medicine, Houston, Tx.
1992 – 1996 Assistant Professor, Department of Biochemistry and Molecular Biology, University of Texas M.D. Anderson Cancer Center, Houston, Tx.
1996 – 2000 Director of DNA Repair, Lexicon Genetics.
2000 – present Associate Professor, Department of Molecular Medicine, University of Texas Health Science Center at San Antonio, Tx.

Awards and Other Professional Activities:

1983 The National Dean's List
1988 – 1990 Postdoctoral Research Fellow of Granada Corporation
1990 – 1992 Postdoctoral Research Fellow of the Cystic Fibrosis Foundation
1993 March of Dimes Basil O'Connor Scholar

Research Projects Ongoing or Completed During the Last 3 Years:

"Investigation of xrcc5 Mutant Mice and Cell Lines
Principal Investigator: E. Paul Hasty, D.V.M.
Agency: National Institutes of Health/National Cancer Institute
Type: R01 CA76317-01, Years 1-4, July 7, 1997 to September 30, 2001
The long-term objective of this project is to investigate the function of Ku80 in tissue culture cells and in mice so that we may better understand the physiological significance of Ku80 for repairing DNA double-strand breaks (DSBs) and monitoring DNA damage.

"Mouse Cancer Models by Regulated Inactivation of Tumor Suppressor genes:
Principal Investigator: (Eva Lee) 04/01/01-03/31/04
One project of Cooperative Agreement Grant (Hasty)
Agency: National Institutes of Health

Relevant Publications:

Hasty, P., Ramirez-Solis, R., Krumlauf, R., and Bradley, A. (1991). Introduction of a subtle mutation into the *Hox-2.6* locus in embryonic stem cells. Nature 350:243-246.

Hasty, P., Rivera-Perez, J., Chang, C., and Bradley, A. (1991). Target frequency and integration pattern for insertion and replacement vectors in embryonic stem cells. Mol. Cell. Biol. 11:4509-4517.

Hasty, P., Rivera-Perez, J., and Bradley, A. (1991). The length of homology required for gene targeting in embryonic stem cells. Mol. Cell. Biol. 11:5586-5591.

Zheng, H., Hasty, P., Brennenman, M., Grompe, M., Gibbs, R., Wilson, J., and Bradley, A. (1991). Fidelity of targeted recombination in human fibroblasts and murine embryonic stem cells. Proc. Natl. Acad. Sci. USA 88:8067-8071.

Hasty, P., Rivera-Perez, J., and Bradley, A. (1992). The role and fate of DNA ends for homologous recombination in embryonic stem cells. Mol. Cell. Biol. 12:2464-2474.

Bradley, A., Hasty, P., Davis, A., and Ramirez-Solis, R. (1992). Modifying the mouse: design and desire. Bio/Technology 10:534-539

Hasty, P., Bradley, A., Morris, J., H., Edmondson, D., G., Venuti, J., M., Olson, E., N., and Klein, W., H. (1993). Muscle deficiency and neonatal death in mice with a targeted mutation in the myogenin gene. Nature 364:501-506.

Hasty, P., Crist, M., Grompe, M., and Bradley, A. (1993). The efficiency of insertion versus replacement vector targeting varies at different chromosomal loci. Mol. Cell. Biol. 14:8385 - 8390.

Rudolph, U., Brabet, P., Kaplan, J., Hasty, P., Bradley, A., and Birnbaumer, L. (1993). Gene targeting of the G_{i2a} gene in ES cells with replacement and insertion vectors. J. Receptor Research 13:619-637.

Rudolph, U., Brabet, P., Hasty, P., Bradley, A., and Birnbaumer, L. (1993). Targeting and intrachromosomal recombination at the G_{i2a} locus in embryonic stem cells. Transgen. Research 2:345-355.\

O'Neil, W.K., Hasty, P., McCray, P.B. Jr., Casey, B., Rivera-Perez, J., Welsh, M.J., Beaudet, A.L., and Bradley, A. (1993). Targeted disruption of the murine cystic fibrosis locus. Human Mol. Genetics 2:1561-1569.

Zhang, H., Hasty, P., and Bradley, A. (1994). Targeting Frequency for Deletion Vectors in Embryonic Stem Cells. Mol. Cell. Biol. 14:2404 - 2410.

Hasty, P., O'Neil, W.K., Liu, Q., Morris, A.P. Bebok, Z., Shumyatsky, G.P. Jilling, T., Sorcher, E.J., Bradley, A., and Beaudet, A.L. (1995). Severe phenotype in mice with a termination mutation in exon of cystic fibrosis gene. Som. Cell. Molec. Gen. 21:177-187.

Mitani, K., Wakamiya, M., Hasty, P., Graham, F.L., Bradley, A., and Caskey, T. (1995). Gene targeting in mouse embryonic stem cells with an adenoviral vector. Som. Cell. Molec. Gen. 21:221-231.

Hasty, P., Rivera-Perez, J., and Bradley, A. (1995). Gene conversion during vector insertion in embryonic stem cells. Neuclic Acids Res. 23:2058-2064.

Zhu, B., Bogue, M. A., Lim, D.-S., Hasty, P., and Roth, D. B. (1996). Ku86-deficient mice exhibit severe combined immunodeficiency and defective processing of V(D(J recombination intermediates. Cell 86:379-389.

Lim D.-L., and Hasty, P. (1996). A mutation in mouse *rad51* results in an early embryonic lethal that is suppressed by a mutation in p53. Mol. Cell. Biol. 16:7133-7143.

Lu, Q., Hasty, P., and Shur, B.D. (1997) Targeted mutation in β1,4-Galactosylt transferase leads to pituitary insufficiency and neonatal lethality. Dev. Biol. 181: 257-267.

Sharan, S. K., Morimatsu, M., Albrecht, U., Lim, D.-S., Regel, E., Dinh, C., Sands, A., Eichele, G., Hasty, P., and Bradley, A. (1997) Embryonic lethality and radiation hypersensitivity mediated by Rad51 in mice lacking Brca2.Nature 386:804-810.

Morimatsu, M., Donoho, G., and Hasty, P. (1998) Cells deleted for *Brca2* COOH terminus exhibit hypersensitivity to radiation and premature senescence. Can. Res. 58:3441-3447.

Vivian, J. L., Klein, W. H., and Hasty, P. (1999) Temporal, Spacial and tissue-specific expression of a myogenin-lacZ transgene targeted to the *Hprt* locus in mice. Biotechniques 27:154-163.

Osipovich, O., Duhe, R., Hasty, P., Durum, S. K. and Muegge, K., (1999) Defining functional domains of Ku80: DNA end binding and survival after radiation. Biochem. and Biophys. Res. Commun. 261:802-807.

Vogel, H., Lim, D-L., Karsenty, G., Finegold, M., and Hasty, P. (1999) Deletion of Ku86 causes early onset of senescence in mice. Proc. Natl. Acad. Sci. 96:10770-10775.

Gu, Y., Sekiguchi, J., Gao, Y., Dikkes, P., Frank, K., Ferguson, D., Hasty, P., Chun, J., and Alt, F. W. (2000) Defective embryonic neurogenesis in Ku-deficient but not DNA-dependent protein kinase catalytic subunit-deficient mice. Proc. Natl. Acad. Sci. 97:2668-2673.

Lim, D-L., Vogel, H., Willerford, D. M., Sands, A., Platt, K. A., and Hasty, P. (2000) Analysis of ku80-mutant mice and cells with deficient levels of p53. Mol. Cell. Biol. 20:3773-3780.

BIOGRAPHICAL SKETCH

Provide the following information for the key personnel in the order listed for Form Page 2.
Photocopy this page or follow this format for each person.

NAME	POSITION TITLE
Sang Eun Lee	Assistant Professor

EDUCATION/TRAINING *(Begin with baccalaureate or other initial professional education, such as nursing, and include postdoctoral training.)*

INSTITUTION AND LOCATION	DEGREE *(if applicable)*	YEAR(s)	FIELD OF STUDY
Seoul National University	M.S.	1990	Molecular Biology
Brown University	Ph.D.	1996	Molecular Biology
Brandeis University	Postdoc	1997-2001	Biology

RESEARCH AND PROFESSIONAL EXPERIENCE: Concluding with present position, list, in chronological order, previous employment, experience, and honors. Include present membership on any Federal Government public advisory committee. List, in chronological order, the titles, all authors, and complete references to all publications during the past three years and to representative earlier publications pertinent to this application. If the list of publications in the last three years exceeds two pages, select the most pertinent publications. **DO NOT EXCEED TWO PAGES.**

PROFESSIONAL POSITIONS

01/97 – 06/01 **Postdoctoral Fellow**, Department of Biology and Rosenstiel Center,m Brandeis University, Waltham, MA

07/01 – Present **Assistant Professor**, Department of Molecular Medicine and Institute of Biotechnology, University of Texas Health Science Center, San Antonio, TX

HONORS AND AWARDS

1997 – 2000 Fellow, Leukemia Society of America
2000 – Present Special Fellow, A. Hildegarde D. Becher Foundation, Leukemia and Lymphoma Society

PUBLICATIONS

Lee, C.G., Kim, C.G., Namkung, R., **Lee, S.E.** and Park, S.D. (1990) Transformation of mouse L cells with thymidine kinase gene of Herpes simplex virus type-I. *Cytotechnology* **3**: 141-147.

Lee, S.E., Pulaski C.R., He, D.-M., Benjamin, D.M., Voss, M.J., Um, J. and Hendrickson, E.A. (1995) Isolation of mammalian cell mutants that are x-ray sensitive, impaired in DNA double-strand break repair and defective for V(D)J recombination. *Mutat. Res.* **339**: 279-291.

Boubnov, N.V., Hall, K.T., Wills, Z., **Lee, S.E.**, He, D.-M., Benjamin, D.M., Pulaski, C.R., Band, H., Reeves, W., Hendrickson, E.A. and Weaver, D.T. (1995) Complementation of the ionizing radiation sensitivity, DNA end binding, and V(D)J recombination defects of double-strand break repair mutants by the p86 Ku autoantigen. *Proc. Natl. Acad. Sci. USA* **92**: 2075-2081.

He, D.-M., **Lee, S.E.** and Hendrickson, E.A. (1996) Restoration of x-ray and etoposide resistance, Ku-end binding activity and V(J)D recombination to the Chinese hamster *sxi*-3 mutant by a hamster Ku86 cDNA. *Mutat Res.* **363**: 43-56.

Lee, S.E., He, D.-M. and Hendrickson, E.A. (1996) Characterization of Chinese hamster cell lines that are x-ray sensitive, impaired in DNA double-strand break repair and defective for V(D)J recombination. In: Current Topics in Microbiology and Immunology, Molecular Analysis of DNA Rearrangements in the Immune System. R. Jessberger ane M. Lieber (eds), Springer-Verlag, Berlin, West Germany, **217**: 133-142.

Lee, S.E., Mitchell, R.A., Cheng, A. and Hendrickson, E.A. (1996) Evidence for DNA-PK dependent and independent DNA double strand break repair pathways in mammalian cells as a function of the cell cycle. *Mol. Cell. Biol.* **17**: 1425-1433.

Myung, K., He, D.-M., **Lee, S.E.** and Hendrickson, E.A. (1997) KARP-1:a novel leucine zipper protein expressed from the Ku86 autoantigen locus is implicated in the control of DNA-dependent protein kinase activity. *EMBO J.* **16**: 3172-3184.

Lee, S.E., Moore, J.K., Holmes, A., Umezu, K., Kolodner, R.D. and Haber, J.E. (1998) *Saccharomyces* Ku70, Mre11/Rad50 and RPA proteins regulate adaptation to G2/M arrest after DNA damage. *Cell* **94**: 399-409.

Lee, S.E., Paques, F., Sylvan, J. and Haber, J.E. (1999) Role of yeast *SIR* genes and mating type in directing DNA double-strand breaks to homologous and non-homologous repair paths. *Curr. Biol.* **9**: 767-770.

Demeter, J., **Lee, S.E.**, Haber, J.E. and Stearns, T.A. (2000) The DNA-damage checkpoint signal in budding yeast is not nuclear-limited. *Mol. Cell* **6**: 487-492.

Pellicioli, A*., **Lee. S.E.***, Foiana, M. and Haber, J.E. (2001) Regulation of *Saccharomyces* Rad53 checkpoint kinase during adaptation from G2/M arrest. *Mol. Cell* 7: 293-300 *(*co first-author).*

Lee, S.E., Pellicioli, A., Malkova, A., Foiana, M. and Haber, J.E. (2001) The *Saccharomyces* recombination protein Tid1p is required for adaptation from G2/M arrest induced by a single double-strand break. *Curr. Biol.* **11**: 1053-1057.

Lee, S.E., Pellicioli, A., Demeter, J., Vaze, M., Gasch, A., Malkova, A. Botstein, D., Brown, P., Stearns, T., Foiani, M and Haber, J.E. (2001) Arrest, adaptation and recovery following a chromosome double-strand break in *Saccharomyces cerevisiae*. *Cold Spring Harbor Symposia on Quantitative Biology*, (in press).

Valencia, M., Bentele, M., Vaze, M.B., Hermann, G., Kraus, E., **Lee, S.E.**, Schar, P. and Haber, J.E. (2001) *NEJ1*: a gene controlling nonhomologous end-joining in yeast. *Nature* (in press).

Lee, S.E., Bressan, D.A., Petrini, J.H. and Haber, J.E. (2001) *In vivo* 5' to 3' resection activity of *mre11* mutants correlates with many mitotic phenotypes. *Mutat. Res.* (in press).

Interaction between PCNA and DNA ligase I is critical for joining of Okazaki fragments and long-patch base-excision repair

David S. Levin*, Allison E. McKenna†, Teresa A. Motycka*, Yoshihiro Matsumoto† and Alan E. Tomkinson*

DNA ligase I belongs to a family of proteins that bind to proliferating cell nuclear antigen (PCNA) via a conserved 8-amino-acid motif [1]. Here we examine the biological significance of this interaction. Inactivation of the PCNA-binding site of DNA ligase I had no effect on its catalytic activity or its interaction with DNA polymerase β. In contrast, the loss of PCNA binding severely compromised the ability of DNA ligase I to join Okazaki fragments. Thus, the interaction between PCNA and DNA ligase I is not only critical for the subnuclear targeting of the ligase, but also for coordination of the molecular transactions that occur during lagging-strand synthesis. A functional PCNA-binding site was also required for the ligase to complement hypersensitivity of the DNA ligase I mutant cell line 46BR.1G1 to monofunctional alkylating agents, indicating that a cytotoxic lesion is repaired by a PCNA-dependent DNA repair pathway. Extracts from 46BR.1G1 cells were defective in long-patch, but not short-patch, base-excision repair (BER). Our results show that the interaction between PCNA and DNA ligase I has a key role in long-patch BER and provide the first evidence for the biological significance of this repair mechanism.

Addresses: *Department of Molecular Medicine, Institute of Biotechnology, The University of Texas Health Science Center at San Antonio, 15355 Lambda Drive, San Antonio, Texas 78245, USA. †Department of Radiation Oncology, Fox Chase Cancer Center, 7701 Burholme Avenue, Philadelphia, Pennsylvania 19111, USA.

Correspondence: Alan E. Tomkinson
E-mail: Tomkinson@uthscsa.edu

Received: **17 May 2000**
Revised: **8 June 2000**
Accepted: **8 June 2000**

Published: **21 July 2000**

Current Biology 2000, 10:919–922

0960-9822/00/$ – see front matter

Results and discussion

We have suggested that interaction of DNA ligase I with PCNA provides a molecular explanation for the unique involvement of this ligase in DNA replication [2]. As the PCNA-binding motif of DNA ligase I also mediates recruitment of the ligase to replication foci [3], PCNA binding could be required for subnuclear targeting to sites of DNA replication but not for the catalytic reactions at the replication fork. We first investigated whether inactivation of PCNA binding had an effect on other biochemical properties of DNA ligase I. Using site-directed mutagenesis, the adjacent phenylalanine residues in the conserved PCNA-binding motif of human DNA ligase I (amino acids 8 and 9) were replaced by alanines. After subcloning into baculovirus expression vectors, wild-type and mutant DNA

Figure 1

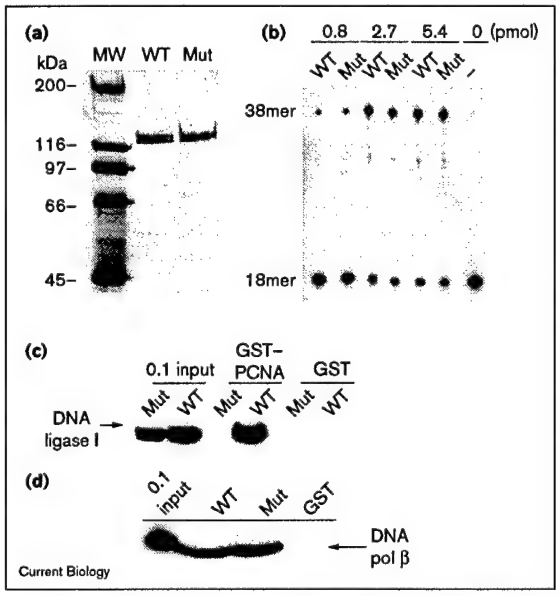

Effect of amino-acid substitutions that inactivate the PCNA-binding site of DNA ligase I on its catalytic and Pol β-binding activities. **(a)** After separation by SDS–PAGE, the wild-type (WT) and mutant (Mut) DNA ligase I purified from baculovirus-infected insect cells were detected by Coomassie blue. Molecular mass standards (in kDa) are on the left. **(b)** DNA joining by recombinant DNA ligase I. WT and mutant DNA ligase I were incubated with a labeled nicked oligonucleotide substrate (see Supplementary material). After separation by denaturing gel electrophoresis, labeled oligonucleotides were detected by autoradiography. The positions of the substrate (18mer) and ligated product (38mer) are indicated on the left. **(c)** Binding of DNA ligase I to PCNA. WT and mutant DNA ligase were incubated with glutathione beads bound by either GST–PCNA or GST (see Supplementary material). Ligase bound to the beads was detected by immunoblotting. **(d)** Binding of DNA ligase I to Pol β. Glutathione beads with the amino-terminal 118 amino acids of DNA ligase I (WT or mutant) fused to GST, or GST alone as the ligand, were incubated with Pol β (see Supplementary material). Pol β bound to the beads was detected by immunoblotting. The lane labeled 0.1 input contained one-tenth of the protein in the binding reactions.

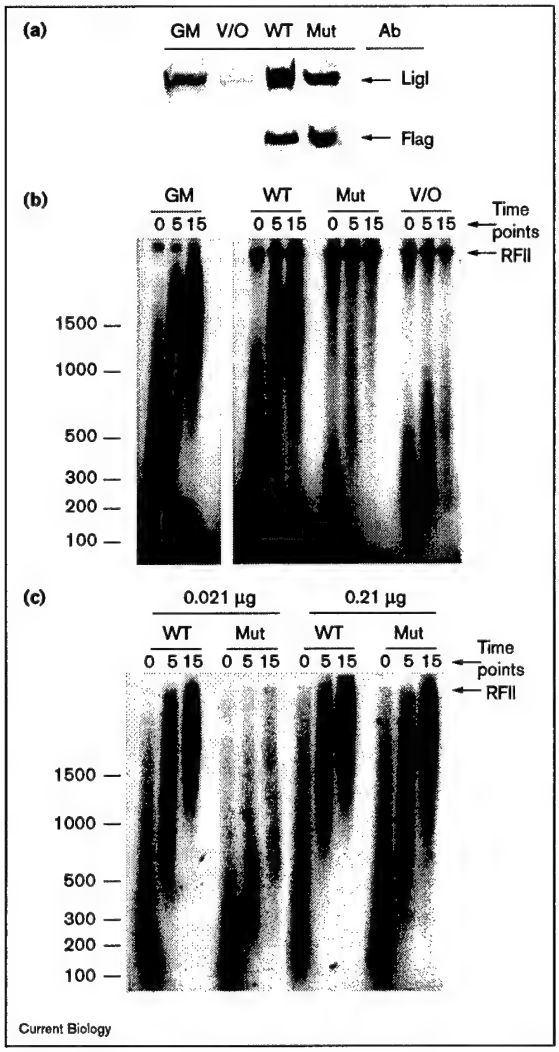

Figure 2

Expression of endogenous and tagged DNA ligase I in 46BR.1G1 cells and the effect of amino-acid substitutions that inactivate the PCNA-binding site of DNA ligase I on Okazaki fragment processing. Whole-cell extracts were prepared from the control cell line GM00847 (GM) and from derivatives of 46BR.1G1 stably transfected with empty expression vector (V/O), plasmid expressing Flag-tagged WT DNA ligase I, or plasmid expressing Flag-tagged mutant DNA ligase I (Mut) (see Supplementary material). **(a)** Endogenous and Flag-tagged DNA ligase I were detected in extracts (60 µg) by immunoblotting with anti-DNA ligase I and anti-Flag antibodies. **(b)** Analysis of DNA replication intermediates by pulse-chase labeling. Aliquots from DNA replication assays with the indicated extracts (360 µg) (see Supplementary material) were collected at the times indicated. **(c)** Aliquots from pulse-chase DNA replication assays supplemented with purified DNA ligase I (WT or Mut) were collected at the times indicated. The position of replicative form II DNA (RFII) is indicated. Positions of molecular mass standards (in nucleotides) are shown. After separation by alkaline agarose gel electrophoresis, labeled DNA replication intermediates were detected by autoradiography.

ligase I were purified to near homogeneity from infected insect cells (Figure 1a). The alanine substitutions abolished PCNA binding ([3] and Figure 1c), but did not alter DNA joining activity (Figure 1b) or inactivate binding to DNA polymerase β (Pol β) (Figure 1d). Nor did the amino-acid changes abolish the ability of DNA ligase I to complement the temperature-sensitive phenotype of the *Escherichia coli lig* strain (see Supplementary material).

To elucidate the role of PCNA binding in the various DNA transactions involving DNA ligase I, we transfected DNA ligase I-deficient 46BR.1G1 cells with cDNAs encoding Flag-tagged versions of either wild-type DNA ligase I or the mutant enzyme that does not interact with PCNA. Figure 2a shows immunoblots of extracts from two stable transfected derivatives of 46BR.1G1 that express comparable amounts of the wild-type and mutant ligase. The level of endogenous ligase in 46BR.1G1 cells is about half that in control GM00847 cells, whereas the levels of tagged DNA ligase I in transfected 46BR.1G1 cells are about five times those of the endogenous protein.

A unique characteristic of 46BR.1G1 cells is the abnormal processing of Okazaki fragments [4,5], which can be revealed by pulse-labeling DNA replication intermediates in the SV40 *ori*-dependent DNA replication assay (Figure 2b) [5]. As expected, the replication intermediates produced by extracts from the 46BR.1G1 derivative expressing wild-type DNA ligase I were essentially identical to those produced by a control cell extract (Figure 2b). In contrast, extracts from 46BR.1G1 expressing the mutant DNA ligase I still exhibited the defect in lagging-strand DNA synthesis (Figure 2b). Addition of 21 nanograms of wild-type DNA ligase I to 46BR.1G1 extracts restored the pattern of replication intermediates to that produced by a control extract, whereas addition of an equivalent amount of mutant DNA ligase I had no effect (Figure 2c). When a 10-fold larger amount of purified ligase protein was added to the 46BR.1G1 extract, both wild-type and mutant DNA ligase I corrected the replication defect, indicating that high levels of DNA ligase protein can suppress the requirement for PCNA binding (Figure 2c). This is the first direct evidence that the interaction between DNA ligase I and PCNA coordinates the synthesis and ligation of Okazaki fragments. The possibility remains, however, that recruitment of DNA ligase I to replication foci via PCNA binding [3] is also important for cellular DNA replication.

As 46BR.1G1 cells are hypersensitive to killing by methyl methanesulfonate (MMS) [6], we compared the ability of wild-type and mutant DNA ligase I to correct this phenotype. Expression of wild-type DNA ligase I complemented the sensitivity to DNA damage (Figure 3),

Figure 3

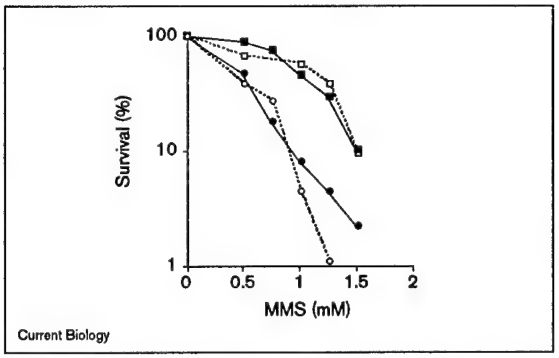

Effect of inactivation of the PCNA-binding site of DNA ligase I on the complementation of the MMS sensitivity of 46BR.1G1 cells. The control cell line GM00847 (open squares) and 46BR.1G1 stably transfected with the empty expression vector (open circles), or WT DNA ligase I cDNA (filled squares), or mutant DNA ligase I cDNA (filled circles) were incubated with MMS (see Supplementary material).

whereas the mutant DNA ligase I had no significant effect (Figure 3). These results show that participation of DNA ligase I in repair of cytotoxic DNA damage induced by MMS is mediated through its interaction with PCNA. It is generally accepted that the major cytotoxic DNA lesion introduced by MMS, 3-methyl adenine, is repaired by BER. Two subpathways of BER can be distinguished on the basis of the length of repair DNA synthesis and the requirement for PCNA [7]; the relative importance of these subpathways for the repair of different base lesions *in vivo* has not been established. As DNA ligase I has been linked with both short-patch BER (one-nucleotide repair) [8] and long-patch BER (repair tract of 2–11 nucleotides) [9], we compared the abilities of 46BR.1G1 extracts to catalyze different BER subpathways. To measure short-patch BER, we used a linear DNA duplex with a single uracil:guanine pair. The linear nature of this substrate makes it refractory to repair by PCNA-dependent BER [10]. In these assays, the 46BR.1G1 extract had essentially the same activity as a control extract both in terms of the amount of ligated product and the patch size, which was predominantly one nucleotide (Figure 4a). Similar results were obtained in assays with extracts from cells expressing either form of DNA ligase I (Figure 4a).

To measure long-patch BER, we used a circular DNA substrate with a single synthetic abasic (AP) site that cannot be repaired by short-patch BER (see Supplementary material). In these assays, the 46BR.1G1 extract generated significantly less repaired product than the control extract (Figure 4b). The addition of purified wild-type DNA ligase I protein to the 46BR.1G1 extract corrected the defect in AP site repair but had no effect on the repair reaction catalyzed by the control cell extract (Figure 4c).

Figure 4

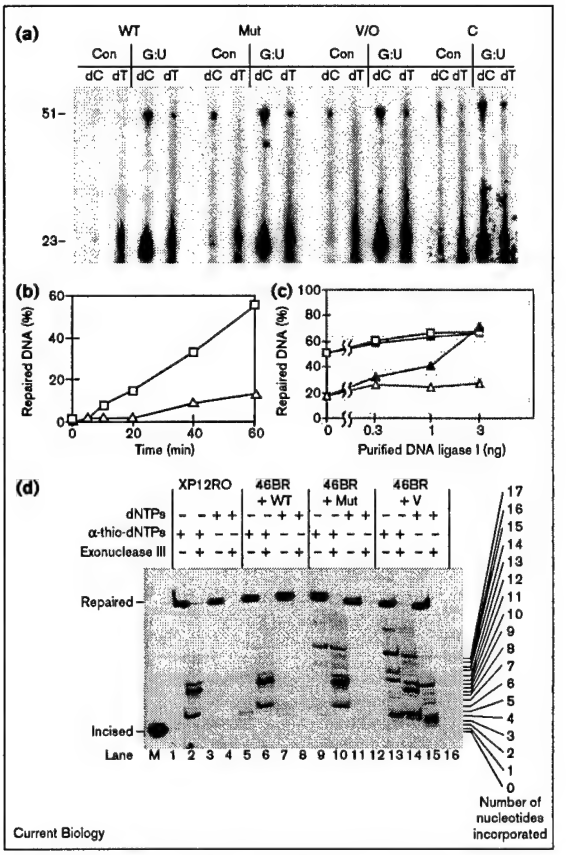

Effect of inactivation of the PCNA-binding site of DNA ligase I on short-patch and long-patch BER. **(a)** Extracts (10 μg) from the control cell line XP12RO (C) and from 46BR.1G1 stably transfected with the empty expression vector (V/O), or expressing WT DNA ligase I (WT), or mutant DNA ligase I (Mut), were assayed for short-patch BER activity using a linear oligonucleotide duplex with (G:U) or without (Con) a single uracil residue (see Supplementary material). Repair reactions contained either [α-^{32}P]dCTP or [α-^{32}P]TTP to detect single or multiple nucleotide incorporation events, respectively. The positions of labeled 23mer reaction intermediates and 51mer ligated products are indicated. **(b)** Extracts (2 μg) from either XP12RO (open squares) or 46BR.1G1 cells (open triangles) were assayed for long-patch BER activity using a labeled circular substrate containing a single synthetic AP site (see Supplementary material). **(c)** Long-patch BER reactions catalyzed by extracts from 46BR.1G1 cells were supplemented with either WT (closed triangles) or mutant (open triangles) purified DNA ligase I. In similar assays, control XP12RO extracts were supplemented with either WT (closed squares) or mutant (open squares) purified DNA ligase I. **(d)** Assays to determine the length of repair DNA synthesis in long-patch BER reactions catalyzed by extracts (5 μg) from control cells (XP12RO, lanes 1–4) and 46BR.1G1 expressing WT DNA ligase I (46BR + WT, lanes 5–8); mutant DNA ligase I (46BR + Mut, lanes 9–12) or containing the empty expression vector (46BR + V, lanes 13–16) (see Supplementary material). The positions of the incised product (lane M) and the repaired product are indicated on the left. DNA repair synthesis events of 0–17 nucleotides are indicated in the right.

In contrast, addition of equal amounts of the mutant form of DNA ligase I had no effect on the efficiency of AP site repair in either 46BR.1G1 or control extract (Figure 4c).

To characterize the defect in long-patch BER, we examined the effect of DNA ligase I deficiency on DNA repair synthesis. Under these reaction conditions (see Supplementary material), the repair reaction catalyzed by the control extract was essentially complete (Figure 4d, lanes 1,2), with most of the repair events having repair synthesis tracts of either two or seven nucleotides (Figure 4d, lane 2). In contrast, incomplete DNA repair events with abnormally long repair synthesis tracts, up to 17 nucleotides, were detected in assays with 46BR.1G1 extracts (Figure 4d, lane 15). This effect was more pronounced in reactions with α-thio-dNTPs (Figure 4d, lanes 13,14). As expected, extracts from 46BR.1G1 cells expressing tagged wild-type DNA ligase I produced the same pattern of repair tracts as the control extract (Figure 4d, lanes 5–8). Extracts from 46BR.1G1 cells expressing mutant DNA ligase I did not show a marked defect in the overall repair reaction (Figure 4d, lane 11). The presence of repair tracts greater than seven nucleotides, however, indicated that the abnormality in DNA repair synthesis was only partially corrected (Figure 4d, lanes 9,10). We conclude that the interaction between PCNA and DNA ligase I has a key role in the coordination of the DNA synthesis and ligation steps that complete long-patch BER. Taken together with the cell survival studies, our observations provide the first strong evidence that long-patch BER is an important DNA repair mechanism *in vivo* and is not functionally redundant with short-patch BER.

Extracts from the cell line EM9, which is deficient in DNA ligase III [11] and also hypersensitive to MMS [12], are defective in short-patch but not long-patch BER [13]. Thus, it appears that short-patch BER is completed by the DNA ligase IIIα–Xrcc1 complex, whereas long-patch BER is completed by DNA ligase I in a PCNA-dependent reaction. The simplest explanation of the alkylation-sensitive phenotypes shown by cell lines deficient in DNA ligase III or I is that these enzymes are involved in functionally distinct BER subpathways that repair different MMS-induced cytotoxic lesions. Alternatively, either DNA ligases I or III might function in DNA repair pathways, other than BER, that repair cytotoxic DNA lesions induced by alkylating agents.

Supplementary material

Supplementary material including additional methodological detail and a figure showing the complementation of the temperature-sensitive phenotype of the *E. coli lig* strain is available at http://current-biology.com/supmat/supmatin.htm.

Acknowledgements

We thank B. Stillman, S. Wilson and R. Schultz for cell lines and reagents. D.S.L. was supported by the training program in the Molecular Basis of Aging. This research was supported by grants GM47251 (A.E.T.), GM57479 (A.E.T.), CA06927 (Y.M.) and CA63154 (Y.M.) from the Department of Health and Human Services and grants from the San Antonio Cancer Institute (A.E.T.).

References

1. Warbrick E: **PCNA binding through a conserved motif.** *Bioessays* 1998, **20**:195-199.
2. Levin DS, Bai W, Yao N, O'Donnell M, Tomkinson AE: **An interaction between DNA ligase I and proliferating cell nuclear antigen: implications for Okazaki fragment synthesis and joining.** *Proc Natl Acad Sci USA* 1997, **94**:12863-12868.
3. Montecucco A, Rossi R, Levin DS, Gary R, Park MS, Motycka TA, *et al.*: **DNA ligase I is recruited to sites of DNA replication by an interaction with proliferating cell nuclear antigen: identification of a common targeting mechanism for the assembly of replication factories.** *EMBO J* 1998, **17**:3786-3795.
4. Prigent C, Satoh MS, Daly G, Barnes DE, Lindahl T: **Aberrant DNA repair and DNA replication due to an inherited defect in human DNA ligase I.** *Mol Cell Biol* 1994, **14**:310-317.
5. Mackenney VJ, Barnes DE, Lindahl T: **Specific function of DNA ligase I in simian virus 40 DNA replication by human cell-free extracts is mediated by the amino-terminal non-catalytic domain.** *J Biol Chem* 1997, **272**:11550-11556.
6. Teo IA, Arlett CF, Harcourt SA, Priestley A, Broughton BC: **Multiple hypersensitivity to mutagens in a cell strain (46BR) derived from a patient with immuno-deficiencies.** *Mutat Res* 1983, **107**:371-386.
7. Frosina G, Fortini P, Rossi O, Carrozzino F, Raspaglio G, Cox LS, *et al.*: **Two pathways for base excision repair in mammalian cells.** *J Biol Chem* 1996, **271**:9573-9578.
8. Prasad R, Singhal RK, Srivastava DK, Molina JT, Tomkinson AE, Wilson SH: **Specific interaction of DNA polymerase β and DNA ligase I in a multiprotein base excision repair complex from bovine testis.** *J Biol Chem* 1996, **271**:16000-16007.
9. Pascucci B, Stucki M, Jonsson ZO, Dogliotti E, Hubscher U: **Long patch base excision repair with purified human proteins. DNA ligase I as patch size mediator for DNA polymerases delta and epsilon.** *J Biol Chem* 1999, **274**:33696-33702.
10. Biade S, Sobol RW, Wilson SH, Matsumoto Y: **Impairment of proliferating cell nuclear antigen-dependent apurinic/apyrimidinic site repair on linear DNA.** *J Biol Chem* 1998, **273**:898-902.
11. Caldecott KW, McKeown CK, Tucker JD, Ljungquist S, Thompson LH: **An interaction between the mammalian DNA repair protein XRCC1 and DNA ligase III.** *Mol Cell Biol* 1994, **14**:68-76.
12. Thompson LH, Brookman KW, Dillehay LE, Carrano AV, Mazrimas JA, Mooney CL, Minkler JL: **A CHO-cell strain having hypersensitivity to mutagens, a defect in strand break repair, and an extraordinary baseline frequency of sister chromatid exchange.** *Mutat Res* 1982, **95**:247-254.
13. Cappelli E, Taylor R, Cevasco M, Abbondandolo A, Caldecott K, Frosina G: **Involvement of XRCC1 and DNA ligase III gene products in DNA base excision repair.** *J Biol Chem* 1997, **272**:23970-23975.

Supplementary material

Interaction between PCNA and DNA ligase I is critical for joining of Okazaki fragments and long-patch base-excision repair

David S. Levin, Allison E. McKenna, Teresa A. Motycka, Yoshihiro Matsumoto and Alan E. Tomkinson

Current Biology 21 July 2000, 10:919–922

Figure S1

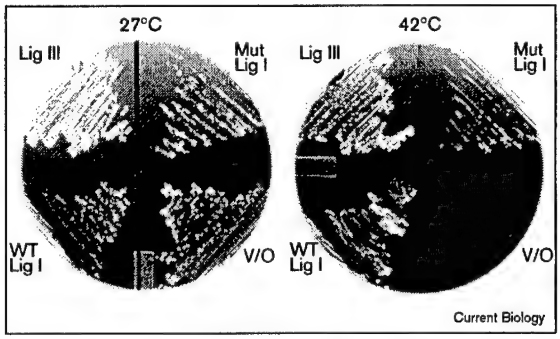

The effect of amino-acid substitutions that inactivate the PCNA-binding site of DNA ligase I on the complementation of the temperature-sensitive phenotype of an *E. coli lig* mutant. The temperature-sensitive *E. coli* strain AK76 *lig* ts7 was transformed with plasmids expressing the following proteins; empty expression vector (V/O); human DNA ligase IIIβ (Lig III); wild type DNA ligase I (WT Lig I); mutant DNA ligase I (Mut Lig I). Cultures were streaked out onto LB-AMP plates containing 2 mM isopropyl-β-D-thiogalactoside and then incubated overnight at the indicated temperatures.

Supplementary materials and methods

Materials

The SV40-immortalized DNA ligase I mutant human fibroblast cell line 46BR.1G1 has been described previously [S1]. SV40-immortalized fibroblast cell lines established from a normal individual, GM00847, and from an individual with xeroderma pigmentosum, XP12RO, were obtained from Roger Schultz. Purified antibodies against human Pol β and Pol β were supplied by Sam Wilson. A recombinant baculovirus encoding SV40 T antigen was a gift from Bruce Stillman. T antigen was purified to near homogeneity from extracts of infected insect cells by a series of column chromatography steps, including phosphocellulose, Resource Q and S (Pharmacia), hydroxylapatite, and gel filtration.

Site-directed mutagenesis of DNA ligase I cDNA and construction of DNA ligase I expression vectors

Human DNA ligase I cDNA was mutated by site-directed mutagenesis using the QuikChange Site-Directed Mutagenesis Kit (Stratagene) according to the manufacturer's instructions. The mutations altered the coding sequence such that alanine residues replaced the phenylalanines at positions 8 and 9 within the DNA ligase I ORF [S2,S3]. After verification of the nucleotide sequence by DNA sequencing, wild-type and mutant DNA ligase I cDNAs were subcloned into the pFastBac expression vector (Gibco BRL). Following infection of Sf9 cells, DNA ligase I was purified as described previously [S4]. The mutant form of DNA ligase I protein behaved identically to the wild-type enzyme during purification.

DNA joining assay

DNA joining assays were performed using an oligonucleotide substrate containing a single defined nick [S5]. DNA ligase I was incubated with ^{32}P-labeled DNA substrate in 60 mM Tris-HCl pH 8.0, 10 mM $MgCl_2$, 5 mM DTT, 1 mM ATP and 50 μg/ml BSA for 20 min at 25°C. Reactions were terminated by the addition of stop solution (40 mM EDTA pH 8.0, and 80% formamide). Labeled oligonucleotides were resolved by denaturing gel electrophoresis and detected by autoradiography.

Pull-down assays

Glutathione beads with either glutathione-*S*-transferase (GST) or GST–PCNA fusion protein as the ligand were incubated with purified DNA ligase I as described [S6]. After washing, proteins bound to the beads were separated by SDS–PAGE. DNA ligase I was detected by immunoblotting with human DNA ligase I antiserum. The binding of Pol β to glutathione beads with either GST or GST fused to the amino-terminal 118 amino acids of DNA ligase I (either wild type or with the alanine substitutions as described above), was detected in similar assays [S6].

Construction of E. coli *expression vectors and complementation of* E. coli lig *mutants*

Wild-type and mutant DNA ligase I cDNAs were subcloned into pQE32 (Qiagen) and then transformed into the temperature sensitive *E. coli* strain AK76 *lig* ts7. Transformants were plated out and grown at the permissive (27°C) or non-permissive (42°C) temperature. Similar experiments were carried out with a pQE plasmid expressing DNA ligase IIIβ cDNA, which complements the temperature-sensitive phenotype [S7].

Isolation of stable derivatives of 46BR.1G1 expressing Flag-tagged DNA ligase I

After the addition of an in-frame Flag tag (Kodak) to the 5′ end of the DNA ligase I ORF, wild-type and mutant DNA ligase I cDNAs were subcloned into the mammalian expression vector pRC/RSV (Invitrogen). 46BR.1G1 cells were transfected with either the DNA ligase I expression constructs or the empty vector using the FuGene transfection reagent (Roche) according to the manufacturer's directions. After selection for resistance to geneticin, the level of DNA ligase I protein in clones was determined by immunoblotting with DNA ligase I antiserum [S6] and an anti-Flag antibody (Sigma).

Cell survival assays

SV40-immortalized fibroblasts (4×10^4 cells) were plated in triplicate in DMEM supplemented with 10% fetal bovine serum. Methyl methanesulfonate (MMS) was added to the medium for 1 h. The drug was removed by extensive washing with PBS, before the addition of fresh media. After 5 days, surviving cells were counted using an improved Neubauer chamber.

Preparation of cell-free extracts

Cell-free extracts for replication and repair assays were prepared as described previously [S8]. Briefly, 10^8–10^9 cells were washed in ice-cold isotonic buffer (20 mM HEPES pH 7.8, 1 mM $MgCl_2$, 5 mM KCl, 250 mM sucrose, 1 mM DTT, 0.1 mM PMSF). Cells were then washed in hypotonic buffer (isotonic buffer lacking sucrose), and then resuspended in hypotonic buffer at 10^8 cells/ml. Following a 45 min incubation on ice, the cells were lysed with 10 strokes from a tight fitting Dounce homogenizer. After incubation on ice for 60 mins, the insoluble debris was removed by centrifugation and the supernatant was aliquoted, flash-frozen and stored at −80°C. Protein concentrations were measured by the method of Bradford using BSA as the standard [S9].

Cell-free DNA replication assay

To monitor replicative DNA synthesis catalyzed by cell-free extracts, DNA replication intermediates were pulse labeled with [α^{32}P]dATP followed by the addition of dATP in DNA replication assays (75 µl) as described previously [S10]. Briefly, 360 µg cell extract was incubated for 20 min at 37°C with 6 µg/ml plasmid DNA containing the SV40 *ori* in 30 mM HEPES pH 7.5, 7 mM $MgCl_2$, 0.5 mM DTT, 3 mM ATP, 40 mM phosphocreatine, 25 µg/ml creatine kinase. For assays containing added purified DNA ligase I, the enzyme was added to the cell extract before the addition of the above buffer, and incubated for 12 min at 37°C. SV40 large T antigen was then added and incubated for 30 min at 37°C. Next, pulse labeling was begun by adding CTP, GTP and UTP to 200 µM each, dCTP, dGTP and TTP to 100 µM each, and 40 µCi/ml [α^{32}P]-dATP. After a 20 sec pulse, dATP was added to a final concentration of 5 mM. Aliquots were collected 0, 5 and 15 min after the cold dATP chase. Reactions were terminated by the addition of SDS to 2% and EDTA to 20 mM. Proteinase K was added, and the mixtures were incubated for 1 h at 37°C. The reactions were then extracted with phenol-chloroform, and the DNA was ethanol precipitated. After separation by alkaline agarose gel electrophoresis, labeled DNA replication intermediates were detected by autoradiography. No labeled DNA replication intermediates were detected in the absence of added T antigen (data not shown).

Base-excision repair (BER) assays

To measure the PCNA-independent single-nucleotide insertion (short patch) subpathway of BER, we utilized a linear DNA oligonucleotide substrate containing a single uracil residue [S11]. Reactions (50 µl), which contained 10 µg of extract, were performed as described previously [S12]. To detect repair patches longer than one nucleotide, [α-^{32}P]TTP was substituted for [α-^{32}P]dCTP. After separation by denaturing gel electrophoresis, labeled oligonucleotides were detected by autoradiography.

To measure the PCNA-dependent long-patch subpathway of BER, we utilized a ^{32}P-prelabeled circular DNA duplex substrate containing a single synthetic abasic (AP) site that cannot be repaired by short-patch BER because the 5′ terminus generated by cleavage of the modified AP site is refractory to removal by Pol β [S13–S15]. For the time-course experiments, repair reactions (20 µl) contained 2 µg of the cell-free extract. For titration of purified DNA ligase I, the repair reactions were supplemented with the indicated amounts of purified DNA ligase I, either wild-type or mutant protein, and incubated for 1 h. After recovery from the reactions, the DNA substrates were digested with *Hin*fI and AP endonuclease for 2 h. Reaction products were separated by denaturing gel electrophoresis and quantified by PhosphorImager analysis. Repair of the AP site yielded a labeled 46mer that is resistant to cleavage by AP endonuclease.

To analyze repair patch size, reactions containing 5 µg of extract were incubated for 2 h in the presence of 40 µM each of the four α-thio-dNTPs instead of the regular dNTPs. After recovery from the reactions, the DNA substrates were digested with *Hae*III, *Pst*I and AP endonuclease for 2 h, followed by 1 h digestion with 8 units of *E. coli* exonuclease III [S13]. The lengths of DNA repair synthesis tracts correspond to the size of exonuclease-generated fragments composed of α-thionucleotides. Reaction products were separated by denaturing gel electrophoresis and visualized by PhosphorImager analysis.

Supplementary references

S1. Barnes DE, Tomkinson AE, Lehmann AR, Webster AD, Lindahl T: **Mutations in the DNA ligase I gene of an individual with immunodeficiencies and cellular hypersensitivity to DNA-damaging agents.** *Cell* 1992, **69**:495-503.

S2. Barnes DE, Johnston LH, Kodama K, Tomkinson AE, Lasko DD, Lindahl T: **Human DNA ligase I cDNA: cloning and functional expression in *Saccharomyces cerevisiae*.** *Proc Natl Acad Sci USA* 1990, **87**:6679-6683.

S3. Montecucco A, Rossi R, Levin DS, Gary R, Park MS, Motycka TA, *et al.*: **DNA ligase I is recruited to sites of DNA replication by an interaction with proliferating cell nuclear antigen: identification of a common targeting mechanism for the assembly of replication factories.** *EMBO J* 1998, **17**:3786-3795.

S4. Wang YC, Burkhart WA, Mackey ZB, Moyer MB, Ramos W, Husain I, *et al.*: **Mammalian DNA ligase II is highly homologous with vaccinia DNA ligase; identification of the DNA ligase II active site for enzyme-adenylate formation.** *J Biol Chem* 1994, **269**:31923-31928.

S5. Tomkinson AE, Tappe NJ, Friedberg EC: **DNA ligase from *Saccharomyces cerevisiae*: physical and biochemical characterization of the *CDC9* gene product.** *Biochemistry* 1992, **31**:11762-11771.

S6. Levin DS, Bai W, Yao N, O'Donnell M, Tomkinson AE: **An interaction between DNA ligase I and proliferating cell nuclear antigen: implications for Okazaki fragment synthesis and joining.** *Proc Natl Acad Sci USA* 1997, **94**:12863-12868.

S7. Mackey ZB, Niedergang C, Murcia JM, Leppard J, Au K, Chen J, *et al.*: **DNA ligase III is recruited to DNA strand breaks by a zinc finger motif homologous to that of poly(ADP-ribose) polymerase. Identification of two functionally distinct DNA binding regions within DNA ligase III.** *J Biol Chem* 1999, **274**:21679-21687.

S8. Brush GS, Kelly TJ, Stillman B: **Identification of eukaryotic DNA replication proteins using simian virus 40 *in vitro* replication system.** *Methods Enzymol* 1995, **26**:522-548.

S9. Bradford MM: **A rapid and sensitive method for the quantitation of microgram quantities of protein utilizing the principle of protein-dye binding.** *Anal Biochem* 1976, **72**:248-254.

S10. Mackenney VJ, Barnes DE, Lindahl T: **Specific function of DNA ligase I in simian virus 40 DNA replication by human cell-free extracts is mediated by the amino-terminal non-catalytic domain.** *J Biol Chem* 1997, **272**:11550-11556.

S11. Singhal RK, Prasad R, Wilson SH: **DNA polymerase beta conducts the gap-filling step in uracil-initiated base excision repair in a bovine testis nuclear extract.** *J Biol Chem* 1995, **270**:949-957.

S12. Klungland A, Lindahl T: **Second pathway for completion of human DNA base excision-repair: reconstitution with purified proteins and requirement for DNase IV (FEN1).** *EMBO J* 1997,**16**:3341-3348.

S13. Matsumoto Y: **Base excision repair assay using *Xenopus laevis* oocyte extracts.** *Methods Mol Biol* 1999, **113**:289-300.

S14. Matsumoto Y, Kim K, Bogenhagen DF: **Proliferating cell nuclear antigen-dependent abasic site repair in *Xenopus laevis* oocytes: an alternative pathway of base excision DNA repair.** *Mol Cell Biol* 1994, **14**:6187-6197.

S15. Biade S, Sobol RW, Wilson SH, Matsumoto Y: **Impairment of proliferating cell nuclear antigen-dependent apurinic/apyrimidinic site repair on linear DNA.** *J Biol Chem* 1998, **273**:898-902.

Completion of Base Excision Repair by Mammalian DNA Ligases

ALAN E. TOMKINSON, LING CHEN, ZHIWAN DONG, JOHN B. LEPPARD, DAVID S. LEVIN, ZACHARY B. MACKEY, AND TERESA A. MOTYCKA

Department of Molecular Medicine
Institute of Biotechnology
The University of Texas Health Science Center at San Antonio
San Antonio, Texas 78245

Three mammalian genes encoding DNA ligases—*LIG1*, *LIG3*, and *LIG4*—have been identified. Genetic, biochemical, and cell biology studies indicate that the products of each of these genes play a unique role in mammalian DNA metabolism. Interestingly, cell lines deficient in either DNA ligase I (46BR.1G1) or DNA ligase III (EM9) are sensitive to simple alkylating agents. One interpretation of these observations is that DNA ligases I and III participate in functionally distinct base excision repair (BER) subpathways. In support of this idea, extracts from both DNA ligase-deficient cell lines are defective in catalyzing BER *in vitro* and both DNA ligases interact with other BER proteins. DNA ligase I interacts directly with proliferating cell nuclear antigen (PCNA) and DNA polymerase β

Progress in Nucleic Acid Research and Molecular Biology, Vol. 68

0079-6603/01 $35.00

(Pol β), linking this enzyme with both short-patch and long-patch BER. In somatic cells, DNA ligase IIIα forms a stable complex with the DNA repair protein Xrcc1. Although Xrcc1 has no catalytic activity, it also interacts with Pol β and poly(ADP-ribose) polymerase (PARP), linking DNA ligase IIIα with BER and single-strand break repair, respectively. Biochemical studies suggest that the majority of short-patch base excision repair events are completed by the DNA ligase IIIα/Xrcc1 complex. Although there is compelling evidence for the participation of PARP in the repair of DNA single-strand breaks, the role of PARP in BER has not been established.

I. Introduction

Phosphodiester bond formation is a common step in many DNA metabolic pathways, including DNA replication, DNA excision repair, and DNA strand-break repair. All the DNA ligation events in the prokaryote *Escherichia coli* are catalyzed by a single species of DNA ligase in an NAD-dependent reaction (*1*). In contrast, mammalian cells contain several distinct species of ATP-dependent DNA ligases (*2*). Except for the different nucleotide cofactor, prokaryotic and eukaryotic DNA ligases employ the same basic three-step reaction mechanism (*1, 2*). Initially, the enzyme reacts with the nucleotide cofactor to form a covalent enzyme–AMP complex, in which the AMP moiety is linked to a specific lysine residue. Next, the AMP group is transferred from the polypeptide to the 5′-phosphate terminus of a DNA nick. Finally, the nonadenylated enzyme catalyzes phosphodiester bond formation between the 3′-hydroxyl and 5′-phosphate termini of the nick, releasing AMP.

Based on their different biochemical properties, it was predicted that the mammalian DNA ligase activities were encoded by different genes (*3, 4*). This has been validated by the identification of three mammalian *LIG* genes: *LIG1*, *LIG3*, and *LIG4* (*5–7*). It seems reasonable to assume that the increased size and complexity of the eukaryotic genome provided the evolutionary driving force for multiple DNA ligases with distinct functions in cellular DNA metabolism. The presence of a conserved catalytic domain within the polypeptides encoded by the mammalian *LIG* genes supports the notion that these genes were generated by duplication events. Insights into the cellular roles of the mammalian *LIG* gene products have been gleaned both from the phenotype of DNA ligase-deficient cell lines and from the identification of proteins that specifically interact with the unique regions that flank the conserved catalytic domain.

In the yeast *Saccharomyces cerevisiae,* the *CDC9* and *DNL4* genes are homologous with the mammalian *LIG1* and *LIG4* genes, respectively (*5, 8–10*). Elegant genetic and biochemical studies have shown that, in addition to its essential role in DNA replication, Cdc9 DNA ligase completes nucleotide and base excision repair pathways (*11, 12*). The assignment of DNA ligases to excision repair pathways in mammalian cells is complicated by the presence

of the *LIG3* gene. Here we will focus on the products of the mammalian *LIG* genes with particular emphasis on the contribution of these enzymes to base excision repair (BER).

II. Mammalian *LIG* Genes and Their Protein Products

The relationship between the mammalian *LIG* genes and their products is shown in Table I and described below.

A. *LIG1*

A full-length cDNA encoding DNA ligase I was identified by screening for human cDNAs that complemented the conditional lethal phenotype of a *S. cerevisiae cdc9* DNA ligase mutant (*5*). The relationship between the 919-amino acid polypeptide encoded by the cDNA and DNA ligase I was confirmed by the alignment of peptide sequences from purified bovine DNA ligase I with sequences within the open reading frame encoded by the cDNA (*5*). A notable feature of the DNA ligase I polypeptide is its high proline content, which causes aberrant mobility during SDS-PAGE. Thus, DNA ligase I has a molecular mass of 125 kDa when measured by SDS-PAGE compared with a calculated molecular weight of 102,000 (*5, 13*).

When compared with other eukaryotic DNA ligases, mammalian DNA ligase I is most closely related to the replicative DNA ligases of *S. cerevisiae* and *Schizosaccharomyces pombe* encoded by the *CDC9* and *CDC17* genes, respectively (*5*). However, the amino acid homology is restricted to the C-terminal catalytic domains of these enzymes. The noncatalytic N-terminal domain of DNA ligase I contains sequences that target this polypeptide to the nucleus and to specific subnuclear locations (*14, 15*). In addition, this domain is phosphorylated *in vivo* and mediates specific protein–protein interactions (*16–18*).

The association of DNA ligase I with DNA replication is further supported by several other observations: (1) The level of DNA ligase I correlates with cell proliferation (*19, 20*); (2) DNA ligase I colocalizes with other replication

TABLE I
MAMMALIAN *LIG* GENES AND THEIR PRODUCTS

Gene	Enzyme
LIG1	DNA ligase I
LIG3	DNA ligase IIIα-nucl
	DNA ligase IIIα-mito
	DNA ligase IIIβ
LIG4	DNA ligase IV

proteins at the sites of DNA synthesis, termed replication foci, in replicating cells (*21*); (3) DNA ligase I copurifies with a high-molecular-weight replication complex (*22*).

B. *LIG3*

This gene was cloned at about the same time by two different approaches—searching an EST database with a motif conserved among eukaryotic DNA ligases, and a conventional cDNA cloning strategy based on partial amino acid sequences from purified bovine DNA ligase III (*6, 7*). The absence of *LIG3* homologs in the genomes of *S. cerevisiae, Drosophila melanogaster,* and *Caenorhabditis elegans* suggests that this gene was a relatively recent addition to the genome of mammals during evolution. In contrast to the *LIG1* and *LIG4* genes, the *LIG3* gene encodes several polypeptides that appear to have distinct cellular functions. Two forms of DNA ligase III, α and β, are produced by an alternative splicing event that results in proteins with different C termini (*23*). The C-terminal 77 amino acids of human DNA ligase IIIα are replaced by a unique 17-amino acid sequence in human DNA ligase IIIβ. The sequence of the C-terminal 100 amino acids of DNA ligase IIIα exhibits homology with the BRCT motif, a putative protein–protein interaction domain that was first identified in the product of the breast cancer susceptibility gene, *BRCA1* (*24, 25*). DNA ligase IIIα mRNA is expressed in all tissues and cells, whereas DNA ligase IIIβ mRNA expression is restricted to male germ cells, specifically pachytene spermatocytes and round spermatids (*23*). The differential expression profiles suggest that DNA ligase IIIα is a housekeeping enzyme, whereas DNA ligase IIIβ participates either in meiotic recombination or postmeiotic DNA repair.

Although the human DNA ligase IIIα open reading frame encodes a 949-amino acid polypeptide, the second in-frame ATG was chosen as the most likely *in vivo* translation initiation site based on homology with the Kozak consensus sequence (*6, 7*). More recently, it was noticed that the preceding 87-amino acid sequence contained a putative mitochondrial targeting signal (*26*). It was assumed that DNA ligase IIIα was a nuclear protein, as this enzyme was purified from nuclear extracts and immunocytochemistry experiments indicated that the majority of DNA ligase IIIα protein is located within the nucleus (*23, 27*). However, fusion of the putative targeting sequence to a heterologous protein resulted in mitochondrial localization of the fusion protein (*26*). Therefore, it appears that mitochondrial and nuclear forms of DNA ligase IIIα are produced in somatic cells by alternative translation initiation. Presumably, mitochondrial DNA ligase IIIα participates in the replication and repair of the mitochondrial genome. At present the mechanism underlying the nuclear localization of DNA ligase IIIα is unknown.

A zinc finger motif at the N terminus of DNA ligase III distinguishes the products of the *LIG3* gene from other eukaryotic DNA ligases. Intriguingly,

the DNA ligase III zinc finger is most closely related to the two zinc fingers located at the N terminus of poly(ADP-ribose) polymerase (PARP) (*7*). PARP is a relatively abundant nuclear protein whose avid binding to both single- and double-strand breaks is mediated by its zinc fingers. DNA binding activates the polymerase activity of PARP, resulting in the ADP-ribosylation of itself and other nuclear proteins (*28*). The single zinc finger of DNA ligase III has similar DNA binding properties in that it mediates the binding of this enzyme to DNA strand breaks with a preference for single-strand breaks (*29*). Although the zinc finger is not required for catalytic activity *in vitro* or for functional complementation of a temperature-sensitive *E. coli lig* mutant, it has a significant effect on the DNA-binding and DNA-joining activities of DNA ligase III at physiological salt concentrations (*29*).

C. *LIG4*

This gene, which was cloned by searching an EST database with a motif conserved among eukaryotic DNA ligases, was identified prior to the detection of the enzyme activity in mammalian cell extracts (*7, 30*). There are several reasons why DNA ligase IV activity escaped detection in the earlier enzyme purification studies: (1) In extracts from proliferating cells, DNA ligase IV is a minor contributor to cellular DNA ligase activity (*30*); (2) both the *LIG3* and *LIG4* genes encode polypeptides with similar electrophoretic mobility (*7, 30*); (3) unlike DNA ligases I and III, a significant fraction of DNA ligase IV remains adenylated during fractionation, making it difficult to label with [α^{32}P]ATP in the adenylation assay (*30*). A unique feature of the *LIG4* gene product compared with the *LIG1* and *LIG3* gene products is its long C-terminal extension beyond the conserved catalytic domain. Furthermore, this C-terminal region contains two BRCT motifs (*7*).

III. DNA Ligase-Associated Proteins

The identification of specific protein partners for each of the DNA ligases (Table II) has provided insights into both the molecular mechanisms by which these enzymes recognize interruptions in the phosphodiester backbone and their cellular functions.

A. DNA Ligase I

Using affinity chromatography with either DNA Pol β antibody or Pol β as the ligand, a multiprotein complex that catalyzed the repair of a uracil-containing DNA substrate was partially purified from a bovine testis nuclear extract (*31*). Subsequent studies revealed that DNA ligase I was a component of this BER complex and that DNA ligase I interacts directly with Pol β (*18, 31*). This interaction occurs between the noncatalytic N-terminal domain of DNA ligase I and

TABLE II
DNA LIGASE INTERACTING PROTEINS [a]

Enzyme	Interacting protein
DNA ligase I	PCNA
	DNA Pol β
DNA ligase IIIα	XRCC1
DNA ligase IIIβ	?
DNA ligase IV	XRCC4

[a]Biochemical and genetic studies indicate that the majority of short-patch BER events are completed by the DNA ligase IIIα/Xrcc1 complex. The contribution of DNA ligase I to short-patch BER via its interaction with Pol β is not known. The interaction of DNA ligase I with PCNA suggests that this enzyme completes the PCNA-dependent long-patch BER subpathway.

the 8-kDa N-terminal domain of Pol β that has DNA binding and 5′-deoxyribose phosphate diesterase activities (*32*, *33*).

Intuitively, an association between two enzymes that catalyze consecutive steps in a reaction pathway suggests that the interaction should enhance the overall rate of the reaction. In Figure 1, we show that gap-filling synthesis and ligation of a DNA substrate with a single nucleotide gap by the concerted action of Pol β and DNA ligase I occurs more rapidly than ligation of a DNA substrate with a single ligatable nick. It should be noted that this experiment does not demonstrate that the increased ligation rate is a direct consequence of the binding of DNA ligase I to Pol β. Nonetheless, it is intriguing that DNA ligase I, which transfers the AMP group to the 5′-phosphate terminus at a nick, interacts with the domain of Pol β that binds to and can modify the 5′ terminus at a nick or short gap in duplex DNA (*32*, *33*).

An association between DNA ligase I and proliferating cell nuclear antigen (PCNA) was also detected by affinity chromatography, in this case using DNA ligase I as the ligand (*17*). The direct interaction of these proteins is mediated by the noncatalytic N-terminal domain of DNA ligase I. Cell biology studies had demonstrated that this region of the protein was required both for nuclear localization and for subnuclear targeting to replication foci (*14*). Subsequent studies mapped these targeting activities to two distinct regions within the N-terminal region of DNA ligase I (*15*). Interestingly, the sequence required for targeting to replication foci was coincident with that required for PCNA binding (*15*). The replication foci targeting/PCNA binding sequence of DNA ligase I exhibits homology with a PCNA binding motif initially identified in the cell division kinase inhibitor p21 and subsequently found in several PCNA binding proteins (*34*). Although these observations indicate that the stable association of

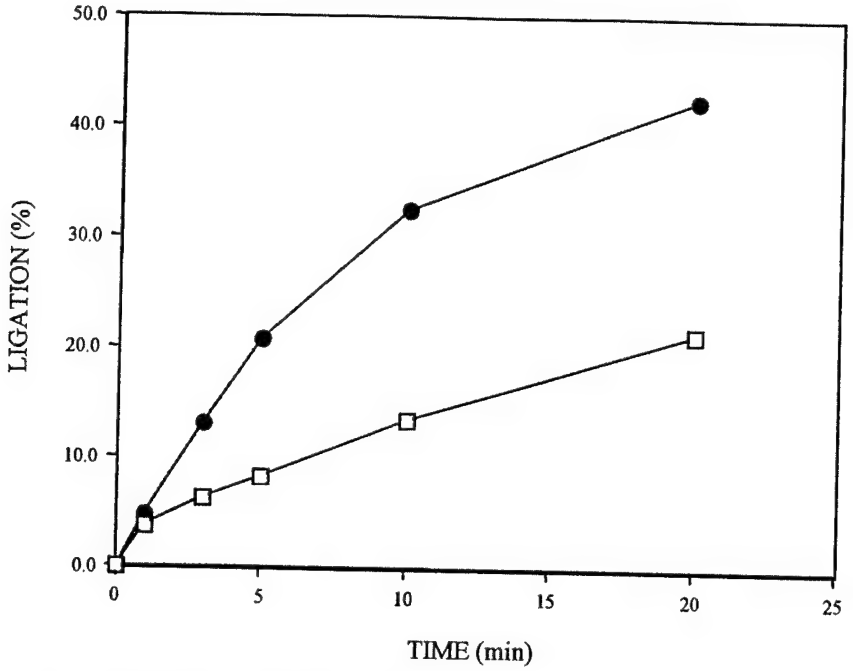

FIG. 1. Repair of a one-nucleotide gap by Pol β and DNA ligase I. DNA ligase I (0.06 pmol) and Pol β (0.12 pmol) were incubated with a labeled linear duplex DNA substrate (4 pmol) containing a one-nucleotide gap in the presence of the 4 dNTPs (filled circles). DNA ligase I (0.06 pmol) was incubated with a labeled linear duplex DNA substrate (4 pmol) containing a single ligatable nick in the presence of the 4 dNTPs (open squares). Aliquots were removed at the times indicated. After separation by denaturing gel electrophoresis, ligated product was detected and quantitated by PhosphorImager analysis. The inclusion of Pol β in assays with the nicked DNA substrate had no effect on the rate of ligation.

DNA ligase I with replication foci is mediated by PCNA binding, they do not address the direct role of PCNA binding in cellular ligation events catalyzed by DNA ligase I. In this regard, the inclusion of PCNA in DNA ligase assays does not stimulate DNA joining by DNA ligase I. However, DNA ligase I will bind to a PCNA molecule that is topologically linked to a circular DNA duplex so PCNA binding could serve to tether DNA ligase I to DNA substrates (*17*).

B. DNA Ligase III

DNA ligase III was identified as a protein that bound specifically to a tagged version of the DNA repair protein Xrcc1 (*35*). The human *XRCC1* gene was identified by its ability to complement the DNA damage hypersensitivity of a mutant Chinese hamster cell line, EM9 (*36*), which is described in more

detail below. Following the discovery of the different forms of DNA ligase III generated by alternative splicing, it was demonstrated that DNA ligase IIIα but not DNA ligase IIIβ formed a complex with Xrcc1 (*23, 37*). Interestingly, complex formation is mediated by an interaction between BRCT motifs present at the C termini of both Xrcc1 and DNA ligase IIIα (*37*). Although Xrcc1 has no catalytic activity, the reduced level of DNA ligase IIIα in the *xrcc1* mutant cell line indicates that Xrcc1 is important for the stability of DNA ligase IIIα (*38*). Moreover, protein–protein interactions between Xrcc1 and both Pol β and PARP have been characterized (*39, 40*). Each of these binding events involves different regions of Xrcc1 that are also distinct from the DNA ligase IIIα binding site, suggesting that Xrcc1 may act as a scaffold for the assembly of a multiprotein complex (*39, 40*).

C. DNA Ligase IV

DNA ligase IV was identified as a protein that specifically coimmunoprecipitated with a tagged version of the DNA repair protein Xrcc4 (*41*). The human *XRCC4* gene was identified by its ability to complement the DNA damage hypersensitivity of a mutant Chinese hamster cell line XR1 (*42*). In contrast to the interaction between DNA ligase IIIα and Xrcc1, the interaction between DNA ligase IV and Xrcc4 is not mediated by BRCT motifs, but instead Xrcc4 binds to the region between the two C-terminal BRCT motifs of DNA ligase IV (*43*). The reduced level of DNA ligase IV protein in *xrcc4* mutant cells suggests that the interaction with Xrcc4 stabilizes DNA ligase IV (*44*). Since Xrcc4 binds to DNA, it is possible that this protein mediates the binding of DNA ligase IV to its DNA substrate (*45*).

IV. Phenotype of DNA Ligase-Deficient Cell Lines

Our understanding of the cellular functions of the mammalian DNA ligases has been greatly enhanced by the isolation of mammalian cell lines deficient in each of the DNA ligases. The phenotypes of these cell lines are summarized below.

A. DNA Ligase I-Deficient Cell Lines

The fibroblast cell line 46BR and an SV40-immortalized derivative 46BR.1G1 were established from an immunodeficient individual who inherited different point mutations in each *LIG1* allele (*46, 47*). One of the mutations abolishes DNA ligase activity, whereas the other mutant allele encodes a polypeptide that is 10- to 20-fold less active than the wild-type enzyme. As expected, the DNA ligase I deficiency results in abnormal joining of Okazaki fragments (*48, 49*). The cell lines are also hypersensitive to the cytotoxic effects of monofunctional

DNA alkylating agents and are moderately sensitive to ultraviolet and ionizing radiation (*50*). These observations are consistent with DNA ligase I participating in strand-break and excision-repair pathways. In support of this idea, 46BR.1G1 extracts are defective in the repair of circular duplex DNA containing a single uracil residue (*48*). Specifically, the DNA ligase I deficiency resulteds in reduced levels of repaired circular product and increased levels of DNA repair synthesis.

B. DNA Ligase III-Deficient Cell Lines

The mutant Chinese hamster ovary cell line EM9 was isolated based on its hypersensitivity to DNA alkylating agents (*51*). Further analysis revealed that this cell line was also moderately sensitive to ionizing radiation and exhibited elevated levels of sister chromatid exchange when grown in the presence of bromodeoxyuridine (*52*). As mentioned previously, expression of the human *XRCC1* gene complemented the DNA damage-sensitive phenotype of the mutant CHO cell line (*36*). Analysis of DNA repair in EM9 cells revealed a defect in events after DNA damage-incision. The interactions of Xrcc1 with both Pol β and DNA ligase IIIα provide a molecular explanation for the participation of Xrcc1 in the DNA synthesis and ligation reactions that complete base excision repair (*35, 40*). In further support of the idea that Xrcc1 plays an important role in BER, extracts from EM9 cells are defective in this type of repair (*53*).

It should be noted that Xrcc1 may function independently of DNA ligase IIIα. As mentioned previously, Xrcc1 interacts with PARP, an enzyme that is not required for the reconstitution of BER *in vitro* (*39*). In addition, a recent study with *xrcc1* mutant cells reported evidence that the DNA ligase IIIα/Xrcc1 complex plays an important role in DNA repair within the G_1 phase of the cell cycle whereas Xrcc1 alone mediates DNA repair events within the DNA synthesis phase of the cell cycle (*54*). The construction and characterization of *lig3* mutant cell lines will facilitate further analysis of the cellular functions of DNA ligase III and Xrcc1.

C. DNA Ligase IV-Deficient Cell Lines

The mutant Chinese hamster cell line XR1 is hypersensitive to ionizing radiation and defective in V(D)J recombination (*42*). Interestingly, the DNA damage hypersensitivity is most pronounced in the G_1 phase of the cell cycle. As noted above, both the repair and V(D)J recombination defects in XR1 cells are complemented by the human *XRCC4* gene whose product forms a stable complex with the *LIG4* gene product (*41, 55*). More recently, the *XRCC4* gene has been deleted in mouse embryonic cells by gene targeting and embryonic fibroblast cell lines established from the resultant *xrcc4*$^{-/-}$ embryos. These cell lines reiterate the phenotype of the XR1 cells (*56*).

Cell lines with mutations in the *LIG4* gene are also available. A radiosensitive human cell line 180BR was established from a leukemia patient who had

severe reactions to both radiotherapy and chemotherapy (*57*). Subsequently, a point mutation was identified within the *LIG4* gene of the 180BR cells (*58*). Interestingly, the leukemia patient did not appear to be immunodeficient, and the 180BR cells, when activated for V(D)J recombination, had no obvious defect in this type of site-specific recombination (*58*). It is possible that the mutant allele encodes a product that retains sufficient activity to complete V(D)J recombination, but not for the repair of DNA damage-induced double-strand breaks. The *LIG4* gene has been deleted in mouse embryonic cells by gene targeting, and embryonic fibroblast cell lines have been established from the resultant *lig4*$^{-/-}$ embryos. These cell lines exhibit the same phenotype as the *xrcc4* mutant cell line in that they are hypersensitive to ionizing radiation and defective in V(D)J recombination (*59*). Based on the results described above and comparable studies in the yeast *S. cerevisiae* (*8–10*), it appears that DNA ligase IV plays a major role in the repair of DNA double-strand breaks by nonhomologous end joining but does not contribute significantly to BER and other excision repair pathways.

V. Involvement of Mammalian DNA Ligases in BER

Biochemical studies using cell-free extracts and purified proteins have identified two pathways of BER that can be distinguished both by the extent of DNA repair synthesis and the requirement for PCNA (*40, 60–63*). At the present time, the spectrum of DNA base lesions repaired *in vivo* by the short-patch (single-nucleotide repair patch, PCNA-independent) and long-patch (repair patches of 2–11 nucleotides, PCNA-dependent) BER subpathways is not known. Thus it is possible that certain base lesions can be repaired by only one of the BER subpathways, whereas other lesions can be effectively repaired by either subpathway.

As mentioned above, cell lines defective in either DNA ligase I or DNA ligase III are hypersensitive to killing by monofunctional alkylating agents such as methyl methanesulfonate (MMS) (*50, 52*). Since the base lesions caused by MMS are thought to be repaired by BER, one explanation of these observations is that there are two functionally distinct BER subpathways, one involving DNA ligase I and the other involving DNA ligase III, that repair different cytotoxic lesions induced by MMS exposure (Fig. 2). In support of this model, extracts from cell lines defective in either DNA ligase I or DNA ligase III exhibit abnormalities in BER assays (*48, 53*). The extracts with reduced DNA ligase III activity are defective in short-patch BER but proficient in long-patch BER (*53*). This suggests that the interaction between Pol β and the Xrcc1 subunit of the Xrcc1/DNA ligase IIIα complex is critical for the completion of short-patch BER (Fig. 2).

Although the interactions of DNA ligase I with both Pol β and PCNA suggest that this enzyme could function in both short- and long-patch BER (*17, 18*), the

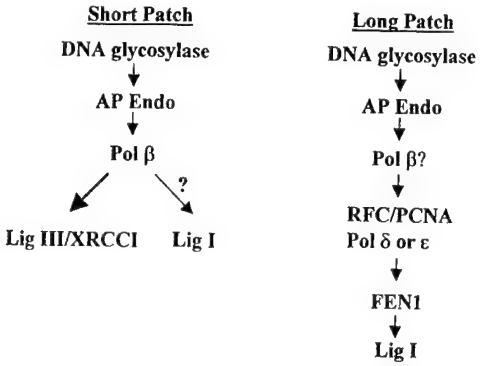

FIG. 2. A model illustrating the participation of DNA ligases I and III in BER.

effect of DNA ligase I deficiency on these subpathways has not been determined. Since DNA ligase III deficiency effects short- but not long-patch BER, it is conceivable that DNA ligase I deficiency will have the opposite effect, causing a defect in long-patch, but not short-patch BER (Fig. 2). If this is the case, the DNA ligase III- and DNA ligase I-deficient cell lines should be useful reagents to determine the spectrum of base lesions repaired *in vivo* by short- and long-patch BER.

VI. Concluding Remarks

Genetic and biochemical studies suggest that both the DNA ligase IIIα/Xrcc1 complex and DNA ligase I play biologically significant roles in BER. Based on currently available evidence, it appears that the DNA ligase IIIα/Xrcc1 complex completes the majority of short-patch BER events (*40, 53*). The interaction of DNA ligase I with PCNA makes this species of DNA ligase the most likely candidate for the long-patch BER subpathway (*17, 60, 63*). Further studies are required to determine the *in vivo* roles of these BER subpathways. At the present time, the biological significance of the interaction between DNA ligase I and Pol β is unclear. Since the 180-kDa BER complex containing these proteins was isolated from extracts of bovine testes (*31*), it is possible that the involvement of DNA ligase I and DNA ligase IIIα/Xrcc1 in short-patch BER is cell type-specific. Further studies are required to elucidate the functional consequence of the interactions between the DNA ligases and Pol β and/or PCNA on the coordination of the reactions that complete BER.

The role of the nuclear protein PARP in BER is controversial. Although both the short- and long-patch BER pathways can be reconstituted *in vitro* without PARP (*40, 60, 61*), the results of BER assays with extracts from $parp^{-/-}$

cells and the interaction between PARP and Xrcc1 suggest that PARP may contribute to the completion of BER (*39, 64*). The involvement of PARP in BER does not appear to be compatible with the current model of BER, in which pairwise interactions between BER proteins mediate the handover of repair intermediates. In fact, this model predicts that PARP would be actively excluded from DNA undergoing BER by the coordinate action of the BER proteins. It is possible that the DNA ligase IIIα/Xrcc1 complex participates in both PARP-dependent repair of DNA single-strand breaks and PARP-independent short-patch BER. Further biochemical and molecular genetic studies are required to clarify the complex relationships between these DNA repair proteins.

ACKNOWLEDGMENTS

Studies in A.E.T.'s laboratory were supported by grants from the Department of Health and Human Services (GM47251 and GM57479), the Nathan Shock Aging Center, and the San Antonio Cancer Institute. D.S.L. and Z.B.M. were supported by the Training Program in the Molecular Basis of Breast Cancer. D.S.L. is supported by the Training Program in the Molecular Basis of Aging. Z.B.M is a UNCF-MERCK fellow.

REFERENCES

1. I. R. Lehman, *Science* **186,** 790–797 (1974).
2. A. E. Tomkinson and Z. B. Mackey, *Mutat. Res.* **407,** 1–9 (1998).
3. A. E. Tomkinson, E. Roberts, G. Daly, N. F. Totty, and T. Lindahl, *J. Biol. Chem.* **286,** 21728–21735 (1991).
4. J. E. Arrand, A. E. Willis, I. Goldsmith, and T. Lindahl, *J. Biol. Chem.* **261,** 9079–9082 (1986).
5. D. E. Barnes, L. H. Johnston, K. Kodama, A. E. Tomkinson, D. D. Lasko, and T. Lindahl, *Proc. Natl. Acad. Sci. U.S.A.* **87,** 6679–6683 (1990).
6. J. Chen, A. E. Tomkinson, W. Ramos, Z. B. Mackey, S. Danehower, C. A. Walter, R. A. Schultz, J. M. Besterman, and I. Husain, *Mol. Cell. Biol.* **15,** 5412–5422 (1995).
7. Y.-F. Wei, P. Robins, K. Carter, K. Caldecott, D. J. C. Pappin, G.-L. Yu, R.-P. Wang, B. K. Shell, R. A. Nash, P. Schär, D. E. Barnes, W. A. Haseltine, and T. Lindahl, *Mol. Cell. Biol.* **15,** 3206–3216 (1995).
8. P. Schär, G. Herrman, G. Daly, and T. Lindahl, *Genes Dev.* **11,** 1912–1924 (1997).
9. S. H. Teo and S. P. Jackson, *EMBO J.* **16,** 4788–4795 (1997).
10. T. E. Wilson, U. Grawunder, and M. R. Lieber, *Nature (London)* **388,** 495–498 (1997).
11. X. Wu, E. Braithwaite, and Z. Wang, *Biochemistry* **38,** 2628– 2635 (1999).
12. D. R. Wilcox and L. Prakash, *J. Bacteriol.* **148,** 618–623 (1981).
13. A. E. Tomkinson, D. D. Lasko, G. Daly, and T. Lindahl, *J. Biol. Chem.* **265,** 12611–12617 (1990).
14. A. Montecucco, E. Savini, F. Weighardt, R. Rossi, G. Ciarrocchi, A. Villa, and G. Biamonti, *EMBO J.* **14,** 5379–5386 (1995).
15. A. Montecucco, R. Rossi, D. S. Levin, R. Gary, M. S. Park, T. A. Motycka, G. Ciarrocchi, A. Villa, G. Biamonti, and A. E. Tomkinson, *EMBO J.* **17,** 3786–3795 (1998).

16. C. Prigent, D. D. Lasko, K. Kodama, J. R. Woodgett, and T. Lindahl, *EMBO J.* **11,** 2925–2933 (1994).
17. D. S. Levin, W. Bai, N. Yao, M. O'Donnell, and A. E. Tomkinson, *Proc. Natl. Acad. Sci. U.S.A.* **94,** 12863–12868 (1997).
18. E. K. Dimitriadis, R. Prasad, M. K. Vaske, L. Chen, A. E. Tomkinson, M. S. Lewis, and S. H. Wilson, *J. Biol.Chem.* **273,** 20540–20550 (1998).
19. J. H. J. Petrini, K. G. Huwiler, and D. T. Weaver, *Proc. Natl. Acad. Sci. U.S.A.* **88,** 7615–7619 (1991).
20. S. Soderhall, *Nature (London)* **260,** 640–642 (1976).
21. D. Wilcock and D. P. Lane, *Nature (London)* **349,** 429–431 (1991).
22. C. Li, J. Goodchild, and E. F. Baril, *Nucleic Acids Res.* **22,** 632–638 (1994).
23. Z. B. Mackey, W. Ramos, D. S. Levin, C. A. Walter, J. R. McCarrey, and A. E. Tomkinson, *Mol. Cell. Biol.* **17,** 989–998 (1996).
24. I. Callebaut and J. P. Mornon, *FEBS Lett.* **400,** 25–30 (1997).
25. E. V. Koonin, S. F. Alschul, and P. Bork, *Nature Genet.* **13,** 266–267 (1996).
26. U. Lakshmipathy and C. Campbell, *Mol. Cell. Biol.* **19,** 3869–3876 (1999).
27. I. Husain, A. E. Tomkinson, W. A. Burkhart, M. B. Moyer, W. Ramos, Z. B. Mackey, J. M. Besterman, and J. Chen, *J. Biol. Chem.* **270,** 9683–9690 (1995).
28. G. de Murcia and J. M. de Murcia, *Trends Biochem. Sci.* **19,** 172–176 (1994).
29. Z. B. Mackey, C. Niedergang, J. M. Murcia, J. Leppard, K. Au, J. Chen, G. de Murcia, and A. E. Tomkinson, *J. Biol. Chem.* **274,** 21679–21687 (1999).
30. P. Robins and T. Lindahl, *J. Biol. Chem.* **271,** 24257–24261 (1996).
31. R. Prasad, R. K. Singhal, D. K. Srivastava, J. T. Molina, A. E. Tomkinson, and S. H. Wilson, *J. Biol. Chem.* **271,** 16000–16007 (1996).
32. Y. Matsumoto and K. Kim, *Science* **269,** 699– 702 (1995).
33. R. Prasad, W. A. Beard, and S. H. Wilson, *J. Biol. Chem.* **269,** 18096–18101 (1994).
34. E. Warbrick, *Bioessays* **20,** 195– 199 (1998).
35. K. W. Caldecott, C. K. McKeown, J. D. Tucker, S. Ljunquist, and L. H. Thompson, *Mol. Cell. Biol.* **14,** 68–76 (1994).
36. L. H. Thompson, K. W. Brookman, N. J. Jones, S. A. Allen, and A. V. Carrano, *Mol. Cell. Biol.* **10,** 6160–6171 (1990).
37. R. A. Nash, K. Caldecott, D. E. Barnes, and T. Lindahl, *Biochemistry* **36,** 5207– 5211 (1997).
38. S. Ljungquist, K. Kenne, L. Olsson, and M. Sandstrom, *Mutat. Res.* **314,** 177–186 (1994).
39. M. Masson, C. Niedergang, V. Schreiber, S. Muller, J. M. de Murcia, and G. de Murcia, *Mol. Cell. Biol.* **18,** 3563–3571 (1998).
40. Y. Kubota, R. A. Nash, A. Klungland, P. Schär, D. E. Barnes, and T. Lindahl, *EMBO J.* **15,** 6662–6670 (1996).
41. U. Grawunder, M. Wilm, X. Wu, P. Kulesza, T. E. Wilson, M. Mann, and M. R. Lieber, *Nature (London)* **388,** 492–495 (1997).
42. Z. Li, T. Otevrel, Y. Gao, H.-L. Cheng, B. Seed, T. D. Stamato, G. E. Taccioli, and F. W. Alt, *Cell (Cambridge, Mass.)* **83,** 1079–1089 (1995).
43. U. Grawunder, D. Zimmer, and M. R. Leiber, *Curr. Biol.* **8,** 873–876 (1998).
44. M. Bryans, M. C. Valenzano, and T. Stamato, *Mutat. Res.* **433,** 53–58 (1999).
45. M. Modesti, J. E. Hesse, and M. Gellert, *EMBO J* **18,** 2008–2017 (1999).
46. D. E. Barnes, A. E. Tomkinson, A. R. Lehmann, A. D. B. Webster, and T. Lindahl, *Cell (Cambridge, Mass.)* **69,** 495–503 (1992).
47. A. D. B. Webster, D. E. Barnes, C. F. Arlett, A. R. Lehmann, and T. Lindahl, *Lancet* **339,** 1508–1509 (1992).
48. C. Prigent, M. S. Satoh, G. Daly, D. E. Barnes, and T. Lindahl, *Mol. Cell. Biol.* **14,** 310–317 (1994).

49. V. J. Mackenney, D. E. Barnes, and T. Lindahl, *J. Biol. Chem.* **272,** 11550–11556 (1997).
50. I. A. Teo, C. F. Arlett, S. A. Harcourt, A. Priestly, and B. C. Broughton, *Mutat. Res.* **107,** 371–386 (1983).
51. L. H. Thompson, T. Shiomi, E. P. Salazar, and S. A. Stewart, *Somat. Cell Mol. Genet.* **14,** 605–612 (1988).
52. L. H. Thompson, K. W. Brookman, L. E. Dillehay, A. V. Carrano, J. A. Mazrimas, C. L. Mooney, and J. L. Minkler, *Mutat. Res.* **95,** 247–254 (1982).
53. E. Cappelli, R. Taylor, M. Cevasco, A. Abbondandolo, K. Caldecott, and G. Frosina, *J. Biol. Chem.* **272,** 23970–23975 (1997).
54. R. M. Taylor, D. J. Moore, J. Whitehouse, P. Johnson, and K. W. Caldecott, *Mol. Cell. Biol.* **20,** 735–740 (2000).
55. S. E. Critchlow, R. P. Bowater, and S. P. Jackson, *Curr. Biol.* **7,** 588–598 (1997).
56. Y. Gao, Y. Sun, K. M. Frank, P. Dikkes, Y. Fujiwara, K. J. Seidl, J. M. Sekiguchi, G. A. Rathbun, W. Swat, J. Wang, R. T. Bronson, B. A. Malynn, M. Bryans, C. Zhu, J. Chaudhuri, L, Davidson, R. Ferrini, T. Stamato, S. H. Orkin, M. E. Greenberg, and F. W. Alt, *Cell (Cambridge, Mass.)* **95,** 891–902 (1998).
57. P. N. Plowman, B. A. Bridges, C. F. Arlett, A. Hinney, and J. E. Kingston, *Br. J. Radiol.* **63,** 624–628 (1990).
58. E. Riballo, S. E. Critchlow, S.-H. Teo, A. J. Doherty, A. Priestly, B. Broughton, B. Kysela, H. Beamish, N. Plowman, C. F. Arlett, A. R. Lehmann, S. P. Jackson, and P. A. Jeggo, *Curr. Biol.* **9,** 699–702 (1999).
59. K. M. Frank, J. M. Sekiguchi, K. J. Seidl, W. Swat, G. A. Rathbun, H. L. Cheng, L. Davidson, L. Kangaloo, and F. W. Alt, *Nature (London)* **396,** 173–176 (1998).
60. A. Klungland and T. Lindahl, *EMBO J.* **16,** 3341–3348 (1997).
61. Y. Matsumoto, K. Kim, J. Hurwitz, R. Gary, D. S. Levin, A. E. Tomkinson, and M. Park, *J. Biol. Chem.* **274,** 33703–33708 (1999).
62. D. K. Srivastava, B. J. Vande Berg, R. Prasad, J. T. Molina, W. A. Beard, A. E. Tomkinson, and S. H. Wilson, *J. Biol. Chem.* **273,** 21203–21209 (1998).
63. G. Frosina, P. Fortini, O. Rossi, F. Carrozzino, G. Raspaglio, L. S. Cox, D. P. Dane, A. Abbondandolo, and E. Dogliotti, *J. Biol. Chem.* **271,** 9573–9578 (1996).
64. C. Trucco, F. J. Oliver, G. de Murcia, and J. Menissier-de Murcia, *Nucleic Acids Res.* **26,** 2644–2649 (1998).

Functional link between ataxia-telangiectasia and Nijmegen breakage syndrome gene products

Song Zhao*†, Yi-Chinn Weng*†, Shyng-Shiou F. Yuan*†‡, Yi-Tzu Lin*†, Hao-Chi Hsu*, Suh-Chin J. Lin*, Elvira Gerbino*, Mei-hua Song*, Małgorzata Z. Zdzienicka§, Richard A. Gatti‖, Jerry W. Shay¶, Yael Ziv#, Yosef Shiloh# & Eva Y.-H. P. Lee*

* *Department of Molecular Medicine/Institute of Biotechnology, The University of Texas Health Science Center at San Antonio, San Antonio, Texas 78245-3207, USA*
§ *MGC-Department of Radiation Genetics and Chemical Mutagenesis, Leiden University, LUMC, Leiden, The Netherlands*
‖ *Department of Pathology, University of California Los Angeles, Los Angeles, California 90095, USA*
¶ *Department of Cell Biology, The University of Texas Southwestern Medical Center, Dallas, Texas 75390-9039, USA*
# *Department of Human Genetics and Molecular Medicine, Sackler School of Medicine, Tel Aviv University, Tel Aviv, Israel*
† *These authors contributed equally to this work*

Ataxia-telangiectasia (A-T) and Nijmegen breakage syndrome (NBS) are recessive genetic disorders with susceptibility to cancer and similar cellular phenotypes[1]. The protein product of the gene responsible for A-T, designated ATM, is a member of a family of kinases characterized by a carboxy-terminal phosphatidylinositol 3-kinase-like domain[2,3]. The NBS1 protein is specifically mutated in patients with Nijmegen breakage syndrome and forms a complex with the DNA repair proteins Rad50 and Mre11[4–7]. Here we show that phosphorylation of NBS1, induced by ionizing radiation, requires catalytically active ATM. Complexes containing ATM and NBS1 exist *in vivo* in both untreated cells and cells treated with ionizing radiation. We have identified two residues of NBS1, Ser 278 and Ser 343 that are phosphorylated *in vitro* by ATM and whose modification *in vivo* is essential for the cellular response to DNA damage. This response includes S-phase checkpoint activation, formation of the NBS1/Mre11/Rad50 nuclear foci and rescue of hypersensitivity to ionizing radiation. Together, these results demonstrate a biochemical link between cell-cycle checkpoints activated by DNA damage and DNA repair in two genetic diseases with overlapping phenotypes.

The cellular response to DNA damage is complex and includes cell-cycle checkpoint activation, DNA repair and changes in gene transcription[8–11]. Cell lines representative of the inherited cancer-prone human diseases ataxia-telangiectasia (A-T) and Nijmegen breakage syndrome (NBS) are hypersensitive to ionizing radiation and have defects in DNA-damage-activated cell-cycle checkpoints[1]. Upon DNA damage, ATM phosphorylates p53 (refs 12, 13), and Brca1 (ref. 14). ATM is required for phosphorylation of Chk2 kinase[15] and Rad51 (refs 16, 17) induced by ionizing radiation. NBS1 is an integral component of the Mre11/Rad50/NBS1 nuclease complex[4–7] which is important in the repair of DNA double-strand breaks[18].

To examine whether a signalling cascade exists between ATM and NBS1, we studied whether NBS1 was posttranslationally modified following treatment with ionizing radiation. The NBS1 monoclonal antibody specifically recognized a protein with a relative molecular mass of 95,000 (M_r 95K) in all human cell lines examined except those established from NBS patients (data not shown). Although the electrophoretic mobility of the 95K NBS1 protein was constant throughout the cell cycle, treatment of cells with 10 Gy γ-irradiation resulted in a slower migrating form of NBS1 (Fig. 1a). The mobility of the altered form of NBS1 immunoprecipitated from irradiated cells reverted to that of NBS1 from undamaged cells upon incubation with phosphatase, indicating that NBS1 becomes phosphorylated in response to DNA damage by ionizing radiation (Fig. 1b, compare lane 6 with lanes 2 and 5).

Cell lines lacking functional ATM protein were used to examine whether ATM is required for phosphorylation of NBS1 after DNA damage. The ionizing radiation- or bleomycin (0.1 U per ml)-induced phosphorylation of NBS1 was not detected in these cells

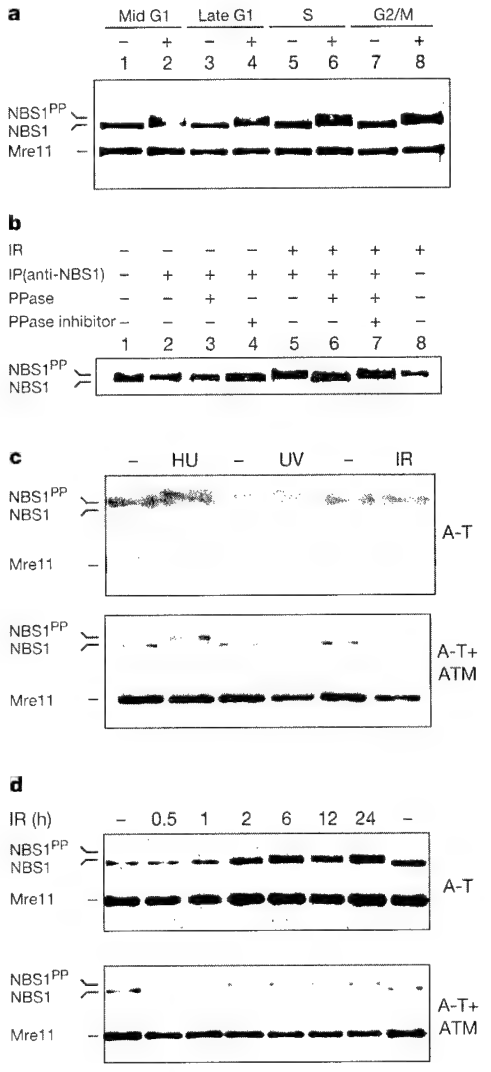

Figure 1 ATM is required for DNA damage-induced phosphorylation of NBS1. **a**, Mobility shift of NBS1 in response to DNA damage during the cell cycle. Synchronized T24 cells were irradiated with 10 Gy γ-irradiation. Lysates (50 μg protein) of untreated cells and cells 1 h after ionizing radiation (IR) treatment were analysed by western blotting with anti-NBS1 antibody. NBS1^{pp}, phosphorylated form of NBS1. Mre11 is included as a protein loading control. **b**, Phosphorylation and mobility shift of NBS1. Lysates from untreated (lanes 1–4) and IR-treated (lanes 5–8) human lymphoblast NAT10 cells were immunoprecipitated with anti-NBS1 antibody. Immunoprecipitates were incubated with phosphatase (PPase) in the absence or presence of phosphatase inhibitor. Lysates from untreated (lane 1) and IR-treated cells (lane 8) were included as control. **c**, Phosphorylation of NBS1 upon DNA damage and replication block in AT22IJE-T/pEBS7 (A-T) and AT22IJE-T/pEBS7-YZ5 (A-T cells complemented with ATM). **d**, Kinetics of IR-induced modification of NBS1. Cell lysates were prepared at the indicated time points after IR treatment.

‡ Present address: Department of Obstetrics and Gynecology, Kaohsiung Medical University, No. 100, Shih-Chuan 1st Road, Kaohsiung 80708, Taiwan.

(Fig. 1c and data not shown). In contrast, the mobility shift induced by treatment with either hydroxyurea (1 mM) or ultraviolet light (10 J m^{-2}) was normal (Fig. 1c). Importantly, re-introduction of the ATM gene into A-T cells[19] restored phosphorylation of NBS1 induced by ionizing radiation (Fig. 1c, bottom) showing that the failure to phosphorylate NBS1 is directly related to a deficiency of the ATM protein. The absence of ATM does not abolish cellular responses to DNA damage but it does result in a significant delay in these responses[20]. We therefore compared the kinetics of phosphorylation of NBS1 induced by ionizing radiation in A-T cells, with that in A-T cells that had also been complemented with the ATM protein. Modification of NBS1 was only detectable 6 h after ionizing radiation in the absence of ATM (Fig. 1d). In contrast, the kinetics of NBS1 phosphorylation in A-T cells complemented with ATM was similar to that of T24 cells, with phosphorylation detectable within 30 min after ionizing radiation (Fig. 1d and data not shown). As the ATM-related kinase, ATR, can phosphorylate p53 with delayed kinetics in the absence of ATM[21], we suggest that the delayed phosphorylation of NBS1 in A-T cells may be attributable to ATR or another related kinase.

The cellular amounts of the ATM and NBS1 proteins remained unchanged following DNA damage (Fig. 2a, left panel). Although ATM was co-immunoprecipitated by NBS1 antibody in extracts from both treated and untreated cells, ionizing radiation increased the amount of ATM in the NBS1-immunoprecipitates (Fig. 2a, middle). Consistent with these results, NBS1 was co-immunoprecipitated by the ATM antibody from untreated cells and in increased quantities from cells treated with ionizing radiation (Fig. 2a, right).

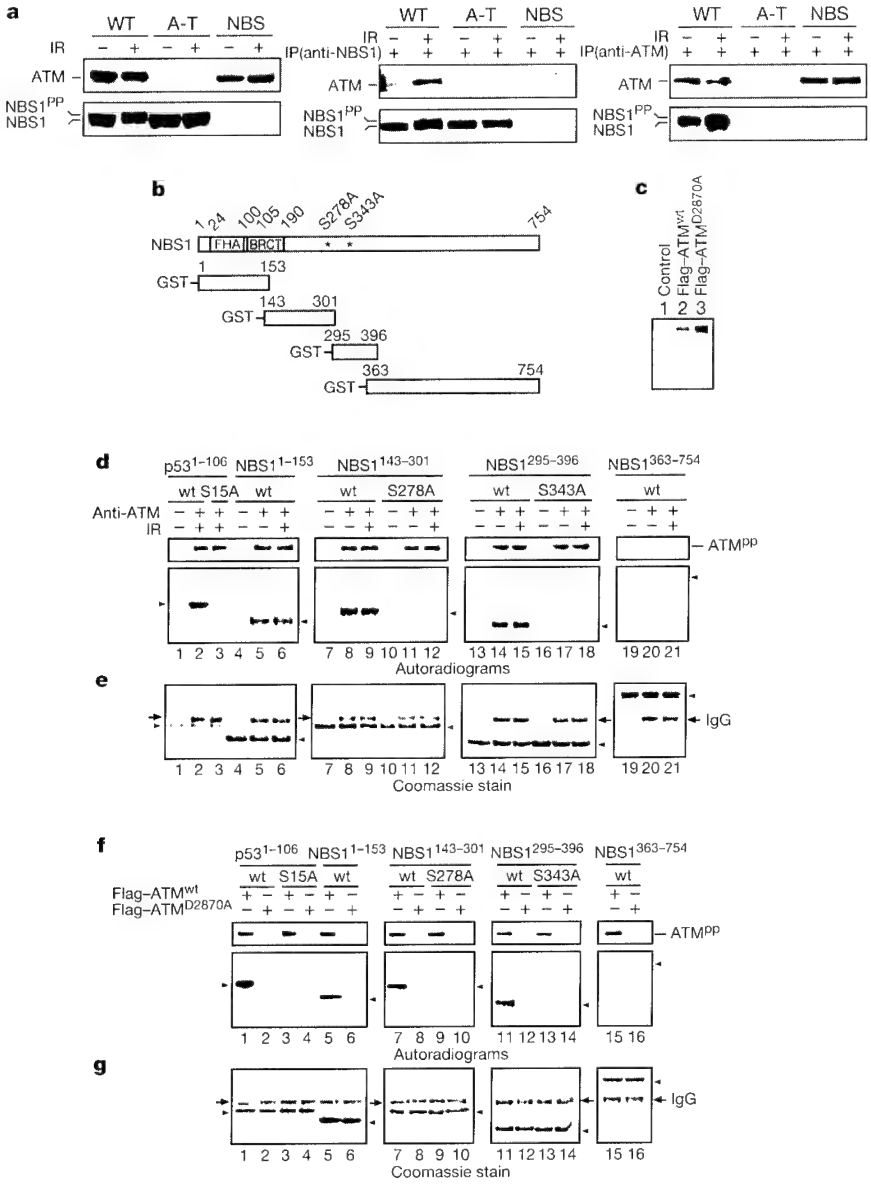

Figure 2 Interaction between ATM and NBS1, *in vivo* and *in vitro* phosphorylation of NBS1 by ATM. **a**, Interaction between ATM and NBS1. Left, direct immunoblotting using cell lysates (100 μg) from mock-treated or 2 h after 10 Gy γ-irradiated cells. T24, A-T (GM09607) and NBS1-LBI cell lines were studied. Middle, co-immunoprecipitation of ATM by anti-NBS1 antibody. Right, co-immunoprecipitation of NBS1 by anti-ATM antibody. **b**, NBS1 structural domains and GST–NBS1 fusion proteins. Asterisk, serine substituted with alanine. **c**, Expression of the recombinant ATM in human 293 cells 24 h after transfection. Immunoblotting with anti-Flag antibody, M5 (Kodak). **d**, Autoradiograms showing ATM autophosphorylation (top) and phosphorylation of GST–NBS1 fusion proteins by the ATM immunoprecipitated from either untreated or IR-treated cells (bottom). Purified fusion proteins were incubated with kinase buffer alone (lanes 1, 4, 7, 10, 13, 16 and 19) or kinase buffer and ATM. p53 is a known substrate of ATM. **e**, Coomassie staining showing the amounts of substrates. **f**, Autoradiograms showing Flag–ATM autophosphorylation (top) and phosphorylation of GST–NBS1 fusion proteins by Flag-ATM and Flag-ATM^{D2870A} immunoprecipitates (bottom). **g**, Coomassie staining. Arrowheads, GST fusion proteins; arrows, IgG.

To determine whether ATM can phosphorylate NBS1 *in vitro*, fragments of NBS1 expressed as glutathione *S*-transferase (GST) fusion proteins in *Escherichia coli* were used as substrates in kinase reactions (Fig. 2b) with either endogenous, recombinant Flag-tagged wild-type ATM or a kinase-inactive form of ATM, ATM^{D2870A} (Fig. 2c). Immunoprecipitated ATM was able to phosphorylate itself (Fig. 2d, top) and the GST–NBS1 fusion proteins tested. All phosphorylation occurred within the amino-terminal 396 residues of NBS1 (Fig. 2d, bottom panel).

ATM phosphorylates Ser 15 of p53 (refs 8, 9). Consistent with this result, GST–$p53^{1-106}$, but not GST–$p53^{S15A}$, was heavily phosphorylated by immunoprecipitated ATM in an *in vitro* kinase assay (Fig. 2d, lanes 2 and 3). Examination of the amino-acid sequences of NBS1 revealed several serine residues followed by glutamines (Q), which are preferred sites for phosphorylation in p53 and c-abl by ATM[8,9,22]. Alanine substitution of these potential phosphorylation sites within the NBS1 protein identified Ser 278 and Ser 343 as sites phosphorylated by ATM *in vitro* (Fig. 2d, lanes 11, 12, 17 and 18). The site(s) of ATM phosphorylation within amino-acid residues 1–153 of NBS1 is not known but does not appear to be Ser 53 or Ser 58 in the FHA domain, as substitution of these residues with alanine did not change the phosphorylation of GST–$NBS1^{1-153}$ significantly (data not shown).

To provide further evidence that ATM phosphorylates Ser 278 and Ser 343 of NBS1, human 293 cells were transfected with either Flag-tagged wild-type or mutant ATM complementary DNA, and the recombinant proteins were immunoprecipitated with anti-Flag antibody (Fig. 2c, f, top). As expected, wild-type ATM (Fig. 2f, bottom, odd lanes) but not ATM^{D2870A} (Fig. 2f, bottom, even lanes) in the anti-Flag immunoprecipitates could phosphorylate Ser 278 and Ser 343 of GST–NBS1 and Ser 15 of GST–p53.

To determine whether Ser 278 and Ser 343 of NBS1 are phosphorylated *in vivo*, NBS1-LBI, a T-antigen immortalized NBS cell line established from a patient carrying the common founder mutation 657del5 (ref. 23) in NBS1, was transfected with plasmids encoding wild-type NBS1 (pCMV-$NBS1^{wt}$); $NBS1^{S278A}$ (pCMV–$NBS1^{S278A}$), $NBS1^{S343A}$ (pCMV–$NBS1^{S343A}$) or $NBS1^{S278A/S343A}$ (pCMV–$NBS1^{S278A/S343A}$). As expected, NBS1 protein was not detectable by immunostaining of untransfected cells but was present in the nuclei of cells transfected with either wild-type or mutant NBS1 constructs (Fig. 3a). Expression of the 95K NBS1 protein was confirmed by immunoblotting of extracts from transfected cells (Fig. 3b). About 20% of the cells were transfected as quantified by immunostaining (data not shown). The protein levels of wild-type and $NBS1^{S343A}$ in the transfected cells are comparable (Fig. 3b, lanes 3–6), but $NBS1^{S278A/S343A}$ expression (Fig. 3b, lanes 9 and 10) was consistently higher than that of the other constructs. Upon treatment with ionizing radiation, the mobility of $NBS1^{wt}$, but not $NBS1^{S278A}$, $NBS1^{S343A}$ or $NBS1^{S278A/S343A}$, was altered (Fig. 3b, compare lanes 5 and 6 with lanes 3 and 4 and 7–10). These data indicate that Ser 278 and Ser 343 are phosphorylated *in vivo*.

Next we examined the effect of NBS1 phosphorylation on cell-cycle checkpoints activated by DNA damage. Both A-T and NBS cells display radioresistant DNA synthesis (RDS)[24]. RDS is likely to be comparable to the DNA damage- but not replication block-induced S-phase checkpoint. These two distinct checkpoint pathways have been found in various eukaryotes including fission and budding yeast, and mammals[2–5]. Plasmids encoding either wild-type or mutant NBS1 were co-transfected with an enhanced green fluorescent protein (EGFP) expression plasmid into the NBS1-LBI cells. 25-bromodeoxyuridine (BrdU) was added to cell cultures immediately after mock or ionizing radiation treatment. The ratio of BrdU-positive/EGFP-positive cells to EGFP-positive cells was determined in untreated and treated cells to assess the effect of phosphorylation of NBS1 on RDS. In comparison with wild-type NBS1, NBS1 mutants with one serine residue replaced with alanine were significantly less effective at inhibiting RDS, and an NBS1 mutant with the double alanine substitution was completely ineffective (Fig. 4a).

We examined the effect of NBS1 phosphorylation on cellular sensitivity to ionizing radiation by counting viable cells 72 h after 5 Gy γ-irradiation. Transfection of NBS1-LBI cells with pCMV–$NBS1^{wt}$ resulted in a significant reduction of cellular sensitivity to ionizing radiation compared with the control vector (Fig. 4b). The reduction in cellular sensitivity was abolished by mutation of both the Ser 278 and Ser 343 phosphorylation sites. Interestingly, the sensitivity of the pCMB-$NBS1^{S278A}$ and -$NBS1^{S343A}$ mutants to ionizing radiation was intermediate, indicating that both phosphorylation events contribute to cell sensitivity. Although stable protein complexes of Mre11/Rad50/NBS1 exist in untreated or ionizing

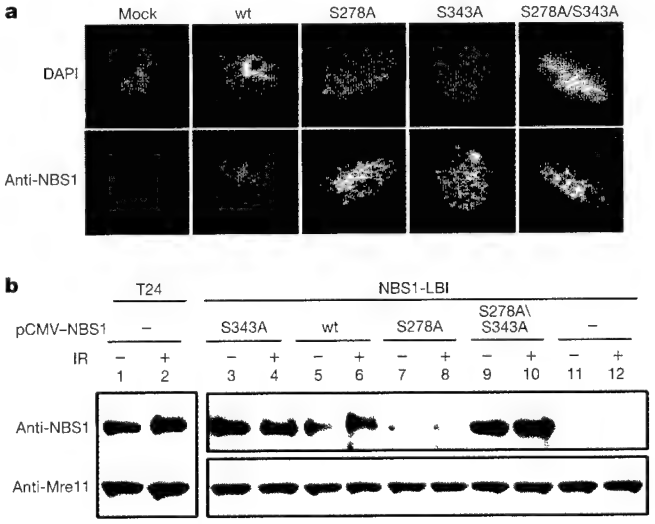

Figure 3 Expression of the full-length wild-type and NBS1 mutant proteins lacking phosphorylation site(s) in NBS1-LBI cells. **a**, Immunostaining of NBS1 proteins in mock or NBS1 expression-plasmid-transfected NBS1-LBI cells. Cells were immunostained with anti-NBS1 monoclonal antibody, MHN1, 36 h after transfection. **b**, Immunoblotting analysis of NBS1 protein in transfected cells. Cells were transfected with expression plasmids (10 μg DNA per 2×10^6 cells). Cell treatment is as described in Fig. 2a and cell lysate (100 μg protein) was analysed. Cell lysates from T24 cells were included as control. Longer exposure is shown to illustrate recombinant NBS1 expression in the transfected NBS1-LBI cells. Shorter exposures are shown for NBS1 and Mre11 in T24 cells, and Mre11 in NBS1-LBI cells.

radiation-treated cells[25], it has been reported that Mre11, Rad50, NBS1 and Brca1 all co-localize within nuclear foci induced only after treatment with ionizing radiation[4,26]. Because NBS1 is required for the formation of foci at DNA damage sites following ionizing radiation[4,27], we examined the role of NBS1 phosphorylation in foci formation. Consistent with previous studies[25], 26.6% of NBS1-LBI cells transfected with pCMV–NBS1^{WT} were foci-positive (Fig. 4c). In contrast, ionizing radiation did not induce foci formation in cells transfected with pCMV–NBS1$^{S278A/S343A}$ (6.0% foci-positive cells after ionizing radiation, 5.4% foci-positive cells in untreated cells). Similar to the result of the ionizing radiation sensitivity assays, inactivation of either serine phosphorylation site partially restored the ability of NBS1 to form foci in response to ionizing radiation. Our results indicate that phosphorylation of Ser 278 and Ser 343 in NBS1 contributes to both cellular resistance to ionizing radiation and formation of foci that contain NBS1 in response to ionizing radiation.

An enhanced interaction between ATM and NBS1 upon DNA damage was seen using different antibodies in the co-immunoprecipitation experiments. However, we did not detect increased co-fractionation of ATM and NBS1 upon DNA damage using gel-filtration chromatography (data not shown). It is unclear whether this is due to the transient nature of the enhanced interaction or whether the increase in complexed ATM and NBS1 is the result of conformational changes induced in the protein complex upon DNA damage. We have mapped two residues of NBS1, Ser 278 and Ser 343, which are phosphorylated by ATM. Inactivation of these phosphorylation sites abolishes NBS1 function in DNA damage-activated cell-cycle checkpoints and DNA repair. Phosphorylation of NBS1 by ATM may be required for signal transduction to downstream effectors of DNA damage-induced S-checkpoint activation, such as Chk1 and Chk2 (refs 8–11). We speculate that phosphorylation of NBS1 is also critical for the assembly of repair proteins at the sites of DNA damage. This is supported by the observation that inactivation of the Ser 278 and Ser 343 phosphorylation sites in NBS1 abolished the formation of Mre11/Rad50/NBS1 foci upon treatment with ionizing radiation. The functional interaction between ATM and NBS1 provides a molecular explanation for similar defects in cell-cycle checkpoints and DNA repair exhibited by NBS and A-T cells. Moreover, these studies provide new insights into the complex relationship between DNA damage-activated cell-cycle checkpoints and DNA repair mechanisms that are involved in the cellular response to DNA double-strand breaks. □

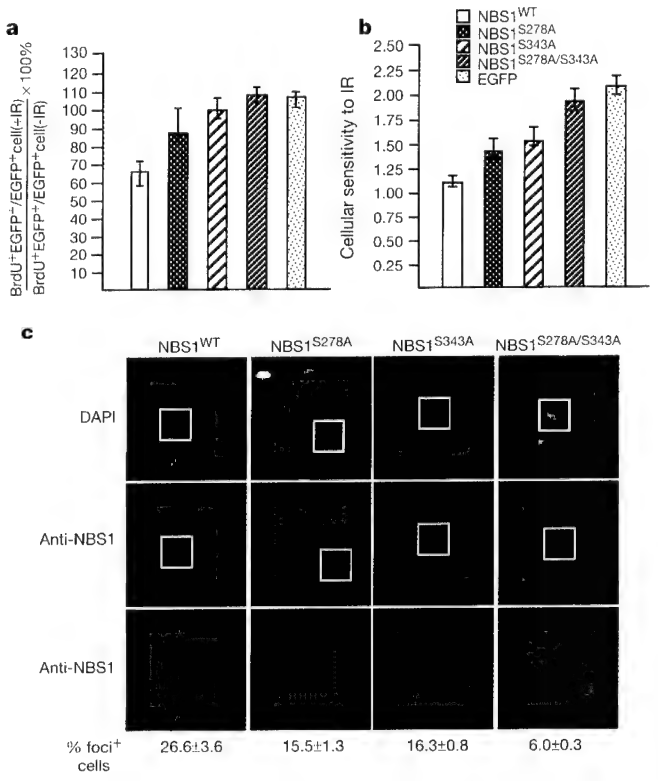

Figure 4 Radioresistant DNA synthesis (RDS) and sensitivity to ionizing radiation by expression of wild-type and NBS1 mutants lacking serine phosphorylation site(s). **a**, RDS. The ratio of BrdU- and EGFP-double positive cells to EGFP-positive cells is determined in untreated and IR-treated cells, respectively. Bar represents the ratio of the IR-treated cells divided by that in the untreated cells multiplied by 100 (>200 fluorescent cells counted per experiment). The mean and s.d. of three experiments is shown. **b**, Cellular sensitivity to IR. Cellular sensitivity to γ-irradiation (5 Gy) was calculated by dividing the number of cells recovered from mock treated cells by the number of cells recovered from the IR-treated cells 72 h after treatment. The mock treated cells have a cellular sensitivity of 1 (>1,000 transfected cells counted per experiment). The mean and s.d. of three experiments is shown. **c**, Formation of IR-induced NBS1 foci in the transfected cells. Three hours after IR (15 Gy), cells were stained with anti-NBS1 monoclonal antibody, MHN1, followed by rhodamine-conjugated anti-mouse antibody. Staining with 4′,6′-diamidino-2-phenylindole (DAPI) identifies nuclei (blue). Bottom, ×500 original magnification; top two panels, ~×31. Percentages of transfected cells with foci are shown. Similar results were obtained with anti-Mre11 antibody.

Methods

Immunoblotting and immunoprecipitation

Cells were lysed in EBC buffer supplemented with protease inhibitors (10 μg ml^{-1} aprotinin, 50 μg ml^{-1} leupeptin, 1 mM phenylmethylsulphonyl fluoride, 100 mM NaF and 1 mM Na_3VO_4). We determined protein concentration by Bradford assay (Biorad). Cell lysates containing 20–100 μg protein were mixed with SDS sample buffer before separation by SDS–7.5% polyacrylamide gel. Proteins were transferred to Immobilon P (Millipore) or nitrocellulose membrane (Schleicher and Schuell). Anti-NBS1 monoclonal antibodies were generated from mice immunized with GST–NBS1$^{363-754}$. Anti-Mre11 antibodies were generated from mice immunized with purified full-length Mre11 expressed in Sf9 insect cells. For co-immunoprecipitation, we incubated protein lysate (2–3 mg) with primary antibodies overnight at 4 °C as described[17] except that we used secondary antibodies cross-linked to magnetic beads (Dynal).

Phosphatase treatment

Cell lysates containing 1 mg of protein from untreated and ionizing radiation-treated human lymphoblast NAT10 cells were incubated with anti-NBS1 antibody. Immunoprecipitates were washed with EBC buffer and were resuspended in λ phosphatase buffer (New England Biolab) with or without 10 mM phosphatase inhibitor, β-sodium glycerol phosphate.

Kinase assay

ATM was immunoprecipitated from non-irradiated or irradiated HeLa cells and used in kinase assays as described[28]. GST fusion proteins (2–10 μg) were added to the ATM–protein G sepharose beads and the kinase reaction was carried out in 20 μl reaction volume containing kinase buffer and 10 μCi of γ^{32}P-ATP. Recombinant ATM was immunoprecipitated from transfected 293 cells 24 h after transfection using anti-Flag M2 antibody (Kodak).

Plasmid construction

Full-length NBS1 cDNA and the cDNA fragment encoding amino acids 343–754 were generated by polymerase chain reaction with reverse transcription (RT-PCR) using RNA isolated from human Raji cells. The full-length NBS1 cDNA was cloned into a pCMV vector. Site-specific mutagenesis was performed using a QuickChange site-directed mutagenesis kit (Stratagene) and was confirmed by DNA sequencing. To construct the pCMV–Flag–ATM expression vector, a 9.2-kilobase (kb) *Sal*I–*Xho*I fragment containing full-length ATM cDNA tagged with a Flag epitope and a His_6 sequence was excised from pFB-YZ5 (ref. 19) and subcloned into a *Xho*I-linearized pCMV vector. Site-specific mutagenesis was performed as described above using a 1.6-kb fragment of the ATM open reading frame as the template. GST–NBS1 and GST–P53 fusion proteins were generated by PCR using full-length cDNAs as templates. The PCR product was cloned into pGEX-4T-3 vector (Pharmacia).

Cell culture and transfection

Primary NBS fibroblasts from Coriell Institute were immortalized with telomerase. The NBS fibroblast cell line NBS1-LBI has been described[24]. Other cell lines were from the American Type Culture Collection. Cells were cultured in Dulbecco's Modified Eagle medium supplemented with 10% fetal bovine serum (Gibco). Human bladder carcinoma T24 cells were synchronized by density arrest. Cells at various cell cycle stages were

collected as described[29]. Cells were irradiated using a ^{137}Cs γ-irradiator at 2.55 Gy per min (Shepherd). Ultraviolet irradiation was performed using UV Stratalinker 2400 (Stratagene). Hydroxyurea (Sigma) was used at 1 mM. Cell lysates were prepared 1 h after treatment with ionizing radiation or ultraviolet unless otherwise specified and after 24 h of hydroxyurea treatment. Transfection was performed using Lipofectamine (Gibco) according to the manufacturer's instructions.

Radioresistant DNA synthesis

NBS1 expression plasmids were co-transfected with pEGFP-N1 (Clontech) in a ratio of 10:1 into the NBS1-LBI cells. Cells were treated with 15 Gy γ-irradiation and immediately incubated in medium containing BrdU for 2 h. We detected BrdU incorporation into DNA using a monoclonal antibody specific for BrdU (Becton-Dickinson) following the immunostaining procedures described below.

Sensitivity to ionizing radiation

Plasmids containing NBS1 cDNA were co-transfected with pEGFP-N1 at a ratio of 10:1 into the NBS1-LBI cells. Cells were treated with 5 Gy γ-irradiation 36 h after transfection. The viable GFP positive cells within 2.9 cm^2 were counted at 72 h after ionizing radiation.

Immunohistochemistry

Immunostaining was carried out as described[17]. Rhodamine-conjugated second antibody was obtained from Jackson Research Laboratories. Slides were mounted in Lipshaw mountant (Immunon) and staining was analysed with a Zeiss AXIOPHOT fluorescence microscope. Images were processed using the software program Adobe Photoshop 5.0.

Received 22 November 1999; accepted 27 March 2000.

1. Shiloh, Y. Ataxia-telangiectasia and the Nijmegen breakage syndrome: related disorders but genes apart. *Annu. Rev. Genet.* **31,** 635–662 (1997).
2. Gatti, R. A. *et al.* Localization of an ataxia-telangiectasia gene to chromosome 11q22–23. *Nature* **336,** 577–580 (1988).
3. Savitsky, K. *et al.* The complete sequence of the coding region of the ATM gene reveals similarity to cell cycle regulators in different species. *Hum. Mol. Genet.* **4,** 2025–2032 (1995).
4. Carney, J. P. *et al.* The hMre11/hRad50 protein complex and Nijmegen breakage syndrome: linkage of double-strand break repair to the cellular DNA damage response. *Cell* **93,** 477–486 (1998).
5. Varon, R. *et al.* Nibrin, a novel DNA double-strand break repair protein, is mutated in Nijmegen breakage syndrome. *Cell* **93,** 467–476 (1998).
6. Trujillo, K. M., Yuan, S. S., Lee, E. Y. & Sung, P. Nuclease activities in a complex of human recombination and DNA repair factors Rad50, Mre11, and p95. *J. Biol. Chem.* **273,** 21447–21450 (1998).
7. Paull, T. T. & Gellert, M. Nbs1 potentiates ATP-driven DNA unwinding and endonuclease cleavage by the Mre11/Rad50 complex. *Genes Dev.* **13,** 1276–1288 (1999).
8. Elledge, S. J. Cell cycle checkpoints: preventing an identity crisis. *Science* **274,** 1664–1672 (1996).
9. Weinert, T. DNA damage and checkpoint pathways: molecular anatomy and interactions with repair. *Cell* **94,** 555–558 (1998).
10. Caspari, T. & Carr, A. M. DNA structure checkpoint pathways in *Schizosaccharomyces pombe*. *Biochimie* **81,** 173–181 (1999).
11. Dasika, G. K. *et al.* DNA damage-induced cell cycle checkpoints and DNA strand break repair in development and tumorigenesis. *Oncogene* **18,** 7883–7899 (1999).
12. Banin, S. *et al.* Enhanced phosphorylation of p53 by ATM in response to DNA damage. *Science* **281,** 1674–1677 (1998).
13. Canman, C. E. *et al.* Activation of the ATM kinase by ionizing radiation and phosphorylation of p53. *Science* **281,** 1677–1679 (1998).
14. Cortez, D., Wang, Y., Qin, J. & Elledge, S. J. Requirement of ATM-dependent phosphorylation of brca1 in the DNA damage response to double-strand breaks. *Science* **286,** 1162–1166 (1999).
15. Matsuoka, S., Huang, M. & Elledge, S. J. Linkage of ATM to cell cycle regulation by the Chk2 protein kinase. *Science* **282,** 1893–1897 (1998).
16. Yuan, Z. M. *et al.* Regulation of Rad51 function by c-Abl in response to DNA damage. *J. Biol. Chem.* **273,** 3799–3802 (1998).
17. Chen, G. *et al.* Radiation-induced assembly of Rad51 and Rad52 recombination complex requires ATM and c-Abl. *J. Biol. Chem.* **274,** 12748–12752 (1999).
18. Haber, J. E. The many interfaces of Mre11. *Cell* **95,** 583–586 (1998).
19. Ziv, Y. *et al.* Recombinant ATM protein complements the cellular A-T phenotype. *Oncogene* **15,** 159–167 (1998).
20. Canman, C. E., Wolff, A. C., Chen, C. Y., Fornace, A. J. Jr & Kastan, M. B. The p53-dependent G1 cell cycle checkpoint pathway and ataxia-telangiectasia. *Cancer Res.* **54,** 5054–5058 (1994).
21. Tibbetts, R. S. *et al.* A role for ATR in the DNA damage-induced phosphorylation of p53. *Genes Dev.* **13,** 152–157 (1999).
22. Baskaran, R. *et al.* Ataxia telangiectasia mutant protein activates c-Abl tyrosine kinase in response to ionizing radiation. *Nature* **387,** 516–519 (1997).
23. Kraakman-van der Zwet, M. *et al.* Immortalization and characterization of Nijmegen Breakage syndrome fibroblasts. *Mutat. Res.* **434,** 17–27 (1999).
24. Young, B. R. & Painter, R. B. Radioresistant DNA synthesis and human genetic diseases. *Hum. Genet.* **82,** 113–117 (1989).
25. Maser, R. S., Monsen, K. J., Nelms, B. E. & Petrini, J. H. hMre11 and hRad50 nuclear foci are induced during the normal cellular response to DNA double-strand breaks. *Mol. Cell. Biol.* **17,** 6087–6096 (1997).
26. Zhong, Q. *et al.* Association of BRCA1 with the hRad50-hMre11-p95 complex and the DNA damage response. *Science* **285,** 747–750 (1999).
27. Nelms, B. E., Maser, R. S., MacKay, J. E., Lagally, M. G. & Petrini, J. H. *In situ* visualization of DNA double-strand break repair in human fibroblasts. *Science* **280,** 590–592 (1998).
28. Ziv, Y., Banin, S., Lim, D.-S., Kastan, M. B. & Shiloh, Y. in *Expression and Assay of Recombinant ATM Kinase* (ed. Keyse, S.) (Humana, New Jersey, 1999).
29. Chen, P. L., Scully, P., Shew, J. Y., Wang, J. Y. & Lee, W. H. Phosphorylation of the retinoblastoma gene product is modulated during the cell cycle and cellular differentiation. *Cell* **58,** 1193–1198 (1989).

Acknowledgements

We thank W.-H. Lee, A. Tomkinson and members of their laboratories for discussion; A. Tomkinson, T. Boyer and P. Sung for critical reading; S.-Y. Lee for assistance on the manuscript; M. Chen for site-specific mutagenesis of ATM; Q. Du for the initial studies of ATM kinase; L. Zheng for technical advice; and S. Deb for the full-length human p53 cDNA. E.L. is supported by grants from NIH NINDS, Texas Advanced Research/Advanced Technology Program and NCI P01. S.Z. is supported by a DOD training grant.

Correspondence and requests for materials should be addressed to E.L. (e-mail: leee@uthscsa.edu).

Oncogene (2001) 20, 7073–7084

www.nature.com/onc

The proliferative and apoptotic activities of E2F1 in the mouse retina

Suh-Chin J Lin[1], Stephen X Skapek[2], David S Papermaster[3], Mark Hankin[4] and Eva Y-HP Lee*,[1]

[1]*Department of Molecular Medicine/Institute of Biotechnology, University of Texas Health Science Center at San Antonio, Texas, TX 78245-3207, USA;* [2]*Department of Hematology/Oncology, St. Jude Children's Research Hospital, Memphis, Tennessee, TN 38105, USA;* [3]*Department of Neuroscience, University of Connecticut Health Science Center, Farmington, Connecticut, CT 06030-3401, USA;* [4]*Department of Anatomy and Neurobiology, Medical College of Ohio, Toledo, Ohio, OH 43614, USA*

The E2F1 transcription factor controls cell proliferation and apoptosis. E2F1 activity is negatively regulated by the retinoblastoma (RB) protein. To study how inactivation of *Rb* and dysregulated E2F1 affects the developing retina, we analysed wild-type and *Rb*$^{-/-}$ embryonic retinas and retinal transplants and we established transgenic mice expressing human E2F1 in retinal photoreceptor cells under the regulation of the IRBP promoter (TgIRBPE2F1). A marked increase in cell proliferation and apoptosis was observed in the retinas of *Rb*$^{-/-}$ mice and *TgIRBPE2F1* transgenic mice. In the transgenic mice, photoreceptor cells formed rosette-like arrangements at postnatal days 9 through 28. Complete loss of photoreceptors followed in the *TgIRBPE2F1* mice but not in the *Rb*$^{-/-}$ retinal transplants. Both RB-deficient and E2F1-overexpressing photoreceptor cells expressed rhodopsin, a marker of terminal differentiation. Loss of *p53* partially reduced the apoptosis and resulted in transient hyperplasia of multiple cell types in the *TgIRBPE2F1* retinas at postnatal day 6. Our findings support the concept that cross-talk occurs between different retinal cell types and that multiple genetic pathways must become dysregulated for the full oncogenic transformation of neuronal retinal cells. *Oncogene* (2001) **20,** 7073–7084.

Keywords: E2F1; p53; RB and retinoblastoma

Introduction

The E2F transcription factor was initially identified as a cellular DNA-binding activity required for the adenovirus E1A-mediated activation of the viral E2 gene (reviewed in Dyson, 1998). E2F functions as a heterodimer consisting of an E2F family member, E2F1 through 6, and a DP protein, DP1 and DP2 (reviewed in Dyson, 1998). E2F can bind to specific regulatory elements in genes required for DNA synthesis including DNA polymerase α, thymidine kinase and dihydrofolate reductase; and cell cycle regulators including cyclin A, cyclin E and cdc2 (Adams and Kaelin, 1995; Slansky and Farnham, 1996). Genetic studies in both *Drosophila* (Duronio *et al.*, 1995) and mammalian cells (Ishizaki *et al.*, 1996; Wu *et al.*, 1996) demonstrate that E2F activity is required for cell proliferation. In addition, overexpression of E2F1 has been shown to be sufficient to drive quiescent cells into S phase *in vitro* (Johnson *et al.*, 1993). E2F1 cooperates with activated Ras to transform fibroblasts (Johnson *et al.*, 1994; Singh *et al.*, 1994; Xu *et al.*, 1995). In mice, expression of E2F1 in the presence of activated Ras results in skin tumor formation (Pierce *et al.*, 1998a). Interestingly, in addition to its role in cell proliferation, overexpression of E2F1 but not other E2F proteins also triggers apoptosis in cells. In the absence of p53, E2F1-induced apoptosis is significantly reduced (DeGregori *et al.*, 1997; Kowalik *et al.*, 1995; Qin *et al.*, 1994; Shan and Lee, 1994; Wu and Levine, 1994). This apoptosis-promoting property of E2F1 likely contributes to the phenotype of E2F1 deficient mice, which are defective in thymocyte apoptosis and predisposed to tumors at an advanced age (Field *et al.*, 1996; Yamasaki *et al.*, 1996).

An understanding of how E2F activity may be regulated in mammalian cells first came from the findings of a functional interaction between E2F1 and the protein product of the retinoblastoma susceptibility gene *Rb* (reviewed in Dyson, 1998). RB may block the transcriptional activity of E2F1 by direct binding to its transactivation domain and preventing its interaction with other components of the transcriptional machinery (Ross *et al.*, 1999). In addition, the presence of histone deacetylases in the E2F/RB complexes could result in transcription repression by a mechanism involving chromatin regulation (Brehm and Kouzarides, 1999). Finally, other RB-interacting proteins have been identified that could mediate transcriptional repression of E2F-dependent genes (Skapek *et al.*, 2000). The physical interaction between RB and E2F is detected during the G_1 phase of the cell cycle. Upon phosphorylation of RB by cyclin-dependent kinases, RB, E2F, and other proteins found in this complex (like HDAC-1) dissociate to allow the activation of the E2F responsive genes (reviewed in Dyson, 1998; Zhang *et al.*, 1999).

Two *Rb*-related genes *p107* and *p130* have also been characterized (reviewed in Mulligan and Jacks, 1998).

*Correspondence: EY-HP Lee; E-mail: Leee@uthscsa.edu
Received 11 August 2000; revised 23 August 2001; accepted 23 August 2001

Protein products of both genes interact with E2F and can act as negative regulators of cell proliferation. Unlike *Rb*, however, mutations of *p107* and *p130* are rarely found in human tumors and mutation of either *p107* or *p130* in mice leads to different phenotypes (reviewed in Lin *et al*., 1996; Mulligan and Jacks, 1998). The different biological functions of different RB family members may be due to their association with specific E2Fs (reviewed in Dyson, 1998; Nevins, 1998). RB interacts with E2F1, E2F2 and E2F3 during late G_1 to S phase. In contrast, p107 preferentially interacts with E2F4 in proliferating cells during S phase whereas p130 binds to E2F4 and E2F5 primarily in G_0 phase. Despite these distinctions, recent studies of mice lacking more than one member of the *Rb* gene family have provided evidence that Rb, p107 and p130 have overlapping as well as distinct function (see below).

That the loss of *Rb* causes retinoblastoma in humans has been well established. On the other hand, how loss of *Rb* affects the retina in mouse models is more confusing. Homozygous $Rb^{-/-}$ mouse embryos show ectopic proliferation and excess apoptosis of the nervous system and die around embryonic day 14.5 (E14.5) (Clarke *et al*., 1992; Jacks *et al*., 1992; Lee *et al*., 1992). Heterozygous $Rb^{+/-}$ mice develop pituitary and thyroid tumors (Hu *et al*., 1994; Jacks *et al*., 1992; Nikitin and Lee, 1996) and all tumors harbor mutations of the wild-type *Rb* allele (Hu *et al*., 1994; Nikitin and Lee, 1996); however, retinoblastoma does not occur. In contrast, multiple dysplastic lesions develop in the photoreceptor cell layer of the retina of $Rb^{+/-}$;*p107*$^{-/-}$ mice but not in $Rb^{+/-}$ or *p107*$^{-/-}$ mice (Lee *et al*., 1996). Retinoblastomas of amacrine cell origin were observed in chimeric mice harboring $Rb^{-/-}$;*p107*$^{-/-}$ cells (Robanus-Maandag *et al*., 1998). Thus, it seems that dysfunction of both RB and p107 are required for retinal tumor formation in mice.

One interpretation of these collective data is that loss of RB and RB-related proteins releases certain E2Fs from suppression to enhance cell proliferation and tumor formation. Consistent with this, inactivation of E2F1 reduces tumorigenesis in $Rb^{+/-}$ mice and extends the survival of $Rb^{+/-}$ mice and $Rb^{-/-}$ embryos (Tsai *et al*., 1998; Yamasaki *et al*., 1998). Furthermore, E2F1 deficiency rescues cell death in *Rb*$^{-/-}$ embryos in tissues undergoing p53-dependent apoptosis (Macleod *et al*., 1996; Morgenbesser *et al*., 1994) including the ocular lens and the central nervous system (Tsai *et al*., 1998). Taken together, these data provide biochemical and genetic support for the regulatory role of RB on E2F1 activities.

We undertook the present series of experiments to study the effects of dysregulated E2F1 activity in photoreceptors. We accomplished this by studying RB-deficient photoreceptors in *Rb*$^{-/-}$ mouse embryos and following transplantation of $Rb^{-/-}$ retinal cells into normal recipient mice. In addition, we have established a transgenic mouse model in which E2F1 is constitutively expressed in maturing photoreceptors. We have used these studies to further understand how loss of regulation of E2F1 and loss of the p53 tumor suppressor contribute, individually or in combination, to photoreceptor development and tumor formation.

Results

Proliferation and apoptosis in Rb-*deficient retinas*

There is aberrant proliferation and extensive apoptosis in the developing nervous system of RB-deficient embryos (Lee *et al*., 1994; Macleod *et al*., 1996). How RB deficiency affects retinal development is not known, in part due to embryonic lethality of $Rb^{-/-}$ mice around E12.5–E14.5 (Lee *et al*., 1992). To begin to study the effects of loss of RB in the retina, we analysed retinal cell proliferation and apoptosis in retinas from E13.5 wild-type and $Rb^{-/-}$ embryos. In normal embryos, the inner layers of the retinal ventricular cells did not incorporate BrdU at E13.5 (Figure 1Aa). In contrast, in $Rb^{-/-}$ embryos, many cells in the same region continued to enter the cell cycle (Figure 1Ab). In wild-type embryos, little TUNEL staining was observed in the normal E13.5 retina (Figure 1Ac), but TUNEL-stained cells were readily detected in $Rb^{-/-}$ retina (Figure 1Ad). Examination of cell proliferation and apoptosis at different embryonic stages (E11.5–E15.5) demonstrated that ectopic BrdU-positive cells appeared in the retina before TUNEL-stained cells (data not shown), a finding that is similar to findings in the spinal cord and dorsal root ganglia of $Rb^{-/-}$ embryos (Lee *et al*., 1994). These data indicate that RB loss causes excessive ectopic cell proliferation and apoptosis in embryonic retinal progenitor layers of the mouse retina.

In addition to regulating cell proliferation and apoptosis, RB is known to facilitate the differentiation of certain types of cells (reviewed in Lipinski and Jacks, 1999). Therefore, we sought to determine how loss of RB affected the differentiation of murine photoreceptors. In wild-type mice, retina development continues after birth. Because loss of RB causes embryonic lethality, to fully address the effect of RB-deficiency on retinal development, we analysed retinal tissue that had been transplanted into normal neonatal mice. It has previously been shown that transplanted embryonic retinal tissue continues to develop and form laminar structures (Hankin *et al*., 1993). Following transplantation of retinas from E11.5–E12.5 embryos into wild-type or $Rb^{+/-}$ neonates, the transplanted retinal tissues formed either sheet-like structures or rosette structures characterized by inside-out, concentric foldings of the donor tissue (Figure 1B). The multi-layered structures were evident in both wild-type and *Rb*-deficient retinal transplants (Figure 1Ba,b). At the cellular level, both wild-type and $Rb^{-/-}$ retinoblasts matured and differentiated into photoreceptors as evidenced by expression of opsin (Figure 1Be,f). Interestingly, using this model of retina development, we confirmed that RB loss causes excess apoptosis. Whereas only a few apoptotic cells were seen in wild-

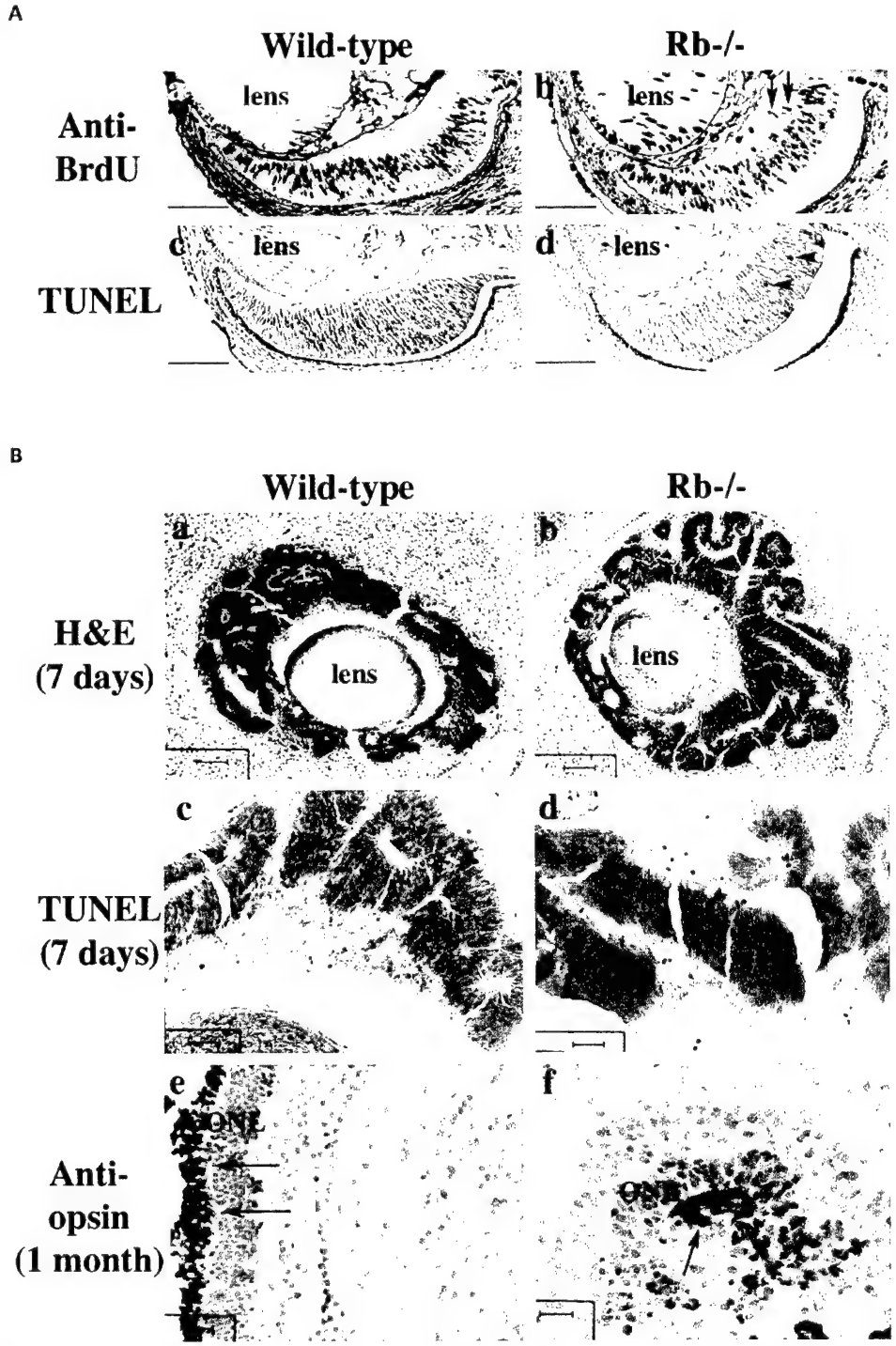

Figure 1 Effects of RB deficiency on proliferation, apoptosis and differentiation of retinal cells. (**A**) Enhanced cell proliferation and cell death in the retina of $Rb^{-/-}$ embryos. Pregnant mice were injected with BrdU. BrdU uptake in the retinas of E13.5 embryos was compared (**a** and **b**). Apoptotic cells were shown using TUNEL assay (**c** and **d**). Arrows indicate ectopic BrdU-positive cells and arrowheads indicate apoptotic cells. Scale bar, 100 μm. (**B**) Cell death and differentiation in the photoreceptor cells of retinal transplants. Retinal tissues of E11.5–12.5 embryos were transplanted intracranially into neonatal $Rb^{+/-}$ or wild-type mice. Sections of retinal transplants were stained with H&E (**a** and **b**), analysed for apoptosis using the TUNEL assay (**c** and **d**), or immunostained with anti-opsin antibodies (**e** and **f**). Arrowheads indicate apoptotic nuclei; arrows indicate opsin expression in the inner/outer segments of the photoreceptor cells. ONL, outer nuclear layer. Scale bar, (**a**,**b**) 100 μm, (**c**,**d**) 40 μm, (**e**,**f**) 15.6 μm. Left panel, wild-type embryos; right panel, $Rb^{-/-}$ embryos

type transplants, abundant apoptotic cells were found in $Rb^{-/-}$ transplants (Figure 1Bc,d). Taken together, these results demonstrate that RB may be required for efficient cell cycle arrest and prevention of apoptosis in

cells in the developing mouse retina, but is not required for the expression of opsin in photoreceptors.

Generation of TgIRBPE2F1 *transgenic mice*

Because the loss of RB appears to alter retinal development in these mouse transplant experiments, and RB is known to regulate E2F1, we established a transgenic mouse model to study the effect of enhanced expression of E2F1 in retinas *in vivo*. To do this, we generated transgenic mice expressing human E2F1 (hE2F1) cDNA under the regulation of IRBP promoter (*TgIRBPE2F1* mice). This promoter directs the expression of the transgene in retinal photoreceptor cells and pinealocytes (Liou *et al*., 1990). Several founder mice were identified using PCR and Southern analyses (data not shown) and two hE2F1 transgenic lines (IRBP-E37 and -E45) were established.

To confirm that the transgene led to ectopic expression of E2F1, we performed immunohistochemical analyses. In normal mice, E2F1 was detectable in the retina of E18.5 embryos (data not shown), but was not detectable after birth (Figure 2A). In the retina of transgenic mice, hE2F1 was expressed in the outer ventricular cell layer, the developing rods, from P0 (day of birth) through P6 (Figure 2A). The hE2F1 was also present in mature photoreceptor cells at later stages (data not shown). All offspring from both lines had similar expression patterns and developed the same phenotype (see below).

Developing neuroretinal cells in TgIRBPE2F1 *transgenic mice continue to synthesize DNA*

During retinal development, the ventricular cells cease proliferation at P6 in the central region and at P11 in the peripheral region of the retina (Young, 1985). The development of post-mitotic cells parallels morphological changes in the developing outer nuclear layer (ONL) of photoreceptors. Active proliferation, as evidenced by BrdU incorporation, was seen throughout the retina of the wild-type mice from P0 to P4 (Figure 2B,C). During this period, there were more BrdU-positive cells in the retina of transgenic mice than in the control retina (Figure 2B,C). By P6, BrdU stained cells were restricted to the peripheral retina in wild-type mice, whereas BrdU-positive cells were detected in the central as well as the peripheral retina in the transgenic mice at P6 (Figure 2B). These data demonstrate that forced expression of E2F1 *in vivo* is sufficient to drive DNA synthesis in the developing retina that should have been filled with post-mitotic photoreceptors. Interestingly, the ectopic BrdU-positive cells in the transgenic mice were different from BrdU-positive cells in the normal mice in two regards. First, they were located near the pigment epithelium (PE) in transgenic mice (Figure 2Bb,d) as opposed to the inner plexiform layer (IPL) in wild-type mice (Figure 2Ba,c). Second, their nuclei were more rounded than the BrdU-positive cells in wild-type mice (data not shown). Their location and nuclear shape suggest that they are differentiating photoreceptors that normally would have excited the cell cycle.

Apoptosis of the neuroretinal cells in TgIRBPE2F1 *transgenic mice*

Despite the increased proliferation observed in retinas from *TgIRBPE2F1* mice, there were fewer photoreceptor cells in the retinas in adult transgenic mice (Figure 5f, discussed below). The decreased number of photoreceptor cells in the retina of the transgenic mice suggests that overexpression of E2F1 may also result in cell death. To better characterize the mechanism by which the photoreceptors were lost, the degree of apoptosis was determined during the early stages of retinal development. In retinas from wild-type mice, apoptotic cells were only occasionally observed during the major period of retinal differentiation (Figure 3A,B; Young, 1984). By contrast, abundant apoptotic cells were found throughout the ventricular layer at all stages in the transgenic mice with greatest apoptosis at P4 and P6 (Figure 3A,B). At later stages, fewer apoptotic cells were seen perhaps in part due to the previous loss of cells in the ONL in the transgenic retinas (Figure 3A). The location of most of the apoptotic cells in the ONL indicates that the dying cells are, in fact, developing photoreceptors.

During normal development, the arrest of cellular proliferation and the initiation of differentiation proceeds from the central to the peripheral retina (Young, 1985). Therefore, we sought to correlate the time course of proliferation and apoptosis with this developmental feature. Proliferation in the central retina was most robust at P0, gradually decreased after birth and ceased at P9 in transgenic mice (Figure 2C). Interestingly, there were more apoptotic cells in the central region compared to the peripheral region in transgenic retinas earlier in postnatal development (Figure 3B), whereas at P9 and P10 there were more apoptotic cells in the periphery (Figure 3A,B). Hence, it appears that the excess cell proliferation caused by E2F1 precedes excess apoptosis and that the apoptosis appears to occur in a developmentally regulated pattern.

Delayed differentiation in the neuroretinal cells in TgIRBPE2F1 *transgenic mice*

During retinal development, multiple cell types are generated and arranged into morphologically distinct layers. To assess the effect of E2F1 expression on development of the multi-layer structure of retina, retina sections of P4–P6 were compared (Figure 4). At P6 the outer plexiform layer (OPL), which is composed of synaptic processes between photoreceptor cells in the ONL and cells in the inner nuclear layer (INL), was evident in the control mice (Figure 4a), but was not apparent in transgenic mice (Figure 4b). However, the OPL was visible at P8 and later stages in transgenic retinas (Figure 3Af,h) when the cells of the ONL were better differentiated. This finding suggests that ectopic

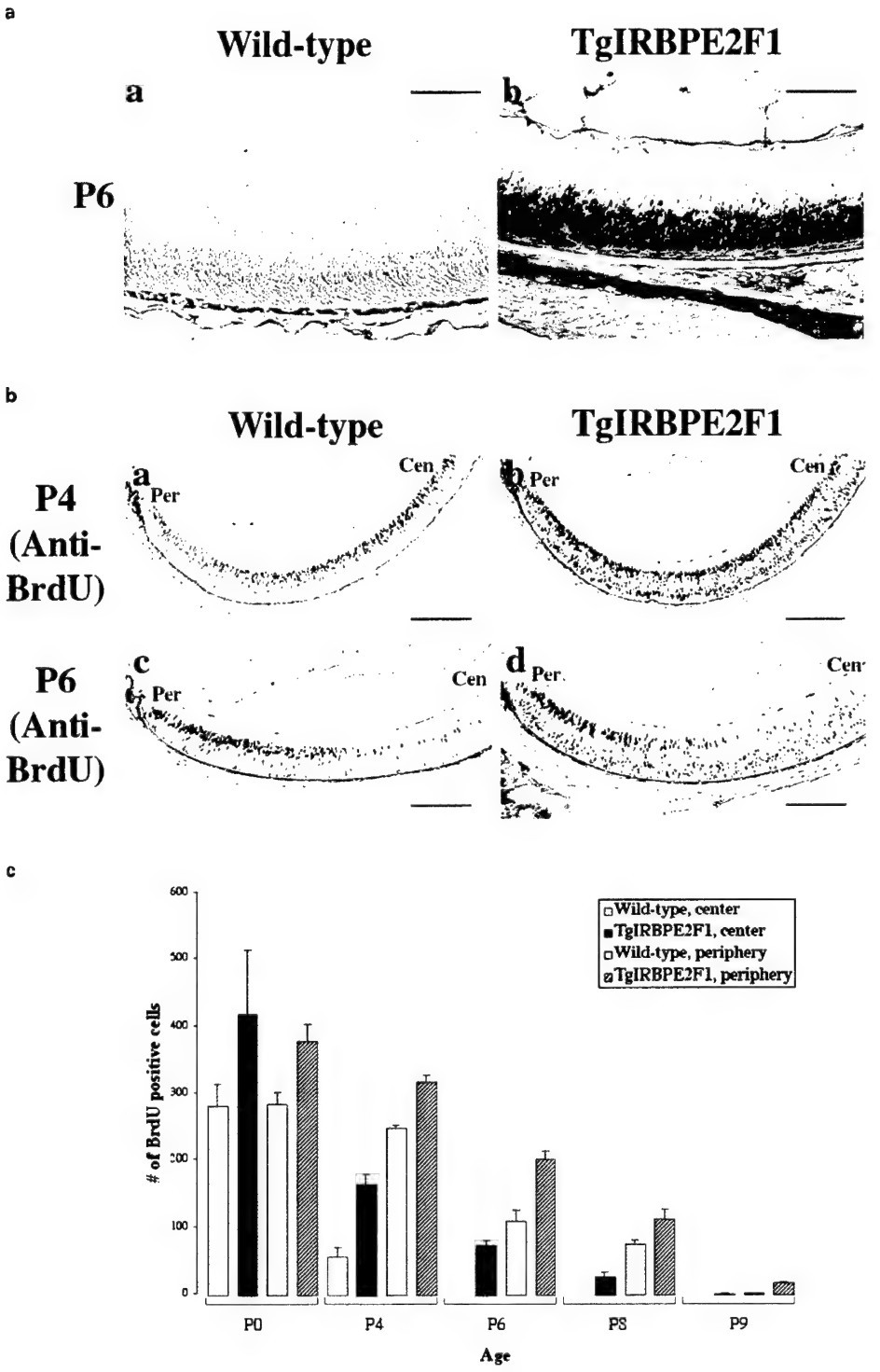

Figure 2 Ectopic E2F1 expression enhances retinal cell proliferation. (**a**) E2F1 expression in the retinas. E2F1 immunostaining was performed on retinal sections of wild-type (left) and *TgIRBPE2F1* retinas (right) of 6-day-old (P6) neonates using anti-E2F1 antibodies. Scale bar, 100 μm. (**B**) BrdU uptake in P4 (**a**,**b**) and P6 (**c**,**d**) retinas of wild-type (left panels) and *TgIRBPE2F1* (right panels) mice. Cen, central retina; Per, peripheral retina; G, Ganglion cell layer; IPL, inner plexiform layer; PE, pigment epithelium. Scale bar, 200 μm. (C) Quantitative comparison of BrdU-positive cells in wild-type and *TgIRBPE2F1* retinas of different ages (P0–P9). BrdU-positive nuclei within a length of 250 μm to optical nerve (center) and to ciliary body (periphery) were counted. The mean $\pm$ s.e. is based on data collected from at least three mice

expression of E2F1 may delay certain aspects of retinal development.

We next sought to determine how ectopic expression of E2F1 altered the differentiation of individual

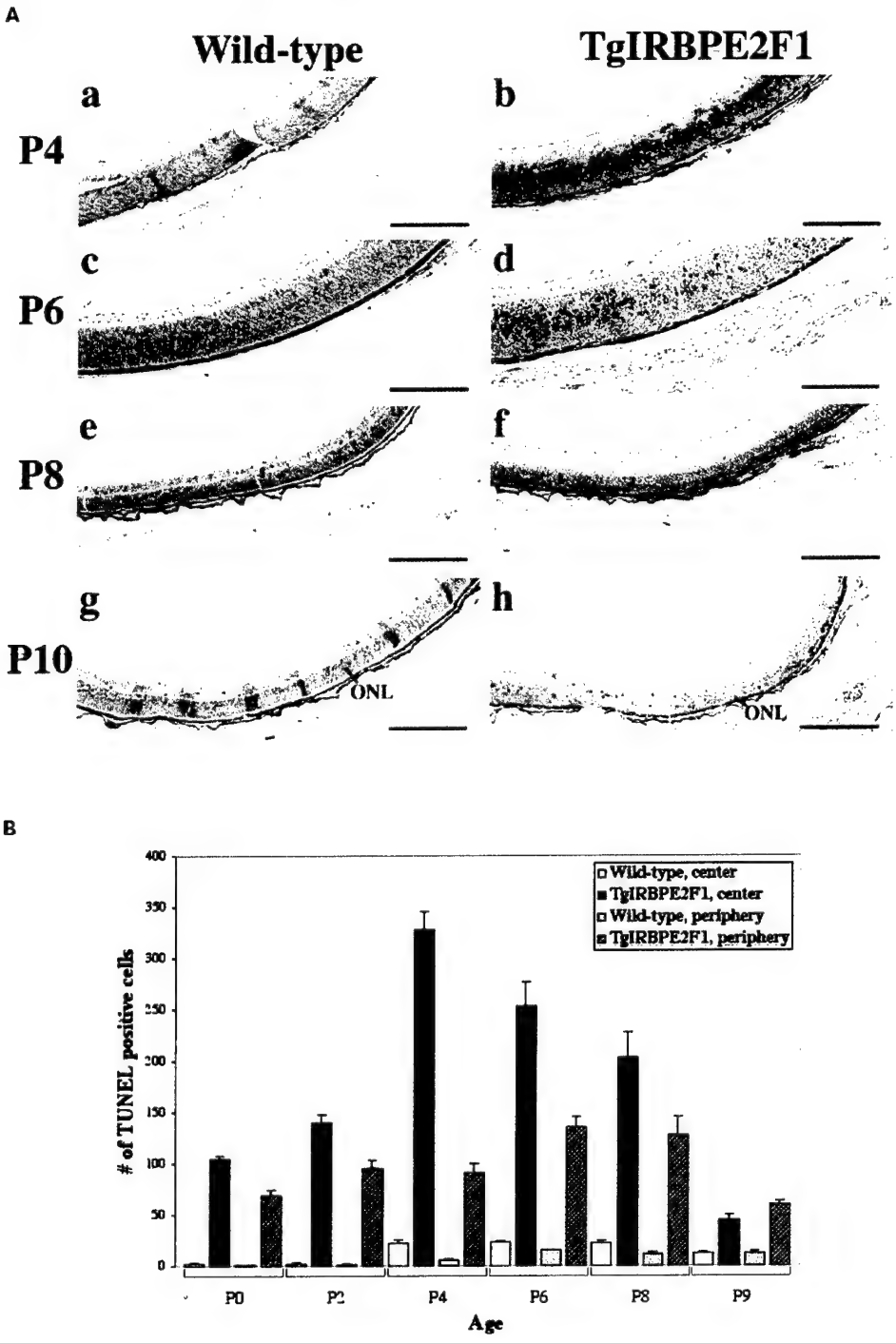

Figure 3 Effects of E2F1 overexpression on retinal apoptosis. (**A**) Apoptotic cells detected by TUNEL assay in wild-type (left panels) and *TgIRBPE2F1* (right panels) retinas of P4–P10 mice. ONL, outer nuclear layer. Scale bar, 200 μm. (**B**) Quantitative comparison of apoptotic cells in wild-type and *TgIRBPE2F1* retinas. Apoptotic nuclei within a length of 250 μm to optical nerve (center) and to ciliary body (periphery) were counted. The mean $\pm$ s.e. is based on data collected from at least three mice

photoreceptors. To accomplish this, opsin protein, which is deposited along the lateral cell membrane and synaptic terminals of the immature rods as shown previously in several other vertebrates (Nir *et al.*, 1984), was detected by immunohistochemical staining. Opsin–positive cells were first detected in the central but not the peripheral retina in wild-type mice at P2 (data not shown). Cells in the peripheral retina were observed to express opsin at later stages. At P4 and P6, levels of opsin expression appeared to be increased in all rod photoreceptor cells (Figure 4c,e). In transgenic mice, opsin-expressing cells were not seen until P6

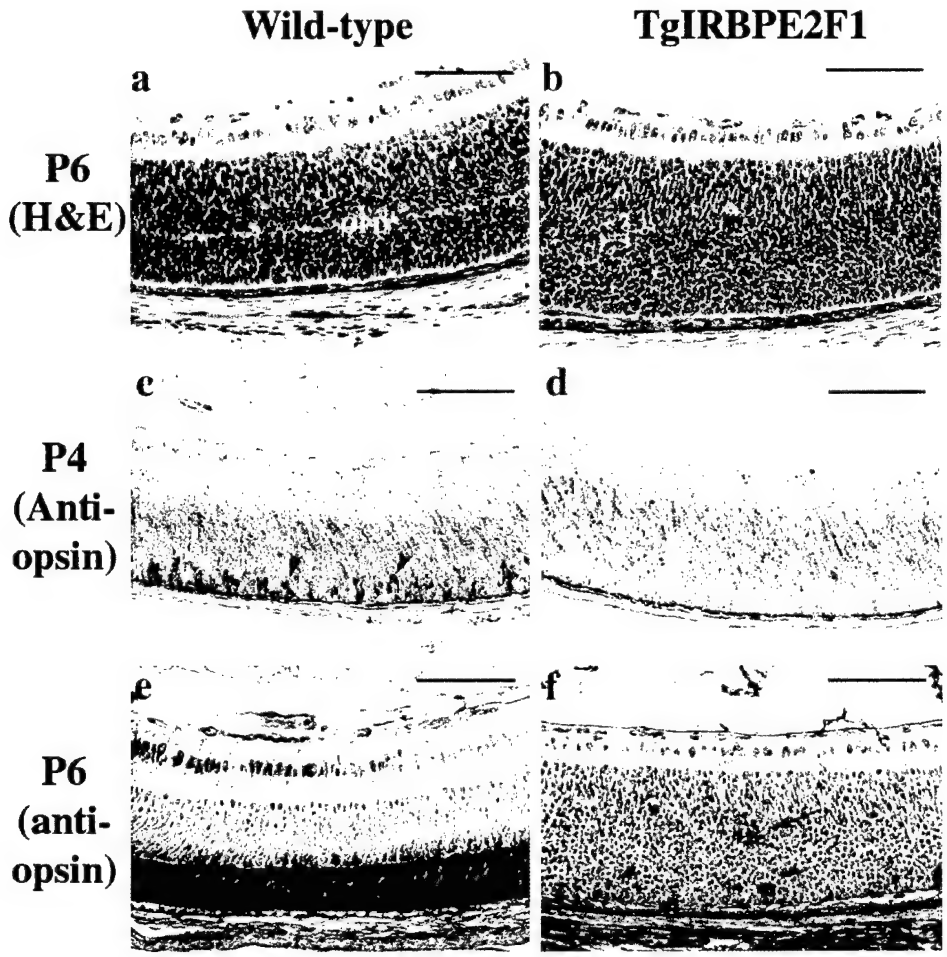

Figure 4 Effects of E2F1 overexpression on photoreceptors cell differentiation. (**a**,**b**) Formation of OPL in the P6 retinas of wild-type (**a**) and *TgIRBPE2F1* (**b**) mice. (**c**–**f**) Expression of opsin in the retinal sections of wild-type (left panel) and *TgIRBPE2F1* (right panel) mice. Arrowheads indicate opsin-expressing cells; arrow indicates clusters of apoptotic cells. OPL, outer plexiform layer. Scale bar, 100 μm

(Figure 4f). At this stage, the opsin expression pattern in the retina of transgenic mice resembles that of the P2 retinas in wild-type mice (data not shown). At later stages, the photoreceptor cells that are present showed robust expression of opsin (see below). In summary, these data indicate that the transgenic expression of E2F1 delays normal development in the retina and the expression of a photoreceptor-specific gene, but does not prevent eventual photoreceptor differentiation.

Dysplasia and degeneration in the neuroretinal cells in TgIRBPE2F1 *transgenic mice*

Although the photoreceptors eventually expressed opsin at apparently normal levels, their differentiation was still altered in the retinas of transgenic mice. Specifically, rosettes were frequently observed in the outer nuclear layer in the retinas of *TgIRBPE2F1* mice, (Figure 5a). These rosettes were composed of at least partially differentiated photoreceptors as evidenced by opsin expression (Figure 5b). The dysplastic lesions were observed from P9 through P28 *TgIRBPE2F1* mice. However, in retinas of 3 month old transgenic mice, at which time most regions were depleted of ONL cells, no rosettes were detected (Figure 5f).

Remarkably, there was a striking hemispheric asymmetry with respect to the dysplastic changes and the apoptosis discussed above. Divided by the optic nerve, multiple layers of photoreceptor cells were arranged into rosette-like structures on one side of the section (Figure 5a), whereas no photoreceptor cells were present in the other side (Figure 5c). The loss of photoreceptor cells was confirmed by the lack of opsin staining (Figure 5d). Such initial side-to-side difference and the final photoreceptor cell loss to the whole retina suggest that there might be a progressive manifestation of the E2F1 effects from one retinal hemisphere to the other; however, the molecular basis for this is not known.

Loss of p53 *promotes both severe dysplasia and hyperplasia in the retina of* TgIRBPE2F1 *mice but does not prevent photoreceptor degeneration*

Because E2F1-mediated cell death has been associated with elevated expression of p53 (Hiebert *et al*., 1995;

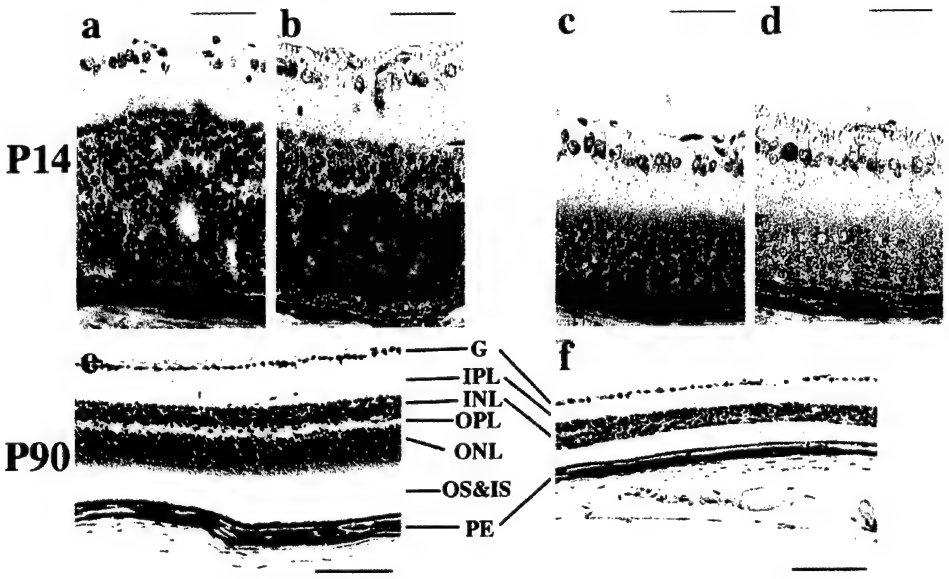

Figure 5 Asymmetric formation of rosette-like structures and loss of photoreceptor cells in a single *TgIRBPE2F1* retina. Retinal sections from different hemispheres of the same *TgIRBPE2F1* retina were stained with H&E (**a**,**c**,**e**,**f**) or immunostained with anti-opsin antibodies (**b**,**d**). (**a**–**e**), *TgIRBPE2F1* retinas; (**f**), wild-type retinas. Ages of the mice are indicated. Arrows indicate the rosettes. G, Ganglion cell layer; IPL, inner plexiform layer; INL, inner nuclear layer; OPL, outer plexiform layer; ONL, outer nuclear layer; OS&IS, outer segment and inner segment; PE, pigment epithelium. Scale bar, (**a**–**d**) 50 μm, (**e**,**f**) 100 μm

Kowalik *et al*., 1998), we tested whether the loss of *p53* affects the phenotype of *TgIRBPE2F1* mice. *TgIRBPE2F1*;$p53^{-/-}$ mice were generated after two rounds of crossings to *p53* null mice (Donehower *et al*., 1992). The loss of *p53* in the *TgIRBPE2F1* mice affected several aspects of the retina phenotype. First, rosette formation in *TgIRBPE2F1*;$p53^{-/-}$ mice appeared earlier (from P6 through P14) and dysplastic lesions were often present in both hemispheres of the retina (Figure 6a,b). Second, in some regions of the retina, multiple layers were not evident. For example, the distinct layered structure of ONL in both wild-type and *TgIRBPE2F1* mice was not observed in *TgIRBPE2F1*;$p53^{-/-}$ mice (Figure 6b). At P10, although the OPL was evident between the INL and the remaining ONL in *TgIRBPE2F1* mice, the OPL was almost undistinguishable in *TgIRBPE2F1*;$p53^{-/-}$ mice (data not shown). The INL was also in disarray as evidenced by focal expansion to nearly 14-cells thick (Figure 6b,c). The loss of layers in the outer two layers of the retina is likely due to focal hyperplasia/dysplasia of multiple cell types, including photoreceptor cells, pigment epithelial cells and cells of the INL. Third, the delayed expression of opsin in the *TgIRBPE2F1* retina was lessened in the *p53* null background. Specifically, at P6, approximately eight photoreceptors cells in every row expressed opsin in wild-type retina (Figure 4e), yet there was only one opsin-positive cell in every 5–20 rows in *TgIRBPE2F1* retina (Figure 4f). However, there were one or two opsin-positive cells in every three or four rows in *TgIRBPE2F1*;$p53^{-/-}$ retina (data not shown). Fourth, the level of cell death in the *TgIRBPE2F1*;$p53^{-/-}$ retinas was much lower than that in the *TgIRBPE2F1* retinas during P6 to P14, although it remained significantly higher than in normal retinas (data not shown). In 3-week-old and adult mice, a similar degree of retinal degeneration occurred in *TgIRBPE2F1* and *TgIRBPE2F1*;$p53^{-/-}$ mice (Figure 6c,d). Thus, although the loss of p53 modifies the degree of apoptosis detectable at any specific time, the loss of photoreceptors in the mature retina of *TgIRBPE2F1* mice is *p53*-independent. These results indicate that loss of *p53* affects multiple aspects of the phenotype induced by dysregulated E2F1 expression, which may allow excessive hyperplasia and disorganization of multiple retinal cell types. However, this is still not sufficient for oncogenic transformation of photoreceptors because significant retinal degeneration still occurs eventually.

Discussion

E2F transcription factors are important targets for RB-dependent control of the cell cycle and tumor formation. We have generated a transgenic mouse model to investigate how the aberrant expression of E2F1 affects photoreceptor cell development and contributes to tumorigenesis. In *TgIRBPE2F1* retinas, ectopic expression of E2F1 resulted in increased DNA synthesis and apoptosis in developing photoreceptor cells, a finding that is similar to what occurs in $Rb^{-/-}$ retinas during embryonic development and in retinal transplant experiments. The differentiation of photoreceptor cells, judging from the delayed appearance of the OPL and opsin expression, was also impaired but not completely blocked. Ultimately, E2F1 deregulation led to photoreceptor cell degeneration rather than

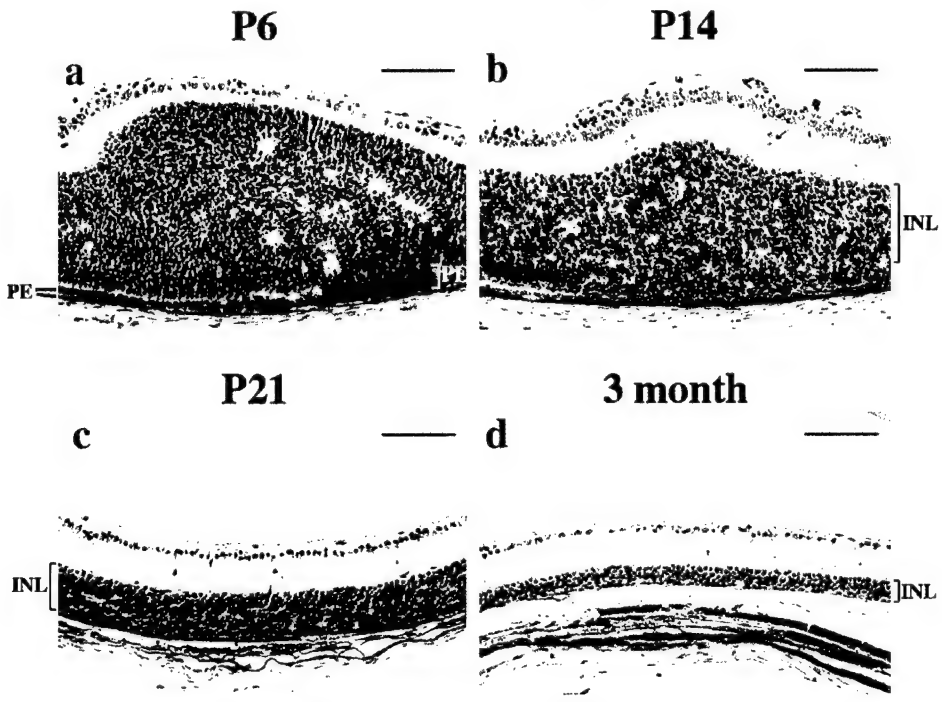

Figure 6 Retinal dysplasia and degeneration in *TgIRBPE2F1*; $p53^{-/-}$ mice. (**a–d**) H&E staining of retinal sections of *TgIRBPE2F1*; $p53^{-/-}$ mice. Note dysplastic photoreceptor cells showing rosette structures in the P6 (**a**) and P14 (**b**) retinas. PE, pigment epithelium; INL, inner nuclear layer. Scale bar, 100 μm

retinoblastoma formation. *p53* deficiency partially rescued the cell death of *TgIRBPE2F1* photoreceptor cells and promoted retinal transient hyperplasia and dysplasia but did not allow macroscopic tumor formation. Together, these studies indicate that normal regulation of E2F1, likely by RB-dependent mechanisms, is required for photoreceptor and retinal development. However, loss of E2F1 regulation is not sufficient for retinal tumor formation.

Several recent studies in other mouse tissues support our conclusions that deregulated E2F1 contributes to the phenotypes associated with *Rb* inactivation. First, aberrant S phase entry and apoptosis in the developing central nervous system and lens of $Rb^{-/-}$ embryos is suppressed in *Rb/E2F1* double mutants (Tsai *et al.*, 1998). Second, mutation of *E2F1* suppresses inappropriate proliferation and cell death of the lens fiber cell compartment induced by the HPV E7 oncoprotein, which binds to and inactivates the RB family proteins (McCaffrey *et al.*, 1999). In these respects, the effects of aberrant expression of E2F1 in mouse photoreceptors are similar to effects in the lens and other areas of the central nervous system. Furthermore, our transgenic mouse model adds further insight into how RB and the RB-related protein p107 affects retinal development. Previous studies have shown that knock out mice and chimeric mice in which all or some of the retina is derived from $Rb^{+/-};p107^{-/-}$ or $Rb^{-/-};p107^{-/-}$ cells have dysplasia (Lee *et al.*, 1996; Robanus-Maandag *et al.*, 1998) that is similar to what we observed in our studies of E2F1. Thus, our data suggest that loss of the *Rb* and *p107* may lead to retinal dysplasia by releasing E2F1 from RB (and p107) mediated repression.

Both *Rb*-deficiency and E2F1 overexpression alter opsin expression in the retinal transplant experiments and transgenic mouse retinas, respectively (Figures 1B and 4). These findings are consistent with previous studies of how loss of RB alters cellular differentiation. For example, the trigeminal ganglia of *Rb*-deficient mice show incomplete differentiation (Lee *et al.*, 1994). In *Rb* heterozygous knockout mice, mutation of the remaining wild-type *Rb* allele alters the differentiation of *Rb*-null melanotrophs in the pituitary gland. These cells fail to become mature melanotrophs and are not innervated by growth inhibitory dopaminergic nerve terminals (Nikitin and Lee, 1996). Finally, *in vitro* and *in vivo* studies have demonstrated that loss of *Rb*, or ectopic expression of E2F1 inhibits the full expression of genes induced during skeletal muscle and adipose differentiation (Chen and Lee, 1999; Chen *et al.*, 1996; Classon *et al.*, 2000; Novitch *et al.*, 1996; Zacksenhaus *et al.*, 1996). Taken together, these data indicate that loss of RB function and ectopic expression of E2F1 is sufficient to prevent normal differentiation of numerous types of cells. Interestingly, it does not completely prevent differentiation *per se* but rather it appears to delay the expression of a differentiation-specific gene in photoreceptors. Although photoreceptors in our transgenic mice eventually show robust opsin expression, we have not performed a quantitative assay to compare the level of expression with normal photoreceptors. At a molecular level, how loss of *Rb* alters differentiation is not known. It has been shown to interact with a

number of transcription factors that mediate cellular differentiation (Chen *et al*., 1996; Gu *et al*., 1993; Lipinski and Jacks, 1999; Schneider *et al*., 1994). On the other hand, it is conceivable that loss of *Rb* indirectly alters the activity of transcription factors that drive cellular differentiation by releasing E2F activity (Wang *et al*., 1995). Finally, it is also conceivable that either loss of *Rb* or aberrant E2F1 expression could influence cellular differentiation by allowing for the accumulation of additional genetic changes. Further experiments will be required to clarify the molecular basis by which loss of Rb or aberrant expression of E2F1 blocks the normal differentiation of photoreceptor cells.

Compared to other models in which E2F1 is ectopically expressed, our study of E2F1-expressing photoreceptor cells offers several new observations. First, hyperplasia was not observed in photoreceptors in our mice whereas transgenic expression of E2F-1 in squamous epithelial cells caused increased cell proliferation and hyperplasia despite increased apoptosis (Pierce *et al*., 1998a). Second, the loss of *p53* only partially abrogates E2F1-mediated cell death and only transiently sustains dysplasia and hyperplasia in photoreceptors of our *TgIRBPE2F1* mice (Figure 6), while E2F1-induced apoptosis in the epidermal cells is largely p53-dependent and its loss allows for the formation of spontaneous skin tumors (Pierce *et al*., 1998b). Similarly, apoptosis *in Rb*-deficient embryos depends on p53 and E2F1 in the central nervous system (Macleod *et al*., 1996; Tsai *et al*., 1998). Finally, we demonstrated that the forced expression of E2F1 alters photoreceptor and retina development (Figures 4 and 5); however, similar forced expression of E2F1 in epidermal cells does not appear to block cellular differentiation (Pierce *et al*., 1998a). In summary, these findings indicate that the effects of deregulated RB/E2F1 on cellular proliferation, differentiation, and apoptosis differ in specific types of cell and tissue.

Although no macroscopic tumors form in *TgIRBPE2F1*;$p53^{-/-}$ mice, there is transient hyperplasia and dysplasia of multiple retinal cell types (Figure 6a,b). This unexpected finding suggests that aberrant expression of E2F1 in photoreceptors may promote proliferation of nearby *p53*-deficient inner retinal cells and pigment epithelial cells through a paracrine mechanism. There is a precedent for paracrine regulation of cells in vertebrate retinas. For example, during development, the seven major types of cells in the retina are derived from a pool of multipotent progenitor cells (Cepko *et al*., 1996). Numerous studies have shown that cell–cell interactions are involved in cell fate determination during this time (Belliveau and Cepko, 1999; Belliveau *et al*., 2000; Cepko *et al*., 1996). Similarly, studies using intact frog retina indicate that the phosphorylation status of rhodopsin is in part regulated by dopamine released from the inner cell layers (Udovichenko *et al*., 1998). Clearly this is minor compared to the phosphorylation induced by light. Thus, it seems reasonable to speculate that the aberrant expression of E2F1 in photoreceptors could alter the cell proliferation of other retinal cells in a p53-dependent manner. However, the molecular mechanisms by which this may occur are not known. It is also plausible that there might be low levels of ectopic E2F1 expression in non-photoreceptor cells and the resultant growth promoting effect is detectable only in the absence of *p53*. Further experiments will be required to clarify the mechanisms involved.

One notable difference between our studies and previous studies of the *RB* gene pathway in the retina is the development of macroscopic retinal tumors, which occurred either in $Rb^{-/-}$;$p107^{-/-}$ chimeric mice (Robanus-Maandag *et al*., 1998) or in the *TgIRBPE7*;$p53^{-/-}$ mice (Howes *et al*., 1994). The molecular basis for the transient dysplasia and hyperplasia that occurs in our *TgIRBPE2F1*;$p53^{-/-}$ mice is not known. It is certainly conceivable that pro-apoptotic mechanisms in the retina are activated in the presence of ectopically expressed E2F1 to prevent tumor formation in the retina. In this regard, it is interesting to note that overexpression of SV40 T antigen under the control of the rhodopsin promoter also results in retinal degeneration in mice (al-Ubaidi *et al*., 1992). However, these photoreceptor cells proliferate in tissue culture and are tumorigenic when implanted subcutaneously into nude mice (al-Ubaidi *et al*., 1992). Furthermore, in the retina of $Rb^{-/-}$ chimeric mice, there was severe cellular degeneration during E16.5–E18.5 (Maandag *et al*., 1994). The contribution of $Rb^{-/-}$ retinal cells was reduced to less than 15% in adult mice (Maandag *et al*., 1994). Similarly, our intracranial $Rb^{-/-}$ retinal transplants exhibited significant apoptosis 1 week after transplantation, a time point equivalent to E18.5 of the donor tissue (Figure 1B). However, transplanted $Rb^{-/-}$ retinal cells were able to survive for more than 2 months (data not shown). Taken together, these results indicate the presence of apoptotic factors *in situ* in the eyes of the transgenic mice. It is conceivable that these pro-apoptotic factors are disrupted in the *TgIRBPE7*;$p53^{-/-}$ mice but not in our *TgIRBPE2F1*;$p53^{-/-}$ mice. Delineating mechanisms underlying phenotypic differences between genetic loss of *Rb* and *p107* (Lee *et al*., 1996; Robanus-Maandag *et al*., 1998) or by expression of IRBP-E7 in the $p53^{-/-}$ background (Howes *et al*., 1994), versus the non-tumorigenic properties of IRBP–E2F1 (even in the absence of *p53*) would likely lead to better understanding of the functions of these gene products and the biology of human retinoblastoma.

Materials and methods

Construction of TgIRBPE2F1 *transgene and generation of transgenic mice*

A plasmid pBSpKCR3 modified from pKCR3 that consists of a 1.9 kb fragment of the murine IRBP promoter, a 1.2 kb part of the rabbit β globin gene including partial exon 2, intron 2, and exon 3, and a polyadenylation site, was provided by Dr Jolene Windle (Howes *et al*., 1994). A 1.5 kb fragment containing the

full-length human E2F1 cDNA was inserted into exon 3 of the rabbit β globin gene of pBSpKCR3. The TgIRBPE2F1 transgene was cut with *Kpn*I and *Xba*I, gel-purified, and microinjected into the male pronucleus of fertilized eggs derived from CB6 F1 × C57BL/6 intercrosses. Transgenic founder mice were identified by Southern blot analysis of tail-derived genomic DNA. Transgenic mice of subsequent generations were identified by PCR using primers derived from the human E2F1 cDNA sequence, 5′ primer (5′-GGAAACT-GACCATCAGTACCTG-3′), and 3′ primer (5′-CCAGCCAC-TGGATGTGGTTCTT-3′). Transgenic lines were established by breeding founders to C57BL/6 mice. Subsequent generations of transgenic mice were maintained on a mixed CB6 F1 × C57BL/6 genetic background.

Histological analysis

Samples were fixed in 10% buffered formalin and processed through paraffin embedding follow standard procedures. Sections (4 μm thick) were cut parallel to the optic nerve and stained with hematoxylin and eosin (H&E) for light microscopy.

E2F1 and opsin immunostaining

Immunostaining was performed using the Vectastain Elite ABC Kit (Vector Laboratories). Briefly, paraffin-embedded sections were rehydrated, fixed in methanol containing 3% hydrogen peroxide for 5 min, and blocked in 1% normal horse serum (NHS) in PBS for 20 min. The sections were incubated with anti-E2F1 monoclonal antibodies (1 : 200, Pharmingen) or mouse anti-opsin antibodies (1 : 2000) diluted in 2% NHS/PBS overnight at 4°C. After washes in PBS, sections were incubated with biotinylated anti-mouse IgG for 30 min. Slides were washed in PBS, incubated with streptavidin/biotinylated peroxidase conjugate, developed by Vector VIP or DAB substrates (Vector Laboratories), and counterstained with methyl green or hematoxylin.

BrdU incorporation and TUNEL assays

Mice received bromodeoxyuridine (BrdU) at a dose of 100 μg/g of body weight by intraperitoneal and subcutaneous injection. After 2 h, retina tissue samples were collected, fixed in formalin, and embedded in paraffin. Tissue sections were treated with 4N HCl/0.2% Triton X-100, and processed for immunostaining as described above using anti-BrdU antibodies (1 : 200, Becton Dickinson). The terminal deoxyribonucleotidyltransferase-mediated dUTP-biotin nick end labeling (TUNEL) assay was performed as described (Howes *et al*., 1994).

Quantification of cells in the neuroretina

Quantification of the number of cells positive for BrdU and TUNEL was performed using light microscopy. The numbers of nuclei in the neuroretina within a length of 250 μm to the optical nerve (the central region) and to the ciliary body (the peripheral region) were counted. At least three mice were examined to obtain the mean and the standard error.

Retinal transplantation methods

Embryos were obtained from anesthetized, timed-pregnant heterozygous *Rb-1*$^{\Delta 20/+}$ mice (Lee *et al*., 1992). Retinas were removed from E11.5–E12.5 embryos and transplanted into the superior colliculus or cerebral cortex of 1-day-old (P1) wild-type or *Rb-1*$^{\Delta 20/+}$ neonates as described (Hankin and Lund, 1987). Briefly, a small glass pipet containing the donor tissue and sterile F10 culture medium (GIBCO BRL) was inserted through a small hole in the cartilagenous skull overlying the recipient midbrain or cortex. The donor tissue was ejected from the pipet with 1 μl of F10.

Acknowledgments
We thank Dr Jolene Windle for the plasmid pBSKCR3, Nancy Ransom for technical advice and Dr CL Cepko for helpful comment. We appreciate Drs NP Hu's, Y Min's, and E Gerbino's contribution in the early phase of the project. We also wish to thank K Bushnell for proof-reading the manuscript. This work was supported by NIH grants CA49649 to E Lee. Histology was performed in part by a core facility of the San Antonio Cancer Institute (grant #P30 CA 54174).

References

Adams PD and Kaelin Jr WG. (1995). *Semin. Cancer Biol.*, **6,** 99–108.
al-Ubaidi MR, Hollyfield JG, Overbeek PA and Baehr W. (1992). *Proc. Natl. Acad. Sci. USA*, **89,** 1194–1198.
Belliveau MJ and Cepko CL. (1999). *Development*, **126,** 555–566.
Belliveau MJ, Young TL and Cepko CL. (2000). *J. Neurosci.*, **20,** 2247–2254.
Brehm A and Kouzarides T. (1999). *Trends Biochem. Sci.*, **24,** 142–145.
Cepko CL, Austin CP, Yang X, Alexiades M and Ezzeddine D. (1996). *Proc. Natl. Acad. Sci. USA*, **93,** 589–595.
Chen G and Lee EY. (1999). *DNA Cell Biol.*, **18,** 305–314.
Chen PL, Riley DJ, Chen Y and Lee WH. (1996). *Genes Dev.*, **10,** 2794–2804.
Clarke AR, Maandag ER, van Roon M, van der Lugt NM, van der Valk M, Hooper ML, Berns A and te Riele H. (1992). *Nature*, **359,** 328–330.
Classon M, Kennedy BK, Mulloy R and Harlow E. (2000). *Proc. Natl. Acad. Sci. USA*, **97,** 10826–10831.
DeGregori J, Leone G, Miron A, Jakoi L and Nevins JR. (1997). *Proc. Natl. Acad. Sci. USA*, **94,** 7245–7250.
Donehower LA, Harvey M, Slagle BL, McArthur MJ, Montgomery Jr CA, Butel JS and Bradley A. (1992). *Nature*, **356,** 215–221.
Duronio RJ, O'Farrell PH, Xie JE, Brook A and Dyson N. (1995). *Genes Dev.*, **9,** 1445–1455.
Dyson N. (1998). *Genes Dev.*, **12,** 2245–2262.
Field SJ, Tsai FY, Kuo F, Zubiaga AM, Kaelin Jr WG, Livingston DM, Orkin SH and Greenberg ME. (1996). *Cell*, **85,** 549–561.
Gu W, Schneider JW, Condorelli G, Kaushal S, Mahdavi V and Nadal-Ginard B. (1993). *Cell*, **72,** 309–324.
Hankin MH and Lund RD. (1987). *J. Comp. Neurol.*, **263,** 455–466.

Hankin M, Sefton AJ and Lund RD. (1993). *Brain Res. Dev. Brain Res.*, **75,** 146–150.
Hiebert SW, Packham G, Strom DK, Haffner R, Oren M, Zambetti G and Cleveland JL. (1995). *Mol. Cell Biol.*, **15,** 6864–6874.
Howes KA, Ransom N, Papermaster DS, Lasudry JG, Albert DM and Windle JJ. (1994). *Genes Dev.*, **8,** 1300–1310.
Hu N, Gutsmann A, Herbert DC, Bradley A, Lee WH and Lee EY. (1994). *Oncogene,* **9,** 1021–1027.
Ishizaki J, Nevins JR and Sullenger BA. (1996). *Nat. Med.*, **2,** 1386–1389.
Jacks T, Fazeli A, Schmitt EM, Bronson RT, Goodell MA and Weinberg RA. (1992). *Nature,* **359,** 295–300.
Johnson DG, Cress WD, Jakoi L and Nevins JR. (1994). *Proc. Natl. Acad. Sci. USA,* **91,** 12823–12827.
Johnson DG, Schwarz JK, Cress WD and Nevins JR. (1993). *Nature,* **365,** 349–352.
Kowalik TF, DeGregori J, Leone G, Jakoi L and Nevins JR. (1998). *Cell Growth Differ.*, **359,** 113–118.
Kowalik TF, DeGregori J, Schwarz JK and Nevins JR. (1995). *J. Virol.*, **69,** 2491–2500.
Lee EY, Chang CY, Hu N, Wang YC, Lai CC, Herrup K, Lee WH and Bradley A. (1992). *Nature,* **359,** 288–294.
Lee EY, Hu N, Yuan SS, Cox LA, Braley A, Lee WH and Herrup K. (1994). *Genes Dev.*, **8,** 2008–2021.
Lee MH, Williams BO, Mulligan G, Mukai S, Bronson RT, Dyson N, Harlow E and Jacks T. (1996). *Genes Dev.*, **10,** 1621–1632.
Lin SC, Skapek SX and Lee EY. (1996). *Semin. Cancer Biol.*, **7,** 279–289.
Liou GI, Geng L, al-Ubaidi MR, Matragoon S, Hanten G, Baehr W and Overbeek PA. (1990). *J. Biol. Chem.*, **265,** 8373–8376.
Lipinski MM and Jacks T. (1999). *Oncogene,* **18,** 7873–7882.
Maandag EC, van der Valk M, Vlaar M, Feltkamp C, O'Brien J, van Roon M, van der Lugt N, Berns A and te Riele H. (1994). *EMBO J.*, **13,** 4260–4268.
Macleod KF, Hu Y and Jacks T. (1996). *EMBO J.*, **15,** 6178–6188.
McCaffrey J, Yamasaki L, Dyson NJ, Harlow E and Griep AE. (1999). *Mol. Cell. Biol.*, **19,** 6458–6468.
Morgenbesser SD, Williams BO, Jacks T and DePinho RA. (1994). *Nature,* **371,** 72–74.
Mulligan G and Jacks T. (1998). *Trends Genet.*, **14,** 223–229.
Nevins JR. (1998). *Cell Growth Differ.*, **9,** 585–593.
Nikitin A and Lee WH. (1996). *Genes Dev.*, **10,** 1870–1879.
Nir I, Cohen D and Papermaster DS. (1984). *J. Cell Biol.*, **98,** 1788–1795.
Novitch BG, Mulligan GJ, Jacks T and Lassar AB. (1996). *J. Cell Biol.*, **135,** 441–456.
Pierce AM, Fisher SM, Conti CJ and Johnson DG. (1998a). *Oncogene,* **16,** 1267–1276.
Pierce AM, Gimenez-Conti IB, Schneider-Broussard R, Martinez LA, Conti CJ and Johnson DG. (1998b). *Proc. Natl. Acad. Sci. USA,* **95,** 8858–8863.
Qin XQ, Livingston DM, Kaelin Jr WG and Adams PD. (1994). *Proc. Natl. Acad. Sci. USA,* **91,** 10918–10922.
Robanus-Maandag E, Dekker M, van der Valk M, Carrozza ML, Jeanny JC, Dannenberg JH, Berns A and te Riele H. (1998). *Genes Dev.*, **12,** 1599–1609.
Ross JF, Liu X and Dynlacht BD. (1999). *Mol. Cell,* **3,** 195–205.
Schneider JW, Gu W, Zhu L, Mahdavi V and Nadal-Ginard B. (1994). *Science,* **264,** 1467–1471.
Shan B and Lee WH. (1994). *Mol. Cell Biol.*, **14,** 8166–8173.
Singh P, Wong SH and Hong W. (1994). *EMBO J.*, **13,** 3329–3338.
Skapek SX, Jansen D, Wei TF, McDermott T, Huang W, Olson EN and Lee EY. (2000). *J. Biol. Chem.*, **275,** 7212–7223.
Slansky JE and Farnham PJ. (1996). *Curr. Top Microbiol. Immunol.*, **208,** 1–30.
Tsai KY, Hu Y, Macleod KF, Crowley D, Yamasaki L and Jacks T. (1998). *Mol. Cell.*, **2,** 293–304.
Udovichenko IP, Newton AC and Williams DS. (1998). *J. Biol. Chem.*, **273,** 7181–7184.
Wang J, Helin K, Jin P and Nadal-Ginard B. (1995). *Cell Growth Differ.*, **6,** 1299–1306.
Wu CL, Classon M, Dyson N and Harlow E. (1996). *Mol. Cell Biol.*, **16,** 3698–3706.
Wu X and Levine AJ. (1994). *Proc. Natl. Acad. Sci. USA,* **91,** 3602–3606.
Xu G, Livingston DM and Krek W. (1995). *Proc. Natl. Acad. Sci. USA,* **92,** 1357–1361.
Yamasaki L, Bronson R, Williams BO, Dyson NJ, Harlow E and Jacks T. (1998). *Nat. Genet.*, **18,** 360–364.
Yamasaki L, Jacks T, Bronson R, Goillot E, Harlow E and Dyson NJ. (1996). *Cell,* **85,** 537–548.
Young RW. (1984). *Cell,* **85,** 537–548.
Young RW. (1985). *Anat. Rec.*, **212,** 199–205.
Zacksenhaus E, Jiang Z, Chung D, Marth JD, Phillips RA and Gallie BL. (1996). *Genes Dev.*, **10,** 3051–3064.
Zhang HS, Postigo AA and Dean DC. (1999). *Cell,* **97,** 53–61.

Phosphorylation of serines 635 and 645 of human Rad17 is cell cycle regulated and is required for G_1/S checkpoint activation in response to DNA damage

Sean Post*, Yi-Chinn Weng*, Karlene Cimprich†, Lan Bo Chen‡, Yang Xu§, and Eva Y.-H. P. Lee*¶

*Deptartment of Molecular Medicine/Institute of Biotechnology, University of Texas Health Science Center, 15355 Lambda Drive, San Antonio, TX 78245; †Department of Molecular Pharmacology, Stanford University, Palo Alto, CA 94305; ‡Dana–Farber Cancer Institute, Harvard Medical School, Boston, MA 02115; and §Department of Biology, University of California at San Diego, La Jolla, CA 92093

Edited by Eric N. Olson, University of Texas Southwestern Medical Center, Dallas, TX, and approved September 18, 2001 (received for review July 16, 2001)

ATR [ataxia–telangiectasia-mutated (ATM)- and Rad3-related] is a protein kinase required for both DNA damage-induced cell cycle checkpoint responses and the DNA replication checkpoint that prevents mitosis before the completion of DNA synthesis. Although ATM and ATR kinases share many substrates, the different phenotypes of ATM- and ATR-deficient mice indicate that these kinases are not functionally redundant. Here we demonstrate that ATR but not ATM phosphorylates the human Rad17 (hRad17) checkpoint protein on Ser^{635} and Ser^{645} *in vitro*. In undamaged synchronized human cells, these two sites were phosphorylated in late G_1, S, and G_2/M, but not in early–mid G_1. Treatment of cells with genotoxic stress induced phosphorylation of hRad17 in cells in early–mid G_1. Expression of kinase-inactive ATR resulted in reduced phosphorylation of these residues, but these same serine residues were phosphorylated in ionizing radiation (IR)-treated ATM-deficient human cell lines. IR-induced phosphorylation of hRad17 was also observed in ATM-deficient tissues, but induction of Ser^{645} was not optimal. Expression of a hRad17 mutant, with both serine residues changed to alanine, abolished IR-induced activation of the G_1/S checkpoint in MCF-7 cells. These results suggest ATR and hRad17 are essential components of a DNA damage response pathway in mammalian cells.

Cell cycle checkpoints activated by stalled replication forks and DNA damage protect genomic integrity by preventing damaged DNA from being replicated and passed on to new daughter cells (1–5). In *Schizosaccharomyces pombe* (*Sp*), conserved checkpoint Rad proteins, including Rad1, Rad3, Rad9, Rad17, Rad26, and Hus1, are required for activation of checkpoint signaling pathways in response to stalled replication forks and DNA damage. Inactivation of any one of the checkpoint *rad* genes abolishes phosphorylation and activation of two downstream kinases, *Sp*Chk1 and *Sp*Cds1 (6, 7), resulting in defective activation of checkpoints. Human homologues of all of the *Sp* checkpoint *rad* genes have been identified, except *rad26*.

The *Sprad3*$^+$ gene, the *Saccharomyces cerevisiae* (*Sc*) *MEC1* gene, and the human *ATM* (ataxia–telangiectasia-mutated) and *ATR* (ATM- and Rad3-related) genes encode related protein kinases (8, 9). ATR and ATM are involved in the replication and DNA damage-induced checkpoints (10–14). Although ATM has been extensively studied, it has been difficult to ascertain ATR function because ATR-deficient cells and embryos are not viable (15, 16). ATM deficiency results in hypersensitivity to ionizing irradiation (IR) in humans and mice (17, 18). Similarly, ATR-deficient blastocysts have increased sensitivity to IR that correlates with chromosomal fragmentation (15). By using cells overexpressing kinase-inactive ATR (ATR^{Ki}) under the regulation of doxycycline, an elevated cellular sensitivity to DNA damage, a defective cell cycle response, and a significant loss of cell viability were observed (13, 19). Cellular substrates of ATM/ATR include p53 (20–23) and BRCA1 (24, 25), but substrates unique to either ATM or ATR are largely unknown. By using random mutagenesis to generate arrays of peptide substrates, preferred substrates of these kinases have been reported (26). The identification of ATR-specific substrates may provide insights into the embryonic lethality of ATR-deficient mice.

The human *Rad17* homologue (27–29), *Sprad17*$^+$, and *ScRAD24* share significant homology to the five genes encoding the replication factor C (RFC) subunits (30), which form a pentimeric clamp-loading complex (CLC) required for loading proliferating cell nuclear antigen (PCNA) onto DNA during DNA replication (31). *Sc*Rad24 has been shown to form a stable complex with the four small RFC subunits (32), suggesting that a DNA damage-specific RFC-like CLC containing *Sc*Rad24 may exist. The putative *Sc*Rad24·RFC·CLC has been proposed to serve as a sensor of DNA damage or replication blocks (33) and/or a loader of the PCNA-like hRad1·hRad9·hHus1 complex (34–36). We show here that ATR but not ATM phosphorylates human Rad17 (hRad17) *in vitro*. There are two modes of regulation of Rad17 phosphorylation, one cell cycle- and the other DNA damage-dependent. We demonstrate that IR-mediated phosphorylation of hRad17 is required for checkpoint activation in response to DNA damage.

Materials and Methods

Cell Culture, Treatment for DNA Damage Induction, and Transfection. AT-22IJE-T-EBS (ATM-deficient) and AT-22IJE-T-YZ5 (ATM-complemented) cell lines, which were gifts from Y. Shiloh (University of Tel Aviv, Israel), were cultured in DMEM supplemented with 10% FCS and 100 μg/ml hygromycin. Tetracycline-inducible wild-type ATR (ATR^{Wt}) and ATR^{Ki} cell lines were cultured in DMEM supplemented with 10% FCS (GIBCO/BRL) and 400 μg/ml G418. All other cell lines were from the American Type Culture Collection. Hydroxyurea was added to cell culture medium at a final concentration of 1 mM for 24 h. Aphidicolin was added to cell culture medium at a final concentration of 5 μg/ml for 20 h. IR was administered by using a ^{137}Cs γ-irradiator (Shepherd, San Fernando, CA) at 2.44 Gy/min. UV irradiation was performed by using UV Stratalinker 2400 (Stratagene). Cell extracts were prepared from mock-, IR-, or

This paper was submitted directly (Track II) to the PNAS office.

Abbreviations: *Sp*, *Schizosaccharomyces pombe*; *Sc*, *Saccharomyces cerevisiae*; ATM, ataxia–telangiectasia-mutated; ATR, ATM- and Rad3-related; hRad17, human Rad17; RFC, replication factor C; CLC, clamp loading complex; IR, ionizing radiation; GST, glutathione *S*-transferase; ATR^{Wt}, wild-type ATR; ATR^{Ki}, kinase-inactive ATR; *Mm*, *Mus musculus*; α-HA, anti-hemagglutinin; EGFP, enhanced green fluorescent protein.

¶To whom reprint requests should be addressed. E-mail: leee@uthscsa.edu.

The publication costs of this article were defrayed in part by page charge payment. This article must therefore be hereby marked "*advertisement*" in accordance with 18 U.S.C. §1734 solely to indicate this fact.

www.pnas.org/cgi/doi/10.1073/pnas.231364598

UV-treated cells 1 h after treatment unless otherwise stated. Transfections of human 293 and MCF-7 cells were performed by using Lipofectamine (GIBCO/BRL) and Fugene-6 (Boehringer Mannheim), respectively, according to the manufacturers' protocols.

Antibodies. ATR monoclonal antibodies were generated in mice immunized with glutathione *S*-transferase (GST)-ATR$^{710-1100}$. Mouse anti (α)-ATM (3E8), and α-hRad17 (31E9) monoclonal antibodies have been described previously (29, 37). Mouse α-HA.11 and α-Flag-M2 antibodies were from Babco (Richmond, CA) and Sigma, respectively. Rabbit α-p53-P-Ser^{15} antibodies were purchased from Cell Signaling (Beverly, MA). Phosphopeptide antibodies were raised against keyhole lymphet hemocyanin-conjugated peptides and were affinity-purified by using a phosphopeptide column after passage of the antiserum through a control non-phosphopeptide column to remove antibodies reacting with the nonphosphorylated antigen peptide and nonspecific antigens.

Immunoprecipitation and Immunoblotting. Cells lysates were prepared in Nonidet P-40 or lysis 250 buffer as described (38). Proteins in the soluble extracts were incubated with the indicated antibodies followed by incubation with protein G Sepharose beads for 2 h. Immunoprecipitates were washed 4 times in cold Nonidet P-40 lysis buffer or lysis 250 buffer and boiled in SDS-sample buffer. Proteins were separated by SDS/8.0% PAGE and transferred to poly(vinylidene difluoride) (Millipore). Membranes were incubated with the indicated antibodies, and proteins were detected by using the enhanced chemiluminescence kit (ECL, Amersham Pharmacia) or the 5-bromo-4-chloro-3-indolyl phosphate/nitroblue tetrazolium (BCIP/NBT) Color Development Substrate (Promega).

Plasmid Construction and Mutagenesis. Substitutions of alanine for serine residues, S180A, S635A, S645A, and S635A/S645A, were generated by using the QuickChange Site-Directed Mutagenesis kit (Stratagene) according to the manufacturer's protocol. hRad17^{Wt} was cloned into pcDNA3.1 (Invitrogen). By using a PCR strategy, an in-frame N-terminal hemagglutinin (HA)-tag was added to pcDNA3.1-hRad17.

Kinase Assays. Endogenous ATR and ATM were immunoprecipitated from HeLa cells mock-treated or exposed to 10 Gy of IR with purified α-ATR (2B5) or α-ATM (3E8) IgGs. Recombinant Flag-ATR^{Wt} and ATR^{Ki} were immunoprecipitated with α-Flag-M2 antibodies. ATR and ATM kinase assays were performed as described (38). Reaction products were separated by SDS/PAGE and analyzed by Coomassie staining and autoradiography.

Collection of Murine Tissues Samples. One-month-old wild-type ($Atm^{+/+}$) and ATM-deficient ($Atm^{-/-}$) mice (18) were treated with 10 Gy of IR. Mice were killed 1 h after treatment, and tissues were collected and frozen in liquid nitrogen. Cell extracts were prepared by grinding frozen tissues before incubation in lysis buffer as described above.

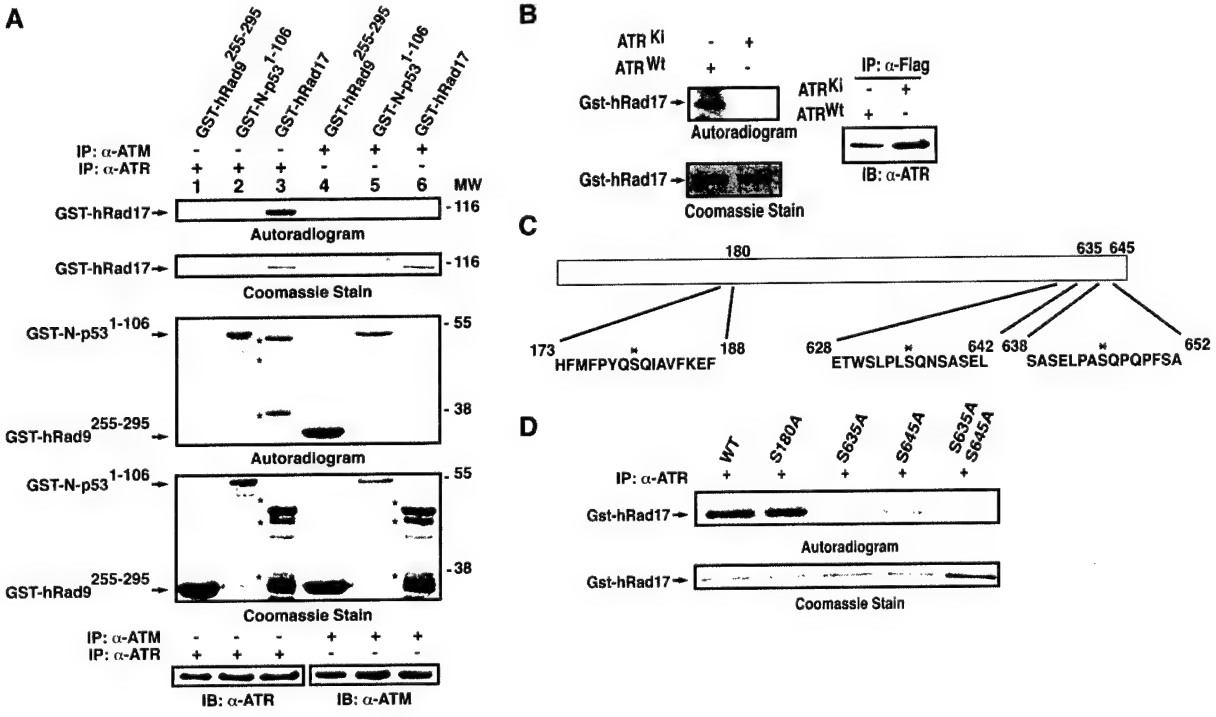

Fig. 1. Phosphorylation of hRad17 on Ser^{635} and Ser^{645} *in vitro*. (*A*) Kinase assays using immunoprecipitated (IP) ATM and ATR. GST-hRad17 was incubated with ATM (*Top Two Panels*, lane 6) and ATR (*Top Two Panels*, lane 3) immunoprecipitated from HeLa cells treated with 10 Gy of IR. GST-N-p53$^{1-106}$, a known substrate of the two kinases, was incubated with ATM (*Bottom Two Panels*, lane 5) or ATR (*Bottom Two Panels*, lane 2). GST-hRad9$^{255-295}$, a known substrate of ATM, was incubated with ATM (*Bottom Two Panels*, lane 4) or ATR (*Bottom Two Panels*, lane 1). Three micrograms of substrate was used in each reaction. The kinase reaction products were separated by SDS/PAGE and analyzed by Coomassie staining and autoradiography. Levels of ATR and ATM in the kinase reactions were determined by immunoprecipitation followed by Western blotting (IB). MW, molecular weight $\times 10^{-3}$. (*B*) Kinase assays using recombinant ATR protein. Human kidney 293 cells were transiently transfected with Flag-tagged ATR^{Wt} or ATR^{Ki}. Cells were treated with 10 Gy of IR 36 h after transfection and lysed 1 h after IR. GST-hRad17 fusion proteins were incubated with recombinant ATR immunoprecipitated with α-Flag antibodies. Immunoprecipitation with α-Flag antibodies followed by immunoblotting with α-ATR antibodies confirmed the presence of recombinant ATR. (*C*) Schematic representation of mutant hRad17 proteins. Site-specific mutation of serine to alanine was confirmed by DNA sequencing. (*D*) Ser^{635} and Ser^{645} of hRad17 are substrate sites of ATR *in vitro*. Wild-type and mutant hRad17 fusion proteins were incubated with ATR and the resultant proteins were analyzed as described in *B*.

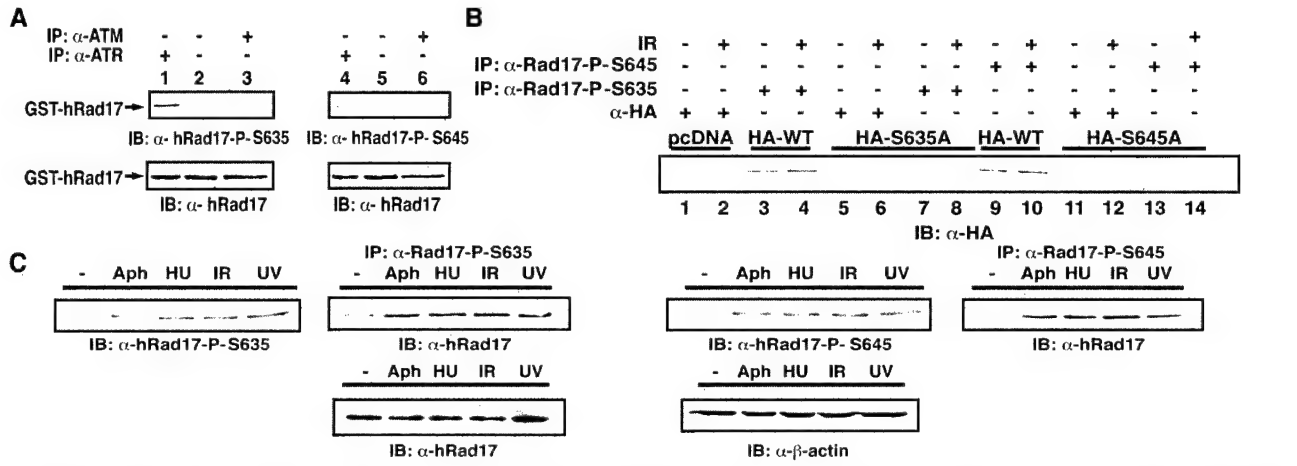

Fig. 2. *In vivo* phosphorylation of hRad17. (*A* and *B*) Specificity of the α-hRad17 phosphospecific antibodies. GST-hRad17 was incubated with ATR (*A*, *Top Two Panels*, lanes 1 and 4) or ATM (*Top Two Panels*, lanes 3 and 6), immunoprecipitated from HeLa cells, and immunoblotted with phosphopeptide antibodies. Human kidney 293 cells transfected with HA-tagged hRad17 plasmid as indicated (*B*). Cells were mock-treated or treated with 10 Gy of IR. Cells were lysed 1 h after treatment, and soluble proteins were immunoprecipitated with α-HA and phosphopeptide antibodies, as indicated. Proteins in the immunoprecipitates were separated by SDS/PAGE and immunoblotted with α-HA antibodies. (*C*) Phosphorylation of hRad17 on Ser^{635} and Ser^{645} *in vivo*. Human fibroblast VA-13 cells were mock-treated, treated with 5 μg/ml aphidicolin (Aph) for 20 h, 1 mM hydroxyurea (HU) for 24 h, 10 Gy of IR, or 50 J/m^2 UV irradiation. Cells lysates were subjected to SDS/PAGE, and immunoblotting was performed by using the indicated antibodies, or lysates were immunoprecipitated with α-hRad17-P^{S635} or α-hRad17-P^{S645} antibodies. Immunoblotting of the immunoprecipitated lysates was performed by using α-hRad17 antibody, 31E9. Western blotting analysis of hRad17 protein in the whole cell extracts. Levels of hRad17 and β-actin remain constant in untreated and treated cells.

G_1/S Checkpoint Assay. The G_1/S checkpoint assay was performed by using modifications of a previously described method (39). Briefly, MCF-7 cells cotransfected with pEGFP [which encodes enhanced green fluorescent protein (pEGFP)] and pcDNA3.1, pcDNA3.1-HA-$hRad17^{Wt}$, or pcDNA3.1-HA-$hRad17^{S635A/S645A}$ (10:1 ratio of pcDNA3.1-HA-Rad17 to pEGFP) were exposed to 10 Gy of IR followed by incubation for 24 h at 37°C. Cells were incubated with 10 μM BrdUrd for 8 h. Immunostaining was performed by using α-BrdUrd antibodies (Becton Dickinson). The percentage of BrdUrd and EGFP double positive cells over EGFP-positive cells was determined for mock- and IR-treated cells, respectively. At least 350 cells were counted from each plate. The mean and SD were calculated from three separate plates.

Results

ATR but Not ATM Phosphorylates Full-Length hRad17 *in Vitro*. To examine whether hRad17 is a substrate of ATR and ATM, *in vitro* kinase assays were performed. Immunoprecipitated ATR, but not ATM, phosphorylated GST full-length hRad17 (Fig. 1*A*, *Upper Two Panels*, lanes 3 and 6). The immunoprecipitated ATM was active, as it phosphorylated known substrates, GST-N-$p53^{1-106}$ and GST-$hRad9^{255-295}$ (Fig. 1*A*, *Bottom Two Panels*, lanes 4 and 5; refs. 23 and 38). ATR also phosphorylated p53 efficiently (23) but did not phosphorylate GST-$hRad9^{255-295}$, an ATM-specific substrate (Fig. 1*A*, *Bottom Two Panels*, lanes 1 and 2; ref. 38). The kinase/substrate relationship between ATR and hRad17 was further confirmed by using recombinant wild-type and kinase-inactive ATR (Flag-ATR^{Wt} and Flag-ATR^{Ki}), only Flag-ATR^{Wt} phosphorylated GST full-length hRad17 (Fig. 1*B*). These results differentiate ATR and ATM substrate specificity *in vitro* and are in agreement with previous reports that used GST-hRad17 peptides as substrates (26) indicating that residues surrounding the consensus serine and glutamine sites affect phosphorylation of the substrate.

hRad17 Is Phosphorylated on Ser^{635} and Ser^{645} *in Vitro* and *in Vivo*. Two consensus ATR/ATM phosphorylation sites, Ser^{635} and Ser^{645}, and a nonpreferred serine and glutamine site, Ser^{180}, are present in hRad17 (Fig. 1*C*) (26). GST full-length $hRad17^{Wt}$ and GST-$hRad17^{S180A}$ were readily phosphorylated by ATR. On the other hand, substitution of alanine Ser^{635} and Ser^{645} greatly reduced, but did not abolish, ATR-mediated phosphorylation of hRad17 (Fig. 1*D*). Taken together, these data demonstrated that GST-hRad17 is phosphorylated mainly on Ser^{635} and Ser^{645} by ATR *in vitro*, but additional target sites may exist in hRad17.

To determine whether hRad17 is phosphorylated *in vivo*, we first used [^{32}P]orthophosphoric acid to label cells and demonstrated that hRad17 is a phosphoprotein (data not shown). To confirm indeed Ser^{635} and Ser^{645} of hRad17 are phosphorylated *in vivo*, phosphospecific antibodies against keyhole limpet hemocyanin-conjugated ETWSLPLS(PO_3)QNSASEL and SASELPAS(PO_3)QPQPFSA peptides were generated, and their specificity was tested by using GST-hRad17. The antibodies react specifically with GST-hRad17 that had been incubated with immunoprecipitated ATR (Fig. 2*A*, lanes 1 and 4) but not with purified GST-hRad17 or GST-hRad17 incubated with immunoprecipitated ATM (Fig. 2*A*, lanes 2, 3, 5, and 6). We generated mammalian expression vectors expressing mutant versions of hRad17. Phosphospecific antibodies for Ser^{635} immunoprecipitated HA-$hRad17^{Wt}$ but not HA-$hRad17^{S635A}$ in extracts of transfected, mock- and 10 Gy of IR-treated cells (Fig. 2*B*, lanes 3, 4, 7, and 8). Similarly, phosphospecific antibodies for Ser^{645} immunoprecipitated HA-$hRad17^{Wt}$ but not HA-$hRad17^{S645A}$ in extracts of transfected, mock- and 10 Gy of IR-treated cells (Fig. 2*B*, lanes 9, 10, 13, and 14). Expression of wild-type and mutant HA-hRad17 was confirmed by immunoprecipitation using α-HA antibodies (Fig. 2*B*, lanes 5, 6, 11, and 12).

Because ATR activities are up-regulated in response to genotoxic stress (40), we examined whether phosphorylation of both sites of endogenous hRad17 is stimulated by various treatment. There were basal levels of Ser^{635} and Ser^{645} phosphorylation in untreated asynchronous human fibroblast VA-13 cells, and treating cells with hydroxyurea, a ribonucleotide reductase inhibitor, aphidicolin, a DNA polymerase inhibitor, IR, or UV-irradiation all resulted in elevated phosphorylation of endogenous hRad17 (Fig. 2*C*). Levels of hRad17 and β-actin remained constant in the untreated or treated cells.

Phosphorylation of hRad17 on Ser^{635} and Ser^{645} *in Vivo* Is Mediated by ATR. We studied Ser^{635} and Ser^{645} phosphorylation in cells expressing ATR^{Ki} under regulation of tetracycline (13, 19). On

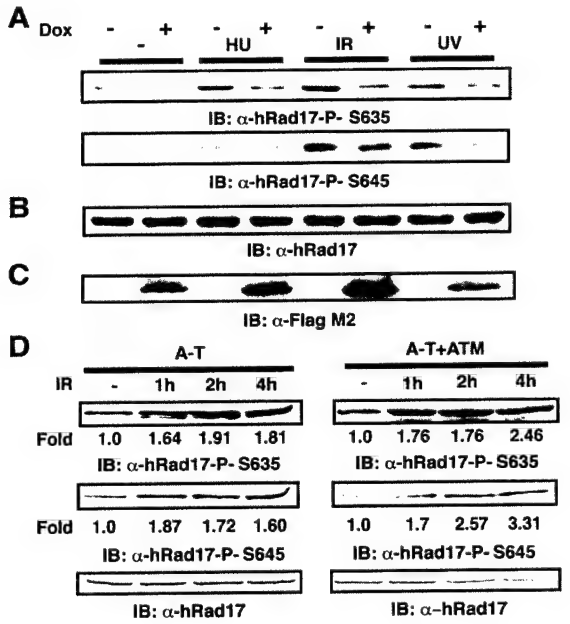

Fig. 3. ATR-dependent phosphorylation of Ser^{635} and Ser^{645} of hRad17. (*A*) Analysis of Ser^{635} and Ser^{645} phosphorylation in cells expressing ATR^{Ki}. Cells expressing ATR^{Ki} under tetracycline regulation were grown in the presence of doxycycline for 72 h. Cells were treated as in Fig. 2*C*. Soluble proteins were prepared and cell extracts were separated by SDS/PAGE. Immunoblotting was performed by using indicated antibodies. (*B*) Immunoblotting analysis of hRad17 before and after DNA damage and replication block. Soluble proteins from treated and untreated cells were subjected to SDS/PAGE and immunoblotted with α-hRad17 antibody 31E9. (*C*) Immunoblotting analysis of recombinant ATR^{Ki} expression. Expression of ATR^{Ki} was determined by SDS/PAGE followed by immunoblotting with α-Flag-M2. (*D*) ATM-independent phosphorylation of Ser^{635} and Ser^{645} of hRad17. EBS and YZ5 cells were mock-treated or treated with 30 Gy of IR and harvested 1, 2, or 4 h after treatment. (*Bottom*) Western blotting analysis of hRad17 in the whole cell extract.

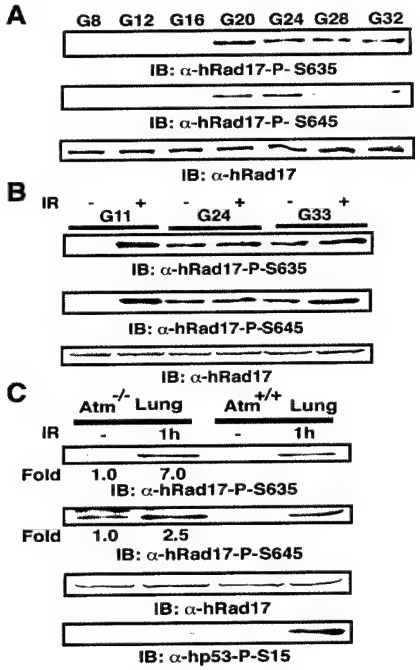

Fig. 4. Cell cycle-dependent phosphorylation of Ser^{635} and Ser^{645} of hRad17. (*A*) Immunoblot analysis of phosphorylation at Ser^{635} and Ser^{645} of hRad17 during the cell cycle. Density-arrested T24 cells were released and harvested at indicated time points G8, G12, G16, G24, G28, and G33 representing 8 h, 12 h, etc. after density release, respectively. Sample analysis was as described in Fig. 2*C*. (*B*) Immunoblot analysis of hRad17 phosphorylation during different cell cycle phases. Density-arrested T24 cells were released for 11, 24, and 33 h and harvested 1 h after treatment. (*C*) Phosphorylation of *Mm*Rad17 in mouse tissues. $Atm^{-/-}$ and $Atm^{+/+}$ mice were mock-treated or treated with 10 Gy of IR and killed 1 h after treatment.

induction of ATR^{Ki}, phosphorylation of Ser^{635} and Ser^{645} was reduced 2- to 10-fold in untreated cells and cells under genotoxic stress based on densitometric analysis (Fig. 3*A* and data not shown). Protein levels of hRad17 did not change in response to DNA damage, replication block, or doxycycline treatment (Fig. 3*B*). Expression of ATR^{Ki} was also similar in untreated and treated cells (Fig. 3*C*). As reported (25), the residual phosphorylation in cells treated with doxycycline is likely because of the remaining endogenous ATR activities. To test whether ATM is required for phosphorylation of hRad17 Ser^{635} and Ser^{645} *in vivo*, we analyzed the phosphorylation events by using extracts from EBS (ATM-deficient) and YZ5 (ATM-complemented) cells prepared from mock treatment or 30 Gy of IR at indicated time points (Fig. 3*D*). Phosphorylation on Ser^{635} of hRad17 was induced 1.61-, 1.91-, and 1.81-fold in response to DNA damage at 1, 2, and 4 h, respectively, in ATM-deficient cells. Phosphorylation on the same serine in ATM-deficient cells expressing recombinant ATM was induced 1.76-, 1.76-, and 2.46-fold at the same time points. Phosphorylation on Ser^{645} of hRad17 was induced 1.87-, 1.72-, and 1.60-fold in response to DNA damage at 1, 2, and 4 h, respectively, in ATM-deficient cells. Phosphorylation on the same serine in ATM-deficient cells expressing recombinant ATM was induced 1.7-, 2.57-, and 3.31-fold at the same time points. The fold induction in ATM-deficient cells at 4 h after IR is not as apparent, which may be relevant to the higher basal phosphorylation seen in these cells in the absence of DNA damage. These data suggest that ATR, but not ATM, is likely to be the kinase responsible for phosphorylating Ser^{635} and Ser^{645} of hRad17 in proliferating cells and in cells under genotoxic stress.

Cell Cycle-Dependent Phosphorylation of hRad17. ATM is activated in all cell cycle phases upon DNA damage (9), though our studies using *Xenopus laevis* (*Xl*) extracts have demonstrated that *Xl*ATR plays a role in the S/M checkpoint in the absence of DNA damage (41). Because basal levels of Ser^{635} and Ser^{645} phosphorylation were detected in asynchronous cell populations without DNA damage (Figs. 2 and 3), we examined whether there is cell cycle-regulated modification of these residues. T24 cells were density arrested, released, and harvested at specific phases of the cell cycle (42). Ser^{635} and Ser^{645} became phosphorylated at the start of S phase, and phosphorylation continued throughout the remainder of the cell cycle (Fig. 4*A*). Protein levels of hRad17 remained constant throughout the cell cycle (Fig. 4*A*). We next determined whether DNA damage-induced phosphorylation of these residues occurs in a cell cycle-dependent manner. Phosphorylated Ser^{635} and Ser^{645} were readily detectable in T24 cells in the G_1 phase (G11) on exposure to IR but not in mock-treated cells (Fig. 4*B*). Similar results were obtained in response to UV treatment (data not shown). In contrast to cells in the G_1 phase, levels of phosphorylation of Ser^{635} and Ser^{645} were not substantially enhanced during mid-S (G24) and G_2 phases (G33) in response to IR. The cell cycle distribution was confirmed by fluorescence-activated cell sorting analysis, showing ≈90% of cells were in G_1 (G11), 60% in S (G24), and 60% in G_2 (G33), respectively, consistent with previous reports (42). To ascertain that the lack of phosphorylation in cells in G_1 phase was not due to prolonged density arrest during cell synchronization, we determined whether *Mus mus-*

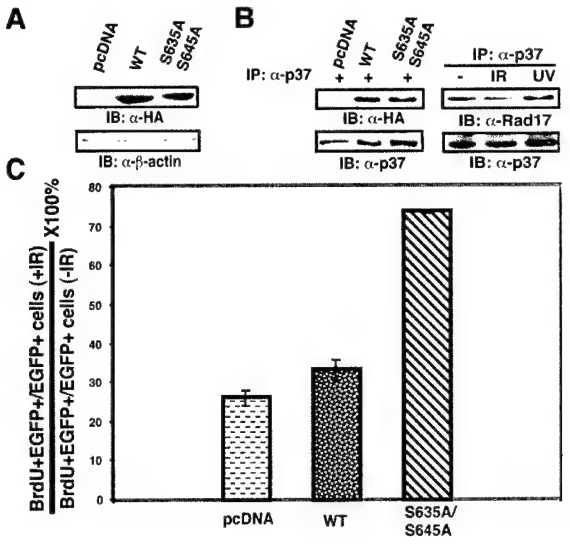

Fig. 5. Effects of expression of hRad17^{S635A} and hRad17^{S645A} on G_1/S checkpoint activation. (*A*) Immunoblotting analysis of recombinant HA-hRad17 expression in the transfected cells. Proteins in the lysates were separated by SDS/PAGE followed by immunoblotting analysis using α-HA antibody. (*B*) Recombinant HA-hRad17 and endogenous hRad17 interact with p37/RFC. Immunoprecipitation was carried out by using α-p37/RFC antibodies, and Western blotting was with antibodies as indicated. (*C*) G_1/S checkpoint activation in response to IR. The ratio of BrdUrd and EGFP double-positive cells to EGFP-positive cells was determined in mock- and IR-treated cells, respectively. At least 350 cells were counted from each plate. The mean and SD were calculated from three separate plates.

culus (*Mm*)-Rad17 is phosphorylated in terminally differentiated tissues of mice. The two sites, Ser^{647} and Ser^{657}, were not phosphorylated in lung and other tissues of the untreated wild-type mice (Fig. 4*C* and data not shown). Phosphorylation on both sites was readily detected 1 h after IR. Similar to studies using cell lines, levels of total *Mm*Rad17 protein remained constant before and after IR (Fig. 4*C*). Additionally, there was enhanced phosphorylation on both sites in *Atm*$^{-/-}$ mice in the absence of DNA damage. In *Atm*-deficient mice, there was a 7.0- and 2.5-fold increase in the phosphorylation of *Mm*Rad17 at Ser^{647} and Ser^{657}, respectively. In contrast to the *Atm*-deficient mice, no basal phosphorylation was seen in *Mm*Rad17 in wild-type mice, consistent with the observation that *h*Rad17 was not phosphorylated in early and mid G_1 cells. There was a dramatic increase in the phosphorylation of *Mm*Rad17 in wild-type mice; however, because the basal phosphorylation was near zero, the fold increase could not be determined. In contrast to the phosphorylation of *Mm*Rad17, but in agreement with published studies, phosphorylation of Ser^{18} of *Mm*p53, the equivalent of Ser^{15} human p53 (43), was greatly compromised in the absence of ATM (Fig. 4*C*; refs. 20–22). Taken together, our data indicate that phosphorylation of Rad17 is enhanced in A-T cells upon IR but the extent of induction may not be optimal, especially at Ser^{645}.

Phosphorylation of hRad17 on Ser^{635} and Ser^{645} Is Required for G_1/S Checkpoint Activation in Response to IR. In subsequent experiments, we determined whether phosphorylation of hRad17 on Ser^{635} and Ser^{645} is required for G_1/S checkpoint activation. Similar levels of recombinant wild-type and mutant HA-hRad17 were detected in cells transfected with pcDNA3.1-HA-hRad17^{Wt} or pcDNA3.1-HA-hRad17$^{S635A/S645A}$ (Fig. 5*A*). Both recombinant wild-type and mutant HA-hRad17 interacted with p37/RFC (Fig. 5*B*). Additionally, unphosphorylated hRad17 from undamaged G_1 synchronized cells and phosphorylated hRad17 from damaged G_1 synchronized cells interacted with p37/RFC (Fig. 5*B*), suggesting that phosphorylation of hRad17 is not required for the CLC formation and that the four small RFC subunits form a stable complex as seen in yeast (32). The effects of Ser^{635} and Ser^{645} phosphorylation on G_1/S checkpoint were assessed by cotransfecting pcDNA3.1, pcDNA3.1-HA-hRad17^{Wt}, or pcDNA3.1-HA-hRad17$^{S635A/S645A}$ and pEGFP at a 10:1 ratio into MCF-7 cells, which express wild-type p53 (44, 45). Overexpression of hRad17$^{S635A/S645A}$ but not vector or wild-type hRad17 (Fig. 5*C*) abolished IR-induced G_1/S checkpoint activation, suggesting phosphorylation of Ser^{635} and Ser^{645} of hRad17 is a critical event required for checkpoint activation following DNA damage (Fig. 5*C*).

Discussion

Our results demonstrate that there are two modes of regulation of phosphorylation on Ser^{635} and Ser^{645} in hRad17; one is cell cycle-dependent and the other is induced by DNA damage or replication block. We have demonstrated that ATR contributes to both modes of regulation. Additionally, phosphorylation of these two residues of hRad17 is required for IR-induced checkpoint activation.

We have showed that hRad17 is phosphorylated on Ser^{635} and Ser^{645} in response to DNA damage and replication inhibitors (Fig. 2). Combining data from budding and fission yeast, it appears that hRad17 may be required for cell cycle checkpoint activation in response to genotoxic stress. In addition to the hyperphosphorylation seen in response to DNA damage, phosphorylation of Ser^{635} and Ser^{645} occurs in undamaged cycling cells during S and G_2/M (Fig. 4). Although it is not clear how ATR activities regulate the S/M checkpoint (46), in *X. laevis* we have shown that *Xl*ATR is associated with chromatin only during S phase (41). Depletion of *Xl*ATR from extracts abrogates the S/M checkpoint in the absence of DNA damage, correlating with inhibition of *Xl*Chk1 phosphorylation (41). It is of interest to test whether chromatin association of ATR controls cell cycle-regulated phosphorylation of hRad17. Studies in yeast have demonstrated that *Sp*Rad17 is required for the activation of Chk1; however, whether hRad17 phosphorylation *per se* is required for the S/M checkpoint has yet to be determined.

Overexpression of hRad17 phosphorylation mutants but not wild-type hRad17 abolishes IR-induced G_1/S checkpoint (Fig. 5). How does hRad17 phosphorylation lead to block of cell cycle progression? Studies in multiple organisms have identified signal cascades involved in genotoxic-induced cell cycle checkpoints (1–5). In mammals, phosphorylation of p53 by ATM and ATR and subsequent up-regulation of p21^{Cip1} lead to G_1 arrest. In addition, phosphorylation cascades involving ATM, ATR, Chk1, Chk2, cyclin-dependent kinases, and Cdc25 phosphatases, as well as their yeast counterparts, have been demonstrated. Whether phosphorylation of hRad17 affects these kinases and phosphatases remains to be tested.

Based on kinase assays performed *in vitro* and studies using cells overexpressing ATR^{Ki}, we conclude that ATR contributes to phosphorylation of Ser^{635} and Ser^{645} of hRad17 with or without genotoxic stress (Figs. 1 and 3). Despite the apparently dispensable role of ATM in hRad17 phosphorylation, it is plausible that optimal phosphorylation of hRad17 may require both kinases, as the reduction of phosphorylation seen in Ser^{645} in ATR^{Ki} cells was not as significant as Ser^{635}. Studies to date suggest that UV- and hydroxyurea-induced phosphorylation of checkpoint proteins are mediated by ATR, and IR-induced phosphorylation is mediated by ATM (23, 25); however, it remains to be seen whether this is true with the expanding list of ATM/ATR substrates.

We consistently observed elevated basal phosphorylation on Ser^{635} and Ser^{645} in cycling and terminally differentiated (G_0) ATM-deficient cells (Figs. 3 and 4). There are several plausible

explanations for these observations. First, low levels of DNA damage may occur in ATM-deficient cells, leading to phosphorylation of hRad17 by ATR. If this explanation is true, it would indicate ATM and ATR might work synergistically to respond to and to repair DNA damage, as the kinase activity of ATR alone cannot result in the repair of the intrinsic DNA damage in these cells. However, there is no increase in basal phosphorylation of *Mm*p53 on Ser^{18} despite the fact that ATR has been shown to be responsible for the delayed phosphorylation of p53 in response to IR (23). Second, the loss of ATM may result in aberrant hyper-recombination (47), yielding unresolved recombination intermediates, which in turn stimulate the phosphorylation of hRad17 by ATR. These recombination intermediates may result in the high basal phosphorylation seen in the ATM-deficient cell line (EBS), $Atm^{-/-}$ mouse embryonic fibroblasts, and $Atm^{-/-}$ tissues. Indeed, recombination intermediates have been shown to activate checkpoints through *Sc*RAD24 (48). Third, ATM may negatively regulate ATR activities during G_0 or G_1 cell cycle phases. In the absence of ATM, deregulated ATR may inappropriately interact with and phosphorylate hRad17.

A possible consequence of IR-induced phosphorylation is the enhancement of interaction among hRad17 and other proteins. We have demonstrated that phosphorylation of Ser^{635} and Ser^{645} of hRad17 is not required for the interaction with p37, one of the small RFC subunits (Fig. 5), suggesting that hRad17 and the four small RFC subunits form a stable complex as seen in budding yeast (32). Because Rad17 and Rad9·Rad1·Hus1 have been placed in the same epistasis group in yeast and we have demonstrated that ATM phosphorylation of hRad9 is required for G_1/S checkpoint activation (38), it is likely that IR-induced phosphorylation of hRad9 and hRad17, mediated by ATM and ATR, respectively, are both required for checkpoint activation. Although the proposed proliferating cell nuclear antigen clamp-like activities of the mammalian hRad9·hRad1·hHus1 complex has yet to be demonstrated, hRad9 is a 3′ to 5′ exonuclease (49), suggesting that this exonuclease complex, likely to be loaded by hRad17·RFC·CLC, may remove DNA lesions. Taken together, these data suggest ATM and ATR may phosphorylate unique substrates but work synergistically to maintain genomic stability.

Note. While this manuscript was in preparation, a study by Bao *et al.* (50) on ATM/ATR and hRad17 was published.

We thank Drs. W.-H. Lee, A. Tomkinson, P. Sung, and K. W. McMahon for critical reading of the manuscript and Drs. W.-H. Lee, A. Tomkinson, and M. Chen for stimulating discussions. We are grateful to Drs. D. Levin, S. Zhao, and S.-C. Lin for technical advice and M.-H. Song for technical assistance. Rabbit α-p37/RFC and mouse α-140/RFC were kind gifts from Drs. J. Hurwitz and B. Stillman, respectively. S.P. is a recipient of a Department of Defense training grant. K.A.C. is supported by American Cancer Society Grant RPG99-241-01CCG. E.Y.-H.P.L. is supported by National Institutes of Health Grant P01CA81020.

1. Weinert, T. (1998) *Curr. Opin. Genet. Dev.* **8,** 185–193.
2. Longhese, M. P., Foiani, M., Muzi-Falconi, M., Lucchini, G. & Plevani, P. (1998) *EMBO J.* **17,** 5525–5528.
3. Dasika, G. K., Lin, S. C., Zhao, S., Sung, P., Tomkinson, A. & Lee, E. Y. (1999) *Oncogene* **18,** 7883–7899.
4. Caspari, T. & Carr, A. M. (1999) *Biochimie* **81,** 173–181.
5. Zhou, B. & Elledge, S. (2000) *Nature (London)* **408,** 433–439.
6. Enoch, T., Carr, A. M. & Nurse, P. (1992) *Genes Dev.* **6,** 2035–2046.
7. O'Connell, M. J., Raleigh, J. M., Verkade, H. M. & Nurse, P. (1997) *EMBO J.* **16,** 545–554.
8. Zakian, V. A. (1995) *Cell* **82,** 685–687.
9. Shiloh, Y. (2001) *Curr. Opin. Genet. Dev.* **11,** 71–77.
10. Painter, R. B. & Young, B. R. (1980) *Proc. Natl. Acad. Sci. USA* **77,** 7315–7317.
11. Canman, C. E., Wolff, A. C., Chen, C. Y., Fornace, A. J., Jr., & Kastan, M. B. (1994) *Cancer Res.* **54,** 5054–5058.
12. Cimprich, K. A., Shin, T. B., Keith, C. T. & Schreiber, S. L. (1996) *Proc. Natl. Acad. Sci. USA* **93,** 2850–2855.
13. Cliby, W. A., Roberts, C. J., Cimprich, K. A., Stringer, C. M., Lamb, J. R., Schreiber, S. L. & Friend, S. H. (1998) *EMBO J.* **17,** 159–169.
14. Guo, Z. & Dunphy, W. G. (2000) *Mol. Biol. Cell* **11,** 1535–1546.
15. Brown, E. J. & Baltimore, D. (2000) *Genes Dev.* **14,** 397–402.
16. de Klein, A., Muijtjens, M., van Os, R., Verhoeven, Y., Smit, B., Carr, A. M., Lehmann, A. R. & Hoeijmakers, J. H. (2000) *Curr. Biol.* **10,** 479–482.
17. Barlow, C., Hirotsune, S., Paylor, R., Liyanage, M., Eckhaus, M., Collins, F., Shiloh, Y., Crawley, J. N., Ried, T., *et al.* (1996) *Cell* **86,** 159–171.
18. Xu, Y., Ashley, T., Brainerd, E. E., Bronson, R. T., Meyn, M. S. & Baltimore, D. (1996) *Genes Dev.* **10,** 2411–2422.
19. Wright, J. A., Keegan, K. S., Herendeen, D. R., Bentley, N. J., Carr, A. M., Hoekstra, M. F. & Concannon, P. (1998) *Proc. Natl. Acad. Sci. USA* **95,** 7445–7450.
20. Banin, S., Moyal, L., Shieh, S., Taya, Y., Anderson, C. W., Chessa, L., Smorodinsky, N. I., Prives, C., Reiss, Y., Shiloh, Y. & Ziv, Y. (1998) *Science* **281,** 1674–1677.
21. Canman, C. E., Lim, D. S., Cimprich, K. A., Taya, Y., Tamai, K., Sakaguchi, K., Appella, E., Kastan, M. B. & Siliciano, J. D. (1998) *Science* **281,** 1677–1679.
22. Khanna, K. K., Keating, K. E., Kozlov, S., Scott, S., Gatei, M., Hobson, K., Taya, Y., Gabrielli, B., Chan, D., Lees-Miller, S. P., *et al.* (1998) *Nat. Genet.* **20,** 398–400.
23. Tibbetts, R. S., Brumbaugh, K. M., Williams, J. M., Sarkaria, J. N., Cliby, W. A., Shieh, S. Y., Taya, Y., Prives, C. & Abraham, R. T. (1999) *Genes Dev.* **13,** 152–157.
24. Cortez, D., Wang, Y., Qin, J. & Elledge, S. J. (1999) *Science* **286,** 1162–1166.
25. Tibbetts, R., Cortez, D., Brumbaugh, K., Scully, R., Livingston, D., Elledge, S. & Abraham, R. (2000) *Genes Dev.* **14,** 2989–3002.
26. Kim, S. T., Lim, D. S., Canman, C. E. & Kastan, M. B. (1999) *J. Biol. Chem.* **274,** 37538–37543.
27. Bluyssen, H. A., Naus, N. C., van Os, R. I., Jaspers, I., Hoeijmakers, J. H. & de Klein, A. (1999) *Genomics* **55,** 219–228.
28. Dean, F. B., Lian, L. & O'Donnell, M. (1998) *Genomics* **54,** 424–436.
29. Bao, S., Chang, M. S., Auclair, D., Sun, Y., Wang, Y., Wong, W. K., Zhang, J., Liu, Y., Qian, X., Sutherland, R., *et al.* (1999) *Cancer Res.* **59,** 2023–2028.
30. Griffiths, D. J., Barbet, N. C., McCready, S., Lehmann, A. R. & Carr, A. M. (1995) *EMBO J.* **14,** 5812–5823.
31. Podust, V. N., Tiwari, N., Stephan, S. & Fanning, E. (1998) *J. Biol. Chem.* **273,** 31992–31999.
32. Green, C. M., Erdjument-Bromage, H., Tempst, P. & Lowndes, N. F. (2000) *Curr. Biol.* **10,** 39–42.
33. Griffiths, D., Uchiyama, M., Nurse, P. & Wang, T. S. (2000) *J. Cell Sci.* **113,** 1075–1088.
34. Rauen, M., Burtelow, M., Dufault, V. & Karnitz, L. (2000) *J. Biol. Chem.* **275,** 29767–29771.
35. Venclovas, C. & Thelen, M. P. (2000) *Nucleic Acids Res.* **28,** 2481–2493.
36. Burtelow, M., Roos-Mattjus, P., Rauen, M., Babendure, J. & Karnitz, L. (2001) *J. Biol. Chem.* **276,** 25903–25909.
37. Chen, G. & Lee, E. (1996) *J. Biol. Chem.* **271,** 33693–33697.
38. Chen, M., Lin, Y., Lieberman, H., Chen, G. & Lee, E. (2001) *J. Biol. Chem.* **276,** 16580–16586.
39. Harrington, E. A., Bruce, J. L., Harlow, E. & Dyson, N. (1998) *Proc. Natl. Acad. Sci. USA* **95,** 11945–11950.
40. Liu, Q., Guntuku, S., Cui, X. S., Matsuoka, S., Cortez, D., Tamai, K., Luo, G., Carattini-Rivera, S., DeMayo, F., Bradley, A., *et al.* (2000) *Genes Dev.* **14,** 1448–1459.
41. Hekmat-Nejad, M., You, Z., Yee, M., Newport, J. & Cimprich, K. (2000) *Curr. Biol.* **10,** 1565–1573.
42. Chen, P. L., Scully, P., Shew, J. Y., Wang, J. Y. & Lee, W. H. (1989) *Cell* **58,** 1193–1198.
43. Chao, C., Saito, S., Anderson, C. W., Appella, E. & Xu, Y. (2000) *Proc. Natl. Acad. Sci. USA* **97,** 11936–11941. (First Published October 17, 2000; 10.1073/pnas.2202522)
44. Gupta, M., Fan, S., Zhan, Q., Kohn, K., O'Connor, P. & Pommier, Y. (1997) *Clin. Cancer Res.* **3,** 1653–1660.
45. Fan, S., Smith, M., Rivet, D., Duba, D., Zhan, Q., Kohn, K., Fornace, A. & O'Connor, P. (1995) *Cancer Res.* **55,** 1649–1654.
46. Nghiem, P., Park, P. K., Kim, Y., Vaziri, C. & Schreiber, S. L. (2001) *Proc. Natl. Acad. Sci. USA* **98,** 9092–9097.
47. Meyn, M. S., Lu-Kuo, J. M. & Herzing, L. B. (1993) *Am. J. Hum. Gen.* **53,** 1206–1216.
48. Klein, H. (2001) *Genetics* **157,** 557–565.
49. Bessho, T. & Sancar, A. (2000) *J. Biol. Chem.* **275,** 7451–7454.
50. Bao, S., Tibbetts, R. S., Brumbaugh, K. M., Fang, Y., Richardson, D. A., Ali, A., Chen, S. M., Abraham, R. T. & Wang, X. F. (2001) *Nature (London)* **411,** 969–974

diabetes or other conditions characterized by renal hypertrophy (2, 4).

In this study, we examined the effect of IGF-I on cultured MCs from glomeruli of rats and evaluated both proliferative and hypertrophic effects. We also examined the signaling pathways activated by IGF-I, including the MAPK and PI3K pathways. In addition, we investigated IGF-I-mediated activation of other pathways, including the calcium-dependent serine/threonine phosphatase, calcineurin. Accordingly, we determined what effect inhibition of these pathways has on IGF-I-mediated hypertrophy and ECM production. Finally, we demonstrated the significance of calcineurin activation by showing IGF-I-mediated nuclear translocation of the calcineurin substrate, nuclear factor of activated T cells- c1 (NFATc1).

EXPERIMENTAL PROCEDURES

Materials

Receptor grade recombinant human IGF-I was purchased from GroPep (Adelaide, Australia), and recombinant human TGFβ1 was obtained from R&D Systems, Inc. (Minneapolis, MN). PD98059 was from Calbiochem (La Jolla, CA). Wortmannin, cyclosporin A, calcium ionophore A23187, and anti-fibronectin antibody were from Sigma Chemical Co. (St. Louis, MO). Anti-collagen type IV antibody was purchased from Chemicon (Temecula, CA), anti-phospho Akt, anti-phospho-Erk1/Erk2, and anti-calcineurin antibodies were from Transduction Laboratories (San Diego, CA), and anti-NFATc1 antibody was from Santa Cruz Biotechnology (Santa Cruz, CA).

Cell Culture

Rat MCs were cultured from glomeruli isolated by differential sieving as previously described (14). Epithelial cells were removed by digestion with collagenase, and glomerular cores were cultured in RPMI (Life Technologies, Inc., Gaithersburg, MD) supplemented with antibiotics and 17% fetal calf serum. For these experiments, rat MCs that have been maintained in our laboratory (University of Texas Health Science Center, San Antonio, TX) were used between passage 26 and 32.

Hypertrophy

FACS—MCs were plated in 60-mm plates and allowed to grow to 80–90% confluency. Medium was then changed to serum-free media (SFM) for 24 h, and the cells were treated as indicated. After treatment, MCs were harvested by trypsinization, washed with 1× PBS, centrifuged at 5000 rpm for 2 min, and then resuspended in ice-cold 70% ethanol added dropwise while vortexing. Ethanol-fixed MCs were then analyzed by forward light scattering on a Becton Dickinson flow cytometer.

Protein/DNA Ratio—MCs were plated in triplicate in 12-well plates and allowed to grow to 80–90% confluence. Medium was changed to SFM for 24 h, and the cells were treated as indicated. Each well was washed, collected by trypsinization, and split into two equal aliquots. Both samples were washed with 1× PBS and centrifuged at 5000 rpm for 2 min. One aliquot was resuspended in TNESV protein lysis buffer (50 mM Tris-HCl, pH 7.4, 2 mM EDTA, 1% Nonidet P-40, 100 mM NaCl, 100 mM sodium orthovanadate, 100 μg/ml leupeptin, 20 μg/ml aprotinin, and 10^{-7} M phenylmethylsulfonyl (PMSF)) and the other in ice-cold 70% ethanol. Protein concentrations were determined by BCA protein assay (Pierce, Rockford, IL). For determination of DNA concentration, Hoescht stain (Sigma, St. Louis, MO) was added to ethanol fixed cells for 30 min at room temperature. DNA was measured at 355-nm excitation and 460-nm emission using a Titertak Flouroskan II fluorometer. For each well the resulting protein determination was divided by the DNA measurement to provide a protein/DNA ratio.

Kinase Assay

MCs were plated in 60-mm plates and allowed to grow to 80–90% confluency (~2 days). Medium was then changed to SFM for 24 h, and the cells were treated as indicated.

Erk1/Erk2 MAPK—Erk1/Erk2 was immunoprecipitated from 100 μg of total protein using anti-Erk1 antibody (Santa Cruz Biotechnology) followed by protein A-Sepharose beads. Immunocomplexes were washed three times in TNESV buffer and resuspended in kinase buffer (10 mM HEPES, pH 7.4, 10 mM $MgCl_2$, 0.5 mM dithiothreitol, and 0.5 mM Na_3VO_4) in the presence of 0.5 mg/ml myelin basic protein (MBP), 25 μM cold ATP, and 1 μCi of [γ-^{32}P]ATP. Reactions were incubated for 30 min at 30 °C followed by 10-min incubation on ice. Phosphorylated MBP was resolved on 12% SDS-PAGE, the gel was dried, and an exposure was made onto film.

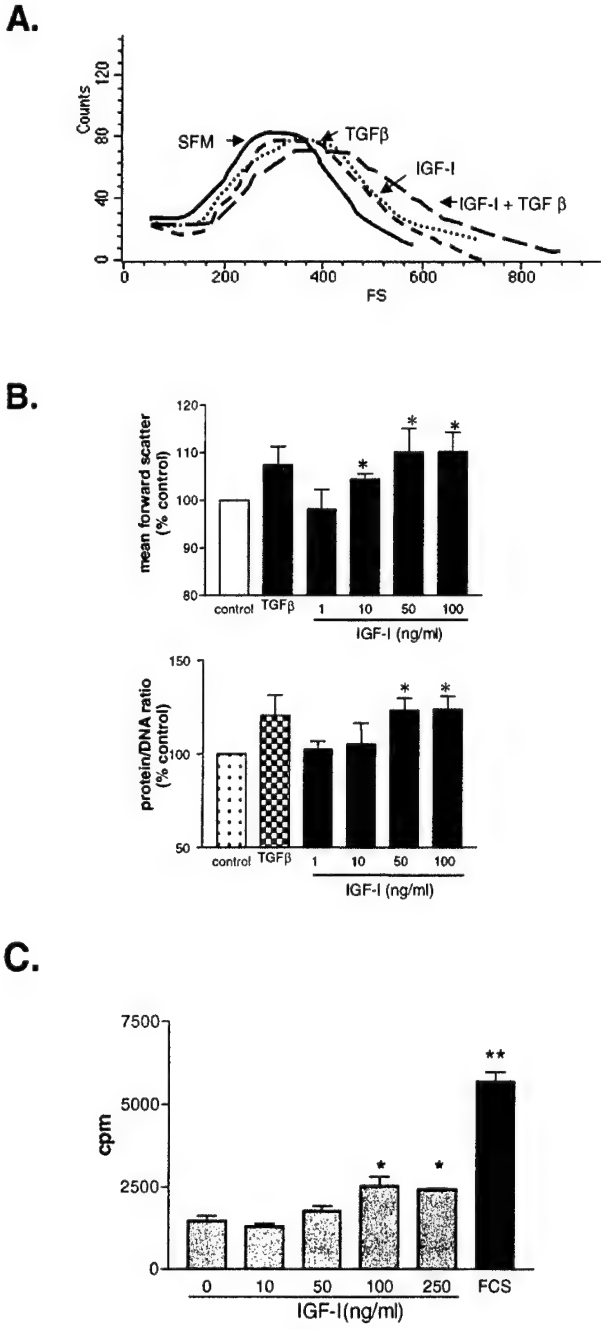

FIG. 1. **IGF-I induces hypertrophy of mesangial cells.** Near-confluent mesangial cells were serum-starved for 24 h and then treated as indicated: *A*, cells were treated with SFM (control), TGFβ (1 ng/ml), or IGF-I (50 ng/ml) for 72 h. Cell size was determined by FACS analysis using forward light scattering. *B*, cells were treated with SFM (control), TGFβ (1 ng/ml), or increasing amounts of IGF-I for 48 h, and then cell size was determined by forward light scattering. *Bars* represent the mean ± S.E. of four independent experiments. Cells were also analyzed for DNA and protein content, and the protein/DNA ratio of triplicate samples ± S.E. was determined. Data shown are representative of at least three independent experiments. *, $p < 0.05$ compared with control. *C*, cells were treated for 24 h with increasing amounts of IGF-I, and then DNA synthesis was measured with ^{3}H-labeled thymidine. Fetal calf serum (*FCS*) was included as a positive control for DNA synthesis. *Bars* represent the mean of triplicate samples ± S.E. Data shown are representative of three independent experiments. *, $p < 0.05$; **, $p < 0.001$ compared with control.

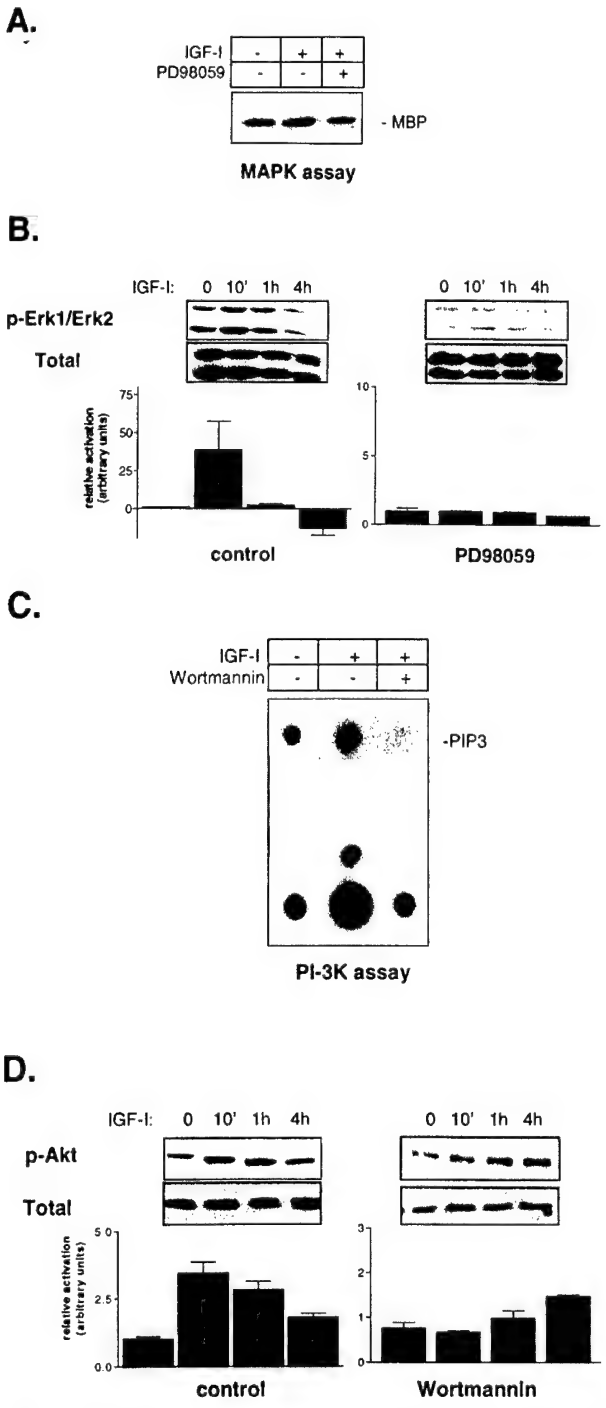

FIG. 3. **IGF-I-mediated hypertrophy is associated with activation of Erk1/Erk2 MAPK and PI3K pathways.** *A*, cells were pretreated with PD98059 (10 μM) and then incubated with IGF-I for 10 min. Erk1/Erk2 MAPK kinase activity was determined by *in vitro* kinase assay with MBP as a substrate. *B*, cells were pretreated with SFM (control) or PD98059 (10 μM) and then treated with IGF-I (50 ng/ml) for the indicated lengths of time. Protein lysates were collected, and phosphorylation of Erk1/Erk2 was determined by immunoblotting with phospho-specific Erk1/Erk2 antibody. Total Erk1/Erk2 was also detected in the same samples using a specific antibody. Relative activation from three separate experiments was quantitated and graphed. *C*, MCs were pretreated with wortmannin (250 nM) and then incubated with IGF-I for 10 min. PI3K activity was determined as described under "Experimental Procedures." *D*, cells were pretreated with SFM (control) or wortmannin (250 nM) and then treated with IGF-I (50 ng/ml) for the indicated lengths of time. Protein lysates were collected, and phosphorylation of Akt was determined by immunoblotting with a phospho-specific Akt antibody. Also, total Akt was detected in the same samples using a specific antibody. Relative activation from three separate experiments was quantitated and graphed.

tion counter. To ensure specificity of the assay for calcineurin activity, okadaic acid was routinely added to the reaction buffer to inhibit any dephosphorylation by serine-threonine phosphatases PP1A and PP2A.

Statistics

Statistical significance was determined by Student's *t* test. A result was considered significant if $p < 0.05$.

RESULTS

In vivo studies demonstrated that IGF-I plays a role in renal hypertrophy (4, 9, 18). However, it is unclear whether IGF-I acts as a proliferative agent for renal cells as it does with many other cells or if IGF-I can directly initiate hypertrophy. Therefore, in this study we examined the effect of IGF-I on cultured mesangial cells (MCs). Hypertrophy was determined as an increase in cell size (without an increase in cell number) and an increase in protein production without an increase in DNA synthesis. Fig. 1*A* shows that IGF-I treatment (50 ng/ml) of MCs resulted in an increase in cell size as determined by FACS analysis. The effect of IGF-I was comparable to the effect of TGFβ (1 ng/ml), which is known to induce hypertrophy in these cells (19). Treatment of MCs with both IGF-I and TGFβ resulted in an additive hypertrophic effect. FACS analysis of these cells showed that there was no difference in the distribution of cells in the cell cycle after IGF-I or TGFβ treatments compared with SFM control (data not shown).

IGF-I induced hypertrophy in a dose-dependent manner, with 50 ng/ml resulting in a significant increase in both cell size and protein/DNA ratio (Fig. 1*B*). The maximal effect of IGF-I was equal to or slightly greater than was seen with TGFβ treatment of these cells. Hypertrophy was discernible as early as 8 h after treatment and was detectable for as long as 72 h after exposure of cells to IGF-I (data not shown). Finally, there was a small increase in DNA synthesis following IGF-I treatment but only at concentrations of 100 ng/ml or greater (Fig. 1*C*).

There are conflicting reports regarding the ability of IGF-I to induce ECM production in renal cells. Previous *in vivo* experiments have shown that overexpression of IGF-I contributes to hypertrophy but is not sufficient for ECM production and development of fibrosis (7). However, other *in vitro* studies have shown that IGF-I does contribute to an increase in ECM (20, 21). In our experiments, MCs were treated with IGF-I or TGFβ for 72 h, and the levels of collagen type IV and fibronectin were determined by both Western blotting (Fig. 2*A*) and immunohistochemistry (Fig. 2*B*). We found that IGF-I induces an increase in both collagen type IV and fibronectin protein levels although not as robustly as does TGFβ. Interestingly, the amount of IGF-I that was sufficient to stimulate an increase in ECM (at least 100 ng/ml) was double that which was required to induce maximal hypertrophy (50 ng/ml). Similar to hypertrophy, IGF-I and TGFβ together resulted in an additive effect on the levels of ECM proteins.

We next examined the signaling pathways activated by IGF-I in MCs. Using an *in vitro* kinase assay with myelin basic protein (MBP) as a substrate for Erk1/Erk2 MAPK, we show that IGF-I treatment results in activation of MAPK in MCs (Fig. 3*A*). This activation was blocked by pretreatment with PD98059, an inhibitor of the Erk1/Erk2 kinase MEK. In addition, we treated MCs with IGF-I for increasing lengths of time and examined phosphorylation of Erk1/Erk2 using a phospho-specific Erk1/Erk2 antibody. Erk1/Erk2 was transiently phosphorylated following addition of IGF-I with maximal activation at 10 min (or less) that was reduced, even to below basal conditions, by 4 h. Pretreatment with PD98059 also blocked phosphorylation of Erk1/Erk2. Total Erk1/Erk2 protein level was determined by direct immunoblotting, and no change in the amount of Erk1/Erk2 protein was found (Fig. 3*B*). Next we

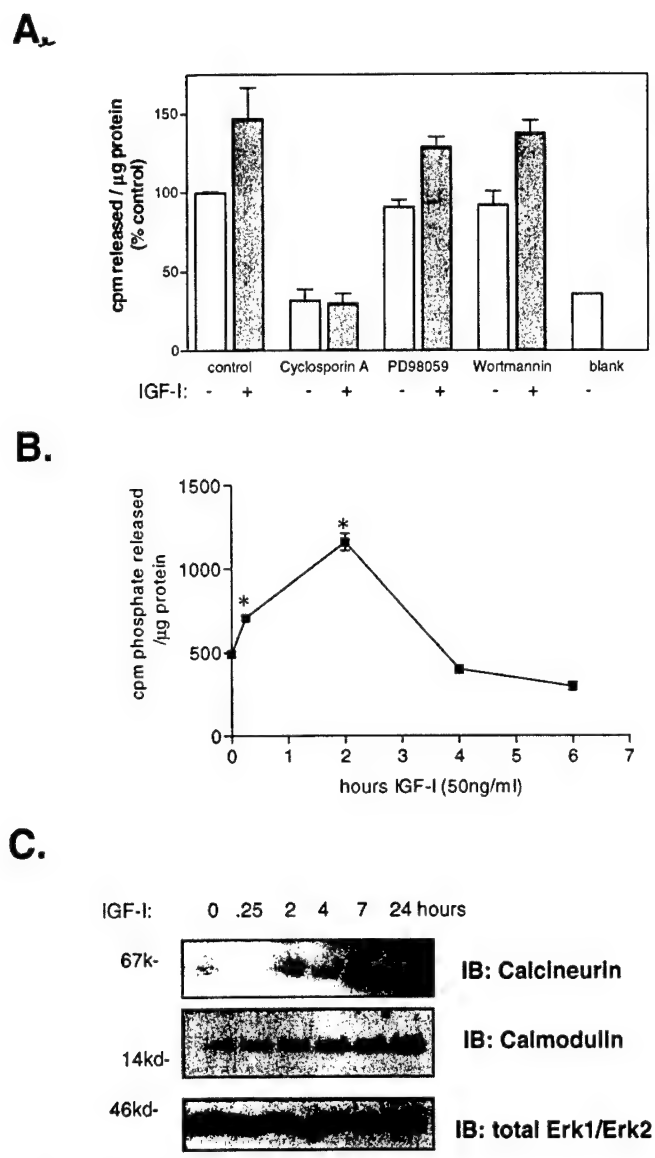

FIG. 5. **IGF-I stimulates calcineurin phosphatase activity and increases calcineurin and calmodulin proteins.** *A*, cells were pretreated with SFM, cyclosporin A (5 µM), PD98059 (10 µM), or wortmannin (250 nM) and then stimulated with IGF-I (50 ng/ml) for 2 h. Protein lysates were collected, and calcineurin phosphatase activity was determined as described under "Experimental Procedures." Data shown are the mean of duplicate assays ± S.E. *B*, calcineruin phosphatase activity was measured determined following treatment with IGF-I for up to 6 h. * $p < 0.01$ compared with 0 h treatment. Data shown are the mean of duplicate assays ± S.E. *C*, cells were treated with IGF-I (50 ng/ml) for up to 24 h and total protein lysates were collected. Calcineurin and calmodulin were detected by direct immunoblotting with specific antibodies. Data shown are representative of at least 3 independent experiments.

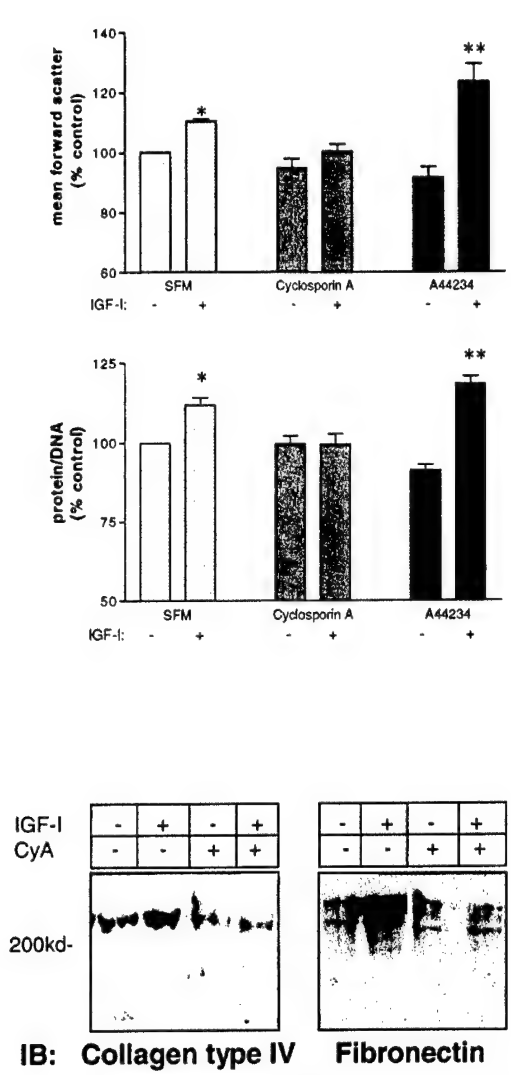

FIG. 6. **Calcineurin is required for IGF-I-mediated hypertrophy and up-regulation of ECM.** *A*, cells were pretreated for 1 h with SFM or cyclosporin A (5 µm) and then incubated with IGF-I for 24 h. Additionally, cells were pretreated with calcium ionophore A23187 (1.5 µm) for 1 h, washed twice with SFM, and then incubated with IGF-I for 24 h. Cells size was determined by mean forward light scatter. Bars represent the mean ± S.E. of four independent experiments. Cells were also analyzed for DNA and protein content and the protein/DNA ratio of triplicate samples ± S.E. was determined. * $p < 0.05$ from control and ** $p < 0.05$ from IGF-I. *B*, cells were pretreated for 1 h with SFM or cyclosporin A (5 µm) and then incubated with IGF-I (100 ng/ml) for 72 h. Total cellular proteins were collected and separated by SDS-PAGE. Collagen type IV and fibronectin were detected by direct immunoblotting. Data shown are representative of at least 3 independent experiments.

inhibit calcineurin activity prior to addition of IGF-I. Both IGF-I-mediated increase in cell size and increase in protein/DNA ratio were blocked following inhibition of calcineurin. Moreover, pretreatment of the cells with calcium ionophore A23187 to increase intracellular calcium significantly increased IGF-I-mediated hypertrophy (Fig. 6*A*). Next we determined if calcineurin was required for IGF-I-mediated induction of ECM. Fig. 6*B* shows that pretreatment with cyclosporin A blocked IGF-I-mediated increase in both collagen type IV and fibronectin protein levels. Cyclosporin A alone had no effect on either total protein synthesis (reflected by protein/DNA ratio) or on basal levels of collagen type IV or fibronectin.

Inhibition of PI3K with wortmannin only abolished Akt phosphorylation at 10 min and had no effect on IGF-I-mediated Akt phosphorylation at 4 h (Fig. 3*D*). The lack of inhibition of the delayed Akt activation by wortmannin suggests a PI3K-independent mechanism of sustained Akt activation. Therefore, in Fig. 7*A*, we examined the role of calcineurin in sustained Akt activation. MC were pretreated with SFM (control), wortmannin (250 nM), or cyclosporin A (5 µm) and then treated with IGF-I for 10 min or 4 h. Phosphorylated Akt was detected by Western blotting with a phospho-specific Akt antibody. At 10 min, wortmannin greatly reduced IGF-I-mediated Akt phosphorylation, as shown before, whereas cyclosporin A had no effect. After 4 h of IGF-I treatment, Akt phosphorylation is still detectable in control cells, and wortmannin pretreatment does not reduce this phosphorylation. However, pretreatment with

role of each signaling pathway in mediating the biological effects of IGF-I remains to be characterized. Although Erk1/Erk2 MAPK was activated by IGF-I in our studies, it does not appear to be required for induction of hypertrophy. It is still possible that the MAPK pathway might be important for other cellular responses to IGF-I, including migration, modulation of DNA synthesis, and cell survival. Treatment of MCs with IGF-I also resulted in the activation of PI3K and Akt kinase. Interestingly, the serine/threonine kinase Akt is activated by IGF-I in a bi-phasic manner. IGF-I induced rapid activation of Akt (10 min) that was inhibited by wortmannin, demonstrating that this activation is mediated by PI3K. However, wortmannin had no effect on the delayed phase of Akt activation, indicating a PI3K-independent mechanism of activation. Inhibition of PI3K by wortmannin or LY294002 had no effect on IGF-I-induced hypertrophy, demonstrating that PI3K is not required for this biological effect of IGF-I. However, the sustained activation of Akt *was* inhibited by cyclosporin A, indicating that activation of calcineurin by IGF-I is responsible for the sustained Akt activation in MCs. Our data support other reports in the literature that calcineurin activation can act in concert with other signaling pathways (31, 32). The consequences of sustained Akt activation by calcineurin and the role of Akt in IGF-I-mediated hypertrophy remain to be evaluated.

Our data show that IGF-I treatment of MCs not only increases the levels of calcineurin protein, but also calmodulin. As calcineurin activation is dependent upon availability of calmodulin (33), one possible consequence of increased calmodulin is sustained activation of other calcium/calmodulin pathways and/or priming of the calcineurin/calmodulin system for activation by other signals. Interestingly, the increase in both calcineurin and calmodulin occurs rapidly following IGF-I treatment, particularly in comparison to the global increase in protein reflected in the protein/DNA ratio. This suggests that the IGF-I-mediated increase in calcineurin and calmodulin protein expression is a specific action of IGF-I and not merely a consequence of the generalized increase in protein synthesis associated with hypertrophy. However, a more dynamic assay of protein synthesis such as incorporation of [^{35}S]methionine into proteins would more accurately address the contribution of global protein synthesis to the increased expression of calcineurin and calmodulin. Moreover, our data do not address the contribution of protein degradation to the modulation of calcineurin/calmodulin levels.

Interestingly, calcineurin activation occurred fairly late after IGF-I treatment. Both Erk1/Erk2 MAPK and Akt are phosphorylated within minutes of IGF-I addition and peak activation has subsided in less than 1 h. Calcineurin activity appears to peak ~2 h following addition of IGF-I and returns to baseline by 4–6 h. Additionally, calcineurin activation precedes a significant increase in calcineurin and calmodulin protein levels, as well as induction of hypertrophy by IGF-I. Our data show that this increase in phosphatase activity is in fact required for IGF-I-mediated hypertrophy. Inhibition of calcineurin with cyclosporin A completely blocks IGF-I-mediated activation of calcineurin phosphatase activity and IGF-I-mediated hypertrophy and ECM accumulation. These effects of cyclosporin A on matrix protein accumulation were specific, because the compound had no effect on total protein synthesis or on the levels of other proteins such as Erk1/Erk2. Of interest is the finding in Fig. 6*A* that increased intracellular calcium due to treatment with ionophore A23187 did not induce hypertrophy. This is consistent with the observation, reported by Musaro *et al.* (34), that calcium alone is actually toxic to some cells. Instead, there appears to be a requirement for an additional IGF-I-mediated signal to generate a hypertrophic response. One possibility is cross-talk with other signaling pathways such as Akt (35, 36).

Several proteins have been identified as targets of calcineurin-mediated dephosphorylation, including NFAT, MEF2A and -2D, and GATA (15, 33). Our data demonstrate that calcineurin is important in IGF-I-mediated hypertrophy. Therefore, calcineurin substrates may also be critical signaling molecules that mediate hypertrophy in MCs. IGF-I induces nuclear localization of NFATc1, which is dependent upon calcineurin activity. Therefore, NFATc1 may be important in transcriptional regulation of hypertrophic response genes, including ECM genes and possibly even of calcineurin and calmodulin. It remains to be seen whether other calcineurin substrates also play a role in the regulation of genes responsible for cell hypertrophy.

The demonstration that IGF-I activates a calcium-dependent serine/threonine phosphatase in mesangial cells introduces a new paradigm in IGF signaling. In addition to its role as a mitogen, requiring primarily the MAPK and PI3K signaling pathways, our work and the work of other groups in this area show that IGF-I elicits relevant biological responses via calcium-dependent signaling pathways, including, but possibly not limited to, calcineurin phosphatase. Similarly, this study demonstrates another potential target tissue for the action of calcineurin. Discovering how growth factors such as IGF-I activate calcineurin and what factors downstream of calcineurin are required for inducing hypertrophy will be important areas for further research. Furthermore, calcineurin represents an intriguing new pathway with substantial relevance in renal disease. Treatment of animal models of cardiac hypertrophy with inhibitors of calcineurin have been successful at preventing hypertrophy (22, 26, 32); therefore, it is possible that calcineurin inhibitors may also be of therapeutic value in renal diseases characterized by hypertrophy.

Acknowledgment—We acknowledge Dr. Goutam Ghosh Choudhury for helpful discussion and review of the manuscript.

REFERENCES

1. Wolf, G., and Ziyadeh, F. N. (1999) *Kidney Int.* **56,** 393–405
2. Gronbaek, H., Volmers, P., Bjorn, S., Osterby, R., Orskov, H., and Flyvbjerg, A. (1997) *Am. J. Physiol.* **272,** E918–E924
3. Verotti, A., Cieri, F., Petitti, M., Morgese, G., and Chiarelli, F. (1999) *Diabetes Nutr. Metab.* **12,** 271–276
4. Flyvbjerg, A. (1997) *Kidney Int.* **52,** S12–S19
5. Feld, S., and Hirschberg, R. (1996) *Endocr. Rev.* **17,** 423–480
6. Sugimoto, H., Shikata, K., Makino, H., Ota, K., and Ota, Z. (1996) *Nephron* **72,** 648–653
7. Doi, T., Striker, L. J., Quaife, C., Conti, F. G., Palmiter, R., Behringer, R., Brinster, R., and Striker, G. E. (1988) *Am. J. Pathol.* **131,** 398–403
8. Quaife, C. J., Mathews, L. S., Pinkert, C. A., Hammer, R. E., Brinster, R. L., and Palmiter, R. D. (1989) *Endocrinology* **124,** 40–48
9. Flyvbjerg, A., Marshall, S. M., Frystyk, J., Hansen, K. W., Harris, A. G., and Orskov, H. (1992) *Kidney Int.* **41,** 805–812
10. Flyvbjerg, A., Bennet, W. F., Rasch, R., Kopchick, J. J., and Scarlett, J. A. (1999) *Diabetes* **48,** 377–382
11. Yenush, L., and White, M. (1997) *Bioessays* **19,** 491–500
12. di Mari, J., Davis, R., and Safirstein, R. (1999) *Am. J. Physiol.* **2777,** F195–F203
13. Horney, M. J., Shirley, D. W., Kurtz, D. T., and Rosenzweig, S. A. (1998) *Am. J. Physiol.* **274,** F1045–F1053
14. Shultz, P., DeCorleto, P., Silver, B., and Abboud, H. (1988) *Am. J. Physiol.* **255,** F674–F684
15. Blaser, F., Ho, N., Prywes, R., and Chatila, T. (2000) *J. Biol. Chem.* **275,** 197–209
16. Choudhury, G. G., Karamitsos, C., Hernandez, J., Gentilini, A., Bardgette, J., and Abboud, H. E. (1997) *Am. J. Physiol.* **273,** F931–F938
17. Fruman, D. A., Pai, S.-Y., Klee, C. N., Burakoff, S. J., and Bierer, B. E. (1996) *Methods Enzymol.* **9,** 146–154
18. Abboud, H. E. (1997) *Kidney Int.* **52,** S3–S6
19. Choi, M., Eung-Gook, K., and Ballerman, B. (1993) *Kidney Int.* **44,** 948–958
20. Schreiber, B., Hughes, M., and Groggel, G. (1995) *Clin. Nephrol.* **43,** 368–374
21. Pricci, F., Pugliese, G., Romano, G., Romeo, G., Locuratolo, N., Pugliese, F., Mene, P., Galli, G., Casini, A., Rotella, C., and Di Mario, U. (1996) *Endocrinology* **137,** 879–885
22. Sussman, M. A., Lim, H. W., Gude, N., Taigen, T., Olsen, E. N., Wieczorek, D. F., and Molkentin, J. D. (1998) *Science* **281,** 1690–1693
23. Molkentin, J., Lu, J., Antos, C., Markham, B., Richardson, J., Robbins, J., Grant, S., and Olsen, E. (1998) *Cell* **93,** 215–228
24. Schreiber, S., and Crabtree, G. (1992) *Immunol. Today* **13,** 136–142
25. Tumlin, J. A. (1997) *Am. J. Kidney Dis.* **30,** 884–895
26. Lim, H. W., De Windt, L. J., Steinberg, L., Taigen, T., Witt, S. A., Kimball,

Effect of Platelet-Derived Growth Factor (PDGF) Isoforms in Rat Metanephric Mesenchymal Cells

Running title: PDGF Signaling in Metanephric Cells

Jill M. Ricono[1,3], Mazan Arar [2], Goutam Gosh Choudhury [4,5], Hanna E. Abboud[1,3,5].

From the Departments of Medicine[1] and Pediatrics [2], and the Department of Molecular Medicine, Institute of Biotechnology [3], The University of Texas Health Science Center and GRECC [4], South Texas Veterans Health Care System[5], San Antonio, TX, 78229-3900.

§To whom all correspondence should be addressed: Hanna E. Abboud, Department of Medicine, The University of Texas Health Science Center, 7703 Floyd Curl Drive, MC 7882, San Antonio, Texas 78229-3900.

Phone: (210) 567-4700: Fax: (210) 567-4712; E-mail: abboud@uthscsa.edu

Abstract

PDGF B-chain or PDGF receptor β-deficient mice lack mesangial cells. To explore potential mechanisms for failure of PDGF A chain to rescue mesangial cell phenotype, we investigated the biologic effects and signaling pathways of PDGF AA and PDGF BB in MM cells isolated from rat kidneys. PDGF AA caused modest cell migration but had no effect on DNA synthesis unlike PDGF BB which potently stimulated migration and DNA synthesis. PDGF AA and PDGF BB significantly increased the activities of PI3-K and MAPK. PDGF BB was more potent than PDGF AA in activating PI3-K or MAPK in these cells. Pretreatment of MM cells with the MEK inhibitor, PD098059, abrogated PDGF BB-induced DNA synthesis, whereas the PI3-K inhibitor, Wortmannin, had a very modest inhibitory effect on DNA synthesis (~Δ 20%). On the other hand, Wortmannin completely blocked PDGF AA and PDGF BB-induced migration, whereas PD098059 had a modest inhibitory effect on cell migration. These data demonstrate that activation of MAPK is necessary for the mitogenic effect of PDGF BB, whereas PI3-K is required for the chemotactic effect of PDGF AA and PDGF BB. Although PDGF AA stimulates PI3-K and MAPK activity, it is not mitogenic and only modestly chemotactic. Collectively the data may have implications related to the failure of PDGF AA to rescue mesangial cell phenotype in PDGF B-chain or PDGF receptor β-deficiency.

Keywords. Kidney, Development, Mesangial cell, Signal transduction.

Introduction

There is evidence that glomerular microvascular cells arise from metanephric mesenchyme (14). The spatial and temporal distribution of Platelet-derived growth factor (PDGF) and its receptors (PDGFR) suggest a role for this growth factor in development of mesangial cells (18) and has been conclusively demonstrated in two studies where PDGF B-chain or PDGFR β-deficient mice lack mesangial cells (16, 21). PDGF is widely expressed in a variety of mesenchymal cells during development. Siefert *et al.* (18) mapped the expression patterns of PDGF ligands and receptors in the developing and adult murine kidney using *in situ* hybridization (Fig. 1). During glomerular development, as the renal vesicle epithelium progresses through the comma and S-shaped stages, both PDGF A-chain and B-chains are expressed in epithelial cells. PDGF A-chain is expressed earlier and is seen even at the renal vesicle stage, whereas PDGF B-chain expression occurs at later stages and at the earliest is seen in the S-shaped bodies of the developing glomerular structures. PDGFR α and PDGFR β are expressed by mesenchymal cells in the metanephric blastema. At later stages, PDGFR α is expressed in cells surrounding the glomerulus and PDGFR β transcripts are present in the mesenchymal/interstitial cells that are recruited into the glomerular cleft which will form the vascular tuft of the mature glomerulus (18). These cells express PDGFR β and PDGF B-chain transcripts at high levels during the later stages of glomerular development when microvasular (capillary) cells begin to fill the glomerular tuft. At this stage, PDGFR α transcripts are barely detectable and PDGF A-chain transcripts are undetectable. Utilizing both immunohistochemistry and *in situ* hybridization, Arar *et al.* (2) showed similar findings in the rat with PDGFR β localizing to metanephric mesenchymal cells at early stages of development, cells within the cleft of the S-shaped bodies of the maturing glomerulus and at later stages in the mature glomerulus. This study also demonstrated that activation of the PDGFR β by PDGF BB

isoform mediates metanephric mesenchymal cell migration and DNA synthesis providing one mechanism by which a subpopulation of these cells potentially develop into mesangial cells. However, the failure of PDGFR α to compensate for the lack of β receptor in the PDGFR β-deficient mice remains unexplained considering that the α receptor, similar to the β receptor, localizes to mesenchymal cells in the metanephric blastema, and PDGF A-chain similar to the B-chain is also expressed in epithelial cells of the maturing glomerulus.

Binding of PDGF dimers to the extracellular domain of the receptor induces the receptor to dimerize and trans-autophosphorylate. Autophosphorylation of the receptor increases its intrinsic tyrosine kinase activity and provides docking sites for downstream signal transduction proteins (1, 9). Many of these tyrosines interact directly or indirectly with the SH2 domains of signaling molecules and are present in homologous positions with respect to the PDGFR α and PDGFR β. Activation of PDGFR initiates several major signal transduction cascades which include activation of PI3-K, PLCγ1, and Ras/Raf/MEK/MAPK (ERK1/2) pathways (3, 5, 8). Expression of mutant PDGFR β whose tyrosine residues are replaced with phenylalanine demonstrated an essential role for PI3-K and PLCγ1 in proliferation and chemotaxis in different cell types (6, 20, 22, 23). Additional studies demonstrated that these responses are cell-specific (12). Because PDGF B-chain and PDGFR β appear to be essential for mesangial cell development, and signaling through the PDGFR α does not seem to compensate for the loss of PDGFR β signaling, we examined the biological effects of PDGF AA and PDGF BB on MM cells and the role of ERK1/2 and PI3-K.

Materials and Methods:

Materials

Tissue culture materials were purchased from GIBCO/BRL (Rockville, MD). Recombinant PDGF-AA and PDGF-BB were obtained from R&D Systems (Minneapolis, MN). Wortmannin and PD098059 were purchased from Alexis (San Diego, CA). Myelin Basic Protein (MBP), Phosphatidylinositol (PI), Collagenase and Collagen type I were obtained from Sigma (Saint Louis, MO). Primary antibodies to PDGFR β (A-3) and PDGFR α (951) were purchased from Santa Cruz Biotechnology Inc. (Santa Cruz, CA). Secondary antibodies conjugated to Cy3 or FITC were obtained from Chemicon (Temecula, CA). Protein measurement and polyacrylamide gel reagents were purchased from Bio-Rad (Hercules, CA). Anti-phosphotyrosine and Erk-1 polyclonal antibody were also purchased from Santa Cruz Biotechnology Inc. (Santa Cruz, CA). Protein A sepharose was obtained from Pierce (Rockford, IL). All other reagents were high quality analytical grade.

Cultured cells

Primary metanephric mesenchymal cell cultures (MM) were prepared as previously described (2, 10). Briefly, pregnant Harlan Sprague-Dawley rats were purchased at 10-11 days of gestation. At gestational day 13, mothers were anesthetized by intramuscular injection of rat mixture (60% Ketamine, 40% Xylazine), and embryos were collected. The age of the embryo was counted from the day of the vaginal plug (day 0). Embryos were dissected in 1X phosphate-buffer saline under a zoom model SZH Olympus stereo microscope. Embryonic kidneys were collected and cells were propagated in Dulbecco's Modified Eagle Medium (GIBCO) including 10% Fetal Calf Serum and grown at 37°C, 5% carbon dioxide.

MAPK assay

MM cells were plated $7.5X10^5$ cells/60mm dish, grown to confluency and serum starved for 48 hours. Respective cells were pretreated with 50 μM PD-098059, a MEK inhibitor, for 45 min. before being stimulated with PDGF-AA or PDGF-BB. Cells were lysed with RIPA buffer (20mM Tris HCl, pH 7.5, 150mM NaCl, 5mM EDTA, 1%NP-40, 1mM Na_3VO_4, 1mM PMSF and 0.1% aprotinin) for 30 minutes at 4°C and centrifuged at 10,000Xg for 20 minutes at 4°C. Protein concentrations were measured in the cell lysates. Equal amounts of protein (100μg) were incubated with ERK-1 polyclonal antibody for 30 minutes on ice. Fifteen microliters Protein A Sepharose beads (50% vol/vol slurry) were added and incubated at 4°C on a rocking platform for two hours. The immunobeads were washed and resuspended in MAPK assay buffer (10mM HEPES, pH 7.4, 10mM $MgCl_2$, 0.5mM dithiothreitol, and 0.5mM Na_3VO_4) in the presence of 0.5 mg/ml myelin basic protein (MBP) and 25μM cold ATP plus 1μCi[γ-^{32}P]ATP. The mixture was incubated at 30°C for 30 minutes followed by a 10 minute incubation on ice. Protein loading buffer was added and reactions were boiled. Samples were then loaded on a 12.5% SDS-PAGE, and phosphorylated MBP was visualized by autoradiography (5).

Western Blotting

Equal amounts of protein from cell lysates were separated on a 12.5% SDS-PAGE and electrophoretically transferred to polyvinyl membrane. The membrane was blocked with 5% nonfat milk prepared in TBST buffer, washed with TBST and incubated with ERK-1 primary antibody (Santa Cruz) (1:200 dilution). The membrane was then washed and incubated with horseradish peroxidase-conjugated goat-anti rabbit IgG. The blot was developed with ECL reagent.

PI3-K assay

MM cells were plated as above. Respective cells were pretreated with 250nM Wortmannin, a PI3-K inhibitor, for 3 hours prior to treatment with PDGF. Cells were lysed and protein analyzed as previously mentioned. 100 μg of protein were incubated with anti-phoshotyrosine antibody for 30 minutes on ice. Fifteen microliters Protein A Sepharose beads (50% vol/vol slurry) were added and incubated at 4°C on a rocking platform for two hours. The immunobeads were washed three times with RIPA, once with PBS, once with buffer A (0.5mM LiCl, 0.1 M Tris-HCl, pH 7.5, 1mM Na_3VO_4), once with double distilled water and once with buffer B (0.1M NaCl, 0.5mM EDTA, 20mM Tris-HCl, pH 7.5). The immunobeads were then resuspended in 50 μl of PI3-K assay buffer (20mM Tris-HCl, pH 7.5, 0.1M NaCl, and 0.5mM EGTA). 0.5ul of 20mg/ml PI was added and incubated at 25°C for 10 minutes. A cocktail of 1μl of 1 M $MgCl_2$ and 10 μCi[γ-^{32}P]ATP was added and incubated at room temperature for 10 minutes. 150μl of a mixture of chloroform, methanol, and 11.6N HCl (50:100:1) was added to stop the reaction, and an additional 100ul of chloroform was added. The organic layer is extracted and washed with methanol and 1N HCl (1:1). The reaction was dried overnight and resuspended in 10μl of chloroform. The samples were separated by Thin Layer Chromatography and developed with $CHCl_3$/MeOH/28%NH_4OH/H20 (129:114:15:21). The spots were visualized by autoradiography (5).

DNA Synthesis

MM cells were plated at $7.5X10^4$ cells/24 well dish, grown to confluency, and serum starved for 48 hours. Cells were either pretreated with PD-098059 or Wortmannin as previously described before stimulation with PDGF isoforms. One μCi/25ml of ^{3}H-TdR was added to each well. DNA synthesis is measured as incorporation of [^{3}H] thymidine into trichoroactic acid-insoluble material (7).

Cell Migration Assay

Cell migration in response to PDGF is determined using Blind well chamber assays. Confluent MM cells were serum starved for 48 hours, then pretreated with PD098059, Wortmannin or LY294002 . The monolayer of cells are trypsinized and resuspended in serum free media. The cell suspension is added to the top chamber, while the PDGF is added to the bottom chamber of the apparatus. A polycarbonate membrane filter coated with collagen I separates the chambers. After 4 hours at 37° C, the cells on the upper surface of the filter are removed with a cotton-tip applicator and migratory cells on the lower surface of the filter are fixed in methanol and stained with Giensa. Migration of cells is analyzed by counting the number of cells that have migrated through the polycarbonate filter using high magnification (X450) (7).

Immunofluorescence

For PDGF receptor α and β double immunoflourescent staining, cells are grown on 8 well cover slips to near confluency. Cells are fixed in methanol and washed in 1X PBS with 0.1% BSA. Primary antibody (PDGFRβ) 1:20 is added and cover slips are incubated for 30 min. at room temperature in a humidifier. Cells are washed 3X for 5min each. Respective secondary antibody (Donkey anti-mouse Cy3 conjugated) 1:30 is added and cover slips are incubated for an additional 30 min at room temperature in a humidifier. For the PDGFR α, cells are washed 3X for 5min each and the primary antibody (PDGFRα) 1:20 is added and cover slips are incubated for 30 min at room temperature in a humidifier. Respective secondary antibody (Donkey anti-Rabbit FITC conjugated) 1:20 is added and cover slips are incubated for an additional 30 min at room temperature in a humidifier. Cells are washed 3X for 5min and mounted with crystal mount. Cells are viewed with respective fluorescent filters with UV light.

Results

Effect of PDGF isoforms on MM cell DNA synthesis and migration

PDGF AA and PDGF BB were examined for their ability to stimulate DNA synthesis as measured by [^{3}H] thymidine incorporation into DNA of quiescent MM cells. When cells were treated with PDGF BB for 24 hours, [^{3}H] thymidine incorporation increased nearly 5 fold above basal levels at concentrations of 10 ng/ml and 100 ng/ml of PDGF BB. However, similar concentrations of PDGF AA did not increase DNA synthesis above basal levels (Fig. 2A). In addition to proliferation, migration is an important biological response during organ development. The same passage MM cells used for the [^{3}H] thymidine incorporation were used for the migration assays. PDGF BB induced migration of MM cells 4-5 fold above base line with a maximal effect seen at a dose of 10 ng/ml. PDGF AA also induced migration in the MM cells approximately 2 fold above basal levels at a dose of both 10 ng/ml and 100 ng/ml, however the response was much weaker than that of PDGF BB (Fig. 2B).

PDGF activation of MAPK in MM cells

Activated PDGFR β is known to associate with Grb2/sos which lies upstream of the Ras/MEK/ERK signaling pathway. In contrast, activated PDGFR α has been reported to associate with Crk adaptor protein which may also lie upstream of Ras/MEK/ERK signaling pathway. To determine if MAPK (ERK1/2) is activated in MM cells, we measured the kinase activity in ERK1/2 immunoprecipitates of PDGF-stimulated MM cells. MM cells were stimulated with PDGF AA or PDGF BB for 5, 10, and 15 minutes. Both PDGF AA and PDGF BB stimulated ERK1/2 activity in MM cells (Fig. 3). Maximal activation was observed at 15 min. and therefore in all subsequent experiments cells were treated for 15 min. with the PDGF isoforms. Dose responses of PDGF–induced ERK1/2 activity showed that PDGF AA induced maximal ERK1/2 activity at 50 ng/ml and100 ng/ml, whereas PDGF BB-induced maximum

activity at 10 ng/ml (Fig. 4). These concentrations correspond to those required to stimulate proliferation and migration (Fig. 2A and B). In some experiments, cells were pretreated with a MEK inhibitor, PD098059 and assayed for ERK1/2 activity (Fig. 5). PD098059 reduced PDGF-induced ERK1/2 activity to near basal levels, indicating ERK1/2 activation in MM cells is mediated by the Ras/Raf/MEK/MAPK pathway. Western blot analysis of the ERK1/2 protein was performed on the same cell lysates as loading controls.

Effect of MAPK inhibitor on PDGF-induced DNA synthesis and migration in MM cells.

To assess the involvement of MAPK signaling pathways in DNA synthesis and migration of the MM cells, cells were pretreated with 50μM PD098095 for 45 min. prior to the addition of PDGF AA or PDGF BB. Pretreatment of cells with the MEK inhibitor abolished PDGF-induced DNA synthesis (Fig. 6A). This suggests that the Ras/Raf/MEK/MAPK pathway is a major contributor of PDGF-induced DNA synthesis in MM cells. Pretreatment of the MM cells with PD098095 significantly decreased migration induced by PDGF BB (Fig. 6B). However, PD098095 did not inhibit migration to basal levels as in PDGF-induced DNA synthesis (Fig. 6A). The same concentration of PD098095 which completely blocked PDGF AA-induced ERK1/2 activity (Fig. 5) did not significantly reduce PDGF AA-induced migration. These data suggest other pathways are involved in PDGF-induced migration.

PDGF activation of PI3-K

PI3-K has previously been shown to associate with tyrosine phosphorylated PDGF receptors. However, it has not been established if signaling by both PDGF isoforms through their respective receptors can activate PI3-K in MM cells. PI3-K activity was determined in anti-phosphotyrosine immunoprecipitates of lysate from PDGF AA or PDGF BB-stimulated cells. The immunoprecipitates were assayed for PI3-K activity as described in Methods. As shown in Fig. 7, both isoforms of PDGF activate PI3-K activity. PDGF BB showed a significant effect at

10ng/ml, whereas 100ng/ml of PDGF AA was necessary to induce significant activation. When cells were pretreated with Wortmaninn, a PI3-K inhibitor, the PDGFR-associated PI3-K activity in MM cells was significantly reduced (Fig. 8).

Effect of PI3-K inhibitor on PDGF-induced DNA synthesis and migration in MM cells.

We have recently shown that activation of PI3-K is necessary for PDGF-induced DNA synthesis and migration in mesangial cells (4). To determine the importance of PI3-K in MM cells, cells were pretreated with 250 nM Wortmannin for 3 hours prior to stimulation with PDGF isoforms. Wortmannin decreased PDGF-induced [^{3}H] thymidine incorporation by approximately 20% (Fig. 9A) unlike complete abolishment of activity when cells were pretreated with PD098059 (Fig. 6A). These data indicate that PI3-K plays a lesser role in PDGF-induced DNA synthesis than MAPK in MM cells. Two structurally dissimialar PI3-K inhibitors, Wortmannin and LY294002, completely block PDGF-induced migration in MM cells (Fig. 9B and 9C), whereas the MEK inhibitor decreased PDGF BB-induced migration by approximately 30% and PDGF AA-induced migration by approximately 15 % (Fig. 6B). These data suggest that PI3-K rather than MAPK, plays a predominant role in PDGF-induced migration.

Expression of PDGF ligands and receptors in MM cells

To study expression of the PDGFR α and β in MM cells immunofluorescence was performed using PDGFR α- and PDGFR β-specific antibodies. Fig. 10 shows abundant expression of both PDGFR α and PDGFR β in the MM cells. This suggests that these cells have the potential to respond to both PDGF isoforms.

Discussion

There are several potential mechanisms by which PDGF acting on metanephric mesenchymal cells leads to development of a subset of these cells into mature differentiated

mesangial cell phenotype. Two mechanisms pertinent to development include cell migration and cell proliferation. This study explored the effects of PDGF AA and BB isoforms on DNA synthesis and migration of MM cells isolated at the earliest stage, embryonic day 13, of the developing rat metanephric blastema. Arar *et al.* (2) have recently demonstrated that PDGF BB stimulates DNA synthesis and migration of these cells. Stimulation of cell migration by PDGF BB was associated with activation of PI3-K and inhibition of PI3-K blocked PDGF BB-induced migration. However, the role of other signal transduction pathways activated by PDGF BB was not explored. More importantly, the role of the PDGF A-chain in activating MM cells is not known. This information is pertinent since the PDGFR α does not appear to compensate for PDGFR β in rescuing mesangial cell phenotype in PDGFR β-deficiency. Moreover, during early stages of development and maturation of the glomerular capillary bed, the PDGF A-chain and PDGFR α have similar spatial and temporal distribution to PDGF B-chain and PDGFR β, respectively (18).

PDGF BB, as reported previously (2), stimulates DNA synthesis and robust migration of MM cells. We now demonstrate that PDGF AA, even at concentration as high as 100 ng/ml, was not mitogenic for these cells and resulted in modest effect on cell migration. Therefore, the lack of mitogenic effect of the PDGF A-chain and its inability to stimulate robust migration are potential mechanisms for failure of the PDGFR α to compensate for the PDGFR β in rescuing mesangial cell phenotype. Mouse chimeras composed of PDGFR β +/+ and -/- cells demonstrated that PDGFR β-/- cells fail to populate the glomerular mesangium whereas PDGFR β +/+ cells do, suggesting a direct permissive role of PDGF BB in mesangial cell development and maturation (17). Studies utilizing BrdU labeling demonstrated active proliferation of mesangial cell progenitors in cup-shaped and S-shaped glomeruli of wild type but not mutant mice. These studies suggested that proliferation of mesangial cell progenitors is a critical step

for mesangial cell development (17). Our finding of failure of PDGF AA to induce proliferation of MM cells support this contention. We next examined the activation of ERK1/2 by PDGF AA or PDGF BB and its involvement in PDGF-induced DNA synthesis and migration of MM cells. PDGF AA and PDGF BB increased ERK1/2 activity in a dose- and time-dependent manner (Fig. 3 and 4) with PDGF BB being slightly more potent than PDGF AA. Pretreatment of MM cells with the MEK inhibitor, PD-098059, at a concentration that abolished MAPK activity resulted in complete inhibition of DNA synthesis. However, the MEK inhibitor only partially blocked PDGF BB-induced cell migration and exerted a small but insignificant effect on PDGF AA-induced cell migration. These data indicate that the Ras/Raf/MEK/MAPK pathway is essential for PDGF BB-induced DNA synthesis in MM cells.

Cells expressing a PDGFR β mutant devoid of the binding sites for PI3-K, *i.e.* lacking Tyr-740 and Tyr-751, show no chemotactic responses to PDGF (15, 24), suggesting a role for PI3-K in cell migration. However, PI3-K regulates growth factor-induced migration in a cell type specific manner. For example, there is evidence that PI3-K does not mediate cell migration in smooth muscle cells activated by PDGF BB (12). PDGFR α-mediated migration also appears to be cell type specific. In lung fibroblasts, Swiss 3T3 and hematopoeitic 32D cells, activation of PDGFR α induces migration (13, 19, 25). However, in other cell types such as aortic endothelial cells and vascular smooth muscle cells, PDGF AA inhibits the chemotactic response. PDGF BB, as well as PDGF AA, induce PI3-K activity in MM cells with the AA isoform resulting in somewhat lesser induction of enzyme activity. Wortmannin, at concentrations that decreased PI3-K enzymatic activity, markedly inhibited PDGF-induced migration of MM cells. In contrast to its potent effect on cell migration, pretreatment of MM cells with Wortmannin reduced PDGF BB-induced DNA synthesis by approximately 20%. The data indicate that migration of MM cells in response to both PDGF isoforms is mediated via PI3-K. It is very

unlikely that the differential effect of PDGF isoforms is due to differential expression of PDGF α and β receptors in the cells, since both receptors were homogenously distributed in MM cells. The data also demonstrate that the lack of biological response to PDGF AA is not due to low number of alpha receptors or poor coupling of the AA ligand with the receptor since PDGF AA was almost as potent as PDGF BB in activating ERK1/2 at wide range of concentrations. Furthermore, PDGF AA isoform potently activated PI3-K almost to a similar degree as did the PDGF BB isoform. However, activation of these pathways, PI3-K and MAPK, by PDGF AA is not sufficient to induce DNA synthesis or robust migration in these cells. These data, taken together with the mesangial cell phenotype in the PDGFR β-deficient mouse suggest that in the absence of significant DNA synthesis, activation of PI3-K and subsequent migration is insufficient for the PDGFR α, which can be activated by PDGF AA or PDGF BB, to compensate for the loss of the PDGFR β. Of interest is the recent observation that mice with a PDGFR β mutant for PI3-K binding sites develop normally and do not exhibit an overt phenotype in the mesangium (11) suggesting that β receptor-mediated signaling through activated PI3-K is only of minor importance during mesangial cell development. Alternatively, other signaling molecules activated by the mutant β receptor are able to compensate for the loss of PI3-K signaling.

In conclusion, in this study we have shown that PDGF AA and PDGF BB activate PI3-K and MAPK enzymatic signaling pathways in metanephric mesenchymal cells. We have also shown that PDGF BB induces DNA synthesis primarily through the MAPK pathway and migration through the PI3-K pathway. The finding that PDGF AA had no effect on DNA synthesis while it stimulates modest migration of the cells suggest that the failure of PDGFR α to compensate for loss of the PDGFR β may be due to its inability to mediate these fundamental biological responses of MM cells. It is tempting to speculate that mesangial cell progenitors that may be stimulated to migrate eventually undergo apoptosis in the absence of the PDGF B-chain

or PDGFR β, or fail to sustain their proliferation or even their survival. A more comprehensive examination of molecules activated by the PDGFR β is required to understand the mechanism by which PDGF BB and PDGFR β activation result in mesangial cell development and maturation.

Footnotes

This study was supported in part by the Dept. Of Veterans Affairs Medical Research Service (G.G.C. and H.E.A.), National Institutes of Diabetes and Digestive and Kidney diseases Grant DK-33665 (to H.E.A) and DK-50190 (to G.G.C.), American Heart Association, Texas Affiliate Grants-in-Aid 97G-439 and Clinical Scientist Award from NKF (to M.A.).

Acknowledgments

We thank Dr. Yves Gorin for critically reading the manuscript and for valuable discussion.

References

1. Abboud, H., B. Bhandari, and G. Gosh Choudhury. Cell biology of platelet-derived growth factor in *Molecular Nephrology. Kidney Function in Health and Disease* Bonventre, J Schlondorf, D., New York: Dekker, 1995, pp. 573-590.

2. Arar, M., Y. C. Xu, I. Elshihabi, J. L. Barnes, G. G. Choudhury, and H. E. Abboud. Platelet-derived growth factor receptor beta regulates migration and DNA synthesis in metanephric mesenchymal cells. *J Biol Chem* 275: 9527-33, 2000.

3. Bazenet, C. E., and A. Kazlauskas. The PDGF receptor alpha subunit activates p21ras and triggers DNA synthesis without interacting with rasGAP. *Oncogene* 9: 517-25, 1994.

4. Choudhury, G. G., G. Grandaliano, D. C. Jin, M. S. Katz, and H. E. Abboud. Activation of PLC and PI 3 kinase by PDGF receptor alpha is not sufficient for mitogenesis and migration in mesangial cells. *Kidney Int* 57: 908-17, 2000.

5. Choudhury, G. G., C. Karamitsos, J. Hernandez, A. Gentilini, J. Bardgette, and H. E. Abboud. PI-3-kinase and MAPK regulate mesangial cell proliferation and migration in response to PDGF. *Am J Physiol* 273: F931-8, 1997.

6. Cospedal, R., H. Abedi, and I. Zachary. Platelet-derived growth factor-BB (PDGF-BB) regulation of migration and focal adhesion kinase phosphorylation in rabbit aortic vascular smooth muscle cells: roles of phosphatidylinositol 3-kinase and mitogen-activated protein kinases. *Cardiovasc Res* 41: 708-21, 1999.

7. Grandaliano, G., A. J. Valente, M. M. Rozek, and H. E. Abboud. Gamma interferon stimulates monocyte chemotactic protein (MCP-1) in human mesangial cells. *J Lab Clin Med* 123: 282-9, 1994.

8. Heldin, C. H. Structural and functional studies on platelet-derived growth factor. *Embo J* 11: 4251-9, 1992.

9. Heldin, C. H., A. Ostman, and L. Ronnstrand. Signal transduction via platelet-derived growth factor receptors. *Biochim Biophys Acta* 1378: F79-113, 1998.

10. Herzlinger, D., C. Koseki, T. Mikawa, and Q. al-Awqati. Metanephric mesenchyme contains multipotent stem cells whose fate is restricted after induction. *Development* 114: 565-72, 1992.

11. Heuchel, R., A. Berg, M. Tallquist, K. Ahlen, R. K. Reed, K. Rubin, L. Claesson-Welsh, C. H. Heldin, and P. Soriano. Platelet-derived growth factor beta receptor regulates interstitial fluid homeostasis through phosphatidylinositol-3' kinase signaling. *Proc Natl Acad Sci U S A* 96: 11410-5, 1999.

12. Higaki, M., H. Sakaue, W. Ogawa, M. Kasuga, and K. Shimokado. Phosphatidylinositol 3-kinase-independent signal transduction pathway for platelet-derived growth factor-induced chemotaxis. *J Biol Chem* 271: 29342-6, 1996.

13. Hosang, M., M. Rouge, B. Wipf, B. Eggimann, F. Kaufmann, and W. Hunziker. Both homodimeric isoforms of PDGF (AA and BB) have mitogenic and chemotactic activity and stimulate phosphoinositol turnover. *J Cell Physiol* 140: 558-64, 1989.

14. Hyink, D. P., D. C. Tucker, P. L. St John, V. Leardkamolkarn, M. A. Accavitti, C. K. Abrass, and D. R. Abrahamson. Endogenous origin of glomerular endothelial and mesangial cells in grafts of embryonic kidneys. *Am J Physiol* 270: F886-99, 1996.

15. Kundra, V., J. A. Escobedo, A. Kazlauskas, H. K. Kim, S. G. Rhee, L. T. Williams, and B. R. Zetter. Regulation of chemotaxis by the platelet-derived growth factor receptor-beta. *Nature* 367: 474-6, 1994.

16. Leveen, P., M. Pekny, S. Gebre-Medhin, B. Swolin, E. Larsson, and C. Betsholtz. Mice deficient for PDGF B show renal, cardiovascular, and hematological abnormalities. *Genes Dev* 8: 1875-87, 1994.

17. Lindahl, P., M. Hellstrom, M. Kalen, L. Karlsson, M. Pekny, M. Pekna, P. Soriano, and C. Betsholtz. Paracrine PDGF-B/PDGF-Rbeta signaling controls mesangial cell development in kidney glomeruli. *Development* 125: 3313-22, 1998.

18. Seifert, R. A., C. E. Alpers, and D. F. Bowen-Pope. Expression of platelet-derived growth factor and its receptors in the developing and adult mouse kidney. *Kidney Int* 54: 731-46, 1998.

19. Siegbahn, A., A. Hammacher, B. Westermark, and C. H. Heldin. Differential effects of the various isoforms of platelet-derived growth factor on chemotaxis of fibroblasts, monocytes, and granulocytes. *J Clin Invest* 85: 916-20, 1990.

20. Smith, R. J., L. M. Sam, J. M. Justen, G. L. Bundy, G. A. Bala, and J. E. Bleasdale. Receptor-coupled signal transduction in human polymorphonuclear neutrophils: effects of a novel inhibitor of phospholipase C-dependent processes on cell responsiveness. *J Pharmacol Exp Ther* 253: 688-97, 1990.

21. Soriano, P. Abnormal kidney development and hematological disorders in PDGF beta-receptor mutant mice. *Genes Dev* 8: 1888-96, 1994.

22. Valius, M., C. Bazenet, and A. Kazlauskas. Tyrosines 1021 and 1009 are phosphorylation sites in the carboxy terminus of the platelet-derived growth factor receptor beta subunit and are required for binding of phospholipase C gamma and a 64-kilodalton protein, respectively. *Mol Cell Biol* 13: 133-43, 1993.

23. Valius, M., J. P. Secrist, and A. Kazlauskas. The GTPase-activating protein of Ras suppresses platelet-derived growth factor beta receptor signaling by silencing phospholipase C-gamma 1. *Mol Cell Biol* 15: 3058-71, 1995.

24. Wennstrom, S., A. Siegbahn, K. Yokote, A. K. Arvidsson, C. H. Heldin, S. Mori, and L. Claesson-Welsh. Membrane ruffling and chemotaxis transduced by the PDGF beta-receptor require the binding site for phosphatidylinositol 3' kinase. *Oncogene* 9: 651-60, 1994.

25. Yu, J. C., M. A. Heidaran, J. H. Pierce, J. S. Gutkind, D. Lombardi, M. Ruggiero, and S. A. Aaronson. Tyrosine mutations within the alpha platelet-derived growth factor receptor kinase insert domain abrogate receptor-associated phosphatidylinositol-3 kinase activity without affecting mitogenic or chemotactic signal transduction. *Mol Cell Biol* 11: 3780-5, 1991.

Figure legends:

Figure 1: Schematic representation of the localization of PDGF ligands and PDGF receptors at various stages of the developing kidney based on data from Siefert *et al* and Arar *et al.*

Figure 2: Effect of Platelet-derived growth factor (PDGF) isoforms on DNA synthesis and migration. *(A)* ^{3}H-thymidine incorporation was measured as an index of DNA synthesis in response to treatment of 10ng/ml or 100 ng/ml of PDGF AA or PDGF BB in quiescent MM cells. Results are mean ±SE of four independent experiments. **$p<0.01$ vs. untreated control. *(B)*Serum-deprived quiescent MM cells were used in cell migration assay in the presence of 10ng/ml or 100 ng/ml of PDGF AA or PDGF BB, as described in Methods. The data represent mean ± SE of three independent experiments. **$p<0.01$ vs. untreated control.

Figure 3: Time Course of Activation of Mitogen-activated protein kinase (MAPK) in PDGF-treated MM cells. Serum-deprived quiescent MM cells were treated with 100 ng/ml of PDGF AA or 10 ng/ml of PDGF BB for various time points, 5, 10 and 15 min. Cleared cell lysates were immunoprecipitated with ERK-1 polyclonal antibody. The immunoprecipitates were then used in a *in vitro* immunecomplex kinase assay in the presence of myelin basic protein (MBP) and [γ-^{32}P]ATP as described in Methods. Phosphorylated MBP was separated on a 12.5%SDS polyacrylamide gel. Western Blot analysis of ERK 1/2 was done on the same cell lysates to determine the loading control. Each barogram represents the ratio of the radioactivity incorporated into the phosphorylated myelin basic protein quantified by Phosphor-Imager analysis factored by the densitometric measurement of ERK1/2 band. The data are expressed as percent of control where the ratio in the untreated cells was defined as 100 %. Values are the means ± S.E. of three independent experiments. ** $p<0.01$ versus control.

Figure 4: Effect of different doses of PDGF AA and BB on MAPK activity in MM cells. Quiescent MM cells were treated with varying concentrations of PDGF AA and BB. Cells were stimulated for 15 minutes with 10, 25, 50 or 100 ng/ml of PDGF AA or BB. Cleared cell lysates were immunoprecipitated with ERK-1 polyclonal antibody. The immunoprecipitates were then used in a *in vitro* immunecomplex kinase assay in the presence of myelin basic protein (MBP) and [γ-^{32}P]ATP as described in Methods. Phosphorylated MBP was separated on a polyacrylamide gel. Western Blot analysis of ERK 1/2 was done on the same cell lysates and used as loading controls. Each barogram represents the ratio of the radioactivity incorporated into the phosphorylated myelin basic protein quantified by Phosphor-Imager analysis factored by the densitometric measurement of ERK1/2 band. The data are expressed as percent of control where the ratio in the untreated cells was defined as 100 %. Values are the means $\pm$ S.E. of three independent experiments. ** $p<0.01$ versus control, *$p<0.05$.

Figure 5: Effect of MEK inhibitor on the Ras/Raf/MEK/ERK pathway. Quiescent MM cells were pretreated with 50μM PD098059 for 45 minutes prior to treatment with 100 ng/ml of PDGF AA or 10 ng/ml of PDGF BB. Cleared cell lysates were immunoprecipitated with ERK-1 polyclonal antibody. The immunoprecipitates were then used in a *in vitro* immunecomplex kinase assay in the presence of myelin basic protein (MBP) and [γ-^{32}P]ATP as described in Methods. Phosphorylated MBP was separated on a 12.5%SDS polyacrylamide gel. Western Blot analysis of ERK 1/2 was done on the same cell lysates and used as loading controls. Each barogram represents the ratio of the radioactivity incorporated into the phosphorylated myelin basic protein quantified by Phosphor-Imager analysis factored by the densitometric measurement of ERK1/2 band. The data are expressed as percent of control where the ratio in the untreated cells was defined as 100 %. Values are the means $\pm$ S.E. of three independent experiments. ** $p<0.01$ versus control

Figure 6. Effect of MEK inhibitor on PDGF-induced DNA synthesis and migration. Quiescent MM cells were pretreated with 50μM PD098059 for 45 minutes prior to treatment with PDGF AA or PDGF BB. *(A)* ^{3}H-thymidine incorporation was measured as an index of DNA synthesis in response to treatment of 10 or 100 ng/ml of PDGF AA or BB in quiescent MM cells. Results are mean ±SE of four independent experiments. **$p<0.01$ vs. untreated and treated with PD098059. *(B)* Serum-deprived quiescent MM cells were used in cell migration assay in the presence of 10 or 100 ng/ml of PDGF AA or BB, as described in Methods. The data represent mean ± SE of three independent experiments. **$p<0.01$ vs. untreated and treated with PD098059.

Figure 7: Activation of phosphatidylinositol 3-kinase (PI3-K) in PDGF-treated MM cells. *(A)* Serum deprived MM cells were treated with 10 or 100 ng/ml PDGF AA or PDGF BB for 15 minutes and cell lysates were immunoprecipitated with antiphosphotyrosine antibody. The immunoprecipitates were then assayed for PI3-kinase activity in the presence of phosphotidyl inositol (PI) and [γ-^{32}P]ATP as described in Methods. The arrow indicates the position of PI3-P spot. *(B)* Each barogram represents the radioactivity incorporated into PI3-P by Phosphor-Imager analysis. The data are expressed as percent of control where the untreated cells were defined as 100 %. Values are the means ± S.E. of three independent experiments, **$p<0.01$ vs. untreated control.

Figure 8: Effect of PI3-K inhibitor on PDGF-activated PI3-K in MM cells. Quiescent MM cells were pretreated with 250nM Wortmannin for 3 hours prior to treatment with PDGF AA or PDGF BB. Cleared cell lysates were immunoprecipitated with antiphosphotyrosine antibody and the immunoprecipitates were then assayed for PI3-kinase activity in the presence of phosphatidylinositol (PI) and [γ-^{32}P]ATP as described in Methods. The arrow indicates the position of PI3-P spot. *(B)* . Each barogram represents the radioactivity incorporated into PI3-P

by Phosphor-Imager analysis. The data are expressed as percent of control where the untreated cells were defined as 100 %. Values are the means ± S.E. of three independent experiments, **p<0.01 vs. untreated and treated with Wortmannin.

Figure 9: Effect of PI3-K inhibitor on PDGF-induced DNA synthesis and migration. Quiescent MM cells were pretreated with 250nM Wortmannin for 3 hours or 25 μM LY294002 for one hour prior to treatment with PDGF AA or PDGF BB. *(A)* ^{3}H-thymidine incorporation was measured as an index of DNA synthesis in response to treatment of 10 or 100 ng/ml of PDGF AA or BB in quiescent MM cells. Results are mean ±SE of four independent experiments. *p<0.05 vs. untreated and treated with Wortmannin. *(B)* Serum-deprived quiescent MM cells were used in cell migration assay in the presence of 10 or 100 ng/ml of PDGF AA or PDGF BB, as described in Methods. The data represent mean ± SE of three independent experiments. **p<0.01 vs. untreated and treated with Wortmannin. . *(C)* Serum-deprived quiescent MM cells were used in cell migration assay in the presence of 100 ng/ml of PDGF AA or 10 ng/ml of PDGF BB, as described in Methods. The data represent mean ± SE of three independent experiments. **p<0.01 vs. untreated and treated with LY294002.

Figure 10: Expression of PDGFR α and β in MM cells. *(A)* Immunofluoresent localization of PDGFR α. *(B)* Immunofluoresent localization of PDGFR β. All MM cells stain for both PDGF α and β receptors. Magnification 40X.

Figure 1

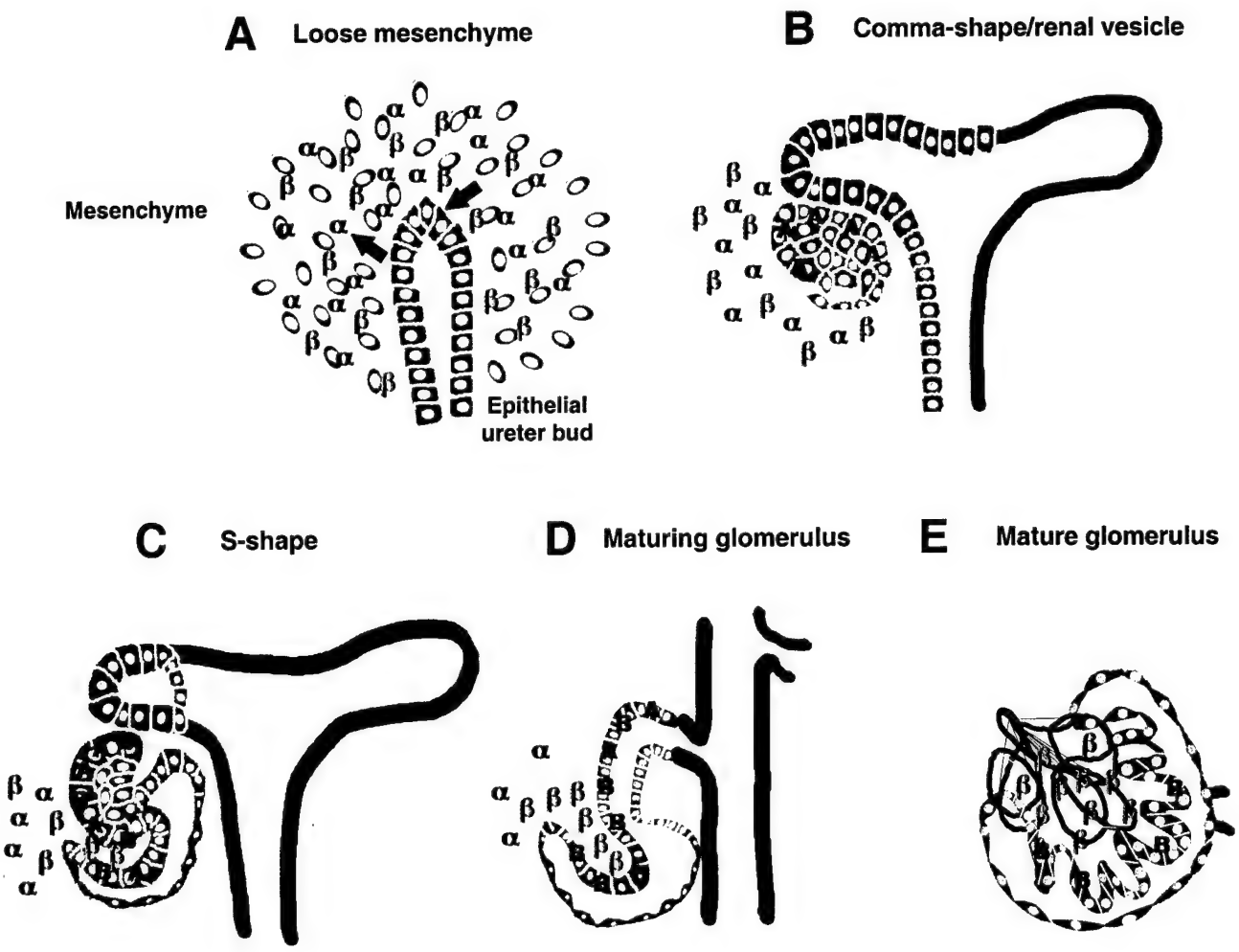

Ricono et al.

Figure 2

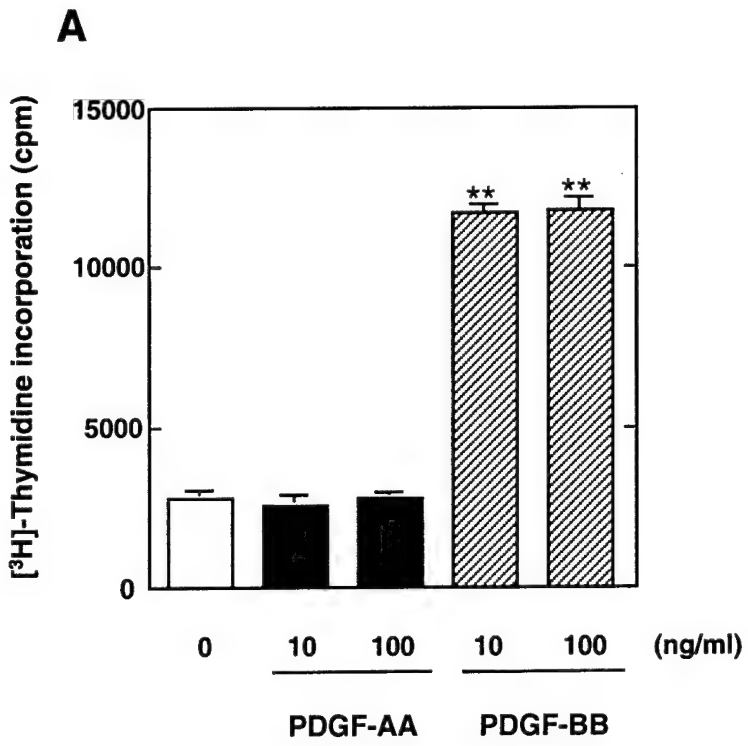

Ricono et al.

Figure 2

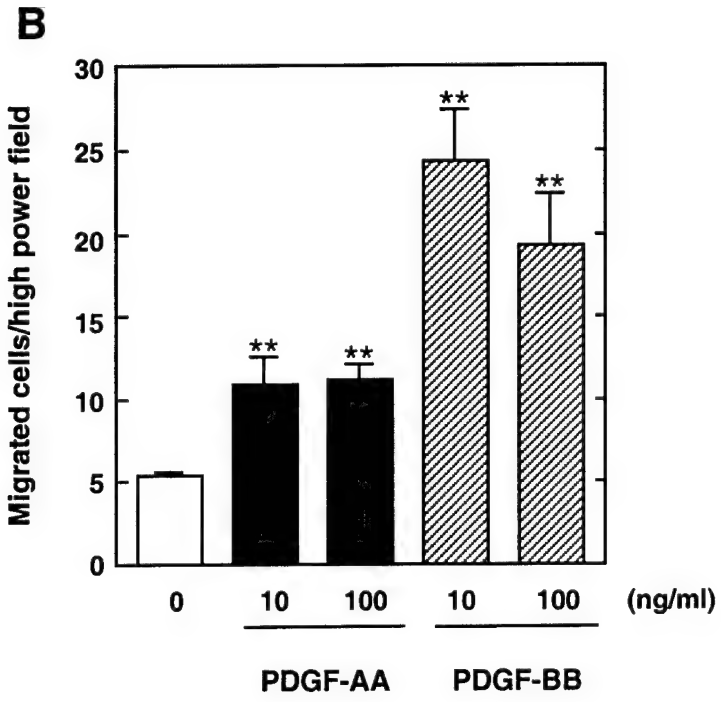

Ricono et al.

Figure 3

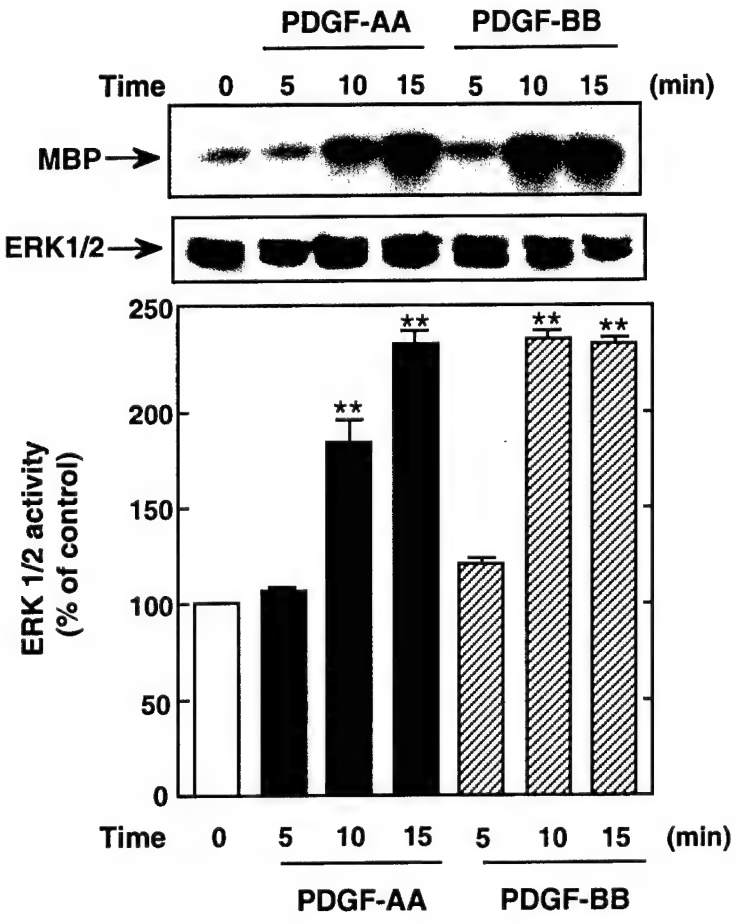

Ricono et al.

Figure 4

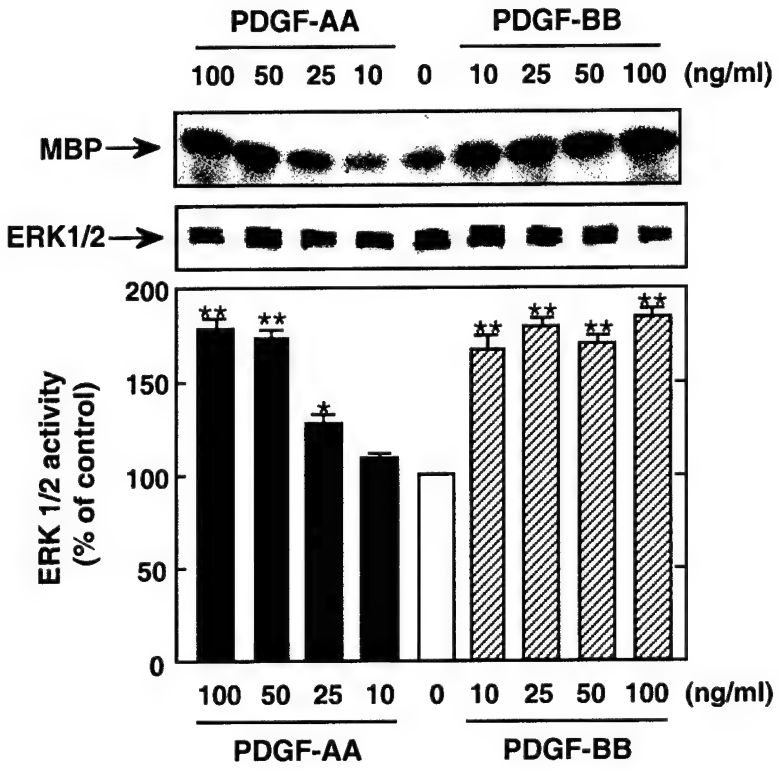

Ricono et al.

Figure 5

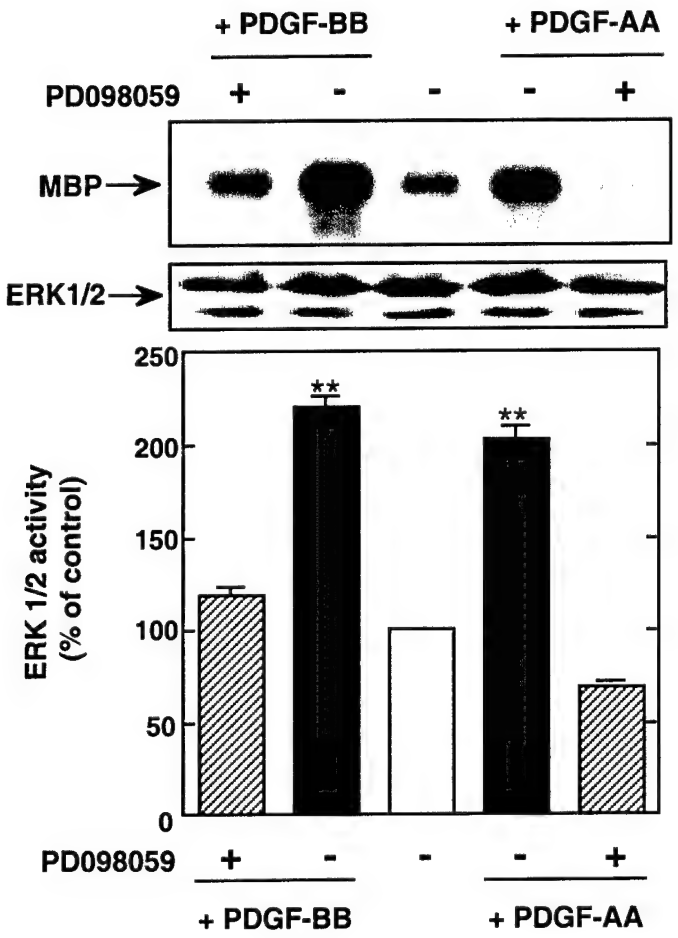

Ricono et al.

Figure 6

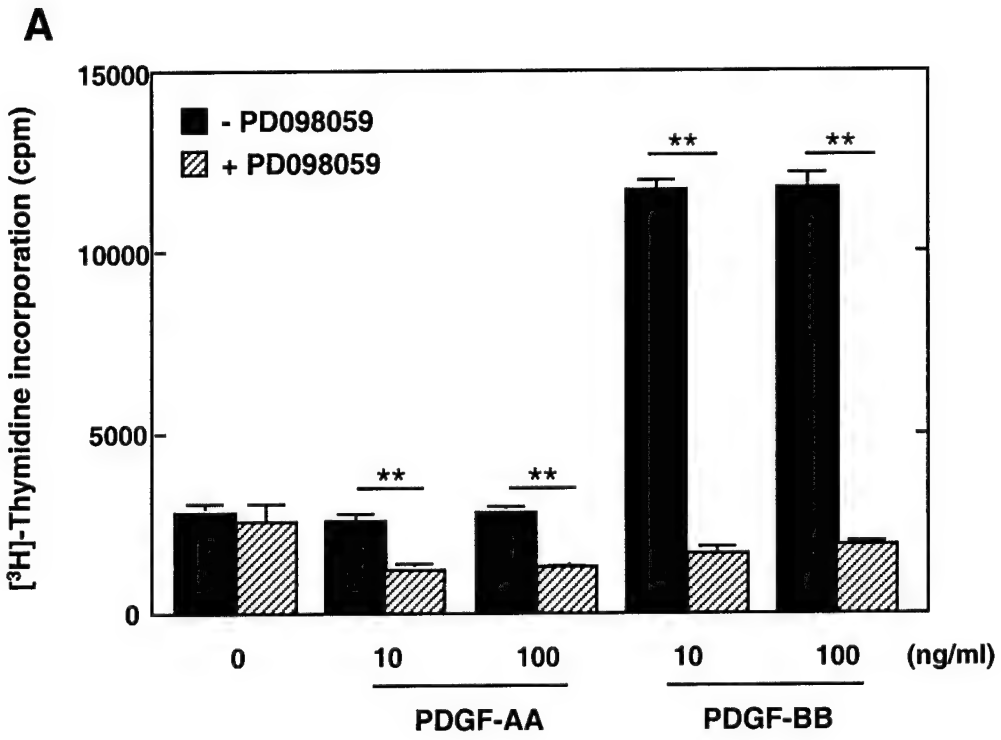

Ricono et al.

Figure 6

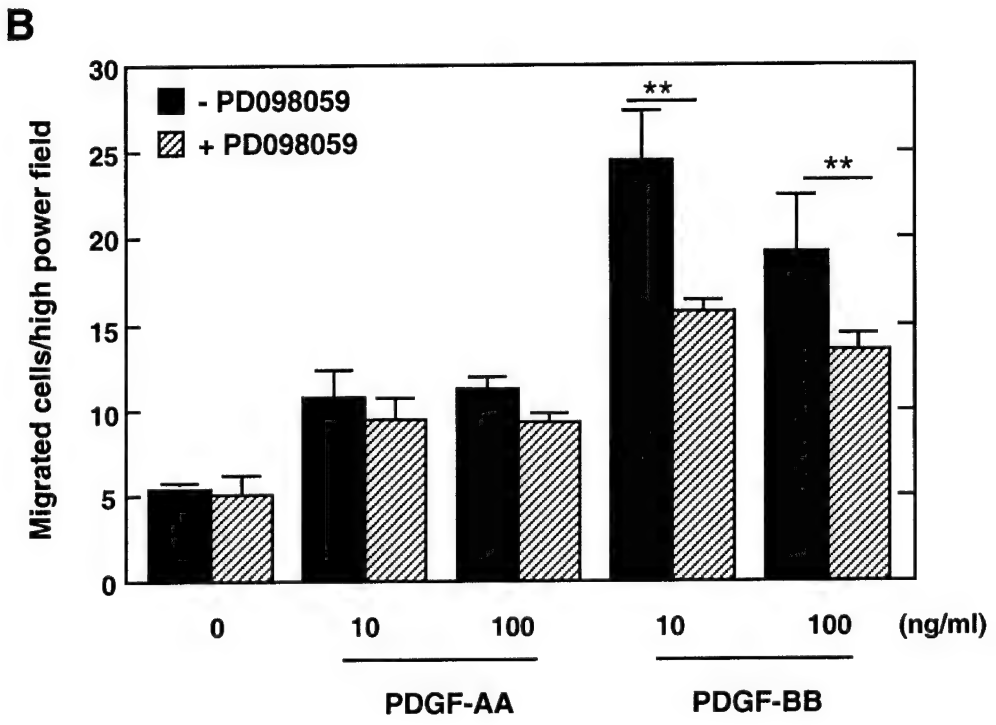

Ricono et al.

Figure 7

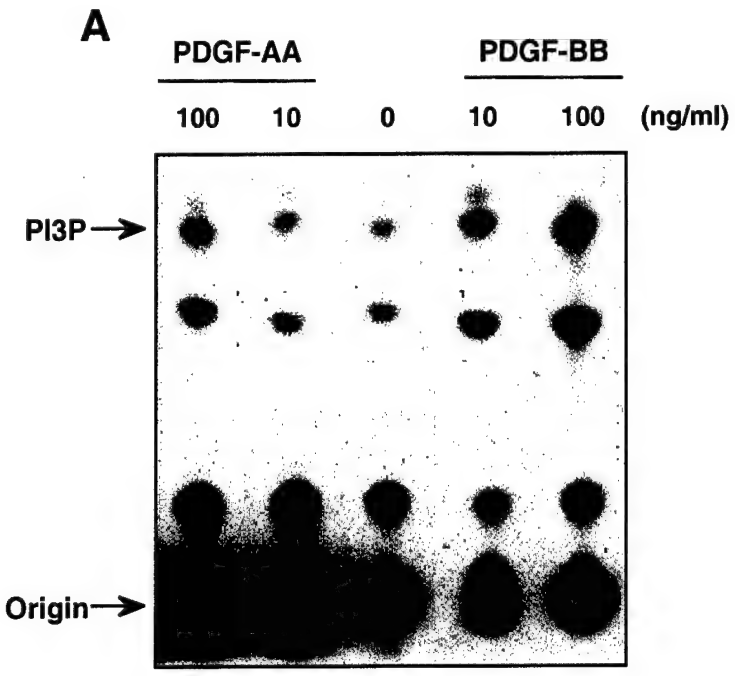

Ricono et al.

Figure 7

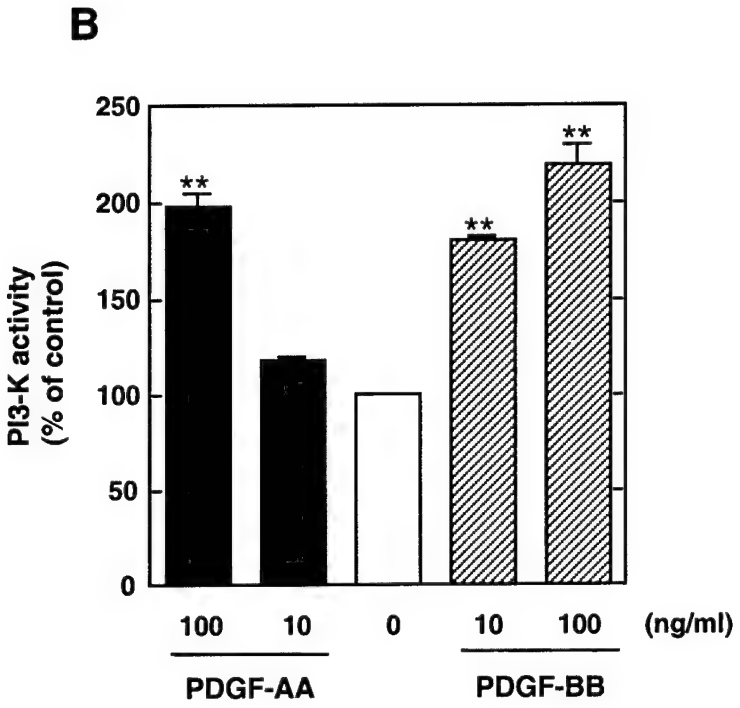

Ricono et al.

Figure 8

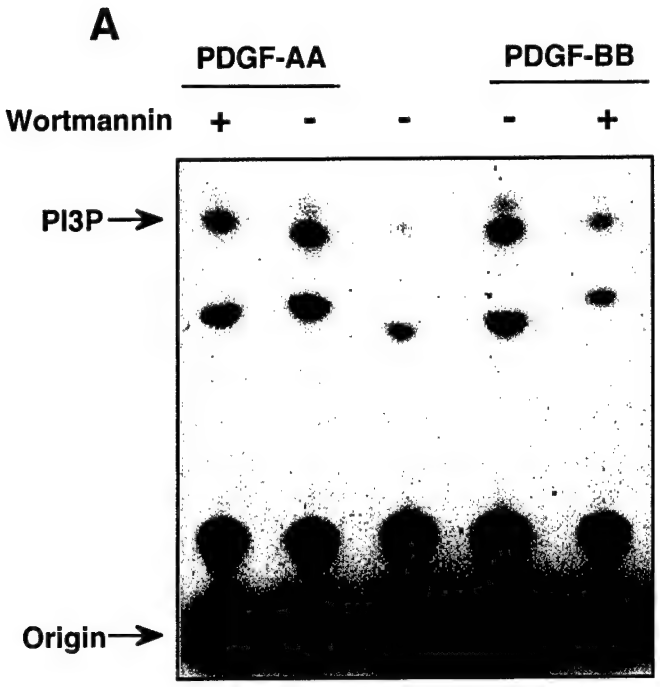

Ricono et al.

Figure 8

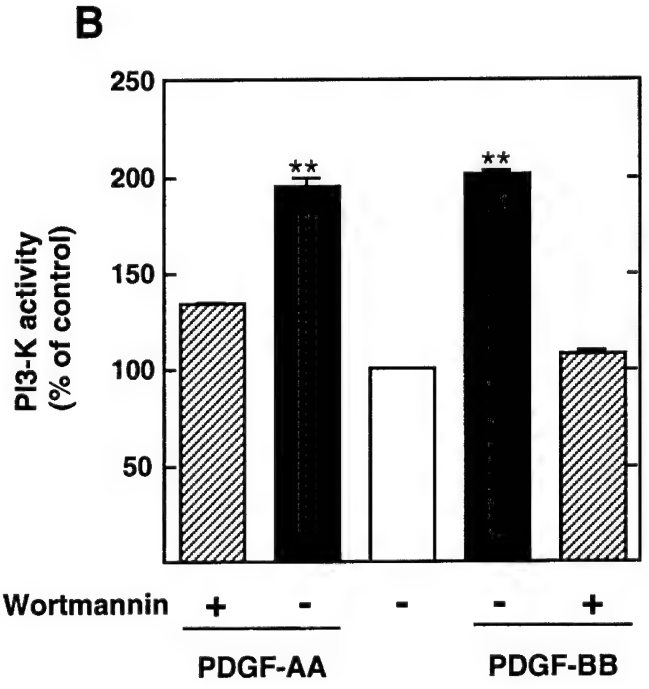

Ricono et al.

Figure 9

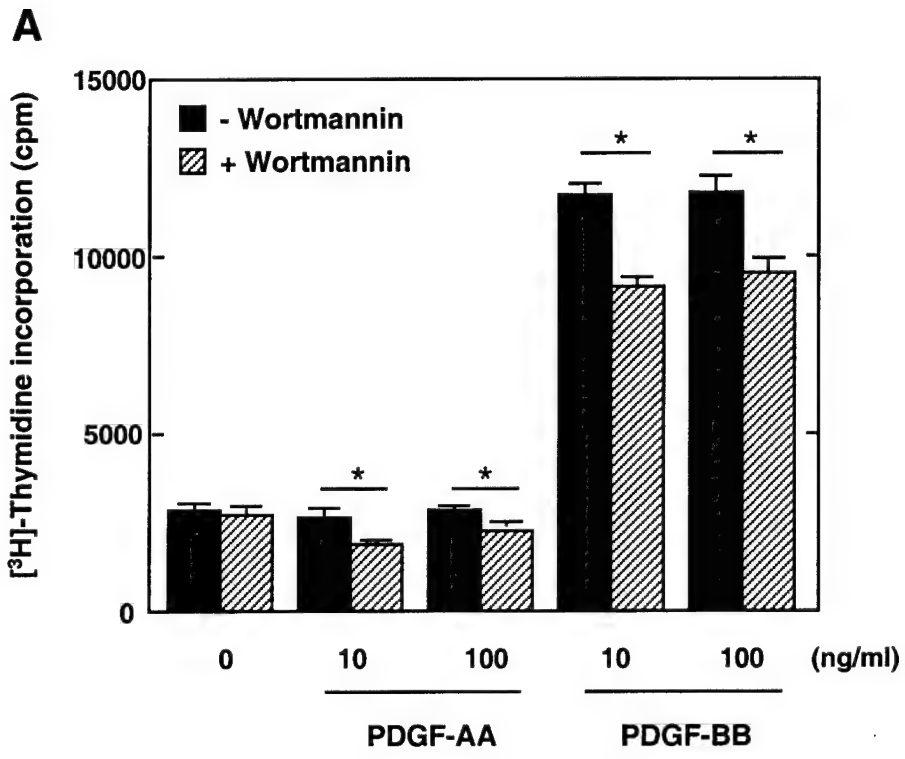

Ricono et al.

Figure 9

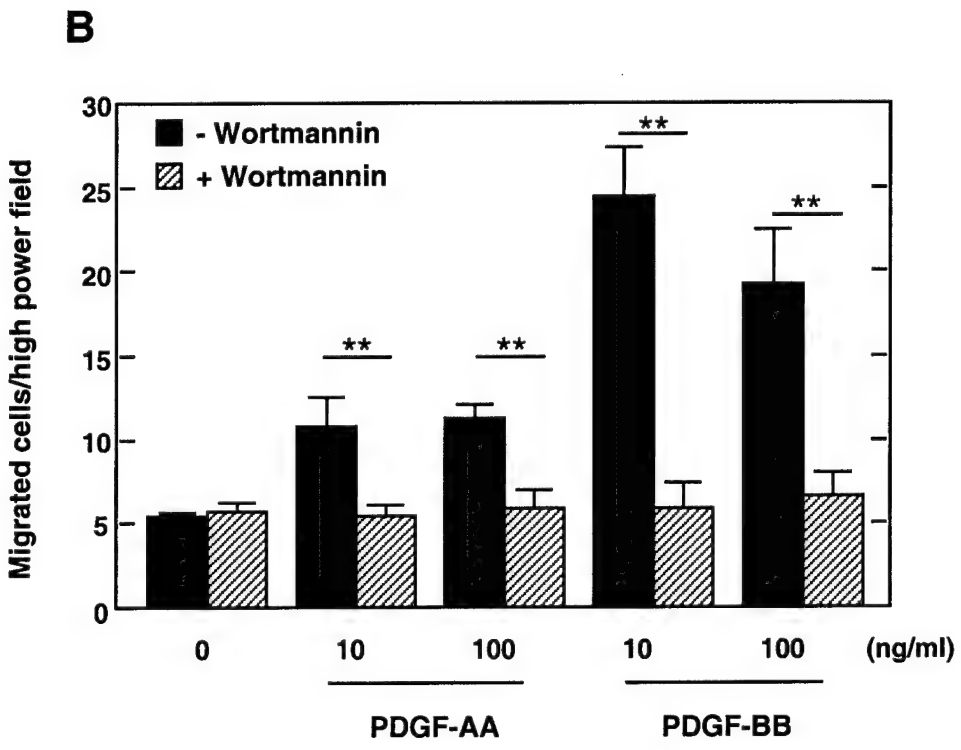

Ricono et al.

Figure 9

C

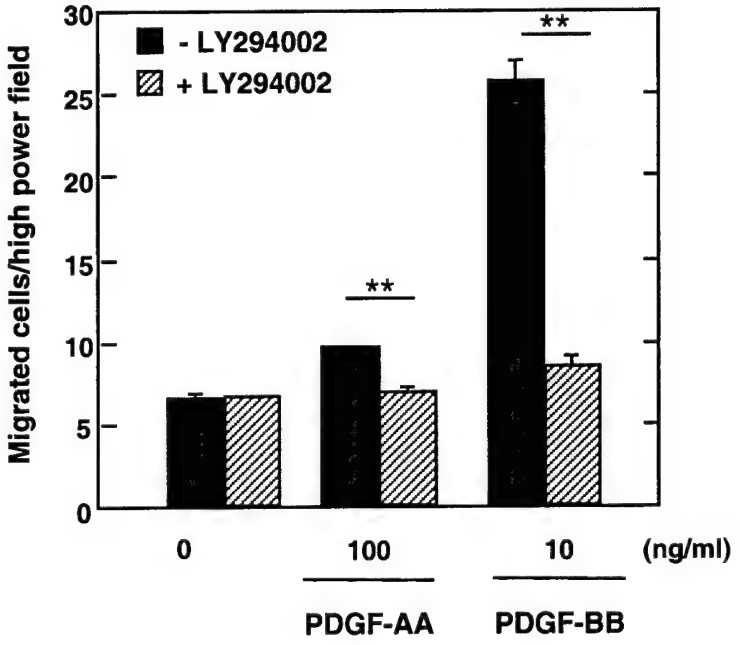

Ricono et al.

Figure 10

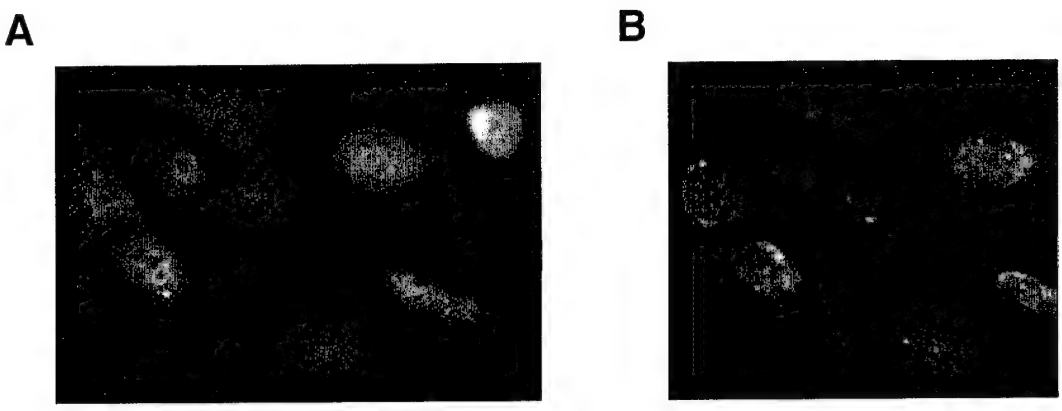

Ricono et al.

Biochemical and Biophysical Research Communications 273, 1069–1077 (2000)
doi:10.1006/bbrc.2000.3081, available online at http://www.idealibrary.com on IDEAL®

Increased Effect of Interferon γ on PDGF-Induced *c-fos* Gene Transcription in Glomerular Mesangial Cells: Differential Effect of the Transcriptional Coactivator CBP on STAT1α Activation

Goutam Ghosh Choudhury* and Jill M. Ricono

*Department of Medicine, University of Texas Health Science Center at San Antonio, Floyd Curl Drive, San Antonio, Texas 78284; and *Geriatric Research, Education and Clinical Center, South Texas Veterans Health Care System, San Antonio, Texas*

Received June 1, 2000

We have previously shown that interferon γ (IFNγ) synergistically increases PDGF-induced DNA synthesis in mesangial cells. To examine the mechanism, we studied its effect on PDGF-induced *c-fos* gene transcription using a reporter mesangial cell in which firefly luciferase gene is driven by *c-fos* promoter. IFNγ significantly enhanced PDGF-induced *c-fos* transcription. We have shown previously that PDGF-induced *c-fos* transcription in mesangial cells is mediated by the ternary complex factor Elk-1. Using a GAL-4 DNA binding-domain-Elk-1 transactivation domain fusion protein-based reporter assay we showed that the increased effect of IFNγ was not mediated by Elk-1 transactivation. Gel mobility shift assay of lysates of mesangial cells treated with a combination of IFNγ and PDGF using *sis*-inducible DNA element (SIE) showed increased STAT1α-SIE complex formation as compared to the PDGF alone. To investigate the transcriptional consequences of this observation, stable reporter mesangial cells in which luciferase gene is driven by four copies of SIE was used. IFNγ and PDGF in combination significantly increased SIE-dependent transcription as compared to PDGF or IFNγ alone. Using an antibody in the gel mobility shift assay we showed that the PDGF-induced SIE-STAT1α complex recruited the transcriptional coactivator CBP. However, the STAT1α-SIE complex formed in the presence of IFNγ and PDGF did not contain CBP. Taken together, our data provide the first evidence that the synergistic effect of IFNγ on PDGF-induced DNA synthesis may be the result of increased *c-fos* gene transcription via SIE. This effect occurs in the presence of increased activation of STAT1α without recruitment of the transcriptional coactivator CBP. © 2000 Academic Press

Key Words: **PDGF; interferon γ; *c-fos;* sis-inducible element.**

Platelet-derived growth factor (PDGF) is a mitogen for many mesenchymal cells, including kidney glomerular mesangial cells, the vascular pericytes of the glomerular microvascular bed (1, 2). Activation of PDGF receptor β (PDGFR) in the multipotent mesenchymal cells during embryogenesis is necessary for development of mesangial cells (3). Binding of PDGF to the extracellular domain of the receptor stimulates dimerization of the receptor complex, leading to transautophosphorylation of the receptor in the kinase domain. This autophosphorylation increases its intrinsic kinase activity to phosphorylate other tyrosine residues located outside the kinase domain. These phosphotyrosine residues in turn serve as the docking sites for different signal transducing proteins containing SH2 domains (2, 4).

Two signal transduction pathways have been implicated in the proliferative response of PDGFR. They are the phosphatidylinositol (PI) 3 kinase and Ras/MAPK pathways (2, 5, 6). Tyrosine phosphorylated and activated PDGFR recruits PI 3 kinase via phosphotyrosine-SH2 domain-mediated interaction. This physical association of PI 3 kinase with PDGFR stimulates its lipid kinase activity. The adaptor protein Grb-2 bound to the guanine nucleotide exchange factor SOS can bind directly to the PDGFR via the SH2 domain or indirectly via other components such as Shc or SHP-2. Thus recruitment of SOS to the receptor activates Ras in the membrane, initiating the kinase cascade, finally activating the mitogen activated protein kinase ERK1/2 (MAPK) (5, 6). PDGF-dependent activation of PI 3 kinase and MAPK integrate in the nucleus to induce the transcription of early response gene, *c-fos* (7, 8). We have recently shown that inhibition of PI 3 kinase and MAPK blocks PDGF-induced DNA synthesis in mesangial cells (9). Inhibition of MAPK activity

0006-291X/00 $35.00

in mesangial cells also results in inhibition of *c-fos* gene transcription (10, 11).

Increased proliferation of mesangial cells during glomerular injury is due to combinatorial effects of PDGF and other growth factors and cytokines present in the microenvironment of glomerulus (12). One such cytokine is interferon γ (IFNγ). Although IFNγ is a potent inhibitor of cell growth, it stimulates proliferation of many cell types including hematopoietic progenitor cells, astrocytes, synovial fibroblasts and smooth muscle cells (13–15). We have shown that interferon γ (IFNγ) potentiates PDGF-induced DNA synthesis in mesangial cells (16). The growth inhibitory and antiviral effects of IFNγ are mediated by the transcription factor STAT1α (signal transducer and activator of transcription α) (17, 18). We have recently shown that PDGF stimulates STAT1α in mesangial cells (19). However, the precise mechanism of this effect of IFNγ and PDGF is not known.

In this report, we show that IFNγ stimulates PDGF-induced *c-fos* gene transcription in mesangial cells in the absence of transactivation of Elk-1, a transcription factor that regulates mitogen-induced *c-fos* gene expression. The increased effect of IFNγ on PDGF-induced *c-fos* transcription is mediated through a *sis*-inducible element (SIE) present in the *c-fos* promoter. IFNγ increased PDGF-induced binding of STAT1α to the SIE. The transcriptional coactivator CBP was recruited in the PDGF-induced STAT1α-SIE complex. On the other hand, in the presence of IFNγ and PDGF, the increased binding of STAT1α to the SIE was independent of recruitment of CBP. Together our data demonstrate that transcriptional activation effect of IFNγ on PDGF-induced *c-fos* gene transcription in mesangial cells is mediated by SIE in the *c-fos* gene promoter without the participation of Elk-1 or CBP.

MATERIALS AND METHODS

Materials. Tissue culture materials were purchased from Gibco. PDGF and IFNγ were obtained from R & D. PDGFR antibody was from UBI. STAT1α and CBP antibodies were obtained from Transduction Laboratories and Santa Cruz respectively. Protein A sepharose CL 4B was obtained from Pharmacia. Lipofectamine plus reagent was purchased from Life Technology. pGL3 promoter-luciferase reporter plasmid, luciferase assay kit and dual luciferase assay kit were obtained from Promega. Oligonucleotides were synthesized in an Applied Biosystem DNA/RNA synthesizer. All other reagents were of analytical grade.

Cell culture. Rat mesangial cells (kindly provided by Dr. Jeff Kreisberg, Department of Pathology) were isolated and characterized as described (10, 11). For the present experiments, cells were used between the 15th and 25th passages. Cells were maintained in RPMI 1640 tissue culture medium supplemented with antibiotic/antifungal solution and 17% fetal bovine serum. Cells were made quiescent by incubation in serum-free RPMI 1640 for 48 h.

Transfection of mesangial cells. 1 μg of GAL-4-firefly luciferase reporter plasmid and 50 ng of GAL-4-DNA binding domain Elk-1 transactivation domain fusion plasmids were cotransfected with 25 ng of CMV-Renilla luciferase reporter plasmid into mesangial cells in 12-well culture plates. The transfected cells were grown to confluency and serum-deprived for 48 h. During the last 24 h of serum starvation, the cells were incubated with 1000 U/ml of IFNγ followed by incubation with 10 ng/ml PDGF for 12 h. This incubation time has been previously shown to be sufficient to give a synergistic effect on PDGF-induced DNA synthesis (16). The luciferase activity was determined in the cell lysate using a dual luciferase assay kit as described before (10, 11). For stable transfection, low passage mesangial cells were cotransfected with the reporter plasmid and pCDNA3; the latter codes for the neomycin resistance gene. Two days post transfection, the cells were split in medium containing 0.4 mg/ml G-418. G-418 resistant colonies were pooled to make mass culture. The locus of integration of reporter construct is likely to be a random event and should vary in different colonies pooled together. Therefore, we decided to use these cultures because the changes in the transcriptional activity due to clonal variation of single colony are eliminated using this method (20). Luciferase activity was determined in the cell lysates to confirm the transcription of the reporter plasmid using the luciferase assay kit. The luciferase activity was corrected with respect to protein concentration.

PDGFR immunecomplex kinase assay and PI 3 kinase assay. PDGFR immunoprecipitates were used for receptor tyrosine kinase activity and PI 3 kinase activity essentially as described before (9, 10, 21, 22).

Gel mobility shift assay (GMSA). To the cell monolayer RIPA buffer (20 mM Tris–HCl, pH 7.5, 150 mM NaCl, 5 mM EDTA, 1 mM Na_3VO_4, 1% NP 40, 1 mM PMSF and 0.1% aprotinin) was added and incubated at 4°C for 30 min, scraped from the plates and centrifuged at 10,000*g* for 30 min at 4°C. Protein concentration was estimated in the supernatant. A SIE DNA probe was labeled by incubating γ^{32}P-ATP and T4 polynucleotide kinase with annealed oligonucleotides 5′-CAGTTCCCGTCAATC-3′ and 5′-CATTGACGGGAACAG-3′. The GMSA was performed using 10–15 μg of each lysate as described previously (19, 20). For supershift analysis the samples were incubated with either STAT1α or CBP antibodies for 30 min on ice before the binding reaction was performed as described before (19, 21, 23).

Construction of SIE reporter plasmid and establishment of MC-SIE reporter mesangial cells. Four tandem repeats of SIE were synthesized with flanking Nhe I and Xho I sites in the 5′ and 3′ ends respectively. The upper strand (5′-CTAGCCATTTCCCGTAAATC-CATTTCCCGTAAATCCATTTCCCGTAAATCCATTTCCCGTAAA-TCC) and lower strand (5′-TCGAGGATTTACGGGAAATGGATT-TACGGGAAATGGATTTACGGGAAATGGATTTACGGGAAATGG) were annealed and ligated to Nhe I and Xho I digested pGL3-prom plasmid in which the luciferase cDNA is under the control of SV 40 TATA box. The resulting pGL3-SIE plasmid was cotransfected with pCDNA 3 into mesangial cells and the G-418 resistant reporter cells (MC-SIE) were established as described above. Data analysis: The data were presented as mean with and without standard error. The significance of the data was assessed by comparison of multiple groups using ANOVA.

RESULTS

Effect of PDGF on c-fos transcription in mesangial cells. We have recently shown that INFγ synergistically activates PDGF-induced DNA synthesis in mesangial cells (16). In many mesenchymal cells, PDGF-induced expression of early response genes such as *c-fos* is directly correlated with its ability to induce DNA synthesis (8). To investigate the effect of PDGF on *c-fos* gene transcription in mesangial cells, we stably transfected a reporter plasmid in which firefly luciferase cDNA is driven by *c-fos* promoter. Addition of PDGF to these reporter mesangial cells (Fos-LUC) in-

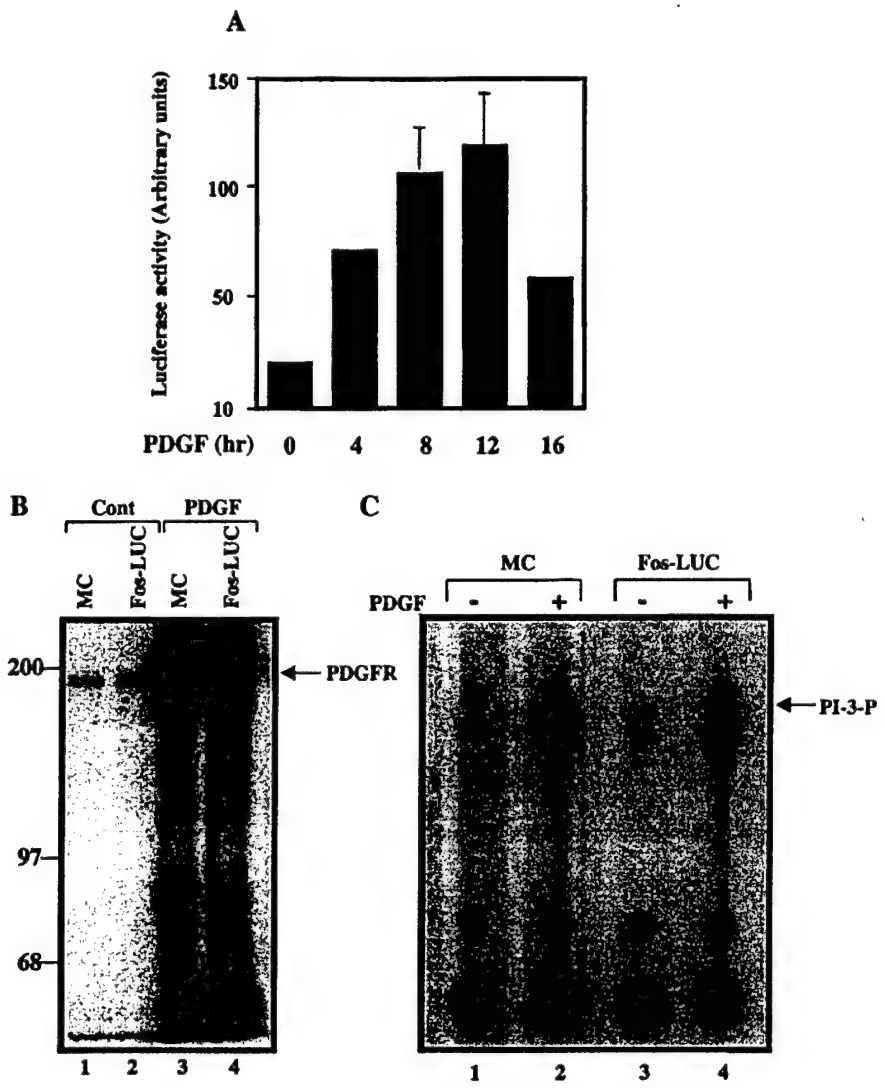

FIG. 1. (A) PDGF stimulates *c-fos* gene transcription in Fos-LUC cells. The cells were serum deprived for 48 h and 10 ng/ml of PDGF was added for different periods of time. Luciferase activity was determined as described under Materials and Methods. (B) Comparison of PDGFR activation between mesangial cells (MC) and Fos-LUC cells. Serum-deprived cells were stimulated with PDGF. 100 μg of cleared RIPA lysates were immunoprecipitated with PDGFR antibody and the immunoprecipitates used in an immunecomplex kinase assay in the presence of γ-^{32}P-ATP. The phosphorylated proteins were separated by SDS gel electrophoresis, dried and autoradiographed. Molecular weight markers are shown in left margin in kDs. The position of PDGFR is shown. (C) Comparison of PDGF-induced PI 3 kinase activity between mesangial cells (MC) and Fos-LUC cells. PDGFR immunoprecipitates were assayed for PI 3 kinase activity with PI as substrate in the presence of γ^{32}P-ATP. The reaction products were separated by thin layer chromatography (22, 24). The position of PI-3-phosphate (PI-3-P) is shown.

creased *c-fos* gene transcription in a time-dependent manner (Fig. 1A). Since we used primary mesangial cells to establish the reporter cells to study PDGF-induced *c-fos* gene transcription, it was necessary to test whether these stably transfected reporter cells changed important and characteristic responses as compared to the parental mesangial cells. We have shown previously that addition of PDGF to mesangial cells increases the tyrosine kinase activity of PDGFR, one of the early events in the PDGF-induced mitogenic signal transduction pathway (24). We tested the effect of PDGF on PDGFR activation in the Fos-LUC cells. Lysates of PDGF-stimulated mesangial cells and Fos-LUC cells were immunoprecipitated with PDGFR specific antibody. The immunoprecipitates were used in an immunecomplex kinase assay. The results show that PDGF increased tyrosine kinase activity of PDGFR in both Fos-LUC cells and the parental mesangial cells to similar degree (Fig. 1B, compare lane 3 with 4). To confirm that the PDGF-induced signaling pathways are intact in Fos-LUC cells, we tested the activation of phosphatidylinositol 3 kinase (PI3 kinase), the activity

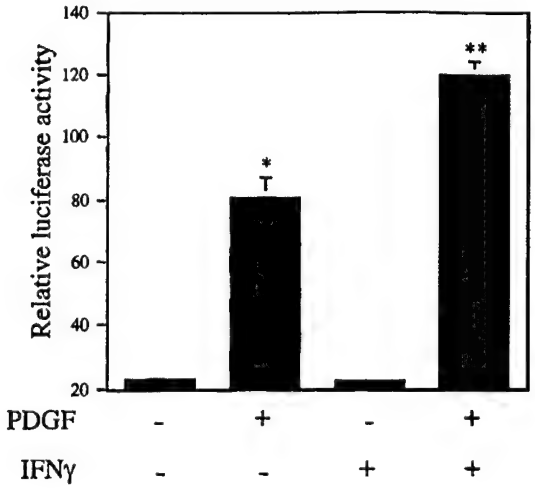

FIG. 2. Effect of PDGF and IFNγ on *c-fos* gene transcription. Serum-deprived Fos-LUC cells were incubated with IFNγ for 24 h before stimulation with PDGF. The lysates were assayed for luciferase activity. * $P < 0.05$ vs untreated control. ** $P < 0.05$ vs PDGF-treated cells.

of which is necessary for DNA synthesis in mesangial cells (9). PDGF increases the activity of PI 3 kinase in both Fos-LUC and mesangial cells again in a similar fashion. Together these data indicate that the reporter mesangial cells behave similarly to the parental mesangial cells. Thus the use of these transfected cells to investigate the mechanism of *c-fos* gene transcription is justified.

Effect of IFNγ on PDGF-induced c-fos gene transcription. Expression of early response genes is associated with mitogenic induction of cells (8). PDGF induces the early response gene *c-fos* as a part of its mitogenic signaling (7, 8, 10). Since IFNγ potentiates PDGF-induced DNA synthesis in mesangial cells (16), we tested its effect on *c-fos* gene transcription using Fos-LUC cells. These cells were preincubated with IFNγ followed by stimulation with PDGF. Luciferase activity was determined as a measure of *c-fos* transcriptional activation. PDGF induced *c-fos* transcription (Fig. 2). IFNγ alone did not have any effect on *c-fos* expression. In contrast, IFNγ significantly increased PDGF-induced transcription of *c-fos* gene (Fig. 2). These data indicate that IFNγ modulates one or more signaling pathways that regulate *c-fos* promoter activity in mesangial cells.

IFNγ does not regulate Elk-1 transcription factor induction of c-fos transcription. *c-fos* gene promoter contains multiple transcriptional regulatory elements including cyclic AMP response element (CRE), serum response element (SRE) and *sis*-inducible element (SIE) among others (7, 25). However, mitogenic growth factors including PDGF stimulate *c-fos* gene expression using SRE (26). We have shown recently in mesangial cells that PDGF-induced DNA synthesis is mediated by MAPK (10). One of the downstream targets of MAPK is the ETS domain transcription factor Elk-1, which after phosphorylation by MAPK, is recruited to SRE along with serum response factor to form a ternary complex to activate *c-fos* transcription (27, 28). We have recently shown that inhibition of MAPK blocks PDGF-induced Elk-1 transactivation in mesangial cells, leading to inhibition of *c-fos* gene transcription (10). To test whether IFNγ utilizes Elk-1 transcription factor to increase PDGF induced *c-fos* transcription, we measured the effect of IFNγ on Elk-1 transactivation. A fusion construct coding for GAL-4 DNA binding domain fused to the Elk-1 transactivation domain was cotransfected into mesangial cells with a reporter plasmid in which luciferase is driven by five copies of GAL-4 DNA elements. These transfected cells were treated with IFNγ followed by PDGF. Luciferase activity was measured in the cell lysates. PDGF stimulated Elk-1-dependent transcription of the reporter gene (Fig. 3). However, IFNγ alone or in combination with PDGF had no effect on Elk-1 transactivation (Fig. 3). These data indicate that IFNγ may not utilize the target sequence SRE in the *c-fos* promoter to induce its additive effect on PDGF-induced *c-fos* transcription.

IFNγ utilizes SIE to exert its stimulatory effect on PDGF-induced c-fos gene transcription. SIE is present in the promoter of *c-fos* gene (8). However, most growth factors do not utilize SIE to promote expression of *c-fos* (29). It has been shown that the STAT family of transcription factors binds this element (18).

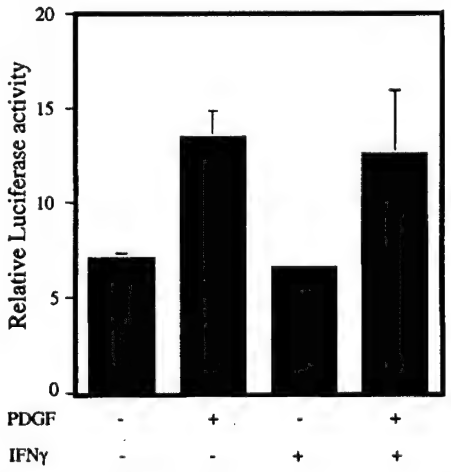

FIG. 3. Effect of IFNγ on PDGF-induced Elk-1-dependent transcription. GAL-4-luciferase reporter plasmid, GAL-4-Elk-1 fusion plasmid and CMV-Renilla luciferase plasmid were cotransfected into mesangial cells as described under Materials and Methods. Serum-starved transfected cells were treated with IFNγ for 24 h followed by treatment with PDGF. Firefly and Renilla luciferase activity were determined using dual luciferase assay kit. The data are expressed as the ratio of Firefly to Renilla luciferase activity.

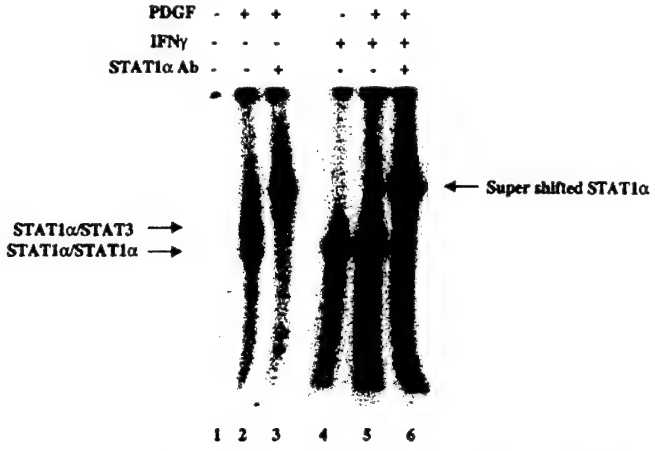

FIG. 4. Effect of IFNγ on PDGF-induced STAT1α activation. Serum-deprived mesangial cells were incubated with IFNγ for 24 h before stimulation with PDGF. The lysates were used in the gel mobility shift assay with labeled SIE probe as described under Materials and Methods. For supershift analysis, the extracts were incubated with STAT1α specific antibody on ice for 30 min before incubation with ^{32}P-labeled SIE probe. The protein-DNA complex was separated by 5% polyacrylamide gel electrophoresis. The arrows in the left margin indicate the position of the STAT1α homodimer and STAT1α/STAT3 heterodimer. The arrow in the right shows the supershifted protein-DNA complex indicating the presence of STAT1α in this complex.

In fact, depending on the cell type, STAT1α and STAT3 homodimers and STAT1α/STAT3 heterodimer bind to this element with high affinity. We and others have shown previously that PDGF stimulates binding of STAT1α with SIE (19, 21). To test whether IFNγ regulates PDGF-induced binding of STAT1α with SIE, lysates of mesangial cells treated with PDGF alone or in combination with IFNγ were used in gel mobility shift assays, with SIE as probe. PDGF stimulated formation of two protein-DNA complexes, STAT1α homodimer and STAT1α/STAT3 heterodimer (Fig. 4, indicated by arrow in the left; compare lane 2 with lane 1). STAT1α-specific monoclonal antibody supershifted both complexes, confirming the presence of STAT1α (lanes 3). These data fit with previous findings in other cell types, where along with STAT1α homodimer and STAT1α/STAT3 heterodimer, STAT3 homodimer also bound to SIE (18, 21). In contrast to PDGF, IFNγ only stimulated the formation of the protein-DNA complex containing STAT1α homodimer alone (lane 4, indicated by lower arrow at left). No binding with STAT1α/STAT3 heterodimer was observed. In the cells incubated with both IFNγ and PDGF, there is an increased binding of STAT1α with the probe as compared to binding in cells stimulated with PDGF or IFNγ alone (compare lane 5 with lanes 4 and 2). These data suggest that the stimulatory effect of IFNγ on PDGF-induced *c-fos* gene transcription may be due to increased transcriptional effect of STAT1α on SIE in the *c-fos* promoter.

Effect of IFNγ on PDGF-induced SIE-dependent transcription. To test SIE-dependent transcription, we synthesized both strands of four tandem repeats of 15 bp SIE sequence (4× SIE) from *c-fos* gene promoter. The double stranded 4× SIE was cloned into the 5′ end of a basal SV40 promoter, which drives the reporter luciferase gene in pGL3 (Fig. 5A). This plasmid was stably transfected into mesangial cells to establish permanent reporter mesangial cells that express luciferase under the control of SIE. Addition of PDGF to these cells increased SIE-dependent transcription (Fig. 5B). To test the effect of IFNγ, these cells were incubated with IFNγ followed by treatment with PDGF. The lysates were then assayed for luciferase activity. The activation of SIE-dependent transcription is in decreasing order with IFNγ > PDGF (Fig. 6). The transcription was increased more than additively with the combination of IFNγ and PDGF than in response to

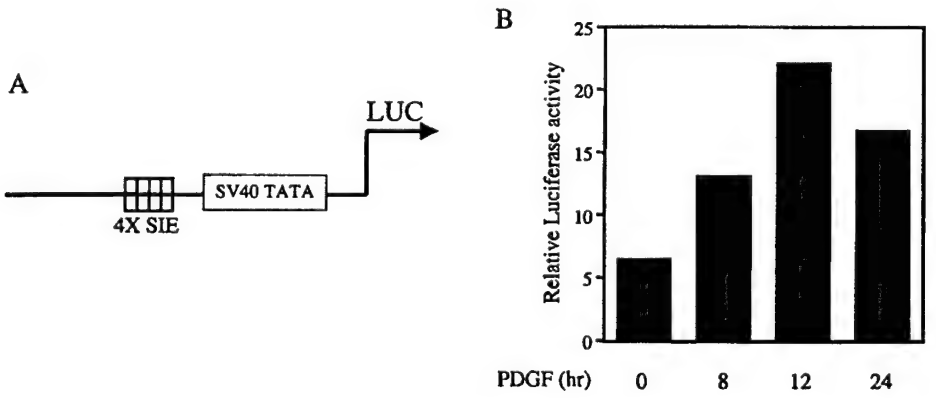

FIG. 5. PDGF stimulates SIE-dependent transcription in mesangial cells. (A) Structure of the pGL3-SIE luciferase reporter plasmid. (B) Stable mesangial cells (MC-SIE) containing pGL3-SIE plasmid were established as described under Materials and Methods. Serum-deprived cells were incubated with PDGF for different periods of time. Luciferase activity was determined in the lysates as described under Materials and Methods.

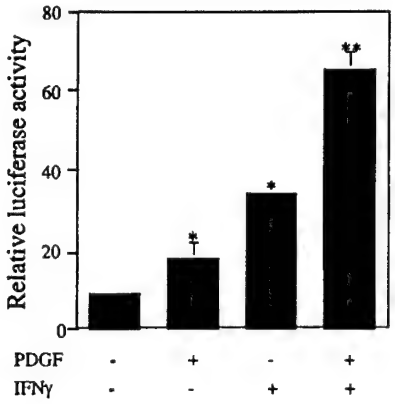

FIG. 6. Effect of IFNγ on PDGF-induced SIE-dependent transcription. Serum-deprived MC-SIE were treated with IFNγ for 24 h followed by 10 ng/ml PDGF. Luciferase activity was determined in the lysate and corrected as described under Materials and Methods. * $P < 0.05$ vs. untreated control. ** $P < 0.05$ vs IFNγ or PDGF alone.

PDGF or IFNγ alone (Fig. 6). This increased combinatorial effect of IFNγ and PDGF on SIE-dependent transcription may be the result of increased STAT1α-SIE complex formation in the presence of both factors as compared to the presence of either one of them alone (Fig. 4, compare lane 5 with lane 2 and lane 4). These data indicate that the SIE present in the *c-fos* promoter may regulate the effect of IFNγ on PDGF-induced *c-fos* gene transcription. To our knowledge, this is the first demonstration of involvement of SIE in *c-fos* gene expression in response to IFNγ.

Differential involvement of transcriptional coactivator CBP in STAT1α activation in mesangial cells. Recent reports indicate that transcriptional coactivators play an important roles in transcription of different genes (30). One such transcriptional coactivator, CBP, has been shown to interact with many transcription factors including STAT1α (31). This transcription factor-mediated recruitment of CBP onto the DNA element increases RNA polymerase II-dependent transcription of genes (30). We tested the effect of PDGF on recruitment of CBP in the DNA-protein complex in mesangial cells. Lysates of mesangial cells treated with PDGF were used in a gel mobility shift assay in the presence of SIE as probe. An antibody that specifically recognizes the transcriptional coactivator CBP was used. PDGF stimulated the formation of protein-DNA complex that contains STAT1α homodimer and STAT1α/STAT3 heterodimer (Fig. 7, lane 2). The presence of CBP antibody significantly blocked the formation of the protein-DNA complexes (Fig. 7, compare lane 3 with lane 2) suggesting the requirement of CBP for optimal association of STAT1α homodimer and STAT1α/STAT3 heterodimer with SIE. IFNγ alone, as well as combination of IFNγ and PDGF, also increased the formation of STAT1α-DNA complex. However, antibody against CBP did not inhibit this protein-DNA complex formation. These data indicate that PDGF-induced STAT1α activation involves recruitment of the transcriptional coactivator CBP in the protein-DNA complex in mesangial cells. However, the increased effect of IFNγ on PDGF-induced STAT1α activity does not involve any recruitment of CBP. Taken together these data suggest that the combined effect of IFNγ and PDGF on STAT1α activation does not require CBP to enhance transcription from SIE.

DISCUSSION

These studies demonstrate that IFNγ has an additive effect on PDGF-induced *c-fos* gene transcription in mesangial cells. This increased effect of IFNγ is not due to increased transactivation of Elk-1, a ternary complex factor that is known to regulate PDGF-induced *c-fos* gene transcription. Increased transcription of *c-fos* is mediated by the combinatorial effect of IFNγ and PDGF on STAT1α activation. The transcriptional coactivator CBP is recruited into STAT1α-SIE complex in response to PDGF. But the STAT1α-SIE complex induced by IFNγ and PDGF together does not contain CBP. These data provide the first evidence that

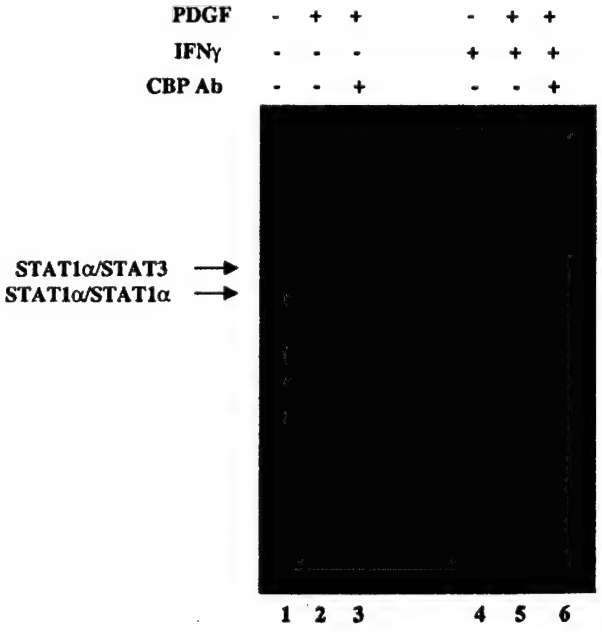

FIG. 7. Recruitment of CBP in the STAT-SIE complex. Lysates of mesangial cells, treated with either IFNγ or PDGF, alone or in combination, were incubated with a specific antibody against CBP for 30 min before incubation with ^{32}P-labeled SIE probe. The protein-DNA complexes were separated as described in the legend to Fig. 4. The arrows indicate the positions of STAT1α homodimer and STAT1α/STAT3 heterodimer. Note that CBP antibody inhibited the binding of SIE to the STAT, indicating the presence of CBP in the protein-DNA complex.

IFNγ activates PDGF-induced *c-fos* gene transcription via STAT1α-SIE interaction in the absence of CBP.

In inflammatory glomerular diseases both PDGF and IFNγ are present in the microenvironment of the glomerulus, along with many other cytokines (1, 32). A pathologic feature of these diseases is the proliferation of mesangial cells in response to the combinatorial effects of these cytokines. Although IFNγ is growth inhibitory for many cells, it can stimulate proliferation of select cells types. Recently, Tellides *et al.* reported that IFNγ induced arteriosclerotic changes by a mechanism involving increased PDGF-induced vascular smooth muscle cell proliferation (VSMC) (33). This increase in VSMC proliferation was the result of increased PDGF and PDGFR expression in response to IFNγ. We have also recently shown that IFNγ stimulates PDGF-induced DNA synthesis in mesangial cells in the absence of PDGFR upregulation or increased PDGFR tyrosine kinase activity (16). These data suggest that other mechanisms exist for the combinatorial effect of IFNγ and PDGF on DNA synthesis in mesangial cells.

A concomitant effect of mitogenic signal transduction is the *de novo* transcription of early response gene *c-fos* (8). To study the effect of IFNγ and PDGF on *c-fos* gene transcription in mesangial cells, we utilized a reporter mesangial cell in which luciferase enzyme is expressed by *c-fos* promoter (Fig. 1A). Use of these cells to investigate the regulation of *c-fos* gene transcription provides a natural chromatin environment and improves reproducibility (34). This is an important advantage when primary and nontransformed cells such as mesangial cells are studied. It should be noted that transfection of an exogenous gene into primary mesangial cells did not change the phenotype of these cells as determined by their responsiveness to PDGF as assessed by PDGFR activation and stimulation of PI 3 kinase activity, two important biological activities necessary for mitogenesis (Figs. 1B and 1C).

IFNγ reportedly does not induce *c-fos* gene expression (26). In mesangial cells IFNγ alone also did not induce *c-fos* transcription, confirming the previous finding (Fig. 2). In different cell types, *c-fos* promoter is regulated by three major transcription factor-binding DNA elements. These are CRE, SRE and SIE (8). Increased cAMP level in the cells stimulates protein kinase A to phosphorylate and activate the transcription factor CREB, which binds to CRE to activate *c-fos* transcription. However, in mesangial cells PDGF does not induce any cAMP production, thus eliminating this element a cause of the observed increase in *c-fos* gene transcription.

The central element for *c-fos* gene expression is the SRE, which binds the serum response factor (SRF) (8). After binding to SRE, SRF recruits another transcription factor, Elk-1, to form a ternary complex on the *c-fos* promoter (26, 27). Elk-1 is a direct substrate of MAPK (28). We have recently shown that growth factors including PDGF and EGF stimulate MAPK activity in mesangial cells and activate Elk-1 transactivation (10, 11). We have also shown that inhibition of MAPK activity results in inhibition of transactivation of Elk-1 (10, 11). This inhibition of Elk-1 activity blocked PDGF-induced *c-fos* gene transcription (10). Therefore, our data here showing the increased effect of IFNγ on PDGF-induced *c-fos* gene transcription (Fig. 2) may be due to increased Elk-1-mediated transcription. To test this possibility, we utilized a reporter assay in which the activation of Elk-1 can be measured in response to PDGF. We therefore provide evidence that IFNγ does not further stimulate PDGF-induced Elk-1-dependent transcription (Fig. 3). Thus we eliminated the involvement of SRE in *c-fos* promoter as a contributor to the observed increased effect of IFNγ on PDGF-induced *c-fos* gene transcription.

The third element in *c-fos* promoter is known to be affected by PDGF induction is the SIE (35). This element binds to the STAT family of transcription factors. After growth factor and cytokine stimulation of cells, the JAK family of cytosolic tyrosine kinases is activated (18). JAKs then phosphorylate STATs in conserved tyrosine residues to induce dimerization. Dimerized STATs then translocate to nucleus and bind specific DNA elements to stimulate transcription of genes. We have recently shown that in mesangial cells PDGF activates STAT1α as measured by binding of this transcription factor to SIE (19). More recently we have shown that PDGFR can directly phosphorylate STAT1α and result in STAT1α activation in mesangial cells (21). We have also demonstrated that IFNγ stimulates STAT1α in these cells (Fig. 4). However, the presence of SIE in the *c-fos* promoter can not induce its transcription by IFNγ in mesangial cells (Fig. 2). These data indicate that SIE is inactive in its context in the *c-fos* promoter. This notion has been suggested before (26). Similarly, growth factor-mediated *c-fos* expression is unaffected in mutant cells lacking STAT1α and in cells from STAT1α knock out mice (36, 37). In the present study, we provide evidence that when both IFNγ and PDGF are used to stimulate mesangial cells, SIE can be activated in an additive or synergistic fashion. SIE activity was assayed by its capability to bind to STAT1α (Fig. 4) but also by its transcriptional activation (Fig. 6). These data provide the first evidence to demonstrate that IFNγ may activate *c-fos* gene transcription using SIE.

The transcriptional coactivator CBP has been shown to interact with STAT1α among many other transcription factors and increases STAT1α-dependent transcription (31). CBP has been shown to interact with the ETS domain transcription factor Elk-1, the activation of which is mediated via phosphorylation by MAPK (38). Horvath *et al.* recently demonstrated that colony-stimulating factor-1-induced MAPK-dependent tran-

scriptional activity of scavenger receptor promoter is inhibited by IFNγ via activation of STAT1α. Since STAT1α has high affinity for CBP, association of CBP with activated STAT1α reduces its abundance so that MAPK-dependent transcriptional activation of scavenger receptor promoter is inhibited (39). In contrast, our data show increased activation of *c-fos* promoter in the presence of IFNγ and PDGF (Fig. 2); the latter is known to activate MAPK-dependent *c-fos* gene transcription (10). In mesangial cells, we demonstrate that CBP is present in PDGF-induced STAT1α-SIE complex (Fig. 7). In the protein-DNA complex formed in the presence of both IFNγ and PDGF, however, CBP is not recruited (Fig. 7). These data indicate that hyperactivated STAT1α by both these factors (Fig. 4), can bind the SIE and result in the release of CBP. This notion is supported by the observation that CBP can directly interact with cyclin E/CDK 2 complex, which is necessary for cells to progress through S-phase (40). Inhibition of cyclin E/CDK 2 activity either by expression of dominant negative CDDK 2 or by ectopic expression of cyclin kinase inhibitor p21 increases the CBP-mediated transcription of a target gene (40). IFNγ has recently been shown to regulate transcription of p21 via a STAT1 element in its promoter (41). It has been postulated that this is one of the mechanisms by which IFNγ inhibits cell proliferation. However, in mesangial cells, IFNγ, which potentiates PDGF-induced DNA synthesis, does not stimulate transcription of p21 (data not shown). On the other hand TGFβ, which is known to increase p21 level and inhibit mesangial cell proliferation, stimulates p21 transcription (data not shown). One possibility to reconcile all these findings is that in the presence of IFNγ and PDGF, when the amount of p21 is low and when there is increased DNA synthesis, CBP is bound to cyclin E/CDK 2 complex. Under this condition, however, increased *c-fos* transcription is mediated by increased recruitment of activated STAT1α onto the SIE in the promoter (Fig. 2 and Fig. 4). More recently it has been shown that phosphorylation of E2F-5 by cyclin E/CDK2 complex during G1/S progression stabilizes the E2F-5/CBP complex for its increased transcriptional potential (42). Since IFNγ synergistically stimulates PDGF-induced DNA synthesis in mesangial cells (16), it is possible that released CBP from STAT1 complex (Fig. 7) may be available to bind to E2F for induction of transcription of genes necessary for DNA synthesis.

Proliferation of mesangial cells is a pathologic feature of many inflammatory glomerular diseases where growth factor and cytokines including PDGF and IFNγ play important roles (32). IFNγ synergistically activates PDGF-induced DNA synthesis in mesangial cells (16). Our data showing that IFNγ activates PDGF-induced *c-fos* gene expression through SIE-dependent transcription in mesangial cells provides a possible mechanism.

ACKNOWLEDGMENTS

We thank Sergio Garcia for help in tissue culture and Cheresa Calhaun for technical help. We thank to Drs. B. S. Kasinath, Nandini Ghosh-Choudhury, and Dan Riley for critically reading the manuscript. This study was supported in part by the Department of Veterans Affairs Medical Research Service Merit Award, a VA REAP Award, and a National Institutes of Diabetes and Digestive and Kidney Diseases Grant DK-50190 (to G. Ghosh Choudhury).

REFERENCES

1. Abboud, H. E. (1995) Role of platelet-derived growth factor in renal injury. *Annu. Rev. Physiol.* **57,** 297–309.
2. Abboud, H. E., Bhandari, B., and Ghosh Choudhury, G. (1995) Cell biology of platelet-derived growth factor. *In* Molecular Nephrology. Kidney Function in Health and Disease (Bonvetre, J., and Schlondorf, D., Eds.), pp. 573–590, Marcel Dekker, Inc., New York.
3. Soriano, P. (1994) Abnormal kidney development and hematological disorders in PDGF beta-receptor mutant mice. *Genes Dev.* **8,** 1888–1896.
4. Heldin, C.-H., and Westermark, B. (1999) Mechanism of action and in vivo role of platelet-derived growth factor. *Physiol. Rev.* **79,** 1283–1316.
5. Heldin, C.-H., Ostman, A., and Ronnstrand, L. (1998) Signal transduction via platelet-derived growth factor receptors. *Biochim. Biophys. Acta* **1378,** F79–F113.
6. Margolis, B., and Skolnik, E. Y. (1994) Activation of Ras by receptor tyrosine kinases. *J. Am. Soc. Nephrol.* **5,** 1288–1299.
7. Wang, Y., Falasca, M., Schlessinger, J., Malstrom, S., Tsichlis, P., Settleman, J., Hu, W., Lim, B., and Prywes, R. (1998) Activation of the c-fos serum response element by phosphatidyl inositol 3-kinase and rho pathways in HeLa cells. *Cell Growth Differ.* **9,** 513–522.
8. Johansen, F. E., and Prywes, R. (1995) Serum response factor: Transcriptional regulation of genes induced by growth factors and differentiation. *Biochim. Biophys. Acta* **1242,** 1–10.
9. Ghosh Choudhury, G., Karamitsos, C., Hernandez, J., Gentilini, A., Bardgette, J., and Abboud, H. E. (1997) PI-3-kinase and MAPK regulate mesangial cell proliferation and migration in response to PDGF. *Am. J. Physiol. Renal Physiol.* **273,** F931–F938.
10. Ghosh Choudhury, G., Kim, Y.-S., Simon, M., Wozney, J., Harris, S., Ghosh-Choudhury, N., and Abboud, H. E. (1999) Bone morphogenetic protein 2 inhibits platelet-derived growth factor-induced c-fos gene transcription and DNA synthesis in mesangial cells: Involvement of mitogen-activated protein kinase. *J. Biol. Chem.* **274,** 10897–10902.
11. Ghosh Choudhury, G., Jin, D.-C., Kim, Y.-S., Celeste, A., Ghosh-Choudhury, N., and Abboud, H. E. (1999) Bone morphogenetic protein-2 inhibits MAPK-dependent Elk-1 transactivation and DNA synthesis induced by EGF in mesangial cells. *Biochem. Biophys. Res. Commun.* **258,** 490–496.
12. Abboud, H. E. (1994) Cytokine mediators of renal inflammation. *Curr. Opin. Nephrol. Hypertens.* **3,** 329–333.
13. Yokota, T., Shimokado, K., Kosaka, C., Sasaguri, T., Masuda, J., and Ogata, J. (1992) Mitogenic activity of interferon gamma on growth-arrested smooth muscle cells. *Arterioscler. Throm.* **12,** 1393–1401.
14. Yong, V. W., Moumdjian, R., Yong, F. P., Ruijs, T. C., Freedman, M. S., Cashman, N., and Antel, J. P. (1991) Gamma interferon promotes proliferation of adult human astrocytes in vitro and reactive gliosis in the adult mouse brain in vivo. *Proc. Natl. Acad. Sci. USA* **88,** 7016–7020.

15. Brinckerhoff, C. E., and Guyre, P. M. (1985) Increased proliferation of human synovial fibroblasts treated with recombinant immune interferon. *J. Immun.* **134,** 3142–3146.
16. Marra, F., Ghosh Choudhury, G., and Abboud, H. E. (1996) Interferon-gamma-mediated activation of STAT1alpha regulates growth factor-induced mitogenesis. *J. Clin. Invest.* **98,** 1218–1230.
17. Schindler, C., and Darnell, J. E. (1995) Transcriptional responses to polypeptide ligands: the JAK-STAT pathway. *Ann. Rev. Biochem.* **64,** 621–651.
18. Leaman, D. W., Leung, S., Li, X., and Stark, G. R. (1996) Regulation of STAT-dependent pathways by growth factors and cytokines. *FASEB J.* **10,** 1578–1588.
19. Ghosh Choudhury, G., Marra, F., Kiyomoto, H., and Abboud, H. E. (1996) PDGF stimulates tyrosine phosphorylation of JAK1 protein tyrosine kinase in human mesangial cells. *Kidney Int.* **49,** 19–25.
20. Alam, J., and Cook, J. L. (1990) Reporter genes: Application to the study of mammalian gene transcription. *Anal. Biochem.* **188,** 245–254.
21. Ghosh Choudhury, G., Ghosh-Choudhury, N., and Abboud, H. E. (1998) Association and direct activation of signal transducer and activator of transcription 1 alpha by platelet-derived growth factor receptor. *J. Clin. Invest.* **101,** 2751–2760.
22. Ghosh Choudhury, G., Grandaliano, G., Jin, D.-C., Katz, M. S., and Abboud, H. E. (2000) Activation of PLC and PI 3 kinase by PDGF receptor alpha is not sufficient for mitogenesis and migration in mesangial cells. *Kidney Int.* 908–917.
23. Bardgette, J., Abboud, H. E., and Ghosh Choudhury, G. (1999) Activation of STAT1a by phosphatase inhibitor vanadate in glomerular mesangial cells: Involvement of tyrosine and serine phosphorylation. *J. Receptor and Signal Transduction Res.* **19,** 865–884.
24. Ghosh Choudhury, G., Biswas, P., Grandaliano, G., Fouqueray, B., Harvey, S. A., and Abboud, H. E. (1994) PDGF-mediated activation of phosphatidylinositol 3 kinase in human mesangial cells. *Kidney Int.* **46,** 37–47.
25. Wang, Y., and Prywes, R. (2000) Activation of c-fos enhancer by the erk MAP kinase pathway through two sequence elements: the c-fos AP-1 and p62TCF sites. *Oncogene* **19,** 1379–1385.
26. Hill, C. S., and Treisman, R. (1995) Differential activation of c-fos promoter elements by serum. *EMBO J.* **14,** 5037–5047.
27. Hill, C. S., Marais, R., John, S., Wynne, J., Dalton, S., and Treisman, R. (1993) Functional analysis of a growth factor-responsive transcription factor complex. *Cell* **73,** 395–406.
28. Whitmarsh, A. J., Shore, P., Sharrocks, A. D., and Davis, R. J. (1995) Integration of MAP kinase signal transduction pathways at the serum response element. *Science* **269,** 403–407.
29. Chen, C., Clarkson, R. W., Xie, Y., Hume, D. A., and Waters, M. J. (1995) Growth hormone and colony-stimulating factor 1 share multiple response elements in the c-fos promoter. *Endocrinology* **136,** 4505–4516.
30. Giordano, A., and Avantaggiati, M. L. (1999) p300 and CBP: Partners for life and death. *J. Cell. Physiol.* **181,** 218–230.
31. Zhang, J. Z., Vinkemeier, U., Gu, W., Chakravarti, D., Horvath, C. M., and Darnell, J. E. (1996) Two contact regions between Stat1 and CBP/p300 in interferon γ signaling. *Proc. Natl. Acad. Sci. USA* **93,** 15092–15096.
32. Schena, F. P., Gesualdo, L., and Monrinaro, V. (1992) Immunopathological aspects of immunoglobulin A nephropathy and other mesangial proliferative glomerulonephritides. *J. Am. Soc. Nephrol.* **10,** S167–S172.
33. Tellides, G., Tereb, D. A., Kirklles-Smith, N. C., Kim, R. W., Wilson, J. H., Schechner, J. S., Lorber, M. I., and Pober, J. S. (2000) Interferon-γ elicits arteriosclerosis in the absence of leukocytes. *Nature* **403,** 207–210.
34. Pondel, M. D., Murphy, S., Pearson, L., Craddock, C., and Proudfoot, N. J. (1995) Sp1 functions in a chromatin-dependent manner to augment human alpha-globin promoter activity. *Proc. Natl. Acad. Sci. USA* **92,** 7237–7241.
35. Wagner, B. J., Hayes, T. E., Hoban, C. J., Cochran, B. H. (1990) The SIF binding element confers sis/PDGF inducibility onto the c-fos promoter. *EMBO J.* **9,** 4477–4484.
36. Leaman, D. W., Pisharody, S., Flickinger, T. W., Commane, M. A., Schlessinger, J., Kerr, I. M., Levy, D. E., and Stark, G. R. (1996) Roles of JAKs in activation of STATs and stimulation of c-fos gene expression by epidermal growth factor. *Mol. Cell. Biol.* **16,** 369–375.
37. Meraz, M. A., White, J. M., Sheehan, K. C. F., Bach, E. A., Rodig, S. J., Dighe, A. S., Kaplan, D. H., Riley, J. K., Greenlund, A. C., Campbell, D., Carver-Moore, K., DuBois, R. N., Clark, R., Auget, M., and Schreiber, R. D. (1996) Targeted disruption of the Stat1 gene in mice reveals unexpected physiologic specificity in the JAK-STAT signaling pathway. *Cell* **84,** 431–442.
38. Janknecht, R., and Nordheim, A. (1996) MAP kinase-dependent transcriptional coactivation by Elk-1 and its cofactor CBP. *Biochem. Biophys. Res. Commun.* **228,** 831–837.
39. Horvath, A. E., Xu, L., Korzus, E., Brard, G., Kalafus, D., Mullen, T-M., Rose, D. W., Rosenfeld, M. G., and Glass, C. K. (1997) Nuclear integration of JAK/STAT and Ras/AP-1 signaling by CBP and p300. *Proc. Natl. Acad. Sci. USA* **94,** 1074–1079.
40. Perkins, N. D., Felzien, L. K., Betts, J. C., Leung, K., Beach, D. H., and Nabel, F. J. (1997) Steroid receptor coactivator-1 interacts with the p50 subunit and coactivates nuclear factor kappaB-mediated transactivations. *Science* **275,** 523–527.
41. Chin, Y. E., Kitagawa, M., Su, W. S., You, Z-H., Iwamoto, Y., and Fu, X-Y. (1996) Cell growth arrest and induction of cyclin-dependent kinase inhibitor $p21^{WAF1/CIP1}$ mediated by STAT1. *Science* **272,** 719–721.
42. Morris, L., Allen, K. E., and Thangue, N. B. L. (2000) Regulation of E2F transcription by cyclin E-Cdk2 kinase mediated through p300/CBP co-activators. *Nature Cell Biol.* **2,** 232–239.

Date: Tue, 08 Jan 2002 14:00:01 -0600
From: "Padilla, Kathy A" <PADILLAK@uthscsa.edu>
Subject: RE:
To: "Hottle, Diana" <HOTTLE@uthscsa.edu>
Cc: "Oyajobi, Babatunde" <OYAJOBI@uthscsa.edu>
MIME-version: 1.0

Diana/Dr. Oyajobi,

Account for supplement has been set up. Account # is K X0J0(22, 25, 29)860 1 17. NAM will be forthcoming.

Kathy Padilla
Accounting Coordinator I
Grants Management
UTHSCSA
210-567-2332 - phone
210-567-2344 - fax
padillak@uthscsa.edu

-----Original Message-----
From: Diana Hottle [mailto:hottle@uthscsa.edu]
Sent: Tuesday, January 08, 2002 12:25 PM
To: padillak@uthscsa.edu
Subject:

Marlayna Brown
Lisa Headlee
Anjana Gupta

Diana L. Hottle
Assistant to the Director
Telephone: 210-567-7204
Fax: 210-567-7277

Date: Tue, 08 Jan 2002 13:37:20 -0600
From: "Aguirre, Linda U" <AGUIRRE@uthscsa.edu>
Subject: RE: liability coverage
To: "Brown, Marlayna" <mbrown@saci.org>
Cc: hottle@uthscsa.edu
MIME-version: 1.0

Effective January 1, 2002 we are terminating Dr. Mundy's liability as I never heard back from you in reference to an account number. His UHS hospital privileges have also expired effective 12/31/01 per Gail Southard at Professional Staff Services as Dr. Mundy never returned his reappointment packet. Please be sure that he is aware of this. If he wants privileges at UHS he will have to complete the initial application packet.

Thanks.

-----Original Message-----
From: Brown, Marlayna [mailto:mbrown@saci.org]
Sent: Thursday, December 13, 2001 10:12 AM
To: aguirre@uthscsa.edu
Cc: grmos@aol.com
Subject: liability coverage

Dear Linda,

Dr. Mundy does want to retain his liability coverage. I am sorry we have missed each other playing phone tag!

What do we need to do?

Ms Marlayna Brown

Executive Assistant to Dr. Greg Mundy,
Director,
Institute for Drug Development,

14960 Omicron Drive
San Antonio, TX 78245

Tel: (210) 677-3890
Fax: (210) 677-3865
email: mbrown@saci.org

Oncogene (2000) 19, 6159–6175

www.nature.com/onc

Lessons learned from BRCA1 and BRCA2

Lei Zheng[1], Shang Li[1], Thomas G Boyer[1] and Wen-Hwa Lee*,[1]

[1]*Department of Molecular Medicine, Institute of Biotechnology, University of Texas Health Science Center at San Antonio, 15355 Lambda Drive, San Antonio, Texas, TX 78245, USA*

BRCA1 and BRCA2 are breast cancer susceptibility genes. Mutations within BRCA1 and BRCA1 are responsible for most familial breast cancer cases. Targeted deletion of Brca1 or Brca2 in mice has revealed an essential function for their encoded products, BRCA1 and BRCA2, in cell proliferation during embryogenesis. Mouse models established from conditional expression of mutant Brca1 alleles develop mammary gland tumors, providing compelling evidence that BRCA1 functions as a breast cancer suppressor. Human cancer cells and mouse cells deficient in BRCA1 or BRCA2 exhibit radiation hypersensitivity and chromosomal abnormalities, thus revealing a potential role for both BRCA1 and BRCA2 in the maintenance of genetic stability through participation in the cellular response to DNA damage. Functional analyses of the BRCA1 and BRCA2 gene products have established their dual participation in transcription regulation and DNA damage repair. Potential insight into the molecular basis for these functions of BRCA1 and BRCA2 has been provided by studies that implicate these two tumor suppressors in both the maintenance of genetic stability and the regulation of cell growth and differentiation. *Oncogene* (2000) **19,** 6159–6175.

Keywords: BRCA1; BRCA2; breast cancer; tumor suppressor; transcription regulation; DNA damage repair

BRCA1 and BRCA2, two genetic models of breast cancer

Breast cancer is one of the most frequent malignancies affecting women. The cumulative lifetime risk of a female for the development of this disease is about 10% (Claus *et al.*, 1991). For this reason, breast cancer has been the subject of intense study; however, the mechanism underlying breast cancer formation is still largely unknown. In the last decade of the 20th century, two breast cancer susceptibility genes, *BRCA1* and *BRCA2*, which together are responsible for most of the hereditary breast cancer cases, were identified (Hall *et al.*, 1990; Miki *et al.*, 1994; Wooster *et al.*, 1994, 1995). Mutations in *BRCA1* account for almost all of the hereditary breast and ovarian cancer cases and up to 40–50% of families with hereditary breast cancer only (Easton *et al.*, 1993). Mutations in *BRCA2* are linked to the other half of inherited breast cancer families and also to male breast cancer (Wooster *et al.*, 1994, 1995). The identification of familial breast cancer susceptibility genes has provided two human genetic models for studies of breast cancer.

To understand how the loss of BRCA1 or BRCA2 function leads to breast cancer formation, mouse genetic models for *BRCA1* or *BRCA2* mutations have been established. This work has revealed that Brca1 homozygous deletions are lethal at early embryonic days (E)5.5–13.5 (Gowen *et al.*, 1996; Hakem *et al.*, 1996; Liu *et al.*, 1996; Ludwig *et al.*, 1997). Three independent groups generated distinct mutations within Brca1, yet nonetheless observed similar embryonic phenotypes, including defects in both gastrulation and cellular proliferation, and death at E6.5 (Hakem *et al.*, 1996; Liu *et al.*, 1996; Ludwig *et al.*, 1997). A fourth group that generated a distinct Brca1 mutation observed embryos that survived until E13.5 and exhibited defects in neural development, including anencephaly and spina bifida to varying degrees (Gowen *et al.*, 1996). A fifth group generated a mouse model with a targeted deletion of Brca1 exon 11. The resultant mutant embryos expressed an exon 11-deletion variant of Brca1 and died at E12–18.5 (Xu *et al.*, 1999b). Collectively, these findings imply a role for the Brca1 gene product in growth and/or differentiation during mouse embryogenesis.

Similarly, three separate groups have demonstrated that mice homozygous for a Brca2 truncation mutation at the 5′ end of exon 11 die at E8.5–9.5 of gestation (Ludwig *et al.*, 1997; Sharan *et al.*, 1997; Suzuki *et al.*, 1997). Prior to growth arrest, the mutant embryos appear to have been differentiating and to be forming mesoderm, suggesting that the influence of Brca2 during mouse embryogenesis is manifest more on proliferation than differentiation. Mice homozygous for a Brca2 truncation mutation at the 3′ end of exon 11 also exhibit progressive proliferative impairment and die prenatally or perinatally; those animals that do survive to adulthood, however, develop lethal thymic lymphomas (Connor *et al.*, 1997; Friedman *et al.*, 1998).

Although these mouse models have revealed a fundamental role for BRCA1 and BRCA2 in embryogenesis, mice carrying heterozygous Brca1 and Brca2 mutations develop normally and are no more susceptible to tumors than their normal littermates. The lack of tumor formation in mice heterozygous for Brca1 or Brca2 has rendered it difficult to study the pathogenesis of breast cancer. However, the recent establishment of a conditional knockout animal model has provided a useful system with which to study early events in breast tumor formation (Deng and Scott, 2000).

By exploiting the mammary epithelium-specific expression of a MMTV-Cre or WAP-Cre transgene to induce a Cre-LoxP mediated deletion of brca1 exon 11 in mammary epithelium, it was reported that five

*Correspondence: W-H Lee

out of 23 MMTV-Cre or WAP-Cre female mice developed diverse mammary tumors by 10–13 months of age (Xu *et al.*, 1999a). Most of the tumors analysed were found to carry p53 mutations, an observation consistent with previous reports from studies of human BRCA1 familial breast tumors (Crook *et al.*, 1997; Eisinger *et al.*, 1997). These observations imply a link between p53 mutation and Brca1-associated mammary tumor development, a notion further supported by a documented acceleration in both the frequency and age of onset of breast tumor formation accompanying inactivation of one germline copy of p53 in these conditional Brca1 knockout mice (Xu *et al.*, 1999a). Collectively, these observations support a role for BRCA1 as a breast cancer suppressor gene.

Evidence to support a role for BRCA2 as a tumor suppressor includes the observation of tumorigenesis in mice homozygous for a Brca2 truncation mutation at the 3′ end of exon 11 (Connor *et al.*, 1997; Friedman *et al.*, 1998). Inactivating mutations in mitotic checkpoint genes such as Bub1, Mad3L and p53, whose products are pressed into action as a consequence of chromosomal damage, are believed to relieve growth arrest caused by BRCA2 deficiency and precipitate neoplastic transformation (Lee *et al.*, 1999). Nevertheless, a suitable breast cancer model for studying the role of BRCA2 in breast cancer development remains to be established.

Both BRCA1 and BRCA2-deficient cells are characterized by cumulative chromosome abnormalities, including chromosomal breaks, aberrant mitotic exchanges and aneuploidy (Lee *et al.*, 1999; Patel *et al.*, 1998; Xu *et al.*, 1999b). Chromosomal instability has been proposed as the pathogenic basis for mammary tumor formation caused by BRCA1 and BRCA2 deficiency. Paradoxically, chromosomal instability is invariably accompanied by growth arrest or increased cell death, and the early embryonic lethality associated with BRCA1 or BRCA2 deficiency has been attributed to these cellular responses. How then might BRCA1 or BRCA2 mutation lead ultimately to uncontrolled cell growth and tumor formation? One answer to this question may lie in the observation that tumors found in Brca1 and Brca2-deficient mice harbor additional inactivating mutations in p53 and mitotic checkpoint genes (Lee *et al.*, 1999; Xu *et al.*, 1999b). Thus, mutational inactivation of p53, which governs the G1/S cell cycle checkpoint, may circumvent the growth arrest that is normally induced upon DNA damage, and also inhibit p53-mediated apoptosis, thereby permitting the survival of cells with severe chromosomal damage. Consistently, the embryonic lethality associated with brca1-null mutations can be partially rescued by targeted deletion of p53 or p21 (Hakem *et al.*, 1997). On the other hand, inactivation of mitotic checkpoint genes could bypass mitotic arrest and permit aberrant chromosomes to segregate into progeny cells. Hence, the cumulative evidence suggests that the genetic instability arising in Brca1- or Brca2-deficient cells plays a pivotal role in tumorigenesis, leading first to compensatory gene mutations that override chromosomal damage-induced cell cycle arrest and apoptosis and, subsequently, to the accrual of functionally inactivating mutations at genetic loci involved in breast tumorigenesis.

Analysis of BRCA1- and BRCA2-deficient cells

The establishment of culture cell lines deficient in either BRCA1 or BRCA2 has facilitated studies designed to define and characterize their corresponding biological activities. Cell lines established from clinical tumor specimens include the BRCA1-deficient human breast adenocarcinoma HCC1937 cell line and the BRCA2-deficient human pancreatic carcinoma CAPAN-1 cell line. Brca1 and Brca2-deficient mouse embryos derived from gene targeting events have also served as an invaluable source of Brca1 and Brca2-deficient stem (ES) and fibroblast (MEF) cell lines for fundamental research purposes.

BRCA1-deficient HCC1937 cells, BRCA1-null ES cells, and Brca1-exon 11 deletion MEF cells are all characterized by radiation hypersensitivity. Increased sensitivity to the radiomimetic agent methyl methanesulfonate (MMS) and ionizing radiation (IR), but not to ultraviolet (UV) radiation, has also been observed in BRCA1-deficient cells (Gowen *et al.*, 1998; Scully *et al.*, 1999; Xu *et al.*, 1999b; Zhong *et al.*, 1999). Reintroduction of a wild-type BRCA1 allele, but not clinically validated BRCA1 missense mutant alleles, can complement the MMS and IR sensitivity of BRCA1-deficient cells, suggesting that the cellular response to DNA damage is compromised in breast cancer patients carrying BRCA1 mutations (Scully *et al.*, 1999; Zhong *et al.*, 1999). BRCA1-null ES cells are defective in the repair of both oxidative DNA damage by transcription-coupled processes (Gowen *et al.*, 1998) and chromosomal double-strand breaks by homologous recombination (Moynahan *et al.*, 1999). Defective control of the DNA-damage induced G2/M checkpoint has also been observed in BRCA1-exon 11 deletion MEFs, thereby implicating BRCA1 in cell cycle checkpoint control (Xu *et al.*, 1999b). Improper centrosome duplication is another prominent characteristic of these cells leading to multipolar spindle formation and consequent unequal chromosomal segregation and micronuclei formation (Xu *et al.*, 1999b). Although a function in centrosome duplication is consistent with the reported localization of the BRCA1 protein to centrosomes (Hsu and White, 1998), multiple centrosomes could be formed as a consequence of accumulated DNA damage in Brca1-deficient cells, as it has been shown that DNA damage can trigger improper centrosome activity followed by micronuclei formation (Sibon *et al.*, 2000; Su and Vidwans, 2000). Nonetheless, improper centrosome duplication is likely to exacerbate pre-existing genomic instability that has arisen from defects in the surveillance and repair of damaged DNA. Taken together, the phenotypic characteristics of BRCA1-deficient cells suggest that BRCA1 occupies a central role in the cellular DNA damage response by virtue of its dual participation in DNA damage repair and cell cycle checkpoint control.

Hypersensitivity to genotoxic agents including UV, MMS, and IR has been reported to be characteristic of BRCA2-deficient cells, including tumor-derived CAPAN-1 cells, Brca2-deficient mouse blastocysts and MEFs (Chen *et al.*, 1998b; Connor *et al.*, 1997; Patel *et al.*, 1998; Sharan *et al.*, 1997). It has also been observed that the level of unrepaired DNA double-strand breaks is abnormally elevated in Brca2-deficient MEFs

following IR-treatment, suggesting that Brca2 is also required for efficient DNA repair (Connor *et al.*, 1997).

Analysis of functional domains recognized in BRCA1 and BRCA2

Genetic studies have revealed *BRCA1* and *BRCA2* to be essential for cell growth and survival, critical for an appropriate cellular response to DNA damage, and important etiological factors in the development of cancer. In parallel, functional analyses of their corresponding gene products have been carried out in order to understand how BRCA1 and BRCA2 execute these functions.

The *BRCA1* gene encodes a nuclear phosphoprotein of 1863 amino acids (Chen *et al.*, 1996b,c; Miki *et al.*, 1994) characterized by the presence of two outstanding structural motifs at each of its flanking termini (Figure 1a). At its amino terminus, BRCA1 harbors a structurally conserved RING finger domain (amino acids 24–64). The RING fingers is a zinc-binding motif characterized by a set of spatially conserved cysteine and histidine residues that follow the linear order C3HC4 within the primary amino acid sequence. The RING finger motif of BRCA1 does not appear to represent a DNA-binding domain, but is apparently involved in protein–protein interactions (Saurin *et al.*, 1996). Two proteins, BARD1 and BAP1, have been identified based on their ability to bind to the BRCA1 RING finger domain (Jensen *et al.*, 1998; Wu *et al.*, 1996).

The C-terminal region of BRCA1 was first characterized as a transactivation domain (Chapman and Verma, 1996; Chen *et al.*, 1996a; Monteiro *et al.*, 1996). This region also contains two tandem BRCT (BRCA1 C-terminal) domains (amino acids 1640–1863). An autonomous folding unit defined by conserved clusters of hydrophobic amino acids, the BRCT domain is found in a diverse group of proteins implicated in DNA repair and cell cycle check-point control (Bork *et al.*, 1997; Callebaut and Mornon, 1997; Koonin *et al.*, 1996). While no specific cellular function has been ascribed to the BRCT domain, this motif is likely to represent a protein interaction surface (Saka *et al.*, 1997). The BRCT domain in BRCA1 mediates its interaction with proteins such as RNA helicase A, CtIP, and histone deacetylases (Table 1) (Anderson *et al.*, 1998; Li *et al.*, 1999b; Wong *et al.*, 1998; Yarden and Brody, 1999; Yu *et al.*, 1998).

Yet another region in BRCA1, which is encoded by the 5′-region of exon 11 appears to have an emerging role as a functionally relevant protein–protein interaction surface (Chen *et al.*, 1999). Although the structure of this region has not yet been defined, it nonetheless mediates the interaction of BRCA1 with many proteins including BRAP2, p53, c-Myc, and RAD50 (Table 1) (Li *et al.*, 1998; Wang *et al.*, 1998; Zhang *et al.*, 1998; Zhong *et al.*, 1999). This region also includes two putative nuclear localization signals, which have been shown to interact with importin α (Chen *et al.*, 1996a).

The BRCA2 gene encodes a nuclear phosphoprotein of 3418 amino acids (Figure 1b) (Bertwistle *et al.*, 1997; Wooster *et al.*, 1995). Sequence analysis has revealed that its exon 3-encoded region shares some sequence similarity with the transactivation domain present in c-Jun, and functional analysis has confirmed the presence of an inherent transactivation function within this region (Milner *et al.*, 1997). A prominent architectural feature resident within the BRCA2 primary amino acid sequence comprises eight tandem copies of a repetitive

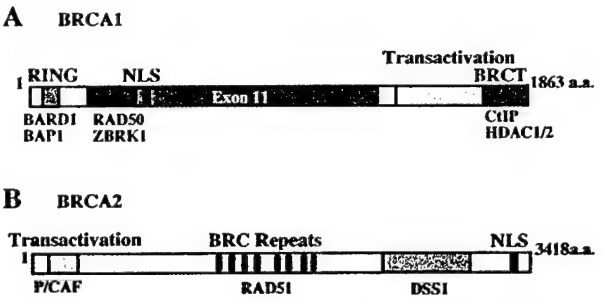

Figure 1 Structural and functional motifs recognized in BRCA1 and BRCA2. (**a**) Schematic structure of BRCA1. RING domain, transactivation domain, BRCT domain, nuclear localization signals (NLS), as well as the exon 11-coding regions are indicated. Representative proteins that interact with BRCA1 in three different regions are indicated. (**b**) Schematic structure of BRCA2. Transactivation domain, BRC repeats, and NLS are indicated. Representative BRCA2-interacting proteins are indicated

Table 1 Putative BRCA1-interacting proteins

BRCA1-interacting protein	*Function*	*Interaction domain*	*Reference*
BARD1	Interacting protein of polyadenylation factor CstF-50	N-terminal RING domain	Wu *et al.*, 1996
BAP1	De-ubiquinating enzyme	N-terminal RING domain	Jensen *et al.*, 1998
RAD50	DSB repair protein	Exon 11 5′-coding region	Zhong *et al.*, 1999
ZBRK1	Sequence-specific transcription repressor	Exon 11 5′-coding region	Zheng *et al.*, 2000
BRAP2	Cytoplasmic retention protein	Exon 11 5′-coding region	Li *et al.*, 1998
p53	Transcription factor tumor suppressor	Exon 11 5′-coding region and 2nd BRCT domain	Zhang *et al.*, 1998; Ouchi *et al.*, 1998 Chai *et al.*, 1999
c-Myc	Transcription factor, oncogene	Exon 11 5′-coding region	Wang *et al.*, 1998
Rb	Cell cycle regulator, Tumor suppressor	Exon 11 5′-coding region	Aprelikova *et al.*, 1999
STAT1	Signal transducer and activator of transcription	Exon 11 5′-coding region	Ouchi *et al.*, 2000
Importin α	Nuclear transportation	Nuclear localization signals	Chen *et al.*, 1996a
RAD51	DSB repair protein	Exon 11 3′-coding region	Scully *et al.*, 1997c
RNA Helicase A	Component of RNA polymerase II holoenzyme	BRCT domains	Anderson *et al.*, 1998
CtIP	Transcription co-repressor, CtBP-interacting protein	BRCT domains	Li *et al.*, 1999b; Yu *et al.*, 1998; Wong *et al.*, 1998
HDAC1/2	Histone deacetylases	BRCT domains	Yarden and Brody, 1999
CBP/p300	Transcription co-activator	BRCT domains	Pao *et al.*, 2000

sequence motif termed the BRC repeat. Each BRC repeat, designated BRC1 to BRC8, is approximately 30 amino acids in length. Among the eight BRC repeats within BRCA2, the sequences of six are highly conserved among the repeats and can mediate the interaction of BRCA2 with RAD51. The two remaining repeats, BRC5 and BRC6, are less conserved and do not bind to RAD51 (Chen *et al.*, 1998b; Wong *et al.*, 1997). A third notable region within the BRCA2 primary amino acid sequence, spanning residues 2472 to 2957, represents a region of higher sequence conservation between human and mouse BRCA2 than the coding sequence as a whole. An evolutionarily conserved protein, DSS1 (deleted in split hand/split foot), has been found to interact with BRCA2 in this region, although the significance of this interaction is not clear (Marston *et al.*, 1999).

Protein interaction studies thus provide independent support for a potential role of BRCA1 and BRCA2 in DNA damage repair by revealing their interactions with RAD50 and RAD51, respectively. Correspondingly, a role for BRCA1 and BRCA2 in transcription regulation is supported by both the identification in each of an autonomous transactivation function, and protein interaction profiling that reveals the interaction of each with a variety of transcriptional activators and repressor proteins.

Molecular basis of BRCA1 and BRCA2 function

BRCA1 in transcription regulation

BRCA1-mediated transcriptional activation A role for BRCA1 in transcriptional regulation was initially indicated by the identification of an acidic domain near the carboxyl-terminus of BRCA1 with an inherent transactivation function that is sensitive to cancer-predisposing mutations (Chapman and Verma, 1996; Chen *et al.*, 1996a; Monteiro *et al.*, 1996). When fused to a heterologous DNA-binding domain, a carboxy-terminal fragment of BRCA1 (amino acids 1560–1863) was observed to exhibit strong transcriptional activity in mammalian cells, and this activity was completely abolished by familial breast cancer-derived BRCA1 mutations (Chapman and Verma, 1996; Monteiro *et al.*, 1996). This region, as well as a second, partially overlapping region (amino acids 1142–1643) was also found to confer similar transactivation activity in yeast cells (Chen *et al.*, 1996a). An inherent transactivation function within this region of BRCA1 is further supported by a recent study showing that this region, when expressed recombinantly with a heterologous DNA binding domain, can activate transcription *in vitro* in a highly purified reconstituted transcription system (Haile and Parvin, 1999). The presence of an autonomous transactivation function within BRCA1, coupled with the absence of demonstrable sequence-specific DNA-binding activity, had led to the hypothesis that BRCA1 functions as a co-activator of transcription.

Biological implications of BRCA1-mediated transcriptional activation Recent studies utilizing gene expression profiling methodologies have revealed that ectopic overexpression of BRCA1 can induce a diverse array of genes implicated in cell growth control, cell cycle regulation, and DNA replication and repair. Included among these are the genes encoding p21, GADD45, EGR1, PCNA, CDC34, Ku70, K80, and GADD153 (Harkin *et al.*, 1999; MacLachlan *et al.*, 2000). As BRCA1 protein levels increase between mid-S and G2 phases of the cell cycle (Chen *et al.*, 1996c), it is possible that BRCA1 overexpression strategies may simulate the status of BRCA1 during these physiological periods and thereby provide at least a limited window onto the spectrum of target genes under its transcriptional control.

While the transactivation function of BRCA1 is likely to contribute to its role in the regulation of gene expression, it is not presently clear how BRCA1 mediates gene-specific transcription control. Since BRCA1 does not appear to bind specific DNA sequences, it seems likely that it must interact with sequence-specific DNA-binding transcription factors in order to target unique genetic loci. As a sequence-specific DNA-binding transcription factor, the universal tumor suppressor p53 may represent an important link between BRCA1 and gene-specific transcription control. p53 lies at the heart of a cell-signaling pathway that is triggered by genotoxic stresses, including DNA damage. Stress-induced p53-initiated cell cycle arrest and/or apoptosis ensures the timely repair or elimination of potentially deleterious genetic lesions. Significantly, p53 and BRCA1 appear to regulate transcription from an overlapping set of DNA damage-inducible target genes, including p21 and GADD45. This observation initially implied a functional interaction between these two important tumor suppressors, a prediction that has since been borne out experimentally. BRCA1 and p53 have been demonstrated to interact physically and synergize functionally to activate transcription through p53 binding sites located in both the *p21* promoter and *GADD45* intron 3 sequences (Chai *et al.*, 1999; Ouchi *et al.*, 1998; Zhang *et al.*, 1998). The ability of BRCA1 to potentiate p53-dependent transcription absent DNA binding has led to the hypothesis that BRCA1 functions as a p53-specific co-activator, possibly linking the biochemical activities of these two proteins to a common pathway of tumor suppression. Nevertheless, BRCA1 can also regulate promoter activity and induce gene expression in a p53-independent manner (Somasundaram *et al.*, 1997; Harkin *et al.*, 1999). Therefore, additional unidentified DNA-binding transcription factors must function to recruit BRCA1 to specific target genes.

Mechanistic basis for BRCA1-mediated transcriptional activation The initiation of RNA polymerase II transcription represents a principal step targeted for regulation within the cell. Gene-specific activators function to stimulate the rate of transcription initiation largely through the recruitment of either chromatin remodeling activities and/or the general transcription machinery in order to override nucleosome-mediated promoter repression and assemble transcription-competent pre-initiation complexes, respectively. While the underlying mechanism by which BRCA1 mediates gene-specific transcriptional activation remains to be established, current experimental observation is consistent with a role for BRCA1 in both of these recruitment steps.

First, BRCA1 could play a role in the recruitment of chromatin remodeling activities. BRCA1 has been demonstrated to interact directly or indirectly with chromatin modifying activities including p300 (Pao *et al*., 2000), hBRG1 (Neish *et al*., 1998), and BRCA2 (Chen *et al*., 1998a) which itself is associated with histone acetyltransferase activity (Fuks *et al*., 1998; Siddique *et al*., 1998). In addition, it has recently been demonstrated that the BRCA1 carboxyl-terminal transactivation domain, when targeted to chromatin via a heterologous DNA-binding domain, can alter local chromatin structure (Hu *et al*., 1999). Significantly, the same cancer-predisposing mutations that abolish its transcriptional activation function also abrogate the ability of this domain to effect chromatin remodeling (Hu *et al*., 1999), perhaps implicating direct recruitment of chromatin modifying activities as a mechanistic basis for the disruptive influence of this region.

A second step at which BRCA1 is likely to function in transcriptional activation involves RNA polymerase II holoenzyme recruitment. This possibility is supported by several studies that link BRCA1 to the RNA polymerase II holoenzyme through demonstrated interactions with constituent holoenzyme components, including RNA helicase A (RHA) (Anderson *et al*., 1998; Scully *et al*., 1997a), CBP/p300 (Pao *et al*., 2000), and RNA polymerase II itself (Schlegel *et al*., 2000). The ability of BRCA1 to bind to RNA helicase A has been shown to be essential for the transactivation activity of BRCA1, suggesting a direct functional link between BRCA1 and the holoenzyme. CBP/p300 has been found to interact with BRCA1 *in vitro* and *in vivo*, and to stimulate BRCA1-directed transcription activation (Pao *et al*., 2000). Recently, BRCA1 has been shown to bind specifically to RNA polymerase II subunits hRPB2 and hRPB10a *in vitro* (Schlegel *et al*., 2000). Moreover, excess recombinant hRPB2 and hRBP10a, but not other polymerase subunits, were found to be capable of blocking activated transcription *in vitro* by the BRCA1 carboxyl-terminal transactivation domain, suggesting that direct interactions between BRCA1 and core RNA polymerase II could potentially mediate BRCA1-dependent transcriptional activation. Taken together, these observations implicate multiple components within the RNA polymerase II holoenzyme for potential contact by BRCA1. Accordingly, a plausible model to account for transcriptional activation by BRCA1 is that gene-specific activators, by virtue of their interaction with BRCA1, recruit the RNA polymerase II holoenzyme onto target promoters in order to effect an increase in the transcription rate of genes under their control.

Yet another mechanism by which BRCA1 could potentially function to stimulate transcription invokes targeting of post-initiation processes, including transcription elongation. The observation that Brca1-deficient ES cells are defective in transcription-coupled repair of oxidative DNA damage (Gowen *et al*., 1998) suggests a link between BRCA1 and RNA polymerase II actively engaged in transcript synthesis. Future studies will be required to more precisely define the potential regulatory role that BRCA1 plays in steps subsequent to RNA polymerase II transcription initiation.

BRCA1-mediated transcriptional repression Somewhat paradoxically, the carboxyl-terminus of BRCA1 that both binds transcriptional coactivators and encodes a potent transactivation domain also mediates the interaction of BRCA1 with transcriptional corepressors including the CtIP/CtBP complex and histone deactylases (HDACs) (Li *et al*., 1999b; Yarden and Brody, 1999). Interestingly, familial breast cancer-derived mutations that compromise its transactivation activity also abolish the binding of BRCA1 to CtIP and HDACs. These observations have prompted the speculation that BRCA1 may function analogously to nuclear receptors, which function both as activators and repressors depending on their associated cofactors (Pao *et al*., 2000). These observations also suggest the intriguing possibility that apparent BRCA1-mediated transcriptional induction may derive, at least in part, from derepression by BRCA1-mediated corepressor titration.

BRCA1 has been shown to repress c-Myc-mediated transcriptional activation (Wang *et al*., 1998) and also to inhibit the transactivation activity of estrogen receptor (Fan *et al*., 1999). The negative effect of BRCA1 on c-Myc-mediated transactivation could derive from transrepression involving inhibition of either Myc-Max heterodimer formation or DNA binding by Myc-Max heterodimers (Wang *et al*., 1998). BRCA1-mediated inhibition of estrogen receptor-mediated transactivation could reflect either direct repressive effects at the promoter or, alternatively, indirect repression through disruption of signaling events that activate the estrogen receptor (Fan *et al*., 1999).

The association of BRCA1 with CtIP/CtBP or HDACs suggests a more direct role for BRCA1 in active repression and, thus provides an alternative explanation for the negative effect of BRCA1 on transcription. A direct role for BRCA1 in transcriptional repression is supported by a recent study showing that BRCA1 can mediate sequence-specific transcriptional repression through its selective recruitment by a novel DNA-binding transcription factor, ZBRK1 (zinc-finger and BRCA1-interacting protein with a KRAB domain). In this study, BRCA1 is shown to mediate ZBRK1-directed repression through a ZBRK1 binding site identified in intron 3 of the GADD45 gene, thus providing a potential mechanistic link between the activities of BRCA1 in gene-specific transcription control, the cellular DNA damage response, and the maintenance of genome integrity (Zheng *et al*., 2000).

Biological implications of BRCA1-mediated transcriptional repression BRCA1 has been reported to repress c-Myc-mediated transcriptional activation from synthetic promoters carrying c-Myc response elements as well as from the natural c-Myc-responsive CDC25A promoter (Wang *et al*., 1998). Furthermore, this BRCA1-mediated transcriptional repression can be correlated with its inhibition of Myc-mediated cellular transformation, thus providing one potential mechanism for BRCA1-mediated tumor suppression (Wang *et al*., 1998).

BRCA1-mediated transcriptional repression has also been implicated in silencing the DNA-damage inducible p21 and GADD45 genes in their uninduced states. Support for this model has been provided by a recent study showing that BRCA1 may be physically tethered and functionally linked to a specific regulatory locus

within GADD45 through the sequence-specific DNA-binding transcription repressor ZBRK1 (Zheng *et al.*, 2000). This study also reveals that relief of ZBRK1-directed GADD45 repression may be achieved by ectopic overexpression of BRCA1, most likely by altering the balance of repression components specifically recruited to DNA-bound ZBRK1. This unexpected observation raises the possibility that activation of GADD45 transcription in the natural setting may reflect the concerted effects of both derepression and true activation.

While derepression by BRCA1 overexpression may accurately reflect some aspect of its function *in vivo*, more physiologically relevant mechanisms for derepression are likely to involve alterations in the phosphorylation and/or protein interaction status of BRCA1. In this regard, DNA damage-induced dissociation of a CtIP-CtBP corepressor complex from BRCA1 could relieve ZBRK1 repression of *GADD45* transcription, thereby leading to *GADD45* induction (Li *et al.*, 2000) in response to DNA damage-induced signaling. A similar mechanism may also underlie p21 induction.

BRCA1-mediated control of p21 and GADD45 gene transcription may contribute to its role in cell cycle checkpoint control, since p21 and GADD45 have been implicated in DNA-damage induced G1/S and G2/M checkpoint control, respectively (el-Deiry *et al.*, 1993; Deng *et al.*, 1995; Brugarolas *et al.*, 1995; Wang *et al.*, 1999). Consistent with this possibility, GADD45 induction in response to MMS or UV has been shown to be dependent on BRCA1 (Harkin *et al.*, 1999). Thus, mutational inactivation of BRCA1 or its associated factors could lead to alterations in the normal induction profile of GADD45 and a resultant failure of cells to achieve an appropriate G2/M arrest. While GADD45 induction triggered by IR has been shown to require ATM and p53 (Kastan *et al.*, 1992), the involvement of BRCA1 is not clear. However, several recent studies have implicated BRCA1 in the IR pathway possibly leading to GADD45 induction. First, it has been shown that BRCA1 can potentiate transcription from p53-response elements within the GADD45 gene in a p53-dependent manner (Harkin *et al.*, 1999). Second, BRCA1 has been identified as a downstream target of ATM in a DNA damage induced signaling pathway following IR (Cortez *et al.*, 1999). Nonetheless, direct supporting evidence of a regulatory role for BRCA1 in GADD45-mediated G2/M checkpoint control is currently lacking.

Gene expression profiling studies have established a number of genes to be downregulated in response to BRCA1 overexpression, thus identifying potential targets of BRCA1-mediated transcriptional repression. Included among these are Cyclin B1 and PIN1 (MacLachlan *et al.*, 2000). Cyclin B1, the activating subunit of cdc2 kinase (reviewed by Nurse, 1994), and PIN1, a peptidyl-prolyl isomerase (Lu *et al.*, 1996), are both involved in mediating cellular progression into and through mitosis. BRCA1-mediated repression of these genes could be expected to arrest cells at the G2/M cell cycle transition phase, thereby providing an additional potential mechanism through which BRCA1 could achieve G2/M cell cycle checkpoint control (MacLachlan *et al.*, 2000). Precisely how DNA damage-induced signaling might activate BRCA1 to effect transcriptional repression of Cyclin B1 or PIN1, however, remains to be elucidated. Alternatively, it is possible that BRCA1 could regulate G2/M phase traversal during the normal cell cycle through regulation of Cyclin B1 and PIN1.

A recent study documenting BRCA1-mediated repression of estrogen receptor transcriptional activity invokes a potential role of BRCA1 in the estrogen-signaling pathway (Fan *et al.*, 1999). This pathway controls multiple aspects of breast and ovarian cell growth, differentiation and homeostasis. Furthermore, estrogen itself is a distinct etiological factor in breast and ovarian cancer. By affecting hormone response pathways, BRCA1 may regulate growth or a differentiation in a cell-type specific manner.

Mechanistic basis for BRCA1-mediated transcriptional repression Insight into the potential mechanism(s) by which BRCA1 mediates the repression of specific target genes has come from protein interaction studies that link BRCA1 to established transcriptional repression activities, including the CtIP/CtBP corepressor complex and histone deacetylases. Human CtBP was initially identified as an adenovirus E1A C-terminal interacting protein - capable of attenuating E1A-mediated transcriptional activation and tumorigenesis (Schaeper *et al.*, 1995). A corepressor function for CtBP was subsequently revealed through the interaction of *Drosophila* CtBP with three transcriptional repressors, Knirps, Snail, and Hairy (Nibu *et al.*, 1998; Poortinga *et al.*, 1998). Mammalian homologs of CtBP have also been found to serve as corepressors for a variety of DNA-binding transcriptional repressors (Furusawa *et al.*, 1999; Postigo and Dean, 1999; Turner and Crossley, 1998). Each of these CtBP-interacting transcriptional repressors harbors a conserved amino acid sequence motif, PLDLS, that was originally identified in E1A and that specifies the association of each with CtBP (Sollerbrandt *et al.*, 1996).

The same sequence motif present in CtBP-interacting transcriptional repressors also specifies the interaction of CtBP with CtIP, a protein initially identified by virtue of this interaction (Schaeper *et al.*, 1998). Remarkably, an interaction between CtIP and BRCA1 was simultaneously identified by several groups (Li *et al.*, 1999b; Wong *et al.*, 1998; Yu *et al.*, 1998), and CtIP was found to link the corepressor CtBP to BRCA1 (Li *et al.*, 1999b). Interestingly, a second tumor suppressor, the retinoblastoma (Rb) protein, as well as one of its associated family members, p130, also interact with CtIP. This observation led to the hypothesis that the transcriptional repression activity of Rb and p130 might be mediated by recruitment of CtBP through CtIP (Meloni *et al.*, 1999). Its specific interaction with two distinct tumor suppressor proteins, BRCA1 and Rb, imply a fundamental role for CtIP in tumor suppression.

Another distinct corepressor complex with which BRCA1 interacts is the histone deacetylase complex (Yarden and Brody, 1999). Initially identified based on its copurification with mSin3, histone deacetylase complex components include two proteins initially identified as Rb-associated proteins, RbAp48 and RbAp46, two histone deacetylases, HDAC1 and HDAC2, two additional polypeptides, SAP18 and

SAP30, and additional unidentified factors (for review, see Pazin and Kadonaga, 1997; and references therein). Sin3 and nuclear receptor corepressors, N-CoR/SMRT, are also components of the histone deacetylase complex and appear to function in establishing the protein–protein links between DNA-bound repressors and the histone deacetylases. The association of N-CoR/SMRT with HDAC1/2 is mediated by mSin3 (Pazin and Kadonaga, 1997). Besides HDAC1 and HDAC2, which comprise class I histone deacetylases, other HDAC family proteins have been identified, including class I HDAC3, and class II HDAC4, HDAC5, HDAC6 and HDAC7. Recently, N-CoR/SMRT have been found to interact directly with class II histone deacetylases, suggesting that these corepressors can recruit histone deacetylases in a mSIN3-independent manner (for review, see Glass and Rosenfeld, 2000; and references therein). BRAC1 has been shown to associate with at least four components of histone, deacetylase complexes, including HDAC1/2 and RbAp46/RbAp48 (Yarden and Brody, 1999). This observation suggests that BRCA1-mediated transcriptional repression may derive, at least in part, from active recruitment of HDACs.

While the precise mechanism by which BRCA1 mediates gene-specific transcriptional repression remains to be established, current experimental observation is consistent with several alternative possibilities (Figure 2). First, BRCA1 corepression could involve targeted chromatin remodeling. For example, BRCA1 could, by virtue of its direct recruitment of HDAC complexes, alter the chromatin structure of its target genes into a repression-favored status. Alternatively, BRCA1 could affect remodeling via its interaction with the CtIP-CtBP corepressor complex. CtBP itself interacts directly with HPC2, the human homolog of *Drosophila* polycomb (Sewalt *et al*., 1999). HPC2 is part of a polycomb group (PcG) protein complex that functions in repression of homeotic gene expression during vertebrate development. The PcG proteins have been proposed to confer heritable and stable transcriptional repression by packaging target genes into heterochromatin-like configurations or, alternatively, by relocalizing target genes into heterchromatic compartments (Sewalt *et al*., 1999). Recently, a histone deacetylase-independent CtBP repression mechanism has been described (Koipally and Georgopoulos, 2000), suggesting the possibility of multiple independent paths to achieve repression through a putative BRCA1-CtIP-CtBP complex. Alternatively, the association of BRCA1 with the RNA polymerase II holoenzyme may evince a distinct mechanism for corepression by which BRCA1 directly targets either the general transcription machinery or interacting coactivators.

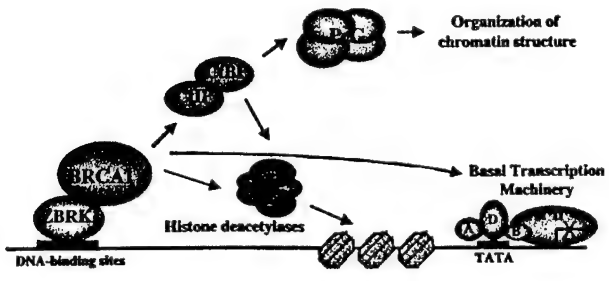

Figure 2 Sequence-specific transcription repression mediated by BRCA1. ZBRK1 represents the sequence-specific transcription repressor that recruits BRCA1 to specific DNA-binding sites in its target genes. BRCA1 mediates transcription repression through three potential mechanisms. First, BRCA1 may recruit CtIP/CtBP to mediate reorganization of higher order chromatin structure. Second, BRCA1 may recruit the histone deacetylase complex to mediate local gene silencing. Third, BRCA1 may repress transcription by regulating the basal transcription machinery

BRCA1 in DNA repair

BRCA1 appears to participate in the cellular DNA damage response at multiple stages. In normal cells, responses to DNA damage include sensing damaged DNA, transducing DNA damage signals, relocating repair machinery to damage sites, completing a repair process, and coordinating cell cycle progression with the DNA repair process. Accumulating evidence suggests that BRCA1 functions not only in association with the DNA repair machinery, but also in DNA-damage induced cell cycle checkpoint control. Additionally, BRCA1 may regulate the expression of genes involved in DNA damage repair and, significantly, it directly participates in the repair process itself. Finally, phosphorylation of BRCA1 upon DNA damage implies a role for BRCA1 in DNA damage-induced signal relay.

The interaction between BRCA1 and the DNA repair machinery BRCA1 has been shown to associate directly with the RAD50/MRE11/NBS1 complex (Zhong *et al*., 1999). Its equivalent complex in yeast, the Rad50/Mre11/Xrs2 complex, functions in both non-homologous end-joining (NHEJ) and homologous recombinational repair of DNA double-strand breaks. Yeast strains deficient in MRE11, RAD50, or XRS2 exhibit a 50- to 100-fold decrease in NHEJ in the absence of the RAD52-dependent homologous recombination pathway (Ivanov *et al*., 1992; Johzuka and Ogawa, 1995). A role in facilitating homologous recombination in mitotic cells has also been established for this complex (Bressan *et al*., 1999). Meanwhile, Mre11, Rad50, and Xrs2 are necessary for introduction of chromosomal double-strand breaks (DSB) that lead to homologous recombination during meiosis in yeast (Ivanov *et al*., 1992; Johzuka and Ogawa, 1995; Ohta *et al*., 1998). In addition, they are involved in other cellular processes including chromatin configuration and telomere maintenance (Boulton and Jackson, 1998; Chamankhah *et al*., 2000; Chamankhah and Xiao, 1999; Gerecke and Zolan, 2000; Nugent *et al*., 1998; Ohta *et al*., 1998). It has been proposed that RAD50/MRE11/XRS2 is responsible for end-processing of double-strand breaks (Tsubouchi and Ogawa, 1998). In support for this idea, recombinant MRE11 proteins and purified human RAD50/MRE11/NBS1 complexes exhibit exonuclease and endonuclease activities (Paull and Gellert, 1998; Trujillo *et al*., 1998). The mechanistic role of RAD50 in this complex is not clear, although it has been shown that the exonuclease activity of MRE11 in complex with RAD50 is moderately increased (Paull and Gellert, 1998). Based on the structural similarity between RAD50 and SMC family proteins, it has been proposed that RAD50 may be a chromatin-associated protein and participate in

chromatin structural reconfiguration (Alani *et al.*, 1989). NBS1, the human equivalent of yeast Xrs2, was identified based on its copurification with RAD50 and MRE11, and simultaneously as the product of the gene mutated in Nijmegen break syndrome (Carney *et al.*, 1998; Varon *et al.*, 1998b). The RAD50/MRE11/NBS1 complex exhibits several activities that are not observed in the absence of NBS1, including partial DNA duplex unwinding and efficient cleavage of fully paired hairpins (Paull and Gellert, 1999). Apart from its role in double-strand break repair, this complex, or individual complex components, may function in other aspects of the DNA damage response. Radio-resistant DNA synthesis (RDS), a hallmark of ataxia telangiectasia (A-T) cells (Painter and Young, 1980), has also been observed in NBS1-deficient cells, implying a role for NBS1 in S phase DNA damage checkpoint control, which could represent a potential mechanism for downregulation of DNA synthesis should DNA be damaged during the early stages of S phase (Painter and Young, 1987).

BRCA1 appears to interact with the RAD50/MRE11/NBS1 complex directly through RAD50 (Zhong *et al.*, 1999). Similar to the formation of the RAD50/MRE11/NBS1 complex, the association of BRCA1 with this complex does not change in response to DNA damage. Rather, the nuclear partitioning of this BRCA1-containing complex changes and BRCA1 forms ionizing irradiation-induced foci (IRIF), which is also a characteristic of RAD50, MRE11 and NBS1 (Maser *et al.*, 1997). Upon IR treatment, BRCA1 nuclear dots originally observed in untreated cells are disrupted, and later gradually reassemble into bright foci, which also colocalize with RAD50 foci in the portion of cells that display both RAD50 and BRCA1 foci (Zhong *et al.*, 1999). It has been suggested that RAD50/MRE11 complexes localize to the sites of DSB upon IR (Nelms *et al.*, 1998); therefore, the colocalization of BRCA1 with this complex implies that BRCA1 is relocated to the sites of DSB upon IR. This dynamic redistribution of BRCA1 could reflect an aspect of the cellular response to DNA damage in a manner analogous to the translocation of RAD50 complexes to the sites of DSBs. Consistently, BRCA1 has been found to be important for efficient formation of IRIF (Zhong *et al.*, 1999). Its association with the RAD50/MRE11/NBS1 complex suggests that BRCA1 could participate directly in the RAD50-mediated DNA repair process. Alternatively, BRCA1 could facilitate the repair of DSBs on chromatin templates through its direct recruitment of chromatin remodeling activities (Hu *et al.*, 1999). The precise role that BRCA1 plays in complex with RAD50/MRE11/NBS1, however, remains to be definitively established.

Besides RAD50/MRE11/NBS1, other components involved in DNA damage repair, such as MSH2, MSH6, MLH1, ATM and BLM, have been found to reside in a large BRCA1-containing DNA repair complex (Wang *et al.*, 2000). In addition, DNA replication factor C and PCNA were also found in this complex (Wang *et al.*, 2000). This complex has been proposed to represent a BRCA1-associated genome surveillance complex (BASC) since many of its constituent proteins individually recognize distinctly abnormal DNA structures, such as double-strand breaks, base-pair mismatches, and stalled replication forks. Many of these proteins are involved in replication or repair of damage that can occur at replication forks. Therefore, the association of BRCA1 with these proteins suggests that BRCA1 may also participate in the resolution of aberrant DNA structures that occur during DNA replication or when DNA replication is stalled (Wang *et al.*, 2000). Consistent with this notion is the previous observation that BRCA1 foci at S phase disperse in response to DNA damage or replication blocks, and relocalize to PCNA-containing structures (Scully *et al.*, 1997b), suggestive of a role for BRCA1 in replicational DNA repair.

BRCA1 has also been proposed to associate, through a region encoded by the 3′ end of exon 11, with RAD51 although it is still not clear whether this association is mediated by direct or indirect interaction (Scully *et al.*, 1997c). This association is supported primarily by the observation that BRCA1 foci partially colocalize with RAD51 foci during S phase, and relocalize to PCNA-containing structures in response to UV-treatment or replication block by hydroxyurea (Scully *et al.*, 1997b). BRCA1 has also been observed in IR-induced RAD51 foci; however, such foci are distinct from those comprising BRCA1 and the RAD50/MRE11/NBS1 complex (Zhong *et al.*, 1999). While the RAD50/MRE11/NBS1 complex has been proposed to function in end-processing, an early step in both homologous recombination and non-homologous end-joining based repair of DNA double-strand breaks, RAD51 is involved in strand-exchange, a later step in homologous recombination (reviewed by Baumann and West, 1998). The biological implications underlying the dual participation of BRCA1 in two distinct steps of homology-based recombinational DSB repair remain to be resolved.

BRCA1 in DNA double-strand break repair Cumulative evidence is consistent with the direct participation of BRCA1 in DNA DSB repair through both homologous recombination and NHEJ. The develop-

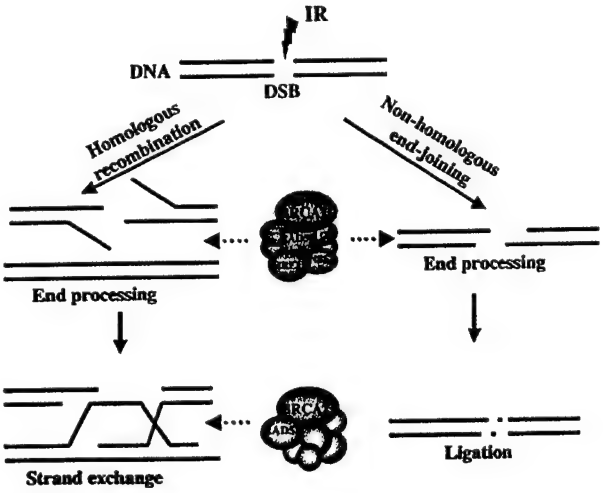

Figure 3 BRCA1 and BRCA2 participate in DSB repair. BRCA1 forms a complex with RAD50, MRE11, NBS1 and other proteins. This complex is involved in both homologous recombination and non-homologous end-joining processes of DSB repair. BRCA2 forms a complex with RAD51, which is involved in DNA strand exchange during homologous recombination

ment of an *in vivo* DSB repair assay system (Moynahan *et al.*, 1999) in which the frequency of repair at a defined DSB may be measured has proven instrumental in elucidating the contribution of BRCA1 to both homologous and nonhomologous recombinational repair pathways (Figure 3). Using this system, Brca1-deficient embryonic stem cells were found to exhibit a significant defect in homologous recombination (Moynahan *et al.*, 1999). A recent study using a similar approach has shown that NHEJ is also severely reduced in Brca1-deficient mouse embryonic fibroblast cells (Zhong *et al.*, submitted) although such a defect was not observed previously in embryonic stem cells (Moynahan *et al.*, 1999). Moreover, retroviral integration, which relies on the NHEJ-dependent repair pathway, is inefficient in Brca1-deficient embryonic fibroblast cells (Zhong *et al.*, submitted). This same study also demonstrated that Brca1-deficient cell extract as well as normal cell extract blocked by BRCA1-specific antibodies both exhibit reduced activity in catalyzing DNA end-joining *in vitro*, suggesting that BRCA1 participates directly in the NHEJ repair process (Zhong *et al.*, submitted).

The involvement of BRCA1 is both homologous recombination and NHEJ is consistent with its interaction with the RAD50/MRE11/NBS1 complex, which is required for both DNA recombination processes. It has been demonstrated that cells with component defects in either of these recombinational repair pathways are prone to radiation hypersensitivity, genetic instability, and increased tumor susceptibility (Difilippantonio *et al.*, 2000; Gao *et al.*, 2000; Varon *et al.*, 1998a).

It is worth noting that both BRCA1 and BRCA2 genes are not evolutionarily conserved, while the basic DSB repair machinery itself is (reviewed by Featherstone and Jackson, 1999; Karran, 2000). BRCA1 is therefore dispensable for normal frequencies of DNA recombination and DSB repair in lower eukaryotes such as *Saccharomyces Cerevisiae*. Thus, BRCA1 is likely to increase the repair efficiency of damaged DNA in the context of a much larger and more complicated chromatin environment such as that of the mammalian genome. Moreover, BRCA1 could additionally function to effect the efficient coordination of DNA repair with other cellular processes that are critical to support metazoan existence.

BRCA1 in transcription-coupled repair Brca1-deficient mouse embryonic stem cells have been shown to be defective in the ability to carry out transcription-coupled repair (TCR), a process in which DNA damage is repaired more rapidly in transcriptionally active DNA than in the genome as a whole (Gowen *et al.*, 1998). DNA damage induced by UV as well as oxidative DNA damage caused by IR or H_2O_2 can be repaired by TCR. It has been demonstrated that Brca1-deficient cells are defective in TCR of oxidative DNA damage, but not in TCR of UV-induced DNA damage. Consistent with this observation, these Brca1-deficient cells are hypersensitive to oxidative DNA damage. Presently, it is not clear whether BRCA1 itself participates directly in TCR or, alternatively, whether it functions as a transcription factor essential for the expression of genes whose products are required for TCR of oxidative damage (Gowen *et al.*, 1998).

The hypersensitivity of BRCA1-deficient cells to IR and H_2O_2 cannot be explained exclusively by a defect in TCR because DSB are also generated following treatments with these two agents. This observation is consistent with the aforementioned role of BRCA1 in recombinational repair of DSBs through both homologous and nonhomologous pathways. Therefore, BRCA1 is involved in multiple DNA repair pathways that ensure global genome stability.

BRCA1 in DNA-damage checkpoint controls DNA repair process must be coordinated with cell cycle control mechanism to ensure that damaged chromosomal DNA is fixed before it is replicated or segregated. BRCA1 appears to play such a role through its dual participation in the repair process of damaged DNA and in cell cycle checkpoint control. Although the underlying mechanism for BRCA1 functioning in checkpoint control has not been clarified, the observations showing the effects of BRCA1 on the transcription of genes involved in cell cycle controls, as aforementioned, may evoke a model for it. Alternatively, BRCA1 may regulate DNA damage-induced checkpoint through its associated DSB repair complexes. Recently, a potential role of Rad50/Mre11 in G2/M checkpoint was suggested by showing that rad50 or mre11 mutants can suppress the adaptation of hdf1, a yeast Ku70 mutant, to G2/M arrest after DNA damage (Lee *et al.*, 1998). Whether the interaction between BRCA1 and the RAD50/MRE11/NBS1 complex is involved in G2/M checkpoint control remains to be examined.

BRCA1 in DNA-damage signaling An important step in the cellular response to DNA damage is to transduce damaged signals to downstream effectors involved in the arrest of cell cycle and repair of damaged DNA. Many kinases have been implicated in the transduction of DNA damage signals. In mammalian cells, several kinases, such as ATM, ATR, DNA-PK, Chk1 and hCds1/Chk2 are activated in response to DNA damage (for review see Dasika *et al.*, 1999; and references therein). Consistently, ATM-deficient cells are defective in DNA damage-induced checkpoint control as well as DNA repair (reviewed by Shiloh, 1997). Chk2, which itself is phosphorylated and regulated by ATM, is essential for G2/M checkpoint control (Matsuoka *et al.*, 1998).

BRCA1 becomes hyperphosphorylated in response to treatment of cells with a variety of DNA damaging agents, including UV, hydroxyurea, mitomycin C, MMS, IR, H_2O_2 and adriamycin (Chen *et al.*, 1996c; Li *et al.*, 1999b; Scully *et al.*, 1997b). Recently, multiple phosphorylation sites at serine (S) residues, including S1330, S1423, S1466, S1524 and S1542, have been detected by mass spectrometry analysis of recombinant BRCA1 peptides phosphorylated *in vitro* by ATM (Cortez *et al.*, 1999). Moreover, S1387 was shown to be phosphorylated by ATM *in vitro* based on a screening of peptides containing potential ATM-phosphorylation sites (Lim *et al.*, 2000). Among these serine residues, S1457, S1524 and S1542 were shown to be phosphorylated *in vivo* by mass spectrometry analysis of transfected BRCA1 in irradiated human 293T cells (Cortez *et al.*, 1999). Furthermore, the phosphorylation-defective mutant of BRCA1 carrying changes of

both serines at residues 1423 and 1524 to alanines failed to rescue radiation hypersensitivity in BRCA1-deficient cells (Cortez *et al.*, 1999). These data suggested that ATM-dependent phosphorylation of BRCA1 on S1423 and S1524 is necessary for BRCA1-mediated DNA damage response.

However, as detected by its mobility shift in SDS gels, hyperphosphorylated forms of BRCA1 still exist in ATM-deficient cells upon DNA damage (Scully *et al.*, 1997c), suggesting that multiple kinase activities are responsible for DNA damage-induced hyperphosphorylation of BRCA1. Consistently, hCds1/ChK2 has been shown to phosphorylate BRCA1 on serine 988 upon IR (Lee *et al.*, 2000). The BRCA1 mutant carrying the S988A mutation also fails to rescue radiation hypersensitivity of BRCA1-deficient HCC1937 cells. It is therefore possible that ATM-dependent and Chk2-dependent phosphorylation of BRCA1 are involved in cellular responses to different levels of DNA damage. Alternatively, two kinase pathways may, through modulating different functions of BRCA1, regulate multiple downstream effectors.

In addition to ATM and hCds1/Chk2, ATR and DNA-PK were shown to phosphorylate BRCA1 *in vitro* (Lim *et al.*, 2000). It remains to be determined whether these kinases are involved in phosphorylation of BRCA1 *in vivo*. Moreover, additional kinases responsible for phosphorylation of BRCA1 upon treatment of cells with other DNA damaging agents such as UV and MMS remains to be identified.

Functional links of ATM and BRCA1 in DNA damage signaling Phosphorylation of BRCA1 is apparently important for a proper DNA damage response. However, it remains unclear how phosphorylation modulates the activities of BRCA1. Since BRCA1 forms IRIF that colocalize with RAD50/MRE11/NBS1 and DNA-damage sites following IR-treatment, it is obvious to speculate that phosphorylation of BRCA1 is involved in this process. Mutation of ATM or hCds1/Chk2 phosphorylation sites on BRCA1, however, did not affect BRCA1 foci formation in response to IR (Cortez *et al.*, 1999; Lee *et al.*, 2000). Therefore, it is likely that ATM or Chk2-mediated phosphorylation of BRCA1 regulates the activities of BRCA1 in DNA repair processes, rather than targeting the BRCA1-RAD50 complexes to damaged sites. Alternatively, phosphorylation of BRCA1 may influence the activities of BRCA1 in transcription regulation of DNA damage responsive genes.

Nevertheless, the kinase activity of ATM has been functionally linked to BRCA1 through the BRCA1-associated protein, CtIP. Recent studies indicated that ATM phosphorylates CtIP *in vitro* and *in vivo* following IR-treatment (Li *et al.*, 2000). This ATM-dependent phosphorylation of CtIP is required for dissociation of the CtIP/CtBP corepressor complex from BRCA1 and, subsequently relieving BRCA1-mediated repression of GADD45 transcription (Figure 4) (Li *et al.*, 2000). Therefore, ATM can modulate the activities of BRCA1, not only through a direct modification on BRCA1, but also through phosphorylation of its binding partner, CtIP. These studies suggest that CtIP mediates one of the functional links between ATM and BRCA1 in DNA-damage signaling pathways.

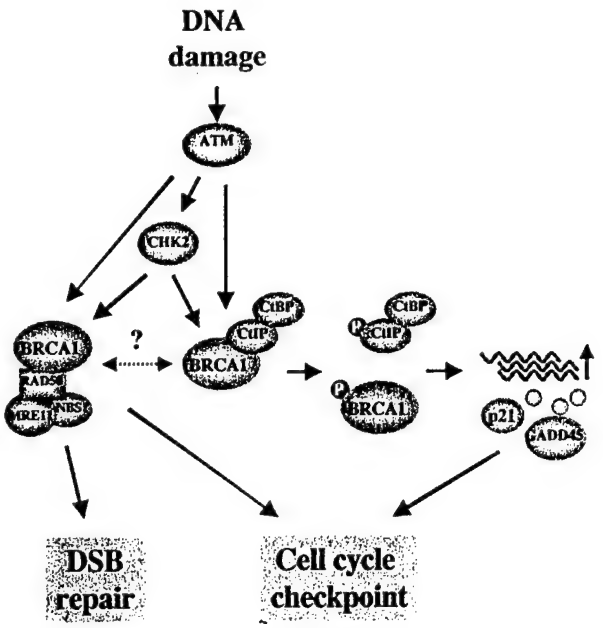

Figure 4 BRCA1 is involved in cellular response to DNA damage. BRCA1 participates in DNA damage repair and cell cycle checkpoint control, and coordinates both cellular processes in response to DNA damage. BRCA1 may directly participate in the DSB repair process through interacting with the RAD50/MRE11/NBS1 complex. BRCA1 may control cell cycle checkpoint by induction of p21 or GADD45 transcription. Upon IR, CtIP is phosphorylated by ATM. Phosphorylated CtIP dissociates from BRCA1, leading to the relief of repression activity of BRCA1 and, thereby, the induction of GADD45 or p21. Induction of p21 or GADD45 results in cell cycle arrest at G1/S or G2/M transition. The BRCA1/RAD50/MRE11/NBS1 complex may be also involved in the cell cycle checkpoint control

An integrated signaling network in BRCA1-mediated DNA-damage response BRCA1 and CtIP are apparently not the only proteins that are phosphorylated by ATM upon IR-treatment. It has been demonstrated that ATM phosphorylates multiple components in BRCA1-containing complexes, including p53 and NBS1. ATM-dependent phosphorylation of p53 is required for G1/S checkpoint and p53-mediated apoptosis (Canman *et al.*, 1998). Phosphorylation of NBS1 by ATM is necessary for the formation of IRIF, suggesting that one function of NBS1 activated by ATM is to relocalize Rad50/Mre11/NBS1 to sites of DNA damage (Zhao *et al.*, 2000). Derivatives of NBS1 carrying mutations in the ATM-phosphorylation sites fail to correct the RDS defect in NBS1-deficient cells, suggesting that another function of NBS1 activated by ATM is in S phase checkpoint control (Gatei *et al.*, 2000; Lim *et al.*, 2000; Wu *et al.*, 2000; Zhao *et al.*, 2000). These BRCA1-associated proteins are also likely to be regulated by other kinases such as ATR and Chk2. Interestingly, MRE11 is also phosphorylated upon DNA damage in an NBS1-dependent manner, although the consequences of this phosphorylation event remains unknown (Dong *et al.*, 1999). It is apparent that a complicated but integrated network is utilized to transmit DNA-damage signals to BRCA1 and its associated proteins, and regulate their functions at different levels.

Other potential functions of BRCA1

BRCA1 also associates with BARD1 (Wu *et al.*, 1996), which functionally interacts with polyadenylation factor CstE-50 (Kleiman and Manley, 1999), and with BAP1 (Jensen *et al.*, 1998), which is a de-ubiquitinating enzyme, suggesting two additional roles of BRCA1 in RNA polyadenylation and in ubiquitin-dependent protein degradation. The potential role of BRCA1 in post-transcriptional RNA processing may coordinate with its role in transcriptional regulation. The N-terminal RING domain of BRCA1 has been suggested to function with or as a ubiquitin–protein ligase (Lorick *et al.*, 1999), which is particularly interesting as protein degradation may influence the processes of transcription and DNA repair. In sum, it remains to be elucidated how BRCA1 participates in these pathways and the biological significance of these functions.

BRCA2 in transcriptional regulation

Contrary to BRCA1, the role of BRCA2 in transcriptional regulation is less certain. However, several lines of evidence support such a role for BRCA2. First, the product of BRCA2 exon 3 (amino acids 23–105), when fused to DNA-binding domains, activates transcription in yeast and mammalian cells (Milner *et al.*, 1997). Consistently, the amino acid sequence of BRCA2 within this region shares some similarity with the transactivation domain present in c-Jun (Milner *et al.*, 1997). Intriguingly, in a breast cancer case of a Swedish patient, a deletion of exon 3 at the BRCA2 allele was found (Nordling *et al.*, 1998). Moreover, a missense mutation (tyrosine 42 to cysteine), identified in a familial breast cancer case, within the primary activating region severely compromised the transactivation activity of BRCA2 (Milner *et al.*, 1997) suggesting that the abrogation of the BRCA2 putative transcription activity may be a predisposition to tumor development. Second, overexpression of exogenous BRCA2 inhibited p53-mediated transcription (Marmorstein *et al.*, 1998). Third, BRCA2 was demonstrated to have histone acetyltransferase activity and consistently, it was found to interact with the transcription co-activator P/CAF (p300/CBP-associated factors), suggesting a role of BRCA2 as a coactivator (Fuks *et al.*, 1998). To date, it remains unclear what the exact role of BRCA2 is in the regulation of transcription. More importantly, it will be critical to understand how the loss of this putative transcriptional activity of BRCA2 contributes to tumorigenesis.

BRCA2 in DNA repair

The interaction between BRCA2 and RAD51 The potential role of BRCA2 in DNA repair was first revealed by identification of its interaction with human or mouse RAD51 in yeast two-hybrid screens (Chen *et al.*, 1998b; Sharan *et al.*, 1997; Wong *et al.*, 1997). Consistently, mouse embryos lacking BRCA2 exhibit similar radiation hypersensitivity to mouse embryos lacking RAD51 (Sharan *et al.*, 1997). Human and mouse RAD51 are mammalian homologs of the *Escherichia coli* protein RecA (Clark, 1996) and of yeast ScRad51 (Shinohara *et al.*, 1992), a member of the RAD52 epistasis group in *Saccharonmyces cerevisiae* (McKee and Lawrence, 1980). All of the proteins in the RAD52 epistasis group are required for the repair of DSB and for mitotic and meiotic recombination in yeast. Eukaryotic RAD51 protein, similar to RecA, has ATP-dependent DNA binding activity and multimerizes to form a nucleoprotein filament on single-stranded DNA. Furthermore, RAD51 can catalyze homologous DNA pairing and DNA strand exchange in an *in vitro* recombination reaction (Baumann *et al.*, 1996; Baumann and West, 1997; Sung, 1994; Sung and Robberson, 1995).

Apparently, multiple discrete regions in BRCA2, including six BRC repeats, mediate its interaction with RAD51 (Chen *et al.*, 1998b; Sharan *et al.*, 1997; Wong *et al.*, 1997). It is, therefore, tempting to hypothesize that BRCA2 may increase the efficiency for RAD51-nucleoprotein filament formation by binding multiple RAD51 subunits. It would be interesting to determine the precise stoichiometry of the BRCA2-RAD51 complex, and examine how BRCA2 influences homologous DNA paring and strand exchange activity of mammalian RAD51. It has been shown that other protein components, such as a single-strand DNA binding protein, replication protein A, RAD52, and RAD55/RAD57 heterodimer are necessary for the formation of the RAD51-filament by enhancing the activity of RAD51 (reviewed by Shinohara and Ogawa, 1999). It is conceivable that BRCA2 is also required for the formation of the RAD51-filament and the proper function of RAD51 (Figure 3). Consistent with this notion, IR-induced RAD51 foci formation is diminished in BRCA2-deficient cells (Yu *et al.*, 2000; Yuan *et al.*, 1999) or in cells in which the interaction between BRCA2 and RAD51 is specifically disrupted (Chen *et al.*, 1998a). Therefore, BRCA2 appears to be necessary for the assembly of RAD51 complexes upon DNA damage.

Interaction between BRCA1 and BRCA2 It has been suggested that BRCA1 and BRCA2 interact *in vivo* (Chen *et al.*, 1998a). A region adjacent to, but not at the extreme C-terminus of BRCA1 was shown to mediate this interaction. BRCA2 also localizes in nuclear dots in mitotic cells at S or G2 phase and, colocalizes with BRCA1 on synaptonemal complexes of meiotic chromosomes (Chen *et al.*, 1998a). As discussed before, BRCA1 colocalizes with RAD51 in a specific period after DNA damage, and this association is distinct from the colocalization of IR-induced BRCA1/RAD50 foci. In short, the functional consequence of the interaction between BRCA1 and BRCA2 remains elusive, although it is possible that this interaction may be involved in coupling the functions of RAD50 and RAD51.

BRCA2 in DSB repair By revealing the interaction between BRCA2 and RAD51, the potential role of BRCA2 in DSB repair through homologous recombination is supported, but direct evidence is still desired. Brca2-truncated mouse lymphocytes are hypersensitive to mitomycin C (MMC) (Yu *et al.*, 2000), which causes DNA interstrand cross-links that are repaired primarily by recombination between homologous sequences (Li *et al.*, 1999a). Other mutant cells lacking DNA recombination genes such as XRCC2 and XRCC3

are also hypersensitive to MMC (Liu *et al.*, 1998). Moreover, gross chromosomal rearrangements and genetic exchange between nonhomologous chromsomes that are observed in BRCA2-deficient cells are proposed to result from a defect in homologous recombination. Taken together, these observations present further evidence for a role of BRCA2 in homologous recombination. Like BRCA1, BRCA2 is not evolutionarily conserved, implying that BRCA2 is not essential for the basic machinery of DSB repair, but is necessary for efficient DNA repair required by higher organisms to ensure the integrity of a more complicated genome.

BRCA2 in DNA-damage induced checkpoint control
Although the enforcement of checkpoints activated by DNA damage is largely preserved in cells from mice homozygous for Brca2 truncations (Patel *et al.*, 1998), tumors formed by these mice display loss of the mitotic spindle checkpoint, presumably due to acquired mutations in BUB1, MAD3L and p53, three genes involved in mitotic checkpoint control (Lee *et al.*, 1999). It is possible that Brca2 truncation at exon 11, retaining the first three BRC repeats, possesses a partial function that is able to rescue the embryonic lethality and preserve an intact DNA damage-induced checkpoint (Chen *et al.*, 1998a). The specific disruption of the interaction between RAD51 and BRCA2 by expressing a peptide containing BRC repeats results in loss of G2/M checkpoint control, thereby, suggesting that the role of BRCA2 in G2/M checkpoint may be associated with its function in DNA repair (Chen *et al.*, 1998a).

Perspectives

Both BRCA1 and BRCA2 have been proposed to be caretakers that function in the maintenance of global genome stability. Although functional inactivation of a caretaker is not sufficient to convert a normal cell to a cancer cell, it destabilizes the genome such that mutations in other genes can accumulate more frequently (Kinzler and Vogelstein, 1997). The subsequent mutational inactivation or deletion of a gatekeeper gene represents the precipitating event that initiates transformation to the neoplastic state. Gatekeepers are exemplified by genes that encode activities that directly regulate cell growth, and loss of gatekeeper activity leads to aberrant control of cell growth or cell death. While this hypothesis has provided a framework for understanding the contribution of inactivation of tumor suppressor genes to the genesis of cancer, its arbitrary distinction between caretakers and gatekeepers may obscure what in actuality represents the contribution of a potentially overlapping set of functional activities. More specifically, it seems evident that classically-defined gatekeepers could reasonably function as caretakers and vice versa. The cases of BRCA1 BRCA2, and p53 provide examples to illustrate this point.

In a variety of model systems, functional inactivation of BRCA1/2 leads to overt global genome instability; BRCA1/2 therefore clearly conform to the class of caretakers. However, while p53 fulfils the definition of a gatekeeper in many instances, other models exist in which it functions more akin to a caretaker. For example, while p53 is likely to play a role in restraining breast cancer formation in BRCA1/2 mutation carriers, the loss of its function does not appear to represent the threshold event that is proposed to accelerate the rate of mutation in cancer development. Rather, in these instances, functional loss of p53 appears only to permit cells with accumulated genetic abnormalities by bypass of checkpoint control and DNA-damage induced apoptosis. A similar effect is observed in a Ku80 deficient mouse tumor model. In this system, the absence of Ku80 precipitates genomic instability, which is not augmented by the additional loss of p53 (Difilippantonio *et al.*, 2000). Under such circumstances, it appears that inactivation of BRCA1/2 (or Ku80) and inactivation of p53 represent two distinct but coordinate events; the first destabilizes the genome, while the second assists the first in evading the custodial effects of cellular surveillance systems such as DNA-damage induced checkpoint control or apoptosis. BRCA1/2 and p53 thus appear to function as a coordinate caretaker; inactivation of both genes will permit cells with unstable genomes to proliferate freely and ultimately become tumorigenic.

Consistent with the possibility that p53 may function as a caretaker, germline inactivation of p53 itself will lead to genome instability and an increased frequency in tumor formation (reviewed by Lane, 1992). Hence, p53 appears to conform to the class of caretakers which are proposed to function as guardians of the genome (Lane, 1992). Genome instability need not necessarily arise through germline inactivation of specific genes such as BRCA1 and BRCA2 that function in the maintenance of chromosomal integrity, but conceivably could arise by spontaneous insult from intrinsic or extrinsic agents. For example, environment, age, diet, or other etiological factors could represent causative agents in the precipitation of chromosomal damage in sporadic cancers, as could sporadic mutations in genes involved in the maintenance of chromosomal integrity. As it represents the most direct means to effect bypass of cellular surveillance systems, p53 mutation is most frequently observed in breast cancers or in familial cancers with BRCA1/2 mutations. However, mutational inactivation of genes that function in p53-mediated pathways, such as p19ARF (de Stanchina *et al.*, 1998; Pomerantz *et al.*, 1998; Zindy *et al.*, 1998), or genes that function in other checkpoint control pathways, such BUB1, have also documented in human cancers (Cahill *et al.*, 1998).

Thus while p53 can evidently fulfill, at least in part, the duties of a caretaker, it must be emphasized that it can also function as a classical gatekeeper. Its dual character likely derives from the fact that p53 exerts its influence over cellular functions other than DNA-damage induced checkpoint conrol and apoptosis. As a sequence-specific transcription factor, p53 regulates multiple genes involved in many cellular pathways (el-Deiry, 1998; Prives and Hall, 1999; Tokino and Nakamura, 2000). Inactivation of p53 could lead to uncontrolled proliferation and/or invasive growth and, in so doing, contribute to a distinct step in malignant transformation. By similar reasoning, it seems plausible that BRCA1/2, which clearly function as caretakers in the sense that their inactivation is invariably accompanied by widespread genome instability, could also fulfill the role of gatekeepers. Indeed, inactivation of

BRCA1/2 apparently accelerates the rate of mutation and increases the incidence of tumor formation, since predisposed individuals who inherit one mutant copy of BRCA1 or BRCA2 experience a 10-fold greater chance of developing breast cancer than non-predisposed individuals (Hall *et al.*, 1990; Wooster *et al.*, 1994). BRCA1/2 function in sequence-specific transcriptional regulation, and it has been demonstrated that BRCA1 can regulate a diverse array of genes involved in cell proliferation, cell cycle control and differentiation. Moreover, BRCA1/2 are unique to metazoans, a fact that distinguishes them from other member genes in the caretaker class. These distinctive features of BRCA1/2 render it possible that their functional inactivation may, apart from their participation in the maintenance of global genome stability, contribute to a critical step in malignant transformation during breast tumorigenesis. Accordingly, it will be important to examine whether reintroduction of BRCA1/2 at levels approaching those occurring physiologically can rescue a transformed cellular phenotype.

In sporadic breast cancers and other cancers, p53 mutations must arise through selection during clonal evolution. This implies that p53 gene mutations are more frequently selected because they either confer growth advantages to tumor cells or, alternatively, that the p53 gene locus is more susceptible to mutation. On the other hand, the fact that somatic mutations in BRCA1/2 are rare events may imply that no growth advantage accompanies the loss of BRCA1/2 function in the adult breast tumor cells, and perhaps even normal adult mammary gland cells. This has raised speculation that BRCA1/2 have distinct functions at different stages of mammary gland development. Consistent with this notion is the observation that expression of BRCA1 and BRCA2 is regulated during this process (Lane *et al.*, 1995; Marquis *et al.*, 1995; Rajan *et al.*, 1996). In this regard, understanding how BRCA1/2 contribute to mammary gland development might weigh equally as important as understanding how their mutational inactivation leads to breast cancer formation.

The rarity of BRCA1/2 gene mutations in sporadic breast and ovarian cancer cases implies that aberrant expression of the BRCA1/2 genes or, alternatively, improperly regulated activity of their encoded products could contribute to non-familial breast cancer formation. Consequently, detailed knowledge of their normal biological function and regulation will be required for a thorough appreciation of how direct or indirect functional inactivation of BRCA1/2 ultimately leads to breast tumorigenesis. Specifically, functional analyses of BRCA1/2-associated proteins and the operative mechanisms underlying their respective roles in transcription regulation and DNA damage repair could contribute to a more complete understanding of the etiological bases of the remaining 90% of breast cancer cases that do not involve germline BRCA1/2 mutations.

Another unsolved question concerns the tissue-specific nature of tumor suppressive properties of BRCA1/2. BRCA1/2 are expressed ubiquitously and participate in universal cellular pathways; however, functional inactivation of BRCA1/2 leads specifically to breast or ovarian cancer formation. One possibility to account for this apparent paradox is that BRCA1/2, apart from their universal activities, exert distinct functions in breast or ovarian tissues. For example, BRCA1/2 may transcriptionally regulate specific genes that are critical for growth control of mammary gland cells. Consequently, a more complete understanding of how BRCA1/2 target specific genes for transcriptional regulation may illuminate unique pathways leading to breast tumorigenesis. Furthermore, the fact that BRCA1 has been implicated in the modulation of estrogen signaling suggests a potential mechanism through which its functional inactivation may impact cells in a specific hormonal environment. It remains to be established whether and how BRCA1 modulates the estrogen response *in vivo* and how its loss affects this cellular response.

An alternative possibility to account for the breast- and ovarian-specific nature of BRCA1/2 tumor suppression is that the activities of BRCA1/2 are more important for tumor suppression in these as opposed to other tissues. BRCA1/2 function ubiquitously in the maintenance of genomic integrity, and it is probable that the DNA damage-induced cellular signaling pathways that converge on them are conserved in most cell types. Indeed, the DNA damage-induced target genes controlled transcriptionally by BRCA1, as well as the components of the DNA double-strand break repair machinery with which it functionally interacts exhibit broad cell type expression profiles. It thus appears likely that BRCA1 occupy a fundamental and universally conserved role in the DNA damage response through their control of transcription and DNA repair. The tissue-specificity of their tumor suppressive properties may therefore lie not within the tissue-specific regulation of BRCA1/2 activity but, rather, in the tissue-specific nature of the DNA damage to which it responds. In this regard, it is significant that specific metabolic byproducts of estrogen itself have been documented to be genotoxic in nature (reviewed by Liehr, 2000). These collective observations raise the intriguing possibility that BRCA1/2 may play a role in protecting breast and ovarian tissue from estrogen-induced DNA damage. Clearly, a precise understanding of the molecular basis underlying the tissue-specificity of the tumor suppressive properties of BRCA1/2 will be essential for the design and implementation of strategies to delay, and ultimately to prevent, breast tumor formation.

Recent advances in the studies of BRCA1/2 have also provided insight into the mechanistic role of DSB repair in the suppression of tumorigenic mutations. It is well-established that cancer-causing mutations such as large deletion mutations, chromosomal translocations, and partial or complete chromosome loss often arise from gross chromosomal rearrangement and lead to loss of heterozygosity which is implicated in the inactivation of tumor suppressor genes (Lasko *et al.*, 1991). Hence, it has been proposed that one role for BRCA1/2 in homologous recombination-based DSB repair is to suppress gross chromosomal rearrangements (GCR) including genetic exchange between nonhomologous chromosomes after chromosome breakage (Moynahan *et al.*, 1999; Yu *et al.*, 2000). However, it is not presently clear whether GCR that are observed in BRCA1/2 mutant cells represent resolution of chromosome breaks by non-homology-

based repair pathways including NHEJ as an error-prone compensation for defective homologous recombination-based mechanisms. On the contrary, it has recently been demonstrated that inactivation of individual NHEJ DNA repair pathway components, such as XRCC4 and Ku, also leads to severe GCR (Difilippantonio *et al.*, 2000; Gao *et al.*, 2000). Moreover, a severe defect in NHEJ has recently been observed in Brca1-deficient MEF cells (Zhong *et al.*, submitted). Thus, both homologous recombination and NHEJ are likely to be required for maintaining genome integrity in the face of chromosome breakage. Defects in either of these repair pathways could result in inefficient and improper repair of damaged chromosomes. These latter studies therefore imply that gross chromosomal rearrangements may not be a consequence of non-homology-dependent DNA repair which is proposed to be error-prone, but due instead to an unknown mechanism that remains to be defined.

Clearly, a more precise understanding of BRCA1/2 function at the mechanistic level will not only provide insight into the pathogenesis of breast cancer, but also enhance our knowledge of the molecular basis by which a cell maintains its genomic integrity. We can also expect that novel therapeutic tools designed to specifically interfere with these molecular events will be developed and tested for tumor suppression in a growing company of genetically defined mammary tumor models.

Acknowledgments

The authors would like to thank members of the Lee laboratory for their contributions of unpublished data and for helpful discussions during the preparation of this review. We especially wish to thank Drs Nicolas Ting, Phang-Lang Chen and Qing Zhong for their insightful discussions and constructive critiques of the manuscript. This work was supported by NIH grants and McDermott endowment funds to W-H Lee. L Zheng and S Li were supported by a predoctoral training grant from the US Army (DAMD17-99-1-9402).

References

Alani E, Subbiah S and Kleckner N. (1989). *Genetics*, **122**, 47–57.

Anderson SF, Schlegel BP, Nakajima T, Wolpin ES and Parvin JD. (1998). *Nat. Genet.*, **19**, 254–256.

Aprelikova ON, Fang BS, Meissner EG, Cotter S, Campbell M, Kuthiala A, Bessho M, Jensen RA and Liu ET. (1999). *Proc. Natl. Acad. Sci. USA*, **96**, 11866–11871.

Baumann P, Benson FE and West SC. (1996). *Cell*, **87**, 757–766.

Baumann P and West SC. (1997). *EMBO J.*, **16**, 5198–5206.

Baumann P and West SC. (1998). *Trends Biochem. Sci.*, **23**, 247–251.

Bertwistle D, Swift S, Marston NJ, Jackson LE, Crossland S, Crompton MR, Marshall CJ and Ashworth A. (1997). *Cancer Res.*, **57**, 5485–5488.

Bork P, Hofmann K, Bucher P, Neuwald AF, Altschul SF and Koonin EV. (1997). *FASEB J.*, **11**, 68–76.

Boulton SJ and Jackson SP. (1998). *EMBO J.*, **17**, 1819–1828.

Bressan DA, Baxter BK and Petrini JH. (1999). *Mol. Cell. Biol.*, **19**, 7681–7687.

Brugarolas J, Chandrasekaran C, Gordon JI, Beach D, Jacks T and Hannon GJ. (1995). *Nature*, **377**, 552–557.

Cahill DP, Lengauer C, Yu J, Riggins GJ, Willson JK, Markowitz SD, Kinzler KW and Vogelstein B. (1998). *Nature*, **392**, 300–303.

Callebaut I and Mornon JP. (1997). *FEBS Lett.*, **400**, 25–30.

Carney JP, Maser RS, Olivares H, Davis EM, Le Beau M, Yates III JR, Hays L, Morgan WF and Petrini JH. (1998). *Cell*, **93**, 477–486.

Canman CE, Lim DS, Cimprich KA, Taya Y, Tamai K, Sakaguchi K, Appella E, Kastan MB and Siliciano JD. (1998). *Science*, **281**, 1677–1679.

Chai YL, Cui J, Shao N, Shyam E, Reddy P and Rao VN. (1999). *Oncogene*, **18**, 263–268.

Chamankhah M, Fontanie T and Xiao W. (2000). *Genetics*, **155**, 569–576.

Chamankhah M and Xiao W. (1999). *Nucleic Acids Res.*, **27**, 2072–2079.

Chapman MS and Verma IM. (1996). *Nature*, **382**, 678–679.

Chen C-F, Li S, Chen Y, Chen P-L, Sharp ZD and Lee W-H. (1996a). *J. Biol. Chem.*, **271**, 32863–32868.

Chen J, Silver DP, Walpita D, Cantor SB, Gazdar AF, Tomlinson G, Couch FJ, Weber BL, Ashley T, Livingston DM and Scully R. (1998a). *Mol. Cell.*, **2**, 317–328.

Chen PL, Chen CF, Chen Y, Xiao J, Sharp ZD and Lee WH. (1998b). *Proc. Natl. Acad. Sci. USA*, **95**, 5287–5292.

Chen Y, Chen PL, Riley DJ, Lee WH, Allred DC and Osborne CK. (1996b). *Science*, **272**, 125–126.

Chen Y, Farmer AA, Chen C-F, Jones DC, Chen P-L and Lee W-H. (1996c). *Cancer Res.*, **56**, 3168–3172.

Chen Y, Lee WH and Chew HK. (1999). *J. Cell. Physiol.*, **181**, 385–392.

Claus EB, Risch N and Thompson WD. (1991). *Am. J. Human Genet.*, **48**, 232–242.

Clark AJ. (1996). *Bioessays*, **18**, 767–772.

Connor F, Bertwistle D, Mee PJ, Ross GM, Swift S, Grigorieva E, Tybulewicz VL and Ashworth A. (1997). *Nat. Genet.*, **17**, 423–430.

Cortez D, Wang Y, Qin J and Elledge SJ. (1999). *Science*, **286**, 1162–1166.

Crook T, Crossland S, Crompton MR, Osin P and Gusterson BA. (1997). *Lancet*, **350**, 638–639.

Dasika GK, Lin SC, Zhao S, Sung P, Tomkinson A and Lee EY. (1999). *Oncogene*, **18**, 7883–7899.

Deng C, Zhang P, Harper JW, Elledge SJ and Leder P. (1995). *Cell*, **82**, 675–684.

Deng CX and Scott F. (2000). *Oncogene*, **19**, 1059–1064.

de Stanchina E, McCurrach ME, Zindy F, Shieh SY, Ferbeyre G, Samuelson AV, Prives C, Roussel MF, Sherr CJ and Lowe SW. (1998). *Genes Dev.*, **12**, 2434–2442.

Difilippantonio MJ, Zhu J, Chen HT, Meffre E, Nussenzweig MC, Max EE, Ried T and Nussenzweig A. (2000). *Nature*, **404**, 510–514.

Dong ZW, Zhong Q and Chen PL. (1999). *J. Biol. Chem.*, **9**, 19513–19516.

Easton DF, Bishop DT, Ford D and Crockford GP. (1993). *Am. J. Human Genet.*, **52**, 678–701.

Eisinger F, Jacquemier J, Guinebretiere JM, Birnbaum D and Sobol H. (1997). *Lancet*, **350**, 1101.

el-Deiry WS. (1998). *Semin. Cancer Biol.*, **8**, 345–357.

el-Deiry WS, Tokino T, Velculescu VE, Levy DB, Parsons R, Trent JM, Mercer WE, Kinzler KW and Vogelstein B. (1993). *Cell*, **75**, 817–825.

Fan S, Wang JA, Yuan R, Ma Y, Meng Q, Erdos MR, Pestell RG, Yuan F, Auborn KJ, Goldberg ID and Rosen EM. (1999). *Science*, **284**, 1354–1356.

Featherstone C and Jackson SP. (1999). *Curr. Biol.*, **9**, R759–R761.

Friedman LS, Thistlethwaite FC, Patel KJ, Yu VP, Lee H, Venkitaraman AR, Abel KJ, Carlton MB, Hunter SM, Colledge WH, Evans MJ and Ponder BA. (1998). *Cancer Res.*, **58**, 1338–1343.

Fuks F, Milner J and Kouzarides T. (1998). *Oncogene*, **17**, 2531–2534.

Furusawa T, Moribe H, Kondoh H and Higashi Y. (1999). *Mol. Cell Biol.*, **19**, 8581–8590.

Gao Y, Ferguson DO, Xie W, Manis JP, Sekiguchi J, Frank KM, Chaudhuri J, Horner J, DePinho RA and Alt FW. (2000). *Nature*, **404**, 897–900.

Gatei M, Young D, Cerosaletti KM, Desai-Mehta A, Spring K, Kozlov S, Lavin MF, Gatti RA, Concannon P and Khanna K. (2000). *Nat. Genet.*, **25**, 115–119.

Gerecke EE and Zolan ME. (2000). *Genetics*, **154**, 1125–1139.

Glass CK and Rosenfeld MG. (2000). *Genes Dev.*, **14**, 121–141.

Gowen LC, Avrutskaya AV, Latour AM, Koller BH and Leadon SA. (1998). *Science*, **281**, 1009–1012.

Gowen LC, Johnson BL, Latour AM, Sulik KK and Koller BH. (1996). *Nat. Genet.*, **12**, 191–194.

Haile DT and Parvin JD. (1999). *J. Biol. Chem.*, **274**, 2113–2117.

Hakem R, de la Pompa JL, Elia A, Potter J and Mak TW. (1997). *Nat. Genet.*, **16**, 298–302.

Hakem R, de la Pompa JL, Sirard C, Mo R, Woo M, Hakem A, Wakeham A, Potter J, Reitmair A, Billia F, Firpo E, Hui CC, Roberts J, Rossant J and Mak TW. (1996). *Cell*, **85**, 1009–1023.

Hall JM, Lee MK, Newman B, Morrow JE, Anderson LA, Huey B and King MC. (1990). *Science*, **250**, 1684–1689.

Harkin DP, Bean JM, Miklos D, Song YH, Truong VB, Englert C, Christians FC, Ellisen LW, Maheswaran S, Oliner JD and Haber DA. (1999). *Cell*, **97**, 575–586.

Hsu LC and White RL. (1998). *Proc. Natl. Acad. Sci. USA*, **95**, 12983–12988.

Hu Y-F, Hao ZL and Li R. (1999). *Genes Dev.*, **13**, 637–642.

Ivanov EL, Korolev VG and Fabre F. (1992). *Genetics*, **132**, 651–664.

Jensen DE, Proctor M, Marquis ST, Gardner HP, Ha SI, Chodosh LA, Ishov AM, Tommerup N, Vissing H, Sekido Y, Minna J, Borodovsky A, Schultz DC, Wilkinson KD, Maul GG, Barlev N, Berger SL, Prendergast GC and Rauscher III FJ. (1998). *Oncogene*, **16**, 1097–1112.

Johzuka K and Ogawa H. (1995). *Genetics*, **139**, 1521–1532.

Karran P. (2000). *Curr. Opin Genet. Dev.*, **10**, 144–150.

Kastan MB, Zhan Q, el-Deiry WS, Carrier F, Jacks T, Walsh WV, Vogelstein B and Fornace Jr AJ. (1992). *Cell*, **71**, 587–597.

Kinzler KW and Vogelstein B. (1997). *Nature*, **386**, 763.

Kleiman FE and Manley JL. (1999). *Science*, **285**, 1576–1579.

Koipally J and Georgopoulos K. (2000). *J. Biol. Chem.*, **13**, 13.

Koonin EV, Altschul SF and Bork P. (1996). *Nat. Genet.*, **13**, 266–267.

Lane DP. (1992). *Nature*, **358**, 15–16.

Lane TF, Deng C, Elson A, Lyu MS, Kozak CA and Leder P. (1995). *Genes Dev.*, **9**, 2712–2722.

Lasko D, Cavenee W and Nordenskjold M. (1991). *Annu. Rev. Genet.*, **25**, 281–314.

Lee H, Trainer AH, Friedman LS, Thistlethwaite FC, Evans MJ, Ponder BA and Venkitaraman AR. (1999). *Mol. Cell.*, **4**, 1–10.

Lee JS, Collins KM, Brown AL, Lee CH and Chung JH. (2000). *Nature*, **404**, 201–204.

Lee SE, Moore JK, Holmes A, Umezu K, Kolodner RD and Haber JE. (1998). *Cell*, **94**, 399–409.

Li L, Peterson CA, Lu X, Wei P and Legerski RJ. (1999a). *Mol. Cell. Biol.*, **19**, 5619–5630.

Li S, Chen PL, Subramanian T, Chinnadurai G, Tomlinson G, Osborne CK, Sharp ZD and Lee WH. (1999b). *J. Biol. Chem.*, **274**, 11334–11338.

Li S, Ku CY, Farmer AA, Cong YS, Chen CF and Lee WH. (1998). *J. Biol. Chem.*, **273**, 6183–6189.

Li S, Ting NEY, Zheng L, Chen P-L, Ziv Y, Shiloh Y, Lee EY-H and Lee W-H. (2000). *Nature*, **406**, 210–215.

Liehr JG. (2000). *Endocr. Rev.*, **21**, 40–54.

Lim DS, Kim ST, Xu B, Maser RS, Lin J, Petrini JH and Kastan MB. (2000). *Nature*, **404**, 613–617.

Liu CY, Flesken-Nikitin A, Li S, Zeng YY and Lee WH. (1996). *Genes Dev.*, **10**, 1835–1843.

Liu N, Lamerdin JE, Tebbs RS, Schild D, Tucker JD, Shen MR, Brookman KW, Siciliano MJ, Walter CA, Fan W, Narayana LS, Zhou ZQ, Adamson AW, Sorensen KJ, Chen DJ, Jones NJ and Thompson LH. (1998). *Mol. Cell*, **1**, 783–793.

Lorick KL, Jensen JP, Fang S, Ong AM, Hatakeyama S and Weissman AM. (1999). *Proc. Natl. Acad. Sci. USA*, **96**, 11364–11369.

Lu KP, Hanes SD and Hunter T. (1996). *Nature*, **380**, 544–547.

Ludwig T, Chapman DL, Papaioannou VE and Efstratiadis A. (1997). *Genes Dev.*, **11**, 1226–1241.

MacLachlan TK, Somasundaram K, Sgagias M, Shifman Y, Muscel RJ, Cowan KH and El-Deiry WS. (2000). *J. Biol. Chem.*, **275**, 2777–2785.

Marmorstein LY, Ouchi T and Aaronson SA. (1998). *Proc. Natl. Acad. Sci. USA*, **95**, 13869–13874.

Marquis ST, Rajan JV, Wynshaw-Boris A, Xu J, Yin GY, Abel KJ, Weber BL and Chodosh LA. (1995). *Nat. Genet.*, **11**, 17–26.

Marston NJ, Richards WJ, Hughes D, Bertwistle D, Marshall CJ and Ashworth A. (1999). *Mol. Cell. Biol.*, **19**, 4633–4642.

Maser RS, Monsen KJ, Nelms BE and Petrini JH. (1997). *Mol. Cell. Biol.*, **17**, 6087–6096.

Matsuoka S, Huang M and Elledge SJ. (1998). *Science*, **282**, 1893–1897.

McKee RH and Lawrence CW. (1980). *Mutat. Res.*, **70**, 37–48.

Meloni AR, Smith EJ and Nevins JR. (1999). *Proc. Natl. Acad. Sci. USA*, **96**, 9574–9579.

Miki Y, Swensen J, Shattuck-Eidens D, Futreal PA, Harshman K, Tavtigian S, Liu Q, Cochran C, Bennett LM, Ding W, Bell R, Rosenthal J, Hussey C, Tran T, McClure M, Frye C, Hattier T, Phelps R, Haugen-Strano A, Katcher J, Yakumo K, Gholalmi Z, Shaffer D, Stone S, Bayer S, Wray C, Bogden R, Dayananth P, Ward J, Tonin P, Narod S, Bristow PK, Norris FJ, Helvering L, Morrison P, Rostek P, Lai M, Barrett JC, Lewis C, Neuhausen S, Cannon-Albright L, Goldgar D, Wiseman R, Kamb A and Skolnick MH. (1994). *Science*, **266**, 66–71.

Milner J, Ponder B, Hughes-Davies L, Seltmann M and Kouzarides T. (1997). *Nature*, **386**, 772–773.

Monteiro ANA, August A and Hanafusa H. (1996). *Proc. Natl. Acad. Sci. USA*, **93**, 13595–13599.

Moynahan ME, Chiu JW, Koller BH and Jasin M. (1999). *Mol. Cell*, **4**, 511–518.

Neish AS, Anderson SF, Schlegel BP, Wei W and Parvin JD. (1998). *Nucleic Acids Res.*, **26**, 847–853.

Nelms BE, Maser RS, MacKay JF, Lagally MG and Petrini JH. (1998). *Science*, **280**, 590–592.

Nibu Y, Zhang H and Levine M. (1998). *Science*, **280**, 101–104.

Nordling M, Karlsson P, Wahlstrom J, Engwall Y, Wallgren A and Martinsson T. (1998). *Cancer Res.*, **58**, 1372–1375.

Nugent CI, Bosco G, Ross LO, Evans SK, Salinger AP, Moore JK, Haber JE and Lundblad V. (1998). *Curr. Biol.*, **8**, 657–660.

Nurse P. (1994). *Cell*, **79**, 547–550.

Ohta K, Nicolas A, Furuse M, Nabetani A, Ogawa H and Shibata T. (1998). *Proc. Natl. Acad. Sci. USA*, **95**, 646–651.
Ouchi T, Lee SW, Ouchi M, Aaronson SA and Horvath CM. (2000). *Proc. Natl. Acad. Sci. USA*, **97**, 5208–5213.
Ouchi T, Monteiro ANA, August A, Aaronson SA and Hanafusa H. (1998). *Proc. Natl. Acad. Sci. USA*, **95**, 2302–2306.
Painter RB and Young BR. (1980). *Proc. Natl. Acad. Sci. USA*, **77**, 7315–7317.
Painter RB and Young BR. (1987). *J. Cell Sci.* (Suppl.), **6**, 207–214.
Pao GM, Janknecht R, Ruffner H, Hunter T and Verma IM. (2000). *Proc. Natl. Acad. Sci. USA*, **97**, 1020–1025.
Patel KJ, Vu VP, Lee H, Corcoran A, Thistlethwaite FC, Evans MJ, Colledge WH, Friedman LS, Ponder BA and Venkitaraman AR. (1998). *Mol. Cell*, **1**, 347–357.
Paull TT and Gellert M. (1998). *Mol. Cell*, **1**, 969–979.
Paull TT and Gellert M. (1999). *Genes Dev.*, **13**, 1276–1288.
Pazin MJ and Kadonaga JT. (1997). *Cell*, **89**, 325–328.
Pomerantz J, Schreiber-Agus N, Leigeois NJ, Silverman A, Alland L, Chin L, Potes J, Chen K, Orlow I, Lee HW, Cordon-Cardo C and DePinho RA. (1998). *Cell*, **92**, 713–723.
Poortinga G, Watanabe M and Parkhurst SM. (1998). *EMBO J.*, **17**, 2067–2078.
Postigo AA and Dean DC. (1999). *Proc. Natl. Acad. Sci. USA*, **96**, 6683–6688.
Prives C and Hall PA. (1999). *J. Pathol.*, **187** 112–126.
Rajan JV, Wang M, Marquis ST and Chodosh LA. (1996). *Proc. Natl. Acad. Sci. USA*, **93**, 13078–13083.
Saka Y, Esashi F, Matsusaka T, Mochida S and Yanagida M. (1997). *Genes Dev.*, **11**, 3387–3400.
Saurin AJ, Borden KL, Boddy MN and Freemont PS. (1996). *Trends Biochem. Sci.*, **21**, 208–214.
Schaeper U, Boyd JM, Verma S, Uhlmann E, Subramanian T and Chinnadurai G. (1995). *Proc. Natl. Acad. Sci. USA*, **92**, 10467–10471.
Schaeper U, Subramanian T, Lim L, Boyd JM and Chinnadurai G. (1998). *J. Biol. Chem.*, **273**, 8549–8552.
Schlegel BP, Green VJ, Ladias JA and Parvin JD. (2000). *Proc. Natl. Acad. Sci. USA*, **97**, 3148–3153.
Scully R, Anderson SF, Chao DM, Wei WJ, Ye LY, Young RA, Livingston DM and Parvin JD. (1997a). *Proc. Natl. Acad. Sci. USA*, **94**, 5605–5610.
Scully R, Chen JJ, Ochs RL, Keegan K, Hoekstra M, Feunteun J and Livingston DM. (1997b). *Cell*, **90**, 425–435.
Scully R, Chen JJ, Plug A, Xiao YH, Weaver D, Feunteun J, Ashley T and Livingston DM. (1997c). *Cell*, **88**, 265–275.
Scully R, Ganesan S, Vlasakova K, Chen J, Socolovsky M and Livingston DM. (1999). *Mol. Cell*, **4**, 1093–1099.
Sewalt RG, Gunster MJ, van der Vlag J, Satijn DP and Otte AP. (1999). *Mol. Cell Biol.*, **19**, 777–787.
Sharan SK, Morimatsu M, Albrecht U, Lim DS, Regel E, Dinh C, Sands A, Eichele G, Hasty P and Bradley A. (1997). *Nature*, **386**, 804–810.
Shiloh Y. (1997). *Annu. Rev. Genet.*, **31**, 635–662.
Shinohara A, Ogawa H and Ogawa T. (1992). *Cell*, **69**, 457–470.
Shinohara A and Ogawa T. (1999). *Mutat. Res.*, **435**, 13–21.
Sibon OC, Kelkar A, Lemstra W and Theurkauf WE. (2000). *Nat. Cell Biol.*, **2**, 90–95.
Siddique H, Zou JP, Rao VN and Reddy ES. (1998). *Oncogene*, **16** 2283–2285.
Sollerbrant K, Chinnadurai G and Svensson C. (1996). *Nucleic Acids Res.*, **24**, 2578–2584.
Somasundaram K, Zhang HB, Zeng YX, Houvras Y, Peng Y, Zhang HX, Wu GS, Licht JD, Weber BL and El-Deiry WS. (1997). *Nature*, **389**, 187–190.
Su TT and Vidwans SJ. (2000). *Nat. Cell Biol.*, **2**, E28–E29.
Sung P. (1994). *Science*, **265**, 1241–1243.
Sung P and Robberson DL. (1995). *Cell*, **82**, 453–461.
Suzuki A, de la Pompa JL, Hakem R, Elia A, Yoshida R, Mo R, Nishina H, Chuang T, Wakeham A, Itie A, Koo W, Billia P, Ho A, Fukumoto M, Hui CC and Mak TW. (1997). *Genes Dev.*, **11**, 1242–1252.
Tokino T and Nakamura Y. (2000). *Crit. Rev. Oncol. Hematol.*, **33**, 1–6.
Trujillo KM, Yuan SS, Lee EY and Sung P. (1998). *J. Biol. Chem.*, **273**, 21447–21450.
Tsubouchi H and Ogawa H. (1998). *Mol. Cell Biol.*, **18**, 260–268.
Turner J and Crossley M. (1998). *EMBO J.*, **17**, 5129–5140.
Varon R, Vissinga C, Platzer M, Cerosaletti KM, Chrzanowska KH, Saar K, Beckmann G, Seemanova E, Cooper PR, Nowak NJ, Stumm M, Weemaes CM, Gatti RA, Wilson RK, Digweed M, Rosenthal A, Sperling K, Concannon P and Reis A. (1998a). *Cell*, **93**, 467–476.
Varon R, Vissinga C, Platzer M, Cerosaletti KM, Chrzanowska KH, Saar K, Beckmann G, Seemanova E, Cooper PR, Nowak NJ, Stumm M, Weemaes CM, Gatti RA, Wilson RK, Digweed M, Rosenthal A, Sperling K, Concannon P and Reis A. (1998b). *Cell*, **93**, 467–476.
Wang Q, Zhang H, Kajino K and Greene MI. (1998). *Oncogene*, **17**, 1939–1948.
Wang XW, Zhan Q, Coursen JD, Khan MA, Kontny HU, Yu L, Hollander MC, O'Connor PM, Fornace Jr AJ and Harris CC. (1999). *Proc. Natl. Acad. Sci. USA*, **96**, 3706–3711.
Wang Y, Cortez D, Yazdi P, Neff N, Elledge SJ and Qin J. (2000). *Genes Dev.*, **14**, 927–939.
Wong AK, Ormonde PA, Pero R, Chen Y, Lian L, Salada G, Berry S, Lawrence Q, Dayananth P, Ha P, Tavtigian SV, Teng DH and Bartel PL. (1998). *Oncogene*, **17**, 2279–2285.
Wong AKC, Pero R, Ormonde PA, Tavtigian SV and Bartel PL. (1997). *J. Biol. Chem.*, **272**, 31941–31944.
Wooster R, Bignell G, Lancaster J, Swift S, Seal S, Mangion J, Collins N, Gregory S, Gumbs C, Micklem G, Barfoot R, Hamoudi R, Patel S, Rice C, Biggs P, Hashim Y, Smith A, Connor F, Arason A, Gudmundsson J, Ficenec D, Kelsell D, Ford D, Tonin P, Bishop DT, Spurr NK, Ponder BAJ, Eeles R, Peto J, Devilee P, Cornelisse C, Lynch H, Narod S, Lenoir G, Egilsson V, Barkadottir RB, Easton FE, Bentley DR, Futreal PA, Ashworth A and Stratton MR. (1995). *Nature*, **378**, 789–792.
Wooster R, Neuhausen SL, Mangion J, Quirk Y, Ford D, Collins N, Nguyen K, Seal S, Tran T, Averill D, Fields P, Marshall G, Narod S, Lenoir GM, Lynch H, Feunteun J, Devilee P, Cornelisse CJ, Menko FH, Daly PA, Ormiston W, McManus R, Pye C, Lewis CM, Cannon-Albright LA, Peto J, Ponder BAJ, Skolnick MH, Easton DF, Goldgar DE and Stratton MR. (1994). *Science*, **265**, 2088–2090.
Wu LJC, Wang ZW, Tsan JT, Spillman MA, Phung A, Xu XL, Yang MCW, Hwang LY, Bowcock AM and Baer R. (1996). *Nat. Genet.*, **14**, 430–440.
Wu X, Ranganathan V, Weisman DS, Heine WF, Ciccone DN, O'Neill TB, Crick KE, Pierce KA, Lane WS, Rathbun G, Livingston DM and Weaver DT. (2000). *Nature*, **405**, 477–482.
Xu X, Wagner KU, Larson D, Weaver Z, Li C, Ried T, Hennighausen L, Wynshaw-Boris A and Deng CX. (1999a). *Nat. Genet.*, **22**, 37–43.
Xu X, Weaver Z, Linke SP, Li C, Gotay J, Wang XW, Harris CC, Ried T and Deng CX. (1999b). *Mol. Cell.*, **3**, 389–395.
Yarden RI and Brody LC. (1999). *Proc. Natl. Acad. Sci. USA*, **96**, 4983–4988.
Yu VP, Koehler M, Steinlein C, Schmid M, Hanakahi LA, van Gool AJ, West SC and Venkitaraman AR. (2000). *Genes Dev.*, **14**, 1400–1406.
Yu X, Wu LC, Bowcock AM, Aronheim A and Baer R. (1998). *J. Biol. Chem.*, **273**, 25388–25392.

Yuan SS, Lee SY, Chen G, Song M, Tomlinson GE and Lee EY. (1999). *Cancer Res.*, **59**, 3547–3551.

Zhang H, Somasundaram K, Peng Y, Tian H, Bi D, Weber BL and el-Deiry WS. (1998). *Oncogene*, **16**, 1713–1721.

Zhao S, Weng YC, Yuan SS, Lin YT, Hsu HC, Lin SC, Gerbino E, Song MH, Zdzienicka MZ, Gatti RA, Shay JW, Ziv Y, Shiloh Y and Lee EY. (2000). *Nature*, **405**, 473–477.

Zheng L, Pan H, Li S, Flesken-Nikitin A, Chen P-L, Boyer TG and Lee W-H. (2000). *Mol. Cell*, **6**, 757–768.

Zhong Q, Chen C-F, Li S, Chen Y, Wang C-C, Xiao J, Chen P-L, Sharp ZD and LEe W-H. (1999). *Science*, **285**, 747–750.

Zindy F, Eischen CM, Randle DH, Kamijo T, Cleveland JL, Sherr CJ and Roussel MF. (1998). *Genes Dev.*, **12**, 2424–2433.

MOLECULAR AND CELLULAR BIOLOGY, May 2000, p. 3529–3537 Vol. 20, No. 10
0270-7306/00/$04.00+0

Retinoblastoma Protein Enhances the Fidelity of Chromosome Segregation Mediated by hsHec1p

LEI ZHENG, YUMAY CHEN, DANIEL J. RILEY, PHANG-LANG CHEN, AND WEN-HWA LEE*

Department of Molecular Medicine and Institute of Biotechnology, University of Texas Health Science Center at San Antonio, San Antonio, Texas 78245

Received 22 September 1999/Returned for modification 17 November 1999/Accepted 14 February 2000

Retinoblastoma protein (Rb) plays important roles in cell cycle progression and cellular differentiation. It may also participate in M phase events, although heretofore only circumstantial evidence has suggested such involvement. Here we show that Rb interacts, through an IxCxE motif and specifically during G_2/M phase, with hsHec1p, a protein essential for proper chromosome segregation. The interaction between Rb and hsHec1p was reconstituted in a yeast strain in which human hs*HEC1* rescues the null mutation of sc*HEC1*. Expression of Rb reduced chromosome segregation errors fivefold in yeast cells sustained by a temperature-sensitive (ts) hs*hec1-113* allele and enhanced the ability of wild-type hsHec1p to suppress lethality caused by a ts *smc1* mutation. The interaction between Hec1p and Smc1p was important for the specific DNA-binding activity of Smc1p. Expression of Rb restored part of the inactivated function of hshec1-113p and thereby increased the DNA-binding activity of Smc1p. Rb thus increased the fidelity of chromosome segregation mediated by hsHec1p in a heterologous yeast system.

Genetic instability is one of the most important hallmarks of cancer. It occurs at two different levels. On one level, increased mutation rates result from defective repair of damaged DNA or replication errors, which leads to missense, nonsense, or other small but functionally important mutations in several types of cancer. On another level, improper segregation of whole chromosomes or pieces of chromosomes during mitosis leads to aneuploidy or translocations, traits commonly observed in cancers (35). Chromosome segregation is controlled by a large group of proteins that together coordinate M phase progression (43, 44, 48, 58). Loss of function of key proteins important for the structure and dynamics of mitotic chromosomes would be expected to lead to cell death and thus to prevent passage of mutations of such fundamental proteins to daughter cells. Loss of function of proteins that play subtler regulatory roles in mitosis, however, may not be immediately lethal but instead may lead to high frequencies of chromosome abnormalities and to neoplasia.

Associations of oncoproteins or tumor suppressors with the process of chromosome segregation provide possible links between carcinogenesis and chromosomal instability. Recent studies suggest that both p53 and retinoblastoma protein (Rb) play important roles in the prevention of aneuploidy in human and rodent cells (12, 28, 34, 56). When treated with microtubule-destabilizing agents, cells lacking functional Rb or p53 do not finish mitosis properly but nonetheless enter a new cell cycle, leading to hyperploidy (28, 34). p53 has been found to be associated with centrosome duplication activity (15) and mitotic or postmitotic checkpoint control (18, 34), loss of these functions would result in aberrant mitosis and contribute to the observed increase in ploidy. Similarly, the propensity of Rb-deficient cells to become hyperploid is most likely due to the loss of a novel function of Rb in M phase of the cell cycle, although supportive evidence remains scarce.

* Corresponding author. Mailing address: Department of Molecular Medicine/Institute of Biotechnology, University of Texas Health Science Center at San Antonio, 15355 Lambda Dr., San Antonio, TX 78245. Phone: (210) 567-7351. Fax: (210) 567-7377. E-mail: leew@uthscsa.edu.

Study of the function of Rb has been centered on the progression of G_1 phase (17, 23, 52). However, accumulating evidence has suggested potential functional roles for Rb during other phases of the cell cycle (27, 31, 46), especially during M phase. First, the functional, hypophosphorylated form of Rb is present at this phase of the cell cycle (8, 38). Second, hypophosphorylated Rb is associated with at least three cellular proteins that have crucial functions in M phase progression (50). One example is the human H-nuc2 (also called hCDC27) protein (9), a subunit of the anaphase-promoting complex that controls the onset of sister chromatid separation and metaphase-anaphase transition by degradation of specific substrates (30, 32). Another Rb-associated protein, protein phosphatase 1α catalytic subunit (13), is important for kinetochore function, chromosome segregation, and M phase progression, as demonstrated by the abnormal phenotype resulting from the mutational inactivation of its yeast homolog (2, 3, 49, 51). Lastly, mitosin (also called CENP-F), a kinetochore protein (60), also interacts specifically with Rb during M phase.

However, the mechanisms by which Rb plays a role in chromosome segregation and M phase progression remain elusive. The current approach of counting total chromosome numbers by karyotyping or detecting a specific chromosome by fluorescent in situ hybridization can only display the status of chromosome instability, which may not necessarily be a direct consequence of a certain gene defect in mammalian cells. To determine whether the loss of a gene function is responsible for improper chromosome segregation, a method for monitoring the dynamic transmission of a specific chromosome marker is required. Any attempt to select for mammalian cells carrying an integrated exogenous chromosome marker, however, bears the risk of immortalizing a primary cell line or making the genetic content of a tumor cell line even more unpredictable. Studies of chromosome segregation in mammalian cells are therefore complicated. On the other hand, methods for monitoring the dynamic transmission of chromosomes in yeast cells are feasible, and the genetic manipulation of a given gene in yeast can be accomplished without affecting the rest of the gene population and chromosome structures. Moreover, the

basic machinery for chromosome segregation is conserved between mammals and yeast (42).

In this study, a yeast assay system for investigating the role of Rb in chromosome segregation was established, based on the study of hsHec1p. hsHec1p, isolated from a screen for proteins interacting with Rb (10, 13), is a coiled-coil protein crucial for proper mitosis (10, 11, 59). Inactivation of hsHec1p leads to disruption of M phase progression (10). The homolog of hsHec1p in *Saccharomyces cerevisiae*, scHec1p (also called Ndc80 or Tid3), has a similar essential function (57, 59), and hs*HEC1* is able to rescue the lethality caused by the null mutation of sc*HEC1* (59). Yeast cells carrying a mutant allele of human or yeast *HEC1* segregate their chromosomes aberrantly (57, 59). At the nonpermissive temperature, significant mitotic delay, unequal nuclear division, and decreased viability were observed in yeast cells carrying hs*hec1-113*, a temperature-sensitive mutant allele of human *HEC1* (59). Increased frequencies of chromosome segregation errors were also detected in the hs*hec1-113* mutant at permissive temperatures. Hec1p has been found to interact physically or genetically with a number of proteins important for G_2/M progression and chromosome segregation, including SMC (structural maintenance of chromosomes) proteins and yeast centromere protein Ctf19p (10, 26, 59). A potential role for Hec1p in modulating chromosome segregation in part through interactions with SMC proteins has been suggested (59). There is no protein with sequence similarity to Rb in the entire *S. cerevisiae* genome. Without interference from endogenous Rb, yeast strains in which the null mutation of sc*HEC1* has been complemented by hs*HEC1* (59) therefore provide useful tools to address the consequence of the interaction between Rb and hsHec1p for chromosome segregation.

The biological significance of the interaction between Rb and hsHec1p is demonstrated here by reconstitution of these proteins in a heterologous in vivo yeast system. Expression of Rb resulted in a decrease in the rate of chromosome segregation errors in cells carrying a mutant form of hsHec1p and an increase in the survival rate of *smc1* mutant cells with defects in chromosome segregation. These results suggest that Rb plays a positive regulatory role in chromosome segregation.

MATERIALS AND METHODS

Strains and plasmids. *S. cerevisiae* haploid and diploid strains carrying the hs*hec1-113* mutant have been described previously (59). A new yeast strain, 4bWHL273 (*matx* ade2 lys2 ura3 trp1 smc1-2::LEU2), is one of the meiotic segregates of the diploid strain from the mating between 3bAS273 (a gift from D. Koshland) and YPH1015 (a gift from P. Hieter). The full-length 2.8-kb *RB* cDNA, or the cDNA for the H209 mutant *RB* derivative (Cys706 changed to Phe), was inserted in two sets of plasmids, p415GAL1 (41) and pESC::*TRP1* (Stratagene), by use of *Bam*HI and *Sal*I. The resultant plasmids were used to transform the above-mentioned strains. By a procedure described previously (21), cells were cultured in 2% raffinose overnight at 25°C before Rb expression was induced in medium containing additional 2% galactose for the indicated number of hours. The YEp195-GC15C plasmid was generated by inserting the *GAL1* promoter, hs*HEC1* cDNA (59), and *CYC1* terminator (41) into the YEplac195 vector (16) for the expression of hsHec1p. The YEp195-GEKC plasmid was generated by site-directed mutagenesis for the expression of the hshec1-EK mutant (Glu234 changed to Lys). To express myc-tagged Smc1p, the full-length *SMC1* was generated by PCR, sequenced, and fused with the c-myc tag in the pESC plasmid.

Immunoprecipitation and immunoblotting. The preparation of yeast cell lysates, immunoprecipitation, and immunoblotting have been described previously (59). Human hsHec1p, *S. cerevisiae* Smc1p, and human Rb were precipitated or immunoblotted with anti-hsHec1p monoclonal antibody (MAb) 9G3, mouse anti-Smc1p antiserum (59), and anti-Rb MAb 11D7, respectively.

Human bladder carcinoma T24 cells were cultured and synchronized at different stages of the cell cycle as described previously (8, 10). Cells were lysed and immunoprecipitated by procedures described previously (8, 10).

For immunoprecipitation and immunoblotting of human SMC1 (hSMC1) from T24 cells, mouse anti-hSMC1 antiserum was obtained from mice immunized with glutathione *S*-transferase (GST) protein fused with the peptide region of hSMC1 isolated from a yeast two-hybrid screen (10, 11, 59).

Colony sectoring assays. Colony sectoring assays were used to measure the frequencies of chromosome missegregation, as described previously (33, 59). Five single pink colonies of each diploid strain that contains a homozygous *ade2-101* ochre color mutation and a dispensable chromosome fragment carrying a copy of *SUP11* were picked and cultured to log phase in histidine-free supplemented minimal medium at 25°C for 3 days. Cells were diluted and incubated at 30°C for 4 h (one generation) in fresh medium supplied with histidine and containing 2% galactose and 2% raffinose to induce the expression of Rb or the H209 mutant. An aliquot of culture was then removed and plated on medium containing 6 mg of adenine per liter. The plates were incubated at 30°C for 6 days and at 4°C overnight before observation. The remaining cultures were used for detecting the expression of Rb or for examining the interaction between Rb and hsHec1p as described above.

Immunoaffinity purification. Yeast cell lysate was prepared as described previously (59). Smc1p was partially purified from this lysate with mouse anti-Smc1p polyclonal antibodies by immunoaffinity chromatography, according to modification of a procedure described previously (25, 29). Antibodies were incubated with 50 μl of protein A-Sepharose beads for 2 h at 4°C and washed twice with 1 ml of Tris-buffered saline (50 mM Tris [pH 8.0], 125 mM NaCl). A 1.5-ml portion of cell lysate (about 50 mg of total protein) was added to the antibody–protein A-Sepharose beads and incubated for another 1 h at 4°C. The mixture was then loaded on a minicolumn and washed sequentially with 4 ml of XBE2 buffer (20 mM potassium HEPES [pH 7.7], 0.1 M KCl, 10% glycerol, 2 mM $MgCl_2$, 5 mM EGTA), 0.5 ml of XBE2 with 0.4 M KCl, and 0.5 ml of XBE2. For elution, 150 μl of XBE2 containing a 4-μg/μl concentration of a GST fusion with the C-terminal region of Smc1p (59) was used. Fifty microliters of elution buffer was first allowed to flow in, and then the other 100 μl was loaded. After incubation at 4°C for 4 h, the elution buffer was allowed to flow through and collected. The elution product was incubated with 100 μl of glutathione-Sepharose that was prewashed with XBE2 for 1 h at 4°C three times to completely remove the GST fusion protein.

For multiple samples in the same experiment, equal numbers of yeast cells that contained comparable amounts of total proteins were lysed. The cell lysates were added to the antibody–protein A-Sepharose beads for immunoaffinity purification as described above. The eluted products from each sample were calibrated with comparable protein concentrations for use in gel shift assays. To minimize the effect of any quantitative variations, the amount of Smc1p in each purified product was adjusted according to the immunoblotting results.

Gel mobility shift assay. Approximately 2 μl of the purified product described above was incubated with the 230-bp M13 replicative-form (RF) DNA fragment in 20 μl of XBE2 buffer with 0.5 mg of bovine serum albumin per ml. The 230-bp M13 RF DNA fragment was digested from the same region of M13 genomic DNA described previously (1), although *Hin*dIII was used instead of *Eco*RI. The DNA fragment was end labeled with [α-^{32}P]dCTP by the fill-in reaction with Klenow enzymes. DNA fragments labeled with 10,000 to 20,000 cpm were used as substrates. For competition, unlabeled 230-bp M13 fragment, a 220-bp pUC19 fragment digested with *Ava*II from a pUC19-derived vector (1), and a 240-bp CEN3 fragment (bp, 113925 to 114168) generated by PCR amplification from yeast genomic DNA with the primers described previously (40) were used. The DNA-protein reaction mixtures were loaded on a 5.5% acrylamide gel and run at 4°C in a buffer containing 20 mM HEPES [pH 7.5] and 0.1 mM EDTA. The results were quantified using a densitometer and ImageQuant v1.1 (Molecular Dynamics).

RESULTS

hsHec1p specifically interacts with Rb through the IxCxE motif. hsHec1p was originally identified using Rb as the bait in a yeast two-hybrid screen (10, 13). In order to determine the specific region of Rb required for binding hsHec1p, a deletion set that had previously been used to delineate the binding domain for protein phosphatase 1α was employed (13). Amino acids 301 to 928 of the Rb protein and several carboxy-terminal deletion mutants, as well as the H209 point mutant with residue 706 changed from cysteine to phenylalanine, were fused with the yeast Gal4 DNA-binding domain. Full-length hsHec1p protein was fused with the Gal4 transactivation domain. The results showed that Rb uses the same T-antigen-binding domain to interact with hsHec1p, and the H209 point mutation abolished this binding (Fig. 1A). hsHec1p sequences required for binding Rb were also determined in a reciprocal manner, using a series of hsHec1p deletion mutants. These mutants showed that the central region of hsHec1p, from amino acids 128 to 251, binds to Rb (Fig. 1B). Two Rb-related

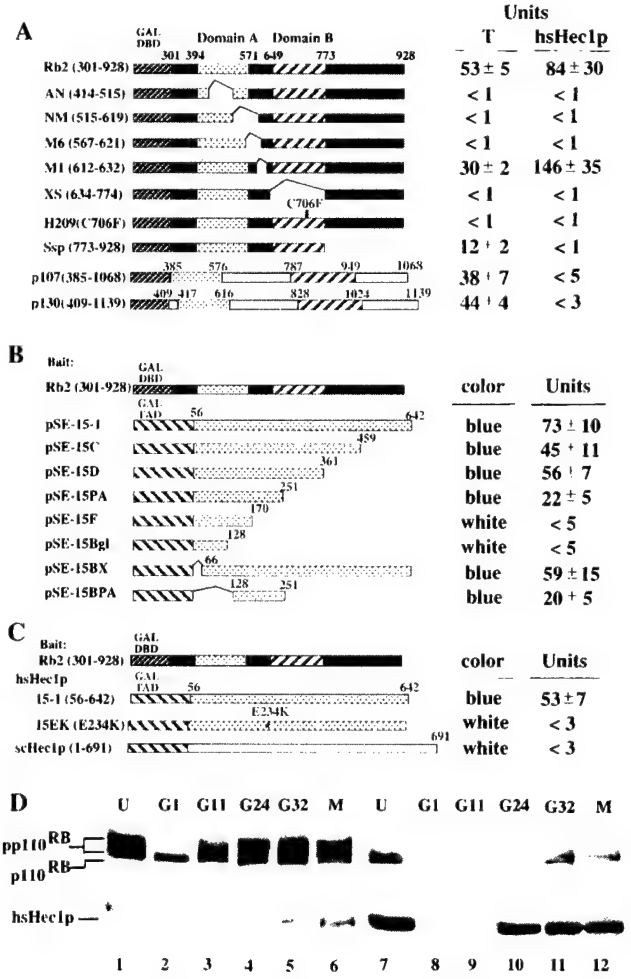

FIG. 1. Specific interaction between Rb and hsHec1p. (A) hsHec1p and T antigen bind to similar regions of the Rb protein. The Gal4 DNA-binding domain (DBD) (amino acids 1 to 147; stippled box) was fused to various Rb mutants, p107 (amino acids 385 to 1068), or p130 (amino acids 409 to 1139). The simian virus 40 T-antigen-binding domains A and B are shown as shaded and hatched boxes, respectively. hsHec1p or T antigen (13) was expressed as a Gal4 transactivation domain fusion protein and used to test for interaction with Rb fusion proteins in yeast two-hybrid assays. Transformants were grown in liquid cultures and used for *o*-nitrophenyl-β-D-galactopyranoside quantitation of β-galactosidase activity as described previously (13). (B) Various hsHec1p mutants were fused with the Gal4 transactivation domain (TAD) (hatched box). Rb (amino acids 301 to 928) was expressed as the fusion with the Gal4 DNA-binding domain used for panel A. (C) Rb was expressed as the same fusion used for panel B. Wild-type hsHec1p (15-1), an hsHec1p mutant with amino acid 234 changed from E to K (15EK), and scHec1p were fused with the Gal4 transactivation domain. (D) Cell cycle-dependent interaction between Rb and hsHec1p. T24 cells were density arrested at G_1 (lanes 2 and 8) and then released for reentry into the cell cycle. At different time points after release as indicated above the lanes, 5×10^6 cells were collected, lysed, and immunoprecipitated with anti-Rb MAb 11D7 (lanes 1 to 6) or with anti-hsHec1p MAb 9G3 (lanes 7 to 12). The immune complexes were then separated by sodium dodecyl sulfate-polyacrylamide gel electrophoresis followed by immunoblotting with MAb 11D7 (upper panel) or with 9G3 (lower panel). G11 represents 11 h after release and corresponds to G_1, G24 marks 24 h after release and corresponds to S, and G32 marks 32 h after release and corresponds to G_2. M phase lysates (lanes 6 and 12) were obtained from cells treated with nocodazole (0.4 μg/ml). Lanes 1 and 7, unsynchronized cells.

proteins, p107 and p130 (14, 20, 36, 39), did not interact with hsHec1p (Fig. 1A).

The region of hsHec1p that binds Rb was not conserved in yeast scHec1p. Thus, it is likely that the interaction between Hec1p and Rb is not conserved in yeast. To test this notion, a yeast two-hybrid assay was performed using the above-described construct, with the Rb sequence fused with the Gal4 DNA-binding domain and a plasmid for the expression of yeast scHec1p sequence fused with the Gal4 transactivation domain. As predicted, yeast scHec1p failed to bind Rb (Fig. 1C).

An examination of the hsHec1p sequence showed that it contains an IxCxE motif, which has been implicated as the specific Rb-binding site in many proteins (reviewed in reference 5). This motif is not found in yeast scHec1p, suggesting that the inability of Rb to bind to scHec1p may be due to the lack of the IxCxE sequence. To verify this possibility, a point mutant with residue 234 changed from glutamic acid to lysine in this motif was tested in a yeast two-hybrid assay. This mutation abolished the ability of hsHec1p to bind to Rb (Fig. 1C). However, hs*hec1-EK*, with this mutation, was able to rescue the yeast sc*hec1* null mutant (data not shown) and generate the strain WHL101EK. This indicated that hsHec1p proteins, with or without an Rb-binding site, are able to perform their essential cellular function in yeast.

Rb and hsHec1p interact at G_2/M phase in mammalian cells. The interaction between Rb and hsHec1p was also examined by coimmunoprecipitation following cell cycle progression. As shown in Fig. 1D, hsHec1p binds to Rb specifically at G_2/M phase in human bladder carcinoma T24 cells, which were synchronized as described previously (8). Similar to most of other Rb-associated proteins, hsHec1p binds specifically to the hypophosphorylated form of Rb that reappears during M phase.

The specific interaction between Rb and hsHec1p is reconstituted in yeast. Wild-type Rb and the H209 mutant Rb were expressed under control of the *GAL1* promoter through *LEU2*-selectable plasmids (p415GAL1) in the same yeast strain that carries an hs*hec1-113* mutant allele (59). As a negative control, wild-type Rb was also expressed in a yeast strain carrying the hs*hec1-113EK* allele, which encodes a hshec1-113p without Rb-binding activity. The hs*hec1-113EK* cells demonstrated no apparent difference in the temperature-sensitive (ts) phenotype compared with the hs*hec1-113* cells (59).

Wild-type Rb coimmunoprecipitated with hshec1-113p but not with hshec1-113EK. The H209 mutant of Rb failed to form a complex with hshec1-113p (Fig. 2A, panel b). Consistent with a previous report (21), both hypophosphorylated and hyperphosphorylated forms of Rb were detected in these unsynchronized cells, but the H209 mutant was deficient in hyperphosphorylated forms. The abundance of hshec1-113p protein did not vary significantly when either Rb or the H209 mutant was expressed (Fig. 2A, panel c). These results suggested that the specific interaction between hsHec1p and Rb could be reconstituted in yeast cells.

To explore whether M phase-specific binding exists in yeast cells expressing Rb, the interaction was examined during cell cycle progression. Cells from the strain carrying the hs*hec1-113* allele were induced to express Rb and then synchronized in early S phase by treatment with hydroxyurea. After release from treatment, an equal aliquot of cells was taken out every 20 min (Fig. 2B; lanes 1 to 10). hshec1-113p was coimmunoprecipitated by anti-Rb MAb in cells that entered M phase, according to DNA content analysis (Fig. 2C and D), and morphology was observed under the microscope. Similarly, hshec1-113p and Rb were coimmunoprecipited in cells synchronized at metaphase with nocodazole (Fig. 2B, lanes 11 and 12) but not in cells released from nocodazole treatment for 1 h. These results indicated that the M phase-specific interaction between Rb and hsHec1p can also be reconstituted in yeast cells.

Rb specifically enhances the fidelity of chromosome segregation. The reconstitution of the specific interaction between Rb and hsHec1p in yeast cells provided an in vivo system for

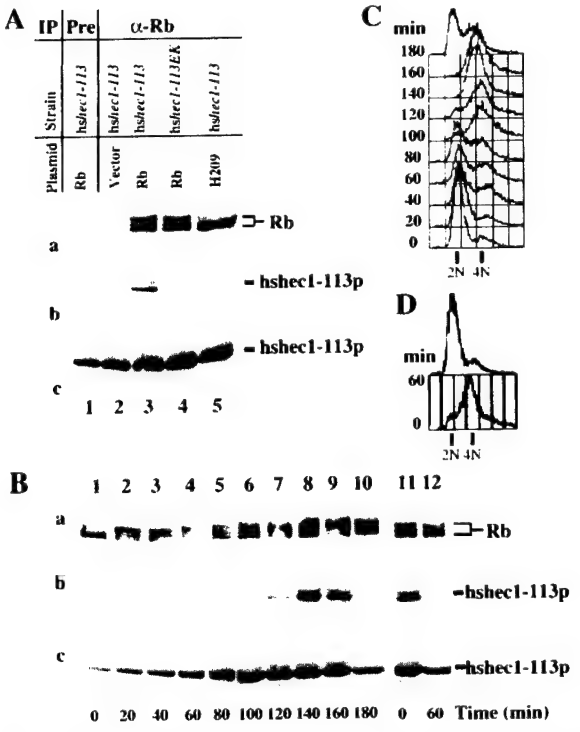

FIG. 2. Reconstitution of the interaction between Rb and hsHec1p in yeast. (A) Specific interaction between hsHec1p and Rb. Yeast cells were diluted to an optical density at 600 nm of 0.75 in fresh medium with 2% galactose and 2% raffinose and then cultured at 30°C for 4 h. Aliquots of cell lysate were immunoprecipitated (IP) with nonspecific IgG (lane 1) or with anti-Rb (α-Rb) MAb 11D7 (lanes 2 to 5) and separated by sodium dodecyl sulfate-polyacrylamide gel electrophoresis. The same blot was probed with MAb 11D7 for Rb (a) or MAb 9G3 for hshec1-113p (b). Panel c shows the endogenous level of hshec1-113p in the cells used in panels a and b. For each lane in panel c, aliquots of the same lysates used in panel a were immunoprecipitated and immunoblotted with 9G3. The yeast strains and plasmids used to express Rb are indicated for each lane. (B) The yeast cells carrying the hs*hec1-113* allele and an Rb expression vector were treated for 5 h with 0.1 M hydroxyurea or 20 μg of nocodazole per ml in medium containing 2% galactose and 2% raffinose. At different time points after release (indicated under each lane [lanes 1 to 10, release from hydroxyurea; lanes 11 and 12, release from nocodazole]), cells were collected, lysed, and immunoprecipitated with α-Rb MAb 11D7. The immunoprecipitates were then separated by sodium dodecyl sulfate-polyacrylamide gel electrophoresis, followed by immunoblotting with 11D7 for Rb (a) or with 9G3 for hshec1-113p (b). Aliquots of the same lysates were immunoprecipitated and immunoblotted with 9G3 (c). hshec1-113p was co-precipitated by Rb specifically at 120 to 160 min after release from hydroxyurea treatment, corresponding to G_2/M phase, or metaphase arrest by nocodazole (time zero, lane 11). (C and D) The DNA content of the same cells used for panel B was analyzed by fluorescence-activated cell sorting as described previously (59).

investigation of the consequence of this interaction. If hsHec1p plays a crucial role in maintaining the fidelity of chromosome segregation as described previously (59), we surmised that Rb modulates hsHec1p and enhances this activity. To test this hypothesis, we examined the rate of chromosome missegregation by using the colony sectoring assay (33) after induction of Rb expression in the hs*hec1-113* diploid strain. This strain was chosen because of its higher rate of chromosome segregation errors during mitosis (59). The total numbers of pink colonies (representing 1:1 segregation of a single dispensable chromosome fragment carried by this yeast strain), half-pink, half-red sectored colonies (representing 1:0 segregation), and half-white, half-red sectored colonies (representing 2:0 segregation) were counted. The rates of chromosome loss and nondisjunction in the first division were determined by the

TABLE 1. Rb reduces chromosome segregation errors

Relevant genotype	Plasmid	No. of colonies[a]	Missegregation rate (%)	
			1:0 events[b]	2:0 events[c]
hs*HEC1*		6,096	0.02	0.01
hs*hec1-113*	Vector	6,687	1.47	0.56
hs*hec1-113*	Rb	12,641	0.31	0.10
hs*hec1-113*	H209	4,299	1.54	0.60
hs*hec1-113EK*	Vector	5,392	1.48	0.46
hs*hec1-113EK*	Rb	6,554	1.51	0.50

[a] Total number of pink colonies.
[b] Number of half-red, half-pink colonies divided by total number of pink colonies.
[c] Number of half-red, half-white colonies divided by total number of pink colonies.

frequencies of half-pink, half-red colonies and half-white, half-red colonies, respectively. As shown in Table 1, Rb expression decreased the frequency of chromosome segregation errors due to chromosome loss or nondisjunction by approximately fivefold. In contrast, expression of the H209 mutant of Rb or the vector alone had no effect. As another control, we examined the influence of Rb expression on the strain carrying the hs*hec-113EK* mutant; it had no significant effect.

The observed difference in the frequencies of chromosome missegregation is not due to the variable cell growth or cell cycle status, because expression of Rb or H209 has no significant effects on these processes in yeast cells carrying either wild-type *HEC1* alleles (21) or the mutant hs*hec1-113* allele (data not shown). Therefore, the fidelity of chromosome segregation is enhanced specifically by interaction between Rb and hsHec1p.

Rb enhances the ability of hsHec1p to suppress lethality caused by an *smc1* mutation. hsHec1p plays an essential role in chromosome segregation in part through interacting with SMC1 protein, which, in a complex with SMC3, is involved in sister chromatid cohesion (24, 37, 54). The mutated hec1p fails to interact with Smc1p physically in the hs*hec1-113* mutant cells at the nonpermissive temperature (59). Overexpression of Hec1p suppresses the lethal phenotype of the *smc1-2* mutant strain (1-1bAS172) at 37°C (55, 59). If Rb enhances the activity of mutated hshec1p in the maintenance of proper chromosome segregation, it is likely that Rb also enhances the activity of wild-type hsHec1p in suppression of defective chromosome segregation due to the *smc1* mutation. To test this hypothesis, we employed the yeast strain 2bAS273, which also carries the *smc1-2* mutant allele and has a lethal phenotype at temperatures above 33°C (D. Koshland, personal communication). The isogenic strain 4bWHL273, carrying the same *smc1-2* allele, was generated from 2bAS273 and transformed by plasmids expressing hsHec1p and Rb under control of the *GAL1* promoter. Cells overexpressing hsHec1p grew at 34°C, a nonpermissive temperature for this *smc1* mutant strain, while cells not overexpressing hsHec1p failed to grow, whether Rb was expressed or not (Fig. 3A). Interestingly, if the temperature was raised further to 35 to 36°C, cells overexpressing hsHec1p also failed to grow. Cells overexpressing both hsHec1p and Rb, however, continued to grow, whereas cells expressing the H209 mutant hardly survived at this higher temperature. Overexpression of hshec1-EK suppressed the *smc1-2* mutant at 34°C, but coexpression of Rb and hshec1-EK did not suppress it if the temperature was raised further (Fig. 3B). These results suggested that the specific interaction between Rb and wild-type hsHec1p results in the enhancement of the fidelity of

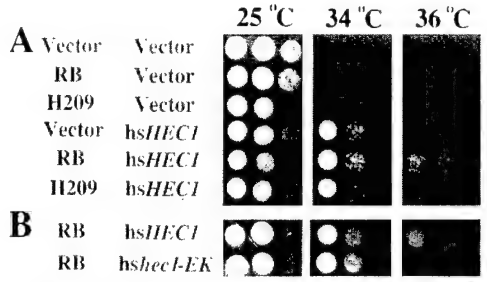

FIG. 3. Rb suppresses the ts phenotype of the *smc1-2* mutant through hsHec1p. (A) 4bWHL273 (*smc1-2*) cells were double transformed by hs*HEC1* in a *GAL1*-inducible and *URA3*-selectable vector (a YEplac195-based vector), by *RB* or the H209 *RB* mutant cDNA in a *GAL1*-inducible and *TRP1*-selectable vector (pESC::*TRP1*), or by the vectors alone. (B) 4bWHL273 cells were double transformed by hs*HEC1* or hs*hec1-EK* in the *GAL1*-inducible and *URA3*-selectable vector and by Rb in the *GAL1*-inducible and *TRP1*-selectable vector. Different dilutions of log-phase cells grown at 25°C were inoculated on three plates with 2% galactose in the same manner and incubated at 25, 34, or 36°C.

chromosome segregation, probably mediated by the interaction between Hec1p and Smc1p.

Specific binding of Smc1p to highly structured DNA. SMC1 protein has been suggested to associate preferentially with highly structured DNA regions of chromatin, such as AT-rich DNA, bent DNA, and scaffold-associated regions (1, 22, 24, 29), and to mediate intermolecular cross-linking in sister chromatid cohesion (24). An in vitro binding assay for investigation of SMC1 DNA-binding activity has been established by using a 230-bp M13 RF DNA fragment (bp 6001 to 6231), which has a very high potential to form secondary structures, e.g., stem-loops, and therefore mimics highly structured DNA regions (1). The carboxyl-terminal region of SMC1 protein had been shown to mediate this specific DNA-binding activity (1).

To partially purify the Smc1p protein complex from yeast cell lysates, anti-Smc1p polyclonal antibodies (59) and a single-step immunoaffinity approach (25, 29) were employed. The affinity-bound proteins were eluted by the use of a highly concentrated GST fusion protein that had been used as the antigen to raise the antibodies (59). Excessive GST fusion protein was subsequently removed with glutathione-Sepharose. The affinity-purified fraction (APF) was incubated with the 230-bp M13 RF DNA fragment. Specific DNA-binding activity for the APF was detected by gel mobility shift assays (Fig. 4A, lanes 1 to 3). The abundance of the specific DNA-protein complex increased when more APF was added. Meanwhile, the mobility of the DNA-protein complex decreased and formed a more slowly migrating band (Fig. 4A, lane 3, bar). This stoichiometric effect is consistent with previous observations for the DNA-binding activity of another SMC-containing complex, the 13S condensin in *Xenopus* (29). This DNA-protein complex is not likely to be contaminated by the eluting antigen, which, encompassing the C-terminal DNA-binding region of Smc1p (1), formed a faster-migrating complex with the same DNA substrate (data not shown).

In order to determine the specificity of this DNA-binding activity, we also tested the APF from the *smc1-2* mutant cells cultured at 37°C, with smc1p inactivated (55). Our observation suggested that this mutated protein is unstable and barely detectable in these mutant cells cultured for 6 h at 37°C (Fig. 4B). No Smc1p-containing complex was obtained from these cells using the same purification procedure (Fig. 4C), and therefore, no DNA-binding activity was detected (Fig. 4A, lanes 4 to 6).

To determine whether this Smc1p-associated activity is spe-

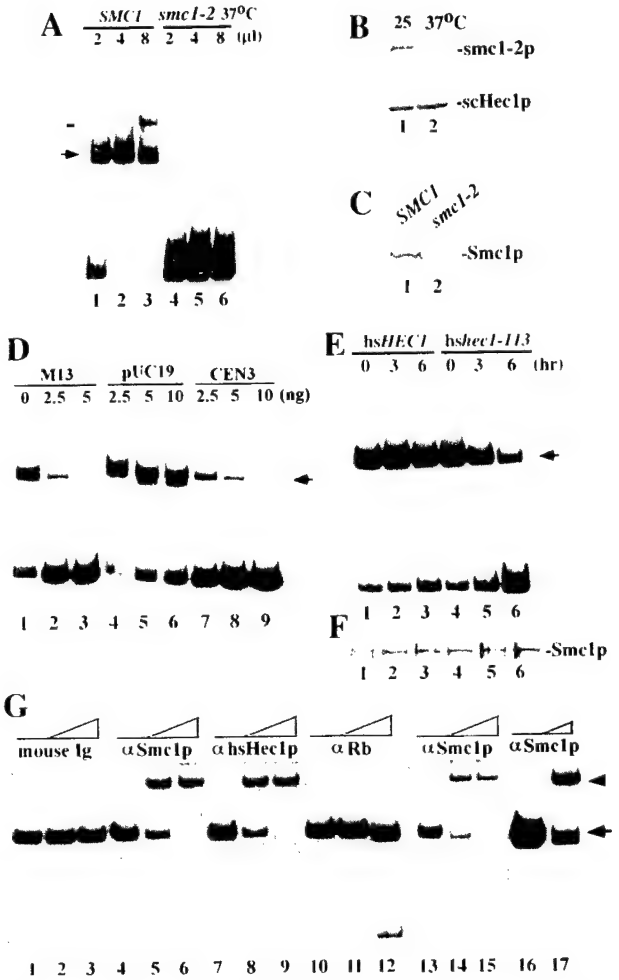

FIG. 4. DNA-binding activity of Smc1p and Hec1p complexes. (A) DNA-binding activity of Smc1p purified from equal numbers of wild-type cells (lanes 1 to 3) and *smc1-2* ts mutant cells (lanes 4 to 6) with a 230-bp M13 RF DNA fragment. The amount of concentrated protein in each lane is shown, and the position of the DNA-protein complex is indicated (arrow). Note that a slower-mobility complex (bar) appeared when more protein was added. (B) Immunoblotting by mouse anti-Smc1p polyclonal antibodies (upper panel) or by anti-scHec1p polyclonal antibodies (lower panel) of lysates from *smc1-2* ts mutant cells cultured at 25°C (lane 1) or 37°C (lane 2) for 6 h. (C) Immunoblotting of Smc1p purified from wild-type (lane 1) or *smc1-2* mutant (lane 2) cells cultured at 37°C for 6 h. (D) Competition of DNA-binding activity by unlabeled DNA fragments. The amount of competitor DNA added in each reaction is indicated above each lane. (E) DNA-binding activity of Smc1p purified from wild-type hs*HEC1* cells (lanes 1 to 3) or from the hs*hec1-113* mutant cells (lanes 4 to 6) with the 230-bp M13 fragment. Cells were cultured at 25°C until log-phase growth and then shifted to 37°C for 0, 3, and 6 h before harvest. (F) Comparable amounts of Smc1p in each of the APFs were measured by immunoblotting with anti-Smc1p antibodies and were used for panel E. (G) Antibody supershift assay. Anti-Smc1p (αSmc1p) antibodies and anti-hsHec1p MAb 9G3 supershifted the DNA-protein complex formed by APF from hshec1-113 cells expressing Rb (lanes 1 to 12), but mouse IgG or anti-Rb MAb 11D7 did not. Anti-Smc1p also supershifted the DNA-binding complex formed by APF from hshec1-113 cells not expressing Rb (lanes 13 to 15) and by APF from the wild-type hsHEC1 cells (lanes 16 and 17). Lanes 1, 4, 7, 10, 13, and 16, no antibodies; lanes 2 and 3, 0.5 and 1 μg of mouse IgG, respectively, lanes 5 and 6, 0.5 and 1 μg anti-Smc1p antibody, respectively; lanes 8 and 9, 0.5 and 1 μg of 9G3, respectively; lanes 11 and 12, 0.5 and 1 μg of 11D7, respectively; lanes 14 and 15, 0.5 and 1 μg of anti-Smc1p antibody, respectively; lane 17, 0.5 μg of anti-Smc1p antibody. The original shift is indicated by an arrow, and the antibody supershift is indicated by an arrowhead.

cific to the highly structured DNA, the DNA-binding activity was competed by unlabeled DNA fragments containing the scaffold-associated region of *S. cerevisiae* CEN3. This centromere region was suggested to be a preferential binding site of SMC proteins and was able to compete with the M13 fragment in the in vitro DNA-binding assay of recombinant SMC1 (1). As shown in Fig. 4D, the Smc1p-associated DNA-binding activity that we detected in the yeast cells can also be competed by unlabeled CEN3 DNA and M13 DNA fragment but not by the region on pUC19 DNA with the least potential to form the secondary structures (1).

We also used a similar procedure to partially purify myc-tagged Smc1p from yeast cells overexpressing myc-Smc1p by use of anti-c-myc MAb and elution with the corresponding peptide. myc-Smc1p has the same DNA-binding activity (data not shown).

Hec1p modulates specific DNA-binding activity of Smc1p. To test whether a deficiency in Hec1p activity affects the function of Smc1p, we examined the activity of Smc1p in the hs*hec1-113* mutant yeast cells and compared it with that in cells expressing wild-type hsHec1p. Cells expressing wild-type hsHec1p or mutant hshec1-113p were cultured at the permissive temperature (25°C) and then shifted to 37°C for different periods of time. Equal numbers of cells were harvested and lysed. The resultant cell lysates from different samples contained comparable amounts of total proteins and were subjected to affinity purification of Smc1p. The DNA-binding activity of Smc1p in the wild-type cells did not change significantly after the cells were shifted to 37°C. In the hs*hec1-113* mutant cells, however, this Smc1p activity dramatically decreased, and only less than 20% remained after 6 h at 37°C (Fig. 4E). The amount of Smc1p expressed in the hshec1-113 cells was comparable to that in the wild-type cells (Fig. 4F), suggesting that the functional defect resulted specifically because of the mutated hec1p. The mobilities of the DNA-binding complexes from the wild-type cells and the mutant hs*hec1-113* cells were very similar; only if gel electrophoresis was prolonged more than usual could they be distinguished (data not shown). It is therefore likely that Hec1p is present in the DNA-binding complex. As shown in Fig. 4G, anti-Hec1p antibodies and anti-Smc1p antibodies, but not anti-Rb antibodies or mouse immunoglobulin G (IgG), were able to supershift the DNA-binding complex. These results suggest that Hec1p is present in the complex with Smc1p to mediate the DNA-binding activity. Similar results were observed with APF from yeast cells expressing the wild-type Hec1p or cells not expressing Rb (Fig. 4G, lanes 13 to 17).

Rb, through hsHec1p, enhances the DNA-binding activity of Smc1p. If Rb enhances the fidelity of chromosome segregation, which may be mediated by the DNA-binding activity of Smc1p through hsHec1p, this Smc1p activity should increase in the cells expressing Rb. To test this hypothesis, we examined the DNA-binding activity of Smc1p in the same Rb-reconstituted yeast strains that had been tested for frequencies of chromosome missegregation. As in the colony sectoring assay, the cells were cultured at 30°C for 8 h while either Rb or the H209 mutant was induced. In the hs*hec1-113* cells carrying only the empty vector, the DNA-binding activity of Smc1p decreased dramatically, to 30 to 40% of the wild-type level (Fig. 5A and C). These results are consistent with the abnormally high frequencies of chromosome missegregation in the same cells at the permissive temperature (Table 1). In cells expressing wild-type Rb, however, Smc1p DNA-binding activity was restored nearly to normal levels. Expression of the H209 mutant had no such effect, nor did wild-type Rb expression alone

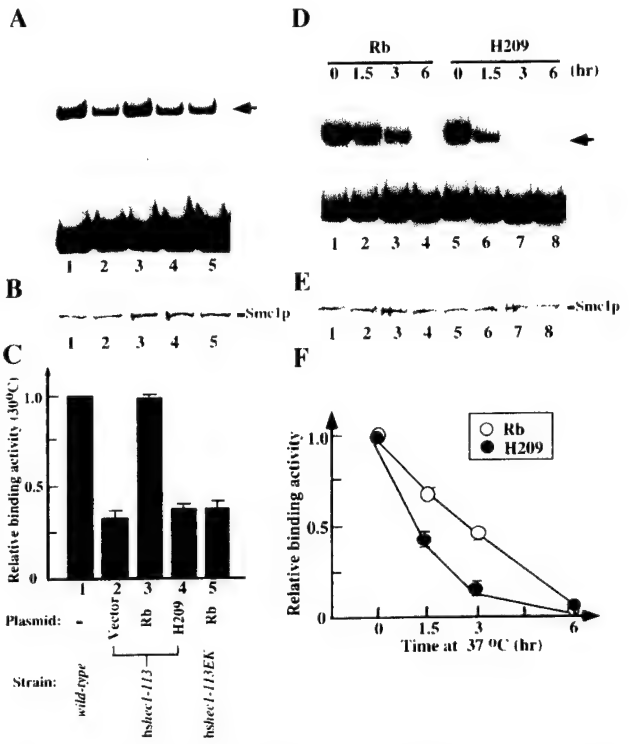

FIG. 5. Rb enhances the DNA-binding activity of Smc1p through hsHec1p. (A) DNA-binding ability of Smc1p purified from equal numbers of cells expressing various forms of Rb and hsHec1p. Expression of Rb and the H209 mutant was induced by addition of 2% galactose to the medium, and cells were cultured at 30°C in this medium for 8 h before harvest. (B) Immunoblot showing that comparable amounts of Smc1p were detected in each of the affinity-purified products used for panel A. (C) Histogram showing relative binding activity of Smc1p in each lane of panel A. (D) DNA-binding ability of Smc1p purified from *hshec1-113* cells expressing Rb (lanes 1 to 4) or the H209 mutant (lanes 5 to 8). Cells were cultured at 25°C in medium containing 2% galactose for 8 h to induce the expression of wild-type Rb or the H209 mutant and then shifted to 37°C for 0, 1.5, 3, or 6 h before harvest. (E) Immunoblot showing comparable amounts of Smc1p in each of the APFs used for panel D. (F) Effect of Rb on the DNA-binding activity of Smc1p in hs*hec1-113* cells. The relative DNA-binding activity of Smc1p indicates the ratio between the quantified density result of each lane in panel D and that of lane 1 for Rb or lane 5 for H209. Bars represent standard errors from three separate experiments.

affect cells carrying the hs*hec1-113EK* allele, which encodes a protein that cannot bind to Rb.

To further corroborate this finding, the dynamic effect of Rb on the activity of hsHec1p was examined. hs*hec1-113* cells were cultured at 25°C in medium containing 2% galactose to induce the expression of Rb or the H209 mutant and then shifted to 37°C for different periods of time. As in the previous experiment (Fig. 4E), the DNA-binding activity of Smc1p began to decrease after cells were shifted to 37°C (Fig. 5D and F). This decrease of Smc1p activity, however, was significantly retarded during the first 3 h at 37°C in the cells expressing Rb compared with the cells expressing H209 mutant (Fig. 5F). By 6 h, Smc1p activity in both strains was very low. This result suggested that Rb can restore much of the activity impaired by mutation of hshec1p but cannot by itself complement the complete loss of hshec1p. Interestingly, Rb was not found in the Smc1p DNA-binding complex, since anti-Rb antibodies were not able to supershift the complex formed by the APF from hs*hec1-113* cells expressing wild-type Rb (Fig. 4G). Rb thus appears to function like a chaperone, consistent with a previous proposal (6).

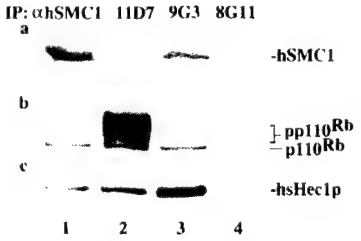

FIG. 6. Rb, hsHec1p, and hSMC1 protein form a complex in human cells. Asynchronous fast-growing human T24 cells (6×10^6) were lysed and immunoprecipitated (IP) by mouse anti-hSMC1 (αhSMC1) antiserum (lane 1), anti-Rb MAb 11D7 (lane 2), anti-hsHec1p MAb 9G3 (lane 3), and anti-GST MAb 8G11 (lane 4). The immunocomplexes were separated by sodium dodecyl sulfate-polyacrylamide gel electrophoresis, followed by immunoblotting with anti-hSMC1 antiserum to detect human SMC1 (a), with 11D7 to detect Rb (b), and with 9G3 to detect hsHec1p (c).

The above results suggest that a potential role of Rb in the modulation of SMC1 through hsHec1p exists and that both Hec1p and SMC1 proteins are functionally conserved from yeast to humans (24, 54, 59). It is therefore likely that Rb, Hec1p, and SMC1 may form a single complex in mammalian cells. To test this notion, hsHec1p and human SMC1 protein were coimmunoprecipitated with each other in human T24 cells (Fig. 6), consistent with our previous observation showing that the Hec1p-SMC1 interaction is conserved (59). Interestingly, the hypophosphorylated form of Rb was also coimmunoprecipitated. As a control, anti-GST MAb 8G11 did not coimmunoprecipitate any of these proteins (Fig. 6). These results suggest that Rb is present in a complex with Hec1p and SMC1 and support a potential role for Rb in modulating the activity of SMC1.

DISCUSSION

In this study, we have employed a yeast system to address the function of Rb in chromosome segregation. Expression of Rb reduced chromosome segregation errors in cells carrying a mutant form of hsHec1p and enhanced the survival rate of *smc1* mutant cells with defects in chromosome segregation. Complexes of Hec1p and Smc1p play essential roles in chromosome segregation. Rb appears to chaperone Hec1p and indirectly to enhance the DNA-binding activity of Smc1p. These results reveal a novel biological activity of Rb intimately linked to its role in carcinogenesis and cancer progression.

The lack of an Rb homolog in yeast allowed us to address Rb function using yeast machinery as a powerful assay tool, without interference from endogenous Rb. Mechanisms similar to those governing Rb phosphorylation in mammalian cells have been demonstrated in yeast (21). However, no significant differences in cell morphology, growth rate, cell cycle progression, or mating pheromone response were observed in yeast cells expressing human wild-type or mutant Rb. These results suggest that Rb does not exert a function when yeast lacks specific cellular mediators of the antiproliferation and differentiation functions of Rb during G_1 phase. Alternatively, potential mediators of such functions in yeast are unable to interact with Rb; such is the case with yeast Hec1p, which has no Rb-binding motif. In either case, the lack of both Rb and mediators of Rb function in yeast made it possible to exploit the yeast cell as an assay system for chromosome segregation and to reconstitute the interaction between hsHec1p and Rb in this system. This assay system ensures that the observed phenomena are direct and specific consequences of Rb expression and are specifically mediated by hsHec1p.

Expression of Rb decreased the frequency of chromosome segregation errors fivefold but was insufficient alone to rescue the yeast cells completely from aberrant mitosis. The fivefold enhancement is likely reminiscent of the physiological effect from a high-level regulator on the basic machinery for chromosome segregation. This improvement in the fidelity of chromosome segregation, however, would be quite significant in higher organisms, considering the millions of cells undergoing mitosis or meiosis daily. In the case of a lack of functional Rb, chromosome segregation errors in mammalian cells are expected to occur at a frequency similar to that for the wild-type yeast. Apparently, a higher fidelity of chromosome segregation is required for higher organisms to avoid errors in the more complicated chromosome segregation.

The biochemical mechanisms by which Rb modulates the activity of Hec1p and by which Hec1p modulates the activity of Smc1p remain to be elucidated. Our studies of DNA-binding activity of Smc1p from cells with different genetic backgrounds have provided some important clues leading to the understanding of these biochemical mechanisms. The DNA-binding activity of SMC1 is suggested to serve as a biochemical basis for its function in the chromatin assembly essential for sister chromatid cohesion and chromosome segregation (24). The modulation of this activity will undoubtedly affect the biological function of SMC1 in chromosome segregation, although other functions of Smc1p may also be influenced. It has been suggested that SMC1 forms complexes with various proteins, most of which, however, have not been revealed (24, 54). Our results indicate that Hec1p is present in the DNA-binding complex of Smc1p and also suggest that Hec1p is important for the biochemical activity of this complex. Consistently, the interaction between Hec1p and Smc1p is critical for proper chromosome segregation (59). Although purified recombinant protein containing the C-terminal region of SMC1 was shown to have the DNA-binding activity (1), it is likely that SMC1 requires other cofactors, such as Hec1p, to enhance its activity for a more stable binding of structured DNA. Rb appears to enhance the DNA-binding activity of Smc1p through Hec1p. This positive regulatory effect of Rb has also been observed in a number of transcription factors, such as MyoD (47), the glucocorticoid receptor (53), C/EBPβ (6), NF-IL6 (7), and c-jun (45). Our results showing that Rb is not a component of the DNA-binding complex formed by Smc1p and Hec1p suggest that Rb may serve as a chaperone for Hec1p, presumably by stabilizing its active conformation. Taken together, the results presented here suggest a potential role of Rb in regulation of SMC1 through hsHec1p.

The functional analysis of Rb in the heterologous yeast system is further supported by the in vivo interaction between Rb, Hec1p, and SMC1 in mammalian cells. The presence of Rb in a complex with Hec1p and Smc1p suggests the relevance of the novel Rb function revealed by the yeast study to mammalian cells where Rb exists. The complex formed between Rb and SMC1 indicates a biological role of Rb in the SMC1 activity, although Rb is not present in the DNA-binding complex of SMC1. Rb thus appears to modulate the activity of SMC1 before SMC1 binds to chromatin DNA. Unlike the activities of Hec1p and SMC1, this M phase activity of Rb does not appear to be required by either yeast or mammalian cells for their basic machinery of chromosome segregation or for cell survival. Nevertheless, such an activity of Rb in regulating SMC1 could be important for higher fidelity of chromosome segregation and higher integrity of mitotic chromosome structures in mammalian cells.

Whether loss of Rb function leads to a decrease in the fidelity of chromosome segregation in mammalian cells re-

mains to be explored. Nonetheless, such an activity for Rb may explain in part the abnormal process of mitosis observed in Rb-deficient fibroblasts and the chromosome abnormalities observed in Rb-deficient tumor cells (12, 28). It may also provide some clues for explaining observations that the majority of human retinoblastomas losing the wild-type allele and reduplicating the mutant allele early in the course of carcingenesis result from nondisjunction and misproportioning of sister chromatids (4, 19). Interestingly, yeast or human cells lacking functional Hec1p complete mitosis with unseparated or unequally separated chromosomes and enter a new cell cycle, leading to hyperploidy and aneuploidy (10, 57, 59). This is similar to the phenomenon observed in Rb-deficient fibroblasts treated with nocodazole (12, 28). Since neither loss of Rb function nor loss of Hec1p function appears to affect the mitotic checkpoint control (28, 59), microtubule-destabilizing agents probably challenge the chromosome segregation process in Rb-deficient cells and thereby induce a high frequency of aberrant mitosis. These results indirectly support the role of Rb in chromosome segregation.

Taken together, the results of this study, using a heterologous yeast system, provide a useful assay and more direct evidence for revealing the mechanistic process of a novel function of Rb in chromosome segregation. The study thereby contributes to explaining a new critical role of Rb in human carcinogenesis.

ACKNOWLEDGMENTS

The first two authors contributed equally to this report.

We thank O. Cohen-Fix, R. D. Gietz, D. Koshland, P. Hieter, C. Holm, A. M. Hoyt, C. Mann, A. Murray, and A. Strunnikov for yeast strains, antibodies, plasmid vectors, and assistance in yeast genetic analysis, and we thank T. Boyer for his critical reading of the manuscript.

This work was supported by NIH grants (EY05758 and CA58318), and L.Z. was supported by a predoctoral training grant from the U.S. Army (DAMD17-99-1-9402).

REFERENCES

1. **Akhmedov, A. T., C. Frei, M. Tsai-Pflugfelder, M. B. Kemper, S. M. Gasser, and R. Jessberger.** 1998. Structural maintenance of chromosome's protein C-terminal domains bind preferentially to DNA with secondary structure. J. Biol. Chem. **273:**24088–24094.
2. **Baker, S. H., D. L. Frederick, A. Bloecher, and K. Tatchell.** 1997. Alanine-scanning mutagenesis of protein phosphatase type 1 in the yeast *Saccharomyces cerevisiae*. Genetics **145:**615–626.
3. **Bloecher, A., and K. Tatchell.** 1999. Defects in *Saccharomyces cerevisiae* protein phosphatase type I activate the spindle/kinetochore checkpoint. Genes Dev. **13:**517–522.
4. **Cavenee, W. K., T. P. Dryja, R. A. Phillips, W. F. Benedict, R. Godbout, B. L. Gallie, A. L. Murphree, L. C. Strong, and R. L. White.** 1983. Expression of recessive alleles by chromosomal mechanisms in retinoblastoma. Nature **305:**779–784.
5. **Chen, P.-L., D. J. Riley, and W.-H. Lee.** 1995. The retinoblastoma protein as a fundamental mediator of growth and differentiation signals. Crit. Rev. Eukaryot. Gene Express. **5:**79–95.
6. **Chen, P.-L., D. J. Riley, and W.-H. Lee.** 1996. Retinoblastoma protein positively regulates terminal adipocyte differentiation through direct interaction with C/EBPs. Genes Dev. **10:**2745–2752.
7. **Chen, P.-L., D. J. Riley, S. Chen-Kiang, and W.-H. Lee.** 1996. Retinoblastoma protein directly interacts with and activates the transcription factor NF-IL6. Proc. Natl. Acad. Sci. USA **93:**465–469.
8. **Chen, P.-L., P. Scully, J.-Y. Shew, J. Y.-J. Wang, and W.-H. Lee.** 1989. Phosphorylation of the retinoblastoma gene product is modulated during cell cycle and cellular differentiation. Cell **58:**1193–1198.
9. **Chen, P.-L., Y.-C. Ueng, T. Durfee, K.-C. Chen, T. Yang-Feng, and W.-H. Lee.** 1995. Identification of a human homologue of yeast nuc2 which interacts with the retinoblastoma protein in a specific manner. Cell Growth Differ. **6:**199–210.
10. **Chen, Y., D. J. Riley, P.-L. Chen, and W.-H. Lee.** 1997. HEC, a novel nuclear protein rich in leucine haptad repeats specifically involved in mitosis. Mol. Cell. Biol. **17:**6049–6056.
11. **Chen, Y., Z. D. Sharp, and W.-H. Lee.** 1997. HEC binds to the seventh regulatory subunit of the 26 S proteasome and modulates the proteolysis of mitotic cyclins. J. Biol. Chem. **272:**24081–24087.
12. **Di Leonardo, A. S., S. H. Khan, S. P. Linke, V. Greco, G. Seidita, and G. M. Wahl.** 1997. DNA rereplication in the presence of mitotic spindle inhibitors in human and mouse fibroblasts lacking either p53 or pRb function. Cancer Res. **57:**1013–1019.
13. **Durfee, T., K. Becherer, P.-L. Chen, S.-H. Yeh, Y. Yang, A. E. Kilburn, W.-H. Lee, and S. J. Elledge.** 1993. The retinoblastoma protein associates with the protein phosphatase type 1 catalytic subunit. Genes Dev. **7:**555–569.
14. **Ewen, M. E., Y. Xing, J. B. Lawrence, and D. M. Livingston.** 1991. Molecular cloning, chromosomal mapping, and expression of the cDNA for p107, a retinoblastoma gene product-related protein. Cell **66:**1155–1164.
15. **Fukasawa, K., T. Choi, R. Kuriyama, S. Rulong, and G. F. Vande Woude.** 1996. Abnormal centrosome amplification in the absence of p53. Science **271:**1744–1747.
16. **Gietz, R. D., and A. Sugino.** 1988. New yeast-E. coli shuttle vectors constructed with in vitro mutagenized yeast genes lacking six-base pair restrictive sites. Gene **74:**527–534.
17. **Goodrich, D. W., N. P. Wang, Y.-W. Qian, E. Y.-H. P. Lee, and W.-H. Lee.** 1991. The retinoblastoma gene product regulates progression through the G1 phase of the cell cycle. Cell **67:**293–302.
18. **Gualberto, A., K. Aldape, K. Kozakiewicz, and T. D. Tlsty.** 1998. An oncogenic form of p53 confers a dominant, gain-of-function phenotype that disrupts spindle checkpoint control. Proc. Natl. Acad. Sci. USA **95:**5166–5171.
19. **Hagstrom, S. A., and T. P. Dryja.** 1999. Mitotic recombination map of 13cen-13q14 derived from an investigation of loss of heterozygosity in retinoblastomas. Proc. Natl. Acad. Sci. USA **96:**2952–2957.
20. **Hannon, G. J., D. Demetrick, and D. Beach.** 1993. Isolation of the Rb-related p130 through its interaction with CDK2 and cyclins. Genes Dev. **7:**2378–2391.
21. **Hatakeyama, M., J. A. Brill, G. R. Fink, and R. A. Weinberg.** 1994. Collaboration of G1 cyclins in the functional inactivation of the retinoblastoma protein. Genes Dev. **8:**1759–1771.
22. **Heck, M. M. S.** 1997. Condensins, cohesins, and chromosome architecture: how to make and break a mitotic chromosome. Cell **91:**5–8.
23. **Hinds, P. W., S. Mittnacht, V. Dulic, A. Arnold, S. I. Reed, and R. A. Weinberg.** 1992. Regulation of retinoblastoma protein functions by ectopic expression of human cyclins. Cell **70:**993–1006.
24. **Hirano, T.** 1999. SMC-mediated chromosome mechanics: a conserved scheme from bacteria to vertebrates? Genes Dev. **13:**11–19.
25. **Hirano, T., R. Kobayashi, and M. Hirano.** 1997. Condensins, chromosome condensation protein complexes containing XCAP-C, XCAP-E and a Xenopus homolog of the Drosophila Barren protein. Cell **89:**511–521.
26. **Hyland, K. M., J. Kingsbury, D. Koshland, and P. Hieter.** 1999. Ctf19p: a novel kinetochore protein in Saccharomyces serevisiae and potential link between the kinetochore and mitotic spindle. J. Cell Biol. **145:**15–28.
27. **Karantza, V., A. Maroo, D. Fay, and J. M. Sedivy.** 1993. Overproduction of Rb protein after the G_1/S boundary causes G_2 arrest. Mol. Cell. Biol. **13:**6640–6652.
28. **Khan, S. H., and G. M. Wahl.** 1998. p53 and pRb prevent rereplication in response to microtubule inhibitors by mediating a reversible G1 arrest. Cancer Res. **58:**396–401.
29. **Kimura, K., and T. Hirano.** 1997. ATP-dependent positive supercoiling of DNA by 13S condensin: a biochemical implication for chromosome condensation. Cell **90:**625–634.
30. **King, R. W., R. J. Deshaies, J. Peters, and M. W. Kirschner.** 1996. How proteolysis drives the cell cycle. Science **274:**1652–1659.
31. **Knudsen, E. S., C. Buckmaster, T.-T. Chen, J. R. Feramisco, and J. Y.-J. Wang.** 1998. Inhibition of DNA synthesis by RB: effects on G1/S transition and S-phase progression. Genes Dev. **12:**2278–2292.
32. **Koepp, D. M., J. W. Harper, and S. J. Elledge.** 1999. How the cyclin became a cyclin: regulated proteolysis in the cell cycle. Cell **97:**431–434.
33. **Koshland, D., and P. Hieter.** 1987. Visual assay for chromosome ploidy. Methods Enzymol. **155:**351–372.
34. **Lanni, J. S., and T. Jacks.** 1998. Characterization of the p53-dependent postmitotic checkpoint following spindle disruption. Mol. Cell. Biol. **18:**1055–1064.
35. **Lengauer, C., K. W. Kinzler, and B. Vogelstein.** 1998. Genetic instability in human cancers. Nature **396:**643–649.
36. **Li, Y., C. Graham, S. Lacy, M. V. Duncan, and P. Whyte.** 1993. The adenovirus E1A-associated 130-kD protein is encoded by a member of the retinoblastoma gene family and physically interacts with cyclins A and E. Genes Dev. **7:**2366–2377.
37. **Losada, A., M. Hirano, and T. Hirano.** 1998. Identification of Xenopus SMC protein complexes required for sister chromatid cohesion. Genes Dev. **12:**1986–1997.
38. **Ludlow, J. W., C. L. Glendening, D. M. Livingston, and J. A. DeCaprio.** 1993. Specific enzymatic dephosphorylation of the retinoblastoma protein. Mol. Cell. Biol. **13:**367–372.
39. **Mayol, X., X. Grana, A. Baldi, N. Sang, Q. Hu, and A. Giordano.** 1993. Cloning of a new member of the retinoblastoma gene family (pRB2) which

Deficiency of Retinoblastoma gene in mouse embryonic stem cells leads to genetic instability

Lei Zheng, Andrea Flesken-Nikitin, Phang-Lang Chen and Wen-Hwa Lee+

Department of Molecular Medicine and Institute of Biotechnology

University of Texas Health Science Center at San Antonio,

15355 Lambda Drive, San Antonio, Texas 78245

+ To whom all correspondence should be addressed.

Email: leew@uthscsa.edu

Tel: 210-567-7351

Fax: 210-567-7377

Supported in part by NIH grant EY 05758 and CA58318.

Abbreviations: LOM: loss of chromosomal marker, FBS: fetal bovine serum, ES: embryonic stem, ICM: inner cell mass, HygTK: fusion gene of the hygromycin phosphotransferase and thymidine kinase, APRT: adenine phosphoribosyltransferase.

ABSTRACT

Genetic instability has been recognized as a hallmark of human cancers. Retinoblastoma tumor suppressor protein (Rb) has an essential role in modulating cell cycle progression. However, there is no direct evidence supporting its role in maintaining genetic stability. Here, we developed a sensitive method to examine the level of chromosome instability by using retrovirus carrying both positive and negative selectable marker that integrated randomly into individual chromosomes, and the frequency of loss of this selectable chromosomal marker (LOM) in normal mammalian cells was measured. Our results showed that normal mouse embryonic stem cells (ES) had a very low frequency of LOM, which was less than 10^{-8}/cell/generation. In Rb-/- mouse ES cells, the frequency was increased to approximately 10^{-5}/cell/generation, while in Rb+/- ES cells, the frequency was approximately 10^{-7}/cell/generation. LOM was mainly mediated through chromosomal mechanisms and not due to point mutations. These results therefore revealed that Rb, with a haploinsufficiency, plays a critical role in the maintenance of chromosome stability. The mystery of why Rb heterozygous carriers have early onset tumor formation with high penetrance can be, at least, partially explained by this novel activity.

INTRODUCTION

Genetic instability is one of the most important hallmarks of cancer (1). Associations of tumor suppressors with the process of chromosome behavior provide possible links between carcinogenesis and genetic instability. Aneuploidy, chromosome structural rearrangements, centrosome amplification, and gene amplification have been observed in p53-deficient cells (2-4) and, more recently, in APC-deficient cells (5,6), supporting a potential role of tumor suppressors in the maintenance of genetic stability.

The roles of Rb in cell cycle regulation and differentiation are well established, and can explain how Rb suppresses tumor growth, but do not completely explain why cancer susceptibility results from loss of Rb function (7). In particular, the mystery behind why the inactivation of Rb leads to multiple genetic alterations that predispose cells to the process of tumorigenesis remains unsolved. In addition to its role in G1 progression, several lines of evidence also suggest that Rb play a significant role at G2/M phases. First, the hypophosphorylated form of Rb, the functional form, is present in these cell cycle stages. It appears that Rb becomes dephosphorylated as Rb interacts with protein phosphatase 1α specifically during G2/M phases (8,9). The yeast homolog of protein phosphatase 1α has been shown to be essential for kinetochore function, execution of mitotic kinetochore/spindle checkpoint, and faithful chromosome segregation (10,11). A regulatory role in the activity of protein phosphatase 1α mediated by Rb would be consistent with other potential activities of Rb in G2/M progression. Second, phosphorylation of Rb in G1/S phases has a coordinated effect on mitotic cyclin induction and degradation in G2/M phases (12). Third, overexpression of Rb in S phase arrests cells at G2 phase (13). Fourth, when

treated with microtubule-destabilizing agents, cells lacking functional Rb do not finish mitosis properly, but exit M phase and undergo a new cycle of DNA replication, leading to hyperploidy (14,15). Finally, p53-mediated G2/M arrest in response to DNA damage requires the presence of functional Rb (16). Taken together, these results suggest that mitotic division cannot be completed in a controlled manner without functional Rb.

Rb may also directly modulate chromosome segregation. Rb has been shown to associate with Hec1, a conserved regulator of multiple mitotic events (17,18). Hec1 interacts with the SMC (structural maintenance of chromosomes) family of proteins, which are chromosome structural proteins essential for establishment of sister chromatid cohesion and chromosome condensation (19). Inactivation of Hec1 in either mammalian cells or yeast cells by either microinjection of specific anti-Hec1 antibodies or by introducing genetic mutations, leads to severe chromosome missegregation resulting lethality (17,20). This essential function of Hec1 appears to be mediated in part by its interaction with SMC family of protein (20). The interaction between Rb and Hec1 occurs specifically in G2/M phase (18). It has been demonstrated that the fidelity of chromosome segregation in yeast cells is enhanced upon induced expression of exogenous human Rb, and this activity requires the specific interaction between Rb and Hec1 (18). However, the role of Rb for maintaining genetic stability in mammalian cells remains to be shown.

Here, we developed a sensitive method to examine the level of chromosome instability in normal mammalian cells by using a retroviral system to integrate randomly a selectable marker on individual chromosomes. The frequency of loss of the chromosomal marker (LOM) was measured, and our results showed increased

frequency of LOM (approximately 10^{-5} per cell per generation) in mouse Rb-/- embryonic stem cells compared with that in Rb+/+ cells. The frequency of LOM in Rb+/- cells was also moderately increased. Further analysis indicated that the loss of the fusion genes is most likely due to gross chromosomal changes.

MATERIALS AND METHODS

Isolation, culture and genotyping of mouse embryonic stem cells

Rb +/+, Rb+/- and Rb-/- ES cells were isolated from blastocysts of the same litter of mouse embryos taken from pregnant intercrossed Rb+/- mice (21) following a previously described procedure (22). Briefly, blastocysts were harvested from pregnant mice on embryonic day 3.5 and cultured on a feeder layer derived from mouse embryonic fibroblasts. The embryos were allowed to hatch for 4-6 days and the inner cell mass (ICM) was moved away from the trophoblast cells, disaggregated and cultured on the feeder layer in the medium containing DMEM, 15% FBS and leukemia inhibitory factors. The pluripotential individual ES colonies were picked and transferred onto a freshly prepared feeder layer and amplified. To determine the genotype of the ES cells, genomic DNA was extracted and PCR was performed as previously described (23).

Selection of individual ES clones infected with HygTK retrovirus

The HygTK fusion gene (24) was inserted between the two long terminal repeats (LTR) derived from Moloney murine leukemia virus in a previously described vector (25). The resultant vector pLHL1-HygTK was transfected into the ecotropic retroviral packaging cell line ϕ2, and the viral supernatant was amplified in the amphotropic packaging cell line PA12. The viral supernatant from the PA12 cell culture was then

used to infect mouse ES cells. Approximately $2x10^6$ ES cells isolated as above described at the twelfth passage with the genotype of Rb+/+, Rb+/- and Rb-/-, respectively, were grown on a hygromysin-resistant feeder layer derived from embryonic fibroblast cells of transgenic mice expressing the hygromycin phosphotransferase gene (Jackson Laboratories). Cells were infected by the HygTK virus for 24 hours in the presence of polybrene and subsequently treated with 250μg/ml hygromycin after another 24 hours. Hygromycin-resistant clones were picked after nine days of selection and maintained in the ES cell culture medium containing 200μg/ml hygromycin afterward. Clones were individually amplified, and PCR analysis indicated that all of the hygromycin resistant colonies carry the integration of the HygTK fusion gene (data not shown).

RESULTS

Establishing a method for measuring the globally genetic instability in mammalian cell

To follow the dynamic changes of individual chromosomes, a selectable marker was permanently integrated on the chromosome by retrovirus mediated gene transfer, which would be expected to harbor a single copy of this marker randomly on individual chromosomes (25). By tracing this marker in multiple virally infected clones, one would have a global view of genetic alterations on chromosomes in general rather than at one specific locus. For the feasibility of detecting the presence or absence of the marker, we chose a fusion gene that combines the hygromycin phosphotransferase gene (Hyg) and herpes simplex virus type 1 thymidine kinase gene (TK) in frame. Translation of this fusion gene into a single bi-functional enzyme protein (designated hereafter as HygTK) confers both resistance to hygromycin and sensitivity to ganciclovir (24), providing both positive and negative selectivity.

The HygTK fusion gene was inserted between two long-terminal repeats (LTR) derived from Moloney murine leukemia virus (25) and, thereby, its expression was under the control of the LTR promoter (Fig. 1A). In an attempt to explore the overall frequencies of LOM regardless of the viral integration loci, more than 50 individual hygromycin-resistant colonies with approximately equal number cells were mixed together. The mixture of cells were maintained in the hygromycin-containing medium, and then transferred to a selection free medium where the cells were propagated for about 10 generations. The cell number after propagation was counted and the number of generations that the cells have been propagated through was calculated (usually between 9-10 generations). In addition, prior to this propagation step, $1x10^7$ cells were also removed from the hygromycin-containing medium and immediately seeded in the ganciclovir-containing medium. Following propagation in the non-selective medium, $1x10^7$ cells were seeded in ganciclovir-containing medium. The ganciclovir-resistant colonies before propagation as well as after propagation were counted after 12 days of ganciclovir-selection to obtain Eo and Ep, respectively (Fig 1B).

The ganciclovir-resistant colonies that arose were from those cells that had lost the functional TK gene and, thus, were no longer sensitive to ganciclovir. Maintaining the cells in the hygromycin-containing medium would prevent the loss of the entire HygTK gene, therefore, ganciclovir-resistant cells were not detected or detected at a frequency less than 10^{-8}. The appearance of ganciclovir-resistant cells before the cells were propagated in non-selective medium would be expected, because accumulation of mutations during this long-term culture could have inactivated the TK gene in some hygromycin-resistant cells. This frequency was however subtracted from that of ganciclovir-resistant cells analyzed after the propagation, and the resultant subtraction

represented the frequency of cells that had the TK gene inactivated during the propagation. Finally, this subtraction was sequentially divided by the total cell number and by the generation numbers to deduce the frequency of LOM at the HygTK-integrated loci in one cell per division generation (Fig. 1C).

Loss of Rb gene increases frequency of LOM.

The above method is ideal for cells with high colony forming efficiency. Normal human fibroblasts and mouse embryonic fibroblasts have poor colony forming efficiency, at about 10^{-3} to 10^{-4}. Therefore, it requires a substantial amount of cells for measuring LOM by this method if the LOM is low. Any immortalized cell lines including cancer cell lines are prone to genetic changes. The selection process in this procedure may create a bias towards certain changes and generate artifacts for this measuring. To circumvent these difficulties, we used ES cells to perform this experiment because of its normalcy and high colony forming efficiency. Three mouse ES cell lines from the same litter were used; one with the wild-type Rb, the other with one allele of Rb mutated at exon 20, and another one with both alleles mutated at exon 20 (21). Our results indicated that the LOM frequency of Rb+/+ cells was lower than 10^{-8}, the frequency of Rb+/- cells was between $10^{-7}$and 10^{-6}, and the frequency of Rb-/- cells was higher than 10^{-5} (Fig. 2). These results therefore suggest that the frequency of LOM is increased in cells homozygous for the null mutation of Rb and moderately increased in cells heterozygous for Rb.

To determine whether the experiments with mixed viral-infected colonies would reveal the average frequencies of LOM regardless of the viral integration loci, we examine the LOM frequencies at individual integration loci. Viral infected cells were selected by hygromycin and hygromycin-resistant clones were randomly picked and

individually cultured. PCR analysis indicated that all of the selected clones carry the integration of the HygTK fusion gene (as shown later in Fig. 4). The ES cells carrying the HygTK fusion gene were maintained in hygromycin-containing medium for at least 6 days before LOM frequency was analyzed following the same procedures for the experiments with the mixed clones.

More than 20 individual clones of each genotype were analyzed to approximately cover one haploid number of chromosomes. The results indicated that individual viral infected clones, though derived from the same parental cells, have different frequency of LOM at the HygTK loci. Similar frequency of LOM was observed with the same clone in repeated experiments. Considering that retroviral infection tends to integrate the HygTK marker in different chromosomal loci, these results implicated that different chromosomal loci vary in the frequency of LOM. We summarized the number of clones with the frequency of LOM that fell in the same logarithm range (Fig. 3A). Results from both sources of Rb+/+ ES cells were combined and showed that approximately 90% of the Rb+/+ clones had a frequency of LOM lower than 10^{-8}, and the rest of clones had a frequency of LOM between 10^{-8} to 10^{-6} (Fig. 3B). However, 80-90% of the Rb-/- clones had a frequency higher than 10^{-6}, and a number of clones (approximately 40%) were higher than 10^{-4}. Interestingly, although none of Rb+/- clones have this frequency higher than 10^{-4}, approximately 60% of these clones were between 10^{-7} and 10^{-5}. These results suggested again that Rb-deficient cells have a significant higher frequency of LOM compared to wild type cells. As shown in Fig. 3B, the majority of clones had a frequency of LOM similar to those of the mixed clones (Fig. 2), suggesting that the assay with the mixed clones was able to reveal the overall frequency of LOM, which closely represented the stability of the whole genome.

It should be noted that the frequency determined by this procedure may be overestimated because the mutated cells may continue to propagate in non-selection medium. However, the relative frequencies of these three different genotype cells are consistent regardless of the different procedures.

Loss of the marker involves larger deletion of chromosomal event instead of point mutation.

To explore the mechanisms underlying the loss of functional TK gene, we examined the status of the HygTK fusion gene in the ganciclovir-resistant cells by PCR. As shown in Fig. 4A and B, PCR was not able to amplify any fragments of the HygTK fusion from genomic DNA of the ganciclovir-resistant clones that were randomly picked. This result indicated that approximately 90% of ganciclovir-resistant clones had lost the entire HygTK fusion gene physically. It also suggested that point mutations or small deletions that could have inactivated the TK gene occurred at a low frequency (about 10%). As previously suggested, potential mechanisms attributed to the loss of a whole gene include chromosomal loss, mitotic recombination, and inter-chromosomal rearrangement, which are all chromosome mechanisms (4, 26). Therefore, increased frequency of LOM observed in Rb-/- cells suggests that Rb-deficiency would lead to chromosome instability.

Interestingly, retaining one wild-type Rb allele does not appear to be sufficient for the maintenance of chromosome stability, as Rb+/- cells also have a moderately increased frequency of LOM compared with the wild type cells. It would be, however, possible that chromosome instability is a consequence of loss of the remaining wild-type Rb allele. To examine this possibility, these ganciclovir-resistant clones derived from Rb+/- cells were genotyped for the wild-type Rb allele by PCR. The result

indicated the clones picked randomly all retained one wild type Rb allele (Fig. 4C), suggesting the haploinsufficiency of Rb in maintaining chromosome stability.

DISCUSSION

Genetic instability in Rb-deficient cells could be responsible for further genetic alterations involved in cancer development. Germline mutations in one Rb allele lead to the development of retinoblastoma in human and pituitary tumors in mouse at very early ages and with nearly complete penetrance (21,27). The remaining wild-type allele is lost as a somatic event and, as suggested, mainly through chromosome mechanisms (26, 28). It has been estimated previously, based on the mean number of tumors occurring in carriers of retinoblastoma, that the mutation rates in both events are nearly equal (27).

In this study, by directly accessing the mutation rate, it suggested that the mutation rate increased when the first Rb allele is inactivated. Chromosome instability in Rb-heterozygous cells could explain the high penetrance of tumor development with loss of the remaining wild-type allele. Nonetheless, the loss of the second Rb allele appears to be the threshold event in tumor development, given that it results in much severe genetic instability, which might account for all of the following genetic alterations essential for tumorigenesis.

It can not be excluded that Rb could also suppress the frequency of point mutations or small deletions, considering that the HygTK gene may not serve as an appropriate reporter for small nucleotide changes. However, our observation implicating a low frequency of point mutations or small deletions in Rb-deficient cells is consistent with previous reports indicating that loss of the remaining Rb allele in the majority of retinoblastoma is mediated by chromosome mechanisms (26, 28). In

addition, chromosome mechanisms appear to be the major cause of loss of heterozygosity during tumorigenesis based on studies with different tumor suppressor genes (4).

In previous studies, reporters such as the adenine phosphoribosyltransferase (APRT) gene at a specific chromosome locus have been used to evaluate the frequency of LOM (4, 29). The new method used in this study, by utilizing retroviral infection to integrate the reporter randomly on different chromosomes, allows us to access comprehensively all chromosome behaviors in cell. In addition, the loss of reporter is prevented by positive selectivity conferred by the same reporter gene; thus, the new method is able to evaluate precisely the level of chromosome instability.

Chromosome abnormality in Rb-deficient fibroblasts has not yet been reported. The average frequency of LOM observed in Rb-/- cells is approximately 10^{-5}. Classical methods such as multiplex fluorescent in situ hybridization (FISH) and spectral karyotyping (SKY) (30) would not be able to catch any aberrance if vast numbers of cells were not subjected to such analysis. By contrast, the new method appears to be more sensitive in evaluating the chromosome instability. However, unlike FISH or SKY, this new method do not reveal the types of chromosome aberrance directly. Our method has to be followed by traditional polymorphism marker analysis on the viral integrated chromosome if one is interested in what types of chromosome mechanisms are involved.

Although non-disjunction is apparently a result of improper chromosome segregation, how other types of chromosome aberrance occur remains to be clarified. Chromosome mechanisms underlying LOM in Rb-deficient cells are most likely comprised of multiple types of chromosome aberrance since Rb appears to be capable of

modulating chromosome metabolisms from different, but intimately-related, aspects including chromosome replication, segregation and structural maintenance (7). Given that Rb is regarded as the prototype for tumor suppressors, it will be even more interesting to examine the role of other tumor suppressors in maintaining chromosome stability by this new method. It is conceivable the other tumor suppressors have a common role in the maintenance of chromosome stability, and such a role may be pivotal for their functions in tumor suppression.

Acknowledgements: We thank Drs. Stanley Cohen for his generosity to provide pLLTX plasmid and Nicholas Ting for his critical reading the manuscript.

Reference

1. Lengauer, C., Kinzler, K.W., & Vogelstein, B., Genetic instabilities in human cancers. Nature 396, 643-649. 1998.
2. Livingstone, L.R., White, A., Sprouse, J., Livanos, E., Jacks, T., & Tlsty, T.D. Altered cell cycle arrest and gene amplification potential accompany loss of wild-type p53. Cell 70, 923-935. 1992.
3. Yin, Y., Tainsky, M. A., Bischoff, F. Z., Strong, L. C. & Wahl, G. M. Wild-type p53 restores cell cycle control and inhibits gene amplification in cells with mutant p53 alleles. Cell 70, 937-948. 1992.
4. Shao C., Deng, L., Henegariu, O., Liang, L., Stambrook, P.J., & Tischfield J.A. Chromosome instability contributes to loss of heterozygosity in mice lacking p53. Proc. Natl. Acad. Sci. USA 97, 7405-7410. 2000.
5. Kaplan, K.B., Burds, A.A., Swedlow, J.R., Bekir, S.S., Sorger, P.K., & Nathke, I.S. A role for the adenomatous polyposis coli protein in chromosome segregation. Nature Cell Biol. 3, 429-432. 2001.
6. Fodde, R., Kuipers, J., Rosenberg, C., Smits, R., Kielman, M., Gaspar, C., van Es, J.H., Breukel, C., Wiegant, J., Giles, R.H., & Clevers H. Mutations in the APC tumour suppressor gene cause chromosomal instability. Nature Cell Biol. 3, 433-438. 2001.
7. Zheng, L., & Lee, W.-H. The retinoblastoma gene: a prototypic and multifunctional tumor suppressor. Exp. Cell Res. 264, 2-18. 2001.
8. Chen, P. -L., Scully, P., Shew, J. Y., Wang, J. Y., & Lee, W. -H. Phosphorylation of the retinoblastoma gene product is modulated during the cell cycle and cellular differentiation. Cell 58, 1193-1198. 1989.

9. Durfee, T., Becherer, K., Chen, P.-L., Yeh, S.-H., Yang, Y., Kilburn, A. E., Lee, W.-H., & Elledge, S. J. The retinoblastoma protein associates with the protein phosphatase type 1 catalytic subunit. Genes Dev. 7, 555-569. 1993.

10. Sassoon, I., Severin, F. F., Andrews, P. D., Taba, M. R., Kaplan, K. B., Ashford, A. J., Stark, M. J., Sorger, P. K., & Hyman, A. A. Regulation of Saccharomyces cerevisiae kinetochores by the type 1 phosphatase Glc7p. Genes Dev. 13, 545-555. 1999.

11. Bloecher, A., & Tatchell, K. Defects in Saccharomyces cerevisiae protein phosphatase type I activate the spindle/kinetochore checkpoint. Genes Dev. 13, 517-522. 1999.

12. Lukas, C., Sorensen, C. S., Kramer, E., Santoni-Rugiu, E., Lindeneg, C., Peters, J. M., Bartek, J., & Lukas, J. Accumulation of cyclin B1 requires E2F and cyclin-A-dependent rearrangement of the anaphase-promoting complex. Nature 401, 815-818. 1999.

13. Karantza, V., Maroo, A., Fay, D., & Sedivy, J. M. Overproduction of Rb protein after the G1/S boundary causes G2 arrest. Mol Cell Biol 13, 6640-6652. 1993.

14. Di Leonardo, A., Khan, S. H., Linke, S. P., Greco, V., Seidita, G., & Wahl, G. M. DNA rereplication in the presence of mitotic spindle inhibitors in human and mouse fibroblasts lacking either p53 or pRb function. Cancer Res 57, 1013-1019. 1997.

15. Khan, S. H., & Wahl, G. M. p53 and pRb prevent rereplication in response to microtubule inhibitors by mediating a reversible G1 arrest. Cancer Res 58, 396-401. 1998.

16. Flatt, P. M., Tang, L. J., Scatena, C. D., Szak, S. T., & Pietenpol, J. A. p53 regulation of G(2) checkpoint is retinoblastoma protein dependent. Mol Cell Biol 20, 4210-23. 2000.

17. Chen, Y., Riley, D. J., Chen, P. -L., & Lee, W. -H. HEC, a Novel nuclear protein rich in leucine heptad repeats specifically involved in mitosis. Mol. Cell. Biol. 17, 6049-6056. 1997.

18. Zheng, L., Chen, Y., Riley, D. J., Chen, P. -L., & Lee, W. -H. Retinoblastoma protein enhances the fidelity of chromosome segregation mediated by hsHec1p. Mol Cell Biol 20, 3529-37. 2000.

19. Koshland, D., & Strunnikov, A. Mitotic chromosome condensation. Annu. Rev. Cell Dev. Biol. 12, 305-333. 1996.

20. Zheng, L., Chen, Y., & Lee, W. -H. Hec1p, an evolutionarily conserved coiled-coil protein, modulates chromosome segregation through interaction with SMC proteins. Mol. Cell. Biol. 19, 5417-5428. 1999.

21. Lee, E. Y., Chang, C. -Y., Hu, N., Wang, Y. -C., Lai, C. -C., Herrup, K., Lee, W. -H., & Bradley, A. A. Mice deficient for Rb are nonviable and show defects in neurogenesis and haematopoiesis. Nature 359: 288-294. 1992.

22. Robertson, E.J. Embryo-derived stem cell lines. In Teratocarcinoma and embryonic stem cells: a practical approach. Ed. Robertson, E.J. (IRL Press, Oxford, England) pp71-112. 1987.

23. Nikitin, A. Y., & Lee, W.-H. Early loss of the retinoblastoma gene is associated with impaired growth inhibitory innervation during melanotroph carcinogenesis in $Rb^{+/-}$ mice. Genes Dev. 10:1870-1879. 1996.

24. Lupton, S.D., Brunton, L.L., Kalberg, V.A., & Overell, R.W. Dominant postive and negative selection using a hygromycin phosphotransferase-thymidine kinase fusion gene. Mol. Cell. Biol. 11, 3374-3378. 1991.

25. Chen, P. -L., Chen, Y., Bookstein, R., & Lee, W.–H. Genetic mechanisms of tumor suppression by the human p53 gene. Science 250, 1576-1580. 1990.

26. Hagstrom, S.A., & Dryja, T.P. Mitotic recombination map of 13cen-13q14 derived from an investigation of loss of heterozygosity in retinoblastoma. Proc. Natl. Acad. Sci. USA 96, 2952-2957. 1999.

27. Knudson, A.G. Mutation and cancer: Statistical study of retinoblastoma. Proc. Natl. Acad. Sci. USA 68, 820-823. 1971.

28. Cavenee, W.K., Dryja, T.P., Phillips, R.A., Benedict, W.F., Godbout, R., Gallie, B.L., Murphree, A.L., Strong, L.C., & White, R.L. Expression of recessive alleles by chromosomal mechanisms in retinoblastoma. Nature 305, 779-784. 1983.

29. Gupta, P.K., Sahota, A., Boyadjiev, S.A., Bye, S., Shao, C., O'Neill, J.P., Hunter, T.C., Albertini, R.J., Stambrook, P.J., & Tishfield, J.A. High frequency in vivo loss of heterozygosity is primarily a consequence of mitotic recombination. Cancer Res. 57, 1188-1193. 1997.

30. Liyanage, M., Coleman, A., du Manoir, S., Veldman, T., McCormack, S., Dickson, R.B., Barlow, C., Wynshaw-Boris, A., Janz, S., Wienberg, J., Ferguson-Smith, M.A., Schrock, E., Ried, T. Multicolour spectral karyotyping of mouse chromosomes. Nature Genetics 14, 312-315. 1996.

Figure Legends

Figure 1 A method for measuring the frequency of LOM using the retroviral-integrated HygTK fusion gene as reporter.

A. Schematic structure of the retroviral provirus carrying the HygTK fusion gene. B. Experimental steps outlined for measuring the frequency of loss of heterozygosity. C. Formula for calculating the frequency of loss of heterozygosity. Feq^{LOM} is the frequency of loss of the marker per cell per generation. Ep and Eo are designated as in B. N is the number of generations.

Figure 2 Increased frequency of LOM in Rb-deficient ES cells.

Three representative dishes selected for ganciclovir-resistant colonies are shown. A mixture of more than 50 individual hygromycin-resistant clones of ES cells infected with the HygTK retrovirus was propagated about 10 generations without any selection. About 10^7 cells of each genotype were seeded on 10-cm dishes and selected for ganciclovir-resistant colonies. Pictures were taken after 12 days of selection. The frequencies of LOM were calculated based on the results collected from multiple dishes

Figure 3 Frequencies of LOM in individual infected clones

A. Number of clones of each genotype of ES cells are listed in the table with frequencies of LOM falling in each indicated logarithm range. B. Histogram showed the percentage of clones falling in each indicated logarithm range deduced from (A).

Figure 4 Genotyping PCR of the HygTK fusion gene and the Rb allele

A. Schematic diagram of the genomic structure of the HygTK-integrated loci. PCR primers for amplifying various regions of the HygTK gene are indicated at their relative

positions. B. Genotyping PCR of the HygTK gene. Lanes 1-5, are representatives of the hygromycin-resistant clones that carry the HygTK fusion gene; lanes 6-15, representatives of ganciclovir-resistant clones. The approximate size of PCR products and corresponding primers used are indicated. In the bottom panel, two pairs of primers as indicated were used in the same reaction. Primers amplifying a region of the Brca1 genome were used as control. C. Genotyping PCR showed that the heterozygosity of the Rb allele was retained. Lanes 1-8, are representatives of hygromycin-resistant clones of Rb+/- ES cells that carry the HygTK fusion gene; lanes 9-27, representative of ganciclovir resistant clones of Rb+/- ES cells that have lost the HygTK fusion gene. 236 bp PCR products were derived from the target allele; 151 bp products derived from the wild-type Rb allele.

Figure 1, Zheng et al

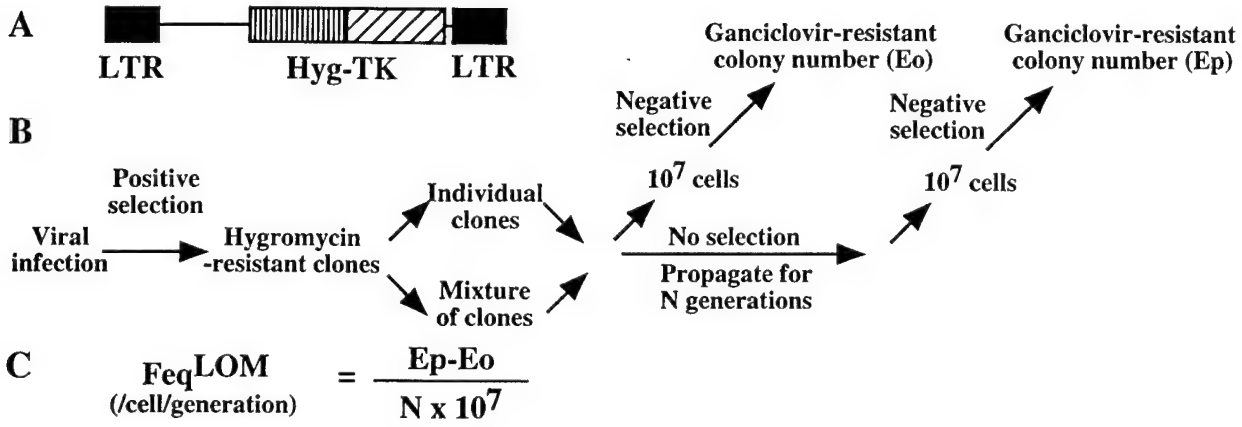

Figure 2, Zheng et al

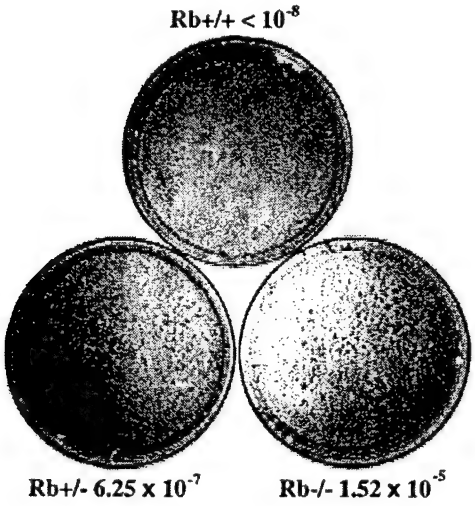

Figure 3, Zheng et al

A

Feq LOM	Numbers of clones		
	Rb-/-	Rb+/-	Rb+/+
$<10^{-8}$	2	7	20
$\sim10^{-8}$	0	4	1
$\sim10^{-7}$	1	6	0
$\sim10^{-6}$	7	4	1
$\sim10^{-5}$	11	4	0
$\sim10^{-4}$	6	0	0
$\sim10^{-3}$	4	0	0
Total	31	25	22

B

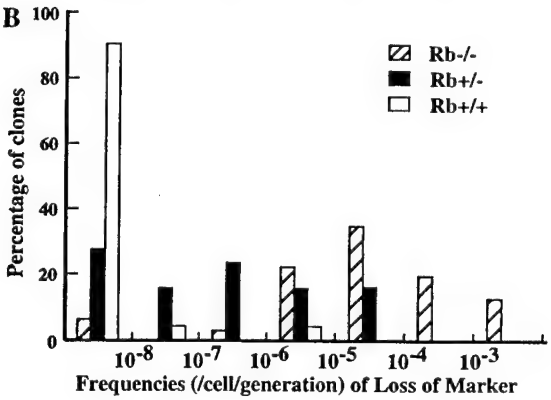

Figure 4, Zheng et al

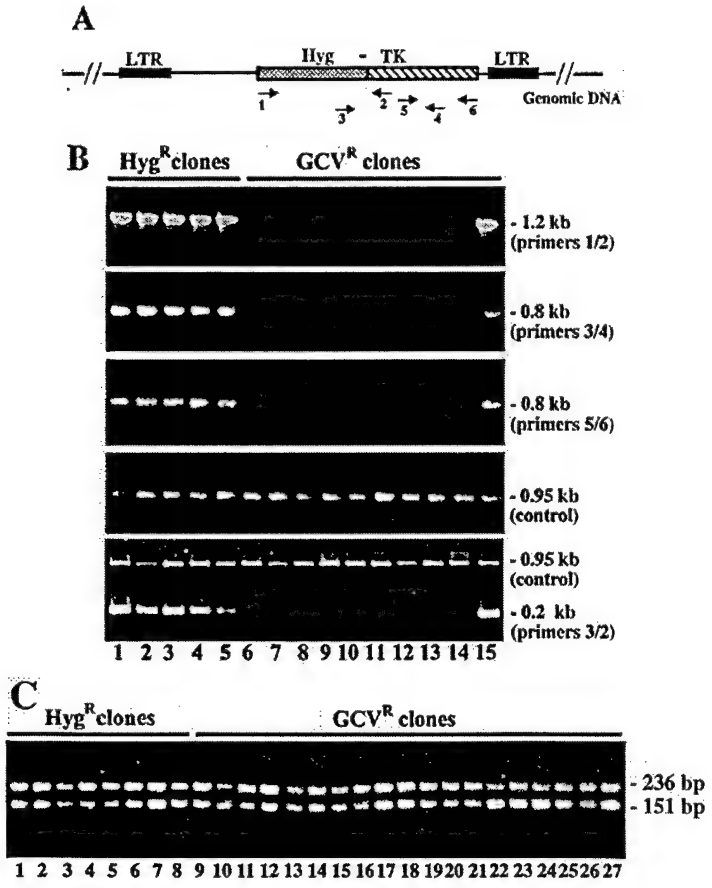

Functional link of BRCA1 and ataxia telangiectasia gene product in DNA damage response

Shang Li*, Nicholas S. Y. Ting*, Lei Zheng*, Phang-Lang Chen*, Yael Ziv†, Yosef Shiloh†, Eva Y.-H. P. Lee* & Wen-Hwa Lee*

** Department of Molecular Medicine/Institute of Biotechnology, University of Texas Health Science Center at San Antonio, San Antonio, Texas 78245, USA*
† Department of Human Genetics and Molecular Medicine, Sackler School of Medicine, Tel Aviv University, Ramat Aviv 69978, Israel

BRCA1 **encodes a familial breast cancer suppressor that has a critical role in cellular responses to DNA damage[1,2]. Mouse cells deficient for *Brca1* show genetic instability, defective G2–M checkpoint control and reduced homologous recombination[3,4]. BRCA1 also directly interacts with proteins of the DNA repair**

machinery[5] and regulates expression of both the *p21* and *GADD45* genes[6–8]. However, it remains unclear how DNA damage signals are transmitted to modulate the repair function of BRCA1. Here we show that the BRCA1-associated protein CtIP[9–12] becomes hyperphosphorylated and dissociated from BRCA1 upon ionizing radiation. This phosphorylation event requires the protein kinase (ATM) that is mutated in the disease ataxia telangiectasia[13]. ATM phosphorylates CtIP at serine residues 664 and 745, and mutation of these sites to alanine abrogates the dissociation of BRCA1 from CtIP, resulting in persistent repression of BRCA1-dependent induction of GADD45 upon ionizing radiation. We conclude that ATM, by phosphorylating CtIP upon ionizing radiation, may modulate BRCA1-mediated regulation of the DNA damage-response *GADD45* gene, thus providing a potential link between ATM deficiency and breast cancer.

BRCA1 interacts with the transcriptional co-repressor complex of CtIP and CtBP through its BRCT domains, and DNA damage-induced dissociation of BRCA1 from this complex may be important for BRCA1 function[9]. To explore the mechanism regulating this interaction, we examined the phosphorylation of CtIP in T24 cells treated with ionizing radiation (IR), ultraviolet or methylmethane sulphonate (MMS). CtIP immunoprecipitated from extracts of treated cells showed slower migrating forms (Fig. 1a, compare lanes 3–5 with lane 2), which were especially prominent in cells γ-irradiated at the dose of 20–40 Gy (Fig. 1a, lane 3; and Fig. 1b). The alteration in electrophoretic mobility was attributed to phosphorylation, as it was sensitive to λ-phosphatase but inhibited by NaF and Na_3VO_4 (Fig. 1c). λ-Phosphatase-treated CtIP migrated faster than the CtIP immunoprecipitated from control cells (Fig. 1c, compare lanes 4 and 2), suggesting that CtIP is a phosphoprotein that becomes hyperphosphorylated after exposure of cells to DNA-damaging agents.

The phosphatidylinositol3-OH kinase [PI(3)K] related family of serine/threonine protein kinases, which includes ATM and DNA-PK (DNA-dependent protein kinase), have been implicated in cell signalling events in response to DNA double-strand breaks[13,14]. It appears that a PI(3)related kinase is involved in the phosphorylation of CtIP, as the IR-induced hyperphosphorylation of CtIP was inhibited in cells treated with the PI(3)K inhibitor, wortmannin (20 μM) (Fig. 1d, lane 4). In two isogenic cell lines, M059J (with deficient DNA-PK activity) and M059K (with normal levels of DNA-PK activity)[15], the IR-induced hyperphosphorylation of CtIP remains unchanged (data not shown); however, the hyper-phosphorylated forms of CtIP appeared only in ATM wild-type GM00637G cells, but not in ATM-deficient GM09607A cells after IR (Fig. 1e). Two other ATM-deficient cell lines, GM05849B and GM02052C, showed identical results (Fig. 1f). Similarly, in two isogenic stable clones derived from ATM-deficient fibroblasts (AT22IJE-T) carrying either vector alone (plasmid pEBS7) or Flag-tagged wild-type ATM (plasmid pEBS7-YZ5)[16], CtIP hyper-phosphorylation was restored only in cells expressing wild-type ATM (Fig. 1g, bottom panel, compare lanes 2 and 4). The presence of wild-type ATM in these cells was confirmed by western blot analysis (Fig. 1g, top panel). These observations suggest that ATM is responsible for the phosphorylation of CtIP following IR.

ATM has been shown to phosphorylate Ser 15 in the highly conserved amino terminus of p53 with the sequence $_{10}$VEPPLSQE$_{17}$ in response to IR[17,18]. The amino-acid sequence of CtIP has six SQ sites bearing similar sequences surrounding Ser 15 of p53. Two of these serines, 664 and 745, are conserved between human and

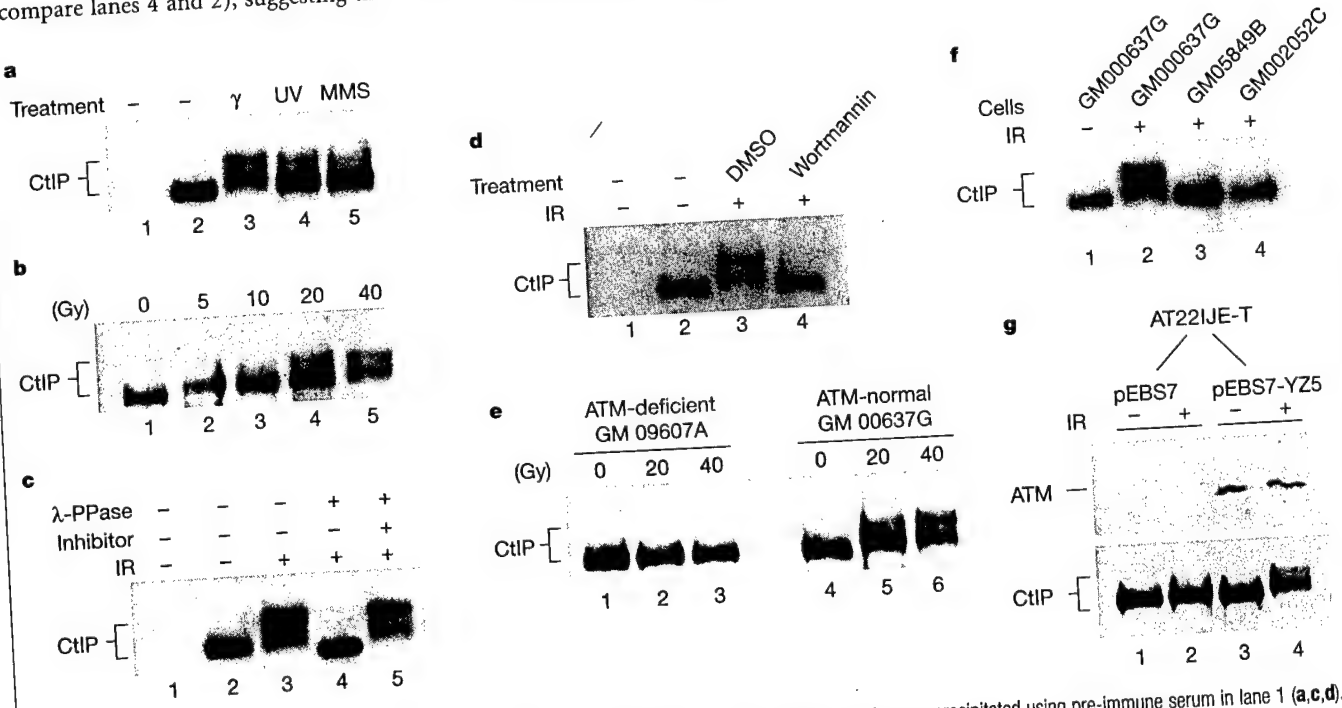

Figure 1 IR-induced phosphorylation of CtIP is ATM dependent. **a**, Change in CtIP gel mobility upon DNA damage. T24 cells were untreated (–) or treated with IR (γ), ultraviolet (UV) or MMS; extracts were immunoprecipitated using anti-CtIP antibody (lanes 2–5) and immunoblotted for CtIP. **b**, Dose-dependent IR phosphorylation of CtIP. T24 cells treated with IR (5–40 Gy) were immunoblotted for CtIP. **c**, Changes in mobility are due to the phosphorylation of CtIP. CtIP immune complexes from untreated (–) or γ-irradiated (+) T24 cells were untreated or treated with λ-phosphatase ± phosphatase inhibitors, as indicated (lanes 2–5), and immunoblotted with anti-CtIP antibodies. **d**, Inhibition of CtIP phosphorylation by wortmannin. T24 cells were untreated (lanes 1 and 2), or pre-incubated with either dimethyl-sulphoxide (DMSO; lane 3) or 20 μM wortmannin (lane 4) before IR (40 Gy); the extracts were then immunoprecipitated and blotted for CtIP (lanes 2–4). Extracts were immunoprecipitated using pre-immune serum in lane 1 (**a**,**c**,**d**). **e**, Phosphorylation of CtIP upon IR is compromised in ATM-deficient cells. Cell extracts from ATM-deficient (GM09607A, lanes 1–3) or normal human fibroblasts (GM00637G, lanes 4–6) treated with IR for the indicated dosages were immunoblotted for CtIP. **f**, Absence of CtIP hyperphosphorylation in additional ATM-deficient cell lines (GM05849B, lane 3; GM02052C, lane 4) upon IR (40 Gy). **g**, Ectopic expression of wild-type ATM in A-T cells restored the phosphorylation of CtIP upon IR. ATM-deficient AT22IJE-T cells were stably transfected with pEBS7 (vector) or pEBS7-YZ5 (carrying Flag-tagged wild-type ATM cDNA). Extracts from IR-treated cells (40 Gy) were immunoblotted with monoclonal antibodies: 2C1, for ATM (top); C11 for CtIP (bottom).

mouse (Fig. 2a), and we mutated these to alanines. Recombinant glutathione *S*-transferase (GST)–CtIP proteins carrying either the double mutations [GST–CtIP(C-S664/745A)] or no mutation [GST–CtIP(C)] were expressed and isolated for *in vitro* ATM kinase assays[17,18]. Immunoprecipitated Flag-tagged wild-type ATM was capable of phosphorylating recombinant GST–CtIP(C), but not GST–CtIP(C-S664/745A) (Fig. 2b, bottom panel, compare lanes 2 and 5), whereas inactive mutant ATM(D2870A) did not phosphorylate either GST–CtIP(C) or GST–CtIP(C-S664/745A) (Fig. 2b, bottom panel, lanes 3 and 6,). The presence of Flag-tagged ATM and ATM(D2870A) was confirmed by immunoblot analysis (Fig. 2b, top panel). These data indicate that ATM may directly phosphorylate CtIP on Ser 664 and Ser 745 *in vitro*.

To determine whether these residues on CtIP are phosphorylated *in vivo*, we transfected Flag-tagged CtIP(WT), CtIP(S664A) or CtIP(S664/745A) into human osteosarcorma U2OS cells and metabolically labelled these cells with inorganic ^{32}P-phosphate. After IR, CtIP(WT), CtIP(S664A) or CtIP(S664/745A) were immunopreci-

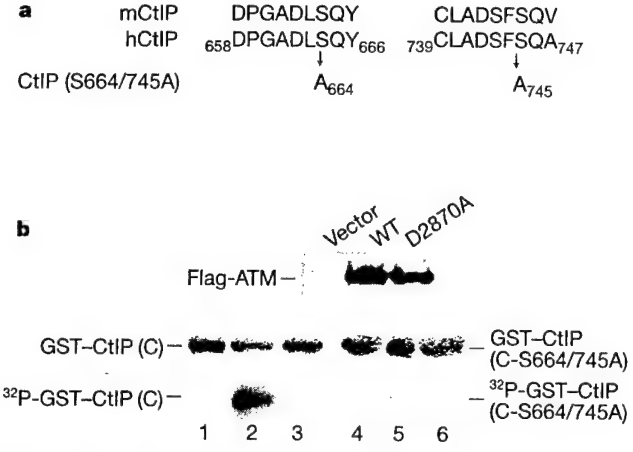

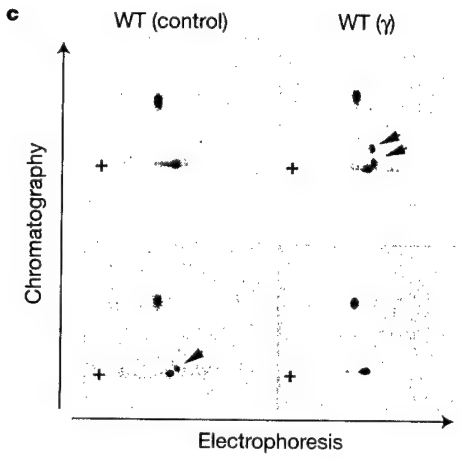

Figure 2 Identification of ATM phosphorylation sites on CtIP. **a**, Sequences of two potential ATM-phosphorylation sites in CtIP and the alignment between human (hCtIP) and mouse (mCtIP) CtIP. For the CtIP phosphorylation site mutant, CtIP(S664/745A), Ser 664 and Ser 745 were mutated to alanine. **b**, Phosphorylation of CtIP by ATM-associated kinase *in vitro*. 293 cells were transiently transfected with vector alone (lanes 1 and 4), or vectors expressing Flag-tagged wild-type ATM (WT) (lanes 2 and 5) or mutated ATM(D2870A) (lanes 3 and 6). Transfected cell extracts were immunoprecipitated with anti-Flag mAb for *in vitro* kinase assay using GST–CtIP(C) (lanes 1–3) and GST–CtIP(C-S664/745A) (lanes 4–6) as substrates. Top, western blot of ectopically expressed ATM using anti-Flag mAb. Middle, Coomassie blue gel of GST–CtIP(C) and GST–CtIP(C-S664/745A). Bottom, autoradiogram of phosphorylated GST–CtIP(C) and CtIP(C-S664/745A). **c**, Phosphorylation of Ser 664 and Ser 745 of CtIP *in vivo* upon IR. U2OS cells transiently transfected with Flag-tagged CtIP(WT), CtIP(S664A) or CtIP(S664/745A) expression vectors, were metabolically labelled with ^{32}P, then either untreated or treated with IR (20 Gy). CtIP was isolated for tryptic phosphopeptide mapping analysis[19]. Two new spots appeared for CtIP(WT) upon IR (arrowheads). Mutation of Ser 664 to alanine resulted in the disappearance of one IR-induced spot, whereas mutation of both Ser 664 and Ser 745 to alanine resulted in the loss of both spots on the tryptic phosphopeptide map.

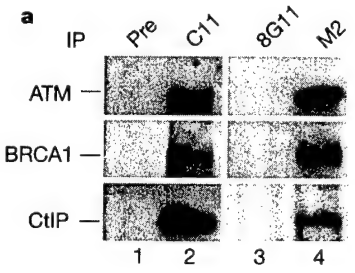

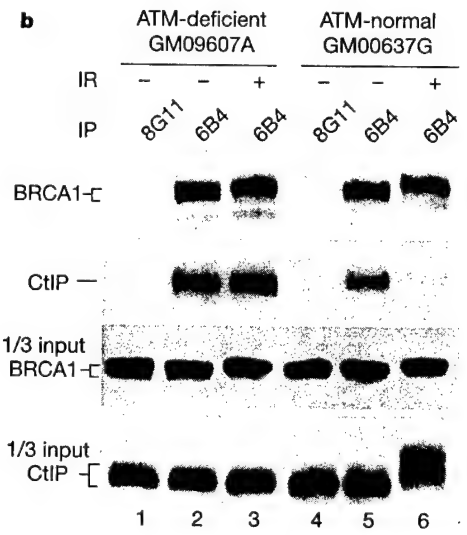

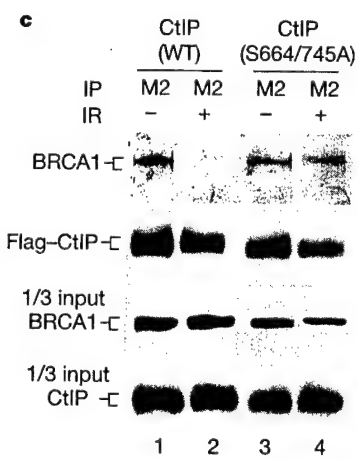

Figure 3 Phosphorylation of CtIP by ATM is essential for dissociation of CtIP from BRCA1 upon IR. **a**, Formation of ATM–BRCA1–CtIP complex *in vivo*. HCT116 cell lysates were immunoprecipitated using pre-immune serum (lane 1) or anti-CtIP polyclonal antibody, C11 (lane 2), and immunoblotted for ATM, BRCA1 or CtIP. In lanes 3 and 4, HCT116 cells were transiently transfected with Flag-tagged ATM expression construct. The lysates were immunoprecipitated using anti-GST (8G11) monoclonal antibody (mAb) as a control or anti-Flag mAb, and immunoblotted for ATM, BRCA1 or CtIP. **b**, Dissociation of BRCA1 and CtIP is abrogated in ATM-deficient cells upon IR. ATM deficient (GM09607A, lanes 1–3) or normal human fibroblasts (GM00637G, lanes 4–6) were untreated (–) or treated with IR (+, 40 Gy). Extracts were immunoprecipitated using control (8G11) mAb or anti-BRCA1 (6B4) mAb, and immunoblotted for BRCA1 (top) or CtIP (bottom). Total input of BRCA1 and CtIP is also shown. **c**, CtIP phosphorylation mutant fails to dissociate from BRCA1 upon IR. Flag-tagged wild-type (lanes 1 and 2) or mutated (lanes 3 and 4) CtIP were transiently transfected into U2OS cells, and the cells were either untreated (–) or treated with IR (40 Gy). The extracts were immunoprecipitated using anti-Flag mAb (M2). Top, immunoblot for BRCA1; bottom, immunoblot for Flag-tagged CtIP. Total input of BRCA1 and Flag-tagged CtIP is also shown.

pitated with anti-Flag antibody (M2), and subjected to two-dimensional tryptic peptide analysis[19]. Two additional tryptic ^{32}P-phosphopeptide spots arose from CtIP(WT) immunoprecipitated from γ-irradiated cells compared with non-irradiated cells (Fig. 2c, top panel, arrows); however, both of these two ^{32}P-phosphopeptide spots were absent in CtIP(S664/745A), and only one of these ^{32}P-phosphopeptides spots was present in CtIP(S664A) (Fig. 2c, bottom panel). Together, these data indicate that both Ser 664 and Ser 745 on CtIP may be phosphorylated *in vivo* in response to IR.

To explore the biological significance of ATM-dependent phosphorylation of CtIP upon IR, we initially tested whether ATM associates with the CtIP and BRCA1 complex *in vivo* by co-immunoprecipitation. BRCA1, CtIP and ATM were co-immunoprecipitated from the human colon carcinoma cell line HCT116 using an anti-CtIP polyclonal antibody (Fig. 3a, compare lanes 1 and 2). As the ATM-specific antibody, 2C1, was not efficient for immunoprecipitation, HCT116 cells were first transfected with a Flag-tagged wild-type ATM expression vector, and subsequently immunoprecipitated with anti-Flag M2 antibody. BRCA1 and CtIP were both co-immunoprecipitated with Flag-tagged ATM (Fig. 3a, lane 4). These data suggest that ATM is present in the previously identified BRCA1–CtIP complex *in vivo*.

We then proceeded to evaluate the consequence of IR-induced ATM-dependent phosphorylation of CtIP on CtIP–BRCA1 complex formation. In the absence of IR, CtIP associated with BRCA1 in both ATM-deficient (GM09607A) and ATM-normal (GM00637G) cells (Fig. 3b, lanes 2 and 5). Upon IR, CtIP dissociated from BRCA1 in ATM-normal cells, but not in ATM-deficient cells (Fig. 3b, compare lanes 3 and 6). Western blot analysis of the cell lysates clearly indicated that IR-induced hyperphosphorylation of CtIP is absent in ATM-deficient cells (Fig. 3b, '1/3 input' panel, compare lanes 3 and 6). Because ATM also phosphorylates BRCA1 (ref. 20), the persistent association of CtIP and BRCA1 in ATM-deficient cells after IR could be attributed to a deficiency in the phosphorylation of BRCA1, of CtIP, or of both. To discriminate between these alternatives, we performed similar experiments with U2OS cells transiently transfected with Flag-tagged CtIP(WT) or CtIP(S664/745A). BRCA1 associated with both CtIP(WT) or CtIP(S664/745A) in the absence of IR (Fig. 3c, lanes 1 and 3), whereas BRCA1 dissociated from CtIP(WT), but remained associated with CtIP(S664/745A) upon IR (Fig. 3c, compare lanes 2–4). Because U2OS cells contain wild-type ATM, IR-induced ATM-dependent phosphorylation of BRCA1 has no apparent effect on the status of the CtIP–BRCA1 complex (Fig. 3c). It should be noted that the change in electrophoretic mobility of Flag-tagged wild-type CtIP was less prominent after IR, perhaps due to the addition of the Flag epitope. These

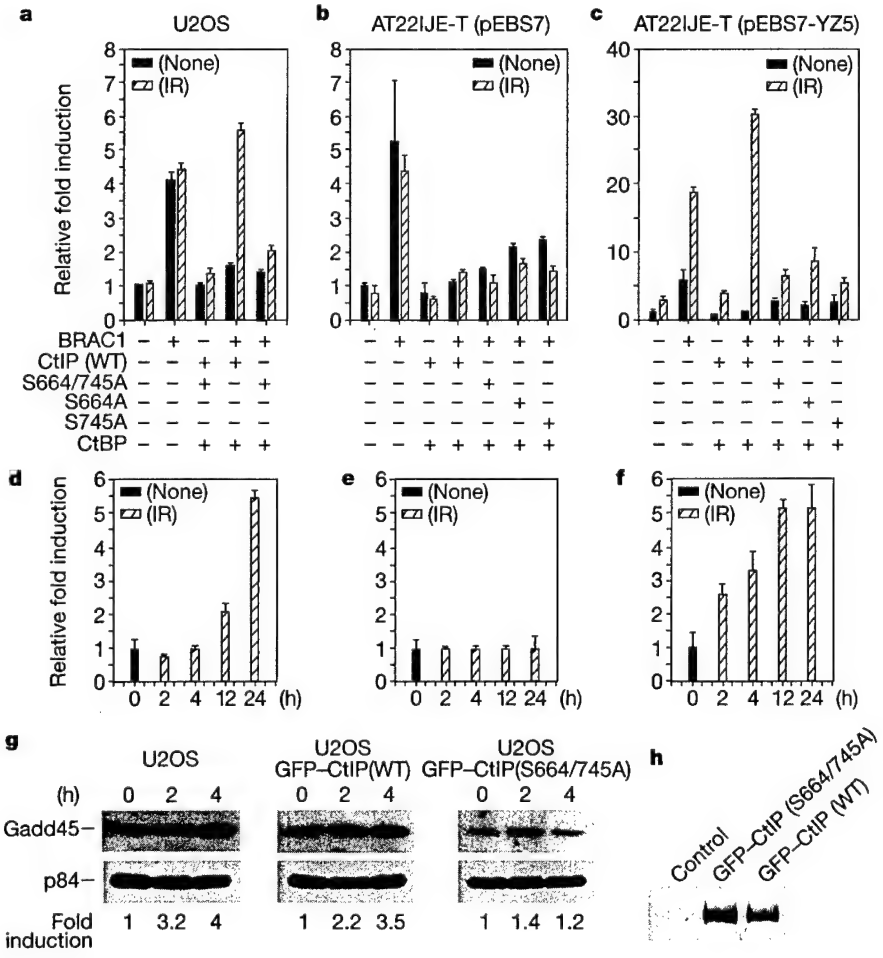

Figure 4 Regulation of GADD45 expression by BRCA1, CtIP and CtBP. **a**–**c**, U2OS, AT22IJE-T (pEBS7) or AT22IJE-T (pEBS7-YZ5) cells were co-transfected with pI-3 (containing *GADD45* intron 3 driving expression of a luciferase reporter gene), pSV40–β-gal (control plasmid) and the plasmids indicated. The luciferase activity was measured and normalized with β-galactosidase activity. Scale in **c** is different from in **a** and **b**. Results were derived from three independent transfection experiments. **d**–**f**, pI-3 reporter activity in U2OS, AT22IJE-T (pEBS7), or AT22IJE-T (pEBS7-YZ5) cells treated with IR. Cells were co-transfected with pI-3 and pSV40–β-gal plasmid, and untreated (solid bar) or treated (hatched bar) with IR (30 Gy) at 36 h after transfection. Transfected cells were then assayed for luciferase activity at the time points indicated. **g**, IR-induced expression of cellular GADD45 protein. U2OS cells stably expressing either GFP–CtIP (WT) or GFP–CtIP(S664/745A) were collected 2 and 4 h after IR and immunblotted for GADD45 and a nuclear matrix protein p84 as an internal control[9]. Blots were developed using an ECL kit and quantified by an SI Densitometer (Molecular Dynamics). The protein ratio of GADD45:p84 is shown. **h**, Immunoblot analysis of ectopically expressed GFP–CtIP(WT) and GFP–CtIP(S664/745A) in the stable cell clones using anti-GFP antibody.

results recapitulate the behaviour of the CtIP–BRCA1 complex in γ-irradiated ATM-deficient cells (Fig. 3b), and suggest that ATM-dependent phosphorylation of CtIP on Ser 664 and Ser 745 is essential for its dissociation from BRCA1 upon IR.

Dissociation of the CtIP–CtBP co-repressor complex from BRCA1, leading to relief of transcription repression, could represent one of the mechanisms regulating the transcriptional activity of BRCA1 upon DNA damage. To test this hypothesis, we examined the effect of CtIP–CtBP on the transactivation activity of BRCA1 on the *GADD45* regulatory element (intron 3 of *GADD45*) which was induced by BRCA1 (ref. 8). Consistently, expression of BRCA1 activated transcription from the reporter plasmid (pI-3) containing intron 3 (+1,553 to +1,695) of *GADD45* by about fourfold compared with the pcDNA3.1 vector alone in U2OS cells (Fig. 4a). Co-expression of CtIP(WT) or CtIP(S664/745A) and CtBP with BRCA1 repressed this BRCA1-induced activity by about 70–80%. After IR, however, CtIP(WT) no longer repressed the activity of BRCA1, whereas CtIP(S664/745A) retained persistent repression (Fig. 4a). The same persistent repression was observed with both CtIP(WT) and CtIP(S664/745A) in ATM-deficient cells [AT22IJE-T(pEBS7)] after IR (Fig. 4b). Re-introduction of wild-type ATM into these cells [AT22IJE-T(pEBS7-YZ5)] eliminated repression mediated by the CtIP(WT)–CtBP complex after IR, whereas CtIP(S664/745A)–CtBP maintained its repression (Fig. 4c). These results suggest that a defect in the ATM-dependent phosphorylation of CtIP(S664/745A) inhibited the dissociation of CtIP(S664/745A) from BRCA1 upon DNA damage, leading to the continuous repression of transcriptional activity from the intron 3 of *GADD45*. Furthermore, it appears that phosphorylation of both Ser 664 and Ser 745 is required for dissociation, as a single mutant form of CtIP(S664A or S745A) maintained its repressive effect after IR treatment (Fig. 4b, c). It was noted that the overall fold induction of the reporter (pI-3) was higher in the AT22IJE-T (pEBS7-YZ5) cells compared with in the U2OS cells in these experiments. This is because the reporter activity 4 h after IR was induced 2–3-fold in AT22IJE-T (pEBS7-YZ5) cells but very little in U2OS cells (Fig. 4d, f). The transcriptional activity of the reporter construct alone in ATM-deficient cells [AT22IJE-T(pEBS7)] remained constant after IR, which is consistent with previous results showing that induction of *GADD45* in response to IR requires ATM (compare Fig. 4e and f)[21]. Together, these data suggest that phophorylation of CtIP by ATM is critical for releasing BRCA1 from its repressive state. Consistently, overexpression of BRCA1 could titrate the endogenous CtIP–CtBP repressor complexes and thereby liberate BRCA1 from repression (Fig. 4a–c).

The persistent repression exerted by CtIP(S664/745A) suggests that it may act as a dominant-negative inhibitor of BRCA1-mediated transcriptional activity following IR. To test this possibility, we created U2OS cells stably expressing green fluorescent protein (GFP) tagged CtIP(WT) or CtIP(S664/745A), challenged these cells with IR, and assessed endogenous expression of GADD45 by immunoblot analysis. Overexpression of CtIP(S664/745A) but not CtIP(WT) inhibited the induction of GADD45 after IR (Fig. 4g). The expression of GFP-tagged CtIP proteins was confirmed by immunoblot analysis (Fig. 4h). These data further support the notion that phosphorylation of CtIP at Ser 664 and Ser 745 is important for BRCA1-mediated induction of GADD45 in response to DNA damage.

In response to genomic insult, ATM probably transduces the DNA damage signal by phosphorylating downstream effector molecules involved in regulating cell-cycle progression or DNA damage repair. For example, IR-induced ATM-dependent phosphorylation of p53 and hMDM2 contributes to the activation of p53, leading to the induction of p21 and GADD45 (refs 17, 18, 22). BRCA1 has also been demonstrated to induce expression of p21 and GADD45 (refs 6–8). Our study suggests another DNA damage-response pathway in which the signal is transmitted through phosphorylation of CtIP by ATM, leading to dissociation of the CtIP–CtBP repressor complex from BRCA1, which in turn, activate transcription of *GADD45* (Fig. 5). This regulatory mechanism may also explain our previous results concerning repression by CtIP/CtBP on the expression of p21 mediated by BRCA1 (ref. 9). Apparently, BRCA1 and p53 are important in p21 and GADD45 expression in response to IR. It is likely that both p53 and BRCA1 mediate synergistic and parallel pathways to ensure a proper cellular response to DNA damage.

These results provide a link between ATM and BRCA1 through CtIP, which may explain the increased risk for breast cancer in certain populations of ataxia telangiectasia heterozygotes[23,24]. In the absence of functional ATM, the activity of BRCA1 may become disregulated leading, in turn, to a defect in the cellular response to DNA damage, concomitant genomic instability and, ultimately, tumorigenesis. □

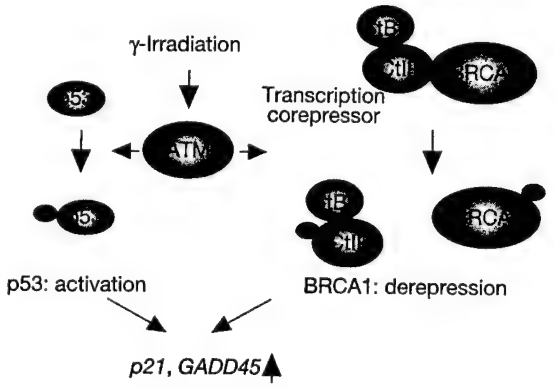

Figure 5 Model showing how ATM modulates the BRCA1 transcriptional regulation of DNA damage-response genes following IR. In response to IR, ATM kinase becomes activated and phosphorylates CtIP to disrupt the CtIP–CtBP–BRCA1 complex. Consequently, BRCA1 is released and participates in the activation of DNA damage-response genes *p21* and *GADD45*.

Methods

Plasmid constructs

The pCNF–CtIP(WT) plasmid that expresses the Flag-tagged CtIP was generated by subcloning Flag-tagged CtIP cDNA into pcDNA3.1 vector (Invitrogen). The pCNF–CtIP(S664/745A) with mutations at Ser 664 and Ser 745 was engineered by site-directed mutagenesis. pCMV–ATM expresses Flag-tagged wild-type ATM, whereas pCMV–ATM(D2870A) expresses mutant ATM with Asp 2,870 changed to alanine by site-directed mutagenesis. GST–CtIP(C) was constructed by inserting the carboxy-terminal fragment of CtIP (amino acids 324–897) into the *Sma*I site of pGEPK3 vector. GFP–CtIP contains the full-length CtIP cDNA downstream of GFP-tagged expression vector[25]. pcDNA–BRCA1, pRcCMV–CtBP and pSV40–β-gal plasmids have been described[9]. The pI-3 plasmid was constructed as described[8].

Cell treatment, immunoprecipitation and western blot analysis

Cells were incubated in fresh medium for 3 h and treated with different dosages of γ-ray (5–40 Gy), ultraviolet (1 mJ cm^{-2}) or 0.01% MMS. The cells were collected 1 h after treatment and lysed in Lysis 250 buffer. Immunoprecipitation and western blots were carried out as described[9]. We used the following antibodies: anti-CtIP mouse polyclonal antibody C11, anti-BRCA1 monoclonal antibody 6B4, anti-GST monoclonal antibody 8G11 (ref. 9), ATM monoclonal antibody 2C1 (GeneTex), anti-Flag monoclonal antibody M2 (Sigma), anti-GADD45 rabbit polyclonal Ab H165 (Santa Cruz Biotechnology) and anti-GFP monoclonal antibody (Clontech).

λ-Phosphatase treatment

Immune complexes containing CtIP were washed in Lysis 250 buffer in the absence of phosphatase inhibitors. Parallel samples were resuspended in λ-phosphatase buffer (New England Biolabs) either in the presence or absence of phosphatase inhibitors, NaF (50 mM final concentration) and Na_3VO_4 (2 mM final concentration). λ-Phosphatase (400 U) was added to each sample followed by incubation at 30 °C for 1 h.

Transfection and luciferase assay

Plasmid DNA including 10 μg of pCMV (vector), pCMV-ATM or pCMV-ATM(D2870A) was transfected into 293 cells (2×10^6 in 10-cm dish) by the calcium phosphate/DNA

Molecular Cell, Vol. 6, 757–768, October, 2000, Copyright ©2000 by Cell Press

Sequence-Specific Transcriptional Corepressor Function for BRCA1 through a Novel Zinc Finger Protein, ZBRK1

Lei Zheng, Hongyi Pan, Shang Li, Andrea Flesken-Nikitin, Phang-Lang Chen, Thomas G. Boyer, and Wen-Hwa Lee*
Department of Molecular Medicine
Institute of Biotechnology
University of Texas Health Science Center at San Antonio
San Antonio, Texas 78245

Summary

BRCA1 has been implicated in the transcriptional regulation of DNA damage–inducible genes that function in cell cycle arrest. To explore the mechanistic basis for this regulation, a novel human gene, *ZBRK1*, which encodes a 60 kDa protein with an N-terminal KRAB domain and eight central zinc fingers, was identified by virtue of its interaction with BRCA1 in vitro and in vivo. ZBRK1 binds to a specific sequence, GGGxxx CAGxxxTTT, within *GADD45* intron 3 that supports the assembly of a nuclear complex minimally containing both ZBRK1 and BRCA1. ZBRK1 represses transcription through this recognition sequence in a BRCA1-dependent manner. These results thus reveal a novel corepressor function for BRCA1 and provide a mechanistic basis for the biological activity of BRCA1 through sequence-specific transcriptional regulation.

Introduction

Potential insight into the molecular basis for the caretaker function of BRCA1 has been provided by studies that implicate this tumor suppressor in both the repair of damaged DNA and the regulation of transcription (Miki et al., 1994; reviewed by Chen et al., 1999; Welcsh et al., 2000). Several lines of evidence support a direct role for BRCA1 in DNA damage repair. First, BRCA1-deficient cells are hypersensitive to ionizing radiation (IR) and characterized by defects in the repair of both oxidative DNA damage by transcription-coupled processes and chromosomal double-strand breaks by homologous recombination (Gowen et al., 1998; Moynahan et al., 1999; Zhong et al., 1999). Second, Brca1 mutant mouse embryo fibroblasts are characterized by genetic instability through improper regulation of centrosome duplication and defective G_2/M checkpoint control (Xu et al., 1999). Third, BRCA1 functionally interacts with the hRad50–hMre11–NBS1 complex that participates in both the DNA damage response and the repair of DNA double-strand breaks (Zhong et al., 1999). Finally, IR-induced phosphorylation of BRCA1 by ATM and hCds1/Chk2 appears to be critical for proper execution of the cellular DNA damage response (Cortez et al., 1999; Lee et al., 2000).

*To whom correspondence should be addressed (e-mail: leew@uthscsa.edu).

A significant body of experimental evidence also implicates BRCA1 in the regulation of transcription. First, the carboxyl terminus of BRCA1 exhibits an inherent transactivation function that is sensitive to cancer-predisposing mutations (Chapman and Verma, 1996; Monteiro et al., 1996; Haile and Parvin, 1999). Second, BRCA1 has been identified as a component of the RNA polymerase II holoenzyme (Scully et al., 1997a; Anderson et al., 1998). Third, BRCA1 has been reported to interact with a variety of transcriptional activators or coactivators, such as p53 and CBP/p300, or corepressors, including CtIP/CtBP and histone deacetylases (HDACs) (Reviewed by Chen et al., 1999; Welcsh et al., 2000). Finally, BRCA1 has been reported to regulate transcription of genes that encode activities involved in cell cycle arrest, including *p21* and *GADD45* (Somasundaram et al., 1997; Harkin et al., 1999).

Thus, while BRCA1 likely ensures global genome stability through its dual participation in transcription and DNA double-strand break repair processes, a number of important issues remain to be resolved. For example, it is not presently clear how BRCA1-mediated transcriptional regulation is functionally linked to its role in DNA damage repair and cell cycle checkpoint control. Furthermore, it is not presently known how BRCA1 mediates gene-specific transcriptional regulation, since BRCA1 itself exhibits no sequence-specific DNA binding activity.

The recent identification of *GADD45* as a target gene transcriptionally induced by BRCA1 overexpression is of interest in this regard (Harkin et al., 1999). GADD45 has been implicated in a variety of growth regulatory processes, including activation of DNA damage–induced G2/M checkpoints (Wang et al., 1999) and maintenance of genome stability (Hollander et al., 1999). The regulatory mechanisms governing *GADD45* gene transcription have in part been revealed by the identification of discrete regulatory elements within its proximal promoter and intron 3 sequences and transcription factors, including p53 and CEB/Pα, capable of activating *GADD45* gene transcription (Kastan et al., 1992; Hollander et al., 1993; Constance et al., 1996). However, a more complete understanding of the regulatory events underlying its inducible control awaits a description of how BRCA1 regulates *GADD45* gene transcription.

Here we identify and characterize a novel zinc finger and *BR*CA1-interacting protein with a KRAB domain, designated ZBRK1. ZBRK1 binds to a specific consensus sequence within intron 3 of the *GADD45* gene through which it functions as a transcriptional repressor. Significantly, we find that this repression activity is mediated by BRCA1.

Results

Isolation of ZBRK1, which Contains a KRAB Domain and Eight Zinc Finger Motifs

ZBRK1 was isolated as a strong positive clone, BRAP12, in a yeast two-hybrid screen for proteins associated

A

```
                                    M I Q A Q E S I T L E  11
D V A V D F T W E E W Q L L G A A Q K D L Y R D V M L E  39
N Y S N L V A V G Y Q A S K P D A L F K L E Q G E Q P W  67
T I E D G I H S G A C S D I W K V D H V L E R L Q S E S  95
L V N R R K P C H E H D A F E N I V H C S K S Q F L L G 123
Q N H D I F D L R G K S L K S N L T L V N Q S K G Y E I 151
K N S V E F T G N G D S F L H A N H E R L H T A I K F P 179
A S Q K L I S T K S Q F I S P K H Q K T R K L E K H H V 207
C S E C G K A F I K K S W L T D H Q V M H T G E K P H R 235
C S L C E K A F S R K F M L T E H Q R T H T G E K P Y E 263
C P E C G K A F L K K S R L N I H Q K T H T G E K P Y I 291
C S E C G K G F I Q K G N L I V H Q R I H T G E K P Y I 319
C N E C G K G F I Q K T C L I A H Q R F H T G K T P F V 347
C S E C G K S C S Q K S G L I K H Q R I H T G E K P F E 375
C S E C G K A F S T K Q K L I V H Q R T H T G E R P Y G 403
C N E C G K A F A Y M S C L V K H K R I H T R E K Q E A 431
A K V E N P P A E R H S S L H T S D V M Q E K N S A N G 459
A T T Q V P S V A P Q T S L N I S G L L A N R N V V L V 487
G Q P V V R C A A S G D N S G F A Q D R N L V N A V N V 515
V V P S V I N Y V L F Y V T E N P                      532
```

B

```
                    A Box                                   B Box
CONSENSUS    VTF DVAV F  EEW  LD  QR LYR VMLENY  LVSL G    KPDL   LEQ    W

ZNF7       2EVVTFGDVAVHFSREEWQCLDPGQRALYREVMLENHSSVAGLAGFLVFKPELISRLEQGEEPW
ZNF90      2GPLEFRDVAIEFSLEEWHCLDTAQQNLYRDVMLENYRHLVFL.GIVVTKPDLITCLEQGKKPF
ZNF85      2GPLTFRDVAIEFSLKEWQCLDTAQRNLYRNVMLENYRNLVFL.GITVSKPDLITCLEQGKEAW
ZNF141     2ELLTFRDVAIEFSPEEWKCLDPDQQNLYRDVMLENYRNLVSL.GVAISNPDLVTCLEQRKEPY
ZNF45      6EAVTFKDVAVVFSEEELQLLDLAQRKLYRDVMLENFRNVVSV.GHOST.PDGLPQLEREEKLW
ZNF10     12TLVTFKDVFVDFTREEWKLLDTAQQILYRNVMLENYKNLVSL.GYQLTKPDVILRLEKGEEPW
ZNF177    12GLLTFQEVFVDFSQEEWGLLDPAQRNLYKDVMLE.FRNLASV.GYQLCRHSLISKVDQEQLKT
ZNF91     12GLLTFRDVAIEFSPEEWQCLDTAQQNLYRNVMLENYRNLAFL.GIALSKPDLIPYLEQGKEPW
ZNF157    24GSVSFEDVAVDFTRQEWHRLDPAQRTMHKDVMLETYSNLASV.GLCVAKPEMIFKLERGEELW
ZNF140     4GSVTFRDVAIDFSQEEWKWLQPAQRDLYRCVMLENYGHLVSL.GLSISKPDVVSLLEQGE.PW

ZBRK1      6ESITLEDVAVDFTWEEWQLLGAAQRDLYRDVMLENYSNLVAV.GYQASKPDALFKLEQGEQPW
```

Figure 1. *ZBRK1* cDNA Encodes a Novel Protein with a KRAB Domain and a Zinc Finger Domain

(A) The ZBRK1 protein sequence. The KRAB domain is underlined, and the Cys and His residues of the C2H2-type zinc fingers are shadowed.

(B) Amino acid sequence alignment of the ZBRK1 KRAB domain with KRAB domains of other zinc finger proteins (Friedman et al., 1996). Conserved residues are indicated by bold letters.

with BRCA1 (Chen et al., 1996). RNA blot analysis using the original 1.2 kb cDNA as a probe revealed a single 2.4 kb mRNA that was expressed in breast epithelial cell lines HBL100, MCF10A, and breast cancer cell lines T47D, MB231, and MCF7 (data not shown). A full-length cDNA was subsequently isolated that encodes a novel human protein of 532 amino acids bearing eight consecutive Krupple-type C2H2 zinc finger motifs within its central region (Figure 1A). The N-terminal region shares significant homology with KRAB domains (Margolin et al., 1994; Witzgall et al., 1994) that have been identified in many zinc finger proteins (Figure 1B). The presence within its predicted coding sequence of these consensus functional motifs (zinc fingers and a KRAB domain) suggests that *ZBRK1* encodes a transcription factor.

ZBRK1 Interacts with BRCA1 In Vitro

To define the ZBRK1 interaction region(s) on BRCA1, in vitro translated ZBRK1 was tested for its ability to bind to different polypeptide fragments of BRCA1 fused to GST (Figures 2A and 2B) as described (Li et al., 1998; Zhong et al., 1999). ZBRK1 bound specifically to GST-BRCA1Bgl, containing BRCA1 amino acid residues 341–748 (aa 341–748), but not to GST-BRCA1N (aa 1–302), GST-BRCA1M (aa 762–1315), or GST-BRCA1C (aa 1316–1863) (Figure 2C).

To confirm this result, different fragments of BRCA1 fused in-frame with the Gal4 DNA-binding domain (Zhong et al., 1999) were individually tested for their respective abilities to interact with full-length ZBRK1 fused to the Gal4 transactivation domain (Figure 2A) by yeast two-hybrid assay (Durfee et al., 1993). Corresponding β-galactosidase activities revealed binding of ZBRK1 to both BRCA1Bgl (aa 341–748), as well as BRCA1-3.5 (aa 1–1142), the original bait used in the yeast two-hybrid screen from which ZBRK1 was first isolated (Chen et al., 1996) (Figure 2D). Fragments corresponding to two regions other than BRCA1Bgl within BRCA1-3.5, BRCA1N (aa 1–302) and BRCA1StuI/PstI (aa 513–914), exhibited little binding activity. These results confirm those of the in vitro binding assays and thus reveal that ZBRK1 binds to BRCA1 aa 341–748.

To map the regions on ZBRK1 required for binding to BRCA1, the BRCA1Bgl region (aa 341–748), carrying a FLAG epitope, was translated in vitro and subsequently tested for binding to different regions of ZBRK1 fused with GST (Figures 2E and 2F). BRCA1Bgl bound to full-length ZBRK1 and to ZBRK1C1 (aa 319–532), but not to ZBRK1N, (aa 1–168) nor to ZBRK1Zn, corresponding to the zinc-finger domain (aa 169–439) (Figure 2G). Interestingly, ZBRK1C2, corresponding to the C-terminal 94 amino acids of ZBRK1 (aa 439–532), was not sufficient for binding to BRCA1, implying that ZBRK1 sequences encoding the last four zinc fingers are also required for BRCA1 binding. Therefore, a C-terminal region corresponding to amino acids 319–532 is required for ZBRK1 to bind to BRCA1.

ZBRK1 Is a 60 kDa Cellular Protein that Interacts with BRCA1 In Vivo

To identify the cellular protein encoded by ZBRK1, we raised mouse polyclonal antibodies specific for ZBRK1 residues 68–208, a less conserved region among KRAB domain–containing zinc finger proteins. These antibod-

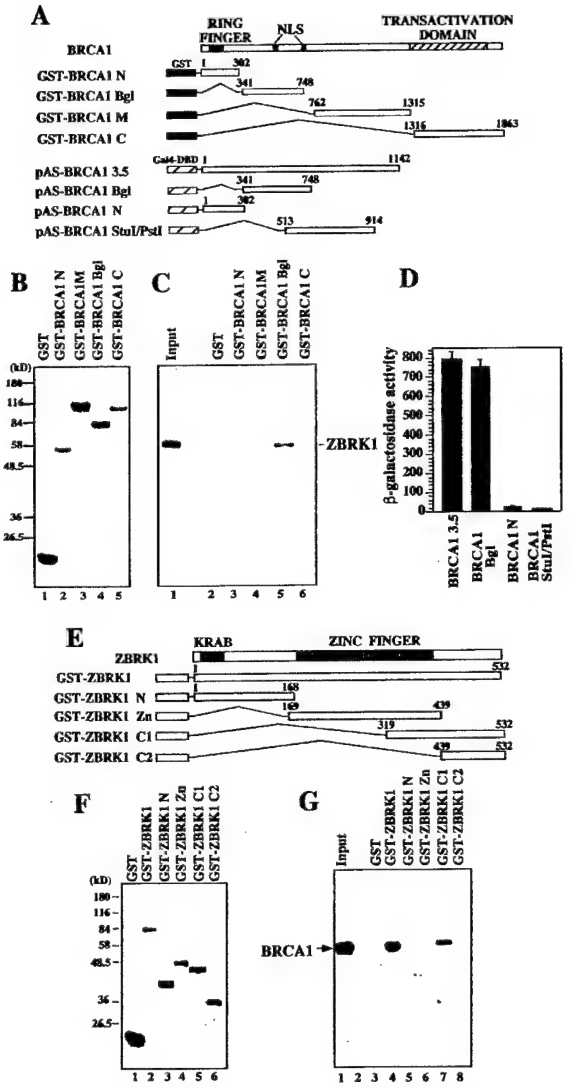

Figure 2. Specific Interaction between ZBRK1 and BRCA1

(A) Schematic diagram of the full-length BRCA1 protein and different BRCA1 polypeptide fragments fused to GST or the Gal4 DNA-binding domain.

(B) Purified GST-BRCA1 fusion proteins were visualized by SDS–PAGE and Coomassie blue staining. Comparable amounts of each fusion protein were used for binding reactions shown in (C).

(C) Specific binding of ^{35}S-methionine-labeled in vitro–translated ZBRK1 to GST-BRCA1Bgl (lane 5) but not to other BRCA1 polypeptide fragments, as detected by SDS–PAGE and subsequent autoradiography. Lane 1 represents the total input of in vitro–translated ZBRK1 used in each binding reaction.

(D) The indicated fragments of BRCA1, expressed as Gal4 DNA-binding domain fusion proteins, were tested for interaction with ZBRK1 fused to the Gal4 transactivation domain in yeast two-hybrid assays. β-galactosidase activities were quantified as described (Durfee et al., 1993).

(E) Schematic diagram of the full-length ZBRK1 and different polypeptide fragments of ZBRK1 fused to GST.

(F) Comparable amounts of each fusion protein were used for binding reactions shown in (G).

(G) Specific binding of in vitro–translated BRCA1 Bgl fragment to the full-length ZBRK1 (lane 4) and the ZBRK1C1 region (lane 7). Lane 1 represents the total input of in vitro–translated BRCA1 Bgl fragment used in each binding reaction.

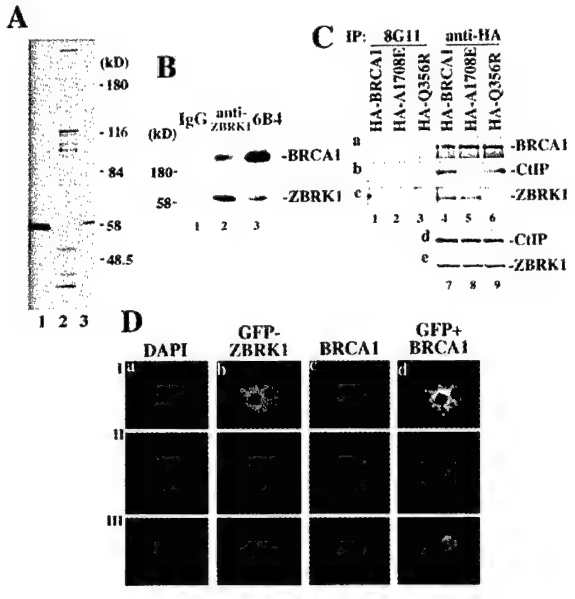

Figure 3. Detection of Cellular ZBRK1 Protein and In Vivo Interaction of ZBRK1 and BRCA1

(A) Detection of cellular ZBRK1 protein. Lysate from ^{35}S-methionine-labeled T24 cells (1.6×10^7) was subjected to immunoprecipitation once by preimmune sera (lane 2) or twice by anti-ZBRK1 antibodies (lane 3). In vitro translated ZBRK1 is indicated in lane 1.

(B) In vivo interaction between ZBRK1 and BRCA1. T24 cell (1.6×10^7) lysate was immunoprecipitated by rabbit IgG (lane 1), anti-ZBRK1 antibodies (lane 2), or anti-BRCA1 mAb 6B4 (lane 3). Immunoprecipitated proteins were eluted by boiling in SDS sample buffer and separated by SDS-7.5% PAGE followed by immunoblot analysis with 6B4 to detect BRCA1 (upper panel) or with anti-ZBRK1 antibodies to detect ZBRK1 (lower panel).

(C) Specific coimmunoprecipitation of ZBRK1 and BRCA1. Myc-GFP-ZBRK1 was cotransfected with either HA-tagged wild-type BRCA1 (lanes 1, 4, and 7), or BRCA1 mutants, A1708E (lanes 2, 5, and 8), or Q356R (lanes 3, 6, and 9). Lysates were immunoprecipitated with anti-GST mAb 8G11 (lanes 1–3) or anti-HA (Santa Cruz) polyclonal antibodies (lanes 4–6). The immune complexes were separated by SDS-7.5% PAGE followed by immunoblot analysis with anti-BRCA1 mAb 6B4 to detect BRCA1 (a), anti-CtIP mAb to detect CtIP (b), and anti-GFP mAb (Clontech) to detect GFP-tagged ZBRK1 (c). Equivalent amount of CtIP or GFP-tagged ZBRK1 was present in the lysates (lanes 7–9) as determined by immunoblot analysis with anti-CtIP mAb (d) and anti-GFP mAb (e).

(D) Nuclear distribution patterns of ZBRK1 and BRCA1. Three representative U2OS cells stably transfected with GFP-ZBRK1 shown in I, II, and III, respectively, were stained with DAPI (row a) and anti-BRCA1 mAb Ab-1 (Oncogene Research Products) followed by Texas red–conjugated secondary antibody (row c), as described elsewhere (Zhong et al., 1999). Row b shows the images of GFP signals, and row d shows the merged images of GFP signals and BRCA1 staining.

ies were subsequently used to immunoprecipitate ZBRK1 from ^{35}S-methionine-labeled cell lysates of human bladder carcinoma T24 cells. As shown in Figure 3A, anti-ZBRK1 antibodies immunoprecipitated a 60 kDa protein that was absent from a parallel immunoprecipitate of the same cells using preimmune serum. This 60 kDa protein exhibits an electrophoretic mobility upon SDS–PAGE similar to that of the product translated in vitro from the *ZBRK1* cDNA and thus appears to represent the cellular ZBRK1 protein.

To test whether BRCA1 and ZBRK1 bind to each other in vivo under physiological conditions, we performed

coimmunoprecipitation analysis of the endogenous proteins in T24 cells. As shown in Figure 3B, both ZBRK1 and BRCA1 were specifically and reciprocally coprecipitated with each other, while rabbit IgG did not precipitate either protein from an equivalent amount of cell lysate. This result demonstrates directly that ZBRK1 is associated with BRCA1 in vivo.

To determine the specificity of this interaction in vivo, we performed coimmunoprecipitation analyses from human osteosarcoma U2OS cells cotransfected with GFP-tagged ZBRK1 and either HA-tagged wild-type BRCA1 or, alternatively, either of two familial breast cancer–derived BRCA1 mutants. One of these, Q356R, carries a mutation within the ZBRK1-binding region of BRCA1, while the second, A1708E, carries a mutation that disrupts CtIP binding activity (Li et al., 1999). ZBRK1 and CtIP were both coimmunoprecipitated along with wild-type BRCA1 using HA epitope–specific antibodies (Figure 3C). Mutant BRCA1-A1708E bound to ZBRK1, but not to CtIP, while mutant BRCA1-Q356R bound to CtIP, but not to ZBRK1. These results thus reveal that BRCA1 and ZBRK1 interact specifically in cells and, furthermore, that this interaction is compromised by a clinically relevant BRCA1 missense mutation identified in familial breast cancer.

Because BRCA1 and ZBRK1 interact in vivo, it was of interest to examine the subcellular distribution of these two proteins. To this end, immunofluorescence analysis was performed on U2OS cells stably expressing GFP-ZBRK1. Within an asynchronously growing culture, approximately 37%–45% of cells exhibited distinct BRCA1 immunoreactive foci against a background of homogeneous BRCA1 nuclear staining (Figure 3D, row c, I and II), consistent with previous observations (Scully et al., 1997b). GFP-ZBRK1 exhibited exclusively a homogeneous distribution throughout the nucleus and did not form foci (row b). In those cells that did not exhibit BRCA1 foci, ZBRK1 and BRCA1 exhibited a similar nuclear distribution pattern. Neither BRCA1 nor GFP-ZBRK1 was localized to nucleoli. Therefore, protein complexes containing both BRCA1 and ZBRK1 are likely to be distributed throughout nuclei, but not specifically localized within either nucleoli or nuclear foci that are more likely relevant to the function of BRCA1 in DNA repair (Scully et al., 1997b; Zhong et al., 1999).

Identification of a Consensus ZBRK1 DNA-Binding Sequence

The zinc finger domain of ZBRK1 conforms to a classic C2H2 zinc finger domain with sequence-specific DNA-binding potential. To identify a binding sequence for ZBRK1, we employed a method for selection and amplification of DNA-binding sites (Blackwell and Weintraub, 1990). Purified GST-ZBRK1Zn was incubated with a random pool of double-stranded 55-mer oligonucleotides, each of which carried 16 base fixed-end sequences flanking 23 central bases of random sequences. Specific GST-ZBRK1Zn-DNA complexes were resolved by EMSA, and bound oligonucleotides were recovered and subjected to PCR amplification using primers corresponding to the 16 fixed bases at both ends of the 55-mer. As shown in Figure 4A, the affinity of GST-ZBRK1Zn for 55-mer pools selected by EMSA following the second, fourth, and sixth rounds of amplification increased with repeated selection. The PCR products from the final round were subcloned and sequenced. A consensus sequence of GGGxxxCAGxxxTTT was derived from sequence alignment of individual subclones (Figure 4B).

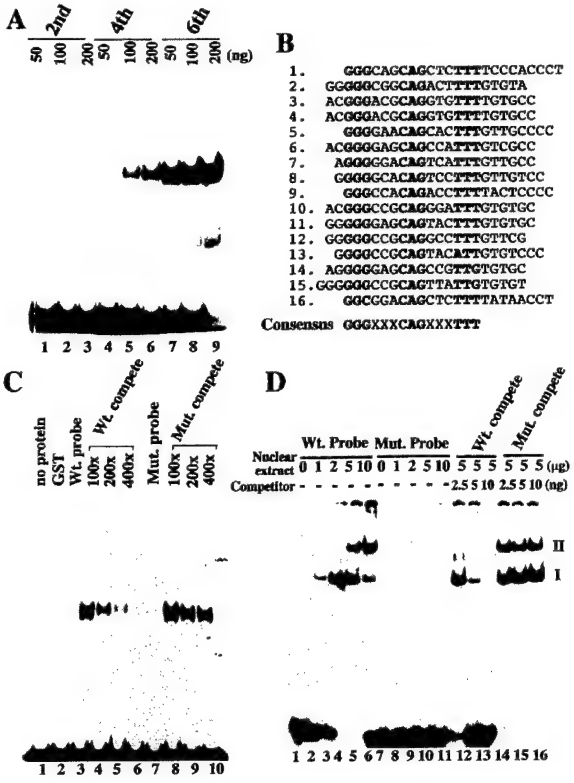

Figure 4. ZBRK1 Binds to a Specific DNA Sequence

(A) Selection and amplification of a ZBRK1-binding site. Equivalent amounts of PCR-amplified DNA derived from each of the second, fourth, and sixth rounds of the SAAB assay were subjected to EMSA using 50, 100, or 200 ng of recombinant GST-ZBRK1Zn protein.

(B) Alignment of individual DNA sequences selected by SAAB assay. The deduced consensus ZBRK1 DNA-binding sequence is indicated below the individually aligned sequences.

(C) Competition EMSA assays. EMSA was performed with Wt. probe, corresponding to the consensus ZBRK1 binding sequence, and either no added protein (lane 1), GST alone (lane 2), or GST-ZBRK1Zn (lanes 3–6 and lanes 8-10). Mut probe, corresponding to a double-stranded oligonucleotide identical in length but differing in sequence from the Wt. probe, was incubated with GST-ZBRK1Zn (lane 7). A 100-, 200-, or 400-fold molar excess of unlabeled Wt. probe (lanes 4–6) or Mut. Probe (lanes 8–10) was added to binding reactions as indicated.

(D) Nuclear complex formation on Wt. probe. EMSA was performed with the indicated amounts of T24 cell nuclear extract and radioactively labeled Wt. probe (lanes 1–5 and 11–16) or Mut Probe (lanes 6–10). A molar excess of unlabeled Wt. probe (lanes 11–13) or Mut probe (lanes 14–16) was added to binding reactions as indicated. DNA–protein complexes I and II are indicated.

To test the binding specificity of ZBRK1 to this consensus sequence, GST-ZBRK1Zn was analyzed by EMSA for its ability to bind to an oligonucleotide containing the consensus sequence GGGxxxCAGxxxTTT (wild-type probe; Wt) or, alternatively, an oligonucleotide identical in length but different in sequence (Mutant probe; Mut) (Figure 4C). Consistently, GST-ZBRK1Zn

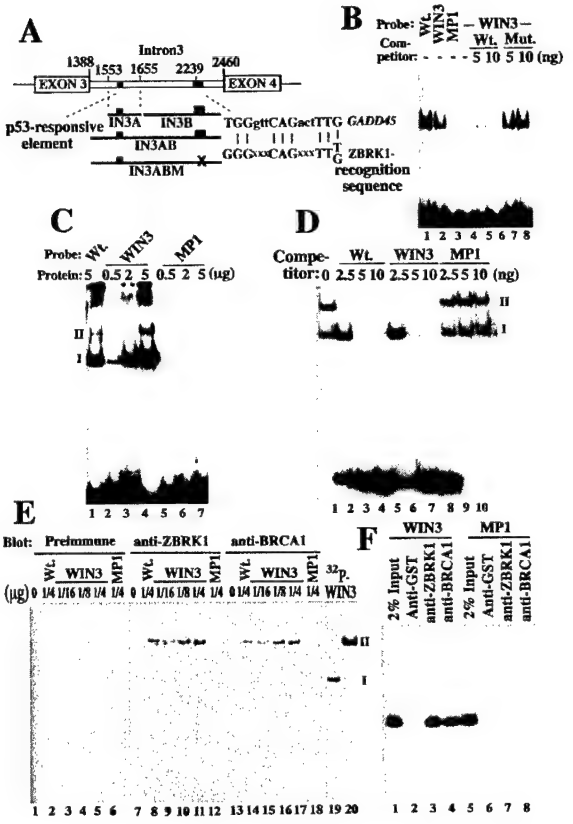

Figure 5. The ZBRK1 Recognition Sequence in *GADD45* Intron 3 Binds to a Nuclear Complex Containing Both ZBRK1 and BRCA1

(A) Schematic diagram of the *GADD45* intron 3 gene region. The p53 responsive element is indicated by a small black box, and the putative ZBRK1 recognition sequence is indicated by a large black box. The consensus ZBRK1 recognition sequence is aligned with *GADD45* intron 3 sequences.

(B) GST-ZBRK1Zn binds to the *GADD45* intron 3–derived ZBRK1 recognition sequence. EMSA performed with 50 ng GST-ZBRK1Zn (lanes 1–3) or GST (lane 4) and radioactively labeled Wt (lane 1), WIN3 (lanes 2 and 4–8), or MP1 (lane 3) probes. Binding reactions included either no specific competitor DNA (lanes 1–4) or the indicated amounts of unlabeled Wt (lanes 5 and 6), or Mut (lanes 7 and 8) probes.

(C) Nuclear complex formation on the *GADD45* intron 3–derived ZBRK1 recognition sequence. EMSA was performed with the indicated amounts (μg) of T24 nuclear extract and radioactively labeled Wt (lane 1), WIN3 (lanes 2–4), or MP1 (lanes 5–7) probes.

(D) Competitive EMSA assays. EMSA was performed with 5 μg T24 nuclear extract and radioactively labeled WIN3 probe. Binding reactions included either no specific competitor DNA (lane 1) or the indicated amounts of unlabeled Wt (lanes 2–4), WIN3 (lanes 5–7), or MP1 (lanes 8–10) probes.

(E) WIN3 probe binds a nuclear complex containing ZBRK1 and BRCA1. Fifty micrograms of nuclear extract in each of lanes 1–18 was incubated with no probe (lanes 1, 7, and 13), the Wt. probe (lanes 2, 8, and 14), indicated amounts of the WIN3 probe (lanes 3–5, 9–11, and 15–17), or the MP1 probe (lanes 6, 12, and 18). Binding reactions were resolved by electrophoresis on a native polyacrylamide gel, and DNA–protein complexes were subsequently analyzed by Western transfer and immunoblotting with anti-ZBRK1 antibodies (lanes 7–12). The blot was stripped of antibodies and sequentially immunoblotted with mouse preimmune serum (lanes 1–6) and anti-BRCA1 mAb 6B4 (lanes 13–18). Control binding reactions using 2 or 50 μg of nuclear extract and radioactively labeled WIN3 probe were run on the same gel to mark the electrophoretic positions of DNA–protein complexes I and II (lanes 19 and 20).

(F) Coimmunoprecipitation of the WIN3 probe with ZBRK1 and BRCA1. Equivalent amounts of nuclear extract were incubated with radioactively labeled WIN3 (lanes 1–4) or MP1 (lanes 5–8) probes, followed by immunoprecipitation with anti-GST mAb 8G11 (lanes 2 and 6), anti-ZBRK1 antibodies (lanes 3 and 7), or anti-BRCA1 mAb 6B4 (lanes 4 and 8). Lanes 1 and 5 indicate 2% of the total amount of each probe used in binding reactions.

bound to the Wt probe (lane 3), but not to the Mut probe (lane 7). The specificity of GST-ZBRK1Zn binding to its consensus sequence was further revealed by testing the ability of a molar excess of unlabeled Wt or Mut probe, respectively, to compete for the binding of GST-ZBRK1Zn to the Wt probe. The results of these competition EMSA assays indicated that the Wt probe, but not the Mut probe, could effectively compete for GST-ZBRK1Zn binding to its Wt consensus sequence (Figure 4C), thereby suggesting that the ZBRK1 zinc fingers comprise a sequence-specific DNA-binding domain.

A Nuclear Protein Complex Binds to the ZBRK1 Recognition Sequence

Should the consensus ZBRK1 binding sequence that we derived represent a biologically relevant motif, it should support the assembly of a DNA–protein complex with one or more cellular proteins. To test this notion, ^{32}P-labeled Wt or Mut probes were used in an EMSA with nuclear extract derived from cultured cells. A DNA–protein complex (complex I) was formed on the Wt probe (Figure 4D, lanes 1–5) but not on the Mut probe (lanes 6–10). Increased nucleoprotein complex formation was observed when the amount of input nuclear extract was increased. Interestingly, a more slowly migrating complex (complex II) appeared as more nuclear extract was used. Consistently, a molar excess of the unlabeled Wt probe could effectively compete for the formation of both complexes I and II (Figure 4D, lanes 11–13). Formation of neither complex I nor II could be efficiently competed by the mutant probe (Figure 4D, lanes 14–16). Immunoblot analysis following EMSA using procedures described for Figure 5E (below) confirmed the presence of ZBRK1 in complex II. These results thus reveal the presence in nuclear extract of one or more activities containing endogenous ZBRK1 capable of binding to the ZBRK1 consensus sequence.

GADD45 Intron 3 Harbors a ZBRK1 Recognition Sequence

Recently, the *GADD45* gene was identified as a major transcriptional target of BRCA1 (Harkin et al., 1999). Because ZBRK1 interacts with BRCA1 in vivo, we reasoned that ZBRK1 might also participate in the regulation of *GADD45* gene transcription. On this basis, we searched the *GADD45* gene and identified within intron 3 a sequence, TGGxxxCAGxxxTTG, which conforms closely to the ZBRK1 consensus sequence (Figure 5A). Interestingly, intron 3 also harbors a functionally important p53 response element residing upstream of this potential ZBRK1-binding site, and the two elements are separated by a nonconserved AT-rich region within intron 3 (Hollander et al., 1993). Significantly, the potential ZBRK1-binding site lies within a region that exhibits

considerable sequence conservation between species (Hollander et al., 1993).

To determine whether ZBRK1 can bind to this potential ZBRK1-binding sequence, GST-ZBRK1Zn was tested by EMSA for its ability to bind to the WIN3 probe, which is identical in sequence to the potential ZBRK1-binding site. As shown in Figure 5B, the WIN3 probe supported the formation of a DNA–protein complex (lane 2) indistinguishable in its electrophoretic mobility from the complex formed on the Wt probe, which contained the consensus ZBRK1 binding sequence (lane 1). Interestingly, GST-ZBRK1Zn did not bind to the MP1 probe that corresponds to a sequence (GATxxxCAGxxxTTT) present in the proximal promoter region of *GADD45* that differs by two nucleotides from the consensus ZBRK1 recognition sequence (lane 3). The binding of GST-ZBRK1Zn to the WIN3 probe could be effectively competed by the addition of a molar excess of unlabeled Wt probe, but not by an equivalent molar excess of the Mut probe (lanes 5–8). These results thus identify the putative ZBRK1 recognition sequence within *GADD45* intron 3 to be an authentic ZBRK1-binding site.

A Nuclear Protein Complex Including ZBRK1 and BRCA1 Binds to the ZBRK1 Recognition Sequence in *GADD45* Intron 3

Next, we determined by EMSA whether the WIN3 probe could serve as a platform for the assembly of proteins present in a crude nuclear extract. As shown in Figure 5C, the WIN3 probe supported the formation of DNA–protein complexes (lanes 2–4) indistinguishable in their electrophoretic mobilities from the complexes formed on the Wt probe (lane 1). By contrast, the MP1 probe did not support the formation of a stable DNA–protein complex (lanes 5–7). Nucleoprotein complex formation on the WIN3 probe was specifically competed by the addition of a molar excess of unlabeled Wt or WIN3 probe, but not by an equivalent molar excess of the MP1 probe (Figure 5D).

To test whether the nuclear complex formed on the WIN3 probe contains both ZBRK1 and BRCA1, we performed EMSA followed by immunoblot analysis (Mueller et al., 1990) using antibodies specific for both ZBRK1 and BRCA1. Parallel binding reactions were assembled using 50 μg of nuclear extract with no probe (Figure 5E; lanes 1, 7, and 13), the Wt. probe (lanes 2, 8, 14), the WIN3 probe (lanes 3–5, 9–11, and 15–17), or the MP1 probe (lanes 6, 12, and 18). Resultant DNA–protein complexes were resolved by native gel electrophoresis and subsequently subjected to Western transfer and immunoblot analysis using mouse preimmune sera (lanes 1–6), anti-ZBRK1 antibodies (lanes 7–12), or anti-BRCA1 mAb 6B4 (lanes 13–18). Control EMSA reactions using two different amounts of nuclear extract and radioactively labeled WIN3 probe were loaded onto the same gel to mark the electrophoretic positions of DNA–protein complexes I and II (lanes 19 and 20). Both ZBRK1 and BRCA1 were detected in complex II in a dose-dependent manner (lanes 9–11 and 15–17). Neither ZBRK1 nor BRCA1 could be detected when EMSA reactions were performed using either no probe or the MP1 probe. Additionally, no immunoblot signal was detected using preimmune sera (lanes 1–6). Because immunodetection required the use of preparative amounts of nuclear extract for individual binding reactions, most of the DNA–protein complex formed on the WIN3 probe represented complex II (compare lane 20 with lane 19). Consequently, we cannot exclude the possibility that complex I also contains BRCA1 and ZBRK1.

To demonstrate further that ZBRK1 and BRCA1 reside within the same complex, DNA coimmunoprecipitation assays (Yew et al., 1994) were performed. Radioactively labeled WIN3 or MP1 probes were incubated with nuclear extract, followed by immunoprecipitation of protein–DNA complexes with antibodies specific for either ZBRK1, BRCA1, or, as a negative control, GST. Immunoprecipitated protein–DNA complexes were deproteinized, and the radioactively labeled probe was subsequently resolved by native gel electrophoresis and detected by autoradiography. As shown in Figure 5F, the WIN3 probe, but not the MP1 probe, was specifically coimmunoprecipitated by both anti-ZBRK1 and anti-BRCA1 antibodies. By contrast, neither the WIN3 probe nor the MP1 probe was immunoprecipitated by anti-GST mAb. Collectively, these results thus reveal the *GADD45* intron 3 ZBRK1 recognition sequence to be a platform for the specific assembly of a nuclear complex containing both ZBRK1 and BRCA1.

ZBRK1 Is a Sequence-Specific Transcriptional Repressor

The presence within ZBRK1 of both zinc finger and KRAB domains indicated that it might function as a sequence-specific transcriptional repressor. To test this possibility, a plasmid containing four copies of the ZBRK1 consensus binding site upstream of the HSV TK promoter driving expression of a CAT reporter gene (pBLcat-E) was engineered and transfected into human osteosarcoma Saos2 cells. The resultant CAT activity was compared with that of an otherwise identical reporter template lacking the four ZBRK1-binding sites (pBLcat). As shown in Figure 6A, the ZBRK1 recognition sequences conferred a 4-fold repression on pBLcat reporter activity. Subsequently, an expression plasmid carrying the *ZBRK1* cDNA driven by the CMV promoter (pCHPL-ZBRK1) was individually cotransfected along with each of the aforementioned CAT reporter templates. Expression of exogenous ZBRK1 caused an additional 2-fold repression of CAT activity from the reporter carrying ZBRK1-binding sites but had no effect on the control CAT reporter. These results thus reveal that the repression activity of ZBRK1 is mediated through its cognate recognition sequence.

ZBRK1 Confers Repression through Intron 3 of the *GADD45* Gene

Intron 3 of the *GADD45* gene, from +1388 to +2460 (where +1 represents the transcription start site), represents a critical regulatory locus that coordinately controls transcription in conjunction with *cis*-acting elements in the proximal promoter region (Hollander et al., 1993). The p53 response element in the *GADD45* gene lies within an intron 3 fragment extending from +1553 to +1655 (herein designated as IN3A; Figure 5A). The ZBRK1-binding site (WIN3) resides in a fragment extending from +1656 to +2460 (herein designated as

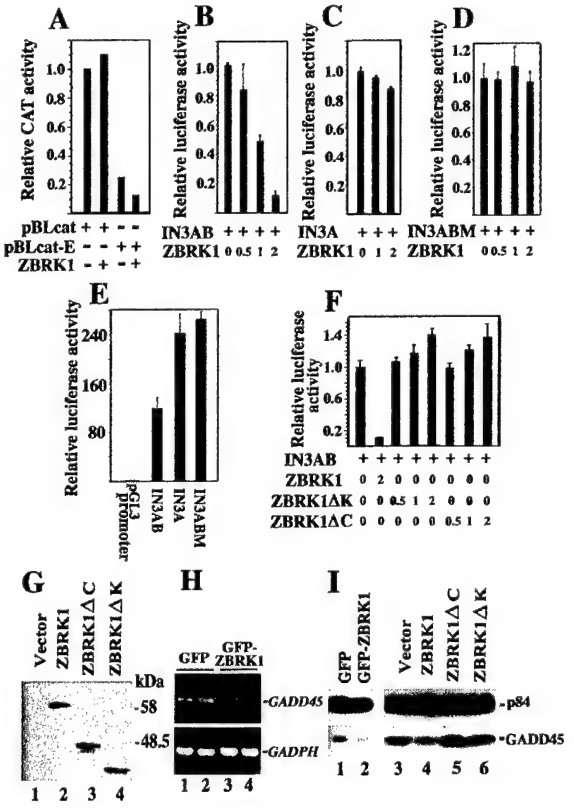

Figure 6. ZBRK1 Is a Transcriptional Repressor through *GADD45* Intron 3

(A) pBLcat or pBLcat-E (containing four copies of the ZBRK1 recognition sequence) was transfected into Saos2 cells either with (+) or without (−) pCHPL-ZBRK1. Resultant CAT activities are expressed relative to the level of CAT activity observed with pBLcat vector–transfected cells.

(B–E) U2OS cells were transfected as indicated with 0.5 μg of pGL3p-IN3AB (B and E), pGL3p-IN3A (C and E), pGL3p-IN3ABM (D and E), or pGL3p (E) along with the indicated amounts (micrograms of DNA) of pCEPF-ZBRK1.

(F) U2OS cells were transfected with pGL3p-IN3AB (0.5 μg) along with the indicated amounts (micrograms of DNA) of either pCNF-ZBRK1, pCNF-ZBRK1ΔK, or pCNF-ZBRKΔC. In (A)–(F), relative CAT or luciferase activities are calculated as the fold increases in CAT or luciferase activities relative to those observed in cells transfected by reporter and CMV vector alone (first lane in each panel). CAT or luciferase activities were normalized to β-galactosidase activity obtained by cotransfection of 1 μg of SV40-β-gal vector as described previously (Li et al., 1999).

(G) Expression of Flag-tagged wild-type ZBRK1 and ZBRK1 mutant derivatives in U2OS cells transiently transfected with pCNF, pCNF-ZBRK1, pCNF-ZBRK1ΔC, and pCNF-ZBRK1ΔK. Flag-tagged proteins were detected by immunoblot analysis using anti-Flag mAb M2 (Sigma).

(H) Semiquantitative RT–PCR analysis of endogenous *GADD45* (upper panel) or *GADPH* (lower panel) mRNAs in U2OS cells stable-expressing GFP (lanes 1 and 2) or GFP-ZBRK1 (lanes 3 and 4). RT–PCR reactions were run in duplicate.

(I) Expression of endogenous GADD45 protein in U2OS cells stable-expressing GFP (lane 1) or GFP-ZBRK1 (lane 2), or transiently transfected with either pCNF, pCNF-ZBRK1, pCNF-ZBRK1ΔC, or pCNF-ZBRK1ΔK (lanes 3–6, respectively). GADD45 (lower panel) or nuclear matrix protein p84 (upper panel, included as an internal loading control [Li et al., 1999]) were detected by immunoblot analysis using rabbit anti-GADD45 antibody H-165 (Santa Crutz), and anti-p84 mAb 5E10, respectively.

IN3B; Figure 5A). Intron 3 in its entirety is designated as IN3AB (Figure 5A).

To address whether the WIN3 sequence represents a functional ZBRK1 response element in its natural context, we constructed pGL3p-IN3AB by inserting IN3AB upstream of the *SV40* promoter driving expression of a luciferase reporter. This reporter template was cotransfected into U2OS cells along with increasing amounts of the ZBRK1-expressing plasmid, pCEPF-ZBRK1. ZBRK1 repressed reporter activity in a dose-dependent manner (Figure 6B). Consistent with a functional requirement for its cognate recognition sequence, ZBRK1 had no effect on the activity of a reporter template containing only the IN3A region (Figure 6C) or on the activity of the IN3ABM reporter template in which the WIN3 sequence was mutated (Figure 6D). Consistently, the reporter activity of IN3AB is lower than that of either IN3A or IN3ABM (Figure 6E). Thus, the *cis*-acting DNA sequence within *GADD45* intron 3 responsible for conferral of ZBRK1-directed transcriptional repression is the ZBRK1-binding site located in the IN3B region.

ZBRK1 Repression Activity Is Mediated Both by Its KRAB Domain and BRCA1-Binding Domain

To understand the mechanism(s) by which ZBRK1 represses transcription, we first sought to determine whether the KRAB domain of ZBRK1 is required. To this end, we engineered ZBRK1ΔK, a deletion derivative of ZBRK1 that carries an N-terminal truncation of the KRAB domain. ZBRK1ΔK was cotransfected along with the IN3AB reporter template into U2OS cells. ZBRK1ΔK failed to repress transcription from the IN3AB reporter template (Figure 6F), indicating that the KRAB domain on ZBRK1 is important for its repression activity. By implication, the KRAB domain–interacting corepressor KAP-1/KRIP-1/TIFβ (Friedman et al., 1996; Kim et al., 1996; Le Douarin et al., 1996; Moosmann et al., 1996) is likely to contribute to ZBRK1-directed repression, although future studies will be required to confirm this prediction.

To assess the requirement of its C-terminal BRCA1-interacting domain for ZBRK1 repression activity, we engineered ZBRK1ΔC, a ZBRK1 deletion derivative lacking its C-terminal 94 amino acid residues. ZBRK1ΔC retains the ZBRK1 KRAB domain and its entire DNA-binding zinc finger domain, but it lacks the C-terminal region of its BRCA1-binding domain. This deletion derivative can therefore bind to its cognate ZBRK1 recognition sequence (Figures 4A and 4C), but it cannot bind to BRCA1 (Figure 2G). Interestingly, ZBRK1ΔC also failed to repress transcription from the IN3AB reporter (Figure 6F).

To test whether the endogenous *GADD45* gene is a target of ZBRK1 regulation, we examined expression of the endogenous *GADD45* gene in U2OS cells stably expressing GFP-ZBRK1 and compared this expression to that in cells stably expressing GFP alone. Results from semiquantitative RT–PCR analysis (De Toledo et al., 1995) indicated that the *GADD45* mRNA level was decreased by approximately 5- to 6-fold in cells expressing GFP-ZBRK1, while the mRNA level of GAPDH was unchanged (Figure 6H). A concordant decrease in the GADD45 protein level was also observed in these

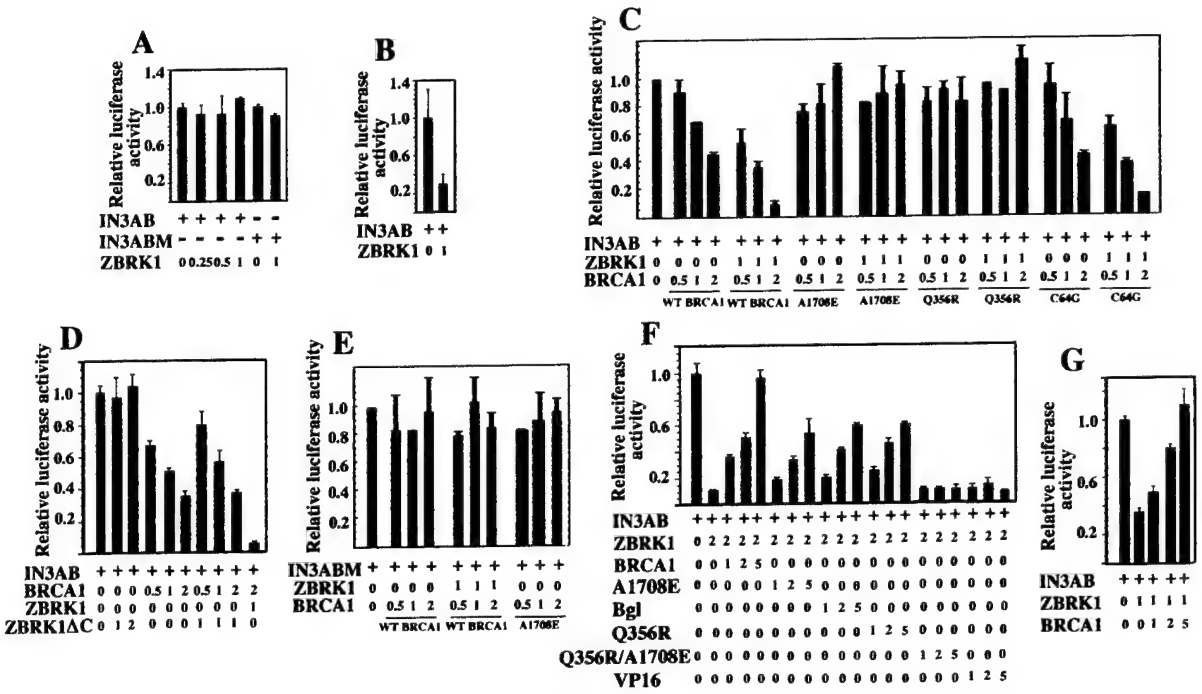

Figure 7. BRCA1 Functions as a ZBRK1 Corepressor through *GADD45* Intron 3

(A) Brca1-deficient (*Brca1*$^{-/-}$; *p53*$^{-/-}$) MEFs were transfected with 2.5 μg of pGL3p-IN3AB or pGL3p-IN3ABM along with the indicated amounts (micrograms of DNA) of pCNF-ZBRK1.

(B) Brca1-proficient (*p53*$^{-/-}$) MEFs were transfected with 2.5 μg of pGL3p-IN3AB along with the indicated amounts (micrograms of DNA) of pCNF-ZBRK1.

(C–E) Brca1-deficient (*Brca1*$^{-/-}$; *p53*$^{-/-}$) MEFs were transfected as indicated with 2.5 μg of pGL3p-IN3AB (C and D) or pGL3p-IN3ABM (E) along with the indicated amounts (micrograms of DNA) of pCNF-ZBRK, pCNF-ZBRK1ΔC, pcDNA3.1-BRCA1, pcDNA3.1-BRCA1A1708E, pcDNA3.1-BRCA1Q356R, or pcDNA3.1-BRCA1C64G.

(F) U2OS cells were transfected with pGL3p-IN3AB (0.5 μg) along with the indicated amounts (micrograms of DNA) of pCNF-ZBRK, pcDNA3.1-BRCA1, pcDNA3.1-BRCA1A1708E, pcDNA3.1-HA-Bgl expressing the ZBRK1-binding region in BRCA1, or pVP16 expressing the VP16 transactivation domain (Li et al., 1999).

(G) *p53*$^{-/-}$ MEFs were transfected with 2.5 μg of pGL3p-IN3AB along with the indicated amounts (micrograms of DNA) of pcDNA3.1-BRCA1 and pCNF-ZBRK1. In (A)–(G), relative luciferase activities are calculated as described in the previous figure.

cells (Figure 6I, lanes 1 and 2). Consistent with these results, the endogenous GADD45 protein level was also decreased by approximately 1- to 2-fold in cells transiently transfected with a wild-type ZBRK1 expression vector when compared to cells transfected with vector alone (Figure 6I, lanes 3–6). By contrast, transient expression of either ZBRK1ΔC or ZBRK1ΔK not only failed to repress but, in fact, moderately activated endogenous *GADD45* expression (Figure 6I). We consider it likely that ZBRK1ΔC and ZBRK1ΔK, both of which retain DNA binding activity, can compete with endogenous ZBRK1 for occupancy of ZBRK1-binding sites and thereby confer dominant-negative effects. Taken together, these results indicate that its KRAB domain and BRCA1-binding domain are both required for ZBRK1-directed repression of *GADD45* transcription.

BRCA1 Mediates the Repression Activity of ZBRK1

The requirement for its BRCA1-binding domain for repression activity is consistent with a functional requirement for BRCA1 in ZBRK1-directed repression. To test this possibility, we examined the ability of ZBRK1 to function as a repressor in Brca1-deficient mouse embryo fibroblasts (MEFs) (*Brca1*$^{-/-}$; *p53*$^{-/-}$). As shown in Figure 7A, ZBRK1 exhibited no repression activity on the IN3AB reporter template in Brca1-deficient MEFs. By contrast, ZBRK1 repression activity was readily observed in Brca1-proficient MEFs (*p53*$^{-/-}$) (Figure 7B). Similar results were obtained in human BRCA1-mutated HCC1937 cells (data not shown).

Significantly, ectopic expression of wild-type BRCA1 in Brca1-deficient MEFs conferred repression on transcription from the IN3AB reporter template (Figure 7C), presumably through endogenous murine ZBRK1 (data not shown). Interestingly, cotransfection of human ZBRK1 along with wild-type BRCA1 provided a synergistic repressive effect on transcription (Figure 7C). Similar to wild-type BRCA1, ectopic expression of a BRCA1 derivative harboring a mutation in the N-terminal ring finger domain (C64G) conferred repression on transcription from the IN3AB reporter template (Figure 7C). By contrast, BRCA1 derivatives harboring mutations in either the C-terminal BRCT domain (A1708E and Y1853term) or the ZBRK1-binding region (Q356R) exhibited no repression activity (Figure 7C and data not shown). These results thus identify the regions important for BRCA1-mediated ZBRK1 repression to include the ZBRK1-binding region and the C-terminal BRCT domain.

Table 1. Potential ZBRK1 Binding Motifs Identified in BRCA1-Targeted Genes

BRCA1-Targeted Genes[a]	Potential ZBRK1 Binding Sequences	Start, End Positions[b]	Genbank Accession No.
	GGGxxxCAGxxxTTT	Consensus	
GADD45	TGGgttCAGactTTG	+2239, +2253	L24498
GADD153	CGGaaaCAGcagCTT	−520, −506	S40707
Ki-67	TGGtctCAGtccCTT	−757, −733	X94762
	GGGacgCAGtccTGT	−781, −757	
Bax	GGGcctCTGagcTTT	+6, +20	AH00538
p21	GGTcacCAGactTCT	−893, −879[c]	U24170
	TGGttgCAGcagCTT	−767, −781[c]	
	AGGacaCAGcacTGT	−288, −302[c]	
EGR1	AGGgaaCAGcctTTC	−930, −916	AJ243425
Amphiregulin	GGTtgtCAGagtTTG	−280, −266	AH002608
Prothymosin	CGGcgcCAGaagCTT	−13, −27	S56449
TIMP-1	TGGcacCAGggtTGT	−842, −856	Y09720
TIMP-2	GGGacgCAGtttTAT	−67, −81	S68860
Topo IIa	GCGagtCAGggaTTG	−79, −65	X66794

[a] Genes that are activated or repressed by overexpression of BRCA1 as described previously (Harkin et al., 1999; MacLachlan et al., 2000).
[b] Positions are relative to transcriptional start sites except those indicated.
[c] Positions are relative to the TATA box.

In contrast to full-length ZBRK1, ZBRK1ΔC failed to synergistically repress transcription when cotransfected with BRCA1 (Figure 7D). Furthermore, in the presence of ectopically expressed wild-type BRCA1, ZBRK1 did not repress transcription from the IN3ABM reporter template, confirming that BRCA1-mediated repression is specific for ZBRK1 (Figure 7E). Collectively, these experiments thus reveal a role for BRCA1 as a transcriptional corepressor of ZBRK1.

BRCA1 Overexpression Relieves ZBRK1-Directed *GADD45* Intron 3–Mediated Repression

Recently, *GADD45* was identified as a gene induced in a p53-independent manner following BRCA1 overexpression (Harkin et al., 1999). Our identification of BRCA1 as a ZBRK1 corepressor led us to question whether this induction could derive from relief of BRCA1-mediated *GADD45* repression. To explore this possibility, we examined whether overexpression of BRCA1 in BRCA1-proficient cells could overcome ZBRK1-directed *GADD45* repression. As shown in Figure 7F, ectopic expression of BRCA1 could efficiently override ZBRK1-mediated repression of transcription from the IN3AB reporter template in a dose-dependent manner. To examine the p53 dependency of this BRCA1-mediated effect, we performed the same experiment in p53-deficient MEFs and obtained similar results (Figure 7G). This observation suggests that induction of IN3AB reporter gene transcription by BRCA1 overexpression is independent of BRCA1-mediated coactivation of p53.

To explore the mechanism for this derepression activity, we tested several BRCA1 mutants for their respective derepression capabilities. BRCA1-BgI, a deletion derivative retaining only the ZBRK1-binding region, as well as missense mutants BRCA1-A1708E and BRCA1-Q356R, could override ZBRK1-directed repression, albeit less effectively than wild-type BRCA1 (Figure 7F). By contrast, no derepression activity was conferred by the double mutant BRCA1-Q356R/A1708E.

Relief of *GADD45* repression by BRCA1 overexpression could derive from either or both of two alternative processes. First, derepression could derive from competitive displacement by ectopically expressed BRCA1 of an endogenous BRCA1-containing repressor complex from DNA-bound ZBRK1. Alternatively, ectopically expressed BRCA1 could titrate other critical corepressors from DNA-bound ZBRK1. If relief of repression derives from competitive displacement, then BRCA1 mutant A1708E, which can bind to ZBRK1 but not to the CtIP/CtBP corepressor complex or HDACs (Li et al., 1999; Yarden and Brody, 1999), would be expected to exhibit derepression activity. On the other hand, if relief of repression derives from repressor titration, then BRCA1 mutant Q356R, which can bind to CtIP/CtBP and HDACs but not to ZBRK1 (Figure 3C), would also be expected to exhibit derepression activity. The observation that both of these BRCA1 single mutants retain derepression activity suggests that both competitive displacement and repressor titration contribute to the derepression activity of wild-type BRCA1. Consistent with this interpretation is the lack of depression activity exhibited by the double mutant BRCA1-Q356R/A1708E, which can bind neither ZBRK1 nor the corepressors CtIP/CtBP or HDACs (Figure 7F).

To eliminate the possibility that BRCA1-mediated *GADD45* derepression occurs simply as a consequence of elevated levels of an activation domain, we overexpressed the potent Herpes simplex virus VP16 activation domain and observed no effect on ZBRK1 repression from the IN3AB reporter (Figure 7F). Collectively, these results suggest that BRCA1 overexpression can lead to induction of *GADD45* transcription through the relief of ZBRK1-directed repression and, furthermore, provide a plausible molecular explanation for the apparent transcriptional activation of *GADD45* gene transcription by BRCA1 overexpression in the absence of p53 (Harkin et al., 1999).

While derepression by BRCA1 overexpression may accurately reflect some aspect of its function in vivo, more physiologically relevant mechanisms for derepression are likely to involve alterations in the phosphorylation and/or protein interaction status of BRCA1. In this

regard, DNA damage–induced dissociation of a CtIP-CtBP corepressor complex from BRCA1 could relieve ZBRK1 repression of *GADD45* transcription, thereby leading to *GADD45* induction (Li et al., 2000).

Discussion

An overriding question concerning the role of BRCA1 in transcription control is how it confers gene-specific regulation in the absence of sequence-specific DNA binding activity. The identification herein of a novel DNA-binding transcription repressor and BRCA1 interaction partner, ZBRK1, suggests a means by which BRCA1 may be physically tethered and functionally linked to specific regulatory loci. Importantly, we demonstrate that genetic ablation of *Brca1* precludes, while its ectopic expression restores, transcriptional repression by ZBRK1. Our results thus reveal a new role for BRCA1 as a corepressor, a prospect consistent with previous reports demonstrating that BRCA1 can not only repress transactivation mediated by the estrogen receptor or c-Myc (Wang et al., 1998; Fan et al., 1999), but also interact with the CtIP/CtBP corepressor and HDAC complexes that mediate transcription repression (Li et al., 1999; Yarden and Brody, 1999). Collectively, these observations suggest that BRCA1 could function more broadly as a corepressor of sequence-specific DNA-binding transcriptional repressors other than ZBRK1.

The interaction between ZBRK1 and BRCA1 is functionally relevant, since mutagenic disruption of cognate interaction surfaces on either protein abrogates ZBRK1 repression activity. Furthermore, familial breast cancer–derived BRCA1 missense mutations that disrupt its interaction with ZBRK1 or BRCT-binding proteins abrogate its corepressor activity, thereby suggesting that its corepressor function may be important for the biological activity of BRCA1 in tumor suppression and/or cell growth and differentiation.

BRCA1 has been proposed to regulate the expression of genes linked to several different aspects of cellular physiology, including cell cycle checkpoint control, proliferation, and differentiation (Harkin et al., 1999; MacLachlan et al., 2000). ZBRK1, through eight Krupple-type zinc fingers, binds to a compositionally flexible recognition sequence, GGGxxxCAGxxxTTT. Interestingly, sequences closely conforming to this recognition sequence lie within the putative regulatory regions of a subset of BRCA1 target genes (Table 1), thus raising the possibility that ZBRK1 and BRCA1 function coordinately to regulate a common class of genes with roles in these cellular processes.

Among these, we have identified *GADD45* to be target of coordinate regulation by both ZBRK1 and BRCA1. Our findings are consistent with a model in which ZBRK1 and its associated corepressors, KAP-1 and BRCA1, largely silence *GADD45* gene transcription in the uninduced state. In response to an appropriate inducing signal(s), *GADD45* would be liberated from this repression, thereby providing the potential for a rapid and robust increase in gene transcription. This model is consistent not only with the observed elevated basal level of endogenous *GADD45* mRNA in BRCA1 mutant HCC1937 cells, but the correspondingly small induction of *GADD45* mRNA in response to MMS in these same cells (Harkin et al., 1999). It must be emphasized that derepression as an operative mechanism in control of *GADD45* gene transcription must be coordinated with additional mechanisms of true activation, since BRCA1 can stimulate transcription, albeit modestly, from reporter templates that do not contain a ZBRK1 response element but that do contain p53 response elements (Harkin et al., 1999). Hence, in the natural setting, *GADD45* induction may reflect the concerted effects of both derepression and true activation. Significantly, BRCA1 appears to play a critical role in both of these transcriptional processes, wherein it functions both as a corepressor and a coactivator (Li et al., 1999; Yarden and Brody, 1999; Pao et al., 2000). Its dual transcriptional activities are likely to contribute to the differential regulation by BRCA1 of a broad spectrum of cellular genes necessary to mediate its tumor suppressor function.

Experimental Procedures

Cell Culture and Generation of *Brca1*$^{-/-}$ *p53*$^{-/-}$ MEFs

Mammalian cells were cultured in the DMEM containing 10% fetal calf serum. For isolation of *Brca1*$^{-/-}$ *p53*$^{-/-}$ and *p53*$^{-/-}$ MEFs, *Brca1*$^{+/-}$ mice (Liu et al., 1996) were crossed with *p53*$^{+/-}$ mice (Jackson Laboratory) to create *Brca1*$^{+/-}$ *p53*$^{+/-}$ mice. The resultant F1 mice were then crossed with each other, and 9.5 day embryos were used to prepare MEFs. The *Brca1*$^{-/-}$ *p53*$^{-/-}$ and *p53*$^{-/-}$ MEFs were obtained from the embryos of the same F2 generation.

RNA Blot and RT–PCR Analysis

Approximately 15 μg of total RNA from indicated cells was subjected to semiquantitive reverse transcription–polymerase chain reaction (RT–PCR) analysis following a procedure previously described for studying *GADD45* expression (De Toledo et al., 1995).

Plasmid Construction

pCEPF-ZBRK1, pCNF-ZBRK1, and pCHPL-ZBRK1, for expressing ZBRK1 in mammalian cells, were constructed, respectively, by subcloning the full-length *ZBRK1* cDNA from pBSK-ZBRK1 into pCEPF (pCEP-Flag; Chen et al., 1996), a pCEP4-based vector (Invitrogen), or into pCNF, a pcDNA3.1-based vector (Invitrogen), or into the pCHPL vector (Li et al., 1998), thereby placing it under control of CMV promoter. pCNF-ZBRK1 expresses ZBRK1 with an N-terminal Flag tag. pCNF-ZBRK1ΔK was constructed by translationally fusing a HincII fragment from the *ZBRK1* cDNA with the N-terminal Flag tag in pCNF. pCNF-ZBRK1ΔC was constructed by introducing a nonsense mutation into the *ZBRK1* cDNA at sequences corresponding to codon 439 in pCNF-ZBRK1. pCHPL-GFP-ZBRK1, which expresses an N-terminal GFP fusion with the full-length ZBRK1, was created by inserting the full-length *ZBRK1* cDNA into pCHPL-GFP, which expresses green fluorescent protein under control of CMV promoter (Li et al., 1998). pcDNA3.1 vector was used to express the wild-type BRCA1 or its mutant derivatives as previously described (Li et al., 1999; Zhong et al., 1999). pcDNA3.1-HA-Bgl, which expresses a HA epitope–tagged Bgl fusion protein was constructed by translationally fusing the ZBRK1-binding region (aa 341–748) in the *BRCA1* cDNA with an N-terminal HA epitope tag.

The pGL3p-IN3AB reporter plasmid was generated by subcloning a 1.1 kb BamHI/PstI fragment from intron 3 of the *GADD45* gene from pHG45 (a gift from A. J. Fornace, Jr.), into the pGL3-promoter vector (Promega). pGL3p-IN3ABM was created by site-directed mutagenesis of the nine-nucleotide ZBRK1 consensus binding sequence in pGL3p-IN3AB. pGL3p-IN3A is equivalent to pI-3 (a gift from D. A. Haber). pBLcat-E was created by subcloning four copies of the consensus ZBRK1 recognition sequence upstream of the chloramphenicol acetyltransferase (CAT) reporter gene in the pBLcat2 vector (Luckow and Schutz, 1987).

Transfection, Immunoprecipitation, and Immunoblot Analysis

For CAT or luciferase reporter assays, Saos2 and U2OS cells (2×10^5) or MEFs (6×10^4) were transfected by conventional calcium phosphate/DNA coprecipitation methods or by lipofectin-based methods, respectively, as described (Li et al., 1999). For generating stable cell lines expressing GFP or GFP-ZBRK1, U2OS cells were selected with 200 μg/ml hygromycin 48 hr after transfection.

Double immunoprecipitation, coimmunoprecipitation, and immunoblot analysis were performed as previously described (Li et al., 1999). For Figure 3B, anti-ZBRK1 antibodies, anti-BRCA1 mAb 6B4, and rabbit IgG were first coupled with protein G– or protein A–Sepharose beads by dimethylpimelimidate as described (Harlow and Lane, 1988).

Generation of Oligonucleotide Library and SAAB

55-mer single-stranded oligonucleotides (5′-GCACTAGCGGATC CGT-N23-CGAAGCTTGGTCACGC-3′) bearing 16-nucleotide fixed-end sequences flanking 23 central random nucleotides were synthesized. A ^{32}P-labeled double-stranded oligonucleotide library was generated by primer extension with the reverse primer (5′-GCG TGACCAAGCTTCG). ^{32}P-α-dCTP was incorporated in the reaction, and the product was purified by electrophoresis on a 15% polyacrylamide gel, followed by elution and precipitation. Selection and amplification of binding sites (SAAB) was performed as previously described (Blackwell and Weintraub, 1990). DNA binding reactions were performed in the buffer containing 25 mM HEPES (pH 7.5), 50 mM KCl, 4 mM $MgCl_2$, 10% glycerol, 25 μM $ZnSO_4$, 250 μg/ml BSA, 1 mM DTT, 250 μg/ml poly dI/dC, and protease inhibitors.

Preparation of Nuclear Extract, EMSA, and DNA Coimmunoprecipitation

Nuclear extracts were prepared from T24 or MCF7 cells as described (Carter et al., 1990). For EMSA, Wt probe was obtained by annealing two complimentary synthesized oligonucleotides, 5′-GATCCACGG GACGCAGGTGTTTTGTGCCG-3′ and 5′-GATCCGGCACAAAACAC CTGCGTCCCGTG-3′. Mut probe was obtained by annealing two complimentary synthesized oligonucleotides, 5′-GATCCACCTCAC GTTCGTGCACTGTGCCG-3′ and 5′-GATCCGGCACAGTGCACGAA CGTGAGGTG-3′. WIN3 probe was obtained by annealing two complimentary synthesized oligonucleotides, 5′-TGGGTTGCATGGGTT CAGACTTTGCAATG-3′ and 5′-TACACATTGCAAAGTCTGAACCCA TGCAA-3′. MP1 probe was obtained by annealing two complimentary synthesized oligonucleotides, 5′-GATCCATGGAGTAGGCA GAAATTTCACCA-3′ and 5′-GATCTGGTGAAATTTCTGCCTACTCC ATG-3′. Each of these double-stranded probes had overhangs at both ends, which were filled in with α-^{32}P-dCTP by Klenow enzyme. In each reaction, 60000 cpm of ^{32}P-labeled probe was mixed with GST-ZBRK1Zn fusion protein or nuclear extract in 40 μl DNA-binding buffer as described in the above SAAB assay. One hundred nanograms of poly dI/dC was added to each reaction. After 30 min of incubation at room temperature, the mixture was loaded onto a 5% polyacrylamide gel in running buffer containing 20 mM HEPES, (pH 7.5), 0.1 mM EDTA.

The DNA immunoprecipitation assay was performed essentially as described (Yew et al., 1994) with slight modifications. Six hundred thousand cpm ^{32}P-labeled WIN3 or MP1 probe was incubated with 60 μg of nuclear extract for 30 min at room temperature in 200 μl DNA-binding buffer with 50 ng/μl of poly dI-dC as described above. Antibody-protein A Sepharose beads were added to the DNA-binding reaction and incubated for 1 hr at room temperature. The reaction was washed twice with DNA-binding buffer, deproteinized, and resolved by electrophoresis in 5% polyacrylamide gel, followed by autoradiography.

Acknowledgments

The first two authors contributed equally to this paper. We thank Dr. D.A. Haber and Dr. A.J. Fornace, Jr. for their generosity in providing plasmids. We thank Dr. Z.D. Sharp and Dr. N. Ting for critical comments, and C.-F. Chen, D. Jones, and P. Garza for technical assistance in plasmid construction and antibody preparation. This work was supported by National Institutes of Health grants and McDermott endowment funds to W.-H. L.; L. Z. and S. L. were supported by a predoctoral training grant from the U.S. Army (DAMD17-99-1-9402).

Received January 27, 2000; revised August 7, 2000.

References

Anderson, S.F., Schlegel, B.P., Nakajima, T., Wolpin, E.S., and Parvin, J.D. (1998). BRCA1 protein in linked to the RNA polymerase II holoenzyme complex via RNA helicase A. Nat. Genet. *19*, 254–256.

Blackwell, T.K., and Weintraub, H. (1990). Differences and similarities in DNA-binding preferences of MyoD and E2A protein complexes revealed by binding site selection. Science *250*, 1104–1110.

Carter, T., Vancurova, I., Sun, I., Lou, W., and DeLeon, S. (1990). A DNA-activated protein kinase from Hela cell nuclei. Mol. Cell. Biol. *10*, 6460–6471.

Chapman, M.S., and Verma, I.M. (1996). Transcriptional activation by BRCA1. Nature *382*, 678–679.

Chen, C.-F., Li, S., Chen, Y., Chen, P.-L., Sharp, Z.D., and Lee, W.-H. (1996). The nuclear localization sequences of the BRCA1 protein interact with the importin-α subunit of the nuclear transport signal receptor. J. Biol. Chem. *271*, 32863–32868.

Chen, Y., Lee, W.-H., and Chew, H.K. (1999). Emerging roles of BRCA1 in transcriptional regulation and DNA repair. J. Cell. Physiol. *181*, 385-392.

Constance, C.M., Morgan, J.I., IV, and Umek, R.M. (1996). C/EBPα regulation of the growth-arrest-associated gene gadd45. Mol. Cell Biol. *16*, 3878–3883.

Cortez, D., Wang, Y., Qin, J., and Elledge, S.J. (1999). Requirement of ATM-dependent phosphorylation of brca1 in the DNA damage response to double-strand breaks. Science *286*, 1162–1166.

De Toledo, S.M., Azzam, E.I., Gasmann, M.K., and Mitchel, R.E.J. (1995). Use of semiquantitative reverse transcription-polymerase chain reaction to study gene expression in normal human skin fibroblasts following low dose-rate irradiation. Int. J. Radiat. Biol. *67*, 135–143.

Durfee, T., Becherer, K., Chen, P.-L., Yeh, S.-H., Yang, Y., Kilburn, A.E., Lee, W.-H., and Elledge, S.J. (1993). The retinoblastoma protein associates with the protein phosphatase type 1 catalytic subunit. Genes Dev. *7*, 555-569.

Fan, S., Wang, J.A., Yuan, R., Ma, Y., Meng, Q., Erdos, M.R., Pestell, R.G., Yuan, F., Auborn, K.J., Goldberg, I.D., and Rosen, E.M. (1999). BRCA1 inhibition of estrogen receptor signaling in transfected cells. Science *284*, 1354–1356.

Friedman, J.R., Fredericks, W.J., Jensen, D.E., Speicher, D.W., Huang, X.-P., Neilson, E.G., and Rauscher, F.J., III. (1996). KAP-1, a novel corepressor for the highly conserved KRAB repression domain. Genes Dev. *10*, 2067–2078.

Gowen, L.C., Avrutskaya, A.V., Latour, A.M., Koller, B.H., and Leadon, S.A. (1998). BRCA1 required for transcription-coupled repair of oxidative DNA damage. Science *281*, 1009–1012.

Haile, D.T., and Parvin, J.D. (1999). Activation of transcription in vitro by the BRCA1 carboxyl-terminal domain. J. Biol. Chem. *274*, 2113–2117.

Harkin, D.P., Bean, J.M., Miklos, D., Song, Y.-H., Truong, V.B., Englert, C., Christians, F.C., Ellisen, L.W., Maheswaran, S., Oliner, J.D., and Haber, D.A. (1999). Induction of GADD45 and JNK/SAPK-dependent apoptosis following inducible expression of BRCA1. Cell *97*, 575–586.

Harlow, E., and Lane, D. (1988). Antibodies: A Laboratory Manual (Cold Spring Harbor, NY: Cold Spring Harbor Press).

Hollander, M.C., Alamo, I., Jackman, J., Wang, M.G., McBride, O.W., and Fornace, A.J., Jr. (1993). Analysis of the mammalian gadd45 gene and its response to DNA damage. J. Biol. Chem. *268*, 24385–24393.

Hollander, M.C., Sheikh, M.S., Bulavin, D.V., Lundgren, K., Augeri-Henmueller, L., Shehee, R., Molinaro, T.A., Kim, K.E., Tolosa, E., Ashwell, J.D., et al. (1999). Genomic instability in Gadd45a-deficient mice. Nat. Genet. *23*, 176–184.

Kastan, M.B., Zhan, Q., El-Deiry, W.S., Carrier, F., Jacks, T., Walsh, W.V., Plunkett, B.S., Vogelstein, B., and Fornace, A.J., Jr. (1992). A mammalian cell cycle checkpoint pathway utilizing p53 and GADD45 is defective in ataxia-telangiectasis. Cell *71*, 587–597.

Kim, S.-S., Chen, Y.M., O'Leary, E., Witzgall, R., Vidal, M., and Bonventre, J.V. (1996). A novel member of the RING finger family, KRIP-1, associates with the KRAB-A transcriptional repressor domain of zinc finger proteins. Proc. Natl. Acad. Sci. USA *95*, 657–662.

Le Douarin, B., Nielsen, A.L., Garnier, J.M., Ichinose, H., Jeanmougin, F., Losson, R., and Chambon, P. (1996). A possible involvement of TIF1α and TIF1β in the epigenetic control of transcription by nuclear receptors. EMBO J. *15*, 6701–6715.

Lee, J.-S., Collins, K.M., Brown, A.L., Lee, C.-H., and Chung, J.H. (2000). hCds1-mediated phosphorylation of BRCA1 regulates the DNA damage response. Nature *404*, 201–204.

Li, S., Ku, C.-Y., Farmer, A.A., Cong, Y.-S., Chen, C.-F., and Lee, W.-H. (1998). Identification of a novel cytoplasmic protein that specifically binds to nuclear localization signal motifs. J. Biol. Chem. *273*, 6183–6189.

Li, S., Chen, P.-L., Subramanian, T., Chinnadurai, G., Tomlinson, G., Osborne, C.K., Sharp, Z.D., and Lee, W.-H. (1999). Binding of CtIP to the BRCT repeats of BRCA1 involved in the transcription regulation of p21 is disrupted upon DNA damage. J. Biol. Chem. *274*, 11334–11338.

Li, S., Ting, N.S.Y., Zheng, L., Chen, P.-L., Ziv, Y., Shiloh, Y., Lee, E.Y.-H., and Lee, W.-H. (2000). Functional link of BRCA1 and ataxia telangiectasia gene product in DNA damage response. Nature *406*, 210–215.

Liu, C. -Y., Flesken-Nikitin, A., Li, S., Zeng, Y., and Lee, W.-H. (1996). Inactivation of the mouse BRCA1 gene led to failure in the morphogenesis of the egg cylinder in early postplantation development. Genes Dev. *10*, 1835–1843.

Luckow, B., and Schutz, G. (1987). CAT constructions with multiple unique restriction sites for the functional analysis of eukaryotic promoters and regulatory elements. Nucleic Acids Res. *15*, 5490.

MacLachlan, T.K., Somasundaram, K., Sgagias, M., Shifman, Y., Muschel, R.J., Cowan, K.H., and El-Deiry, W.S. (2000). BRCA1 effects on the cell cycle and the DNA damage response are linked to altered gene expression. J. Biol. Chem. *275*, 2777–2785.

Margolin, J.F., Friedman, J.R., Meyer, W.K., Vissing, H., Thiesen, H.J., and Rauscher, F.J., III. (1994). Krupple-associated boxes are potent transcriptional repression domain. Proc. Natl. Acad. Sci. USA *91*, 4509–4513.

Miki, Y., Swensen, J., Shattuck-Eidens, D., Futreal, P.A., Harshman, K., Tavtigian, S., Liu, Q., Cochran, C., Bennett, L.M., Ding, W., et al. (1994). A strong candidate for the breast and ovarian cancer susceptibility gene BRCA1. Science *266*, 66–71.

Monteiro, A.N.A., August, A., and Hanafusa, H. (1996). Evidence for a transcriptional activation function of BRCA1 C-terminal region. Proc. Natl. Acad. Sci. USA *93*, 13595–13599.

Moosmann, P., Georgiev, O., Le Douarin, B., Bourquin, J.-P., and Schaffner, W. (1996). Transcriptional repression by RING finger protein TIF1β that interacts with the KRAB repression domain of KOX1. Nucleic Acid Res. *24*, 4859–4867.

Moynahan, M.E., Chiu, J.W., Koller, B.H., and Jasin, M. (1999). Brca1 controls homology-directed DNA repair. Mol. Cell *4*, 511–518.

Mueller, C.R., Maire, P., and Schibler, U. (1990). DBP, a liver-enriched transcriptional activator, is expressed late in ontogeny and its tissue specificity is determined posttranscriptionally. Cell *61*, 279–291.

Pao, G.M., Janknecht, R., Ruffner, H., Hunter, T., and Verma, I.M. (2000). CBP/p300 interact with and function as transcriptional coactivators of BRCA1. Proc. Natl. Acad. Sci. USA *97*, 1020–1025.

Scully, R., Anderson, S.F., Chao, D.M., Wei, W., Ye, L., Young, R.A., Livingston, D.M., and Parvin, J.D. (1997a). BRCA1 is a component of the polymerase II holoenzyme. Proc. Natl. Acad. Sci. USA *94*, 5605–5610.

Scully, R., Chen, J., Ochs, R.L., Keegan, K., Hoekstra, M., Feunteun, J., and Livingston, D.M. (1997b). Dynamic changes of BRCA1 subnuclear location and phosphorylation state are initiated by DNA damage. Cell *90*, 425–435.

Somasundaram, K., Zhang, H., Zeng, Y.X., Houvras, Y., Peng, Y., Zhang, H., Wu, G.S., Licht, J.D., Weber, B.L., and El-Deiry, W.S. (1997). Arrest of the cell cycle by the tumor suppressor BRCA1 requires the CDK-inhibition p21(Waf1/Cip1). Nature *389*, 187–190.

Wang, Q., Zhang, H., Kajino, K., and Greene, M.I. (1998). BRCA1 binds c-Myc and inhibits its transcriptional and transforming activity in cells. Oncogene *17*, 1939–1948.

Wang, X.W., Zhan, Q., Coursen, J.D., Khan, M.A., Kontny, U., Yu, L., Hollander, M.C., O'Conner, P.M., Fornace, A.J., Jr., and Harris, C. (1999). GADD45 induction of a G2/M cell cycle checkpoint. Proc. Natl. Acad. Sci. USA *96*, 3706–3711.

Welcsh, P.L., Owens, K.N., and King, M.C. (2000). Insights into the functions of BRCA1 and BRCA2. Trends Genet. *16*, 69–74.

Witzgall, R., O'Leary, E., Leaf, A., Onaldi, D., and Bonventre, J.V. (1994). The Kruppel associated box-A (KRAB) domain of zinc finger proteins mediates transcriptional repression. Proc. Natl. Acad. Sci. USA *91*, 4514–4518.

Xu, X., Weaver, Z., Linke, S.P., Li, C., Gotay, J., Wang, X.W., Harris, C.C., Ried, T., and Deng, C.-X. (1999). Centrosome amplification and a defective G2-M cell cycle checkpoint induce genetic instability in BRCA1 exon 11 isoform-deficient cells. Mol. Cell *3*, 389–395.

Yarden, R.I., and Brody, L.C. (1999). BRCA1 interacts with components of the histone deacetylase complex. Proc. Natl. Acad. Sci. USA *96*, 4983–4988.

Yew, P.R., Liu, X., and Berk, A.J. (1994). Adenovirus E1B oncoprotein tethers a transcription repression domain to p53. Gene Dev. *8*, 190–202.

Zhong, Q., Chen, C.-F., Li, S., Chen, Y., Wang, C.-C., Xiao, J., Chen, P.-L., Sharp, Z.D., and Lee, W.-H. (1999). BRCA1 is essential for DNA damage response mediated by the Rad50/Mre11/p95 complex. Science *285*, 747–750.

GenBank Accession Number

The GenBank accession number for the *ZBRK1* sequence is AF295096.

THE JOURNAL OF BIOLOGICAL CHEMISTRY
Vol. 275, No. 39, Issue of September 29, pp. 30618–30622, 2000
Printed in U.S.A.

NBS1 and TRF1 Colocalize at Promyelocytic Leukemia Bodies during Late S/G_2 Phases in Immortalized Telomerase-negative Cells

IMPLICATION OF NBS1 IN ALTERNATIVE LENGTHENING OF TELOMERES*

Received for publication, June 20, 2000
Published, JBC Papers in Press, July 25, 2000, DOI 10.1074/jbc.C000390200

Guikai Wu‡, Wen-Hwa Lee, and Phang-Lang Chen§

From the Department of Molecular Medicine and Institute of Biotechnology, University of Texas Health Science Center at San Antonio, San Antonio, Texas 78245

Nijmegen breakage syndrome, a chromosomal instability disorder, is characterized in part by cellular hypersensitivity to ionizing radiation. The *NBS1* gene product, p95 (NBS1 or nibrin) forms a complex with Rad50 and Mre11. Cells deficient in the formation of this complex are defective in DNA double-strand break repair, cell cycle checkpoint control, and telomere length maintenance. How the NBS1 complex is involved in telomere length maintenance remains unclear. Here we show that the C-terminal region of NBS1 interacts directly with a telomere repeat binding factor, TRF1, by both yeast two-hybrid and *in vivo* DNA-coimmunoprecipitation assays. NBS1 and Mre11 colocalize with TRF1 at promyelocytic leukemia (PML) nuclear bodies in immortalized telomerase-negative cell lines, but rarely in telomerase-positive cell lines. The translocation of NBS1 to PML bodies occurs specifically during late S to G_2 phases of the cell cycle and coincides with active DNA synthesis in these NBS1-containing PML bodies. These results suggest that NBS1 may be involved in alternative lengthening of telomeres in telomerase-negative immortalized cells.

Telomeres comprise tracts of noncoding chromosomal hexanucleotide repeat sequences that, in combination with specific proteins, prevent degradation, rearrangement, and chromosomal fusion events (1). Telomere length is maintained by the *de novo* addition of telomere repeats by telomerase (2). In mammals, telomerase expression is ubiquitous in embryonic tissues and down-regulated in somatic adult tissues. There are, however, exceptions such as in regenerative tissues or tumor cells (3).

Recombination can lengthen telomeres in the absence of telomerase. For example, when the yeast telomerase RNA component, TLC1, is deleted, telomeres become shortened and most cells die (4). However, gene conversion mediated by the RAD52 pathway subserves telomere lengthening in rare surviving cells (5). Genetic studies in yeast have also implicated the Rad50-Mre11-Xrs2 complex in telomere length maintenance, aside from its additional roles in homologous and nonhomologous recombinational repair, DNA damage assessment, and/or cell cycle checkpoint regulation (6). The Rad50-Mre11-Xrs2 complex has been proposed to function in the preparation of DNA ends for telomerase-mediated replication and is therefore implicated in telomerase-dependent telomere length maintenance, rather than in protection of telomeric ends.

In mammalian cells, Mre11 and Rad50, together with NBS1 (p95) form a complex (7–9) comparable in mass to a similar assemblage in *Saccharomyces cerevisiae* containing Rad50, Mre11, and Xrs2. The *NBS1* gene mutated in Nijmegen breakage syndrome, a chromosomal instability disorder, encodes a 95-kDa protein (NBS1) with two functional modules found in cell cycle checkpoint proteins, a forkhead-associated domain and an adjacent BRCA1 C-terminal (BRCT) repeat (10). Rad50 is a coiled coil SMC (for structural maintenance of chromosomes)-like protein with ATP-dependent DNA binding activity (11). Mre11 has been proposed to have both structural (end-holding) and catalytic activities including double-stranded DNA 3′ to 5′ exonuclease and single-stranded endonuclease activity (9, 12–15). Despite their similar size (95 kDa), NBS1 and Xrs2p are quite dissimilar in sequence, although it remains possible that they will be functional analogues or early related homologues (16).

The function of NBS1 is unknown although there is speculation that it might recognize signals from a DNA damage-sensing complex that could be in the form of phosphorylation of serine or threonine residues that are, in turn, recognized by the forkhead-associated domain in NBS1 (16). Mre11 colocalizes to subnuclear regions containing DNA breaks within 30 min after irradiation of normal human diploid fibroblasts (17). In NBS[1] cells, a deficiency of NBS1 is correlated with an inability to form Mre11-Rad50 nuclear foci in response to ionizing radiation (8). Together, these observations point to a major role for the Mre11-Rad50-NBS1 complex in repair of DNA double-strand breaks. The NBS1 protein is essential for Mre11 phosphorylation upon DNA damage (18). In addition, NBS1 function has been linked to ATM by the observation that phosphorylation of NBS1 in response to radiation exposure is ATM-dependent (19–21). Whether the mammalian Rad50-

* This work was supported in part by National Institutes of Health Grants CA85605 (to P. L. C.) and CA81020 (to W. H. L.), and a grant from the V Foundation for Cancer Research. The costs of publication of this article were defrayed in part by the payment of page charges. This article must therefore be hereby marked "*advertisement*" in accordance with 18 U.S.C. Section 1734 solely to indicate this fact.

‡ Supported by Predoctoral Training Grant DAMD17-99-1-9402 from the Department of Defense.

§ To whom correspondence should be addressed: Dept. of Molecular Medicine and Inst. Of Biotechnology, University of Texas Health Science Center at San Antonio, 15355 Lambda Dr., San Antonio, TX 78245. Tel.: 210-567-7353; Fax: 210-567-7377; E-mail: chenp0@uthscsa.edu.

[1] The abbreviations used are: NBS, Nijmegen breakage syndrome; PML, promyelocytic leukemia; ATM, ataxia telangiectasia mutated; CPRG, chlorophenol red-β-D-galactopyranoside; PBS, phosphate-buffered saline; FITC, fluorescein isothiocyanate; DAPI, 4′,6′-diamino-2-phenylindole; mAB, monoclonal antibody; GST, glutathione *S*-transferase; BrdUrd, bromodeoxyuridine.

polyclonal antibodies were obtained by using bacterially expressed and purified GST-TRF1 fusion protein as antigen.

Isolation of GM847 Cell Clones with Inducible Expression of the GFP-TRF1—To establish cell clones that express a GFP-TRF1 fusion protein, we have used the inducible expression system controlled by a *tet*-responsive promoter. A cDNA fragment containing GFP-TRF1 fusion protein was subcloned into an expression plasmid (pUHD10–3) driven by a core cytomegalovirus promoter linked to a *tet* operator heptad (pUHD10–3-GFP-TRF1) (29). This plasmid was cotransfected into GM847 cells with pCHTV, bearing a hygromycin-resistance gene and a cytomegalovirus-controlled tetracycline repressor-VP16 fusion transcription unit, and *hygro*-resistant clones were subsequently isolated. Several cell clones that express the GFP-TRF1 fusion protein upon removal of tetracycline were obtained.

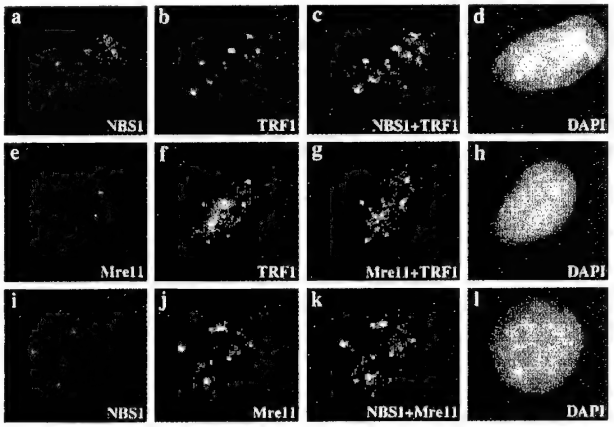

FIG. 2. **NBS1 and Mre11 colocalize with TRF1 in GM847 cells.** Actively growing GM847 cells were fixed and immunostained using a conventional protocol as described. NBS1 colocalizes with TRF1 (*a–d*). Mre11 colocalizes with TRF1 (*e–h*). NBS1 also colocalizes with Mre11 (*i–l*). For *a* and *b*, cells were costained with a rabbit polyclonal NBS1 antibody and a mouse polyclonal TRF1 antibody. A rabbit polyclonal Mre11 antibody co- stained cells with anti-TRF1 (*e* and *f*). In *i* and *j*, cells were costained with rabbit NBS1 antiserum and 12D7, a monoclonal Mre11 antibody. The first antibodies were detected with a goat anti-rabbit antibody conjugated with Texas Red and a goat anti-mouse antibody conjugated with FITC. *c*, *g*, and *k* are the merged images. DNA was stained with DAPI, shown in *blue* (*d*, *h*, and *l*).

RESULTS AND DISCUSSION

To explore the potential biological function(s) of NBS1, we used near full-length NBS1 as the bait in a yeast two-hybrid screen to recover interacting proteins encoded by a human lymphocyte cDNA library. One of the clones thus isolated corresponded to a near full-length cDNA for the telomeric DNA-binding protein TRF1. TRF1 consists of an acidic N terminus followed by a dimerization domain and a Myb-like DNA-binding domain at its C terminus (30). To determine the specific domain(s) of TRF1 required for binding to NBS1, various regions of TRF1 fused to the GAL4-transactivation domain were individually tested for their respective abilities to interact with NBS1 fused to the GAL4-DNA-binding domain by yeast two-hybrid assay. As shown in Fig. 1*A*, none of the isolated TRF1 fragments exhibited significant binding activity, suggesting that full-length TRF1 is required for efficient binding to NBS1. Reciprocally, a series of NBS1 deletion mutants fused to the GAL4-DNA-binding domain were tested for their abilities to interact with full-length TRF1. Interestingly, the C-terminal region of NBS1 (amino acids 534 to 754) is required for TRF1 binding, and its binding activity appears much stronger than that of the near full-length clone (Fig. 1*B*). It is possible that one or more inhibitory motifs reside N-terminally of amino acid 534 within NBS1 and that the NBS1-TRF1 interaction is enhanced by release of this inhibitory function by post-translational modification such as phosphorylation. In this regard, we note that there are multiple potential phosphorylation sites in this region, some of which are subject to regulation by the ATM kinase during the DNA damage response (19–21).

Because NBS1 forms a complex with Mre11, Rad50, and BRCA1 (28), we next tested whether TRF1 binds to any of these proteins in a yeast two-hybrid assay. As shown in Fig. 1*C*, TRF1 exhibits very little binding activity toward any one of these three proteins. These results suggest that TRF1 may bind to the Rad50-Mre11-NBS1 triplex through NBS1.

To determine whether the complex of TRF1 and NBS1 exists in human cells, telomeric DNA repeats were radioactively labeled

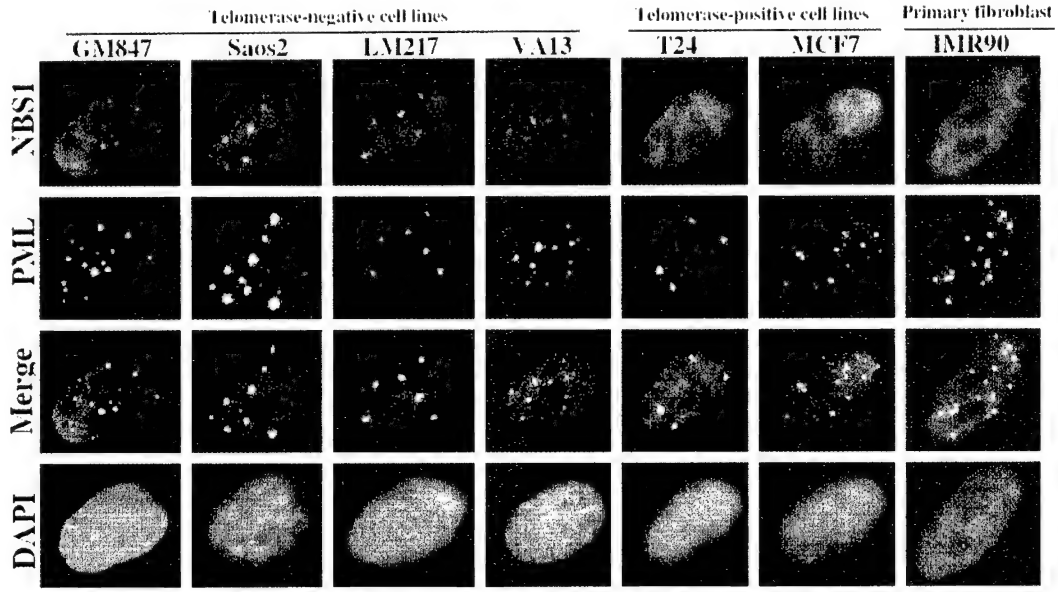

FIG. 3. **NBS1 colocalizes with PML bodies in telomerase-negative immortal cell lines but not in telomerase-positive immortal cell lines or primary fibroblasts.** Actively growing cells were fixed and costained for NBS1 with a rabbit NBS1 antibody (*row 1*) and for PML with a monoclonal PML antibody (*row 2*). In telomerase-negative immortal cells (GM847, Saos2, LM217, and VA13), NBS1 foci were detectable in about 5% of cells within a randomly growing culture; these NBS1 foci colocalize with PML bodies. NBS1 foci were not detected or evident in telomerase-positive immoral cell lines (T24 and MCF7) or a primary cell line (IMR90). PML bodies were readily detected in all cells tested. Cells in *row 1* were stained with Texas Red and in *row 2* with FITC. *Row 3* corresponds to merged images of NBS1 and PML. *Row 4* corresponds to DAPI staining, which indicates nuclei. Note that these NBS1 foci, whose number usually ranges from 2 to 15, are generally larger and more distinctive than ionizing radiation-induced foci. In VA13, NBS1 foci are smaller than those in the other telomerase-negative immortal cell lines.

Mre11-NBS1 complex also plays a role in the maintenance of telomere length has not yet been demonstrated. To address this issue, we have undertaken to identify cellular interacting partners of NBS1 by yeast two-hybrid screening. Here we report the identification of a telomere repeat binding factor, TRF1, as an interaction partner of NBS1. We show that NBS1 and Mre11 colocalize with TRF1 in PML nuclear bodies in telomerase-negative immortalized cells during G_2 phase of the cell cycle. Significantly, the NBS1/TRF1 foci undergo active BrdUrd incorporation during late S/G_2 transition, thus suggesting a novel role for NBS1 in telomere lengthening in telomerase-negative immortalized cell lines.

EXPERIMENTAL PROCEDURES

Yeast Two-hybrid Interaction System—Full-length NBS1 cDNAs (minus the first 12 amino acids) were fused to the DNA-binding domain of GAL4 in the pAS2–1 vector and used as the bait in two-hybrid screens using human lymphocyte cDNA library. Detailed screening procedures were described previously (22). Similarly, a cDNA fragment containing Rad50 (amino acid 753 to 1312), Mre11 (amino acid 1–680), or BRCA1 (amino acid 1–1315) was fused to the DNA-binding domain of GAL4 in the pAS2–1 vector. To map the binding regions, various truncated forms of TRF1 and NBS1 were generated and fused to the GAL4 activation domain of pGAD10 and DNA-binding domain of pAS2–1, respectively, and cotransformed into Mav203 with full-length NBS1 and TRF1, respectively. β-Galactosidase activity was quantified with chlorophenol red-β-D-galactopyranoside (CPRG) as the substrate (22).

Cell Lines, Culture Conditions, Synchronization, and BrdUrd Labeling—T24, a human bladder carcinoma cell line, MCF7, a human breast cancer cell line, HeLa, a human cervical carcinoma cell line, Saos2, a human osteosarcoma cell line, and IMR90, a human fetal lung primary fibroblast are from ATCC (America Type Culture Collection). SV40-immortalized human fibroblast cell lines, VA13, GM847, and LM217, were kindly provided by J. Shay and J. P. Murnane. Cells were cultured in Dulbecco's modified Eagle's medium supplemented with 10% fetal bovine serum (10% CO_2). Cell synchronization by double thymidine block in G_1/S boundary was performed as described with modification (23). Cells blocked at G_1/S transition were released and fixed at different time points (0–13 h). For an additional arrest at early G_2 by Hoechst 33342, cells were released from double thymidine block for 2 h, incubated with Hoechst 33342 at the final concentration of 0.2 μg/ml for 11 more h, washed with PBS, fixed, and processed for staining (24). For BrdUrd pulse labeling, cells were released from double thymidine block for 13 h, labeled with BrdUrd for 30 min with a cell proliferation kit (Amersham Pharmacia Biotech, RPN20), fixed, and stained as described.

DNA Coimmunoprecipitation Assay—The procedure was performed essentially as described (25). Briefly, cell nuclear extracts were prepared as described previously (26). A telomeric DNA-containing $TTAGGG^{11}$ repeat sequence was labeled with ^{32}P-dCTP by Klenow filling and purified in 5% polyacrylamide gel. For each reaction, 50 μg of nuclear extract was incubated with the telomere probe (30,000 cpm) in a binding buffer (20 mM HEPES, pH 7.9, 150 mM KCl, 1 mM $MgCl_2$, 5% glycerol, 4% Ficoll, 1 mM dithiothreitol, 1 mM phenylmethylsulfonyl fluoride) at room temperature for 30 min. The protein-DNA complex was then immunoprecipitated by specific antibody and protein A beads and washed 3 times with binding buffer. The complex was digested by proteinase K and extracted with phenol/chloroform. The telomere probe was then precipitated by ethanol and electrophoresed in 5% native polyacrylamide gel and autoradiographed.

Immunostaining—This immunostaining procedure was adapted from the previous published work of Durfee *et al.* (27). Briefly, cells were grown on coverslips in tissue culture dishes and collected at various time points as indicated (random populated or synchronized). The cells were washed with PBS and fixed for 30 min in 3.7% formaldehyde in PBS plus 0.1% Triton X-100. Cells were then permeated with 0.05% Saponin at room temperature for 30 min, followed by washing five times with PBS. After being blocked with 10% goat serum in PBS/0.5% Nonidet P-40 at room temperature for 30 min, cells were incubated with primary antibodies at 4 °C for overnight. After five PBS washes, cells were incubated with FITC or Texas Red-conjugated secondary antibodies (Southern Biotechnology Associates, Inc.) for 30 min. Cells were then washed extensively in PBS/0.5% Nonidet P-40, further stained with DAPI (1 μg/ml in H_2O, Fisher), and mounted in Permafluor (Lipshaw-Immunonon, Inc). Immunofluorescence microscopy was performed with a Nikon Eclipse TE300 immunofluorescence microscope. Images captured were processed with Adobe Photoshop.

Antibodies—Rabbit polyclonal antibodies specific for NBS1 and Mre11 were obtained from Novus Biologicals (Littleton, CO). PML mAB PG-M3 was from Santa Cruz Biotechnology (Santa Cruz, CA). 12D7 mAB specific for Mre11 has been described before (28). Mouse α-TRF1

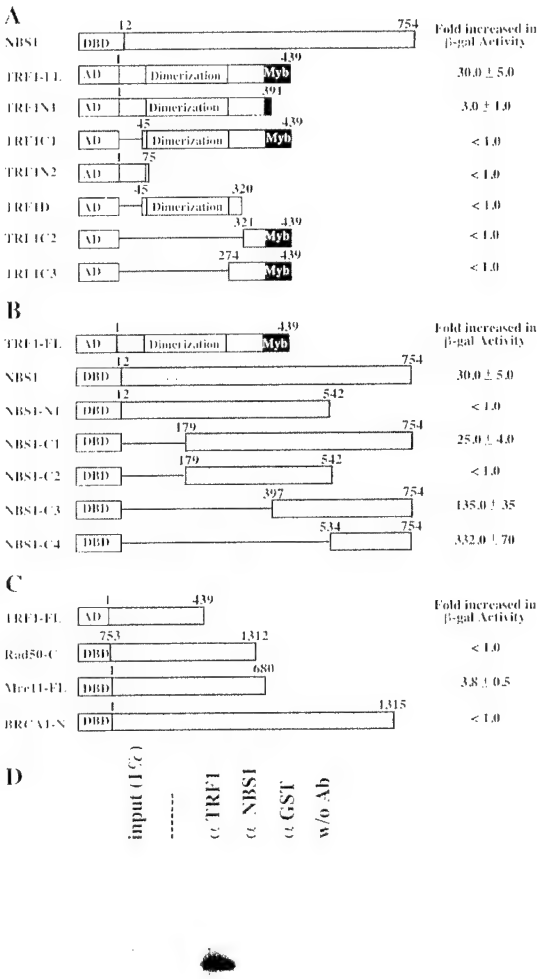

FIG. 1. **NBS1 interacts with TRF1.** *A–C*, NBS1 interacts with TRF1 in a yeast two-hybrid assay. β-Galactosidase activities were quantified using CPRG as the substrate. *A*, a near full-length NBS1 cDNA was fused to the GAL4 DNA-binding domain (*DBD*) of pAS2–1. Six truncated TRF1 fragments were fused to the GAL4 activation domain (*AD*) of pGAD10 and cotransformed into Mav203 with pAS2–1-NBS1, respectively. Only TRF1N1 showed detectable but low binding activity. *B*, various NBS1 fragments were fused to the GAL4 DNA-binding domain of pAS2–1 and cotransformed together with pGAD10-TRF1-FL into Mav203, respectively. The results showed that NBS1-C4 (amino acid 534–754) is responsible for binding to TRF1. With this fragment, the β-galactosidase activity was increased by 10-fold, when compared with the near full-length NBS1. *C*, Mre11, Rad50, and BRCA1 showed no or very little binding activity with TRF1 in the same system. The N-terminal region of Rad50 and C-terminal region of BRCA1 were removed, because they exhibit transactivation activity in yeast two-hybrid assays. Full-length Mre11 showed low binding activity with TRF1. *D*, NBS1 associates with telomere repeat sequences in an *in vivo* DNA coimmunoprecipitation assay. A $TTAGGG^{11}$ telomeric DNA fragment radioactively labeled by ^{32}P was coprecipitated specifically with NBS antibodies (*lane 4*) and TRF1-antibodies (*lane 3*, positive control) but not GST antibodies (*lane 5*, negative control). *Lane 1* shows 1% input of labeled DNA, whereas *lane 6* shows a precipitation reaction performed in the absence of antibodies.

and incubated with nuclear extracts. The labeled telomeric DNA repeats were specifically coimmunoprecipitated by antibodies against either TRF1 or NBS1 but not control antibodies against GST (Fig. 1*D*). These results further suggest that NBS1 binds to TRF1 in human cells and, furthermore, that the complex has the ability to bind the telomeric DNA repeats.

It has been well documented that the Rad50-Mre11-NBS1 triplex is involved in DNA double-strand break repair and, moreover, that specific nuclear foci positive for Rad50-Mre11-NBS1 are formed after ionizing radiation (8). Previous reports have suggested that, in the absence of DNA damage, no evident NBS1/Mre11 foci can be detected. Interestingly, we found that NBS1/Mre11 foci could be detected in about 5% of an asynchronously growing culture of human GM847 cells even in the absence of DNA damage treatment. These DNA damage-independent NBS1/Mre11 foci colocalize with TRF1 by immunostaining (Fig. 2), further supporting an *in vivo* association of NBS1 and TRF1 in human cells.

Yeager *et al.* (31) reported that TRF1 is associated with PML bodies in several telomerase-negative immortalized cell lines. Telomere length maintenance in this type of cells requires a telomerase-independent mechanism, previously designated as alternative lengthening of telomeres (ALT) (32). Coincidentally, the cell lines in which we observed DNA damage-independent NBS1/Mre11 foci are deficient in telomerase activity and immortalized through the ALT pathway. We therefore reasoned it likely that NBS1 might associate with PML bodies in these ALT cells. To determine whether this is the case, we examined a panel of telomerase-negative and -positive cell lines for the colocalization of NBS1 with PML bodies. As shown in Fig. 3, NBS1 colocalized with PML bodies in telomerase-negative immortalized cell lines including human GM847, Saos2, LM217, and VA13. However, in either telomerase-positive immortalized cell lines, such as T24 and MCF7, or human primary fibroblasts (IMR90), whereas PML bodies were detected, neither NBS1 foci nor NBS1 colocalization with PML bodies could be detected (Fig. 3).

Because only a small fraction of cells within a randomly growing telomerase-negative cell culture contain NBS1/Mre11 foci, it is likely that NBS1 foci formation is cell cycle stage-specific, perhaps during G_2 phase. To test this possibility, cells synchronized at the G_1/S boundary by a double thymidine block were released into the cell cycle and then fixed at specific time points post-release for immunostaining with NBS1-specific antibodies. As shown in Fig. 4, NBS1 foci formation in telomerase-negative immortalized cells occurs during late S/G_2 phase. This cell cycle-specific formation of NBS1 foci was not observed in telomerase-positive cell lines. To more accurately establish the point at which NBS1 foci formation occurs during S/G_2 phase, cells released from a double thymidine block were subsequently treated with Hoechst 33342, which specifically arrests cells at G_2 phase. A significantly higher percentage of NBS1 foci-containing cells were observed in ALT cell lines but not in T24, MCF7, or HeLa cells (Fig. 4). These results suggest that NBS1 specifically translocates to PML bodies in ALT cells at G_2 phase.

Telomere repeat sequences have been found in TRF1-containing PML bodies (31) and, as demonstrated above, NBS1 is localized to such PML bodies. It is therefore very likely that these PML bodies represent sites for maintaining telomere length in ALT cells. To test this possibility, a GFP-TRF1-expressing GM847 cell line was enriched for late S/G_2 phase cells, pulse-labeled with BrdUrd for 30 min, and immunostained with an anti-BrdUrd antibody. GM847 cells were also subjected to an identical procedure and immunostained with anti-BrdUrd and anti-NBS1 antibodies. As shown in Fig. 5, the PML bodies in a

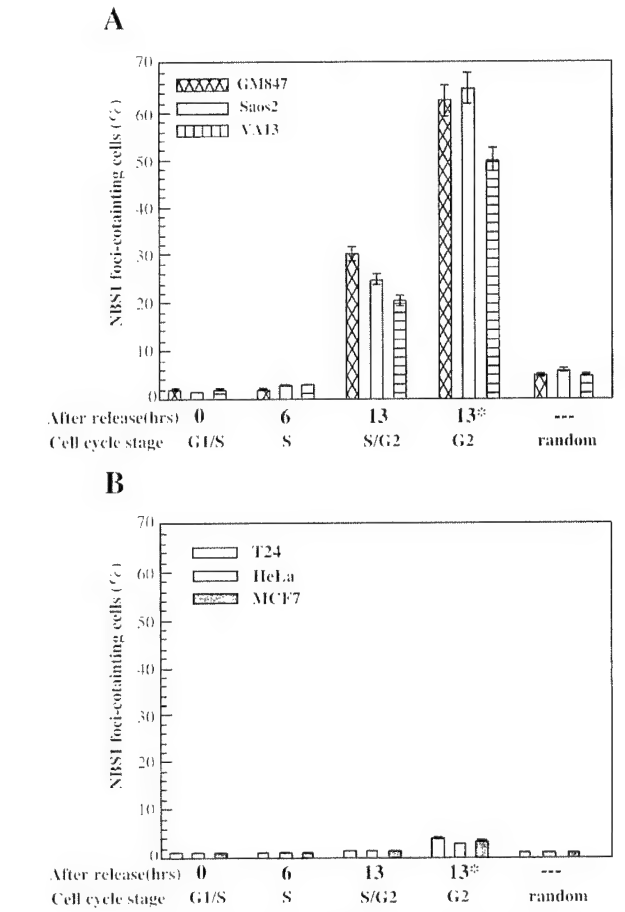

FIG. 4. **Cell cycle-dependent NBS1 foci formation in immortalized telomerase-negative cells.** Cells from a randomly growing population, or from the specified time points following release from a double thymidine block, were fixed and processed for immunostaining. The asterisk (*) shows an additional block by Hoechst 33342, in addition to the double thymidine treatment, which enriches G_2 cells more efficiently than double thymidine block alone. Cells were stained for NBS1. The percentage of NBS1 foci-containing cells are shown as Y coordinates in *A* and *B*. For every time point and for each cell line, at least 180 cells were scored, and the results are summarized from two or three independent experiments. In telomerase-negative immortal cells (GM847, Saos2, and VA13), NBS1 foci are most prominent at the late S/early G_2 boundary (*A*), whereas in telomerase-positive immortal cells (T24, MCF7, and HeLa), there is no significant NBS1 foci formation at any time point, compared with a random cell population (*B*). Therefore, NBS1 foci formation is cell cycle-dependent. This is also true for Mre11 (data not shown).

fraction of GM847 cells, as indicated by NBS1 immunostaining or GFP-TRF1 immunofluorescence, underwent active BrdUrd incorporation at late S/G_2 phase. By contrast, no BrdUrd incorporation could be observed in MCF7 cells following a similar labeling procedure. These results imply that the telomere lengthening process in ALT cells that requires DNA synthesis occurs in PML bodies at G_2 phase of the cell cycle.

NBS1 is an apparent multi-functional protein, with demonstrated roles in DNA double-strand break repair and S-phase checkpoint control (8, 19). The interaction between TRF1 and the NBS1 complex suggests that NBS1 may be involved in telomere length maintenance in ALT cells. A homologous recombination-mediated mechanism has been proposed for telomere length maintenance in telomerase-negative cells in organisms ranging from human to yeast (32). Interestingly, Rad51, Rad52, RPA, and NBS1/Mre11 are localized to PML bodies (see Ref. 31 and this report). Given that multiple key players in homologous recombination are localized to PML

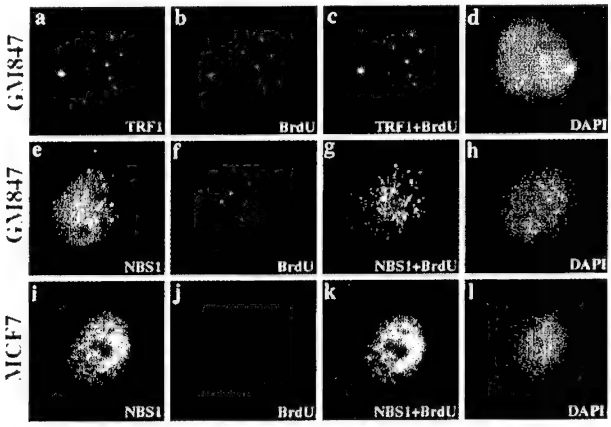

FIG. 5. **TRF1/NBS1 foci undergo active BrdUrd incorporation in late S/G_2 phase, suggestive of telomere lengthening.** All cells were subjected to a double thymidine block and then labeled with BrdUrd for 30 min at 13 h post-release. Subsequently cells were fixed and stained as described. A GFP-TRF1-inducible clone of GM847 was stained with a monoclonal BrdUrd antibody (*a–d*). A fraction of cells (5–10%) showed foci-like BrdUrd staining (*b*) that colocalize with TRF1 (*a*). In GM847 cells (*e–h*), this type of BrdUrd foci (*f*) also colocalize with NBS1 foci (*e*) and PML bodies by deduction. However, these BrdUrd foci were not observed in the telomerase-positive cell line MCF7 (*I–l*), which barely incorporated BrdUrd (*j*) and had relatively homogeneous NBS1 staining (*i*). *Panels b* and *f* indicate staining with Texas Red, and *e* and *i* with FITC. Panels *c*, *g*, and *k* indicate merged images. Panels *d*, *h*, and *l* are stained with DAPI.

bodies in telomerase-negative immortalized cells, it is reasonable to speculate that active DNA synthesis in these nuclear domains in late S/G_2 may reflect a telomere-maintenance process potentially involving a homologous recombination. However, the mechanistic details of how these factors work in concert remains to be investigated.

It has been reported that yeast Rad50-Mre11-XRS2 is important for telomere maintenance in a telomerase-dependent manner, perhaps by making DNA ends available for telomerase to replicate (33). The equivalent mammalian complex, Rad50-Mre11-NBS1, may share a similar activity, although it remains to be demonstrated. Electron microscopic analysis has revealed that mammalian telomeres end in a large duplex loop (34). Binding of TRF1 and single-strand-binding protein suggested that t loops be formed by invasion of the 3′ telomeric overhang into the duplex telomeric repeat array. It is possible that the association between TRF1 and NBS1 provides a bridge between the telomere repeat sequences and the nuclease complex of Mre11 that could make telomere ends available for replication. However, it remains to be shown that the NBS1-Mre11-Rad50 triplex is located at the telomere ends for this purpose.

NBS is a disorder characterized in part by an aging phenotype, and NBS1-deficient cells show accelerated telomere shortening *in vitro*. The link between NBS1 and TRF1 in telomere length maintenance provides a plausible explanation for these phenotypes.

Acknowledgments—We thank Drs. John Murnane and Jerry Shay for providing cell lines, Paula Garza and Diane Jones for antibody preparation, Chi-Fen Chen for technical assistance, Qing Zhong for helpful discussion, and Dr. Tom Boyer for critical reading of the manuscript.

REFERENCES

1. Shore, D. (1998) *Science* **281,** 1818–1819
2. Prescott, J. C., and Blackburn, E. H. (1999) *Curr. Opin. Genet. Dev.* **9,** 368–373
3. Colgin, L. M., and Reddel, R. R. (1999) *Curr. Opin. Genet. Dev.* **9,** 97–103
4. Prescott, J., and Blackburn, E. H. (1997) *Genes Dev.* **11,** 528–540
5. Le, S., Moore, J. K., Haber, J. E., and Greider, C. W. (1999) *Genetics* **152,** 143–152
6. Haber, J. E. (1998) *Cell* **95,** 583–586
7. Dolganov, G. M., Maser, R. S., Novikov, A., Tosto, L., Chong, S., Bressan, D. A., and Petrini, J. H. (1996) *Mol. Cell. Biol.* **16,** 4832–4841
8. Carney, J. P., Maser, R. S., Olivares, H., Davis, E. M., Le Beau, M., Yates, J. R., III, Hays, L., Morgan, W. F., and Petrini, J. H. (1998) *Cell* **93,** 477–486
9. Trujillo, K. M., Yuan, S. S., Lee, E. Y., and Sung, P. (1998) *J. Biol. Chem.* **273,** 21447–21450
10. Varon, R., Vissinga, C., Platzer, M., Cerosaletti, K. M., Chrzanowska, K. H., Saar, K., Beckmann, G., Seemanova, E., Cooper, P. R., Nowak, N. J., Stumm, M., Weemaes, C. M., Gatti, R. A., Wilson, R. K., Digweed, M., Rosenthal, A., Sperling, K., Concannon, P., and Reis, A. (1998) *Cell* **93,** 467–476
11. Raymond, W. E., and Kleckner, N. (1993) *Nucleic Acids Res.* **21,** 3851–3856
12. Furuse, M., Nagase, Y., Tsubouchi, H., Murakami-Murofushi, K., Shibata, T., and Ohta, K. (1998) *EMBO J.* **17,** 6412–6425
13. Moreau, S., Ferguson, J. R., and Symington, L. S. (1999) *Mol. Cell. Biol.* **19,** 556–566
14. Paull, T. T., and Gellert, M. (1998) *Mol. Cell* **1,** 969–979
15. Usui, T., Ohta, T., Oshiumi, H., Tomizawa, J., Ogawa, H., and Ogawa, T. (1998) *Cell* **95,** 705–716
16. Featherstone, C., and Jackson, S. P. (1998) *Curr. Biol.* **8,** R622–625
17. Maser, R. S., Monsen, K. J., Nelms, B. E., and Petrini, J. H. (1997) *Mol. Cell. Biol.* **17,** 6087–6096
18. Dong, Z., Zhong, Q., and Chen, P.-L. (1999) *J. Biol. Chem.* **274,** 19513–19516
19. Lim, D. S., Kim, S. T., Xu, B., Maser, R. S., Lin, J., Petrini, J. H., and Kastan, M. B. (2000) *Nature* **404,** 613–617
20. Wu, X., Ranganathan, V., Weisman, D. S., Heine, W. F., Ciccone, D. N., O'Neill, T. B., Crick, K. E., Pierce, K. A., Lane, W. S., Rathbun, G., Livingston, D. M., and Weaver, D. T. (2000) *Nature* **405,** 477–482
21. Zhao, S., Weng, Y. C., Yuan, S. S., Lin, Y. T., Hsu, H. C., Lin, S. C., Gerbino, E., Song, M. H., Zdzienicka, M. Z., Gatti, R. A., Shay, J. W., Ziv, Y., Shiloh, Y., and Lee, E. Y. (2000) *Nature* **405,** 473–477
22. Durfee, T., Becherer, K., Chen, P.-L., Yeh, S. H., Yang, Y., Kilburn, A. E., Lee, W.-H., and Elledge, S. J. (1993) *Genes Dev.* **7,** 555–569
23. Detke, S., Lichtler, A., Phillips, I., Stein, J., and Stein, G. (1979) *Proc. Natl. Acad. Sci. U. S. A.* **76,** 4995–4999
24. Tobey, R. A., Oishi, N., and Crissman, H. A. (1990) *Proc. Natl. Acad. Sci. U. S. A.* **87,** 5104–5108
25. Yew, P. R., Liu, X., and Berk, A. J. (1994) *Genes Dev.* **8,** 190–202
26. Zhong, Z., Shiue, L., Kaplan, S., and de Lange, T. (1992) *Mol. Cell. Biol.* **12,** 4834–4843
27. Durfee, T., Mancini, M. A., Jones, D., Elledge, S. J., and Lee, W.-H. (1994) *J. Cell Biol.* **127,** 609–622
28. Zhong, Q., Chen, C. F., Li, S., Chen, Y., Wang, C. C., Xiao, J., Chen, P.-L., Sharp, Z. D., and Lee, W.-H. (1999) *Science* **285,** 747–750
29. Chen, P.-L., Riley, D. J., Chen, Y., and Lee, W.-H. (1996) *Genes Dev.* **10,** 2794–2804
30. Chong, L., van Steensel, B., Broccoli, D., Erdjument-Bromage, H., Hanish, J., Tempst, P., and de Lange, T. (1995) *Science* **270,** 1663–1667
31. Yeager, T. R., Neumann, A. A., Englezou, A., Huschtscha, L. I., Noble, J. R., and Reddel, R. R. (1999) *Cancer Res.* **59,** 4175–4109
32. Reddel, R. R., Bryan, T. M., and Murnane, J. P. (1997) *Biochemistry (Mosc.)* **62,** 1254–1262
33. Nugent, C. I., Bosco, G., Ross, L. O., Evans, S. K., Salinge, A. P., Moore, J. K., Haber, J. E., and Lundblad, V. (1998) *Curr. Biol.* **8,** 657–660
34. Griffith, J. D., Comeau, L., Rosenfield, S., Stansel, R. M., Bianchi, A., Moss, H., and de Lange, T. (1999) *Cell* **97,** 503–514

THE JOURNAL OF BIOLOGICAL CHEMISTRY
Vol. 276, No. 12, Issue of March 23, pp. 8798–8806, 2001
Printed in U.S.A.

Basis for Avid Homologous DNA Strand Exchange by Human Rad51 and RPA*

Received for publication, November 3, 2000, and in revised form, December 12, 2000
Published, JBC Papers in Press, December 20, 2000, DOI 10.1074/jbc.M010011200

Stefan Sigurdsson, Kelly Trujillo, BinWei Song, Sabrina Stratton, and Patrick Sung‡

From the Department of Molecular Medicine and Institute of Biotechnology, University of Texas Health Science Center at San Antonio, San Antonio, Texas 78245-3207

Human Rad51 (hRad51), a member of a conserved family of general recombinases, is shown here to have an avid capability to make DNA joints between homologous DNA molecules and promote highly efficient DNA strand exchange of the paired molecules over at least 5.4 kilobase pairs. Furthermore, maximal efficiency of homologous DNA pairing and strand exchange is strongly dependent on the heterotrimeric single-stranded DNA binding factor hRPA and requires conditions that lessen interactions of the homologous duplex with the hRad51-single-stranded DNA nucleoprotein filament. The homologous DNA pairing and strand exchange system described should be valuable for dissecting the action mechanism of hRad51 and for deciphering its functional interactions with other recombination factors.

Genetic studies in various eukaryotic organisms have indicated that homologous recombination processes are mediated by a group of evolutionarily conserved genes known as the *RAD52* epistasis group. As revealed in studies on meiotic recombination and mating type switching in *Saccharomyces cerevisiae*, DNA double-strand breaks are formed and then processed exonucleolytically to yield long single-stranded tails with a 3′ extremity. Nucleation of various *RAD52* group proteins onto these ssDNA[1] tails renders them recombinogenic, leading to the search for a homologous DNA target (sister chromatid or homologous chromosome), formation of DNA joints with the target, and an exchange of genetic information with it. The repair by recombination of DNA double-strand breaks induced by ionizing radiation and other DNA damaging agents very likely follows the same mechanistic route, as it too is dependent on genes of the *RAD52* epistasis group (reviewed in Refs. 1 and 2).

Among members of the *RAD52* group, the *RAD51*-encoded product is of particular interest because of its structural and functional similarities to the *Escherichia coli* recombination protein RecA (2–5). RecA promotes the pairing and strand exchange between homologous DNA molecules to form heteroduplex DNA (4, 5), an enzymatic activity believed to be germane for the central role of RecA in recombination and DNA repair processes. Likewise, homologous DNA pairing and strand exchange activities have been shown for *S. cerevisiae* Rad51 (yRad51) (6). Under optimized conditions, the length of heteroduplex DNA joints formed by yRad51 and RecA can extend over quite a few kilobase pairs (4, 5, 7).

In published studies, human Rad51 (hRad51) was found to have the ability to make DNA joints but the maximal potential for forming only about 1 kilobase pairs of heteroduplex DNA (8–11). Furthermore, while yRad51 and RecA require their cognate single-strand DNA binding factors, SSB and yRPA, for optimal recombinase activity, hRPA has been suggested to stimulate the hRad51-mediated homologous pairing and strand exchange reaction only when the hRad51 concentration is suboptimal (9, 10).

Given the central role of hRad51 in recombination processes and the fact that the activities of hRad51 are apparently subject to modulation by tumor suppressor proteins such as BRCA2 (reviewed in Ref. 12), establishing an efficient hRad51-mediated DNA strand exchange system will be important for dissecting the functional interactions among hRad51, other recombination factors, and tumor suppressors. In this work, a variety of reaction parameters that could influence the recombinase activity of hRad51 were explored. We demonstrate that under certain conditions, hRad51 makes DNA joints avidly and promotes highly efficient strand exchange over at least 5.4 kilobase pairs. Importantly, under the new reaction conditions, the efficiency of the hRad51-mediated DNA strand exchange reaction is strongly dependent on hRPA over a wide range of Rad51 concentrations tested.

EXPERIMENTAL PROCEDURES

DNA Substrates—φX174 viral (+)-strand was purchased from New England Biolabs and φX174 replicative form I DNA was from Life Technologies, Inc. The replicative form I DNA was linearized with *Apa*LI. The pBluescript DNA was prepared from *E. coli* XL-1 Blue (Stratagene), purified by banding in cesium chloride gradients, and linearized with *Bsa*I. The oligonucleotides (83-mer) used in strand exchange were: oligo 1, 5′-AAATGAACATAAGATAAATAAGTATAAGGATAATACAAAATAAGTAAATGAATAAACATAGAAAATAAAGTAAAGGATATAAA; oligo 2, the exact complement of oligo 1. Oligo 2 was labeled at the 5′ end with [γ-^{32}P]ATP and T4 polynucleotide kinase and then annealed to oligo 1. The labeled duplex was purified from 10% polyacrylamide gels by overnight diffusion at 4 °C into TAE buffer (40 mM Tris acetate, pH 7.4, 0.5 mM EDTA). DNA substrates were stored in TE (10 mM Tris-HCl, pH 7.5, with 0.5 mM EDTA).

Plasmids—Plasmid pRh51.1 consists of human *RAD51 K313* cDNA under the control of the T7 promoter in vector pET11 (Novagen). Plasmid pRh51.1 was then subject to *in vitro* mutagenesis using the QuikChange kit (Stratagene), to change Lys^{313} (AAA codon) to a glutamine residue (CAA codon). The resulting plasmid, pRh51.2, was sequenced to ensure that no other undesired change has occurred in the *RAD51* sequence. Plasmid p11d-tRPA (13), which coexpresses all three subunits of hRPA, was used for purification of this factor.

Cell Growth—Plasmids pRh51.1 and pRh51.2 were introduced into the RecA-deficient *E. coli* strain BLR (DE3) with pLysS. Following transformation, single clones were picked and grown for 15 h in 30 ml of Luria broth. The starter culture was diluted 200 times with fresh

* This work was supported by United States Public Health Service Grants RO1 ES07061, RO1GM57814, and PO1 CA81020, Army Research Grant DAMD 17-98-1-8247, and Army Training Grant DAMD17-99-1-9402. The costs of publication of this article were defrayed in part by the payment of page charges. This article must therefore be hereby marked "*advertisement*" in accordance with 18 U.S.C. Section 1734 solely to indicate this fact.

‡ To whom correspondence should be addressed. Tel.: 210-567-7216; Fax: 210-567-7277; E-mail: sung@uthscsa.edu.

[1] The abbreviations used are: ssDNA, single-stranded DNA; dsDNA, double-stranded DNA.

Luria broth and incubated at 37 °C. When the A_{600} of the cultures reached 0.6 to 1, isopropyl-1-thio-β-D-galactopyranoside was added to 0.4 mM and the induction of hRad51 continued at 37 °C for 4 h. Cells were harvested by centrifugation and stored frozen at −70 °C. Plasmid p11d-tRPA was introduced into *E. coli* strain BL21 (DE3) and the induction of hRPA was carried out as described previously (13).

Protein Purification—All the following steps were carried out at 4 °C. For the purification of hRad51 Lys^{313} and hRad51 Gln^{313} proteins, *E. coli* cell paste, 30 g from 20 liters of culture, was suspended in 150 ml cell breakage buffer (50 mM Tris-HCl, pH 7.5, 5 mM EDTA, 200 mM KCl, 2 mM dithiothreitol, 10% sucrose, and the following protease inhibitors: aprotinin, chymostatin, leupeptin, and pepstatin A at 3 μg/ml each, and 1 mM phenylmethylsulfonyl fluoride) and then passed through a French press once at 20,000 p.s.i. The crude lysate was clarified by centrifugation (100,000 × *g*, 120 min), and the supernatant (Fraction I) was treated with ammonium sulfate at 0.23 g/ml to precipitate hRad51 and about 20% of the total extract protein. The ammonium sulfate pellet was dissolved in 300 ml of T buffer (30 mM Tris-HCl, pH 7.4, 10% glycerol, 0.5 mM EDTA, 0.5 mM dithiothreitol) with the set of protease inhibitors used in extract preparation, and then clarified by centrifugation (10,000 × *g* for 30 min). The cleared protein solution (Fraction II) was then applied onto a column of Q-Sepharose (2.6 × 6 cm; total 30-ml matrix) equilibrated in T buffer with 100 mM KCl and eluted with a 400 ml of gradient of 100 to 600 mM KCl in T buffer. The peak of hRad51 (Fraction III), eluting at about 330 mM KCl (60 ml), was dialyzed against T buffer with 100 mM KCl and then fractionated in a column of Affi-Gel Blue (Bio-Rad; 1.6 × 5 cm; total 10-ml matrix) with a 100-ml gradient of 100 to 2000 mM KCl in T buffer. The hRad51 protein eluted from Affi-Gel Blue at 800 to 1200 mM KCl, and the pool of which (Fraction IV; 20 ml) was dialyzed against T buffer with 100 mM KCl and fractionated in a column of Macro hydroxyapatite (Bio-Rad; 1 × 7.5 cm; total 6-ml matrix) with a 100-ml 30 to 320 mM KH_2PO_4 gradient in buffer T. hRad51 eluted from 150 to 220 mM KH_2PO_4, and the peak fractions were pooled (Fraction V; 15 ml containing 7.5 mg of hRad51), dialyzed against T buffer with 50 mM KCl, and applied onto a Mono S column (HR5/5), which was developed with a 30-ml 100 to 400 mM KCl gradient in buffer T. The Mono S fractions containing the peak of hRad51, eluting at about 250 mM KCl, were pooled (Fraction VI; 4 ml containing 6 mg of hRad51), diluted with an equal volume of 10% glycerol and then fractionated in Mono Q (HR 5/5) with a 30-ml 100 to 600 mM KCl gradient. The final pool of hRad51 (Fraction VII; 3 ml containing 5 mg of hRad51 in ~350 mM KCl) was concentrated in Centricon-30 microconcentrators and stored at −70 °C. The hRad51 concentration was determined using the calculated molar extinction coefficient of 12,800 M^{-1} cm^{-1} at 280 nM (10).

For the purification of hRPA, extract was made from *E. coli* BL21 (DE3) harboring the plasmid p11d-tRPA (13) and subjected to the purification procedure we have used for yRPA (14). The concentration of hRPA was determined by comparison of multiple loadings of hRPA against known amounts of bovine serum albumin and ovalbumin in a Coomassie Blue R-stained polyacrylamide gel.

DNA Strand Exchange System That Uses φX174 DNA—All the reaction steps were carried out at 37 °C. In Fig. 2, the reaction (50 μl final volume) was assembled by mixing hRad51 (7.5 μM) added in 2 μl of storage buffer and φX174 viral (+)-strand (30 μM nucleotides) added in 2 μl in 40 μl of buffer R (40 mM Tris-HCl, pH 7.8, 2 mM ATP, 1 mM $MgCl_2$, 1 mM dithiothreitol, and an ATP regenerating system consisting of 8 mM creatine phosphate and 28 μg/ml creatine kinase). After a 5-min incubation, hRPA (2 μM) in 2 μl of storage buffer was added, followed by a 5-min incubation, and then 5 μl of ammonium sulfate (1 M stock, final concentration of 100 mM), followed by another 1-min incubation. To complete the reaction, linear φX174 replicative form I DNA (30 μM nucleotides) in 3 μl of TE and 4 μl of 50 mM spermidine (4 mM) were incorporated. At the indicated times, 4.5-μl portions were withdrawn, mixed with 7 μl of 0.8% SDS and 800 μg/ml proteinase K, incubated for 15 min before electrophoresis in 0.9% agarose gels in TAE buffer. The gels were stained in ethidium bromide (2 μg/ml in H_2O) for 1 h, destained for 12 to 18 h in a large volume of water, and then subjected to image analysis in a NucleoTech gel documentation station equipped with a CCD camera using Gel Expert for quantification of the data. Unless stated otherwise, the reaction mixtures in other experiments were assembled in the same manner with the indicated amounts and order of addition of reaction components, except that they were scaled down two and one-half times.

DNA Strand Exchange System That Employs Oligonucleotides—The reaction mixture had a final volume of 12.5 μl and the steps were carried out at 37 °C. hRad51 (7.5 μM) was incubated with oligonucleotide 2 (30 μM nucleotides) in 10 μl of buffer R. The reaction mixture was completed by adding ammonium sulfate in 1 μl, 1 μl of 50 mM spermidine, and the radiolabeled duplex (30 μM nucleotides) in 0.5 μl. At all the times indicated, a 3-μl portion of the reaction mixture was deproteinized as described above and then subjected to electrophoresis in 10% polyacrylamide gels run in TAE buffer. The level of DNA strand exchange was determined by PhosphorImager analysis of the dried gels.

Examination of Interaction between hRad51-ssDNA Filament and Duplex DNA—Oligonucleotides F1 and F1b (Midland) both have the sequence 5′-TGGCTTGAACGCGTCATGGAAGCGATAAAACTCTGCA-GGTTGGATACGCCAATCATTTTTATCGAAGCGCGCCGCCC-3′, except that the latter also contains a biotin molecule positioned at the 5′ terminus. In these oligonucleotides, nucleotide residues 11 to 72 are complementary to positions 5348 to 23 of the φX (+)-strand DNA. These oligonucleotides were hybridized to φX (+)-strand by incubating a 3 M excess of the oligonucleotide with the latter in buffer containing 50 mM Tris-HCl, pH 7.5, 10 mM $MgCl_2$, 100 mM NaCl, and 1 mM dithiothreitol. The F1-φX (+)-strand and F1b-φX (+)-strand hybrids (30 μM nucleotides) were mixed with 10 μl of magnetic beads containing streptavidin (Roche Molecular Biochemicals) in binding buffer containing 10 mM Tris-HCl, pH 7.5, 100 mM KCl, and 1 mM EDTA for 10 min at 37 °C. About 70% of the F1b-(+)-strand hybrid was immobilized on the beads, whereas, as expected, less than 5% of the F1-(+)-strand hybrid was retained. To assemble hRad51 filament on the immobilized φX (+)-strand, magnetic beads preloaded with the F1b-φX (+)-strand hybrid were incubated with 4 μM hRad51 in 20 μl of buffer R. Reproducibly, ~85% of the hRad51 was bound to the magnetic beads under the stated conditions, as determined by eluting the bound hRad51 with 2% SDS followed by SDS-polyacrylamide gel electrophoresis and staining with Coomassie Blue; this procedure gave an immobilized hRad51-ssDNA nucleoprotein complex of ~3 nucleotides/hRad51 monomer. The magnetic beads containing hRad51-ssDNA complex was then washed once each with 20 μl of buffer R with 0.01% Nonidet P-40 and 20 μl buffer R, before being incubated with linear φX duplex (8 μM nucleotides) for 3 min at 37 °C in 20 μl of buffer R containing 4 mM spermidine and the indicated concentrations of ammonium sulfate. The beads were treated with 20 μl of 2% SDS at 37 °C for 5 min to elute bound duplex and hRad51. The supernatants and SDS eluates were analyzed in agarose gels followed by staining with ethidium bromide to quantify DNA and in polyacrylamide gels with Coomassie Blue staining to determine the amount of hRad51. As controls, magnetic beads alone, magnetic beads preincubated with the F1-φX (+)-strand hybrid, and magnetic beads preincubated with F1b but without φX (+)-strand were similarly incubated with the linear φX duplex and then processed for analyses.

RESULTS

Recombination Factors—The cDNA for hRad51 was amplified from a human B-cell cDNA library. Sequencing of the *hRAD51* cDNA insert revealed that it was identical to one of the published *hRAD51* sequences (15) but differed from the other sequence (16) at amino acid residue 313; the former has a lysine (an AAA codon) while the latter has a glutamine (a CAA codon) at this position. The cloned cDNA was subjected to targeted mutagenesis to change lysine 313 to glutamine. Both hRad51 Lys^{313} and hRad51 Gln^{313} variants were expressed in *E. coli* and purified to near homogeneity (Fig. 1*A*). The two hRad51 isoforms behaved identically during purification and gave indistinguishable results in all the enzymatic assays described here. Only the results with hRad51 Lys^{313} are shown. We presume that the two hRad51 isoforms correspond to naturally occurring polymorphic variants. For DNA strand exchange experiments, the human ssDNA binding factor replication protein A (hRPA), a heterotrimer of 70-, 32-, and 14-kDa subunits, was also purified to near homogeneity (Fig. 1*B*) from *E. coli* cells harboring a plasmid which coexpresses all three subunits of this factor (13).

System for ATP-dependent Homologous DNA Pairing and Strand Exchange—For characterizing the homologous DNA pairing and strand exchange activity of hRad51, we used as substrates φX 174 viral (+)-strand and linear duplex that are 5.4 kilobase pairs in length (Ref. 6; schematic shown in Fig. 2*A*). In this system, hRad51 is preincubated with the (+)-strand, followed by the addition of hRPA, and the linear duplex

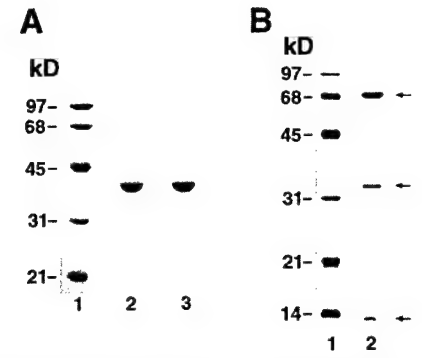

FIG. 1. **Recombination factors.** *A*, purified hRad51 Lys^{313} (*lane 2*) and hRad51 Gln^{313} (*lane 3*), 3 μg each, were analyzed in an 11% SDS-polyacrylamide gel and stained with Coomassie Blue. *B*, purified hRPA, 3 μg in *lane 2*, was analyzed in a 12.5% SDS-polyacrylamide gel and stained with Coomassie Blue. The three subunits of hRPA are denoted by the *arrows*.

is incorporated last. Pairing between the DNA substrates yields a joint molecule, and branch migration, if successful, over 5.4 kilobase pairs produces nicked circular duplex as product (Fig. 2*A*). We have examined a variety of reaction conditions including the levels of magnesium, pH, and various types of salt on the hRad51 recombinase activity. As documented below, the most dramatic effects were seen with the addition of salts.

We tested the effects of increasing concentrations of potassium acetate, potassium chloride, potassium phosphate, potassium sulfate, ammonium chloride, and ammonium sulfate, and found that while all of these salts were stimulatory, ammonium sulfate produced the most stimulation, followed by potassium sulfate. *Panel I* in Fig. 2*B* shows a time course experiment in which 7.5 μM hRad51 was used with 2 μM hRPA, ϕX (+)-strand (30 μM nucleotides), and ϕX linear duplex (30 μM nucleotides) in pH 7.8 buffer and 100 mM ammonium sulfate. Following the published conditions of Baumann and West (9, 10), another reaction was also carried out in which hRad51, at 5 μM, was used with 1 μM hRPA and the same concentrations of DNA substrates and 80 mM potassium acetate at pH 7.5 (Fig. 2*B*, *panel II*). The results showed a much higher level of DNA strand exchange under the new conditions. Specifically, whereas no full strand exchange product (nicked circular duplex) was detected under the published conditions (Fig. 2, *B*, *panel II*, and *C*, *panel I*) (9, 10), the inclusion of ammonium sulfate resulted in conversion of ~30 and ~60% of the linear duplex to nicked circular duplex after 30 and 60 min, respectively (Fig. 2, *B*, *panel I*, and *C*, *panel I*). Overall, there was a 3–4-fold increase in total products (joint molecules plus nicked circular duplex) in the reaction that employed ammonium sulfate (Fig. 2*C*, *panel II*). Even though 100 mM ammonium sulfate was found to be optimal, highly significant levels of homologous DNA pairing and complete DNA strand exchange were seen at reduced concentrations (50 and 75 mM) of the salt (data not shown).

In published studies (9, 10), 80 mM potassium acetate was employed. In agreement with the published work (9, 10), neither higher (up to 200 mM in 20 mM increments) nor lower concentrations of potassium acetate would improve homologous DNA pairing and strand exchange efficiency beyond the level seen in *panel II* of Fig. 2*B*. As expected from published work (8), omission of ATP from the reaction abolished strand exchange, either under our reaction conditions (Fig. 2*B*, *panel I*, *lanes 10–12*) or the published conditions (Fig. 2*B*, *panel II*, *lanes 11–13*) (9, 10).

Thus, the inclusion of ammonium sulfate renders hRad51-mediated ATP-dependent homologous DNA pairing and strand exchange highly efficient. Under the new reaction conditions, the optimal levels of hRad51 for pairing and strand exchange were found to be between 2 and 4 nucleotides/protein monomer. Increasing hRad51 above 2 nucleotides/protein monomer resulted in gradual inhibition (data not shown), which was likely due to binding of hRad51 to the duplex and its sequestration from pairing with the hRad51-ssDNA complex (7, 9).

Dependence on hRPA—In the yRad51-mediated DNA strand exchange reaction that uses plasmid length DNA substrates, a strong dependence of the reaction efficiency on yRPA has been observed (2, 4). However, in the published work, when hRad51 was used at the optimal ratio of 3 nucleotides of ssDNA/hRad51 monomer, hRPA has no stimulatory effect on the reaction efficiency, and relatively high levels of hRPA were in fact strongly inhibitory (9, 10). We have examined whether under the newly devised reaction conditions, hRPA is required for strand exchange efficiency. Fig. 3 summarizes the results obtained with 7.5 μM hRad51, 30 μM nucleotides of ssDNA, 100 mM ammonium sulfate, and increasing concentrations of hRPA, from 0.4 to 4.0 μM. Whereas only negligible pairing and strand exchange was seen in the absence of hRPA, increasing concentrations of hRPA gave progressively higher levels of products (Fig. 3, panels I and *II*). The optimal level of hRPA was ~2 μM, although addition of as little as 0.4 μM hRPA gave highly notable stimulation. Importantly, increasing the hRPA concentration to 4 μM did not lower the level of products, which is very different from published studies (10) in which concentrations of hRPA $\geq$0.8 μM were found to be strongly inhibitory.

Additional experiments revealed that at levels of hRad51 higher (2 nucleotides/hRad51 monomer) or lower (6 nucleotides/hRad51 monomer) than that (4 nucleotides/hRad51 monomer) used in Fig. 3, there is also a similar dependence of homologous pairing and strand exchange on hRPA. Likewise, at ammonium sulfate levels higher and lower than that used in prior experiments, we have also observed a similar dependence of the strand exchange reaction on hRPA. Control experiments confirmed that hRPA by itself does not have homologous pairing and strand exchange activity under the new conditions (data not shown). In summary, under our reaction conditions, there is a uniform dependence of DNA strand exchange on hRPA, regardless of the amount of hRad51 used.

Effect of Order of Addition of Salt and Heterologous DNA—In the experiments described thus far, ammonium sulfate was added to the reaction mixture after hRad51 had already nucleated onto the ssDNA but before the incorporation of hRPA. We have also examined whether the addition of ammonium sulfate at other stages would affect the reaction efficiency, as such an endeavor could yield important clues as to the basis of stimulation. As shown in Fig. 4, similar levels of homologous DNA pairing and strand exchange were observed when ammonium sulfate was added at the beginning with hRad51, after hRad51 but before the incorporation of hRPA (as in the standard reaction), and after hRPA but before the incorporation of the duplex. Interestingly, when ammonium sulfate was incorporated a few minutes after the duplex, there was little product formed even at the reaction end point of 60 min (Fig. 4*A*, *lanes 11–13*). Since dsDNA coated with hRad51 or yRad51 has been found to be inactive in the DNA strand exchange reaction (7, 9), we considered the possibility that perhaps the suppression of DNA strand exchange seen with ammonium sulfate being added after the duplex might have stemmed from free hRad51 binding to the duplex (7). However, two lines of evidence strongly suggest that this was not the main reason for the lack of strand exchange stimulation. First, even at levels of hRad51 (6 nucleotides and 9 nucleotides of ssDNA/hRad51 monomer) lower than that (4 nucleotides ssDNA/hRad51 monomer) used in Fig.

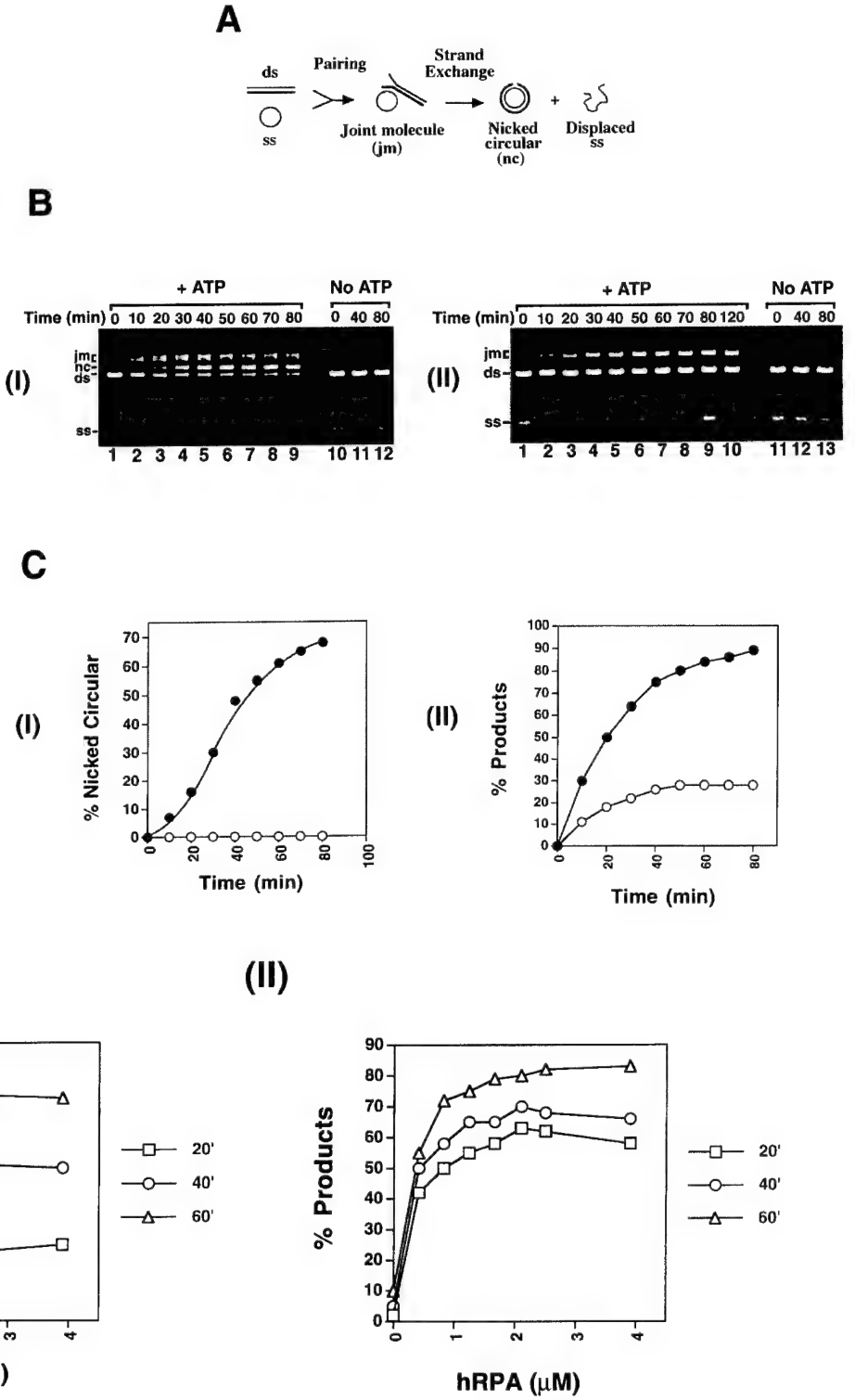

FIG. 2. **Homologous DNA pairing and strand exchange by hRad51 and hRPA.** *A*, schematic of the reaction. The ϕX174 viral (+)-strand (*ss*) is paired with the linear homologous duplex (*ds*) to form joint molecules (*jm*), and strand exchange over the length of the DNA (5.4 kilobase pairs) yields nicked circular duplex (*nc*) and linear ssDNA as products. *B*, hRad51-mediated homologous DNA pairing and strand exchange. *Panel I* shows reactions carried out with ammonium sulfate as salt and with ATP (*lanes 1–9*) or without ATP (*lanes 10–12*). The reactant concentrations were: 7.5 μM hRad51, 2 μM hRPA, 30 μM (in nucleotides) each of ssDNA and dsDNA. *Panel II* shows reactions carried out as described by Baumann and West (9, 10), with ATP (*lanes 1–10*) or without it (*lanes 11–13*). The reactant concentrations were: 5 μM hRad51, 1 μM hRPA, and 30 μM (in nucleotides) each of ssDNA and dsDNA. *C*, in *panel I*, the time courses of conversion of the input linear duplex into nicked circular duplex in the experiments in *panels I* (●) and *II* (○) of *B* are graphed. In *panel II*, the time courses of conversion of the input linear duplex into total products (joint molecules and nicked circular duplex) in the experiments in *panels I* (●) and *II* (○) of *B* are graphed.

FIG. 3. **Dependence of homologous DNA pairing and strand exchange on hRPA.** hRad51 at 7.5 μM was incubated with 30 μM ϕX ssDNA with or without increasing concentrations of hRPA, and the resulting hRad51-ssDNA nucleoprotein filaments were reacted with linear ϕX dsDNA for 20 (□), 40 (○), and 60 (△) min. In *panel I*, the level of full DNA strand exchange, as measured by the percent conversion of the input linear duplex to nicked circular duplex, was graphed. In *panel II*, the level of total products, joint molecules plus nicked circular duplex, was graphed.

4 and with much longer preincubation of hRad51 with ssDNA to minimize the level of free hRad51, addition of ammonium sulfate before the duplex molecule is still necessary to see significant strand exchange (data not shown). Second, an excess of a heterologous duplex (pBluescript) added together with the homologous duplex or before the homologous duplex, in an attempt to titrate out any free hRad51, also did not compensate for the stimulatory effect of adding ammonium sulfate before the homologous duplex (see below). Taken together, the results strongly suggested that the lack of DNA strand exchange when ammonium sulfate was incorporated after the homologous duplex was due to a reason other than free hRad51 coating the duplex molecule.

Interestingly, whereas the incorporation of increasing

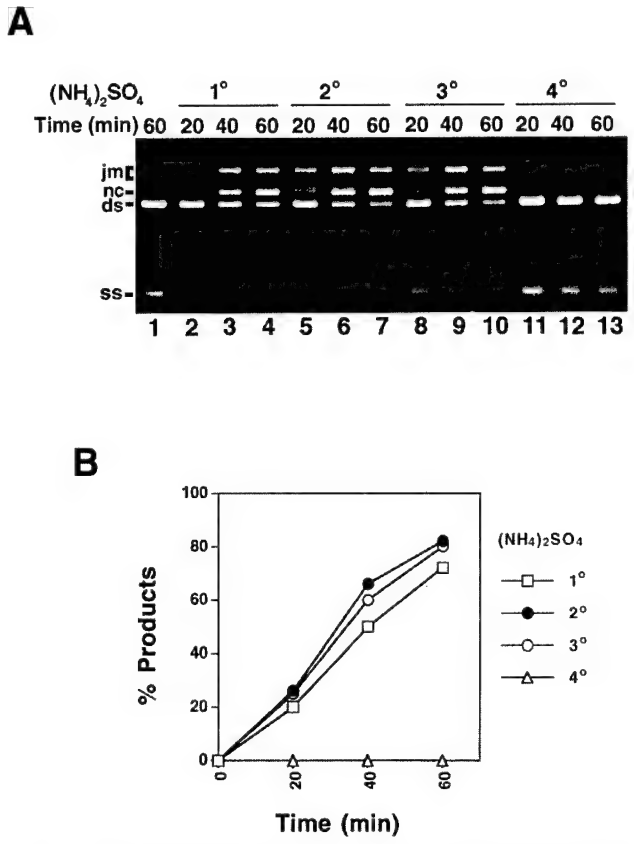

FIG. 4. **Order of addition of salt is critical for reaction efficiency.** *A*, ammonium sulfate (100 mM) was added at the same time as hRad51 to ϕX ssDNA (1°), after ϕX ssDNA had been preincubated with hRad51 (2°), after ϕX ssDNA had been preincubated first with hRad51 and then with hRPA (3°), or added 3 min after the duplex had already been incorporated into the reaction (4°). The complete reaction mixtures were incubated for 20, 40, and 60 min and processed for gel analysis. In *lane 1*, DNA substrates were incubated in the absence of recombination proteins. The reactant concentrations were: hRad51 at 7.5 μM, ϕX ssDNA at 30 μM nucleotides, hRPA at 2 μM, and ϕX dsDNA at 30 μM nucleotides. *B*, the levels of total products, joint molecules plus nicked circular duplex, were graphed.

amounts of the heterologous pBluescript duplex in the presence of ammonium sulfate lowered the reaction efficiency only slightly (Fig. 5, *A, panel I*, and *B, panel I*), the addition of pBluescript duplex before ammonium sulfate resulted in much more pronounced inhibition (Fig. 5, *A, panel II*, and *B, panel II*). These results, coupled with those presented above, indicated that binding of duplex to the hRad51-ssDNA nucleoprotein filament, regardless of whether the duplex is homologous to the ssDNA situated in the hRad51 filament, has a strong suppressive effect on pairing and strand exchange, unless salt is already present.

In summary, the results have revealed a strict dependence of homologous DNA pairing and strand exchange efficiency on ammonium sulfate being incorporated into the reaction prior to the duplex, and they suggest that ammonium sulfate exerts its stimulatory effect via modulation of the interactions between the hRad51-ssDNA nucleoprotein complex and the incoming duplex molecule. This premise is further tested and verified in the experiments below.

Dependence of Strand Exchange Efficiency on Interactions between Duplex and hRad51-ssDNA Complex—Extensive biochemical studies conducted with RecA have revealed that the incoming duplex molecule is bound only transiently within the RecA-ssDNA nucleoprotein filament (4, 5, see "Discussion"). We reasoned that if the hRad51-ssDNA filament has a relatively high affinity for the duplex, then the DNA homology search process might occur efficiently only when the association of the duplex molecule and the hRad51-ssDNA nucleoprotein filament is rendered transient, which could conceivably be realized by salt inclusion.

Intrinsic to this hypothesis are two predictions. First, it might be expected that the salt dependence of the homologous DNA pairing and strand exchange process would be lessened with reduction in the length of the DNA substrates, such as when oligonucleotides are used (11) (see Fig. 6*A* for schematic). This is because the extent of interactions of a short duplex with the limited length of hRad51-ssDNA nucleoprotein filament assembled on a short single-strand would not be extensive. Furthermore, the search for DNA homology with short DNA substrates would not be as rate-limiting as when ϕX DNA substrates are used, because the probability of productive collisions between two short substrates leading to their homologous registry should be considerably higher. As predicted, when the DNA substrates used were based on 83-mer oligonucleotides, the rate of homologous pairing between the substrates was the same in the absence of salt as when ammonium sulfate was present at 25 mM, and higher levels of ammonium sulfate were in fact inhibitory (Fig. 6, *B* and *C*).

Second, if salt indeed acted to weaken the interaction between the duplex and the hRad51-ssDNA nucleoprotein complex, then we would expect to see lessened binding of the duplex molecule to the hRad51-ssDNA complex when ammonium sulfate was present. To test this premise experimentally, we examined the interaction of ϕX linear dsDNA with hRad51-ϕX ssDNA complex immobilized on streptavidin magnetic beads via a short biotinylated oligonucleotide, called F1b, which is complementary to a portion of the ϕX (+)-strand (see schematic in *panel I* of Fig. 7*A* and "Experimental Procedures"). Analysis of the SDS eluate of the magnetic beads allowed us to determine the amount of duplex DNA that had bound to the immobilized hRad51-ssDNA complex (Fig. 7*A, panel I*). As shown in Fig. 7*A, lanes 1* and *2* in *panel II*, incubation of the duplex with bead-immobilized hRad51-ssDNA complex in the absence of ammonium sulfate resulted in >90% retention of the duplex on the beads. Binding of the duplex to the magnetic beads was due to its interaction with the immobilized hRad51-ssDNA complex, because little retention of the duplex DNA occurred with magnetic beads pretreated with hRad51 and ϕX (+)-strand hybridized to an oligonucleotide, F1, that had identical sequence to F1b but lacked the biotin tag of the latter (Fig. 7*A, lanes 3* and *4* in *panel II*). As expected, only the background level of duplex retention was seen with beads containing the F1b-ϕX (+)-strand hybrid but without hRad51, with DNA-free beads preincubated with hRad51, and with beads that contained only the F1b oligonucleotide and preincubated with hRad51 (Fig. 7*A, lanes 5–10* in *panel II*).

Once the utility of the assay system was verified, we proceeded to test the effect of ammonium sulfate on the interactions of duplex DNA with the immobilized hRad51-ssDNA complex. The results revealed gradual weakening of the duplex/hRad51-ssDNA complex interactions by increasing levels of ammonium sulfate. Specifically, whereas greater than 90% retention of the duplex occurred in the absence of ammonium sulfate, less than 10% of the duplex was bound at 100 mM of the salt (Fig. 7, *B, upper panel*, and *C*). Analysis of the amount of hRad51 in the various SDS eluates showed that even the highest concentration of ammonium sulfate did not cause significant turnover of hRad51 from the bound ssDNA (Fig. 7*B, lower panel*). Taken together, we concluded that ammonium sulfate indeed weakens the binding of duplex DNA to the hRad51-

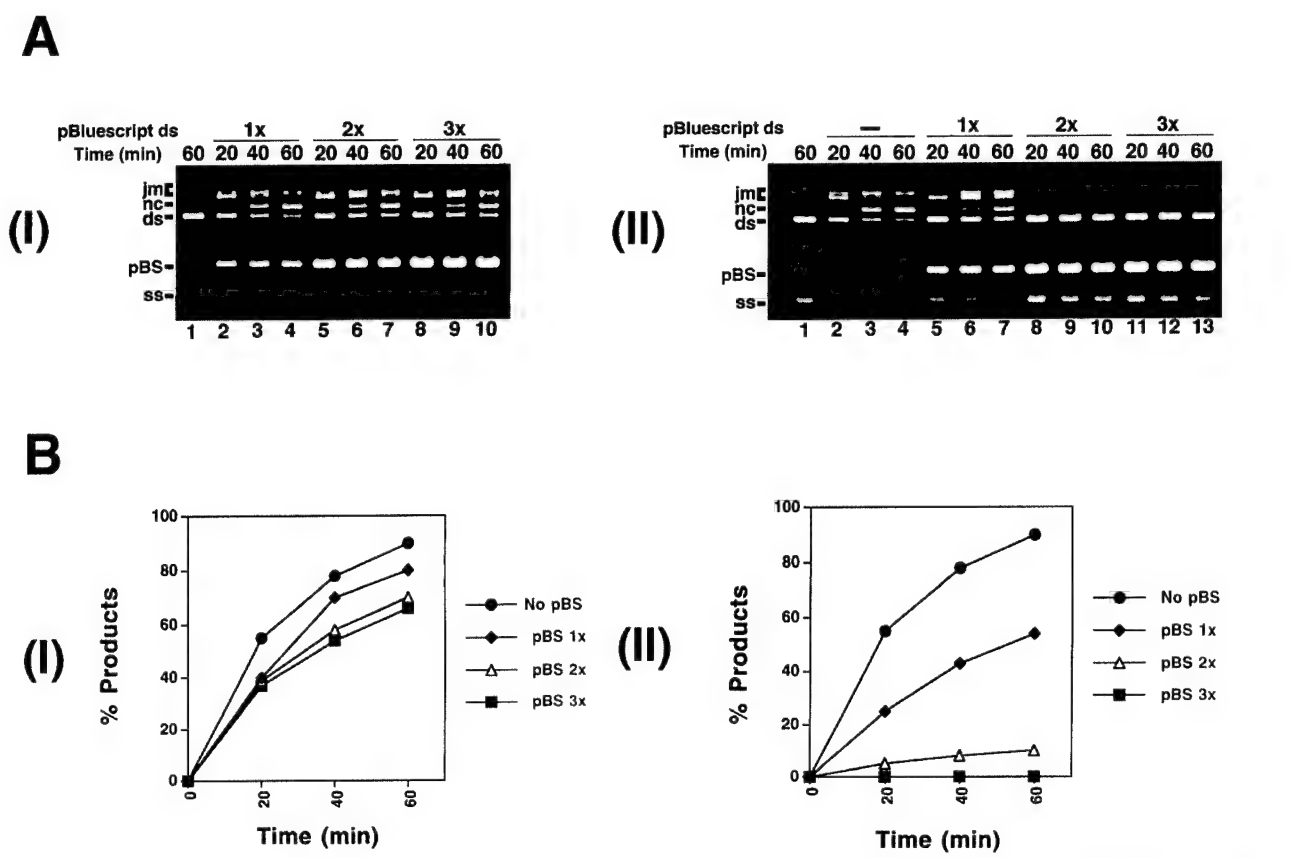

FIG. 5. **Effect of heterologous duplex.** *A*, increasing concentrations of pBluescript (1 to 3 times the concentration of ϕX dsDNA) was added in the presence of ammonium sulfate (*panel I*) or 3 min before the incorporation of ammonium sulfate (*panel II*) to presynaptic complex assembled with hRad51 (7.5 μM), hRPA (2 μM), and ϕX ssDNA (30 μM nucleotides). Following the incorporation of ϕX duplex (30 μM nucleotides), the reaction mixtures were incubated for the indicated times. The concentration of ammonium sulfate was 100 mM. In *lane 1* of both panels, DNA substrates were incubated in the absence of recombination proteins. *B*, the levels of total products, joint molecules plus nicked circular duplex, in *A* were graphed. *Panel I* shows the levels of products (joint molecules and nicked circular duplex) when pBluescript was added after ammonium sulfate and *panel II* shows the levels of products when pBluescript was added before ammonium sulfate.

ssDNA complex. Other experiments revealed that pBluescript duplex also binds to the immobilized hRad51-ϕX ssDNA complex in a manner that is reduced by ammonium sulfate (data not shown), indicating that the hRad51-ssDNA complex can interact with both homologous and heterologous duplex molecules.

Interestingly, potassium acetate lessened the interaction between the duplex and the immobilized hRad51-ssDNA complex only slightly (Fig. 7*C*), and as expected, the hRad51-ssDNA complex was stable to potassium acetate (data not shown). Since potassium acetate is much less effective in the homologous pairing and strand exchange reaction (Fig. 2) (9, 10), the observation in Fig. 7*C* is again consistent with the suggestion that ammonium sulfate stimulates homologous pairing and strand exchange by attenuating the affinity of the hRad51-ssDNA nucleoprotein filament for the incoming duplex.

In the DNA strand exchange experiments, we found that the order of addition of ammonium sulfate relative to duplex DNA was important for ensuring strand exchange efficiency, such that if duplex DNA was added before ammonium sulfate, only negligible pairing and strand exchange was observed (see Fig. 4). Given this observation, we wanted to test whether the level of duplex retention by bead-immobilized hRad51-ssDNA complex would change with the order of addition of ammonium sulfate. To examine this, we used three different concentrations of ammonium sulfate (25, 50, and 100 mM) and added the salt either before the incorporation of duplex or after the duplex had already been preincubated with the bead-immobilized hRad51-ssDNA complex. The results from this experiment revealed that more of the duplex becomes associated with the hRad51-ssDNA complex with preincubation of duplex and Rad51-ssDNA complex prior to salt addition (Fig. 7*D*).

The experiments in Fig. 7 were conducted with hRad51-ssDNA nucleoprotein complex assembled in the absence of hRPA. We have obtained similar results when hRPA was included in the binding reaction (data not shown).

DISCUSSION

Homologous DNA Pairing and Strand Exchange by hRad51 and hRPA—Both hRad51 and yRad51 are related in amino acid sequence and biological function to *E. coli* RecA. Like RecA, yRad51 forms nucleoprotein filaments on ssDNA and dsDNA in an ATP-dependent manner. Biochemical studies have indicated that the search for DNA homology in the incoming duplex DNA molecule and formation of heteroduplex joints with the duplex occur within the confines of the RecA-ssDNA and yRad51-ssDNA nucleoprotein filaments, which are also referred to presynaptic filaments. The assembly of the recombinase-ssDNA nucleoprotein filaments and the efficiency of subsequent homologous pairing and strand exchange are stimulated by the single-strand binding factor, SSB for RecA and yRPA for yRad51 (2, 4, 5). In the presence of ATP, hRad51 also forms a filament on ssDNA similar in structure to the equivalent nucleoprotein filaments assembled with RecA and yRad51 (3–5). However, published studies have suggested that hRad51 has only a modest ability to make DNA joints and an even lower capacity to promote DNA strand exchange. These published observations have suggested that either hRad51 partic-

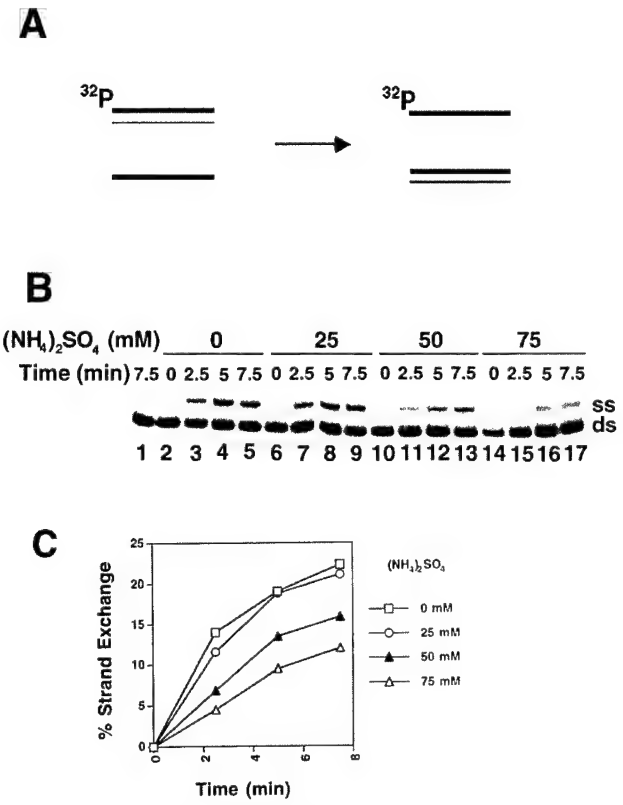

FIG. 6. **Homologous pairing with oligonucleotide-based substrates is independent of salt.** *A*, pairing and strand exchange between the unlabeled single-stranded oligonucleotide with the ^{32}P-labeled duplex results in displacement of the radiolabeled single strand. *B*, hRad51 was incubated with the 83-mer oligonucleotide and the resulting nucleoprotein filament was reacted with the homologous duplex in the absence of salt or with increasing concentrations of ammonium sulfate, as indicated. In *lane 1*, DNA substrates were incubated in the absence of hRad51. *C*, the results from PhosphorImager analysis of the gel in *B* were plotted.

ipates in making DNA joints without catalyzing much DNA strand exchange, as discussed before (3), or that other reaction conditions are in fact required to reveal the strand exchange activity in hRad51. To entertain the latter possibility, we have explored a variety of reaction parameters for their effect on the hRad51 recombinase activity, and have shown that when ammonium sulfate is included, an avid capability of hRad51 to catalyze DNA joint formation and strand exchange is revealed. Moreover, formation of nicked circular duplex, the product of full DNA strand exchange, becomes completely dependent on hRPA. The dependence of homologous DNA pairing and strand exchange on hRPA is seen over a wide range of hRad51 concentrations, from below and above the optimal level. The requirement for hRPA in homologous DNA pairing and strand exchange is very likely due to its ability to minimize secondary structure in DNA, thus facilitating the assembly of a contiguous hRad51-ssDNA filament, as suggested in previous studies (2–5).

In summary, the results presented here demonstrate an intrinsic ability of hRad51 to form DNA joints efficiently and to catalyze a substantial amount of DNA strand exchange. These findings also reveal the functional dependence of hRad51 recombinase on the ssDNA binding factor hRPA. The ability of hRad51 and hRPA to promote DNA joint formation and extension of nascent heteroduplex joints by strand exchange is likely to be indispensable for various recombination reactions *in vivo*.

Possible Basis for Salt Stimulation of Homologous DNA Pairing and Strand Exchange—Extensive biochemical studies have revealed the presence of two distinct DNA-binding sites in the RecA protein filament, with the initiating ssDNA substrate viewed as being situated within the "primary" site, while the incoming duplex molecule is bound within the "secondary" site of the presynaptic filament (4, 5). The search for DNA homology in the duplex DNA occurs by way of reiterative binding and release of the duplex until homology is located. For this random collision mode of DNA homology search to work efficiently, the incoming duplex molecule must be retained only transiently within the secondary site of the recombinase-ssDNA filament. Consistent with this deduction, evidence has been presented to suggest that the RecA-ssDNA filament has modest affinity for duplex DNA (4).

Given the structural and functional similarities between hRad51 and RecA, it seems reasonable to suggest that DNA homology conducted by the hRad51-ssDNA presynaptic filament also occurs by means of random association/dissociation of the duplex molecule with the former, with efficient homology search to be dictated by transient, rather than stable, association of the incoming duplex with the presynaptic filament. We have presented two lines of evidence to support the notion that salt exerts its remarkable stimulatory effect by weakening the interactions of the duplex molecule with the hRad51-ssDNA filament, thereby enhancing the rate of turnover and the efficiency at which the duplex can be sampled for homology. First, we have shown that the dependence of the homologous DNA pairing and strand exchange process on salt is alleviated if the length of the DNA substrates is reduced, as when oligonucleotides are used. This is likely due to the increased probability for productive collisions between the two oligonucleotide substrates that lead to homologous registry and also because the interactions between the duplex and the short presynaptic filament of hRad51 assembled on the ss oligonucleotide are similarly minimized. Furthermore, we have provided direct evidence that binding of a duplex molecule to hRad51 presynaptic filament is weakened by the inclusion of ammonium sulfate.

In summary, we surmise from the biochemical results that the hRad51-ssDNA filament binds duplex DNA in the available secondary site with high affinity, thus limiting efficient sampling of the duplex molecule for DNA homology. Accordingly, stimulation of homologous DNA pairing is realized by salt addition, with the degree of stimulation being dependent on the effectiveness of a particular salt to weaken the affinity of the hRad51-ssDNA nucleoprotein filament for the duplex molecule. We further suggest that the stimulation of strand exchange efficiency by ammonium sulfate is also due to increased turnover of the duplex DNA from the secondary DNA-binding site, as the ease with which the initial DNA joint can be extended by branch migration may be expected to be critically dependent on the hRad51-ssDNA nucleoprotein filament being free of stably bound duplex DNA molecules as well. These suggestions are summarized in our working model in Fig. 8.

It is reasonable to ask whether the requirement for a high level of salt for revealing the catalytic potential of the hRad51 recombinase is physiological. Concerning this point, it is important to note that the *in vivo* salt concentration is between 0.17 and 0.24 M (17). The specific stimulation of hRad51 strand exchange activity by salts could also be reflecting the requirement for a small molecule (a polyanion, for instance), a certain post-translational modification of hRad51 (phosphorylation, for instance), or the involvement of other recombination factors (see discussion below) in modulating the affinity of the hRad51-ssDNA filament for the incoming duplex DNA molecule.

Significance of the in Vitro DNA Strand Exchange System—Studies on yRad51 using plasmid length DNA molecules as

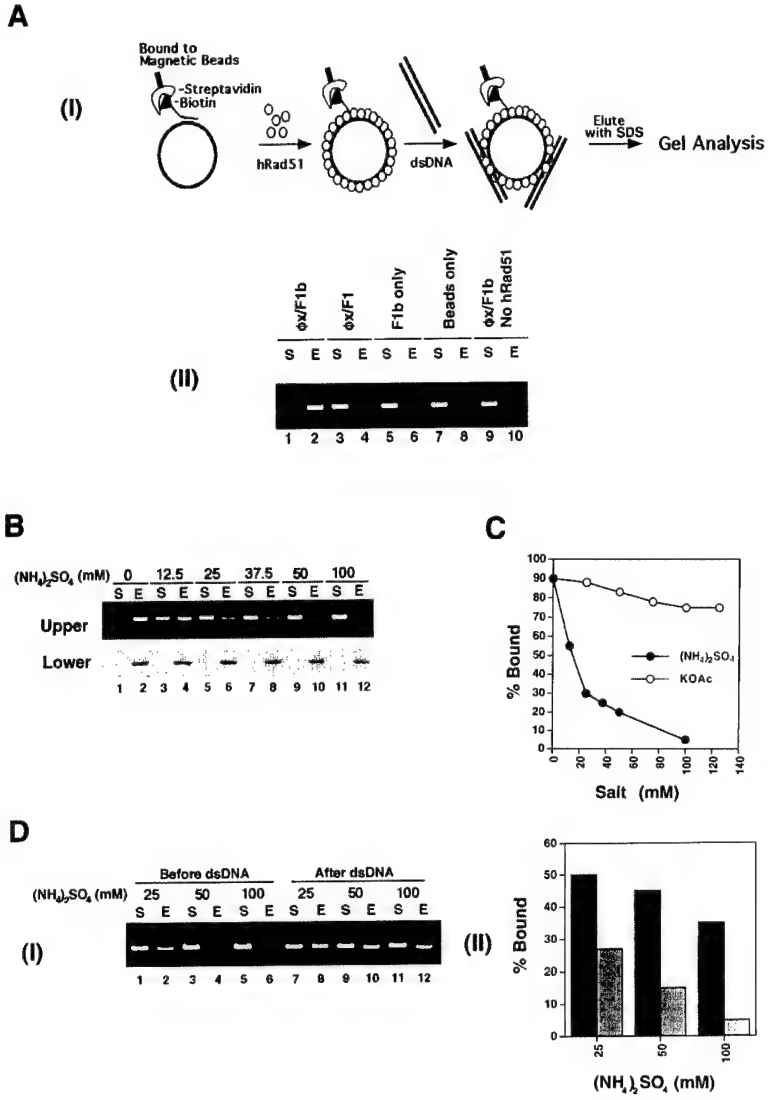

FIG. 7. **Salt lessens interactions between duplex and hRad51-ssDNA nucleoprotein filament.** *A, panel I,* the assay scheme is summarized. Briefly, ϕX (+)-strand hybridized to the biotinylated oligonucleotide F1b is immobilized on streptavidin magnetic beads via the biotin tag. hRad51 filament is assembled on the (+)-strand and then mixed with ϕX duplex DNA. The bound duplex and hRad51 are eluted by SDS and analyzed. To verify the utility of the assay (*panel II*), beads containing ϕX (+)-strand-F1b hybrid (*ϕX-F1b*; *lanes 1* and *2*), beads preincubated with ϕX (+)-strand hybridized to the nonbiotinylated oligonucleotide F1 (*ϕX-F1*; *lanes 3* and *4*), beads with F1b but no ϕX (+)-strand (*F1b only*; *lanes 5* and *6*), and beads that contained neither ϕX (+)-strand nor F1b (*beads only; lanes 7* and *8*) were incubated with hRad51 and then mixed with ϕX duplex. As an additional control, ϕX duplex DNA was incubated with beads containing the ϕX (+)-strand-F1b hybrid without hRad51 (*ϕX/F1b, No hRad51; lanes 9* and *10*). The supernatants (*S*) and the SDS eluates (*E*) from the reactions were analyzed in an agarose gel for their content of duplex DNA. *B,* salt weakens interaction of duplex with the hRad51-ssDNA filament. Duplex ϕX DNA was incubated with the hRad51 filament assembled on the immobilized ϕX (+)-strand with increasing concentrations of ammonium sulfate. The supernatants (*S*) and SDS eluates (*E*) from the binding reactions were analyzed for their contents of DNA duplex (*upper panel*) and hRad51 (*lower panel*). *C,* the results in *B* are graphed (●), as are results from binding reactions in which potassium acetate was used (○). *D,* effect of order of addition of ammonium sulfate. Duplex DNA was added to binding reactions 3 min before or immediately after the incorporation of increasing levels of ammonium sulfate (*panel I*). The results with adding ammonium sulfate before (*shaded bar*) and after (*dark bar*) the incorporation of duplex are presented in the histogram in *panel II*.

substrates have been instrumental for formulating biochemical models for understanding the functions of various *RAD52* group proteins. For instance, in addition to the well documented stimulatory role of yRPA in yRad51-mediated DNA strand exchange, experiments which varied the order of addition of reaction components have revealed that yRPA, if added with or before yRad51 to the ssDNA substrate, can also compete with yRad51 for binding sites on the ssDNA and consequently suppress the assembly of yRad51-ssDNA nucleoprotein filament (2). The yeast *RAD52* encoded product and the heterodimeric molecule of yRad55 and yRad57 proteins, referred to as recombination mediators, promote the assembly of the yRad51-ssDNA filament and help overcome the suppression of DNA strand exchange caused by coaddition of yRPA with yRad51 to the ssDNA substrate or by preincubation of ssDNA with yRPA (2, 18).

We have verified that preincubation of ssDNA with hRad51 before the incorporation of hRPA is in fact critical for homologous pairing and strand exchange efficiency,[2] providing evidence that hRPA competes with hRad51 for binding sites on ssDNA. This observation suggests the existence of specific mediators in the human recombination machinery for promoting hRad51-ssDNA filament assembly when there is the need for hRad51 to compete with other single-strand binding factors for sites on the initiating ssDNA substrate. A possible mediator

[2] S. Sigurdsson and P. Sung, unpublished observations.

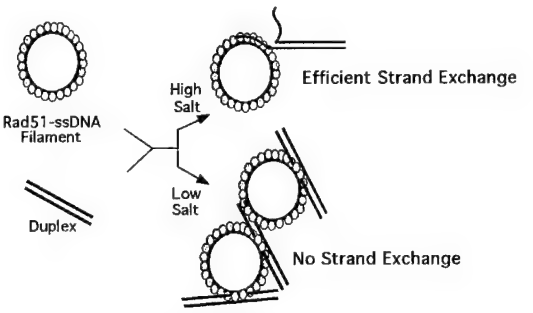

FIG. 8. **Model for hRad51-mediated DNA strand exchange.** The results suggest that duplex DNA molecules stably bound to the hRad51-ssDNA nucleoprotein filament present a strong impediment to the different reaction steps, including DNA homology search, DNA pairing, and branch migration of the nascent DNA joint, that lead to successful recombination between the DNA substrates. Efficient DNA pairing and strand exchange is realized by lessening the duplex/hRad51-ssDNA interactions, achieved by the inclusion of salt.

function may exist in various human recombination factors including hRad52 and a number of Rad55/Rad57-like proteins, namely XRCC2, XRCC3, Rad51B, Rad51C, and Rad51D, which are all known to be involved in recombination and either directly, or through another recombination factor, physically interact with hRad51 (3, 19). Furthermore, it remains a distinct possibility that some of these other recombination factors are in fact integral components of the presynaptic filament, and as such, may modulate the dynamics of the presynaptic filament to facilitate sampling of duplex DNA for homology and to promote the formation of DNA joints once homology is located. The *in vitro* DNA strand exchange system with the defined biochemical parameters described herein should be well suited for examining the function of various recombination factors and the role of post-translational modifications of these recombination factors in the DNA strand exchange reaction.

Recently, hRad51 was shown to interact with the breast tumor suppressor BRCA2 (12). In the Capan-1 cell line defective in BRCA2 function, the DNA damage-induced formation of hRad51 nuclear foci is defective, suggesting the possibility that BRCA2 helps deliver hRad51 to the DNA substrate (12). Whether or not BRCA2 functions as a mediator to promote hRad51 nucleoprotein filament assembly can be tested with the *in vitro* DNA strand exchange system described herein.

Acknowledgments—We are very grateful to Wen-Hwa Lee and Phang-Lang Chen for kindly providing the *hRAD51 K313* cDNA and Marc Wold for the gift of plasmid p11d-tRPA.

REFERENCES

1. Paques, F., and Haber, J. E. (1999) *Microbiol. Mol. Biol. Rev.* **63,** 349–404
2. Sung, P., Trujillo, K., and Van Komen, S. (2000) *Mutat. Res.* **451,** 257–275.
3. Baumann, P., and West, S. C. (1998) *Trends Biochem. Sci.* **23,** 247–251
4. Bianco, P. R., Tracy, R. B., and Kowalczykowski, S. C. (1998) *Front. Biosci.* **3,** D570–603
5. Roca, A. I., and Cox, M. M. (1997) *Prog. Nucleic Acids Res. Mol. Biol.* **56,** 129–223
6. Sung, P. (1994) *Science* **265,** 1241–1243
7. Sung, P., and Robberson, D. L. (1995) *Cell* **82,** 453–461
8. Baumann, P., Benson, F. E., and West, S. C. (1996) *Cell* **87,** 757–766
9. Baumann, P., and West, S. C. (1997) *EMBO J.* **16,** 5198–5206
10. Baumann, P., and West, S. C. (1999) *J. Mol. Biol.* **291,** 363–374
11. Gupta, R. C., Bazemore, L. R., Golub, E. I., and Radding, C. M. (1997) *Proc. Natl. Acad. Sci. U. S. A.* **94,** 463–468
12. Dasika, G. K., Lin, S. C., Zhao, S., Sung, P., Tomkinson, A., and Lee, E. Y. (1999) *Oncogene* **18,** 7883–7899
13. Henricksen, L. A., Umbricht, C. B., and Wold, M. S. (1994) *J. Biol. Chem.* **269,** 11121–11132
14. Sung, P. (1997) *Genes Dev.* **11,** 1111–1121
15. Yoshimura, Y., Morita, T., Yamamoto, A., and Matsushiro, A. (1993) *Nucleic Acids Res.* **21,** 1665
16. Shinohara, A., Ogawa, H., Matsuda, Y., Ushio, N., Ikeo, K., and Ogawa, T. (1993) *Nat. Genet.* **4,** 239–243
17. Kao-Huang, Y., Revizin, A., Butler, A. P., O'Conner, P., Noble, D. W., and Von Hippel, P. H. (1977) *Proc. Natl. Acad. Sci. U. S. A.* **74,** 4228–4232
18. Beernink, H. T., and Morrical, S. W. (1999) *Trends Biochem. Sci.* **24,** 385–389
19. Schild, D., Lio, Y., Collins, D. W., Tsomondo, T., and Chen, D. J. (2000) *J. Biol. Chem.* **275,** 16443–16449

Molecular Cell, Vol. 6, 563–572, September, 2000, Copyright ©2000 by Cell Press

Superhelicity-Driven Homologous DNA Pairing by Yeast Recombination Factors Rad51 and Rad54

Stephen Van Komen,† Galina Petukhova,†‡ Stefan Sigurdsson, Sabrina Stratton, and Patrick Sung*
Department of Molecular Medicine and Institute of Biotechnology
University of Texas Health Science Center at San Antonio
15355 Lambda Drive
San Antonio, Texas 78245

Summary

Yeast Rad51 recombinase has only minimal ability to form D loop. Addition of Rad54 renders D loop formation by Rad51 efficient, even when topologically relaxed DNA is used as substrate. Treatment of the nucleoprotein complex of Rad54 and relaxed DNA with topoisomerases reveals dynamic DNA remodeling to generate unconstrained negative and positive supercoils. DNA remodeling requires ATP hydrolysis by Rad54 and is stimulated by Rad51-DNA nucleoprotein complex. A marked sensitivity of DNA undergoing remodeling to P1 nuclease indicates that the negative supercoils produced lead to transient DNA strand separation. Thus, a specific interaction of Rad54 with the Rad51-ssDNA complex enhances the ability of the former to remodel DNA and allows the latter to harvest the negative supercoils generated for DNA joint formation.

Introduction

Saccharomyces cerevisiae genes of the *RAD52* epistasis group, consisting of *RAD50, RAD51, RAD52, RAD54, RAD55, RAD57, RAD59, MRE11, XRS2,* and *RDH54/TID1*, are indispensable for homologous recombination and the repair of DNA double-strand breaks induced by ionizing radiation and other DNA damaging agents. Because of a requirement for meiotic recombination to effect the proper disjunction of homologous chromosomes in meiosis I, mutations in the *RAD52* group genes often lead to meiotic abnormalities, including lethality (reviewed in Petes et al., 1991; Paques and Haber, 1999; Sung et al., 2000).

Much of our current understanding of homologous recombination in eukaryotes has been garnered from studies on mating type switching and meiotic recombination in *S. cerevisiae*. In both types of recombination, DNA double-strand breaks are generated in a developmentally programmed fashion. Once formed, the ends of these breaks are processed nucleolytically to yield long ssDNA overhangs. These ssDNA tails are then utilized by the recombination machinery to invade an intact DNA homolog, either the sister chromatid or homologous chromosome, to form a heteroduplex DNA joint called D loop. The recombination event is completed by DNA synthesis primed from the D loop and the resolution of DNA intermediates. The repair of DNA double-strand breaks induced by ionizing radiation very likely follows the same mechanistic route, as it too shows a dependence on the same *RAD52* epistasis group genes (Petes et al., 1991; Paques and Haber, 1999; Sung et al., 2000). Cloning studies have revealed a high degree of functional and structural conservation of the components of the recombination machinery, from yeast to humans. Emerging evidence has implicated the homologous recombination machinery in cancer prevention in mammals, underscoring the importance of dissecting the functional and mechanistic intricacies of this machinery (reviewed in Dasika et al., 1999).

The enzymatic process that leads to the formation of heteroduplex DNA during recombination is referred to as "homologous DNA pairing and strand exchange" (reviewed in Kowalczykowski et al., 1994; Roca and Cox, 1997; Sung et al., 2000). *RAD51*, a key member of the *RAD52* group, encodes a protein homologous to the *Escherichia coli* homologous DNA pairing and strand exchange enzyme RecA. Even though Rad51 catalyzes homologous DNA pairing and strand exchange in model systems that involve oligonucleotides or plasmid length circular ssDNA and linear duplex molecules, it has little ability to pair a linear ssDNA and a covalently closed duplex molecule to form D loop (Petukhova et al., 1998; Mazin et al., 2000). Previous studies have indicated that the *RAD54* encoded product, a member of the *RAD52* group and a Swi2/Snf2-like factor (see Eisen et al., 1995, for a discussion), promotes efficient D loop formation by Rad51 (Petukhova et al., 1998; Mazin et al., 2000).

Rad54 interacts with Rad51 in two-hybrid analysis and in vitro (Jiang et al., 1996; Clever et al., 1997; Petukhova et al., 1998). Rad54 also possesses a robust ATPase function that is completely dependent on DNA, dsDNA in particular, for activation (Petukhova et al., 1998; Swagemakers et al., 1998). Upon ATP hydrolysis, Rad54 induces a linking number change in the DNA that can be trapped by treatment of relaxed DNA with calf thymus topoisomerase I or nicked circular duplex with DNA ligase, indicating that Rad54 remodels DNA (Petukhova et al., 1999; Tan et al., 1999). However, the nature of DNA remodeling and the manner in which Rad51 and Rad54 functionally cooperate to make D loop have remained mysterious. Here, we show that Rad54 supercoils DNA and report on the synergistic cross-talk between Rad51 and Rad54 in DNA supercoiling and D loop formation. Our results highlight the main distinctions between the prokaryotic and eukaryotic recombination machineries in effecting DNA strand invasion to form DNA joints, and they also suggest a novel general principle for a protein machinery to promote DNA strand opening via supercoiling rather than unwinding.

Results

Rad51/Rad54-Mediated D Loop Formation

For examining D loop formation (Figure 1A, schematic), we made covalently closed duplex DNAs with different

*To whom correspondence should be addressed (e-mail: sung@uthscsa.edu).
†These authors contributed equally to this work.
‡Present address: National Institutes of Health, NIDDK, Building 10, Room 9D17, 9000 Rockville Pike, Bethesda, Maryland 20892.

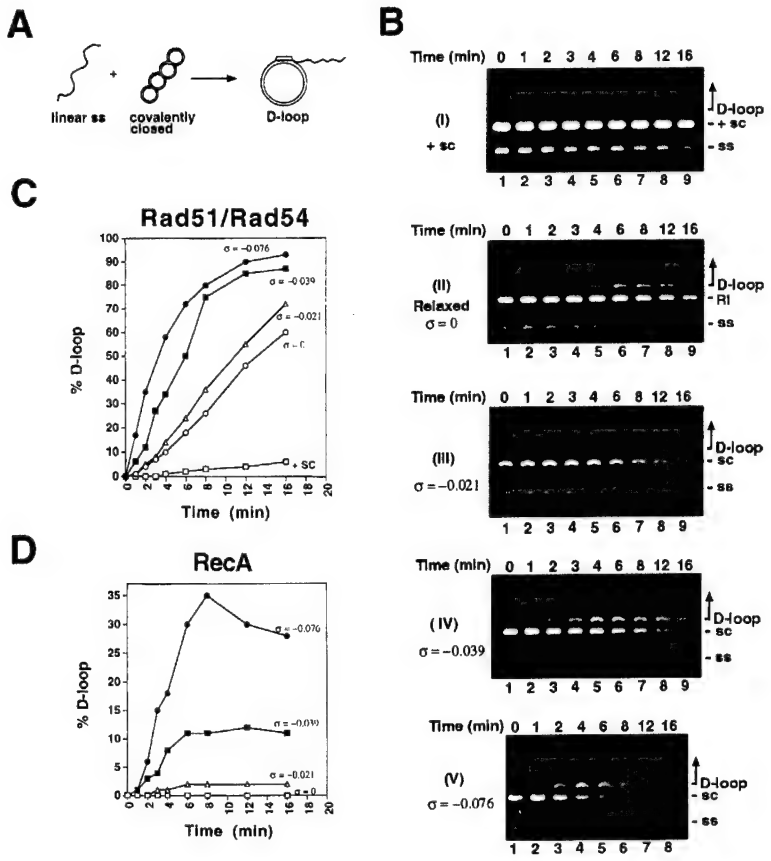

Figure 1. Effect of Superhelicity on D Loop Formation

(A) Schematic of the D loop reaction. Linear ssDNA is paired with a covalently closed duplex, such as a negatively supercoiled species as shown, to yield the D loop. A variety of covalently closed duplex substrates differing in their topological state were employed in the present study (see below).

(B) Superhelicity and D loop formation. In (I) through (V), a preassembled nucleoprotein complex of Rad51-RPA-ssDNA was mixed with Rad54 and duplex DNA substrates that were positively supercoiled (+SC in [I]), relaxed (RI in [II]), and with σ values of −0.021 (III), −0.039 (IV), and −0.076 (V), as indicated. The reaction mixtures were analyzed in agarose gels containing 10 μM ethidium bromide to effect the separation of D loop species from other DNA species (nicked circular duplex and linear duplex, which are not marked). At later time points, more complex D loop species appeared, which likely corresponded to multiple molecules of ssDNA and dsDNA paired together. The linear single-strand is designated as ss.

(C) The results in (B) are plotted.

(D) Results from D loop reactions in which RecA-SSB-ssDNA complex was reacted with duplex substrates of the indicated topological state are plotted.

topological states (see Experimental Procedures for technical details), ranging from positively supercoiled, relaxed (average $\sigma = 0$), to negatively supercoiled (average σ values of −0.021, −0.039, and −0.076). In addition to yeast Rad51/Rad54/RPA, *E. coli* RecA was also used in conjunction with *E. coli* SSB. The reaction temperature used for examining D loop formation was 23°C, as this relatively low temperature enabled us to more easily follow the reaction kinetics.

Rad51, at 3 nucleotides/monomer and 23°C, was unable to form D loop with the entire range of DNA substrates used, including the most highly negatively supercoiled DNA with $\sigma = -0.076$. This conclusion was validated with a wide range of Rad51 concentrations from 60 nucleotides/monomer to 1 nucleotide/monomer and at the higher reaction temperatures of 30°C and 37°C (data not shown). We next characterized the effect of adding Rad54 on D loop formation with the same DNA substrates, using an amount of Rad51 protein corresponding to 20 nucleotides per protein monomer. This ratio of Rad51 to ssDNA was used because even although 3 nucleotides/Rad51 monomer was optimal for DNA joint formation in the model reaction that employs circular ssDNA and linear duplex (Sung and Robberson, 1995), increasing Rad51 to this level in fact resulted in about 2- to 3-fold reduction in D loop formation (S. V. K. and P. S., unpublished data). As shown in Figure 1B, addition of Rad54 protein rendered the formation of D loop by Rad51 robust, as even with relaxed DNA as substrate, about half of the input DNA had been converted into D loop species at the reaction endpoint of 16 min. Compared to the relaxed DNA substrate, a significantly higher level of D loop was seen when the σ value of the substrates decreased to −0.039 and −0.076, but only a small enhancement in the rate and extent of D loop formation was detected with the slightly negatively supercoiled substrate with $\sigma = -0.021$ (Figures 1B and 1C). The result with the relaxed substrate (Figures 1C and 1D) was rather surprising, as RecA protein requires a high level of negative supercoiling in the DNA substrate for D loop formation (Kowalczykowski et al., 1994; see later).

D loop formation by the combination of Rad51 and Rad54 requires that ATP is hydrolyzed by Rad54, as the substitution of Rad54 with mutant variants (Petukhova et al., 1999) of Rad54 either defective in ATP hydrolysis (rad54 K341A) or greatly attenuated for its ATPase activity (rad54 K341R) abolished D loop formation with the entire range of DNA substrates that differed in their topological state (data not shown). RPA is needed for optimal D loop formation (Petukhova et al., 1998), and other experiments have shown that Rad54 does not replace RPA in DNA joint formation, nor does it promote D loop formation without Rad51 (Petukhova et al., 1998; S. V. K. and P. S., unpublished data). In addition, no D loop was formed if we preincubated Rad51 with the duplex, indicating that DNA joint formation requires that Rad51 is bound to the ssDNA substrate (data not shown).

Figure 1D presents the results obtained with the combination of *E. coli* RecA and SSB proteins. As reported before, RecA makes D loop, in a manner that is strongly dependent on the topological state of DNA, such that a dramatic increase in the yield of D loop occurred with decreasing σ (reviewed in Kowalczykowski et al., 1994).

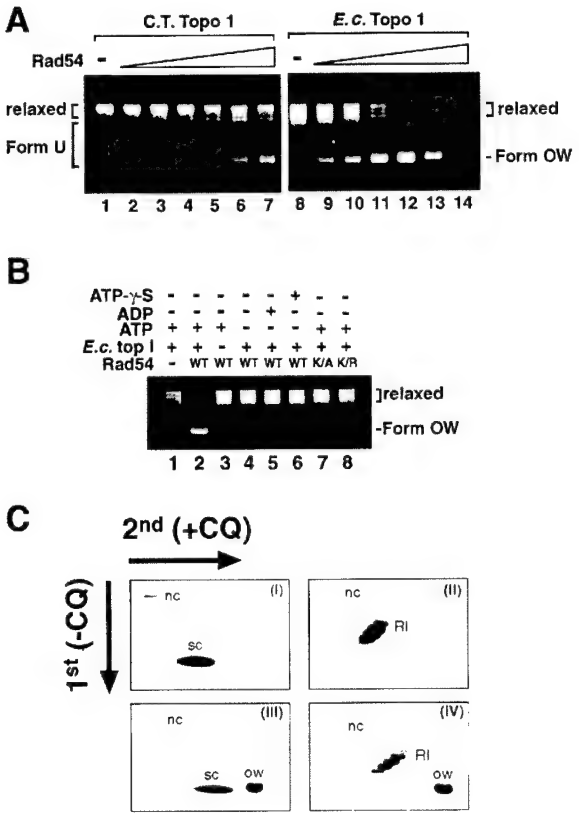

Figure 2. DNA Remodeling by Rad54 as Revealed by Topoisomerase Treatment

(A) Increasing concentrations of Rad54 protein (0.045, 0.09, 0.23, 0.45, 0.9, and 1.8 μM in lanes 2 to 7 and lanes 9 to 14, respectively) were incubated with relaxed DNA and with either calf thymus topoisomerase I (lanes 2 to 7) or *E. coli* topoisomerase I (lanes 9 to 14), as indicated. In lanes 1 and 8, DNA was incubated in buffer with topoisomerase but no Rad54 protein. The novel DNA species generated by the combination of Rad54 and topoisomerase I is designated as Form OW, and the heterogeneous novel DNA species generated by the combination of Rad54 and calf thymus topoisomerase I are collectively designated as Form U. The DNA concentration was 18.5 μM base pairs, and all the reactions were incubated at 37°C for 10 min.

(B) Formation of Form OW DNA requires ATP hydrolysis. Rad54 (0.3 μM) was incubated with relaxed DNA and *E. coli* topoisomerase I in the presence of ATP (lane 2), ADP (lane 5), ATP-γ-S (lane 6), or in the absence of a nucleotide (lane 4), as indicated. The reaction in lane 1 contained relaxed DNA without Rad54, and in lane 3, relaxed DNA was incubated with Rad54 and ATP without topoisomerase. In lanes 7 and 8, rad54 K341A (K/A) and rad54 K341R (K/R) mutant proteins, 0.3 μM each, were incubated with relaxed DNA, *E. coli* topoisomerase I, and ATP, as indicated. The DNA concentration was 18.5 μM base pairs, and the reactions were carried out at 37°C for 10 min.

(C) Two-dimensional gel analysis of Form OW DNA. In (I) and (II), negatively supercoiled ϕX DNA isolated from cells ($\sigma = -0.06$) without (I) or with (II) prior treatment with *E. coli* topoisomerase I was subject to two-dimensional gel analysis. In (III) and (IV), a mixture of negatively supercoiled ϕX DNA and purified Form OW DNA without (III) or with (IV) prior treatment with *E. coli* topoisomerase I was subject to two-dimensional gel analysis. Note in (IV) that the negatively supercoiled DNA, but not Form OW DNA, was relaxed by *E. coli* topoisomerase I. OW, Form OW DNA; SC, negatively supercoiled DNA; RI, relaxed DNA; and nc, nicked circular DNA. In these gel analyses, the first dimension was conducted in the absence of chloroquine (- CQ) and the second dimension in the presence of chloroquine (+CQ).

Importantly, no D loop was formed by RecA with topologically relaxed DNA or positively supercoiled DNA. Even with the supercoiled substrate with $\sigma = -0.021$, only a trace of D loop was seen. These results demonstrate that topological constraints in the relaxed and less negatively supercoiled DNA molecules prevent the formation of a stable joint with the linear ssDNA molecule by RecA protein. Importantly, addition of Rad54 protein did not enhance the ability of RecA to make D loop with the negatively supercoiled DNA, nor did it enable RecA to promote D loop formation with relaxed or positively supercoiled substrate (data not shown). These results suggest that the physical interaction noted between Rad51 and Rad54 (Jiang et al., 1996; Clever et al., 1997; Petukhova et al., 1998) is likely to be functionally important in the D loop reaction.

In summary, unlike RecA, negative supercoiling alone does not appear to compensate for a deficit in the ability in Rad51 to form D loop. Addition of Rad54 overcomes this deficit and in fact renders D loop formation efficient even with relaxed DNA, indicating a specific role of Rad54 in overcoming the topological constraint inherent in DNA joint formation. The experiments described below begin to address the mechanism by which Rad54 promotes DNA joint formation with Rad51.

Rad54 Generates Both Negatively and Positively Supercoiled Domains in DNA

We have shown that incubation of yeast Rad54 with topologically relaxed DNA and calf thymus topoisomerase I results in a change in the DNA linking number (Petukhova et al., 1999; Figure 2A, lanes 1 to 7), in a manner that is completely dependent on ATP hydrolysis by Rad54 (Petukhova et al., 1999). The product of the DNA remodeling reaction that uses calf thymus topoisomerase I, which removes both negative and positive supercoils efficiently, is negatively supercoiled and was designated Form U (underwound) (Petukhova et al., 1999). In this reaction, a relatively high concentration of Rad54 protein (≤ 50 base pairs per Rad54 monomer) is required to see any linking number change (Petukhova et al., 1999; Figure 2A, lanes 1 to 7), suggesting that either Rad54 protein produces only limited unwinding of the DNA double-helix or that in fact both negative and positive supercoils are produced by low concentrations of Rad54, but that both types of supercoils are removed by calf thymus topoisomerase I. To distinguish between these possibilities, we have used *E. coli* topoisomerase I, which removes negative supercoils but is completely inactive toward positive supercoils in DNA, together with Rad54 and relaxed DNA substrate in the DNA remodeling reaction.

Incubation of the relaxed ϕX DNA substrate, Rad54, and *E. coli* topoisomerase I resulted in the formation of a novel DNA species that migrated ahead of the relaxed DNA (Figure 2A, lanes 8 to 14). Since subsequent analyses showed that this DNA species was positively supercoiled, we have designated it Form OW (overwound) DNA. Formation of Form OW DNA was completely dependent on ATP hydrolysis by Rad54, as revealed by either the omission of ATP or its substitution by ADP and the nonhydrolyzable analog ATP-γ-S (Figure 2B). Consistent with this result, neither rad54 K341A nor rad54 K341R was active in the DNA remodeling reaction (Figure 2B). That Form OW DNA was positively supercoiled was revealed by two-dimensional gel analysis (Figure 2C, panel III) and by the finding that while it can

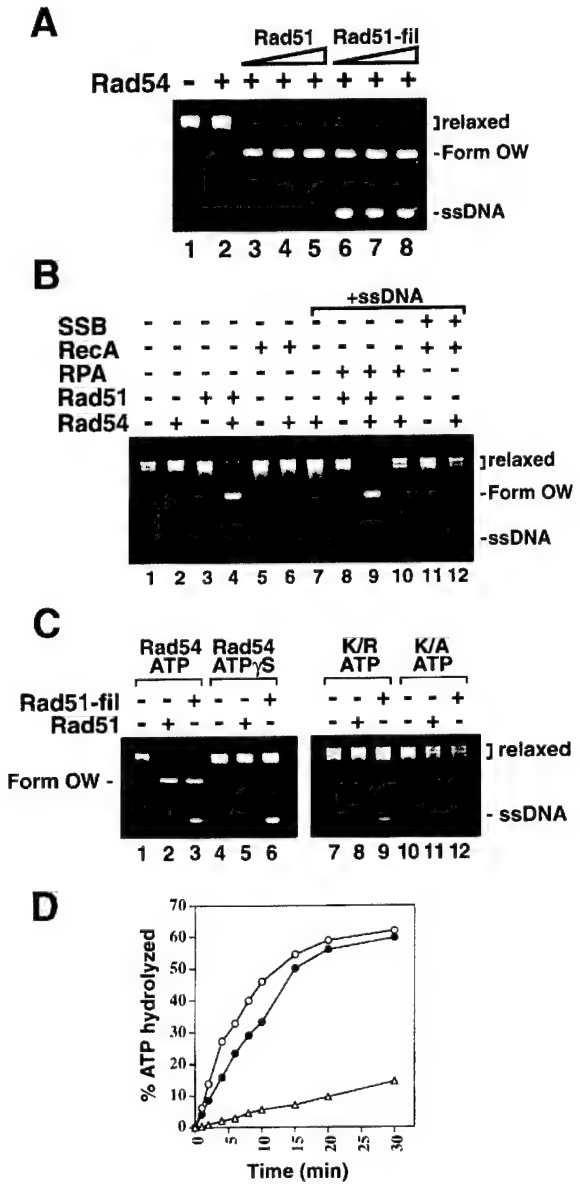

Figure 3. Effect of Rad51 on the Rad54 DNA Supercoiling and ATPase Activities

(A) Stimulation of DNA supercoiling by Rad51 and Rad51-RPA-ssDNA complex. Rad54, at 22.5 nM (lanes 2 to 8), was incubated with relaxed ϕX DNA (18.5 μM base pairs, lanes 1 to 8), *E. coli* topoisomerase I (lanes 1 to 8), and increasing amounts of Rad51 (120, 240, and 360 nM in lanes 3 to 5) or nucleoprotein complexes of Rad51-RPA-ssDNA (Rad51-fil) containing a constant amount of RPA (2 μM) and pBluescript ssDNA (30 μM nucleotides) but an increasing level of Rad51 (60, 120, and 240 nM in lanes 6 to 8) at 23°C for 10 min.

(B) RecA does not stimulate DNA supercoiling. Relaxed DNA (lanes 1 to 12) was incubated with *E. coli* topoisomerase I (lanes 1 to 12), Rad54 (lanes 2, 4, 6, 7, 9, 10, and 12), Rad51 (lanes 3 and 4), Rad51-RPA-ssDNA complex (lanes 8 and 9), RecA (lanes 5 and 6), and RecA-SSB-ssDNA complex (lanes 11 and 12), all in the presence of ATP. The concentrations of the reaction components were Rad54, 90 nM; Rad51, 120 nM; RPA, 2 μM; pBluescript ssDNA, 30 μM nucleotides; relaxed ϕX DNA, 18.5 μM base pairs; RecA, 1 μM; and SSB, 6 μM. The reaction mixtures were incubated at 23°C for 10 min.

(C) Dependence of DNA supercoiling on ATP hydrolysis. Relaxed DNA (lanes 1 to 6) was incubated with *E. coli* topoisomerase I (lanes 1 to 6), Rad54 (lanes 1 to 6), and Rad51 (lanes 2 and 5) or a nucleoprotein complex of Rad51, RPA, and ssDNA (Rad51-fil; lanes 3 and 6) in the presence of ATP (lanes 1 to 3) or ATP-γ-S (lanes 4 to 6), as indicated. Likewise, relaxed DNA (lanes 7 to 12) was incubated with *E. coli* topoisomerase I (lanes 7 to 12), rad54 K341R (K/R; lanes 7 to 9), and rad54 K341A (K/A; lanes 10 to 12) and either Rad51 (lanes 8 and 11) or the Rad51-RPA-ssDNA complex (Rad51-fil; lanes 9 and 12), all in the presence of ATP. The concentrations of the reaction components were Rad54, rad54 K341A, and rad54 K341R proteins, 90 nM; relaxed ϕX DNA, 18.5 μM base pairs; Rad51, 120 nM; RPA, 2 μM; and pBluescript ssDNA, 30 μM nucleotides. The reaction mixtures were incubated at 23°C for 10 min.

(D) Rad51 and Rad51-RPA-ssDNA complex stimulate Rad54 ATPase activity. Rad54, at 50 nM, was incubated with radiolabeled ATP and relaxed ϕX DNA without other protein (open triangles), with Rad51 (closed circles), or with Rad51-RPA-ssDNA complex (open circles) at 23°C.

be fully relaxed by calf thymus topoisomerase I (data not shown) it is refractory to *E. coli* topoisomerase I (Figure 2C, panel IV).

It is important to note that at relatively low Rad54 concentrations where no significant DNA linking number change was observed with calf thymus topoisomerase I (Figure 2A, lanes 2 to 4), Rad54 was very much adept at generating Form OW DNA with *E. coli* topoisomerase I (Figure 2A, lanes 9 to 11). For instance, while 90 nM of Rad54 (corresponding to 205 base pairs per Rad54 monomer) produced a substantial amount of Form OW DNA (Figure 2A, lane 10), this concentration of Rad54 did not cause any linking number change in DNA when calf thymus topoisomerase I was used (Figure 2A, lane 3). At 225 nM of Rad54 (corresponding to 82 base pairs per Rad54 monomer), while the majority of the input substrate was converted to Form OW DNA (Figure 2A, lane 11), only a trace of Form U DNA was seen (Figure 2A, lane 4). These results strongly suggest that equivalent levels of both unconstrained negative and positive supercoils are generated during DNA remodeling by relatively low levels of Rad54 (up to 225 nM), and treatment with *E. coli* topoisomerase I removes only the negative supercoils, thus resulting in the accumulation of the positive supercoils and the formation of Form OW DNA. At these relatively low concentrations of Rad54, little or no linking number change in the DNA is seen with calf thymus topoisomerase I, because both the unconstrained negative and positive supercoils are removed by the eukaryotic topoisomerase. Results from these analyses have also allowed us to deduce that at concentrations of 225 nM of Rad54 and above, some of the negative supercoils produced as a result of DNA remodeling become constrained, as revealed by the formation of Form U DNA in the reaction that uses calf thymus topoisomerase I (Figure 2A, lanes 4 to 7). This deduction is also supported by the observation that at high concentrations of Rad54, the formation of Form OW DNA with *E. coli* topoisomerase I in fact becomes progressively inhibited (Figure 2A, lanes 13 and 14). The constraining of negative supercoils seen at high concentrations of Rad54 (Figure 2A, lanes 5 to 7) is likely due to secondary binding of Rad54 to the regions that contained these supercoils.

DNA Remodeling Is Stimulated by Rad51

Since Rad54 physically interacts with Rad51 and cooperates with the latter in the formation of DNA joints, it was of considerable interest to examine whether the

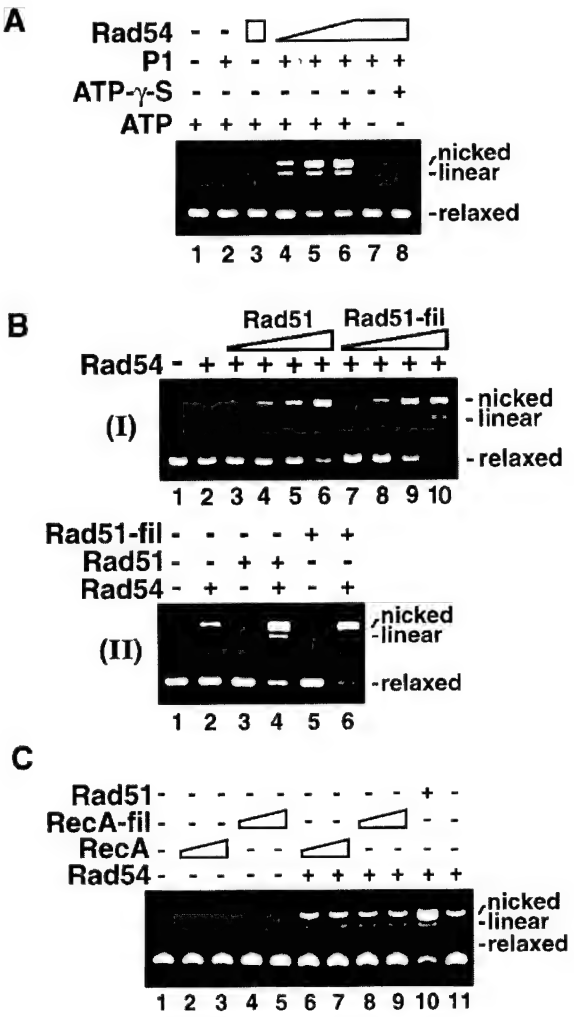

Figure 4. DNA Supercoiling Leads to DNA Strand Opening

(A) Rad54 renders topologically relaxed DNA sensitive to P1 nuclease. Relaxed DNA (18.5 μM base pairs, lanes 1 to 8) was incubated at 23°C for 10 min with P1 nuclease and increasing concentrations of Rad54 protein (90, 250, and 500 nM in lanes 4 to 6, respectively) in the presence of ATP. In lane 3, Rad54 (500 nM) was incubated with relaxed DNA in the presence of ATP but without P1, and in lanes 7 and 8, Rad54 (500 nM), relaxed DNA, P1 nuclease were incubated in the absence of ATP or with ATP-γ-S, as indicated.

(B) Rad51 enhances P1 sensitivity. In (I), relaxed ϕX DNA (18.5 μM base pairs in lanes 1 to 10) was incubated with P1 nuclease (lanes 1 to 10), Rad54, (50 nM; lanes 2 to 10), and increasing amounts of Rad51 (60, 120, 240, and 360 nM in lanes 3 to 6, respectively) or nucleoprotein complexes containing pBluescript ssDNA (30 μM nucleotides), RPA (2 μM), and increasing amounts of Rad51 (60, 120, 240 and 360 nM in lanes 7 to 10, respectively) at 23°C for 10 min. In lane 1, relaxed DNA and P1 nuclease were incubated in the absence of Rad51 and Rad54. In (II), relaxed ϕX DNA (18.5 μM base pairs in lanes 1 to 6) was incubated with P1 nuclease (lanes 1 to 6), Rad54 (50 nM in lanes 2, 4, and 6), and Rad51 (360 nM in lanes 3 and 4) or a nucleoprotein complex of Rad51-RPA-ssDNA (Rad51-fil, consisting of 360 nM Rad51, 2 μM RPA, and 30 μM pBluescript ssDNA; lanes 5 and 6), as described in (I).

(C) RecA does not promote DNA strand opening. Relaxed ϕX DNA (18.5 μM base pairs; lanes 1 to 11), P1 nuclease (lanes 1 to 11), Rad54 (50 nM in lanes 6 to 11), and Rad51 (360 nM, lane 10), RecA (525 nM in lanes 2 and 6, and 2.6 μM in lanes 3 and 7), or nucleoprotein complexes of RecA-SSB-ssDNA (RecA-fil; lanes 4, 5, 8, and 9) consisting of a fixed amount of SSB (6 μM), pBluescript ssDNA (30 μM nucleotides), but an increasing level of RecA (525 nM in lanes 4 and 8, and 2.6 μM in lanes 5 and 9). The analyses in (A) through (C) were carried out in 0.85% agarose gels containing 10 μM ethidium bromide.

DNA remodeling ability of Rad54 is influenced by Rad51. For this purpose, we examined Form OW DNA formation by incubating increasing amounts of Rad51 or nucleoprotein complexes preassembled with pBlueScript ssDNA, RPA, and increasing amounts of Rad51 with a quantity of Rad54 (22.5 nM, corresponding to 822 base pairs/Rad54 monomer) that by itself gave only a trace of Form OW DNA. Both Rad51 alone or Rad51/RPA prebound to ssDNA markedly stimulated the ability of Rad54 to produce Form OW DNA (Figure 3A). Control experiments showed that Rad51 or the complex of Rad51-RPA-ssDNA alone was devoid of DNA remodeling ability (Figure 3B, lanes 3 and 8), and the complex of RPA on ssDNA without Rad51 did not stimulate the DNA remodeling ability of Rad54 (Figure 3B, lane 10). Interestingly, ssDNA alone inhibited the ability of Rad54 to remodel duplex DNA (Figure 3B, compare lane 7 to lane 2), and other experiments have suggested that this is due to preferential binding of Rad54 to ssDNA and its sequestration from the DNA remodeling reaction (data not shown). In the presence of Rad51 or Rad51-RPA-ssDNA complex, DNA remodeling is also dependent on ATP hydrolysis by Rad54, as revealed by the substitution of Rad54 with either rad54 K341A or rad54 K341R mutant protein (Figure 3C). Consistent with the results from DNA remodeling experiments, Rad51 and Rad51-RPA-ssDNA both stimulated the dsDNA-dependent ATPase activity of Rad54 significantly (Figure 3D). As expected, RPA-ssDNA complex alone has no stimulatory effect on the Rad54 ATPase activity. A similar degree of stimulation of the Rad54 supercoiling and ATPase activities was observed when we used ϕX ssDNA instead of pBluescript ssDNA for assembling the Rad51-RPA-ssDNA complex (data not shown), indicating that DNA homology is not required for stimulation.

We have also examined whether a nucleoprotein complex of RecA-SSB-ssDNA has the ability to remodel DNA and to stimulate the Rad54 DNA remodeling and ATPase activities. The results indicated that RecA and the RecA-SSB-ssDNA nucleoprotein complex are devoid of the ability to remodel DNA (Figure 3B, lanes 5 and 11), and in addition that RecA and the RecA-SSB-ssDNA complex do not stimulate the DNA remodeling capability of Rad54 (Figure 3B, lanes 6 and 12) or its ATPase activity (data not shown). Taken together, the above observations indicate a specific cooperation between Rad51 and Rad54 in DNA remodeling, consistent with the physical interaction noted between these two proteins (Jiang et al., 1996; Clever et al., 1997; Petukhova et al., 1998).

Nuclease P1 Sensitivity Reveals DNA Strand Separation by Rad51/Rad54-Mediated Supercoiling

Since formation of a heteroduplex DNA joint involves the melting of the target duplex to facilitate invasion by the initiating ssDNA substrate (Gupta et al., 1999), we wished to determine whether the negative supercoiling induced by Rad54 leads to DNA strand separation. We addressed this point by asking if treatment of a relaxed duplex with Rad54 would render the DNA sensitive to the single-strand-specific nuclease P1. Relaxed DNA by

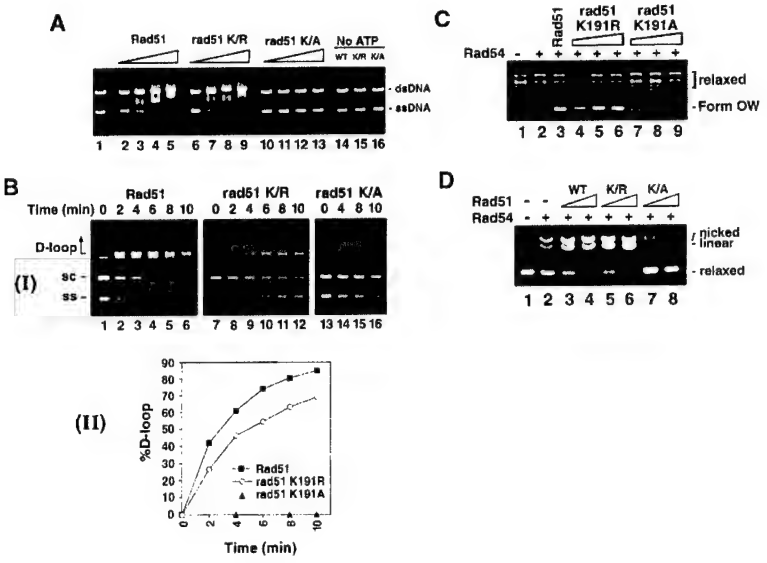

Figure 5. DNA Binding by Rad51 Is Required for DNA Supercoiling and D Loop Formation

(A) DNA binding ability of wild-type Rad51 and mutant rad51 proteins. Rad51 (1, 2, 4, and 6 μM in lanes 2 to 5, and 6 μM in lane 14), rad51 K191R (1, 2, 4, and 6 μM in lanes 6 to 9, and 6 μM in lane 15), and rad51 K191A (1, 2, 4, and 6 μM in lanes 10 to 13, and 6 μM in lane 16) were incubated with a mixture of ϕX viral (+) strand (30 μM nucleotides) and linear duplex (20 μM base pairs), either in the presence (lanes 1 to 13) or absence of ATP (14 to 16), for 10 min at 23°C. The reaction mixtures were run in a 0.9% agarose gel to detect the mobility shift of the DNA substrates.

(B) rad51 K191R but not rad51 K191A forms D loop with Rad54. Time courses of D loop formation (I) with Rad51 (1.5 μM), rad51 K191A (1.5 μM), and rad51 K191R (1.5 μM) using ϕX linear ssDNA (ss) and negatively supercoiled DNA (sc) with $\sigma = -0.06$ isolated from cells as substrates. The details are given in the Experimental Procedures. The datapoints from image analysis of the gels are plotted (II).

(C) rad51 K191R but not rad51 K191A cooperates with Rad54 in supercoiling DNA. The relaxed ϕX DNA substrate (18.5 μM) was incubated with Rad54 (90 nM in lanes 2 to 9), *E. coli* topoisomerase I (lanes 1 to 9), Rad51 (120 nM, lane 3), rad51 K191R (120, 240, and 360 nM in lanes 4, 5, and 6, respectively), and rad51 K191A (120, 240, and 360 nM in lanes 7, 8, and 9, respectively) for 10 min at 23°C, as indicated.

(D) Enhancement of DNA strand opening by rad51 K191R but not rad51 K191A. Relaxed ϕX DNA (18.5 μM base pairs) was incubated with P1 nuclease and the following components at 23°C for 10 min before gel analysis: Rad54 (90 nM in lanes 2 to 8), Rad51 (WT; 240 and 360 nM in lanes 3 and 4, respectively), rad51 K191R (K/R; 360 and 480 nM in lanes 5 and 6, respectively), and rad51 K191A (K/A; 360 and 480 nM in lanes 7 and 8, respectively), as indicated. The analyses in (D) were carried out in 0.85% agarose gels containing 10 μM ethidium bromide.

itself was, as expected, impervious to the action of P1 nuclease due to the lack of single-stranded nature in the DNA (Figure 4A, lane 2). Interestingly, treatment of the relaxed substrate with Rad54 rendered it sensitive to P1 nuclease, as revealed by the presence of nicked DNA in the gel analysis, with the level of P1-digested DNA increasing with the amount of Rad54 added (Figure 4A, lanes 4 to 6). The sensitivity of relaxed DNA to P1 nuclease is completely dependent on ATP hydrolysis by Rad54, as the omission of ATP or its substitution with ATP-γ-S abolished the sensitivity of the DNA substrate to P1 nuclease (Figure 4A, lanes 7 and 8), and even high levels of the ATPase defective rad54 K341A and rad54 K341R mutant proteins did not render the DNA substrate sensitive to P1 nuclease (data not shown).

Since in the topoisomerase-linked DNA remodeling reaction stimulation of the Rad54 DNA remodeling ability by either Rad51 or Rad51-RPA-ssDNA filament was seen (Figure 3), it became important to establish whether the P1 sensitivity of the relaxed DNA substrate undergoing remodeling is also similarly enhanced. To do this, we used exactly the same incubation conditions as those employed in the topoisomerase-linked DNA remodeling experiments (Figure 3), with the exception that P1 nuclease was used instead of topoisomerase. The results from these experiments indicated that either the addition of free Rad51 or a preassembled complex of Rad51-RPA-ssDNA results in a marked increase of the DNA sensitivity to P1 nuclease (Figure 4B, panel I). Control experiments showed that neither free Rad51 nor Rad51-RPA-ssDNA complex alone has any ability to promote scission of DNA by P1 nuclease (Figure 4B, panel II). In addition, RecA and the RecA-SSB-ssDNA complex are also devoid of the ability to promote P1 scission of DNA (Figure 4C, lanes 2 to 5), nor do they significantly enhance the ability of Rad54 to make DNA sensitive to P1 (Figure 4C, lanes 6 to 9). The synergistic action of Rad51/Rad54 and Rad51-RPA-ssDNA/Rad54 in the P1 sensitivity assay is completely dependent on the ability of Rad54 to hydrolyze ATP, as verified by substitution of Rad54 with the rad54 K341A and rad54 K341R mutant proteins (data not shown). Taken together, the results from the analyses conducted with P1 nuclease provide direct evidence that ATP hydrolysis-driven negative supercoiling of DNA by the combination of Rad51 and Rad54 leads to transient DNA strand opening.

D Loop Formation and DNA Remodeling Require DNA Binding by Rad51

Rad51 protein, like RecA, assembles onto ssDNA to form a nucleoprotein filament in which the search for DNA homology in the incoming homologous duplex and formation of DNA joints with the duplex occur. The assembly of the Rad51-ssDNA nucleoprotein filament requires ATP binding (reviewed in Bianco et al., 1998; Roca and Cox, 1997; Sung et al., 2000). We have previously described mutant variants of Rad51 altered in their ability to interact with ATP: rad51 K191A, which does not bind ATP, and rad51 K191R, which retains the ability to bind ATP but has greatly attenuated ATPase activity (Sung and Stratton, 1996). As shown in previous studies (Zaitseva et al., 1999) and reiterated here, wild-type Rad51 binds DNA in a mobility shift assay in an ATP-dependent manner (Figure 5A). While the rad51 K191A mutant is defective in DNA binding, the rad51 K191R mutant, as expected, retains the ability to bind DNA with a dependence on ATP (Figure 5A).

We next examined the ability of the two mutant rad51 proteins to promote D loop formation. The results, as shown in Figure 5B, indicated that while rad51 K191R cooperates with Rad54 in forming D loop, rad51 K191A mutant is defective in this reaction. Importantly, rad51 K191R stimulated the ability of Rad54 protein to remodel DNA structure, as measured by the formation of Form OW DNA in the *E. coli* topoisomerase I-linked reaction (Figure 5C) and by the assay that examines sensitivity of relaxed DNA to P1 nuclease (Figure 5D). The same results were obtained when rad51 K191R was preassembled into a nucleoprotein complex with RPA and ssDNA (data not shown). On the other hand, rad51 K191A (Figures 5C and 5D) and the mixture of rad51 K191A and RPA-ssDNA complex (data not shown) were incapable of stimulating the DNA remodeling ability of Rad54, as judged by both of the available criteria of DNA supercoiling (Figure 5C) and sensitivity to P1 nuclease (Figure 5D). Taken together, the results suggest that the DNA binding ability of Rad51 is indispensable for D loop formation and for stimulating the DNA remodeling activity of Rad54.

Discussion

Biochemical Requirements for D Loop Formation in Eukaryotic Recombination

Rad51 by itself has negligible D loop–forming ability (Petukhova et al., 1998; Mazin et al., 2000). In this work and other studies (Petukhova et al., 1998; Mazin et al., 2000), Rad54 has been shown to have a strong dsDNA-dependent ATPase activity and to promote robust D loop formation with Rad51 protein. Importantly, ATP hydrolysis by Rad54 is indispensable for the D loop reaction, in that rad54 K341A and rad54 K341R, which are, respectively, defective and greatly attenuated in ATPase activity (Petukhova et al., 1999), are inactive in the D loop reaction. Consistent with the in vitro results, genetic studies have revealed that the ATPase activity of Rad54 is required for DNA repair and recombination (Clever et al., 1997; Petukhova et al., 1999).

In the present work, we have also demonstrated that the ATP binding defective rad51 K191A mutant is inactive in D loop formation. On the other hand, rad51 K191R, which is greatly attenuated in ATPase activity but retains the ability to bind ATP and functions with the latter in making D loop. We have also provided evidence that rad51 K191R but not the rad51 K191A mutant binds DNA in an ATP-dependent manner. This result strongly suggests that the defect of rad51 K191A mutant in the D loop reaction is due to its inability to bind DNA. Accordingly, the results from genetic experiments have indicated that rad51 K191R is biologically active, whereas the rad51 K191A mutant is defective in recombination functions (Shinohara et al., 1992; Sung and Stratton, 1996).

DNA Remodeling by Rad51 and Rad54

In previous studies, no DNA helicase activity was detected in yeast and human Rad54 proteins (Petukhova et al., 1998; Swagemakers et al., 1998). Yeast Rad54 also does not exhibit a DNA helicase activity in combination with yeast Rad51 (Petukhova et al., 1998). We have now shown that the free energy from ATP hydrolysis is used by Rad54 to remodel DNA structure in such a fashion that both negatively and positively supercoiled domains are generated in the DNA template. Within the concentration range of Rad54 employed for the D loop reaction, the negative and positive supercoils generated as a result of DNA remodeling by Rad54 are relatively unconstrained, as indicated by the fact that whereas treatment of *E. coli* topoisomerase I results in the formation of a positively supercoiled DNA species termed Form OW, similar incubation with calf thymus topoisomerase I did not result in a noticeable change in the DNA linking number. As shown in this work and in an earlier study (Petukhova et al., 1999), at much higher concentrations of Rad54, some of the negative supercoils become constrained, probably due to the preferential binding of Rad54 protein to the negatively supercoiled regions, resulting in the formation of Form U DNA upon treatment with calf thymus topoisomerase I.

We have also employed the single-strand-specific nuclease P1 to demonstrate DNA strand opening by Rad54. P1 does not act on topologically relaxed DNA, but negatively supercoiled DNA is susceptible to this nuclease, with the degree of sensitivity being proportional to the extent of negative supercoiling in the substrate. Incubation of topologically relaxed DNA with Rad54 renders the DNA sensitive to P1 nuclease in a manner that is completely dependent on ATP hydrolysis by Rad54, consistent with the suggestion that the negative supercoils induced by Rad54 lead to DNA strand opening.

Our results have shown a marked stimulation of the Rad54 DNA supercoiling ability by Rad51. Specifically, the formation of Form OW DNA in the *E. coli* topoisomerase I–linked reaction is enhanced by Rad51, and the sensitivity of the DNA substrate to P1 nuclease is similarly increased. The ability to stimulate the DNA supercoiling reaction is rather unique to Rad51, as RecA protein, either free or applied as a preassembled RecA-SSB-ssDNA complex, is devoid of the ability to enhance this Rad54-mediated DNA remodeling reaction. Taken together with our observation that the Rad54 has no stimulatory effect on the RecA-catalyzed D loop reaction, we conclude that the specific interaction noted between Rad51 and Rad54 (Jiang et al., 1996; Clever et al., 1997; Petukhova et al., 1998) is indispensable for the synergistic interactions between these two factors in DNA remodeling and D loop formation.

Basis for Rad51/Rad54-Mediated DNA Supercoiling

A number of proteins, including type I restriction enzymes, DNA helicases, and RNA polymerase II, have been shown to be capable of simultaneously inducing positive and negative supercoils in duplex DNA. The supercoiling induced by these protein factors is thought to result from tracking of these factors along duplex DNA. In particular, the supercoiling produced by RNA polymerase II has been discussed in the context of the "twin-supercoiled-domain" model. In this model, RNA polymerase in the transcript elongation mode tracking along DNA produces a positively supercoiled domain ahead of the polymerase and a negatively supercoiled domain behind it (Wu et al., 1988). Based on these precedents, we speculate that the supercoiling function of Rad54 also stems from an ability of this protein to track along DNA, similarly producing positively and negatively supercoiled domains that are unconstrained, as revealed in the present study by treatment with eukaryotic and prokaryotic topoisomerases.

Our work has also shown stimulation of the DNA remodeling ability of Rad54 by Rad51 and by the Rad51-RPA-ssDNA complex. Based on DNA binding results with the rad51 K191R and rad51 K191A mutants, we further suggest that the ability of Rad51 to stimulate Rad54 DNA remodeling activity requires DNA binding by Rad51. Thus, it seems likely that in the case of free Rad51 being added to the remodeling reaction, Rad51 stimulates DNA remodeling by first binding to the relaxed DNA used as substrate or to the supercoiled domains created by Rad54. We envision two different possibilities of how the Rad51-DNA complex stimulates DNA remodeling. First, it is possible that the complex of Rad51/Rad54 assembled on DNA has a higher intrinsic ability to remodel DNA. Alternatively, or in addition, the Rad51-dsDNA complex may facilitate the formation of closed DNA loops in the duplex via incorporation of the duplex molecule into the secondary binding site of the Rad51-ssDNA complex (Roca and Cox, 1997; Bianco et al., 1999; Sung et al., 2000). The establishment of such closed DNA loops is expected to further constrain the negative and positive supercoils formed by Rad54.

Mechanism for D Loop Formation

Based on the findings from this study, we consider the following model for the observed cooperation between Rad51 and Rad54 in making D loop. In this model, the first step in the D loop reaction is the assembly of an active nucleoprotein complex on ssDNA that involves the binding of Rad51 protein and RPA to ssDNA and the incorporation of Rad54 protein via a specific interaction with Rad51. We propose this sequence of events because we have found that when Rad51 is first allowed to nucleate onto dsDNA, instead of the ssDNA, then D loop formation is suppressed in a Rad51 concentration-dependent manner. It should be noted that the role of RPA in the D loop reaction is less specific, as *E. coli* SSB can substitute for RPA at least partially (data not shown). In addition, we have found that the optimal amount of Rad51 protein (20 nucleotides per Rad51 monomer) for D loop formation is substantially lower than that required to saturate the ssDNA (3 nucleotides per Rad51 monomer), indicating that the most active form of the nucleoprotein filament contains short filaments of Rad51 with Rad54 protein bound to the filaments, with the remainder of the ssDNA substrate being covered with RPA. These biochemical results suggest that during recombination in vivo, efficient formation of D loop can in fact occur prior to the assembly of a contiguous Rad51 filament on the ssDNA tails generated as a result of the nucleolytic end-processing of the DNA break.

We envision that the DNA remodeling activity of Rad51-Rad54 could have two major consequences on the efficiency of the homologous DNA pairing reaction. First, an ability of Rad54 already associated with the Rad51-ssDNA nucleoprotein complex to thread the duplex through its fold (i.e., tracking) will enhance the rate at which the incoming duplex molecule is sampled for homology. Importantly, the transient DNA strand opening that occurs in the negatively supercoiled domain generated by Rad54 can be expected to facilitate the formation of a nascent DNA joint, when homology is located in the duplex. This latter suggestion is supported by our observation that Rad54 enables Rad51 to utilize even relaxed DNA substrate for efficient DNA joint formation. The nascent joint molecule formed will be paranemic in nature, if it is located within the interior of the initiating linear ssDNA molecule. However, if DNA joint formation occurs near one of the ends of the linear ssDNA molecule, then it has the potential of being converted into a plectonemic linkage or stabilizing a preexisting plectonemic joint.

Experimental Procedures

Recombination Proteins

Rad51, rad51 K191A, and rad51 K191R were purified from yeast strain tailored to overproduce these factors to near homogeneity, as described (Sung, 1994; Sung and Stratton, 1996). Rad54, rad54 K341, and rad54 K341R were purified to near homogeneity from overproducing yeast strains, as described (Petukhova et al., 1998, 1999). RPA was purified from *E. coli* cells transformed with a plasmid that simultaneously expresses all three subunits of this factor (He et al., 1996), using the purification procedure described in Sung (1997). RecA was a gift from Michael Cox, and SSB was purchased from Gibco/BRL.

DNA Substrates

Replicative form I ϕX 174 DNA (Gibco/BRL) was relaxed with an excess of calf thymus topoisomerase I (Gibco/BRL) in buffer T (50 mM Tris-HCl [pH 7.5], 30 mM KCl, 0.5 mM DTT, and 10 mM $MgCl_2$) at 37°C. To make negatively supercoiled DNA, replicative form I DNA (120 μM base pairs) was incubated with 60 units of calf thymus topoisomerase I in 400 μl buffer T containing 5, 10, or 20 μM of ethidium bromide at 37°C for 2 hr. To make positively supercoiled DNA, topologically relaxed DNA (50 μM base pairs) was treated with Rad54 (400 nM) and 5 μg *E. coli* topoisomerase I in 500 μl of buffer R (in 35 mM Tris-HCl [pH 7.2], 2.5 mM ATP, 3 mM $MgCl_2$, 100 μg/ml bovine serum albumin, 1 mM DTT, 50 mM KCl, and an ATP regenerating system consisting of 30 mM creatine phosphate and 28 μg/ml phosphocreatine kinase) at 37°C for 15 min. To purify the DNA substrates, reaction mixtures were extracted with phenol and then run on 0.8% agarose gels without ethidium bromide (for positively supercoiled DNA and DNA negatively supercoiled with 10 and 20 μM ethidium bromide) or with 10 μM ethidium bromide (for relaxed DNA and DNA negatively supercoiled with 5 μM ethidium bromide). The DNA bands of interest were visualized by staining with ethidium bromide, excised, and purified using the Geneclean kit (Bio 101). DNA substrates were filter dialyzed in Centricon 30 microconcentrators into TE (10 mM Tris-HCl [pH 7.5] and 0.5 mM EDTA). The superhelical densities of the DNA substrates were determined by one-dimensional and two-dimensional gel analyses. The negatively supercoiled DNA species made with 5, 10, and 20 μM ethidium bromide had superhelical densities of −0.021, −0.039, and −0.076, respectively. The ϕX (+) strand DNA substrate used in the D loop assay was linearized by hybridizing a 26-mer oligonucleotide to create a PstI site, followed by treatment with an excess of this restriction enzyme. The linearized (+) strand was purified as described above.

Rad51/Rad54-Mediated D Loop Formation

The reaction mixture (50 μl final volume) was assembled by mixing 3.3 μg Rad51 (1.5 μM) and 500 ng of linear ϕX viral (+) strand (30 μM nucleotides) in 40 μl of buffer R containing 50 mM KCl. After a 3 min incubation at 37°C, 12 μg RPA (2 μM) in 2 μl was added, followed by a 3 min incubation at 37°C, and then 1.2 μg Rad54 (220 nM) in 1 μl was incorporated, followed by a 3 min incubation at 23°C. To complete the reaction mixture, 600 ng ϕX174 DNA (18.5 μM base pairs) in 3 and 4 μl of 50 mM spermidine (4 mM) was incorporated. The reaction mixture was incubated at 23°C, and 5 μl portions were withdrawn at the indicated times and processed (Petukhova et al., 1998) for electrophoresis in 0.85% agarose gels containing 10 μM ethidium bromide in TAE buffer at 23°C. The gels were stained in ethidium bromide and then subjected to image analysis in a Nucleotech gel documentation station equipped with a CCD camera. The size of the reaction mixtures was scaled down

appropriately for other experiments, but, unless stated otherwise, the procedure for assembling the reaction mixtures was the same. In the analysis of rad51 K191R and rad51 K191A (Figure 5B), the reaction mixtures had a final volume of 50 μl and contained 3.3 μg (1.5 μM) of Rad51, rad51 K191R, or rad51 K191A and 2.4 μg Rad54 (440 nM).

RecA-Mediated D Loop Formation

RecA (7.8 μM) was incubated with 500 ng of ϕX174 viral (+) strand (30 μM nucleotides) in 40 μl of buffer R for 5 min at 37°C, followed by the addition of 5.5 μg of *E. coli* SSB (6 μM) in 3 μl of storage buffer and a 5 min incubation at 37°C. The reaction mixture (50 μl final volume) was completed by adding 4 μl of 120 mM $MgCl_2$ and 600 ng ϕX174 replicative form I DNA (18.5 μM base pairs) in 3 μl. Samples were processed for agarose gel electrophoresis as described above for the Rad51/Rad54-mediated reaction.

Topoisomerase I–Linked DNA Remodeling

The indicated concentrations of Rad54 were incubated with 120 ng of relaxed ϕX 174 DNA (18.5 μM base pairs) for 3 min at 23°C in 9.5 μl of buffer R with 50 mM KCl, followed by the addition of 4 units of calf thymus topoisomerase I (Gibco/BRL) or 100 ng of *E. coli* topoisomerase I in 0.5 μl. Reactions were incubated at 37°C for 10 min, deproteinized by treatment with SDS (0.5%) and proteinase K (1 mg/ml) for 15 min at 37°C. DNA species were resolved in 0.8% agarose gels run in TAE buffer at 23°C and stained with ethidium bromide. To examine the effect of Rad51, rad51 K191R, and rad51 K191A on DNA remodeling, these proteins were incubated with Rad54 and 120 ng of relaxed ϕX 174 DNA (18.5 μM base pairs) in 9.5 μl of buffer R for 3 min at 23°C, before the incorporation of *E. coli* topoisomerase I. For testing the effect of Rad51-RPA-ssDNA filament on DNA remodeling, the indicated concentration of Rad51 was incubated with pBluescript ssDNA (30 μM nucleotides) in 7.7 μl buffer R for 3 min at 37°C, and then 2.4 μg RPA (2 μM) was added in 0.5 μl storage buffer. After 3 min of incubation at 37°C, Rad54 in 0.5 μl storage buffer and 120 ng of relaxed ϕX 174 DNA (18.5 μM base pairs) in 0.8 μl TE were added, followed by a 3 min incubation at 23°C, before the incorporation of *E. coli* topoisomerase I. To analyze the effect of RecA or RecA-SSB-ssDNA, the same procedures were used to assemble the reaction. The completed reaction mixtures were incubated at 23°C for 10 min and then analyzed as described above.

Two-Dimensional Gel Analysis of Form OW DNA

Kodak BioMax MP1015 agarose gel units were used for electrophoresis. The first dimension of the electrophoresis was carried out in 0.9% gels in TAE buffer at 110 mA and 23°C for 6 hr. The gels were soaked for 18 hr at 4°C in 30 gel volumes of TAE buffer containing 30 μM chloroquine diphosphate, and then subject to a second electrophoresis step in TAE containing 30 μM chloroquine diphosphate at 110 mA and 23°C for 6 hr. The DNA species were stained with ethidium bromide. The DNA samples in panels II and IV of Figure 3 were treated with 50 ng of *E. coli* topoisomerase I in buffer T for 10 min at 37°C prior to electrophoresis. The amount of negatively supercoiled DNA and Form OW DNA used in all the panels was 200 ng.

P1 Sensitivity

Increasing concentrations of Rad54 were incubated with 120 ng of relaxed ϕX DNA (18.5 μM base pairs) in 9.5 μl of buffer R with 50 mM KCl for 2 min at 23°C, followed by the addition of 0.4 units of P1 nuclease (Roche) in 0.5 μl. Reaction mixtures were incubated at 23°C or 37°C for 10 min, quenched by 0.5% SDS, and treated with proteinase K (1 mg/ml) for 15 min at 37°C. Reactions products were resolved in agarose gels containing 10 μM ethidium bromide in TAE buffer at 23°C, followed by staining with ethidium bromide. For testing the effect of Rad51, Rad51-RPA-ssDNA complex, RecA, and RecA-SSB-ssDNA complex on P1 sensitivity, the procedures used in the topoisomerase I-linked DNA remodeling experiments described earlier were employed, except that 0.4 units of P1 nuclease replaced the topoisomerase.

ATPase Assay

Rad54 (50 nM) was incubated with 120 ng of relaxed ϕX DNA (18.5 μM base pairs) in 10 μl of buffer A (30 mM Tris-HCl [pH 7.2], 5 mM $MgCl_2$, 1 mM DTT, 50 mM KCl, and 100 μg/ml BSA) and 1.5 mM [γ-^{32}P] ATP for the indicated times at 23°C, and the level of ATP hydrolysis determined by thin layer chromatography, as described (Petukhova et al., 1998). For testing the effect of Rad51 (360 nM) and Rad51-RPA-ssDNA (360 nM Rad51, 2 μM RPA, and 30 μM nucleotides of pBluescript ssDNA) complex on Rad54 ATPase, the procedures followed those described for the DNA supercoiling experiments earlier, except that Rad54 was preincubated with the other reaction components at 0°C instead of 23°C.

DNA Mobility Shift

A mixture of ϕX174 viral (+) strand (30 μM nucleotides) and PstI-linearized ϕX replicative form (20 μM nucleotides) substrates were used with the indicated amounts of Rad51, rad51 K191R, or rad51 K191A in 10 μl buffer G (35 mM Tris-HCl [pH 7.2], 1 mM DTT, 3 mM $MgCl_2$, and 100 μg/ml BSA, with or without 2.5 mM ATP, as indicated). Following incubation at 23°C for 10 min, the reaction mixtures were mixed with 2 μl of loading buffer (0.1% orange G in 50% glycerol), subjected to electrophoresis in 0.9% agarose gels in TAE buffer at 23°C, and stained with ethidium bromide.

Acknowledgments

We are grateful to John Diffley for discussions, to James Wang and Sue-Jane Chen and also to Yuk-Ching Tse-Dinh for their kind gifts of *E. coli* topoisomerase I, and to Michael Cox for the gift of RecA protein. This work was supported by National Institutes of Health research grants RO1GM57814 and RO1ES07061 and by training grants T32AG00165 from the National Institutes of Health (G. P.) and DAMD17-99-1-9402 from the US Army (S. S.).

Received June 20, 2000; revised July 21, 2000.

References

Bianco, P.R., Tracy, R.B., and Kowalczykowski, S.C. (1998). DNA strand exchange proteins: a biochemical and physical comparison. Front Biosci. *3*, D570–D603.

Clever, B., Interhal, H., Schmuckli-Maurer, J., King, J., Sigrist, M., and Heyer, W.-D. (1997). Recombinational repair in yeast: functional interactions between Rad51 and Rad54 proteins. EMBO J. *16*, 2535–2544.

Dasika, G.K., Lin, S.C., Zhao, S., Sung, P., Tomkinson, A., and Lee, E.Y. (1999). DNA damage-induced cell cycle checkpoints and DNA strand break repair in development and tumorigenesis. Oncogene *18*, 7883–7899.

Eisen, J.A., Sweder, K.S., and Hanawalt, P.C. (1995). Evolution of the SNF2 family of proteins: subfamilies with distinct sequences and functions. Nucleic Acid Res *23*, 2715–2723.

Gupta, R.C., Folta-Stogniew, E., O'Malley, S., Takahashi, M., and Radding, C.M. (1999). Rapid exchange of A:T base pairs is essential for recognition of DNA homology by human Rad51 recombination protein. Mol. Cell *4*, 705–714.

He, Z., Wong, J.M.S., Maniar, H.S., Brill, S.J., and Ingles, C.J. (1996). Assessing the requirements for nucleotide excision repair proteins of *Saccharomyces cerevisiae* in an in vitro system. J. Biol. Chem. *271*, 28243–28249.

Jiang, H., Xie, Y., Houston, P., Stemke-Hale, K., Mortensen, U.H., Rothstein, R., and Kodadek, T. (1996). Direct association between the yeast Rad51 and Rad54 recombination proteins. J. Biol. Chem. *271*, 33181–33186.

Kowalczykowski, S.C., Dixon, D.A., Eggleston, A.K., Lauder, S.D., and Rehrauer, W.M. (1994). Biochemistry of homologous recombination in *E. coli*. Microbiol. Rev *58*, 401–465.

Mazin, A.V., Zaitseva, E., Sung, P., and Kowalczykowski, S.C. (2000). Tailed duplex DNA is the preferred substrate for Rad51 protein-mediated homologous pairing. EMBO J. *19*, 1148–1156.

Paques, F., and Haber, J.E. (1999).Multiple pathways of recombination induced by double-strand breaks in *Saccharomyces cerevisiae*. Microbiol. Mol. Biol. Rev. *63*, 349–404.

Petes, T.D., Malone, R.E., and Symington, L.S. (1991). Recombination in yeast. In The Mol. Cell. Biol. of the Yeast Saccharomyces: Genome Dynamics, Protein Synthesis, and Energetics. J.R. Broach, E.W. Jones, and J.R. Pringle, eds. (Cold Spring Harbor Laboratory Press), pp 407–521.

Petukhova, G., Stratton, S., and Sung, P. (1998). Catalysis of homologous DNA pairing by yeast Rad51 and Rad54 proteins. Nature *393*, 91–94.

Petukhova, G., Van Komen, S., Vergano, S., Klein, H., and Sung, P. (1999). ATP hydrolysis-dependent duplex DNA unwinding and promotion of Rad51 catalyzed homologous DNA pairing by yeast Rad54 protein. J. Biol. Chem. *274*, 29453–29462.

Roca, I.A., and Cox, M.M. (1997). RecA protein: structure, function, and role in recombinational DNA repair. Prog. Nucleic Acid Res. Mol. Biol. *56*, 129–223.

Shinohara, A., Ogawa, H., and Ogawa, T. (1992). Rad51 protein involved in repair and recombination in *S. cerevisiae* is a RecA-like protein. Cell *69*, 457–470.

Sung, P. (1994). Catalysis of ATP dependent homologous DNA pairing and strand exchange by the yeast Rad51 protein. Science *265*, 1241–1243.

Sung, P. (1997). Function of Rad52 protein as mediator between RPA and the Rad51 recombinase. J. Biol. Chem. *272*, 28194–28197.

Sung, P., and Robberson, D.L. (1995). DNA strand exchange mediated by a Rad51-ssDNA nucleoprotein filament with polarity opposite to that of RecA. Cell *83*, 453–461.

Sung, P., and Stratton, S.A. (1996). Yeast Rad51 recombinase mediates polar DNA strand exchange in the absence of ATP hydrolysis. J. Biol. Chem. *271*, 27983–27986.

Sung, P., Trujillo, K., and Van Komen, S. (2000). Recombination factors of *Saccharomyces cerevisiae*. Mutat. Res. *451*, 257–275.

Swagemakers, S.M.A., Essers, J., de Wit, J., Hoeijmakers, J.H.J., and Kanaar, R. (1998). The human Rad54 recombinational DNA repair protein is a double-stranded DNA-dependent ATPase. J. Biol. Chem. *273*, 28292–28297.

Tan, T.L., Essers, J., Citterio, E., Swagemakers, S.M., de Wit, J., Benson, F.E., Hoeijmakers, J.H., and Kanaar, R. (1999). Mouse Rad54 affects DNA conformation and DNA-damage-induced Rad51 foci formation. Curr. Biol. *9*, 325–328.

Wu, H.Y., Shyy, S.H., Wang, J.C., and Lui, L.F. (1988). Transcription generates positively and negatively supercoiled domains in the template. Cell *53*, 433–440.

Zaitseva, E.M., Zaitsev, E.N., and Kowalczykowski, S.C. (1999). The DNA binding properties of Saccharomyces cerevisiae Rad51 protein. J. Biol. Chem. *274*, 2907–2915.

Reprinted from

MUTATION RESEARCH

Fundamental and Molecular Mechanisms of Mutagenesis

Mutation Research 451 (2000) 257–275

Review

Recombination factors of *Saccharomyces cerevisiae*

Patrick Sung *, Kelly Miguel Trujillo, Stephen Van Komen

Department of Molecular Medicine and Institute of Biotechnology, University of Texas Health Science Center at San Antonio, 15355 Lambda Drive, San Antonio, TX 78245-3207, USA

Received 21 September 1999; received in revised form 3 December 1999; accepted 16 December 1999

ELSEVIER

Aims and scope

MUTATION RESEARCH, Fundamental and Molecular Mechanisms of Mutagenesis publishes complete research papers in all areas of mutation research which focus on fundamental mechanisms underlying phenotypic and genotypic expression of genetic damage, molecular mechanisms of mutagenesis including the relationship between genetic damage and its manifestation as hereditary diseases and cancers, as well as aging. Additional 'special issues', which bring together original research and review papers written from a particular viewpoint on a central theme of topical interest, will also appear in this section. Topics for special issues are developed by the Special Issues Editors.

Instructions to Authors and addresses for the submission of articles are provided at the back of each issue and at the website http://www.elsevier.com/locate/molmut

ELSEVIER

Mutation Research 451 (2000) 257–275

Fundamental and Molecular Mechanisms of Mutagenesis

www.elsevier.com/locate/molmut
Community address: www.elsevier.com/locate/mutres

Review

Recombination factors of *Saccharomyces cerevisiae*

Patrick Sung *, Kelly Miguel Trujillo, Stephen Van Komen

Department of Molecular Medicine and Institute of Biotechnology, University of Texas Health Science Center at San Antonio, 15355 Lambda Drive, San Antonio, TX 78245-3207, USA

Received 21 September 1999; received in revised form 3 December 1999; accepted 16 December 1999

Abstract

The budding yeast *Saccharomyces cerevisiae* has been an excellent genetic and biochemical model for our understanding of homologous recombination. Central to the process of homologous recombination are the products of the *RAD52* epistasis group of genes, whose functions we now know include the nucleolytic processing of DNA double-stand breaks, the ability to conduct a DNA homology search, and the capacity to promote the exchange of genetic information between homologous regions on recombining chromosomes. It is also clear that the basic functions of the *RAD52* group of genes have been highly conserved among eukaryotes. Disruption of this important process causes genomic instability, which can result in a number of unsavory consequences, including tumorigenesis and cell death.

1. Prologue

In addition to creating genetic diversity, homologous recombination is also an important tool for repairing DNA double-strand breaks (DSBs). Furthermore, meiotic recombination helps establish stable interactions between chromosomal homologs, and as such, is indispensable for the proper disjunction of chromosomes in the first meiotic division (reviewed in Refs. [47,71,82]).

Much of our understanding of homologous recombination processes in eukaryotes has originated from studies conducted in the budding yeast *Saccharomyces cerevisiae*. The common denominator of many recombination processes in *S. cerevisiae* (henceforth referred to as yeast) is a DNA DSB, formed either as a result of exposure of cells to break-inducing radiation and chemicals or as part of developmental programs. The most notable examples of the latter class of recombination processes are mating type switching, being initiated by a site-specific DSB made by the HO endonuclease, and meiotic recombination, which occurs by way of DSBs introduced by a complex of proteins including Spo11 as the catalytic subunit. Once a DSB is formed, the ends of the break are subjected to processing by exonucleolytic activities and the single-stranded DNA tails thus formed will be channeled into one of a number of homologous recombination pathways as discussed below and elsewhere [66]. Alternatively, the DNA ends can simply be rejoined via the non-homologous DNA end-joining pathway, with or without further processing. A synopsis of the major homologous recombination pathways and their genetic and biochemical requirements is given below. Comprehensive reviews on non-homologous DNA

* Corresponding author. Tel.: +1-210-567-7215; fax: +1-210-567-7277.
E-mail address: sung@uthscsa.edu (P. Sung).

0027-5107/00/$ - see front matter
PII: S0027-5107(00)00054-3

end-joining have been published recently [32,107], and this topic will not be dealt with here.

2. Recombination processes

2.1. Classical recombination

In classical recombination, the DSB is processed by an exonuclease activity, digesting away a substantial portion of the DNA strands that contain the 5′ ends of the break. This end-processing reaction results in long (as long as 1 kb or more) ssDNA tails that have a 3′ extremity. These ssDNA tails are utilized for the nucleation of a number of recombination factors to yield a nucleoprotein complex that has the ability to conduct a DNA homology search to locate an intact DNA homolog, which could be either the sister chromatid or the homologous chromosome. Invasion of the homolog in a reaction called ''homologous DNA pairing and strand exchange'' yields a joint between the recombining molecules (Fig. 1). When the recombining DNA molecules encompass different alleles of the same gene, then DNA mismatches will form in the DNA joint, giving rise to heteroduplex DNA. Correction of the DNA mismatches results in the conversion of one of the recombining alleles to the other. Heteroduplex DNA formation followed by DNA mismatch correction represents an important means for gene conversion in yeast, although it is not the only route. In considering this well recognized DNA DSB repair model for homologous recombination (variants of this model have been discussed by Paques and Haber [66]), one important point to bear in mind is that the 3′ ssDNA tails arising through DSB end-processing, rather than the DSB per se, are in fact the substrate utilized by the recombination machinery for mediating subsequent reactions.

While meiotic recombination mainly involves chromosomal homologs, it is believed that most of the recombination events during mitotic growth occur in the late S and G2 phases and involve the sister chromatids. However, in yeast, there is considerable capacity to carry out allelic (interchromosomal) recombination during mitotic growth, and allelic recombination appears to have a somewhat different genetic requirement than sister chromatid-based recombination ([66]; see later). Mutations in genes

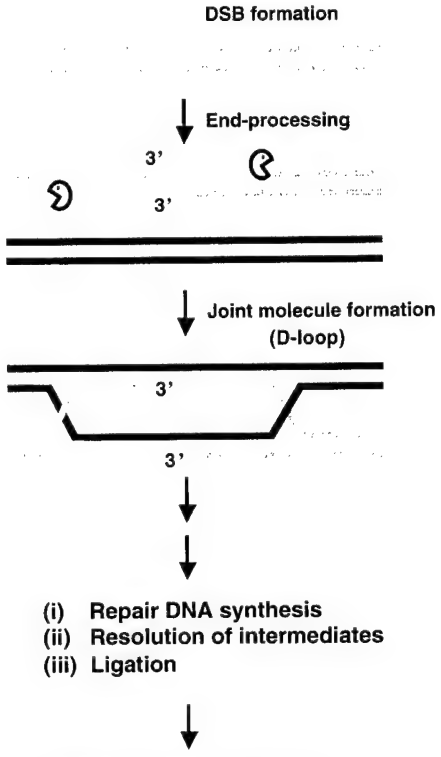

Fig. 1. Recombination induced by DNA DSBs. The ends of DNA DSBs are processed nucleolytically to yield long 3′ single-strand tails. Nucleation of recombination factors onto the single-strand tails leads to a search for a DNA homolog and pairing with the homolog to form a joint molecule called D-loop. Concurrent and subsequent steps include DNA synthesis to replace the genetic information eliminated during end-processing, resolution of the Holliday intermediates, and DNA ligation to complete the recombination process.

(e.g., *RAD50*, *MRE11*, and *XRS2*) that are believed to mediate sister chromatid-based recombination could in fact lead to higher levels of recombination between homologs. It has been suggested that when sister chromatid-based recombination is inactivated, the recombinogenic DNA substrates are channeled more often into interchromosomal recombination pathways.

2.1.1. The players in classical homologous recombination: RAD52 epistasis group

Genetic screens based mainly on sensitivity to ionizing radiation have identified a large number of genetic loci required for the repair of DNA breaks,

and many of these genes have subsequently been shown to be needed for efficient mating type switching, mitotic recombination, and meiotic recombination. These genes — *RAD50*, *RAD51*, *RAD52*, *RAD54*, *RAD55*, *RAD57*, *RAD59*, *RDH54/TID1*, *MRE11*, and *XRS2* — are collectively known as the *RAD52* epistasis group [6,29,48,66,71,90]. Below, we provide a synopsis of the biochemistry of the products of these genes and their likely roles in enzymatic reactions that lead to the formation of recombinants.

2.1.1.1. Biochemistry of homologous recombination DNA end-processing

Role of Rad50, Mre11, and Xrs2 in end-processing. A good body of evidence has linked *RAD50*, *MRE11*, and *XRS2* to DSB end-processing during recombination processes [66]. Rad50 is a highly conserved member of the Structural Maintenance of Chromosomes (SMC) family of proteins, which functions in different aspects of chromosomal metabolism (reviewed in Ref. [35]). Mre11 is also a highly conserved protein and shows homology to phosphodiesterases. Rad50 and Mre11 are the respective homologs of *Escherichia coli* SbcC and SbcD [84], which combine to form a complex that has ssDNA endonuclease and ATP-dependent exonuclease activities, and also an ability to open DNA hairpins; SbcD is the catalytic subunit of this nuclease complex [20]. Consistent with these observations, Mre11 from both yeast [28,60,108] and humans [69,106] exhibits ssDNA endonuclease activity, a 3′ to 5′ exonuclease activity, and hMre11 also possesses an ability to cleave DNA hairpins [69,70]; whether yMre11 acts on DNA hairpins remains to be determined. hMre11 combines with hRad50, and the resulting complex has enhanced exonuclease activity [69]. The exonuclease activity of hRad50–hMre11 complex is not stimulated by ATP, thus marking a major difference between this human complex and the bacterial SbcC–SbcD complex. Mre11 from both yeast and humans, like its bacterial counterpart SbcD, specifically requires manganese for the activation of its nuclease activity.

The human Rad50–Mre11 complex combines, primarily or exclusively through Mre11 [70], with a third protein called p95 [22]. Recently, p95 was found to be mutated in the cancer prone disease Nijmegen breakage syndrome (NBS), and is now also called NBS1 or nibrin [16,110]. NBS1/nibrin modulates the nuclease function of the Rad50–Mre11 complex, making it possible for the complex containing the protein trio to act efficiently on different types of DNA hairpins and also endonucleolytically and in an ATP-dependent manner, on 3′ ssDNA tails that border a duplex region. The Rad50–Mre11–NBS1 complex has a modest ability to unwind duplex DNA, resulting in DNA strand separation. DNA unwinding is stimulated by ATP, and mutating the nucleotide binding fold in Rad50 renders the mutant Rad50 containing protein complex insensitive to ATP in DNA unwinding and nuclease functions [70]. NBS cells, like ataxia telangiectasia (AT) cells, appear to be defective in different cell cycle checkpoints. Based on this phenotype of NBS cells, it has been proposed that NBS1 relays the detection of DNA lesions to the cell cycle checkpoint machinery (reviewed in Ref. [88]). However, the results of Paull and Gellert [70] have clearly demonstrated that NBS1 is in fact also important for the expression of the full repertoire of biochemical activities of the Mre11-associated complex.

In yeast, Xrs2 combines with the Rad50–Mre11 complex through the Mre11 subunit [43,108]. Although Xrs2 is considered the yeast equivalent of NBS1, Xrs2 is only distantly related to NBS1 in amino acid sequence, with homology noted only in the amino-termini of the two factors where putative protein–protein interaction domains are located (reviewed in Ref. [27]). There is no information available as to the biochemical functions of Xrs2 and its role in modulating the activities of Rad50 and Mre11.

Possible means for processing DNA ends. Studies in yeast have clearly indicated that the ends of DNA DSBs are processed to yield 3′ ssDNA tails (Fig. 1), predicting a 5′ to 3′ exonuclease activity in the end-processing reaction. It was therefore rather surprising to find that hMre11 and yMre11 both have a 3′ to 5′ exonuclease activity but are apparently devoid of a significant 5′ to 3′ exonuclease activity [28,60,69,106,108]. To reconcile this paradox, it has been suggested that the Mre11-associated complex functionally cooperates with a DNA helicase to unwind DNA from the ends, creating an open structure for the endonucleolytic function of Mre11 to act on (Fig. 2). Since a short single-stranded region may be

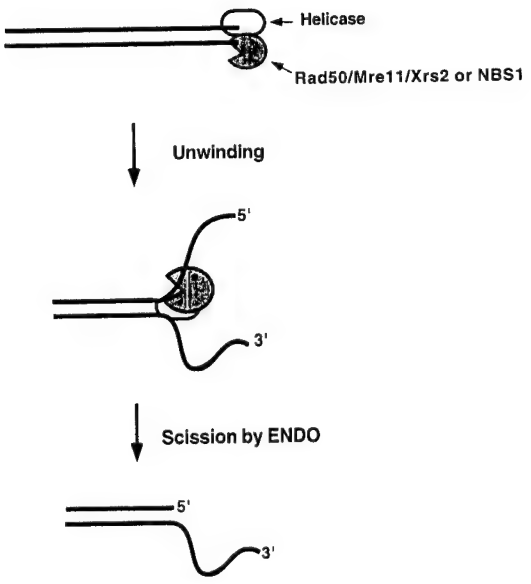

Fig. 2. Possible mechanism for DSB end-processing. It is postulated that a higher order complex of a DNA helicase and the trio of Rad50, Mre11, and Xrs2 is recruited to the DNA ends. DNA strand separation by the helicase then creates a splayed DNA structure, the 5′ overhang of which is then excised by the endonucleolytic activity of Mre11 to generate the 3′ ssDNA tail observed in genetic experiments.

required for the loading of a DNA helicase and activation of DNA unwinding, it seems possible that the 3′ to 5′ exonuclease activity of Mre11 may, at least under some circumstances, be involved in generating a short 5′ ssDNA overhang for the loading and activation of the DNA helicase.

Genetic results have clearly indicated that Mre11 is not the only nuclease capable of processing DNA ends during mitotic recombination, and that the Mre11 complex must play another role in recombination [66]. Since the sister chromatid appears to be the preferred DNA homolog used in directing recombinational repair, one plausible idea is that Mre11 together with Rad50 and Xrs2 mediate the type of sister–sister chromatid interactions indispensable for the efficient repair of lesions by sister chromatid-based recombination ([66]; John Petrini, personal communication).

Unlike the situation in mitotic cells, the processing of DNA DSBs during meiotic recombination is largely or completely dependent on the Mre11-associated nuclease activity. As discussed elsewhere [10,49], a putative topoiosmerase activity in Spo11 is likely to be responsible for the generation of meiosis-specific DSBs, and Spo11 has been shown to remain covalently attached to the 5′ termini of the DNA breaks [49]. Thus, it appears that only the Mre11-associated protein complex is capable of removing Spo11 covalently attached to the 5′ termini of the meiosis-specific DSBs.

Multifunctional nature of Rad50, Mre11, and Xrs2. Genetic analyses have revealed that Rad50, Mre11, and Xrs2 work in conjunction with Spo11 to introduce meiosis specific DNA DSBs. Truly remarkable are the observations that the trio of Rad50, Mre11, and Xrs2 are also required for the maintenance of telomere length and for non-homologous DNA end joining. Notably, the Mre11 nuclease activity appears to be dispensable for its functions in meiotic DSB formation, telomere maintenance, and DNA end-joining. The readers can find more information on these topics in recent reviews [32,66,107].

Heteroduplex DNA formation

Roles of Rad51, Rad52, Rad54, Rad55, Rad57, Rdh54 / Tid1, and RPA in heteroduplex DNA formation. Genetic and biochemical studies have revealed a role for Rad51, Rad52, Rad54, Rad55, Rad57, Rdh54, and RPA in the utilization of recombinogenic ssDNA substrates for the formation of heteroduplex DNA (reviewed in Ref. [66]). Here, we will describe in some detail the homologous DNA pairing and strand exchange reaction that is responsible for the generation of heteroduplex DNA, and will summarize the current state of knowledge of the biochemical functions of these recombination factors. The properties and salient features of the various recombination factors are also given in Table 1.

Rad51 recombinase. The *RAD51* encoded product is homologous to the *E. coli* general recombinase RecA [2,9,89], most notably in the regions of the latter that are concerned with catalytic functions, including the motifs involved in DNA binding and in nucleotide binding and hydrolysis [11,81]. Genetic studies have clearly implicated *RAD51* in recombination processes, and *rad51* mutants exhibit the type of phenotypes expected for eukaryotic homolog of RecA [2,9,89]. Direct evidence supporting the notion that Rad51 is a true functional RecA homolog has come from biochemical studies which demonstrated that (i) in the presence of ATP, Rad51 assem-

Table 1
The recombination factors of yeast

Protein	Size	Biochemical function	*E. coli* homolog	Human homolog	Notable features
Rad50	152,545	DNA-binding	SbcC	hRad50	Member of SMC family; forms complex with Mre11 and Xrs2
Mre11	77,630	ssDNA endonuclease 3′ to 5′ exonuclease	SbcD	hMre11	Homology to phosphodiesterases; forms complex with Rad50 and Xrs2
Xrs2	96,366	not known	none	NBS1	Forms complex with Rad50 and Mre11
Rad51	42,943	ATP-dependent homologous DNA pairing and strand exchange	RecA	hRad51	Forms nucleoprotein filaments; forms complexes with Rad52 and Rad54
Rad52	56,064	ssDNA binding and annealing	none	hRad52	Mediator of strand exchange; required for single strand annealing and BIR
Rad54	101,776	DNA-dependent ATPase	none	hRad54	Member of Snf2 family; promotes homologous DNA pairing by Rad51
Rad55	46,347	ssDNA binding	none	XRCC2, XRCC3, Rad51B, Rad51C, Rad51D	Forms heterodimer with Rad57; Rad55–Rad57 heterodimer functions as mediator in strand exchange
Rad57	52,242	ssDNA binding	none	XRCC2, XRCC3, Rad51B, Rad51C, Rad51D	Forms heterodimer with Rad55; Rad55–Rad57 heterodimer functions as mediator in strand exchange
Rad59	26,632	ssDNA binding and annealing	none	not known	Homology to Rad52; required for single strand annealing
Dmc1	36,606	ATP-dependent homologous DNA pairing[a]	RecA	hDmc1	Interacts with Rdh54/Tid1 in two-hybrid system
Rdh54/Tid1	108,058	not known	none	hRad54	Member of Snf2 family; interacts with Dmc1 and Rad51 in two-hybrid system
RPA	70,339	ssDNA binding	none	hRPA	Removes secondary structure in ssDNA during the presynaptic phase of strand exchange
	29,921				
	13,810				

[a]Based on results with hDmc1 [52].

bles into a nucleoprotein filament on both ssDNA and dsDNA that is almost identical to the equivalent RecA-DNA nucleoprotein filament in overall dimensions and structure [65,98] and (ii) like RecA, Rad51 exhibits a homologous DNA pairing and strand exchange activity that yields joints between two DNA molecules [97].

Outside of the central homologous core of about 220 amino acids, RecA and Rad51 actually differ significantly, with Rad51 bearing an amino-terminal extension of about 120 amino acids, but is shorter than RecA by about 90 amino acids at the carboxyl-terminus. In addition, yeast Rad51 has a putative leucine zipper motif ($L–X_6–L–X_6–L–X_6–F$) from residues 296–317. These structural distinctions between RecA and Rad51 could account for the functional differences between the two proteins and could perhaps also reflect the unique sets of evolutionarily divergent recombination factors with which the two recombinases have to interact to accomplish their biological roles. Like RecA, Rad51 has a DNA-dependent ATPase activity. Maximal ATP hydrolysis

by Rad51 is seen with ssDNA, with duplex DNA being 5–10-fold less effective in activating ATP hydrolysis [97]. The kcat for ATP hydrolysis with ssDNA as cofactor is less than 1/min, which is about 40-fold lower than what has been observed for RecA [95,97].

Homologous DNA pairing and strand exchange mediated by Rad51. The homologous DNA pairing and strand exchange reaction has been studied in vitro using a variety of available systems, some of which are described in Fig. 3. The common feature of all of these in vitro systems is that there is a single DNA strand, which is the equivalent of the 3′ ssDNA tail generated via DNA end-processing in vivo, and a homologous duplex DNA molecule that is either linear or covalently closed, which can be considered the prospective DNA homolog, i.e. the homologous chromosome or sister chromatid. The reaction is initiated via the assembly a Rad51-ssDNA nucleoprotein complex, into which the homologous duplex DNA molecule is incorporated for DNA homology search and DNA joint formation with the single strand.

The reaction phase in which assembly of the Rad51-ssDNA nucleoprotein complex occurs is called the ''presynaptic'' phase, a process that is simple conceptually but in reality surprisingly complex, being dependent on the single-strand DNA binding factor RPA and molecular ''mediators'', as described in more detail below. Later, reaction steps which collectively lead to stable pairing between the recombining DNA molecules occur in the ''synaptic'' phase, which is also described in some detail below. Once a stable joint is formed between the two recombining DNA molecules, branch migration extends the length of the joint, resulting in formation of a substantial amount of heteroduplex DNA (see below).

Distinct phases of the homologous DNA pairing and strand exchange reaction

The presynaptic phase. In the presence of ATP, Rad51 polymerizes onto ssDNA [98] and dsDNA [65] to form helical nucleoprotein filaments that are right-handed [65]. Formation of the Rad51 filament on ssDNA is stimulated by the heterotrimeric ssDNA binding factor RPA [98], whereas Rad51 filament

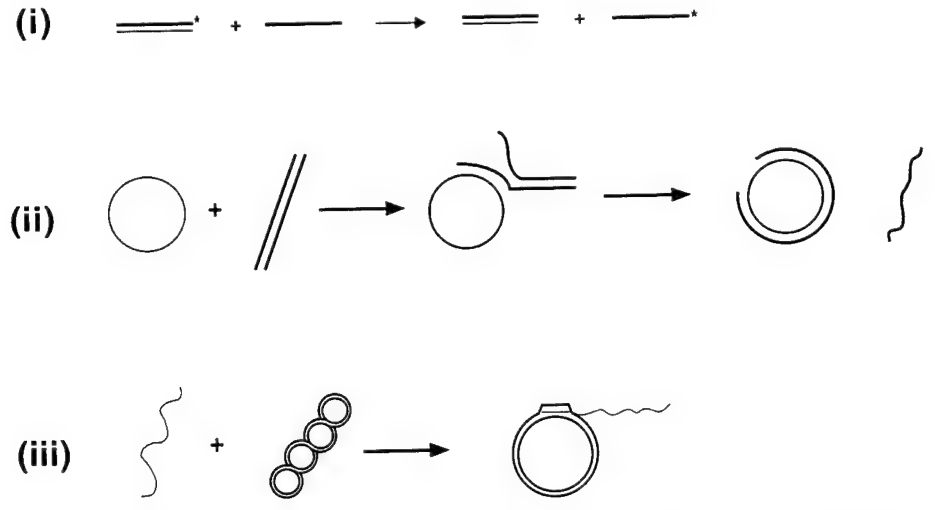

Fig. 3. Systems for studying the homologous DNA pairing and strand exchange reaction. (i) This prototypical system that uses oligonucleotides is quite sensitive, and it allows one the option of examining the influence of DNA sequence context on homologous DNA pairing. Because of the short length of the substrates, this system is not very useful for studying the strand exchange or branch migration reaction. (ii) This system employs the viral (+) strand and linear duplex form of DNA from a bacteriophage, and is used frequently for examining homologous DNA pairing and strand exchange by RecA and Rad51. (iii) To measure D-loop formation, one employs a linear single strand and a covalently closed duplex, normally a supercoiled molecule. The D-loop is the first DNA intermediate formed in vivo, and studies with yeast proteins have indicated that formation of D-loop requires Rad54, in addition to Rad51 and RPA (Petukhova et al., 1998). The readers can find more information on in vitro homologous DNA pairing and strand exchange systems in other review articles [50,81]. Portions of this figure were adapted from Camerini-Otero and Hsieh [15].

assembly on dsDNA shows no dependence on RPA [65,98]. The formation of Rad51 filament on either ssDNA or dsDNA requires ATP [65,98], although ATP binding alone appears to be sufficient for assembly [99]. The Rad51 nucleoprotein filament on circular dsDNA has been analyzed by three-dimensional reconstruction [65], and the results indicate that the Rad51 filament is almost identical in overall dimensions and appearance to the equivalent filament of RecA, with a pitch of 99 Å and 18.6 base pairs of DNA per helical turn. The most notable feature about the Rad51-dsDNA filament is that the DNA is held in a highly extended conformation, as reflected in the axial rise of 5.1 Å per base pair as compared to 3.4 Å per base pair encountered in normal B-form DNA [65]. The Rad51 filament formed on ssDNA has not been analyzed in as much detail, but it also shows the same extended conformation and shares similar overall dimensions as the Rad51-dsDNA filament [98].

Biochemical analyses have indicated that the homologous DNA pairing and strand exchange reaction occurs within the confines of the Rad51-ssDNA nucleoprotein filament, whereas the Rad51 filament on dsDNA is not capable of mediating this reaction [98]. The extent of Rad51 filament assembly on ssDNA can be followed by electron microscopy, but much more conveniently by simply measuring the level of ssDNA dependent ATPase activity [95]. Although RPA is important for the assembly of a contiguous filament on ssDNA and is therefore an important cofactor in the strand exchange reaction [95,97], an excess of RPA can in fact suppress this reaction [100]. This inhibitory effect of RPA has been attributed to competition with Rad51 for binding sites on the ssDNA. Two factors, Rad52 and Rad55–Rad57, help Rad51 overcome the competition posed by RPA, as described below.

The synaptic phase. Once the Rad51-ssDNA nucleoprotein filament is assembled, it is capable of taking up another DNA molecule, which could be a single-strand or a duplex. In this regard, the ssDNA molecule onto which the Rad51 filament has assembled may be viewed as being bound within a primary site within the filament, and the incoming homologous duplex molecule bound within a secondary site in the filament [50,81]. For stable pairing between the ssDNA and the duplex to occur, homologous contacts need to be established between the two recombining DNA molecules within the nucleoprotein filament. By reason of probability, the initial contact points between the ssDNA and the duplex are not at homologous locales. Exactly how the Rad51 nucleoprotein filament samples the incoming duplex to locate DNA homology is not known at this juncture. In the case of the RecA filament, it is believed that DNA homology search is relatively rapid and involves random collisions of the two DNA molecules [50,81]. In theory, binding of the duplex to the secondary site in the RecA filament has to be transient for a random collision mechanism to work efficiently. In support of this deduction, Mazin and Kowalczykowski [58] have provided evidence that the secondary binding site in the RecA filament indeed has only modest affinity for a duplex molecule. Experimental evidence does not support extensive sliding between the two DNA molecules within the RecA filament as a major means for locating DNA homology [3]. Given the precedent with RecA, it seems reasonable to propose that DNA homology search conducted by the Rad51-ssDNA nucleoprotein filament may primarily go through the random collision mode as well.

Once DNA homology is found, alignment of the two recombining molecules is established through a series of transient joints called paranemic joints (Fig. 4A). In RecA studies, the exact nature of the paranemic joint is still a subject of debate. Some have argued that the paranemic linkage involves a DNA triplex structure (i.e. all three strands are held together via novel non-Watson–Crick bonding), whereas other investigators believe that DNA strand switch occurs in the paranemic joint, with the extent of the strand switch being limited by topological constraints and dependent on the local nucleotide sequence context. Regardless of the true nature of the paranemic joint, it has been demonstrated in a number of studies, and although the paranemic joints dissociate readily when the RecA filament is disrupted (by deproteinization treatment, for instance), they are believed to be an important DNA intermediate that serves to capture the duplex and bring the two recombining DNA molecules into homologous registry [50,78,81].

When the two recombining DNA molecules are aligned, then there is the potential for the formation

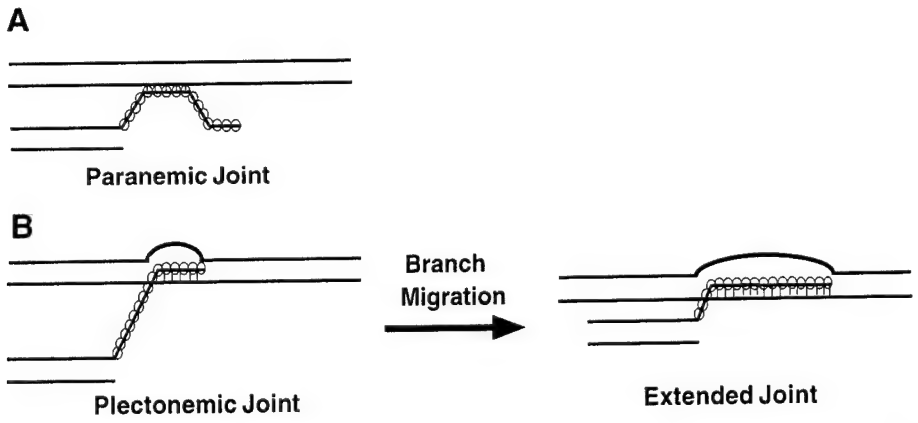

Fig. 4. DNA joints in the formation of heteroduplex DNA. (A) The first homologous joints formed between the recombining DNA molecules are paranemic. The paranemic joints are unstable but are believed to be important intermediates which lead to the formation of a stable joint molecule. The exact nature of the paranemic joint remains a subject of debate (see text and Roca and Cox [81]). (B) Once a free DNA end is located, the formation of a stable plectonemic linkage ensues. The reaction in which the plectonemic joint is extended is called branch migration or strand exchange. The circles in (A) and (B) denote Rad51 molecules. It should be noted that the nucleoprotein complex that conducts the reaction steps very likely contains other factors of the *RAD52* group, including Rad52, Rad54, and Rad55–Rad57 (see text).

of a stable joint molecule. This occurs when a free DNA end is present either in the ssDNA or the dsDNA molecule to allow for intertwining of the ssDNA strand with the complementary strand in the duplex partner. The plectonemic joint that results is much more stable than the paranemic linkage, because the two DNA molecules in the plectonemic joint are not only base-paired but are also topologically linked. In the branch migration reaction, the length of the plectonemic joint is extended (Fig. 4B). In the case of the Rad51 filament, branch migration proceeds 3′ to 5′ with respect to the initiating single strand, a reaction polarity opposite to that of RecA [98]. However, other results have suggested that branch migration within the Rad51 filament can also proceed in the 5′ to 3′ direction [63]. It is clear that branch migration mediated by the Rad51 filament does not need ATP hydrolysis [99], although based on the RecA model, one suspects that ATP hydrolysis could increase the bias for branch migration in a certain direction [81].

Recombination factors that function in the presynaptic phase

RPA. As alluded to above, the heterotrimeric ssDNA binding factor RPA is required for the efficient assembly of the Rad51 presynaptic filament, as verified by electron microscopy [98] and by examining the level of Rad51 ssDNA-dependent ATPase activity [95]. *E. coli* single-strand DNA binding protein (SSB) is as effective as yeast RPA in stimulating the ssDNA dependent ATPase and the DNA strand exchange activities of Rad51. Since Rad51 and SSB are not expected to interact physically, the results suggest that the major functional role of RPA in presynapsis is to remove the secondary structure in the ssDNA substrate [95]. This conclusion is directly supported by the observation that homopolymeric DNA species which are devoid of secondary structure are significantly more effective than natural ssDNA species in activating ATP hydrolysis by Rad51 [95].

In Rad51-mediated strand exchange, the stimulatory effect of RPA is seen most clearly when it is incorporated into the reaction after Rad51 has already nucleated onto the ssDNA. If an excess of RPA is added before or with Rad51 to the ssDNA substrate, suppression of strand exchange ensues [100]. RPA inhibits the ssDNA-dependent ATPase activity of Rad51 under conditions where it suppresses strand exchange [91,95]. Taken together, the results indicate that RPA can interfere with the assembly process by competing for binding sites on the

ssDNA substrate. Since RPA is at least as abundant as Rad51 in yeast cells, it seems likely that specific ancillary factors function with Rad51 in vivo to overcome the competition posed by RPA. Indeed, Rad52 and the Rad55–Rad57 complex have been shown to facilitate the assembly of the Rad51-ssDNA nucleoprotein filament when RPA is competing for DNA binding sites, as described in greater detail below.

Rad52, a mediator in strand exchange. RAD52 encoded product does not show obvious homology to any of the known recombination proteins in bacteria, and therefore appears to be unique to eukaryotes. Rad52 from yeast and humans binds to DNA as a ring-shaped multimer [92,109], showing higher affinity for ssDNA than dsDNA [61,92]. Recently, Van Dyck et al. [109] reported that human Rad52 binds specifically to DNA-ends.

Rad52 is of lower cellular abundance than Rad51, and forms a stable, stoichiometric, and co-immunoprecipitable complex with Rad51 [101]. Rad51–Rad52 complex has a mean size of greater than 1 MDa in gel filtration and its formation is not influenced by ATP (B.W. Song and P. Sung, unpublished results). Although Rad52 has been reported to interact with RPA in solution [92] and when RPA is bound to DNA [96], a stable complex between RPA and Rad52 cannot be demonstrated in cell extract or when purified Rad52 and RPA are mixed (B.W. Song and P. Sung, unpublished results). As described earlier, an excess of RPA added with Rad51 to the ssDNA substrate suppresses nucleoprotein filament assembly and compromises strand exchange efficiency. Under this circumstance, addition of Rad52 effectively overcomes the inhibition posed by RPA [64,92,100], and an amount of Rad52 approximately one tenth of Rad51 is already optimal for restoring strand exchange [101]. Although Rad52 is a ssDNA binding protein, it does not replace RPA in the strand exchange reaction [64,91,101]. Thus, Rad52 plays a highly specific role in the homologous pairing and strand exchange reaction, mediating a productive interaction between the recombinase Rad51 and the ssDNA binding factor RPA [101]. Because of this function of Rad52, it has been coined a "mediator" of DNA strand exchange [45,100]. How Rad52 exerts its mediator function is not known at present, but it seems reasonable to propose that Rad52 targets Rad51 to ssDNA, which can then act as the nucleation sites for filament growth.

Genetic studies have indicated that Rad52 also functions in at least two other pathways of recombination, namely, single-strand annealing (SSA) and DNA break induced replication (BIR), which are discussed in more detail below. The involvement of *RAD52* in multiple recombination pathways could be the reason why it appears to be the most important recombination factor in mitotic cells. Thus, although null mutations in *RAD52* essentially eliminate all the cellular ability to carry out recombination, it could be due to the cumulated effects of defects in different recombination pathways and does not necessarily mean that a certain recombination mechanism is more dependent on Rad52 than on other members of the *RAD52* group. Interestingly, the *RAD52* homolog in vertebrates does not appear to be nearly as indispensable in recombination and repair [80,112], suggesting that either Rad52 is not involved in as many different recombination pathways in higher organisms, or another recombination factor, a Rad52-homologous protein perhaps, provides parallel functions in other eukaryotes.

Rad55–Rad57 complex, and its mediator function. RAD55 and *RAD57* genes are unique among the *RAD52* group members in that their mutants, including null mutants, are cold sensitive for recombination and for sensitivity to ionizing radiation [55]. The recombination defects in the *rad55 rad57* double mutant are no more severe than those in single mutants, indicating a tight epistatic relationship between the two genes. Interestingly, Rad55 and Rad57 share some limited homology to RecA and Rad51, particularly in the sequence motifs involved in the binding of nucleoside triphosphates [54], and have in fact been referred to as RecA homologs. Rad55 and Rad57 interact in the yeast two-hybrid system [34,41]. In agreement with the two-hybrid results, Rad55 and Rad57 coimmunoprecipitate from cell extract and co-purify chromatographically. Sizing experiments revealed that the majority of Rad55–Rad57 is heterodimeric [101]. Interestingly, although Rad51 was shown to interact strongly with Rad55 in the yeast two-hybrid assay [34,41], Rad55–Rad57 complex does not co-immunoprecipitate with Rad51 from cell extract and purified Rad55–Rad57 heterodimer binds only weakly to Rad51 immobilized on Affi-gel beads

[100]. Mutations in the Walker type A nucleotide binding motif of Rad55 interfere with its recombination functions, whereas the equivalent mutations in Rad57 have little or no effect [41].

Addition of Rad55–Rad57 complex to the strand exchange reaction also effectively overcomes the competition posed by RPA, indicative of a mediator function of the heterodimer [101]. Like Rad52, the Rad55–Rad57 heterodimer is of lower cellular abundance than Rad51, and amounts of Rad55–Rad57 substoichiometric to that of Rad51 are already sufficient to effect the optimal level of mediator function. Although Rad55–Rad57 heterodimer has a ssDNA binding activity, it does not replace RPA in strand exchange and does not appear to possess strand exchange activity [101].

Since a mediator function has been identified in Rad52 as well [64,91,100], it is possible that Rad55–Rad57 heterodimer acts via a different mechanism or assists Rad51 at a stage in the assembly of the presynaptic filament temporally distinct from the reaction step that is dependent on Rad52. Alternatively, or in addition, Rad52 and Rad55–Rad57 complex may provide parallel, overlapping functions to ensure that the assembly of the Rad51 nucleoprotein filament occurs efficiently in vivo.

Recombination factors that function in the synaptic phase

Rad54. The *RAD54* encoded product belongs to the Swi2/Snf2 protein family, members of which are involved in diverse chromosomal processes including transcription, nucleotide excision repair, and post-replicative repair (reviewed in Ref. [25]). Consistent with the presence of Walker type nucleotide binding motifs in Rad54 [26], purified Rad54 has a robust ATPase activity (kcat $\sim$ 1000 min^{-1}) that is completely dependent on DNA, dsDNA in particular, for its activation. However, Rad54 does not possess a DNA helicase activity [72a]. Rad54 is a monomer in solution, but in the presence of DNA assembles into higher order species, as revealed by protein cross-linking [72]. Rad54 is of lower cellular abundance than Rad51 [40] and physically interacts with Rad51 [19,40,72a]. The addition of Rad54 to a homologous DNA pairing reaction consisting of circular ssDNA and linear duplex (systems (i) and (ii) in Fig. 3) results in strong stimulation of the homologous pairing rate [72a]. The first DNA intermediate predicted in the DNA DSB repair model for recombination is a D-loop structure formed between the initiating ssDNA tail and the DNA homolog (see Fig. 1). While Rad51 is incapable of mediating D-loop formation in vitro (system (iii) in Fig. 3), the inclusion of Rad54 renders D-loop formation possible [72a]. Rad54 by itself does not have homologous DNA pairing activity, nor does it replace RPA in this reaction [72a].

Rad54 from both yeast and humans mediates an alteration in duplex DNA conformation that results in a DNA linking number change [72,102]. This reaction has a strict dependence on ATP hydrolysis, as indicated from biochemical studies using the non-hydrolyzable ATP analog ATP-γ-S and substitution of Rad54 with mutant variants (hrad54 K189R, yrad54 K341A, and yrad54 K341R) that do not hydrolyze ATP [72,102]. Whether the DNA conformational change entails DNA strand separation is not known at this point. It seems reasonable to propose that the ability to alter DNA conformation in a manner that is dependent on ATP hydrolysis is a conserved property of Rad54, and that this property is germane for the recombination function of Rad54.

The *rad54 K341A* and *rad54 K341R* alleles, which habor mutations in the highly conserved lysine residue in the Walker type A sequence, have been shown to encode mutant rad54 proteins defective in ATP hydrolysis [72]. Clever et al. [19] found that whereas overexpression of wild type *RAD54* gene suppresses the ultraviolet and MMS sensitivities of a *rad51Δ* mutant, overexpression of the *rad54 K341R* allele has no such effect. The *rad54 K341R* allele in a *rad54Δ* background is also defective in the repair of DNA lesions induced by MMS, intrachromosomal gene conversion in haploid *rad54Δ* cells, and in meiosis. The *rad54 K341A* mutant gene behaves like the *rad54 K341R* allele phenotypically [72]. Taken together, it seems clear that the Rad54 ATPase function is indispensable for *RAD54* dosage-dependent suppression of the DNA repair defects of the *rad51Δ* mutation [19] and also for different types of mitotic and meiotic recombination [72].

The *rad54* null mutant is not as affected in diploid interchromosomal gene conversion as in haploid gene conversion [48]. One possible explanation is that the *RAD54* related gene *RDH54/TID1* (see

below) provides the ability to carry out most of the diploid interchromosomal gene conversions, with only a small fraction being effected through *RAD54* ([48]; see below). Interestingly, diploid mitotic gene conversion was not significantly decreased in the *rad54K341A* and *rad54K341R* mutants [72]. This result suggests that either *rad54K341A* and *rad54K341R* mutants could promote diploid mitotic gene conversion on their own, or Rad54, but not its ATPase activity, is required for the integrity of a higher order complex important for gene conversion in diploid cells [72]. Since many members of the Swi2/Snf2 family of proteins function to remodel chromatin, it is an open possibility that Rad54 also has a chromatin remodeling function.

Rdh54 / Tid1. Based on computer search, a homolog of *S. cerevisiae RAD54*, *RDH54*, has been identified [48,90]. *RDH54* was independently isolated as a gene whose product interacts with the meiosis-specific Rad51 homolog Dmc1 in a yeast two-hybrid screen, and was named *TID1* [24]. Rdh54/Tid1 also interacts with Rad51 in the two-hybrid assay, albeit with a lower apparent affinity than with Dmc1 [24]. Rdh54 shows about 35% sequence identity to Rad54. Although the *rdh54Δ* mutation confers only slightly sensitivity to MMS in haploid cells, it greatly sensitizes the MMS sensitivity of a *rad54Δ* haploid strain. Likewise, the *rad54Δ rdh54Δ* double mutant is more impaired in meiosis than either single mutant alone [48,90]. Interestingly, diploid yeast strains harboring homozygous deletions of *RAD54* and *RDH54* are severely growth retarded, and this impairment can be overcome by simultaneously deleting *RAD51*, strongly suggesting that the growth deficiency stems from attempted, but incomplete recombination. A diploid strain harboring homozygous deletions of *RDH54* and *SRS2* is inviable, and the lethality is also overcome by simultaneously deleting *RAD51* [48].

Superficially, it might appear that Rdh54 is simply providing a recombination function redundant to that of Rad54 during mitotic growth. However, Klein [48] discovered that diploid *rdh54Δ* cells are much more defective in interchromosomal gene conversions than diploid *rad54Δ* cells, indicating a specialized function of Rdh54 in interchromosomal recombination. Whether this specificity stems from a unique ability of Rdh54 to interact with proteins required for interchromosomal recombination, or because Rdh54 provides a specific enzymatic function during interchromosomal recombination, remains to be determined.

Given the structural similarity of Rdh54 to Rad54 and its involvement in recombination processes, it is a distinct possibility that Rdh54 also possesses biochemical functions similar to what have been reported for Rad54 [72,72a]) and affects heteroduplex DNA formation by a similar mechanism. The interaction of Rdh54 with Dmc1 and Rad51 could mean that Rdh54 functions with both recombinases to promote heteroduplex DNA formation. Whether Rdh54 has a chromatin remodeling function is an interesting possibility that needs to be tested.

Other recombination factors

Rad59. Bai and Symington [6] identified a mutant, called *rad59*, which lowers the level of intrachromosomal recombination in a *rad51* mutant background. The *rad59* mutant exhibits sensitivity to γ-ray, which was used as the basis for cloning the *RAD59* gene. *RAD59* has a meiotic function, as indicated by a synergistic decline in sporulation efficiency when combining a leaky mutation in *RAD52*, *rad52 R70K*, with the *rad59Δ* mutation [7]. Interestingly, Rad59 shows homology to the amino-terminal region of Rad52, and overexpression of Rad52 suppresses the γ-sensitivity of the *rad59* mutant [6]. More recently, both the Symington group [7] and the Haber group (personal communication) have found that Rad59 is required for recombination by SSA. Rad59 has a ssDNA binding activity and, consistent with its involvement in SSA, mediates the annealing of complementary DNA strands in vitro [73]. Bai and Symington [6] have envisioned that Rad59 functions in the context of a complex with Rad51, Rad52, and other recombination factors to ensure that ssDNA substrates are channeled efficiently into recombination pathways, and that Rad52 together with Rad59 may have the ability to promote strand invasion [7]. These ideas need to be tested with purified proteins.

Dmc1. The yeast *DMC1* encoded product is homologous to RecA [13,94] and much more so to Rad51 [13]. *DMC1* gene is required for normal levels of meiotic recombination and is therefore important for chromosomal disjunction during meiosis I. The expression of *DMC1* is restricted to meiosis, and consistent with this expression pattern, a *dmc1Δ*

mutation produces no discernible mitotic phenotype [13]. From gene knockout experiments in mice, it is clear that the Dmc1 homolog in mammals also has important meiotic functions [75,113]. Human Dmc1 has been purified and shown by Li et al. [52] to possess homologous DNA pairing activity. Dmc1 forms octameric rings, which stack on DNA, but does not apparently form a helical nucleoprotein filament [57,67].

Cell biological tool for studying recombination. The use of cell biological techniques to study recombination in yeast is a relatively new and exciting development. Because of the availability of yeast mutants defective in various stages of recombination processes, their analyses are often revealing as to their effect on the assembly of recombination protein complexes. The patterns of nuclear redistribution of various recombination factors during meiosis and following DNA damaging treatment have been examined [12,30,56,108]. For instance, the assembly of meiotic nuclear foci of Rad51 has been shown to be dependent on *RAD52*, *RAD55*, *RAD57*, and on genes that control the formation of meiotic DSBs [30], results which very nicely corroborate mechanistic predictions based on genetic and biochemical analyses. Currently, the cell biological approach is as close as one can get to visualizing recombination processes in situ. This approach will continue to provide valuable information concerning the temporal sequence and genetic requirements for the assembly of higher order recombination protein complexes in vivo.

Repair DNA synthesis and resolution of recombination intermediates. Based on the observation that during conversion of the mating type information at *MAT*, the repair DNA synthesis step requires the concerted action of DNA polymerases α, δ, and ε, Holmes and Haber [37] have suggested that the repair synthesis reaction entails the establishment of both leading and lagging DNA strands. Whether the results of Holmes and Haber on mating type switching apply to other recombination processes and how the various DNA synthesis factors are recruited to sites of recombination are interesting subjects that need to be addressed.

Two genes, *MSH4* and *MSH5*, which encode proteins with considerable homology to the mismatch repair factors Msh2 and Msh3, are required for wild type levels of crossover recombination during meiosis [36,83]. In the *msh4* and *msh5* mutants, the levels of meiotic gene conversion and post meiotic segregation appear to be normal at the majority of the loci examined, indicating no overt defect in mismatch repair in these mutants. Because of the deficiency in crossover recombination, *msh4* and *msh5* mutants exhibit a defect in chromosome disjunction during meiosis I, resulting in a sporulation deficit and low spore viability. The *MSH4* and *MSH5* genes are epistatic to each other in meiotic crossover recombination, consistent with the suggestion that their encoded products function in the same biological pathway or reaction [36], and also with the observation that the two proteins are associated as a stable complex [77]. Other results have indicated a role for the mismatch repair protein Mlh1 in the Msh4–Msh5 dependent pathway of meiotic crossover recombination [38]. Since Msh proteins have the ability to bind DNA mismatches and specific DNA structures [4], it is possible that Msh4–Msh5 complex in conjunction with Mlh1 may specifically recognize and stabilize a DNA intermediate, such as the Holliday junction, critical for the formation of crossover recombinants. Expression of *MSH4* and *MSH5* is restricted to meiosis, and in yeast strains mutated for these two genes, no mitotic phenotypes can be discerned [36,83].

Aside from a possible function of the Msh4–Msh5 complex in Holliday junction recognition and perhaps its stabilization, little is known about other recombination factors that promote branch migration of Holliday junctions. Although a mitochondrial Cruciform Cutting Endonuclease, CCE1, has been described [86], the resolvases that process Holliday junctions and other DNA intermediates in nuclear chromosomal recombination have not been identified.

2.2. Recombination by SSA

As the name implies, this mechanism involves the annealing or hybridization of two complementary DNA single strands to yield a recombinant. SSA has mostly been studied using plasmid or chromosomal constructs that carry direct repeats of a genetic element, but the work of Haber and Leung [33] has indicated that SSA can in fact occur across chromo-

somes. Genetically, SSA is less complex than classical recombination, being dependent on *RAD52* [66] and *RAD59* ([7]; Jim Haber, personal communication), but the other *RAD52* group members are apparently dispensable.

Consistent with the genetic data implicating *RAD52* in SSA, Rad52 anneals complementary DNA strands in vitro [61]. Interestingly, single strand annealing by Rad52 is stimulated by RPA [92,96], which is thought to remove secondary structure in the single strands and directs Rad52 to the bound single strands via specific protein–protein interactions [96]. As alluded to earlier, Rad59 possesses an ability to bind ssDNA and anneals complementary DNA strands. However, DNA annealing by Rad59 does not appear to depend on RPA [73]. In fact, relatively high concentrations of RPA inhibit the Rad59-mediated DNA strand annealing reaction. Rothstein et al. previously isolated a mutant of the *RFA1* gene which encodes the largest subunit of RPA and found that this mutation, *rfa1-D228Y*, allows SSA in a *rad52* mutant background. Interestingly, SSA in the *rfa-D228Y* mutant occurs much more frequently than in the isogenic wild type strain, which suggests that a normal level of RPA in fact suppresses SSA in vivo [93].

In addition to Rad52 and Rad59, genetic studies have implicated the DNA structure-specific endonuclease Rad1–Rad10 in trimming the non-homologous, unhybridized ssDNA overhangs during SSA (see Fig. 5). Interestingly, the mismatch repair factors Msh2 and Msh3 also appear to play a role in some SSA events, and it is possible that these factors serve to stabilize the annealed DNA structure and to target the Rad1–Rad10 endonucleolytic activity to the ssDNA overhangs [66]. It is not known whether the single-strand gaps after trimming of ssDNA overhangs are filled by a particular DNA polymerase. In addition to an involvement in SSA, Rad1 and Rad10 also seem to play a role in other mitotic recombination events [39,85]. Interestingly, the Rad1 homolog in Drosophila, Mei-9, is important for meiotic recombination as well [87].

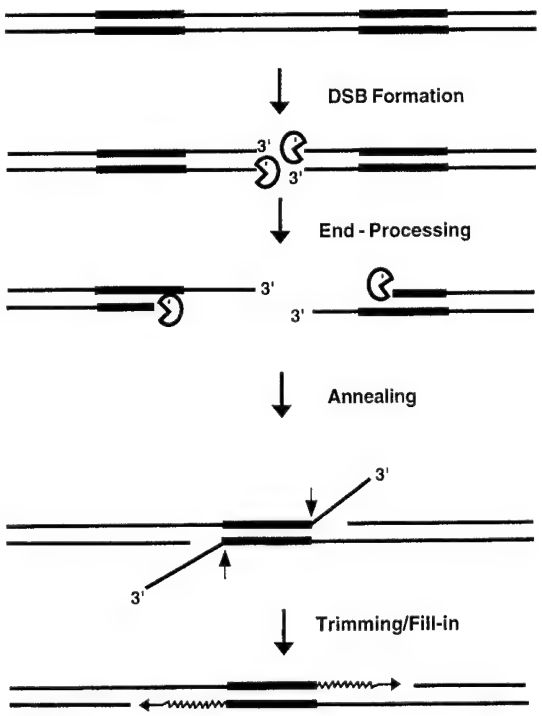

Fig. 5. Conceptual model for recombination by SSA. A DSB formed between direct repeats (represented by the dark lines) of a genetic element is processed exonucleolytically to yield 3′ ssDNA tails. Because of the presence of DNA homology, the DNA tails can anneal to each other to form a joint. After strand annealing, nucleolytic trimming of the overhanging ssDNA tails and fill-in by a DNA polymerase yield a recombinant that has some of the original DNA sequence deleted.

2.3. Recombination by BIR

A pathway of very long tract gene conversion has been described, which entails the formation of a short DNA joint between an initiating ssDNA substrate and a DNA molecule at a site where there is localized homology between the DNA molecules, followed by DNA synthesis to copy information contained within the DNA homolog. This pathway of recombination is dependent on *RAD52*, but not on *RAD51* [66]. It is possible that the DNA strand annealing activity of Rad52 is germane for establishing the initial DNA joint to prime DNA synthesis during BIR. Given the similarities between Rad52 and Rad59, it is tempting to speculate that perhaps BIR is also dependent on *RAD59* gene. The manner in which DNA joint formation and DNA synthesis are coupled in BIR and the relative contributions of the various DNA polymerases in the DNA synthesis reaction during BIR remain to be determined.

2.3.1. Some major unresolved problems

2.3.1.1. Meiotic DNA DSB formation. It remains a real mystery how the meiotic cell decides when to order the introduction of DNA DSBs at various "hotspots". Is this process controlled by the synthesis of a critical protein factor at a certain stage of the meiotic program, or is it due to post-translational modifications of preexisting factors? Likewise, the mechanism by which Spo11, Rad50, Mre11, Xrs2, and other protein factors function to make the meiotic DNA DSBs is completely unknown at this point. Addressing these issues will require a combination of genetic, cell biological, and biochemical analyses.

2.3.2. Channeling of DSBs into recombination or non-recombination pathways

How is the decision made at the cellular level for channeling a DNA DSB into a certain recombination pathway or into non-homologous DNA end-joining? Is it possible that this decision is influenced by the cell cycle stage or is dependent on post-translational modifications of key protein components? Given that the trio of Rad50, Mre11, and Xrs2 are involved in both homologous recombination and non-homologous DNA end-joining, could they have a role in executing the cellular command to conduct either recombination or end-joining? These are interesting questions that again can be addressed genetically and biochemically.

2.3.3. Coupling of steps in recombination

It seems plausible that DNA end-processing, heteroduplex joint formation, and DNA synthesis are not distinct steps that occur independently, but rather that they are coupled to one another. This idea predicts a hierarchy of functional and physical interactions among factors traditionally thought of being required only in one or the other step of recombination. This idea can be tested, now that purified recombination factors are becoming available.

2.3.4. Chromatin structure

How does the recombination machinery deal with chromatin packing when conducting its business? The initiating ssDNA substrate that triggers recombination can be as long as 1 kb or more. Assuming that all of this ssDNA is utilized for heteroduplex DNA formation, then an extensive region of chromatin probably needs to be remodeled to allow strand invasion, branch migration, and subsequent reactions to occur. How is chromatin remodeling mediated during recombination and repair? Do Rad54 and Rdh54/Tid1 play a role in chromatin remodeling?

2.3.5. Recombination in higher organisms

From the phenotypes of other eukaryotic cells mutated for recombination genes, from animal models, and from biochemical analyses of human recombination factors, it is apparent that the functions of the *RAD52* group genes have been highly conserved. However, it is becoming clear that the genetic requirements for recombination are more complex and subject to additional layers of control in higher organisms. For instance, five Rad51-homologous proteins, Rad51B [5,79], Rad51C [23], Rad51D [76], XRCC2 [17,53], and XRCC3 [53] have already been identified in human cells. Evidence that at least some of these Rad51-homologous proteins have a role in recombination and repair has come from analysis of Chinese hamster ovary cell lines irs1 and irs1SF, which are, respectively, defective in *XRCC2* and *XRCC3* [44,105,104]. These cell lines show a marked deficiency in the repair of DNA DSBs through recombination. Transient transfection of XRCC2 and XRCC3 restores recombinational repair to near wild-type levels [42,74]. XRCC3 interacts with Rad51 in the yeast two-hybrid system and co-immunoprecipitates with Rad51 from cell extract [53], while Rad51C interacts with both XRCC3 and Rad51B in two-hybrid studies [23]. XRCC3 has also been shown in the Bishop laboratory to be required for the formation of DNA damage-induced Rad51 nuclear foci [14]. Given what we know about yeast Rad55 and Rad57, which are also homologous to Rad51, it seems possible that Rad51B, Rad51C, Rad51D, XRCC2, and XRCC3 also form complexes with one another and function to enhance hRad51-ssDNA nucleoprotein filament assembly. It is not known whether these human Rad51-homologous proteins are all required simultaneously for efficient recombination or whether they play specific recombination roles in certain cell types or at certain cell cycle or developmental stages.

There is growing evidence that the recombination machinery is subjected to modulation by genes that have a tumor suppression function. In addition to *NBS1*, which encodes an integral component of the Mre11-associated nuclease complex as described at the beginning of this article, recent work has implicated the gene mutated in AT (*ATM*) and the breast tumor suppressor genes *BRCA1* [62] and *BRCA2* in modulating the efficiency of recombination. Specifically, BRCA1 has recently been shown to associate with the hRad50–hMre11–Nbs1 complex and colocalizes with hRad50 in discrete nuclear foci upon irradiation [114]. In addition to its checkpoint function, ATM may be directly involved in DNA repair processes, as AT cells remain hypersensitive to ionizing radiation under conditions where the checkpoint function is dispensable [103]. AT patients and all Atm-deficient mice are infertile due to the absence of mature gametes (reviewed by Ref. [51]). Detailed analysis of Atm-deficient mice indicates that ATM is required for an early stage of meiosis [8].

Several lines of recent evidence have implicated the breast tumor suppressor *BRCA2* in DNA repair by recombination. Cultured cells become sensitive to γ-irradiation upon down-regulation of BRCA2 [1], and the pancreatic adenocarcinoma Capan-1 cells, which lack one copy of the *BRCA2* gene and contain a truncating mutation (617delT) in the other *BRCA2* allele [31], are hypersensitive to various DNA damaging agents. In addition, fibroblasts derived from mutant mouse embryos deleted for *Brca2* are specifically sensitive to γ-irradiation [21,59,68]. Most importantly, several laboratories have reported the association of BRCA2 with Rad51, and the interaction domain has been mapped to the BRC repeat in BRCA2 [18,46,111]. These observations appear to point to a role for BRCA2 in recombinational repair by influencing the activities of Rad51.

3. Epilogue

In every measurable way, *S. cerevisiae* has served as an excellent model for learning about the genetics and biochemistry of recombination processes, and there are good reasons to believe that studies in this organism will continue to yield answers to fundamental questions concerning recombination. The emergence of various tumor suppressors as potential modulators and regulators of recombination processes in mammals is an exciting recent development that has captivated investigators who otherwise work outside of the recombination field. Aficionados of recombination mechanisms can now legitimately declare that what they have loved to study is not only fascinating, but is also germane for human health.

Acknowledgements

We are grateful to Jim Haber, John Petrini, and Lorraine Symington for communicating results, and would like to thank Sabrina Stratton for artwork preparation. The studies in the laboratory of the authors have been supported by grants from the NIH (ES07061 and GM57814) and the US Army Medical Research and Material Command (DAMD17-94-J-4147).

References

[1] D.W. Abbott, M.L. Freeman, J.T. Holt, Double-stand break repair deficiency and radiation sensitivity in BRCA2 mutant cancer cells, J. Natl. Cancer Inst. 90 (1998) 978–985.

[2] A. Aboussekhra, R. Chanet, A. Adjiri, F. Fabre, Semidominant suppressors of Srs2 helicase mutations of *Saccharomyces cerevisiae* map in the RAD51 gene, whose sequence predicts a protein with similarities to procaryotic RecA proteins, Mol. Cell. Biol. 12 (1992) 3224–3234.

[3] K. Adzuma, No sliding during homology search by RecA protein, J. Biol. Chem. 273 (1998) 31565–31573.

[4] E. Alani, S. Lee, M.F. Kane, J. Griffith, R.D. Kolodner, *Saccharomyces cerevisiae* MSH2, a mispaired base recognition protein, also recognizes Holliday junctions in DNA, J. Mol. Biol. 265 (1997) 289–301.

[5] J.S. Albala, M.P. Thelen, C. Prange, W. Fan, M. Christensen, L.H. Thompson, G.G. Lennon, Identification of a novel human RAD51 homolog, RAD51B, Genomics 46 (1997) 476–479.

[6] Y. Bai, L.S. Symington, A Rad52 homolog is required for *RAD51*-independent mitotic recombination in *Saccharomyces cerevisiae*, Genes Dev. 10 (1996) 2025–2037.

[7] Y. Bai, A.P. Davis, L.S. Symington, A novel allele of *RAD52* that causes severe DNA repair and recombination deficiencies only in the absence of *RAD51* or *RAD59*, Genetics (1999) in press.

[8] C. Barlow, M. Liyanage, P.B. Moens, M. Tarsounas, K. Nagashima, K. Brown, S. Rottinghaus, S.P. Jackson, D.

Tagle, T. Ried, A. Wynshaw-Boris, Atm deficiency results in severe meiotic disruption as early as leptonema of prophase I, Development 125 (1998) 4007–4017.
[9] G. Basile, M. Aker, R.K. Mortimer, Nucleotide sequence and transcriptional regulation of the yeast recombinational repair gene RAD51, Mol. Cell Biol. 12 (1992) 3235–3246.
[10] A. Bergerat, B. de Massy, D. Gadelle, P.-C. Varoutas, A. Nicolas, P. Forterre, An atypical topoisomerase II from archaea with implications for meiotic recombination, Nature 386 (1997) 414–417.
[11] P.R. Bianco, R.B. Tracy, S.C. Kowalczykowski, DNA strand exchange proteins: a biochemical and physical comparison, Front. Biosci. 3 (1998) D570–603.
[12] D.K. Bishop, recA homologs Dmc1 and Rad51 interact to form multiple nuclear complexes prior to meiotic chromosome synapsis, Cell 79 (1994) 1081–1092.
[13] D.K. Bishop, D. Park, L. Xu, N. Kleckner, DMC1: a meiosis-specific yeast homolog of *E. coli recA* required for recombination, synaptonemal complex formation, and cell cycle progression, Cell 69 (1992) 439–456.
[14] D.K. Bishop, U. Ear, A. Bhattacharyya, C. Calderone, M. Beckett, R.R. Weichselbaum, A. Shinohara, Xrcc3 is required for assembly of Rad51 complexes in vivo, J. Biol. Chem. 273 (1998) 21482–21488.
[15] R.D. Camerini-Otero, P. Hsieh, Homologous recombination proteins in prokaryotes and eukaryotes, Annu. Rev. Genet. 29 (1995) 509–552.
[16] J.P. Carney, R.S. Maser, H. Olivares, E.M. Davis, M. Le Beau, J.R. Yates, L. Hays, W.F. Morgan, J.H. Petrini, The hMre11/hRad50 protein complex and Nijmegen Breakage Syndrome: linkage of double-strand break repair to the cellular DNA damage response, Cell 93 (1998) 477–486.
[17] R. Cartwright, C.E. Tambini, P.J. Simpson, J. Thacker, The XRCC2 DNA repair gene from human and mouse encodes a novel member of the recA/RAD51 family, Nucl. Acids Res. 26 (1998) 3084–3089.
[18] P.L. Chen, C.F. Chen, Y. Chen, J. Xiao, Z.D. Sharp, W.-H. Lee, The BRC repeats in BRCA2 are critical for Rad51 binding and resistance to methyl methanesulfonate treatment, Proc. Natl. Acad. Sci. U. S. A. 95 (1998) 5287–5292.
[19] B. Clever, H. Interhal, J. Schmuckli-Maurer, J. King, M. Sigrist, W.-D. Heyer, Recombinational repair in yeast: functional interactions between Rad51 and Rad54 proteins, EMBO J. 16 (1997) 2535–2544.
[20] J.C. Connelly, L.A. Kirkham, D.R. Leach, The SbcCD nuclease of *Escherichia coli* is a structural maintenance of chromosomes (SMC) family protein that cleaves hairpin DNa, Proc. Natl. Acad. Sci. U. S. A. 95 (1998) 7969–7974.
[21] F. Connor, D. Bertwistle, J. Mee, G.M. Ross, S. Swift, E. Grigorieva, V. Tybulewicz, A. Ashworth, Tumorigenesis and a DNA repair defect in mice with a truncating Brca2 mutation, Nat. Genet. 17 (1997) 423–430.
[22] G.M. Dolganov, R.S. Maser, A. Novikov, L. Tosto, S. Chong, D.A. Bressan, J.H. Petrini, Human Rad50 is physically associated with human Mre11: identification of a conserved multiprotein complex implicated in recombinational DNA repair, Mol. Cell Biol. 16 (1996) 4832–4841.
[23] M.K. Dosanjh, D.W. Collins, W. Fan, G.G. Lennon, J.S. Albala, Z. Shen, D. Schild, Isolation and characterization of RAD51C, a new human member of the RAD51 family of related genes, Nucl. Acids Res. 26 (1998) 1179–1184.
[24] M.E. Dresser, D.J. Ewing, M.N. Conrad, A.M. Domingues, R. Barstead, H. Jiang, T. Kodadek, *DMC1* functions in a *Saccharomyces cerevisiae* meiotic pathway that is largely independent of the *RAD51* pathway, Genetics 147 (1997) 533–544.
[25] J.A. Eisen, K.S. Sweder, P.C. Hanawalt, Evolution of the SNF2 family of proteins: subfamilies with distinct sequences and functions, Nucl. Acids Res. 23 (1995) 2715–2723.
[26] H.S. Emery, D. Schild, D.E. Kellogg, R.K. Mortimer, Sequence of *RAD54*, a *Saccharomyces cerevisiae* gene involved in recombination and repair, Gene 104 (1991) 103–109.
[27] C. Featherstone, S.P. Jackson, DNA repair: the Nijmegen breakage syndrome protein, Curr. Biol. 8 (1998) R622–R625.
[28] M. Furuse, Y. Nagase, H. Tsubouchi, K. Murakami-Murofushi, T. Shibata, K. Ohta, Distinct roles of two separable in vitro activities of yeast Mre11 in mitotic and meiotic recombination, EMBO J. 17 (1998) 6412–6425.
[29] J.C. Game, DNA double-strand breaks and the *RAD50–RAD57* genes in *Saccharomyces*, Sem. Cancer Biol. 4 (1993) 73–83.
[30] S.L. Gasior, A.K. Wong, Y. Kora, A. Shinohara, D.K. Bishop, Rad52 associates with RPA and functions with rad55 and rad57 to assemble meiotic recombination complexes, Genes Dev. 12 (1998) 2208–2221.
[31] M. Goggins, M. Schutte, J. Lu, C.A. Moskalukm, C.L. Weinstein, G.M. Peterson, C.J. Yeo, C.E. Jackson, H.T. Lynch, R.H. Hruban, S.E. Kern, Germline BRCA2 gene mutations in patients with apparently sporadic pancreatic carcinomas, Cancer Res. 56 (1996) 5360–5364.
[32] J.E. Haber, Sir-Ku-itous routes to make ends meet, Cell 97 (1999) 829–832.
[33] J.E. Haber, W.Y. Leung, Lack of chromosome territoriality in yeast: promiscuous rejoining of broken chromosome ends, Proc. Natl. Acad. Sci. U. S. A. 93 (1996) 13949–13954.
[34] S.L. Hays, A.A. Firmenich, P. Berg, Complex formation in yeast double-strand break repair: participation of Rad51, Rad52, Rad55, and Rad57 proteins, Proc. Natl. Acad. Sci. U. S. A. 92 (1995) 6925–6929.
[35] T. Hirano, SMC-mediated chromosome mechanics: a conserved scheme from bacteria to vertebrates?, Genes Dev. 13 (1999) 11–19.
[36] N.M. Hollingsworth, L. Ponte, C. Halsey, MSH5, a novel MutS homolog, facilitates meiotic reciprocal recombination between homologs in *Saccharomyces cerevisiae* but not mismatch repair, Genes Dev. 9 (1995) 1728–1739.
[37] A.M. Holmes, J.E. Haber, Double-strand break repair in yeast requires both leading and lagging strand DNA polymerase, Cell 96 (1999) 415–424.
[38] N. Hunter, R.H. Borts, Mlh1 is unique among mismatch

repair proteins in its ability to promote crossing-over during meiosis, Genes Dev. 11 (1997) 1573–1582.
[39] E.L. Ivanov, J.E. Haber, *RAD1* and *RAD10*, but not other excision repair genes, are required for double-strand break-induced recombination in *Saccharomyces cerivisiae*, Mol. Cell Biol. 15 (1995) 2245–2251.
[40] H. Jiang, Y. Xie, P. Houston, K. Stemke-Hale, U.H. Mortensen, R. Rothstein, T. Kodadek, Direct association between the yeast Rad51 and Rad54 recombination proteins, J. Biol. Chem. 271 (1996) 33181–33186.
[41] R.D. Johnson, L.S. Symington, Functional differences and interactions among the putative RecA homologs Rad51, Rad55, and Rad57, Mol. Cell Biol. 15 (1995) 4843–4850.
[42] R.D. Johnson, N. Liu, M. Jasin, Mammaliam XRCC2 promotes the repair of DNA double-strand breaks by homologous recombination, Nature 401 (1999) 397–399.
[43] K. Johzuka, H. Ogawa, Interaction of Mre11 and Rad50: two proteins required for DNA repair and meiosis-specific double-strand break formation in *Saccharomyces cerevisiae*, Genetics 139 (1995) 1521–1532.
[44] N.J. Jones, Y. Zhao, M.J. Siciliano, L.H. Thompson, Assignment of the XRCC2 human DNA repair gene to chromosome 7q36 by complementation analysis, Genomics 26 (1995) 619–622.
[45] R. Kanaar, J.H.J. Hoeijmakers, From competition to collaboration, Nature 391 (1998) 335–337.
[46] T. Katagiri, H. Saito, A. Shinohara, H. Ogawa, N. Kamada, Y. Nakamura, Y. Miki, Multiple possible sites of BRCA2 interacting with DNA repair protein Rad51, Genes, Chromosomes Cancer 21 (1998) 217–222.
[47] N. Kleckner, Meiosis: how could it work?, Proc. Natl. Acad. Sci. U. S. A. 93 (1996) 8167–8174.
[48] H. Klein, *RDH54*, a *RAD54* homologue in *Saccharomyces cerivisiae*, is required for mitotic diploid-specific recombination and repair and for meiosis, Genetics 147 (1997) 1533–1543.
[49] S. Keeney, N. Giroux, N. Kleckner, Meiosis-specific DNA double-strand breaks are catalyzed by Spo11, a member of a widely conserved protein family, Cell 88 (1997) 375–384.
[50] S.C. Kowalczykowski, D.A. Dixon, A.K. Eggleston, S.D. Lauder, W.M. Rehrauer, Biochemistry of homologous recombination in *E. coli*, Microbiol. Rev. 58 (1994) 401–465.
[51] M.F. Lavin, Y. Shiloh, The genetic defects in ataxia-telangiectasia, Annu. Rev. Immunol. 15 (1997) 177–202.
[52] Z. Li, E.I. Golub, R. Gupta, C.M. Radding, Recombination activities of HsDmc1 protein, the meiotic human homolog of RecA protein, Proc. Natl. Acad. Sci. U. S. A. 94 (1997) 11221–11226.
[53] N. Liu, J.E. Lamerdin, R.S. Tebbs, D. Schild, J.D. Tucker, M.R. Shen, K.W. Brookman, M.J. Siciliano, C.A. Walter, W. Fan, L.S. Narayana, Z.Q. Zhou, A.W. Adamson, K.J. Sorensen, D.J. Chen, N.J. Jones, L.H. Thompson, XRCC2 and XRCC3, new human Rad51-family members, promote chromosome stability and protect against DNA cross-links and other damages, Mol. Cell 1 (1998) 783–793.
[54] S.T. Lovett, Sequence of the *RAD55* gene of *Saccharomyces cerivisiae*: similarity of *RAD55* to prokaryotic RecA and other RecA like proteins, Gene 142 (1994) 103–106.
[55] S.T. Lovett, R.K. Mortimer, Characterization of null mutants of the *RAD55* gene of *Saccharomyces cerevisiae*: effects of temperature, osmotic strength, and mating type, Genetics 116 (1987) 547–553.
[56] D. Lydall, Y. Nikolsky, D.K. Bishop, T. Weinert, A meiotic recombination checkpoint controlled by mitotic DNA damage checkpoint genes, Nature 383 (1996) 840–843.
[57] J.Y. Masson, A.A. Davies, N. Hajibagheri, E. Van Dyck, F.E. Benson, A.Z. Stasiak, A. Stasiak, S.C. West, The meiosis-specific recombinase hDmc1 forms ring structure and interacts with hRad51, EMBO 18 (1999) 6552–6560.
[58] A.V. Mazin, S.C. Kowalczykowski, The function of the secondary DNA-binding site of RecA protein during DNA strand exchange, EMBO J. 17 (1998) 1161–1168.
[59] M. Morimatsu, G. Donoho, P. Hasty, Cells deleted for Brca2 COOH terminus exhibit hypersensitivity to gamma-radiation and premature senescence, Cancer Res. 58 (1998) 3441–3447.
[60] S. Moreau, J.R. Ferguson, L.S. Symington, The nuclease activity of Mre11 is required for meiosis but not for mating type switching, end joining, or telomere maintenance, Mol. Cell Biol. (1999) In press.
[61] U.H. Mortensen, C. Bendixen, I. Sunjevaric, R. Rothstein, DNA strand annealing is promoted by the yeast Rad52 protein, Proc. Natl. Acad. Sci. U. S. A. 93 (1996) 10729–10734.
[62] M.E. Moynahan, J.W. Chiu, B.H. Koller, M. Jasin, Brca1 controls homology-directed DNA repair, Mol. Cell 4 (1999) 511–518.
[63] E.A. Namsaraev, P. Berg, Branch migration during Rad51-promoted strand exchange proceeds in either direction, Proc. Natl. Acad. Sci. U. S. A. 95 (1998) 10477–10481.
[64] J.H. New, T. Sugiyama, E. Zaitseva, S.C. Kowalczykowski, Rad52 protein stimulates DNA strand exchange by Rad51 and replication protein A, Nature 391 (1998) 407–410.
[65] T. Ogawa, X. Yu, A. Shinohara, E.H. Egelman, Similarity of the yeast Rad51 filament to the bacterial RecA filament, Science 259 (1993) 1896–1899.
[66] F. Paques, J.E. Haber, Multiple pathways of recombination induced by double-strand breaks in *Saccharomyces cerevisiae*, Microbiol. Mol. Biol. Rev. 63 (1999) 349–404.
[67] S.I. Passy, X. Yu, Z. Li, C.M. Radding, J.Y. Masson, S.C. West, E.H. Egelman, Human DMC1 protein binds DNA as an octameric ring, Proc. Natl. Acad. Sci. U. S. A. 96 (1999) 10684–10688.
[68] K.J. Patel, V. Yu, H. Lee, A. Corcoran, F.C. Thistlethwaite, M.J. Evans, W.H. Colledge, L.S. Friedman, B. Ponder, A.R. Venkitaraman, Involvement of Brca2 in DNA repair, Mol. Cell 1 (1998) 347–357.
[69] T.T. Paull, M. Gellert, The 3′ to 5′ exonuclease activity of Mre11 facilitates repair of DNA double-strand breaks, Mol. Cell 1 (1998) 969–979.
[70] T.T. Paull, M. Gellert, Nbs1 potentiates ATP-driven DNA unwinding and endonuclease cleavage by the Mre11/Rad50 complex, Genes Dev. 13 (1999) 1276–1288.

[71] T.D. Petes, R.E. Malone, L.S. Symington, Recombination in yeast, in: J.R. Broach, E.W. Jones, J.R. Pringle (Eds.), The Molecular and Cellular Biology of the Yeast Saccharomyces: Genome Dynamics, Protein Synthesis, and Energetics, Cold Spring Harbor Laboratory Press, New York, 1991, pp. 407–521.

[72] G. Petukhova, S. Van Komen, S. Vergano, H. Klein, P. Sung, ATP hydrolysis-dependent duplex DNA unwinding and promotion of Rad51 catalyzed homologous DNA pairing by yeast Rad54 protein, J. Biol. Chem. 274 (1999) 29453–29462.

[72a] G. Petukhova, S. Stratton, P. Sung, Catalysis of homologous DNA pairing by yeast Rad51 and Rad54 proteins, Nature 393 (1998) 91–94.

[73] G. Petukhova, S.A. Stratton, P. Sung, Single strand DNA binding and annealing activities in yeast recombination protein Rad59, J. Biol. Chem. 274 (1999) 33839–33842.

[74] A.J. Pierce, R.D. Johnson, L.H. Thompson, M. Jasin, XRCC3 promotes homology-directed repair of DNA damage in mammalian cells, Genes Dev. 13 (1999) 2633–2638.

[75] D.L. Pittman, J. Cobb, K.J. Schimenti, L.A. Wilson, D.M. Cooper, E. Brignull, M.A. Handel, J.C. Schimenti, Meiotic prophase arrest with failure of chromosome synapsis in mice deficient for *Dmc1*, a germline-specific RecA homolog, Mol. Cell 1 (1998) 697–705.

[76] D.L. Pittman, L.R. Weinberg, J.C. Schimenti, Identification, characterization, and genetic mapping of Rad51d, a new mouse and human RAD51/RecA-related gene, Genomics 49 (1998) 103–111.

[77] P. Pochart, D. Woltering, N.M. Hollingsworth, Conserved properties between functionally distinct MutS homologs in yeast, J. Biol. Chem. 272 (1997) 30345–30349.

[78] C.M. Radding, Helical interactions in homologous pairing and strand exchange driven by RecA protein, J. Biol. Chem. 266 (1991) 5355–5358.

[79] M.C. Rice, S.T. Smith, F. Bullrich, P. Havre, E.B. Kmiec, Isolation of human and mouse genes based on homology to REC2, a recombinational repair gene from the fungus *Ustilago maydis*, Proc. Natl. Acad. Sci. U. S. A. 94 (1997) 7417–7422.

[80] T. Rijkers, J. Van Den Ouwel, B. Morolli, A.G. Rolink, W.M. Baarends, P.P. Van Sloun, P.H. Lohman, A. Pastink, Targeted inactivation of mouse RAD52 reduces homologous recombination but not resistance to ionizing radiation, Mol. Cell Biol. 18 (1998) 6423–6429.

[81] A.I. Roca, M.M. Cox, RecA protein: structure, function, and role in recombinational DNA repair, Prog. Nucl. Acid Res. Mol. Biol. 56 (1997) 129–223.

[82] G.S. Roeder, Meiotic chromosomes: it takes two to tango, Genes Dev. 11 (1997) 2600–2621.

[83] P. Ross-Macdonald, G.S. Roeder, Mutation of a meiosis-specific MutS homolog decreases crossing over but not mismatch correction, Cell 79 (1994) 1069–1080.

[84] G.J. Sharples, D.F.R. Leach, Structural and functional similarities between the SbcCD proteins of *Escherichia coli* and the Rad50 and Mre11 (Rad32) recombination and repair proteins of yeast, Mol. Microbiol. 17 (1995) 1215–1217.

[85] R.H. Schiestl, S. Prakash, RAD1, an excision repair gene of *Saccharomyces cerevisiae*, is also involved in recombination, Mol. Cell Biol. 8 (1988) 3619–3626.

[86] M.J. Schofield, D.M. Lilley, M. White, Dissection of the sequence specificity of the Holliday junction endonuclease CCE1, Biochemistry 37 (1998) 7733–7740.

[87] J.J. Seklsky, K.S. McKim, G.M. Chin, R.S. Hawley, The Drosophila meiotic recombination gene mei-9 encodes a homologue of the yeast excision repair protein Rad1, Genetics 141 (1995) 619–627.

[88] Y. Shiloh, Ataxia-telangiectasia and the Nijmegen breakage syndrome: related disorders but genes apart, Annu. Rev. Genet. 31 (1997) 635–662.

[89] A. Shinohara, H. Ogawa, T. Ogawa, Rad51 protein involved in repair and recombination in *S. cerevisiae* is a RecA-like protein, Cell 69 (1992) 457–470.

[90] M. Shinohara, E. Shita-Yamaguchi, J.M. Buerstedde, H. Shinagawa, H. Ogawa, A. Shinohara, Characterization of the roles of the *Saccharomyces cerevisiae RAD54* gene and a homologue of *RAD54, RDH54/TID1*, in mitosis and meiosis, Genetics 147 (1997) 1545–1556.

[91] A. Shinohara, T. Ogawa, Stimulation by Rad52 of yeast Rad51-mediated recombination, Nature 391 (1998) 404–407.

[92] A. Shinohara, M. Shinohara, T. Ohta, S. Matsuda, T. Ogawa, Rad52 forms ring structures and co-operates with RPA in single-strand DNA annealing, Genes Cells 3 (1998) 145–156.

[93] J. Smith, R. Rothstein, An allele of RFA1 suppresses RAD52-dependent double-strand break repair in *Saccharomyces cerivisiae*, Genetics 151 (1999) 447–458.

[94] R.M. Story, D.K. Bishop, N. Kleckner, T.A. Steitz, Structural relationship of bacterial RecA proteins to recombination proteins from bacteriophage T4 and yeast, Science 26 (1993) 1892–1896.

[95] T. Sugiyama, E.M. Zaitseva, S.C. Kowalczykowski, A single-stranded DNA binding protein is needed for efficient presynaptic complex formation by the *Saccharomyces cerevisiae* Rad51 protein, J. Biol. Chem. 272 (1997) 7940–7945.

[96] T. Sugiyama, J.H. New, S.C. Kowalczykowski, DNA annealing by RAD52 protein is stimulated by specific interaction with the complex of replication protein A and single-stranded DNA, Proc. Natl. Acad. Sci. U. S. A. 95 (1998) 6049–6054.

[97] P. Sung, Catalysis of ATP dependent homologous DNA pairing and strand exchange by the yeast Rad51 protein, Science 265 (1994) 1241–1243.

[98] P. Sung, D.L. Robberson, DNA strand exchange mediated by a Rad51-ssDNA nucleoprotein filament with polarity opposite to that of RecA, Cell 83 (1995) 453–461.

[99] P. Sung, S.A. Stratton, Yeast Rad51 recombinase mediates polar DNA strand exchange in the absence of ATP hydrolysis, J. Biol. Chem. 271 (1996) 27983–27986.

[100] P. Sung, Yeast Rad55 and Rad57 proteins form a heterodimer that functions with RPA to promote DNA strand exchange by Rad51 recombinase, Genes Dev. 11 (1997) 1111–1121.

[101] P. Sung, Function of Rad52 protein as mediator between RPA and the Rad51 recombinase, J. Biol. Chem. 272 (1997) 28194–28197.
[102] T.L. Tan, J. Essers, E. Citterio, S.M. Swagemakers, J. de Wit, F.E. Benson, J.H. Hoeijmakers, R. Kanaar, Mouse Rad54 affects DNA conformation and DNA-damage-induced Rad51 foci formation, Curr. Biol. 9 (1999) 325–328.
[103] J. Thacker, Cellular radiosensitivity in ataxia-telangiectasia, Int. J. Radiat. Biol. 66 (1994) s87–s96.
[104] J. Thacker, C.E. Tambini, P.J. Simpson, L.C. Tsui, S.W. Scherer, Localization to chromosome 7q36.1 of the human XRCC2 gene, determining sensitivity to DNA-damaging agents, Hum. Mol. Genet. 4 (1995) 113–120.
[105] R.S. Tebbs, Y. Zhao, J.D. Tucker, J.B. Scheerer, M.J. Siciliano, M. Hwang, N. Liu, R.J. Legerski, L.H. Thompson, Correction of chromosomal instability and sensitivity to diverse mutagens by a cloned cDNA of the XRCC3 DNA repair gene, Proc. Natl. Acad. Sci. U. S. A. 92 (1995) 6354–6358.
[106] K.M. Trujillo, S.-S.F. Yuan, E.Y.-H.P. Lee, P. Sung, Nuclease activities in a complex of human recombination and repair factors Rad50, Mre11, and p95, J. Biol. Chem. 273 (1998) 21447–21450.
[107] Y. Tsukamoto, H. Ikeda, Double-strand break repair mediated by DNA end-joining, Genes Cells 3 (1998) 135–144.
[108] T. Usui, T. Ohta, H. Oshiumi, J. Tomizawa, H. Ogawa, T. Ogawa, Complex formation and functional versatility of Mre11 of budding yeast in recombination, Cell 95 (1998) 705–716.
[109] E. Van Dyck, A.Z. Stasiak, A. Stasiak, S.C. West, Binding of double-strand breaks in DNA by human Rad52 protein, Nature 398 (1999) 728–731.
[110] R. Varon, C. Vissinga, M. Platzer, K.M. Cerosaletti, K.H. Chrzanowska, K. Saar, G. Beckmann, E. Seemanova, P.R. Cooper, N.J. Nowak, M. Stumm, C.M.R. Weemaes, R.A. Gatti, R.K. Wilson, M. Digweed, A. Rosenthal, K. Sperling, P. Concannon, A. Reis, Nibrin, a novel DNA double-strand break repair protein, is mutated in Nijmegen Breakage Syndrome, Cell 93 (1998) 467–476.
[111] A. Wong, R. Pero, P.A. Ormonde, S.V. Tavtigian, P.L. Bartel, Rad51 interacts with the evolutionarily conserved BRC motifs in the human breast cancer susceptibility gene brca2, J. Biol Chem. 272 (1997) 31941–31944.
[112] Y. Yamaguchi-Iwai, E. Sonoda, J.M. Buerstedde, O. Bezzubova, C. Morrison, M. Takata, A. Shinohara, S. Takeda, Homologous recombination, but not DNA repair, is reduced in vertebrate cells deficient in RAD52, Mol. Cell Biol. 18 (1998) 6430–6435.
[113] K. Yoshida, G. Kondoh, Y. Matsuda, T. Habu, Y. Nishimune, T. Morita, The mouse *RecA*-like gene *Dmc*1 is required for homologous chromosome synapsis during meiosis, Mol. Cell. 1 (1998) 707–718.
[114] Q. Zhong, C.F. Chen, S. Li, Y. Chen, C.C. Wang, J. Xiao, P.L. Chen, Z.D. Sharp, W.H. Lee, Association of BRCA1 with the hRad50-hMre11-p95 Complex and the DNA Damage Response, Science 285 (1999) 747–750.

Publication information: *Mutation Research, Fundamental and Molecular Mechanisms of Mutagenesis* (ISSN 0027-5107). For 2000 volumes 447–457 are scheduled for publication. Subscription prices are available upon request from the Publisher. Subscriptions are accepted on a prepaid basis only and are entered on a calendar year basis. Issues are sent by surface mail except to the following countries where Air delivery via SAL mail is ensured: Argentina, Australia, Brazil, Canada, Hong Kong, India, Israel, Japan, Malaysia, Mexico, New Zealand, Pakistan, PR China, Singapore, South Africa, South Korea, Taiwan, Thailand, USA. For all other countries airmail rates are available upon request. Claims for missing issues should be made within six months of our publication (mailing) date.

Orders, claims, and product enquiries: please contact the Customer Support Department at the Regional Sales Office nearest you:
New York, Elsevier Science, P.O. Box 945, New York, NY 10159-0945, USA. phone: (+1) 212-633-3730, [Toll free number for North American Customers:1-888-4ES-INFO (437-4636)], fax: (+1) 212-633-3680, e-mail: usinfo-f@elsevier.com
Amsterdam, Elsevier Science, P.O. Box 211, 1000 AE Amsterdam, The Netherlands. phone: (+31) 20-485-3757, fax: (+31) 20-485-3432, e-mail: nlinfo-f@elsevier.nl
Tokyo, Elsevier Science, 9-15, Higashi-Azabu 1-chome, Minato-ku, Tokyo 106, Japan. phone: (+81) 3-5561-5033, fax: (+81) 3-5561-5047, e-mail: info@elsevier.co.jp
Singapore, Elsevier Science, No. 1 Temasek Avenue, #17-01 Millenia Tower, Singapore 039192. phone: (+65) 434-3727, fax: (+65) 337-2230, e-mail: asiainfo@elsevier.com.sg
Rio de Janeiro: Elsevier Science, Rua Sete de Setembro 111/16 Andar, 20050-002 Centro, Rio de Janeiro - RJ, Brazil; phone: (+55) (21) 509 5340; fax: (+55) (21) 507 1991; e-mail: elsevier@campus.com.br [Note (Latin America): for orders, claims and help desk information, please contact the Regional Sales Office in New York as listed above]

Enquiries concerning manuscripts and proofs: questions arising after acceptance of the manuscript, especially those relating to proofs, should be directed to the Publisher, Elsevier Science B.V., Log-in Department, P.O. Box 2759, 1000 CT Amsterdam, The Netherlands (phone: (+31)-20 4853628; fax: (+31)-20-4853239).

Electronic manuscripts: Electronic manuscripts have the advantage that there is no need for the rekeying of text, thereby avoiding the possibility of introducing errors and resulting in reliable and fast delivery of proofs.

For the initial submission of manuscripts for consideration, hardcopies are sufficient. For the processing of accepted papers, electronic versions are preferred. After final acceptance, your disk plus one, final and exactly matching printed version should be submitted together. Double density (DD) of high density (HD) diskettes are acceptable. It is important that the file saved is in the native format of the wordprocessor program used. Label the disk with the name of the computer and wordprocessing package used, your name, and the name of the file on the disk. Further information may be obtained from the Publisher.

US mailing notice — Mutation Research, Fundamental and Molecular Mechanisms of Mutagenesis (ISSN 0027-5107) is published on a triweekly basis by Elsevier Science B.V. (P.O. Box 211, 1000 AE Amsterdam, The Netherlands). Annual combined subscription price for the full set in the U.S.A. US$7622.00 (valid in North, Central and South America), including air speed delivery. Periodicals postage is paid at Jamaica, NY 11431.

USA POSTMASTERS: Send address changes to MUTATION RESEARCH, Publications Expediting, Inc., 200 Meacham Avenue, Elmont, NY 11003.

Airfreight and mailing in the U.S.A. by Publications Expediting.

Authors in Japan please note: Upon request, Elsevier Science K.K. will provide authors with a list of people who can check and improve the English of their paper (*before submission*). Please contact our Tokyo office: Elsevier Science K.K., 1-9-15 Higashi-Azabu, Minato-ku, Tokyo 106; phone (03)-5561-5032; fax (03)-5561-5045.

Manuscripts can be submitted to a Managing Editor of the appropriate section (for addresses see the Instructions to Authors; last pages of this issue.

This Journal has adopted the ADONIS System. Copies of individual articles can be printed out from CD-ROM on request. An explanatory leaflet can be obtained by writing to ADONIS B.V., P.O Box 17005, 1001 JA Amsterdam, The Netherlands.

***Mutation Research* has no page charges**

Printed in The Netherlands

♾ The paper used in this publication meets the requirements of ANSI/NISO Z39.48-1992 (Permanence of Paper)

Mediator function of the human Rad51B–Rad51C complex in Rad51/RPA-catalyzed DNA strand exchange

Stefan Sigurdsson,[1] Stephen Van Komen,[1] Wendy Bussen,[1] David Schild,[2] Joanna S. Albala,[3] and Patrick Sung[1,4]

[1]Department of Molecular Medicine/Institute of Biotechnology, University of Texas Health Science Center at San Antonio, San Antonio, Texas 78245-3207, USA; [2]Life Science Division, Lawrence Berkeley National Laboratory, Berkeley, California 94720, USA; [3]Biology and Biotechnology Research Program, Lawrence Livermore National Laboratory, Livermore, California 94551-0808, USA

Five Rad51-like proteins, referred to as Rad51 paralogs, have been described in vertebrates. We show that two of them, Rad51B and Rad51C, are associated in a stable complex. Rad51B–Rad51C complex has ssDNA binding and ssDNA-stimulated ATPase activities. We also examined the functional interaction of Rad51B–Rad51C with Rad51 and RPA. Even though RPA enhances Rad51-catalyzed DNA joint formation via removal of secondary structure in the ssDNA substrate, it can also compete with Rad51 for binding to the substrate, leading to suppressed reaction efficiency. The competition by RPA for substrate binding can be partially alleviated by Rad51B–Rad51C. This recombination mediator function of Rad51B–Rad51C is likely required for the assembly of the Rad51-ssDNA nucleoprotein filament in vivo.

[*Key Words:* DNA double-strand break repair; tumor suppression]

Received August 7, 2001; revised version accepted October 17, 2001.

Studies in *Saccharomyces cerevisiae* have identified a large number of genetic loci required for mitotic and meiotic recombination. These genes, comprising *RAD50, RAD51, RAD52, RAD54, RAD55, RAD57, RAD59, RDH54/TID1, MRE11,* and *XRS2* are collectively known as the *RAD52* epistasis group. The *RAD52* group of genes are also intimately involved in the repair of DNA double-strand breaks induced by exogenous agents such as ionizing radiation (Paques and Haber 1999; Sung et al. 2000) and for telomere maintenance in the absence of telomerase.

Cloning, genetic, and biochemical studies have indicated that the structure and function of the *RAD52* group genes are highly conserved among eukaryotes, from yeast to humans (Sung et al. 2000; Thompson and Schild 2001). Interestingly, in mammals, the efficiency of recombination and DNA double-strand break repair is contingent upon the integrity of the tumor suppressors BRCA1 and BRCA2 (Dasika et al. 1999; Moynahan et al. 1999, 2001; Thompson and Schild 2001), underscoring the importance for deciphering the mechanistic basis of the recombination machinery.

[4]Corresponding author.
E-MAIL sung@uthscsa.edu; FAX (210) 567-7277.
Article and publication are at http://www.genesdev.org/cgi/doi/10.1101/gad.935501.

In recombination processes that involve the formation of a DNA double-strand break, the ends of the DNA break are processed to yield single-stranded DNA tails. These DNA tails are utilized by the *RAD52* group recombination factors for the formation of DNA joints with a homologous DNA template, contained within the sister chromatid or the chromosomal homolog. The nascent DNA joints are then extended in length by branch migration, followed by resolution of DNA intermediates to complete the recombination process (Paques and Haber 1999; Sung et al. 2000).

The *RAD51* encoded product is the functional homolog of *Escherichia coli* RecA protein, and like RecA, possesses the ability to promote the homologous DNA pairing and strand exchange reaction that forms heteroduplex DNA joints. In mediating homologous DNA pairing and strand exchange, Rad51 must first assemble onto ssDNA as a nucleoprotein filament, in which the DNA is held in a highly extended conformation (Ogawa et al. 1993; Benson et al. 1994; Sung and Robberson 1995). Assembly of the Rad51-ssDNA nucleoprotein filament is rate-limiting and strongly inhibited by secondary structure in the ssDNA template. The removal of secondary structure can be effected by the single-strand DNA binding protein RPA, which has proved to be indispensable for homologous DNA pairing and strand exchange effi-

ciency, especially when a plasmid-length ssDNA template is used as the initiating substrate (Sung et al. 2000; Sigurdsson et al. 2001).

Even though RPA is an important accessory factor for Rad51-mediated homologous DNA pairing and strand exchange, it can also compete with Rad51 for binding sites on the ssDNA template, which, when allowed to occur, suppresses pairing and strand exchange efficiency markedly (Sung et al. 2000). Here we demonstrate that the stoichiometric complex of the human Rad51B and Rad51C proteins, homologs of the *S. cerevisiae* Rad55 and Rad57 proteins (Sung et al. 2000), can partially overcome the suppressive effect of hRPA on hRad51-catalyzed DNA pairing and strand exchange, thus identifying the Rad51B–Rad51C complex as a mediator of recombination.

Results

Rad51B and Rad51C are associated in a stable complex

Because Rad51B and Rad51C interact in two-hybrid studies (Schild et al. 2000), we wished to address whether they are associated in human cells. For detecting Rad51B and Rad51C, we raised antibodies against these proteins expressed in *E. coli* and purified from inclusion bodies by preparative SDS-PAGE. The specificity of the anti-Rad51B and anti-Rad51C antibodies is shown in Figure 1A, in the left and right panels, in which extracts from yeast cells harboring the empty protein expression vector and plasmids expressing Rad51B and Rad51C were probed with the antibodies. A single 40-kD Rad51B and 42-kD Rad51C species was detected. The observed sizes of Rad51B and Rad51C are in good agreement with the predicted values of 39 kD for Rad51B and 42 kD for Rad51C. Furthermore, Rad51B and Rad51C endogenous to human HeLa cells have the same gel sizes as proteins expressed in yeast cells (see below). In both the immunoblot analysis (Fig. 1A) and immunoprecipitation (data not shown), the anti-Rad51B antibodies did not cross-react with Rad51C protein, nor did the anti-Rad51C antibodies cross-react with Rad51B protein.

To identify Rad51B and Rad51C endogenous to human cells, an extract from HeLa cells was fractionated in a Q Sepharose column, and the column fractions were subjected to immunoblotting analysis. In this analysis, we used extracts from yeast cells expressing Rad51B and Rad51C (Fig. 1B, lane 10 in both panels) to aid in the identification of the endogenous proteins. The results (Fig. 1B) showed that Rad51B and Rad51C coeluted from Q Sepharose precisely, from fractions 8 to 16. To investigate whether Rad51B and Rad51C in the Q Sepharose fractions were stably associated, we examined whether they could be coimmunoprecipitated. As shown in Figure 1C, anti-Rad51B antibodies precipitated not only Rad51B, but also Rad51C. Similarly, Rad51B coprecipitated with Rad51C in the anti-Rad51C immunoprecipitation (Fig. 1C). Importantly, the quantity of Rad51B and Rad51C that coprecipitated with the other protein was similar to the amount of these proteins precipitated by their cognate antibodies, suggesting that Rad51B and Rad51C in the Q column fractions were associated as a stable complex. Neither Rad51B nor Rad51C was precipitated by control antibodies raised against yeast Srs2 protein (Fig. 1C). Rad51C also forms a complex with XRCC3 (Schild et al. 2000; Kurumizaka et al. 2001; Mas-

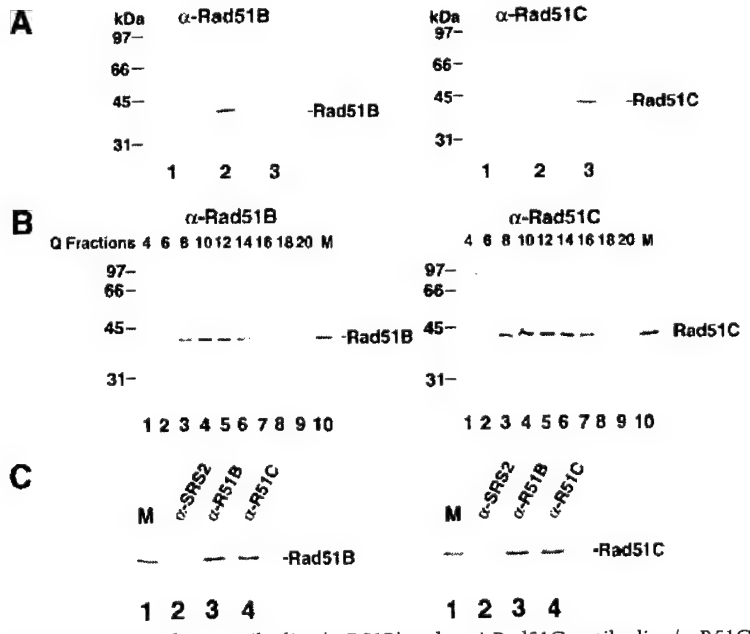

Figure 1. Rad51B and Rad51C form a stable complex. (*A*) Specificity of antibodies. Yeast cells harboring the empty expression vector pPM231 (*2μ, GAL-PGK;* lane *1*), the Rad51B expression plasmid pR51B.1 (*2μ, GAL-PGK-RAD51B;* lane *2*), and the Rad51C expression plasmid pR51C.1 (*2μ, PGK-RAD51C;* lane *3*) were run in an 11% polyacrylamide gel and then subjected to immunoblot analysis with either anti-Rad51B (αRad51B; *left* panel) or anti-Rad51C antibodies (αRad51C; *right* panel). (*B*) Rad51B and Rad51C are associated in a complex in human cells. HeLa cell extract was fractionated in a Q Sepharose column, and the indicated fractions were run in an 11% gel and then subjected to immunoblot analysis with anti-Rad51B antibodies (α-Rad51B; *left* panel) or anti-Rad51C antibodies (α-Rad51C; *right* panel). Yeast extracts containing Rad51B (lane *10* in *left* panel, marked M) or Rad51C (lane *10* in *right* panel, marked M) were used to help identify these proteins in the Q column fractions. (*C*) Coimmunoprecipitation of Rad51B and Rad51C from the Q column fractions. The Q Sepharose pool (fractions 8–16) was subjected to immunoprecipitation with protein A beads containing anti-ySrs2 antibodies (α-SRS2), anti-Rad51B antibodies (α-R51B) and anti-Rad51C antibodies (α-R51C). Proteins bound to the various immunobeads were eluted by SDS treatment and analyzed for their content of Rad51B (*left* panel) and Rad51C (*right* panel).

son et al. 2001), and it remains possible that a portion of Rad51C in the Q Sepharose fractions was bound to XRCC3 or that the XRCC3-Rad51C complex was not retained on the Q column.

The results above indicated that Rad51B and Rad51C are associated in a stable complex in HeLa cell extract, but they could not address whether association of these two proteins was due to direct interaction between them or whether an intermediary is required. To determine whether Rad51B and Rad51C interact directly, we carried out immunoprecipitation using extracts from yeast cells that expressed these two factors. As expected, Rad51B and Rad51C were precipitated by their cognate antibodies but not by antibodies specific for the other protein (data not shown). Importantly, upon mixing of the extracts containing Rad51B and Rad51C, coprecipitation of the two proteins occurred (data not shown). Direct interaction between Rad51B and Rad51C was demonstrated another way. In this case, we constructed recombinant baculoviruses that encoded a six-histidine-tagged form of Rad51B and an untagged form of Rad51C. The expression of Rad51B and Rad51C in insect cells infected separately with these baculoviruses was verified by immunoblotting (Fig. 2A). Because Rad51B was tagged with a six-histidine sequence, we could in this instance use affinity binding of the six-histidine tag to nickel-NTA agarose as criterion for protein–protein interaction when extracts were mixed. As summarized in Figure 2B, untagged Rad51C alone did not bind the nickel matrix, whereas a significant portion of it was retained on the affinity matrix in the presence of six-histidine-tagged Rad51B. Taken together, these results made it clear that Rad51B and Rad51C form a stable complex via direct interaction. The results presented below further indicated that the complex of Rad51B and Rad51C is highly stable, and contains stoichiometric amounts of the two proteins.

Rad51C expressed in insect cells consists of two closely spaced species (Fig. 2A,B), with the top band having the same gel mobility as Rad51C seen in extract from HeLa cells or yeast cells expressing this protein (data not shown). The slower migrating species of the two Rad51C immunoreactive bands is likely full-size Rad51C, whereas the faster migrating form, which represents ~60% of the total Rad51C amount, could be a proteolytic product or the result of an aberrant expression in insect cells.

Expression and purification of the Rad51B–Rad51C complex

We used insect cells as the medium for the purification of the Rad51B–Rad51C complex for the following two reasons: (1) much larger amounts of Rad51B–Rad51C complex can be obtained from insect cells infected with the recombinant baculoviruses than from HeLa cell extract or yeast cells harboring the Rad51B and Rad51C expression plasmids, and (2) the six-histidine tag engineered in the recombinant Rad51B baculovirus allowed

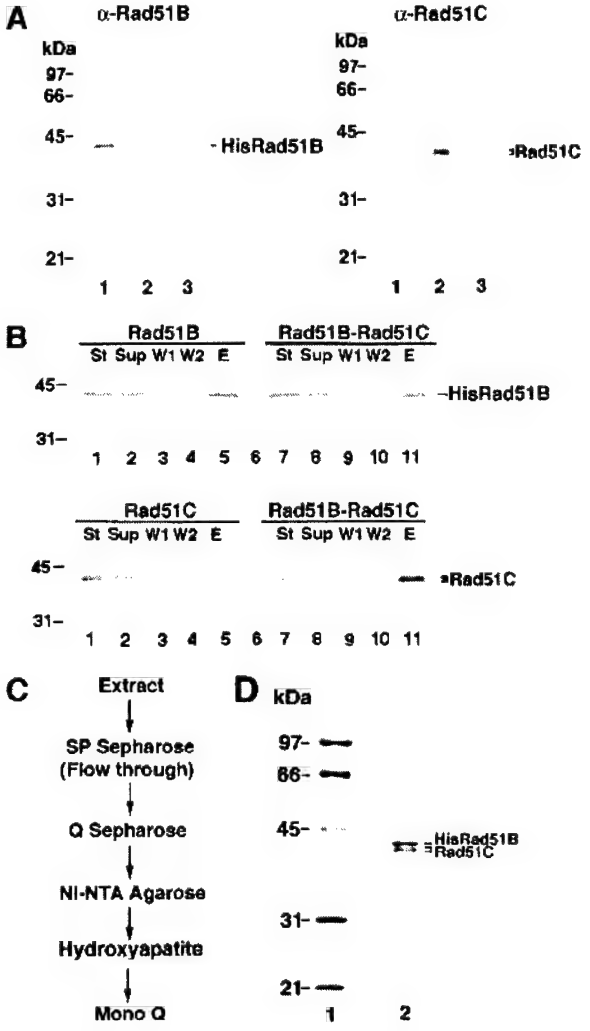

Figure 2. Purification of Rad51B and Rad51C from insect cells. (*A*) Expression of six-histidine-tagged Rad51B and Rad51C in insect cells. Nitrocellulose blots containing extracts from insect cells without any baculovirus (lane *3* of both panels) and infected with the recombinant 6His-tagged Rad51B baculovirus (lane *1* of both panels) or Rad51C baculovirus (lane *2* of both panels) were probed with either anti-Rad51B antibodies (αRad51B; *left* panel) or anti-Rad51C antibodies (αRad51C; *right* panel). (*B*) Complex formation between 6His-tagged Rad51B and Rad51C. Extracts from insect cells expressing 6His-tagged Rad51B (Rad51B), Rad51C (Rad51C), and the mixture of these extracts (Rad51B–Rad51C) were incubated with nickel-NTA agarose beads, which were washed with 10 mM, 20 mM, and then with 150 mM imadazole. The starting fractions (St), the supernatants containing unbound proteins (Sup), the 10 mM (W1) and 20 mM (W2) imidazole washes, and the 150 mM imidazole eluate (E) were subjected to immunoblotting to determine their content of Rad51B (*upper* panel) and Rad51C (*lower* panel). (*C*) Purification scheme for Rad51B–Rad51C complex. (*D*) Purity analysis. The purified Rad51B–Rad51C complex, 1.5 μg in lane *2*, was run alongside molecular size markers (lane *1*) in an 11% denaturing polyacrylamide gel and stained with Coomassie blue.

us to use nickel-NTA agarose as an affinity step to facilitate the purification of this complex.

We initially attempted to purify Rad51B and Rad51C individually, but our efforts were hampered by the complications that a significant portion (>75%) of these two proteins was insoluble and the soluble portion gave broad peaks during chromatographic fractionation procedures. To determine whether the Rad51B–Rad51C complex might be more amenable to purification than the individual components, we coinfected the Rad51B and Rad51C recombinant baculoviruses into insect cells. Interestingly, coexpression of Rad51B and Rad51C improved the solubility of these two proteins, even though the overall protein amounts in the infected insect cells remained relatively unchanged (data not shown). Importantly, the Rad51B–Rad51C complex eluted from various chromatographic matrices as relatively well defined peaks, thus enabling us to obtain substantial purification of the complex. Through many small-scale trials, a procedure was devised to encompass fractionation of insect cell extract containing the Rad51B–Rad51C complex in SP Sepharose, Q Sepharose, Hydroxyapatite, Mono Q, and affinity chromatography on nickel-NTA agarose (Fig. 2C) to purify this complex to near homogeneity (Fig. 2D). Stoichiometric amounts of Rad51B and Rad51C cofractionated during the entire purification procedure, indicating a high degree of stability of the complex. Using the aforementioned purification protocol, we could obtain about 100 µg of Rad51B–Rad51C complex from one liter of insect cell culture. Three independent preparations of Rad51B–Rad51C complex gave similar results in the experiments described below.

Rad51B–Rad51C complex binds DNA and hydrolyzes ATP

Because Rad51B and Rad51C are involved in recombination, we tested the purified Rad51B–Rad51C complex for binding to DNA. For this, an increasing amount of Rad51B–Rad51C complex was incubated with either ϕX ssDNA or dsDNA. The reaction mixtures were run in agarose gels, followed by staining with ethidium bromide to detect shifting of the DNA species. As shown in Figure 3A, while clear shifting of the ssDNA occurred at the lowest Rad51B–Rad51C concentration of 0.15 µM (DNA to protein ratio of 80 nucleotides/protein complex; see lane 2 of panel I), no shifting of the dsDNA was seen until the Rad51B–Rad51C concentration reached 0.6 µM (7 base pairs/protein complex; see lane 5 of panel II). These observations suggested that Rad51B–Rad51C complex binds ssDNA readily but has a lower affinity for dsDNA. To validate this conclusion, we repeated the DNA binding experiment by coincubating the ssDNA and dsDNA with the same concentration range of Rad51B–Rad51C used before. The results (Fig. 3A, panel III) revealed that Rad51B–Rad51C complex preferentially shifted the ssDNA without binding significantly to the dsDNA. In these experiments, ATP was included in the buffer used for the binding reaction, but the exclusion of ATP or its substitution with the nonhydrolyzable ATP-γ-S did not affect the binding results appreciably (data not shown). Taken together, these findings led us to conclude that the Rad51B–Rad51C complex binds ssDNA preferentially. We also examined ssDNA binding by Rad51B–Rad51C as a function of the ionic strength. To

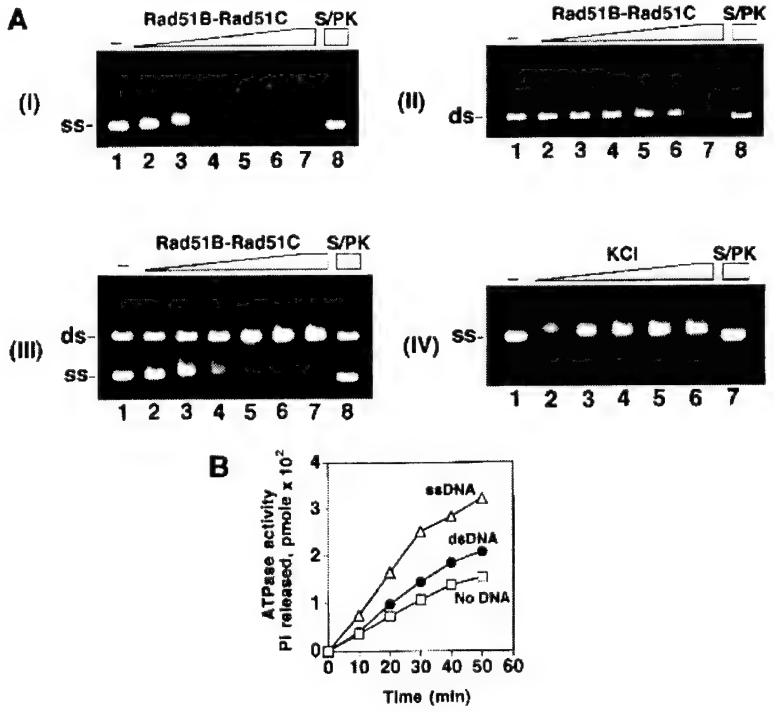

Figure 3. Rad51B–Rad51C binds DNA and hydrolyzes ATP. (*A*) Rad51B–Rad51C complex (0.15, 0.3, 0.45, 0.6, 0.75, and 0.9 µM in lanes *2–7*, respectively) was incubated with ϕX ssDNA (12 µM nucleotides in panel *I*; designated as ss), ϕX dsDNA (4 µM base pair in panel *II*; designated as ds), or with both the ssDNA and dsDNA (panel *III*) for 10 min at 37°C and then run in a 0.9% agarose gel. The DNA species were stained with ethidium bromide. In lane *8* of all three panels, the nucleoprotein complex formed with 0.9 µM of Rad51B–Rad51C complex was treated with 0.5% SDS and 500 µg/mL proteinase K at 37°C for 5 min before loading onto the agarose gel. In lane *1* of all three panels, DNA was incubated in buffer without protein. In panel *IV*, Rad51B–Rad51C complex (0.3 µM) was incubated with ssDNA (12 µM nucleotides) in the presence of increasing concentrations (50, 100, 150, 200, and 250 mM in lanes *2–6*, respectively) of KCl at 37°C for 10 min and then analyzed. (*B*) Rad51B–Rad51C, 1.8 µM, was incubated with 1 mM ATP in the absence of DNA (designated by the squares) and in the presence of ssDNA (20 µM nucleotides; designated by the triangles) or dsDNA (20 µM base pairs; designated by the closed circles) for the indicated times at 37°C.

do this, a fixed quantity of Rad51B–Rad51C complex (0.3 μM) was incubated with the ssDNA (12 μM nucleotides) in the presence of increasing concentrations (50, 100, 150, 200, and 250 mM) of KCl. The results (Fig. 3A, panel IV) showed that ssDNA binding was not diminished significantly by even the highest concentration of KCl (250 mM), indicating a high degree of avidity of Rad51B–Rad51C complex for the DNA.

Both Rad51B and Rad51C contain Walker ATP binding motifs, suggestive of an ability to bind and hydrolyze ATP (Sung et al. 2000; Thompson and Schild 2001). For this reason, we examined the purified Rad51B–Rad51C complex for ATPase activity. As shown in Figure 3B, Rad51B–Rad51C complex possesses an ATP hydrolytic activity that is stimulated by DNA. Reproducibly, ssDNA was more effective at stimulating ATP hydrolysis than was dsDNA. The kcat values for the Rad51B–Rad51C ATPase were found to be 0.15/min in the absence of DNA, and 0.19/min and 0.3/min in the presence of dsDNA and ssDNA, respectively.

Effects of RPA on Rad51-mediated DNA joint formation

Human Rad51 (hRad51) can make joints between homologous single-stranded and double-stranded DNA molecules, but was thought to have only limited DNA strand exchange activity (Baumann and West 1997, 1999; Gupta et al. 1997). We recently described a DNA strand exchange system (Fig. 4A) wherein hRad51 mediates a substantial amount of DNA strand exchange (Sigurdsson et al. 2001). In this new system, the efficiency of homologous DNA pairing and strand exchange is strongly dependent on the heterotrimeric ssDNA binding factor RPA. To assemble the reaction, hRad51 is preincubated with circular ssDNA at the optimal ratio of 4 nucleotides per protein monomer, followed by the addition of

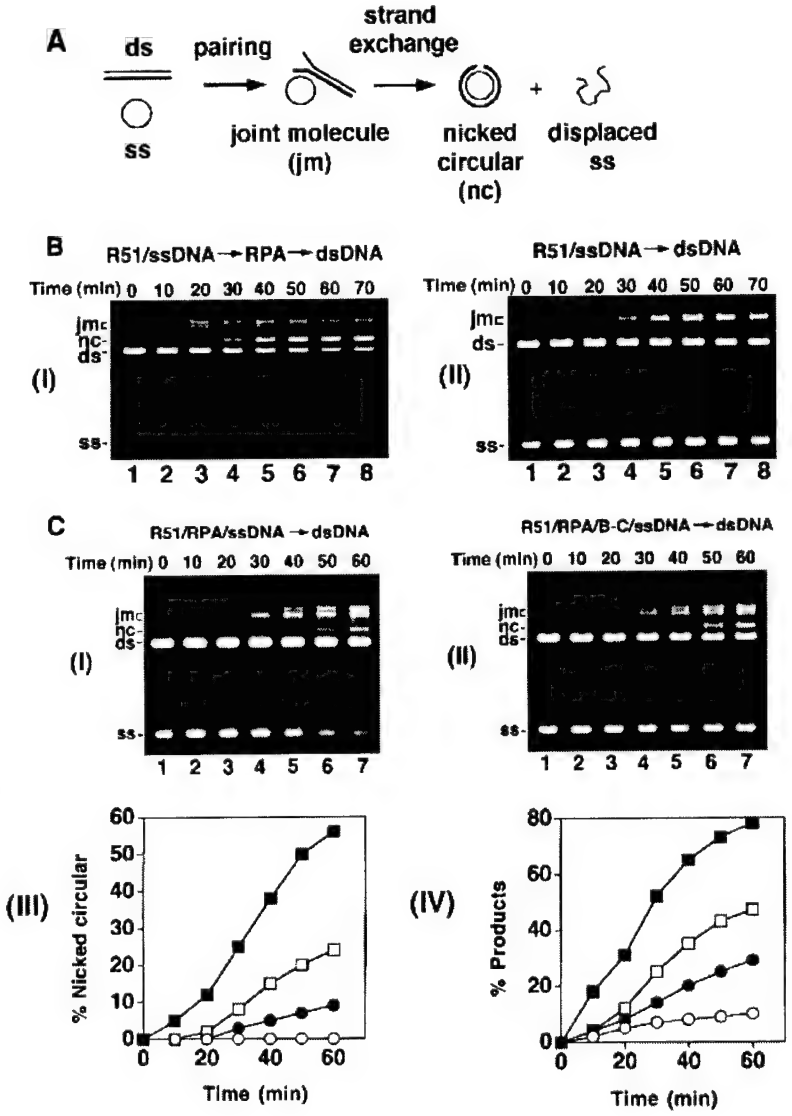

Figure 4. Mediator function of Rad51B–Rad51C. (*A*) Schematic of the homologous DNA pairing and strand exchange reaction using ϕX174 DNA substrates. Linear duplex is paired with the homologous ssDNA circle to yield a joint molecule. DNA strand exchange, if successful over the length (5.4 kb) of the DNA molecules, results in the formation of the nicked circular duplex. (*B*) Rad51-mediated DNA pairing and strand exchange was carried out with RPA (panel *I*) or without it (panel *II*). In panel *I*, the ssDNA was preincubated with Rad51 (R51) before RPA was added. The concentrations of the reaction components were: Rad51, 7.5 μM; RPA, 1.5 μM; ssDNA, 30 μM nucleotides; linear duplex, 15 μM base pairs. (*C*) In the DNA strand exchange reaction in panel *I*, the ssDNA was incubated with both Rad51 (R51) and RPA simultaneously, and in the reaction in panel *II*, the ssDNA was incubated with Rad51, RPA and Rad51B–Rad51C (*B–C*) simultaneously. The concentration of Rad51B–Rad51C was 0.8 μM, while the concentrations of the other components were exactly as those in *B*. In panel *III*, the amounts of nicked circular duplex in the reactions represented in *B* panel *I* (filled squares) and panel *II* (open circles) and in *C* panel *I* (filled circles) and panel *II* (open squares) are plotted. In panel *IV*, the amounts of total reaction products (sum of joint molecules and nicked circular duplex) in the reactions represented in *B* panel *I* (filled squares) and panel *II* (open circles) and in *C* panel *I* (filled circles) and panel *II* (open squares) are plotted.

hRPA at 20 nucleotides per protein monomer and the homologous linear duplex substrate (Fig. 4A). The reaction products, that is, joint molecules and nicked circular duplex (Fig. 4A), are separated from the input substrates by agarose gel electrophoresis and visualized by staining with ethidium bromide. An example of this reaction is shown in Figure 4B, panel I. As reported earlier (Sigurdsson et al. 2001) and reiterated here, omission of RPA from the reaction reduced the amount of products markedly (Fig. 4B, panel II). Importantly, little or no nicked circular duplex, the product of full strand exchange, was generated in the reaction that did not contain RPA (Fig. 4B, panel II).

Interestingly, coaddition of RPA with Rad51 to the ssDNA to mimic what may be expected to occur in vivo resulted in a marked reduction in reaction efficiency (Fig. 4C, panels I, III, and IV). Specifically, while ~38% and ~56% of the input linear duplex substrate had been converted into nicked circular duplex after 40 min and 60 min in the standard reaction (Fig. 4B, panel I and 4C, panel III), coaddition of hRPA with hRad51 to the ssDNA yielded only 5% and 9% of nicked circular duplex after these reaction time (Fig. 4C, panels I and III). In the homologous DNA pairing and strand exchange reaction mediated by *E. coli* RecA or yeast Rad51, SSB/yRPA added to the ssDNA template before or at the same time as the recombinase causes a notable suppression of the reaction as well (Umezu et al. 1993; Sung 1997a; New et al. 1998; Shinohara and Ogawa 1998). In these cases, suppression of the reaction efficiency by SSB/yRPA is due to competition of these ssDNA binding factors with RecA/yRad51 for sites on the ssDNA template. Based on the paradigm established with the *E. coli* and yeast recombination systems (Bianco et al. 1998; Sung et al. 2000), we also attribute the suppression of hRad51-mediated DNA pairing and strand exchange by hRPA to the exclusion of hRad51 from the ssDNA template.

Rad51B–Rad51C complex has a presynaptic mediator function

Rad51B and Rad51C are both required for recombination and DNA double-strand break repair in vivo. In chicken DT40 cells deleted for either Rad51B or Rad51C, the assembly of Rad51 nuclear foci in response to DNA damage is compromised (Takata et al. 2000, 2001). Based on these results, we wished to test whether Rad51B–Rad51C could promote homologous DNA pairing and strand exchange by Rad51 with RPA competing for binding sites on the initiating ssDNA substrate. To do this, we added Rad51B–Rad51C complex (0.8 μM) with Rad51 (7.5 μM) and RPA (1.5 μM) during the preincubation with ssDNA (30 μM), and then completed the reaction mixture by adding the homologous duplex. Importantly, upon inclusion of the Rad51B–Rad51C complex, significantly higher amounts of the reaction products were seen (Fig. 4C, panels II, III, and IV). In particular, the level of the nicked circular duplex, product of complete strand exchange (see Fig. 4A), was formed at a significantly higher rate than in the absence of Rad51B–Rad51C (Fig. 4C, panels II and III). We also examined whether amounts of Rad51B–Rad51C below and above that used before would lead to different levels of homologous DNA pairing and strand exchange. As shown in Figure 5, the optimal concentration of Rad51B–Rad51C was from 0.4 to 1.0 μM, and amounts of Rad51B–Rad51C above the optimal level in fact led to gradual inhibition of the reaction (Fig. 5; data not shown).

One possible explanation for the stimulatory effect of Rad51B–Rad51C complex (Fig. 5) is that this protein complex promotes homologous DNA pairing and strand exchange regardless of the order of addition of RPA. To test this possibility, we used the same amount of Rad51B–Rad51C complex (0.8 μM) that afforded the maximal restoration of DNA pairing and strand exchange (see Fig. 5A,B) in reactions wherein the protein complex was (1) added with Rad51 to the ssDNA substrate, followed by RPA; (2) added with RPA after Rad51 had already nucleated onto the ssDNA substrate; and (3) added after the ssDNA had first been incubated with Rad51 and then with RPA. No measurable effect of the Rad51B–Rad51C complex on the rate of formation of joint molecules and nicked circular duplex was recorded in any of these experiments (data not shown). We also tested whether the inclusion of Rad51B–Rad51C complex would alter the concentration of Rad51 needed for optimal pairing and strand exchange, determined previously to be from 3 to 4 nucleotides per Rad51 monomer (Baumann and West 1997, 1999; Gupta et al. 1997; Sigurdsson et al. 2001). However, Rad51B–Rad51C did not change the concentration of Rad51 needed for optimal reaction efficiency (data not shown).

To examine whether the Rad51B–Rad51C complex can substitute for RPA in the DNA pairing and strand exchange reaction, we used a range of Rad51B–Rad51C concentrations (0.4, 0.8, 1.2, and 2.0 μM) with a fixed concentration of Rad51 (7.5 μM) and ssDNA (30 μM) without RPA. Rad51B–Rad51C did not promote the formation of nicked circular duplex (Fig. 6) even after 60 min of reaction (data not shown), showing that it cannot substitute for RPA, which is highly effective in enabling Rad51 to make nicked circular duplex (Fig. 4; Sigurdsson et al. 2001). Interestingly, we observed an increase in joint molecules at 0.8 and 1.2 μM of Rad51B–Rad51C complex (Fig. 6). Specifically, after 30 min, the level of DNA joint molecules increased from ~5% in the absence of Rad51B–Rad51C to ~10% upon the inclusion of 1.2 μM Rad51B–Rad51C. As with the earlier strand exchange restoration experiment (Fig. 5), suppression of DNA joint molecule formation was seen at higher concentrations of the Rad51B–Rad51C complex (Fig. 6A,B; data not shown). In other experiments, over the range of Rad51B–Rad51C concentration from 3 to 45 nucleotides/protein complex, we did not detect any DNA joint molecule with the ϕX substrates, regardless of whether RPA was present (data not shown). These observations suggested that the Rad51B–Rad51C complex is devoid of homologous DNA pairing activity.

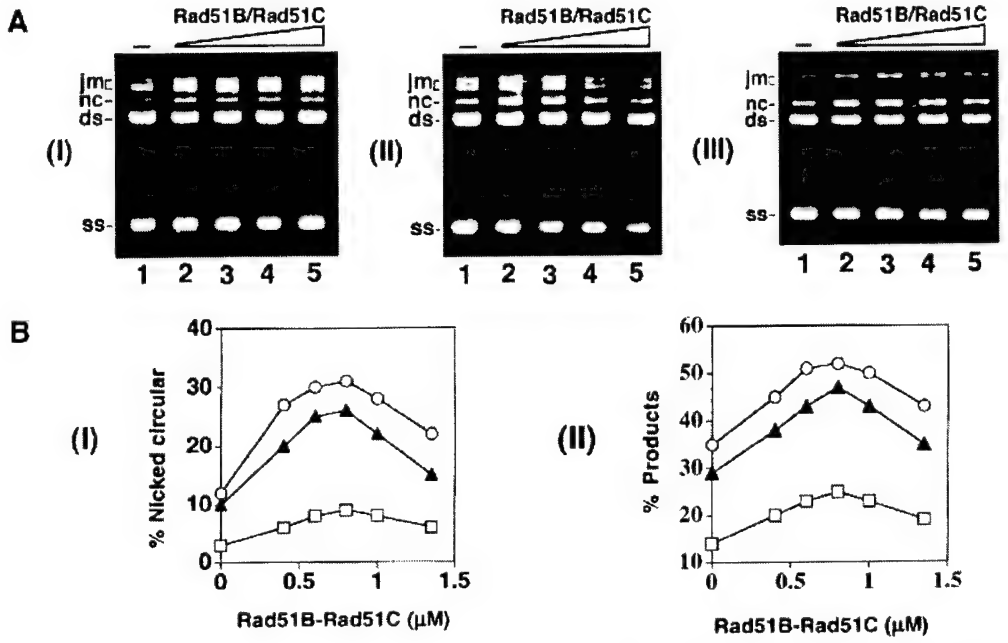

Figure 5. Mediator activity as a function of Rad51B–Rad51C concentration. (*A*) The ϕX174 ssDNA template (30 μM nucleotides) was incubated with Rad51 (7.5 μM), RPA (1.5 μM), and increasing concentrations of Rad51B–Rad51C (0, 0.6, 0.8, 1.0, and 1.4 μM in lanes *1–5*, respectively) for 10 min before the ϕX174 linear duplex (15 μM base pairs) was incorporated to complete the reaction mixtures. Portions of the reaction mixtures were withdrawn at 30 min (panel *I*), 60 min (panel *II*), and 80 min (panel *III*) and then processed for agarose gel electrophoresis. (*B*) The results from *A* and from two other independent experiments performed under the same reaction conditions were compiled and graphed. Symbols: results from the 30 min timepoint (squares), the 60 min timepoint (filled triangles), and the 80 min timepoint (circles). Panel *I* shows the levels of nicked circular duplex formed, and panel *II* shows the amounts of total reaction products (joint molecules and nicked circular duplex).

Discussion

Paradoxical effects of RPA on homologous DNA pairing and strand exchange

Like other members of the RecA/Rad51 class of recombinases (Ogawa et al. 1993; Sung and Robberson 1995; Roca and Cox 1997; Bianco et al. 1998), hRad51 assembles onto ssDNA to form a nucleoprotein filament in an ATP-dependent manner (Benson et al. 1994). Extensive biochemical studies with RecA have indicated that the search for DNA homology, DNA joint formation, and DNA strand exchange all occur within the confines of the RecA-ssDNA nucleoprotein filament. The assembly of the recombinase-ssDNA nucleoprotein filament is therefore the critical first step in the homologous DNA pairing and strand exchange reaction, and is generally referred to as the presynaptic phase of this reaction (Roca and Cox 1997; Bianco et al. 1998; Sung et al. 2000).

For RecA and yeast Rad51, the assembly of the presynaptic filament on plasmid-length DNA molecules is dependent on the cognate single-strand binding protein, *E. coli* SSB or yeast RPA, which acts to minimize the secondary structure in the DNA template and hence renders extension of the nascent nucleoprotein filament facile. In most experimental systems, the single-strand DNA binding factor is added subsequent to the recombinase, that is, after nucleation of the recombinase onto the ssDNA substrate has already commenced. Interestingly, precoating of the ssDNA template with the single-strand binding protein (Umezu et al. 1993; Sugiyama et al. 1997; New et al. 1998; Shinohara and Ogawa 1998) or coincubation of RPA, Rad51, and the ssDNA substrate (Sung 1997a,b) results in pronounced suppression of the reaction efficiency. We have shown in the present study that the hRad51 recombinase activity is similarly suppressed by RPA during the presynaptic phase. Taken together, the results indicate that the single-strand binding protein, while important for secondary structure removal in the ssDNA template, can interfere with the nucleation of the recombinase onto the DNA template and can thus prevent the formation of a contiguous presynaptic filament.

Mediator function in the Rad51B–Rad51C complex

Exploiting the paradoxical behavior of the single-strand DNA binding protein in the assembly of the presynaptic recombinase filament, various recombination mediator proteins capable of overcoming the suppressive effect of the single-strand binding protein have been identified in prokaryotes and yeast cells (Umezu et al. 1993; Sung 1997a,b; New et al. 1998; Shinohara and Ogawa 1998; Beernink and Morrical 1999). In yeast, two such mediators—Rad52 and the Rad55–Rad57 complex—have been

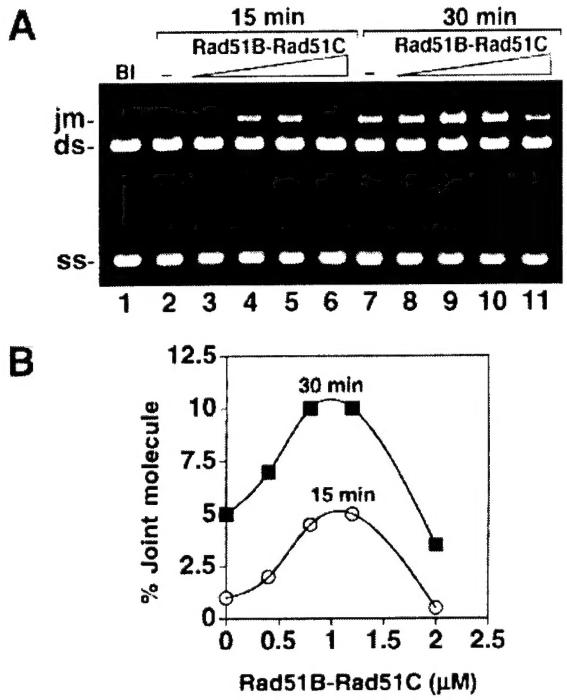

Figure 6. Rad51B–Rad51C stimulates DNA joint formation but does not replace RPA in DNA strand exchange. (*A*) Rad51 and Rad51B–Rad51C were used in the homologous DNA pairing and strand exchange reaction without RPA. The concentrations of the reaction components were: Rad51, 7.5 μM; Rad51B–Rad51C, 0.4 to 2 μM, as indicated; ssDNA, 30 μM nucleotides; linear duplex, 15 μM base pairs. (*B*) Graphic representation of the results from the experiment in *A*.

described. Rad55 and Rad57 are similar to Rad51B and Rad51C in that they too exhibit homology to Rad51 and form a stable stoichiometric complex via direct interaction (Sung et al. 2000). Importantly, both Rad51B–Rad51C and Rad55–Rad57 complexes are needed for the assembly of Rad51 nuclear foci in response to DNA damaging treatment (Gasior et al. 1998, 2001; Takata et al. 2000, 2001), which are thought to correspond to the sites of ongoing DNA damage repair.

We show here that purified Rad51B–Rad51C complex has single-strand DNA binding and ssDNA-stimulated ATPase activities. Importantly, Rad51B–Rad51C can promote the Rad51-mediated homologous DNA pairing and strand exchange reaction under conditions wherein Rad51 must contend with the competition by RPA for binding sites on the initiating ssDNA substrate. In addition, DNA joint formation by Rad51 in the absence of RPA is also enhanced by Rad51B–Rad51C. We asked whether Rad51B–Rad51C could stimulate the rate of DNA pairing and strand exchange, but did not uncover a postsynaptic role (Roca and Cox 1997; Bianco et al. 1998; Sung et al. 2000) in this protein complex. Rad51B–Rad51C complex did not pair the ϕX DNA substrates used, nor did it lower the concentration of Rad51 needed to attain optimal reaction efficiency. Thus, the results of our study suggest a specific role of Rad51B–Rad51C in promoting the assembly of the presynaptic Rad51 filament, identifying it as a mediator of recombination, in a manner analogous to what has been described for the yeast Rad55–Rad57 complex (Sung et al. 2000). Given that both Rad51B and Rad51C are indispensable for recombination and DNA repair and needed for the normal assembly of Rad51 nuclear foci after DNA damaging treatment, we surmise that the Rad51B–Rad51C mediator function likely contributes to the recruitment of hRad51 to sites of recombination and DNA damage repair.

Role of other Rad51 paralogs in recombination processes

Aside from Rad51B and Rad51C, three additional Rad51 paralogs, namely, XRCC2, XRCC3, and Rad51D, have been described (Thompson and Schild 2001). XRCC3 and Rad51C also form a stable complex that has DNA binding activity (Kurumizaka et al. 2001; Masson et al. 2001). Rad51D (also called Rad51L3) has DNA binding and ssDNA-stimulated ATPase activities, and it forms a stable complex with XRCC2 (Braybrooke et al. 2000). Whether the XRCC2–Rad51D and XRCC3–Rad51C complexes also have a recombination mediator function remains to be determined. However, that the formation of DNA damage-induced Rad51 nuclear foci is impaired in mutants of all five of the Rad51 paralogs would seem to suggest that they all play a role in the delivery of Rad51 to DNA lesions in vivo. It thus seems possible that some combination of complexes of the Rad51 paralogs could have an enhanced mediator function in the Rad51-catalyzed homologous DNA pairing and strand exchange reaction. In fact, our observation that Rad51B–Rad51C only partially overcomes the suppressive effect of RPA is consistent with such a scenario. It remains to be seen whether the other two Rad51 paralog pairs, either by themselves or in combination with each other and with Rad51B–Rad51C, may also function in the postsynaptic phase of the pairing and strand exchange reaction by enhancing the efficiency of DNA joint formation and promoting DNA branch migration.

Materials and methods

Antibodies

Rad51B protein was expressed in *E. coli* BL21 (DE3) using the T7 promoter in the vector pET11a. The insoluble Rad51B protein was purified by preparative SDS-PAGE, dialyzed into phosphate-buffered saline (10 mM NaH_2PO_4 at pH 7.2, 150 mM NaCl), and then used as antigen for production of antisera in rabbits. A GST–Rad51C fusion protein was expressed in *E. coli* BL21 (DE3) using the vector pGEX-2T. The GST–Rad51C fusion protein is also insoluble and was purified for antibody production in rabbits as described for Rad51B. The antigens were covalently conjugated to cyanogen bromide activated Sepharose 4B (Pharmacia-LKB) for use as affinity matrices to purify monospecific antibodies from rabbit antisera (Sung et al. 1987).

DNA substrates

ϕX174 viral (+) strand was purchased from New England Biolabs, and the ϕX174 replicative form I DNA was from GIBCO BRL. The replicative form I DNA was linearized with *Apa*LI. All of the DNA substrates were stored in TE (10 mM Tris-HCl at pH 7.5, 0.5 mM EDTA).

Fractionation of HeLa cell extract

To make extract, 10.4 g of HeLa S3 cells (National Cell Culture Center) was suspended in 15 mL of cell breakage buffer (50 mM Tris/HCl at pH 7.5, 2 mM EDTA, 10% sucrose, 100 mM KCl, 1 mM dithiothreitol and the following protease inhibitors: aprotinin, chymostatin, leupeptin, pepstatin, all at 3 μg/mL, and 1 mM phenylmethylsulfonyl fluoride) and passed through a French Press at 20,000 psi. After centrifugation (100,000*g* for 1 h), the clarified extract (20 mL) was loaded onto a column of Q-Sepharose (4 mL), which was fractionated with a 45 mL gradient of KCl from 100 to 600 mM in K buffer (20 mM KH_2PO_4 at pH 7.4, 0.5 mM EDTA, 1 mM DTT, and 10% glycerol) collecting 30 fractions. To identify the Rad51B and Rad51C proteins, the Q-Sepharose fractions (8 μL) were subjected to immunoblot analyses with anti-Rad51B and anti-Rad51C antibodies after SDS-PAGE in 11% gels.

Expression of Rad51B and Rad51C in yeast cells

The *RAD51B* gene was placed under the control of the *GAL-PGK* promoter in vector pPM231 (*2μ, GAL-PGK, LEU2d*) to yield pRad51B.1 (*2μ, GAL-PGK-RAD51B, LEU2d*) and *RAD51C* were placed under the control of the *PGK* promoter in vector pPM255 (*2μ, PGK, URA3*) to yield pRad51C.1 (*2μ, PGK-RAD51C, URA3*). The empty expression vector, pR51B.1, and pR51C.1 were introduced into the protease-deficient yeast strain BJ5464 (*MATα, ura3-52, trp-1, leu2Δ1, his3Δ200, pep4::HIS3, prbΔ1.6R*). Induction of Rad51B and Rad51C followed the protocol of Petukhova et al. (2000). Extracts (2 mL of buffer per gram of yeast cells) were prepared using a French press and clarified by centrifugation, as described above.

Purification of the Rad51B–Rad51C complex

Six-histidine (6His)-tagged Rad51B and untagged Rad51C recombinant baculoviruses were constructed by cloning the cDNAs for these proteins into the baculovirus transfer vector pVL1393 (Invitrogen). Amplification of the recombinant viruses was carried out in Sf9 cells and for protein expression, High-Five insect cells (Invitrogen) were infected with the 6His-tagged Rad51B and Rad51C baculoviruses at an MOI of 5. The insect cells were harvested 36–48 h postinfection. For the purification of the Rad51B–Rad51C complex, High-Five cells were coinfected with the Rad51B and Rad51C baculoviruses at an MOI of 5 for both viruses. The insect cells were harvested 36–48 h postinfection.

All the protein purification steps were carried out at 0 to 4°C. Cell lysate was prepared from 1 L of insect cell culture (15 g) using a French press in 60 mL of cell breakage buffer. The lysate was clarified by centrifugation (100,000*g* for 1 h) and the supernatant was applied on a 10 mL SP-Sepharose column. The flow-through from SP-Sepharose was then fractionated in a column of Q-Sepharose (10 mL of matrix) with a 30 mL, 100 to 600 mM KCl gradient in buffer K. Rad51B–Rad51C eluted from 200–300 mM KCl, and the peak fractions were pooled and mixed with 0.6 mL of Ni-NTA agarose for 2 h, followed by fractionation with a 15 mL, 0 to 250 mM imidazole in buffer K. The Rad51B–Rad51C peak fractions were pooled and further fractionated in a column of Macro-hydroxyapatite (0.5 mL matrix) with a 15 mL, 0 to 180 mM KH_2PO_4 gradient in buffer K. The peak fractions were pooled and dialyzed against buffer K with 50 mM KCl and applied onto a Mono Q column (HR5/5), which was developed with a 15 mL gradient from 100 to 800 mM KCl in buffer K. Rad51B–Rad51C from the Mono Q step was concentrated in a Centricon-30 microconcentrator to 2 mg/mL and stored at −70°C.

Immunoprecipitation

Affinity-purified anti-Rad51B, anti-Rad51C, and anti-ySrs2 antibodies, 1.0 mg each, were coupled to 300 μL protein A agarose beads as described previously (Sung 1997a). In Figure 1C, 0.3 mL of the Q-Sepharose pool (fractions 8 to 16) containing the Rad51B–Rad51C peak was mixed with 10 μL of protein A beads containing anti-Rad51B, anti-Rad51C, or anti-ySrs2 antibodies at 4°C for 5 h. The beads were washed twice with 200 μL of buffer K containing 1 M KCl and once with 200 μL of buffer K, before being eluted with 20 μL of 2% SDS at 37°C for 10 min. The SDS eluates, 2 μL each, were analyzed by immunoblotting to reveal their content of Rad51B and Rad51C.

Affinity binding of the Rad51B–Rad51C complex to nickel-NTA agarose

Extract from 0.5 mL packed cell volume of High-Five insect cells harboring either the six-histidine-tagged Rad51B or Rad51C recombinant baculovirus was prepared as described above, using 3 mL of cell breakage buffer. After ultracentrifugation (100,000*g* for 1 h), 0.25 mL of the Rad51B and Rad51C containing extracts were mixed either with each other or with 0.25 mL of extract from insect cells that did not contain any recombinant baculovirus. After incubation on ice for 1 h, the various mixtures were subjected to ultracentrifugation (100,000*g* for 1h), and then rocked gently with 50 μL of nickel-NTA agarose beads (QIAGEN) at 4°C for 3 h. The beads were washed sequentially with 0.2 mL of 10 mM and 20 mM imidazole, and then with 0.1 mL of 150 mM imidazole. The starting fractions, supernatants after nickel-binding, and the three imidazole washes, 5 μL each, were subjected to immunoblot analysis to determine their content of Rad51B and Rad51C.

Other recombination proteins

Human Rad51 (hRad51 Lys^{313}) was expressed in and purified from *E. coli* as described (Sigurdsson et al. 2001). Human RPA was purified from *E. coli* cells transformed with a plasmid that co-overexpresses the three subunits of this factor (Henricksen et al. 1994), as described (Sigurdsson et al. 2001). Both hRad51 and hRPA were nearly homogeneous.

Homologous DNA pairing and strand exchange reactions

All the reaction steps were carried out at 37°C. The reaction buffer was 40 mM Tris-HCl (pH 7.8), 2 mM ATP, 1 mM $MgCl_2$, and 1 mM DTT, and contained an ATP regenerating system consisting of 8 mM creatine phosphate and 28 μg/mL creatine kinase. The standard reaction had a final volume of 12.5 μL, and was assembled by first incubating hRad51 (7.5 μM) added in 0.5 μL of storage buffer and ϕX174 viral (+) strand (30 μM nucleotides) added in 1 μL for 5 min. After this, hRPA (1.5 μM) in 0.5 μL of storage buffer was added and following a 5 min incubation, 1.25 μL of ammonium sulfate (1 M stock, final concentration of

100 mM) was incorporated. Immediately afterward, linear ϕX174 replicative form I DNA (15 μM base pairs) in 1 μL was added to complete the reaction. At the indicated times, 5 μL portions were withdrawn, mixed with 7.5 μL of 0.8% SDS and 800 μg/mL proteinase K, incubated for 15 min at 37°C, before being run in 0.9% agarose gels in TAE buffer (40 mM Tris acetate at pH 7.4, 0.5 mM EDTA). The gels were stained in ethidium bromide (2 μg/mL in H_2O) for 1 h, destained for 12 to 18 h in a large volume of water at 4°C, and then subjected to image analysis in a NucleoTech gel documentation station equipped with a CCD camera. In some experiments, the reaction was scaled up appropriately to accommodate the increased number of timepoints used. In Figure 4B, panel II, storage buffer was added instead of RPA, but otherwise the reaction was assembled in exactly the same manner as the standard reaction. In Figure 5A, panel I, Rad51 and RPA were added together to ssDNA at the beginning of the reaction and incubated for 10 min with the latter, but otherwise the additions of the ammonium sulfate and linear ϕX duplex followed the procedure described for the standard reaction. In Figure 5A, panel II and in Figure 5B, Rad51, RPA, and the indicated amounts of Rad51B–Rad51C were incubated with the ssDNA for 10 min, but otherwise the additions of the ammonium sulfate and linear ϕX duplex followed the procedure described for the standard reaction. In Figure 6, Rad51 and the indicated amounts of Rad51B–Rad51C were incubated with the ssDNA for 10 min, but otherwise the additions of the ammonium sulfate and linear ϕX duplex followed the procedure described for the standard reaction.

DNA mobility shift and ATPase assays

The indicated amounts of Rad51B–Rad51C complex were incubated with ϕX ssDNA (12 μM nucleotides), dsDNA (4 μM base pairs), or both ssDNA (12 μM nucleotides) and dsDNA (4 μM base pairs) in reaction buffer (50 mM Tris-HCl at pH 7.8, 1 mM DTT, 100 μg/mL BSA, 1 mM $MgCl_2$, 1 mM ATP, and 100 mM KCl) for 10 min at 37°C. After electrophoresis in 0.9% agarose gels in TAE buffer at 4°C, the gels were stained in ethidium bromide (2 μg/mL in H_2O) for 1 h and destained at 4°C for 12 to 18 h, before being subjected to image analysis in the gel documentation station.

Rad51B–Rad51C (1.8 μM) was incubated in the absence or presence of ssDNA (20 μM nucleotides) or dsDNA (20 μM base pairs) in 10 μL of reaction buffer (50 mM Tris-HCl at pH 7.8, 1 mM DTT, 1 mM $MgCl_2$) containing 1 mM [γ-^{32}P]ATP for the indicated times at 37°C. The level of ATP hydrolysis was determined by thin layer chromatography as described previously (Petukhova et al. 2000).

Acknowledgments

We thank Susie Zhang for constructing the Rad51C recombinant baculovirus. This work was supported by Public Health Service grants PO1CA81020, GM57814, ES07061, GM30990, CA81019-01 and by California Breast Cancer Research Program grant 5KB-0123. S.S. was supported in part by U.S. Army Training Grant DAMD17-99-1-9402 and Predoctoral Fellowship DAMD-17-01-1-0412. S.V.K. was supported in part by U.S. Army Predoctoral Fellowship DAMD-17-01-1-0414.

The publication costs of this article were defrayed in part by payment of page charges. This article must therefore be hereby marked "advertisement" in accordance with 18 USC section 1734 solely to indicate this fact.

References

Baumann, P. and West, S.C. 1997. The human Rad51 protein: Polarity of strand transfer and stimulation by hRP-A. *EMBO J.* **16:** 5198–5206.

———. 1999. Heteroduplex formation by human Rad51 protein: Effects of DNA end-structure, hRP-A and hRad52. *J. Mol. Biol.* **291:** 363–374.

Beernink, H.T. and Morrical, S.W. 1999. RMPs: Recombination/replication mediator proteins. *Trends. Biochem. Sci.* **24:** 385–389.

Benson, F.E., Stasiak, A., and West, S.C. 1994. Purification and characterization of the human Rad51 protein, an analogue of *E. coli* RecA. *EMBO J.* **23:** 5764–5771.

Bianco, P.R., Tracy, R.B., and Kowalczykowski, S.C. 1998. DNA strand exchange proteins: A biochemical and physical comparison. *Front. Biosci.* **3:** D570–D603.

Braybrooke, J.P., Spink, K.G., Thacker, J., and Hickson, I.D. 2000. The Rad51 family member, Rad51L3, is a DNA-stimulated ATPase that forms a complex with XRCC2. *J. Biol. Chem.* **275:** 29100–29106.

Dasika, G.K., Lin, S.C., Zhao, S., Sung, P., Tomkinson, A., and Lee, E.Y. 1999. DNA damage-induced cell cycle checkpoints and DNA strand break repair in development and tumorigenesis. *Oncogene* **18:** 7883–7899.

Gasior, S.L., Wong, A.K., Kora, Y., Shinohara, A., and Bishop, D.K. 1998. Rad52 associates with RPA and functions with rad55 and rad57 to assemble meiotic recombination complexes. *Genes & Dev.* **12:** 2208–2221.

Gasior, S.L., Olivares, H., Ear, U., Hari, D.M., Weichselbaum, R., and Bishop, D.K. 2001. Assembly of RecA-like recombinases: Distinct roles for mediator proteins in mitosis and meiosis. *Proc. Natl. Acad. Sci.* **98:** 8411–8418.

Gupta, R.C., Bazemore, L.R., Golub, E.I., and Radding, C.M. 1997. Activities of human recombination protein Rad51. *Proc. Natl. Acad. Sci.* **94:** 463–468.

Henricksen, L.A., Umbricht, C.B., and Wold, M.S. 1994. Recombinant replication protein A: Expression, complex formation, and functional characterization. *J. Biol. Chem.* **269:** 11121–11132.

Kurumizaka, H., Ikawa, S., Nakada, M., Eda, K., Kagawa, W., Takata, M., Takeda, S., Yokoyama, S., and Shibata, T. 2001. Homologous-pairing activity of the human DNA-repair proteins Xrcc3–Rad51C. *Proc. Natl. Acad. Sci.* **98:** 5538–5543.

Masson, J.Y., Stasiak, A.Z., Stasiak, A., Benson, F.E., and West, S.C. 2001. Complex formation by the human Rad51C and XRCC3 recombination repair proteins. *Proc. Natl. Acad. Sci.* **98:** 8440–8446.

Moynahan, M.E., Chiu, J.W., Koller, B.H., and Jasin, M. 1999. Brca1 controls homology-directed DNA repair. *Mol. Cell* **4:** 511–518.

Moynahan, M.E., Pierce, A.J., and Jasin, M. 2001. BRCA2 is required for homology-directed repair of chromosomal breaks. *Mol. Cell* **2:** 263–272.

New, J.H., Sugiyama, T., Zaitseva, E., and Kowalczykowski, S.C. 1998. Rad52 protein stimulates DNA strand exchange by Rad51 and replication protein A. *Nature* **391:** 407–410.

Ogawa, T., Yu, X., Shinohara, A., and Egelman, E.H. 1993. Similarity of the yeast RAD51 filament to the bacterial RecA filament. *Science* **259:** 1896–1899.

Paques, F. and Haber, J.E. 1999. Multiple pathways of recombination induced by double-strand breaks in *Saccharomyces cerevisiae*. *Microbiol. Mol. Biol. Rev.* **63:** 349–404.

Petukhova, G., Sung, P., and Klein, H. 2000. Promotion of Rad51-dependent D-loop formation by yeast recombination factor Rdh54/Tid1. *Genes & Dev.* **14:** 2206–2215.

Roca, A.I., and Cox, M.M. 1997. RecA protein: Structure, function, and role in recombinational DNA repair. *Prog. Nucleic. Acid. Res. Mol. Biol.* **56:** 129–223.

Schild, D., Lio, Y., Collins, D.W., Tsomondo, T., and Chen, D.J. 2000. Evidence for simultaneous protein interactions between human Rad51 paralogs. *J. Biol. Chem.* **275:** 16443–16449.

Shinohara, A. and Ogawa, T. 1998. Stimulation by Rad52 of yeast Rad51-mediated recombination. *Nature* **391:** 404–407.

Sigurdsson, S., Trujillo, K., Song, B., Stratton, S., and Sung, P. 2001. Basis for avid homologous DNA strand exchange by human Rad51 and RPA. *J. Biol. Chem.* **276:** 8798–8806.

Sugiyama, T., Zaitseva, E.M., and Kowalczykowski, S.C. 1997. A single-stranded DNA-binding protein is needed for efficient presynaptic complex formation by the *Saccharomyces cerevisiae* Rad51 protein. *J. Biol. Chem.* **272:** 7940–7945.

Sung, P. 1997a. Function of yeast Rad52 protein as a mediator between replication protein A and the Rad51 recombinase. *J. Biol. Chem.* **272:** 28194–28197.

———. 1997b. Yeast Rad55 and Rad57 proteins form a heterodimer that functions with replication protein A to promote DNA strand exchange by Rad51 recombinase. *Genes & Dev.* **11:** 1111–1121.

Sung, P. and Robberson, D.L. 1995. DNA strand exchange mediated by a RAD51-ssDNA nucleoprotein filament with polarity opposite to that of RecA. *Cell* **82:** 453–461.

Sung, P., Prakash, L., Matson, S.W., and Prakash, S. 1987. RAD3 protein of *Saccharomyces cerevisiae* is a DNA helicase. *Proc. Natl. Acad. Sci.* **84:** 8951–8955.

Sung, P., Trujillo, K., and Van Komen, S. 2000. Recombination factors of *Saccharomyces cerevisiae*. *Mutat. Res.* **451:** 257–275.

Takata, M., Sasaki, M.S., Sonoda, E., Fukushima, T., Morrison, C., Albala, J.S., Swagemakers, M.A., Kanaar, R., Thompson, L.H., and Takeda, S. 2000. The Rad51 paralog Rad51B promotes homologous recombinational repair. *Mol. Cell. Biol.* **20:** 6476–6482.

Takata, M., Sasaki, M.S., Tachiiri, S., Fukushima, T., Sonoda, E., Schild, D., Thompson, L.H., and Takeda, S. 2001. Chromosome instability and defective recombinational repair in knockout mutants of the five Rad51 paralogs. *Mol. Cell. Biol.* **21:** 2858–2866.

Thompson L.H. and Schild, D. 2001. Homologous recombinational repair of DNA ensures mammalian chromosome stability. *Mutat. Res.* **477:** 131–153.

Umezu, K., Chi, N.W., and Kolodner, R.D. 1993. Biochemical interaction of the *Escherichia coli* RecF, RecO, and RecR proteins with RecA protein and single-stranded DNA binding protein. *Proc. Natl. Acad. Sci.* **90:** 3875–3879.